

Computational Models for Civil Engineering

C.Ionescu, A.H.Bărbat
R.Scînteie, A.Nicuță
Editors



COMPUTATIONAL MODELS FOR CIVIL ENGINEERING

Constantin Ionescu, Alex Horia Bărbat,
Rodian Scînteie, Alina Mihaela Nicuță
editors



Editura Societății Academice "Matei - Teiu Botez"
Iași 2008

Proceedings of the Sixth International Symposium

" Computational Civil Engineering 2008"

Iași, Romania, May 30, 2008

Descrierea CIP a Bibliotecii Naționale a României

Computational models for civil engineering / ed.: C.

Ionescu, A. H. Bărbat, R. Scînteie, A. Nicuță. - Iași :
Editura Societății Academice "Matei - Teiu Botez",
2008

Bibliogr.

ISBN 978-973-8955-41-7

I. Ionescu, C. (ed.)

II. Bărbat, A. H. (ed.)

III. Scînteie, Rodian (ed.)

IV. Nicuță, A. (ed.)

004:624

**THE VIth INTERNATIONAL SYMPOSIUM
"COMPUTATIONAL CIVIL ENGINEERING 2008"**

ORGANIZERS

**Academic Society "Matei - Teiu Botez"
Academy of Romanian Scientists
Faculty of Civil Engineering and Installations**

Co-ordination committee

Prof. Eng. Constantin Ionescu - president
Prof. Eng. Nicolae Țăranu
Prof. Eng. Horia Alexandru Barbat
Prof. Eng. Mihai Budescu

Scientific commission

Dr. Eng. Rodian Scînteie - co-ordinating
Prof. Eng. Elena Axinte
Prof. Eng. Doina Ștefan
Prof. Eng. Andrei Radu
Associate Prof. Eng. Irina Lungu
Associate Prof. Eng. Marinela Bărbuță
Associate Prof. Eng. Liliana Bejan
Secretary - Drd. Ec. Alina Nicuță

Organizing commission

Dr. Eng. Ionică Modoi - co-ordinating
Drd. Arh. Tudor Grădinaru
Drd. Eng. Cristian Ciobanu
Drd. Eng. Gabriela Covatariu
Secretary – Eng. Nicoleta Peșehonov

Table of Contents

1. L. Bejan Computational Science and Civil Engineering	1
2. Irina Baran Computational Modeling In Civil Buildings	11
3. O. Rosca, M. Budescu Advanced Computer Based Structural Design	18
4. M. Barbuta, D. Lepadatu Concrete and Reinforced Concrete Structures	28
5. R. Andrei, C. Ionescu, A. Nicuta Soft Computing in Transportation and Civil Engineering	37
6. Irina Lungu Trends in soil improvement to accommodate constructions of high class importance in urban restrictive zones	41
7. D. Stefan, V.E. Chitan Dynamic And Seismic Analysis Of Some Structures	46
8. A.H. Barbat, P. Mata, S. Oller, R. Boroschek, J.C. Vielma Computational model for buildings with energy dissipators subjected to seismic Action	54
9. Cosmina Geanina Adam, Iulian Gabriel Mihai Minimum weight buildings design best evaluation using inequalities method automatic evaluation program	70
10. Ion Anghel, Popa Constantin, Pavel Alecsandru Application of computer modeling in civil fire safety engineering. Glass breakage in fire.	78
11. Valeriu Banut, Mircea-Eugen Teodorescu Stability plane structure analysis program by correction functions	89
12. Renáta Bašková Automation of building process time structure models	98
13. Dalibor Beneš Masonry mortar development based on fluid fly ashes	109
14. Huseyin Bilgin, Hasan Kaplan, Salih Yilmaz Seismic assessment of existing R.C. Public Buildings in Turkey – An overview with a case Study	115
15. Jiří Brožovský, Jiří Brožovský, Jr. and Jiří Bydžovský Aggregates types impact on features of fresh and hardened concrete using gypsum free cement	131
16. Cristina Cosma Available Scheduling software for linear repetitive construction projects	138

17. Irene Daprà, Giambattista Scarpi Numerical solution for unsteady Couette flow of viscoplastic fluids	155
18. L. De Doncker, P. Troch, R. Verhoeven, N. Desmet, K. Buis, P. Meire Computational Aspects of River Hydraulics	168
19. Adrian Doloca, Oana Țănculescu Epiqr energy – A New Software For the Evaluation of Thermal Energy Consumption in Buildings	178
20. Amos Dufka Problems with determination of degradation level of reinforced elements from fire affected constructions	185
21. Mihai Iancovici, Cristian Gavrilesco Database-assisted seismic analysis of tall buildings subjected to long predominant period Vrancea earthquakes	194
22. Pavol Juhás, Mohamad Al Ali, Zuzana Kokoruďová The elastic-plastic load-carrying capacity of thin-walled steel members with quasi-homogenous and hybrid cross-sections	207
23. Saeed Khorram Numerical Simulation of Wave Transformation in the Fars Gulf	221
24. Saeed Khorram Modeling of light Non-aqueous phase liquids Spreading and Migration to fate of oil and Locate the Source, case study in Estahban	228
25. Ludovic Kopenetz, Alexandru Cătărig Structural Analysis of High Rise Building Structures	236
26. Ludovic Kopenetz, Ferdinand-Zsongor Gobesz Expert Study of Bearing Structures, Using Intelligent Control Systems Based on Fuzzy Logi	246
27. Mária Kozlovská, Assoc. Prof. PhD, Lukáš Sabol, Eng. Building projects control by software products	256
28. Helena Křišíková The theoretic base for simulation and calculation of boreholes	265
29. Helena Křišíková The soil thermal analysis in the neighbor of ground source heat exchanger of the heat pump	272
30. Helena Křišíková The thermal behavior of the water to water heat pump	280
31. Ciprian Lamatic, Nicolae Ungureanu, Mihai Vrabie The analysis of the liquid-filled cylindrical tank's wall flexibility	287
32. Ferencz Lazar-Mand, Dragoș Florin Lișman Practical Aspects about Linear Dynamic Analysis of Cable Structures	298
33. Daniel Lepădatu, Marinela Bărbuța Optimal mix design of polymer concrete using generalized reduced gradient algorithm	311
34. Tomáš Melichar Glass addition influence on cement-bound composite materials' strength characteristics	325
35. Horatiu Alin Mociran, Alexandra Denisa Stan The influence of damping ratios on earthquake response of steel frame structures	334

36. Mohamad Al Ali	
The simulation of weakening of steel columns` cross-sections caused by welding when strengthening under load	342
37. M. Moradi, A.H. Alavi, M.A. Pashabavandpour, A.H. Gandomi, A. Askarinejad	
Soft computing based approaches for lime-microsilica stabilized clayey soils	350
38. Roman Musil	
People Presence Stochastic Model for Building Energy Simulations	366
39. Roman Musil	
People Behaviour Influence for Total Yearly Energy need in one Person Office Room	378
40. Mihai Nedelcu	
Seismic analysis using Robot Millennium	383
41. Alina Mihaela Nicuță	
Computational Approaches for Life Cycle Cost Analysis	393
42. Eugen Pamfil, Vasile Iacob, Ioan Paul Voda	
Comparative study regarding three standardized European methods for estimation on horizontal loads that act on formworks	403
43. Popa Constantin, Ion Anghel, Valeriu Panaitescu	
Modeling and simulation of ventilation in fire emergency situations	421
44. David Procházka, Dalibor Beneš	
Gamma Radiation Shielding	430
45. Irina Radinschi, Cristian Damoc	
Computer Simulations for Physics Laboratory	441
46. Voichița Roib	
Computer Simulations for Physics Laboratory	448
47. Claudiu Romanescu, Cristina Romanescu, Rodian Scînteie	
Simplified Inventory for Road Culverts and Bridges	458
48. Claudiu Romanescu, Cristina Romanescu, Rodian Scînteie	
Analysis of repair works assignment to create the BMS works database	462
49. Victoria E. Roșca, Lictor M.A. Leitão	
Numerical implementation of meshless methods for beam problems	476
50. Salim Sadi	
Pushover analysis of reinforced concrete structures (Damage theory)	486
51. Meisam Safari Gorji, Masoud Taribakhsh, Amirhossein Gandomi	
Seismic Assessment and Strengthening of Intermediate Moment Resisting Concrete Frames	497
52. Jaroslav Smutny, Lubos Pazdera, Ivo Moll	
The Comparison of the Dynamic Parameters of the Rail Fastening Vossloh W 14 and Pandrol FC	512
53. Jaroslav Smutny, Lubos Pazdera, Ivo Moll, Miroslav Bajer	
The Analysis of Dynamic Effects in Turnout Structures by the Method of Quadratic Time and Frequency Invariant Transformations	518
54. Alexandra Stan, Horațiu Mociran	
Modeling lateral earth pressure on concrete retaining walls	525
55. Doina Stefan, Gabriela Covatariu	
The seismic force development related to romanian designing codes	531

56. Jerzy Szolomicki Different numerical methods using for analysis of historical masonry structures	541
57. George Țăranu, Mihai Budescu Slab stiffness influence in design of reinforced concrete frame system	547
58. Teodorescu Mircea-Eugen, Topala Cristina-Alexandra The detection of singular points in the stability analysis of structures	558
59. Nicolae Ungureanu, Mihai Vrabie, Iancu Bogdan Teodoru The Seismic Soil-Structure Interaction Effect for Pile-Raft Systems	568
60. Ioan Paul Voda, Nicolae Florea, Vasile Iacob Numerical implementation of meshless methods for beam problems	578
61. Iulia Brîndușa Ciobanu Computational modeling development for radionuclide decay study	588
62. Photo	603

Computational Science and Civil Engineering

Liliana Bejan¹

¹*Department of Theoretical Mechanics,
Technical University “Gh.Asachi” Iasi, 700050, Romania*

Computational science (or scientific computing) is the field of study concerned with constructing mathematical models and numerical solution techniques and using computers to analyse and solve scientific, social scientific and engineering problems. In practical use, it is typically the application of computer simulation and other forms of computation to problems in various scientific disciplines. Scientists and engineers develop computer programs, application software, that model systems being studied and run these programs with various sets of input parameters. Problem domains for computational science/scientific computing include:

Numerical simulations which have different objectives depending on the nature of the task being simulated:

- Reconstruct and understand known events (e.g., earthquake, tsunamis and other natural disasters).
- Predict future or unobserved situations (e.g., weather, sub-atomic particle behaviour).

Model fitting and data analysis

- Appropriately tune models or solve equations to reflect observations, subject to model constraints (e.g. oil exploration geophysics, computational linguistics)
- Use graph theory to model networks, especially those connecting individuals, organizations, and websites.

Optimization

Computational science application programs often model real-world changing conditions, such as weather, air flow around a plane, automobile body distortions in a crash, the motion of stars in a galaxy, an explosive device, etc. Such programs might create a 'logical mesh' in computer memory where each item corresponds to an area in space and contains information about that space relevant to the model. Computational science is now commonly considered a third mode of science, complementing and adding to experimentation/observation and theory. The benefits of using computer simulations in production and research are indisputable, and include more efficient utilisation of resource and cost saving from this increased efficiency. Indeed, in many fields, computer simulation is integral and therefore essential to business and research. Computer simulation provides the capability to enter fields that are inaccessible to traditional experimentation and methods of inquiry. As computers become faster and computationally more

powerful, the range of application for computer simulation and modelling has also expanded.

Civil engineering involves planning, research, and design related to the construction of bridges, tunnels, airports, skyscrapers, pipelines, highways, railways, dams, towers, and buildings for commerce and industry, as well as water supply and waste-management systems. As the complexity of civil engineering systems has increased, computers have been used increasingly for simulation, visualization, and design. However, nationwide surveys of employers have clearly demonstrated the inadequacy of current conventional computer science training programs in meeting the need of civil engineering firms and engineering-application-oriented software companies. The software training of the computer science program with the civil engineering training in engineered structures and systems, offer the possibility to perform sophisticated computer simulations of engineering systems and develop appropriate software for various engineering applications.

One of application is the problem of light Non-aqueous phase liquids (LNAPL) spreading and migration was studied by **Saeed Khorram** in the paper **Modeling of light Non-aqueous phase liquids Spreading and Migration to fate of oil and Locate the Source**, case study in Estahban. A common problem associated with oil refineries is the subsurface contamination resulted from leaking of light non-aqueous phase liquids (LNAPL), released from storage tanks and underground facilities. LNAPL transport on the water table is modeled numerically to simulate the extent of current oil contamination plumes over the groundwater and to investigate the future fate of the contamination by finding possible suitable locations for their treatment. The model proposed assumes a sharp interface between the LNAPL and groundwater that takes into account the groundwater velocity and pertinent soil parameters. Analyses are carried out considering presence and absence of the leaking sources. The results show that, migration is relatively small when a LNAPL leaks above an unconfined aquifer, the NAPL migrates through the unsaturated zone as a separate phase under the dominant influence of gravity, leaving residual droplets in the unsaturated zone. Once it reaches the water table, the LNAPL forms a free-product mound floating on the water table The governing partial differential equation which describe spreading and migration of LNAPL is solved numerically using a finite difference technique of 2-D governing equation through classical Implicit, Alternate Direction Implicit (ADI), or explicit finite difference methods. A computer program was developed to incorporate the above-mentioned algorithm in order to simulate the migration and spreading of LNAPL mounds. Computer program was developed in "MATLAB" environment. Two computer programs were developed: Program #1: Solves the governing differential equation assuming a continuous LNAPL source with a prescribed discharge value to predict LNAPL spreading and migration in the solution domain with time. Program #2: Solves the governing differential equation

in the absence of a continuous LNAPL source. This program is capable of simulating migration and spreading of LNAPL mound on an ambient groundwater surface by taking into account the residual mass loss, which is left behind in the pores. Results obtained using sharp interface model for the case studied, are discussed into two different parts:

A- Speculation of previous history and pattern of leaks,

B- Prediction of future LNAPL plumes spreading and migration with time:

- spreading and migration of current LNAPL mounds considering a continuous leaking source.
- spreading and migration of LNAPL mounds with no leaking source

LNAPL mounds were simulated and duration and pattern of leaks leading to the existing condition were estimated. According to model results, further migration of LNAPL mounds was small. Consequently, sources of LNAPL contamination were expected to be located in the proximity of maximum LNAPL thicknesses for each mound. This fact helped locating possible source of leakage at the site.

Another numerical simulation in the same field of fluid mechanics was developed by the same **Saeed Khorram** in his paper **Numerical Simulation of Wave Transformation in the Fars Gulf**. for the simulation of wave transformations applicable to irregular bottom topographies. It was developed a numerical model based on nonlinear parabolic mild slope equation that could simulate wave shoaling, refraction, diffraction together. The numerical model has been solved by Mac Cormack Method with using Point Gauss Seidel Iteration Method. Wave phase gradient of Ebersole has been used to determine local wave number in the model. The model is applicable to arbitrary varying bottom topographies. Unidirectional waves are considered for the numerical model. Model predictions are compared with the physical experiment over semicircular shoaling area. The study has been applied to Fars Gulf located on the Mediterranean Sea Coast of Iran. MacCormack method is a multistep method and are using Point Gauss Seidel iteration m. Firstly, forward finite difference approximations are used to obtain the predictor and then backward finite difference approximations are applied to the governing equation to find the corrector. This method gives more realistic results than the other methods since it assures static stability. Point Gauss Seidel Iteration provides to reach the convergence more rapidly because the current variables of dependent variable are used to compute the neighbouring points as soon as they are available.

The nonlinear parabolic model has been used in this study so as to overcome caustics problems of the linear theory. The use of wave phase gradient provides more accurate results to obtain the local wave number. The model can be successfully used over arbitrary bathymetries in the prespecified direction.

Computational physics is the study and implementation of numerical algorithms in order to solve problems in physics for which a quantitative theory already exists. It is often regarded as a subdiscipline of theoretical physics but some consider it an intermediate branch between theoretical and experimental physics. Physicists often have a very precise mathematical theory describing how a system will behave. Unfortunately, it is often the case that solving the theory's equations ab initio in order to produce a useful prediction is not practical. This is especially true with quantum mechanics, where only a handful of simple models have complete analytic solutions. In cases where the systems only have numerical solutions, computational methods are used.

An example of applications of computational physics is the paper **Computational modeling development for radionuclide decay study** by **Iulia Brîndușa Ciobanu**. The contribution of this work is to perform a computational program in C++ language, adapted to the study of beta radiation interaction with substance. The program computes the linear absorption coefficient, mass absorption coefficient of beta radiation, maximum mass range, and maximum distance of radiation penetration into substance as well as maximum energy. The program was run for a set of experimental data obtained by measurements with the help of a Geiger type radiation counter, using a Cs-137 radionuclide source and as absorbent substance, aluminum (Al). The parameters of the two equivalent linear representations of radionuclide decay law were calculated, that derive by logarithmation of disintegration law. The processing of experimental data is computed by using the least squares method. Experiments have shown that all radioactive radiations cause chemical effects, blacken photographic plates, ionize gases and, sometimes, condensed materials on passing through them, and cause some solids and liquids to fluoresce. This computational method can be used for nondestructive density measurements of cylindrical specimens. This method has several important applications in civil engineering. Many specimens in civil engineering laboratory testing are usually in the form of cylinders. One can show that for solid cylindrical specimens of the materials tested, the radiation attenuation law is satisfied to a very high degree.

Many problems in CFD, Computational Physics etc., involve the numerical solution of a set of equations in a complicated shape domain. The solution of such problems requires the domain to be discretized to produce a set of points on which the numerical algorithm can be based. For some problems, the generation of a suitable grid/mesh can be as demanding as the effort required to perform the computations for which the grid was intended. In recent times, considerable attention has been focused on the discretization process, which is commonly called mesh generation.

The paper **IITGEN System - Mesh Generation and Analysis System for 2D Surfaces** by **Ioan Pavaloi, Florin Rotaru, Cristina Nita Dan Diaconu** begins with an introduction in the mesh generation and the general concepts involved. It

also describes some various generation of the techniques. Numerical mesh generation has now become a fairly common tool for use in the numerical solution of PDEs on arbitrarily shaped regions. This is especially true in CFD, from which came much of Finite element analysis for pre-stressed concrete structures is an important part of the whole design process. The advantages of quadrilateral isoparametric elements versus triangles are numerous and well-known in this domain. The paper after a general presentation of the IITGEN system describes the features provided by the system, focuses especially on editing, processing and mesh analyzing.

In engineering and science, one often has a number of data points, as obtained by sampling or some experiment, and tries to construct a function, which closely fits those data points. The so-called meshless methods construct approximations from a set of nodal data without the need for any (finite - element) a priori connectivity information between the nodes. The authors **Victoria E. Roşca, Vitor M.A. Leitão** present in their paper a **Numerical implementation of meshless methods for beam problems** a flexible computational procedure for solving 1D linear elastic beam problems that currently uses two forms of approximation function (moving least squares and kernel approximation functions) and two types of formulations, namely the weak form and collocation technique, respectively, to reproduce Element Free Galerkin (EFG) and Smooth Particle Hydrodynamics (SPH) meshless methods.

Materials science or materials engineering is an interdisciplinary field involving the properties of matter and its applications to various areas of science and engineering. This science investigates the relationship between the structure of materials and their properties. It includes elements of applied physics and chemistry, as well as chemical, mechanical, civil and electrical engineering. With significant media attention to nanoscience and nanotechnology in recent years, materials science has been propelled to the forefront at many universities. It is also an important part of forensic engineering and forensic materials engineering, the study of failed products and components. The basis of all materials science involves relating the desired properties and relative performance of a material in a certain application to the structure of the atoms and phases in that material through characterization. The major determinants of the structure of a material and thus of its properties are its constituent chemical elements and the way in which it has been processed into its final form. These, taken together and related through the laws of thermodynamics, govern a material's microstructure, and thus its properties. An old adage in materials science says: "materials are like people; it is the defects that make them interesting. “.

Fire is one of the factors that might be the cause of considerable failure on constructional objects and in extreme cases they might cause the collapse of the whole construction. It is possible that extreme temperatures connected with the outbreak of fire degraded building materials by expansion pressures of water

steam, linear respectively volume changes etc. with physically chemical principles (degradation of material swage, modification changes etc.). The paper **Problems with determination of degradation level of reinforced elements from fire affected constructions** by **Amos Dufka** present degradation of material as a consequence of synergistic action occurs at the fire affected reinforced concrete constructions of both physical (temperature shocks, expansion pressures of water steam etc.), and physically chemical mechanisms (decomposition of cement swage, modification changes in aggregate etc.). With regard to these facts it is obvious that correct judgement of state respectively measure of disruption of constructions interfered this way makes demands on measure of tests and analysis realised in the frame of constructional technical research.. This work treats

- the problems with choosing diagnostic procedures that are required for correct judgement of state of reinforced concrete constructions
- diagnostic processes whose aim is to judge succinctly the state of reinforced concrete constructions struck by fire and especially securing the data for statical judgement of constructions evaluated.

Both physically mechanical parameters of concrete are watched (especially its bastion characterisation) and physically chemical analyses are made (with an aim to judge the state of cement swage) and the state of steel reinforcement is monitored as well. The autor recommend unambiguously expanding the results of statement of tensile strength of surface layers of concrete by carrying out tests of concrete tensile strength (tests on core holes) for a more complex judgement of state of constructional elements.

Many researches focused to study the domain of structures deformation capability, conductive heat transfer and thermic deformation capacity (respectively, elastic deformation of structures created by dynamic variation of temperature). The paper **Using WinFidias System for Temperature Distribution Computing** by **Dan Diaconu, Ioan Pavaloi** study this problem using finite elements method. This is motivated by current trends in present legislative environment regarding fire security of buildings exposed to large variations of temperature, especially to fire hazard. The calculus of temperatures distribution in bars structures, both in 1D, 2D and in 3D structures, both in stationary and non-stationary state is based on Fidias routines package Fidias, developed in Iasi, at Faculty of Civil Engineering and also on WinMesh system, developed in Iasi, at Institute for Computer Science. The result is the WinFidias system. This paper present

- a general WinFidias system' presentation software package that provides facilities of editing, meshing, temperature distribution calculus and final results display and printing.
- the way of technical accomplishment of objective is to analyze stationary heat transfer at discretizeable structures
- a model for the analysis of structures modelled by using two-dimensional elements (quadrilaterals).

Another very important application in the civil engineering is the study of the seismic effects on the buildings. The seismic calculus researches in the past 50 years also based on experimental recordings are led to changes in the building design standards. The recent devastating earthquakes have exposed the vulnerability of the existing public buildings.

The paper Seismic Assessment of Existing R.C. Public Buildings in Turkey – An Overview with a Case Study by Huseyin Bilgin, Hasan Kaplan and Salih Yilmaz, aims to evaluate the seismic performance of a public building with the selected template design in Turkey considering the nonlinear behavior of reinforced concrete members. Seismic performance evaluation will be carried out in accordance with the recently published Turkish Earthquake Code-2007 that has many similarities with FEMA 356 guidelines. This study has evaluated the seismic performance of a typical (hospital) building in Turkey using TEC-2007 and determine the various seismic retrofit techniques.. In order to compute global structural parameters, such as stiffness, strength and deformation capacity; pushover analysis was conducted for the case hospital building. This study evaluated seismic capacity of a typical hospital building considering nonlinear behaviour of reinforced concrete components. The results of the pushover analysis were investigated according to TEC-2007 requirements for evaluating the seismic response of this building. Finally, different possible retrofitting solutions able to improve the seismic behaviour of non-seismically designed public buildings have been discussed. The building has a typical structural system, and no structural irregularities. For modelling and the structural analysis of the case, the computer program SAP2000NL, Nonlinear Version 8.2.3 was employed (program for performing static and dynamic finite element analyses of structures). The observations and findings of the current study are briefly summarized as following:

- that concrete quality and detailing has significant role in displacement and lateral strength capacity of buildings either in both directions
- the difference of poor (C10 and s250) and average (C16 and s150) conditions on lateral strength capacity is limited, the difference in displacement capacity is noteworthy.
- shear failures of columns are common problems for poor concrete and low amount of transverse reinforcement, resulting in brittle failure for existing hospital buildings.
- as material quality gets better, performance of buildings improves
- the amount of transverse reinforcement increases the displacement capacity increases as well and therefore the sustained damage decreases.
- adding of shear walls increases lateral load capacity and decreases displacement demands significantly

Other issues were presented in the work **The seismic force development related to romanian designing codes** by **Doina Stefan, Gabriela Covatariu**. This paper aims evolution of global seismic coefficient for 3 types of structures situated in Iasi and Bucharest. By analyzing the results of the seismic force calculus according to the present standards one it can notice the major increase of the seismic force value according to the P100-2006 Standard, in comparison with the former ones. Seismic force values representing 40-60% of the seismic force according to P100-2006 for various types of buildings designed in period 1963 - 1992 can be alarming. Analyzing the results of the seismic force calculus according to the present standards it can notice the major increase of the seismic force value according to the P100-2006 Standard, in comparison with the former ones. The structures of the buildings have been more or less affected by those earthquakes. This can be proved with the results obtained after the evaluations on various types of buildings made before 1992. Thus:

- structures made of bearing brick masonry - the bearing capacity being reduced with 22%.
- structures with reinforced concrete prefabricated diaphragms - real medium reduction of 25 to 28% (major problems with joints);
- reinforced concrete framed structures - real reduction of almost 6% (constant degradation mainly present in beams).

By corroborating the effects of the designing standards changes with the degradations caused by the earthquakes it could draw the alarming conclusion for the heritage witch was built before 1992 – the most of the buildings do not meet the terms of seismic insurance.

In order to perform an optimal economic evaluation of a construction project the research institutes have considered necessary to develop different computer software. This is due to the great diversity of information and for the facilitation of man's work. This is why in the last years have been created complex databases with different price information, construction details and other.

The paper **Computational Approaches for Life Cycle Cost Analysis** by **Nicuta Alina Mihaela**. present some of the software which realizes computer analysis of investments and cost – benefit analysis for construction projects. The software programs in the area of construction cost analysis addresses the needs of the transportation agency during a particular phase in the construction life cycle. The software programs presented in this paper have the role of explaining the evolution of the cost analysis for construction works. Some of the main economic analysis software models was presented, like:

- HERS and HERS-ST, Highway Economic Requirements System (HERS) is an analysis system for cost – benefit analysis developed by the Office of Goods Management from the Federal Administration of Highway Infrastructure.

- HDM 4, Highway Development and Management Tools (HDM-4) has been developed by the World Bank consequently after a serial of previous versions. It is used to estimate the benefits of roads users, infrastructure costs
- APA model - asphalt pavement analysis
- CES - Cost Estimation System
- The Cost Estimation System (CES) is the primary Transport module for construction cost estimation.
- ESTIMATOR- Highway Cost Estimation Workstation Transport Estimator is an interactive, PC-based, stand-alone cost estimation system for transportation construction that provides a graphical user interface for the preparation of detailed estimates.
- TRACER- Transportation Cost Estimator, Earth Tech and the American Association of State Highway & Transportation Officials (AASHTO) have developed a new cost estimating tool that will make it easier and more time efficient to estimate transportation project costs.
- BridgeLCC-Life cycle cost software for bridge design. BridgeLCC is user-friendly life-cycle costing software developed by the National Institute of Standards and Technology (NIST) to help bridge engineers assess the cost effectiveness of new, alternative construction materials.
- DARWin 3.1 is metric-compliant AASHTOWare computer software that conforms to and is compliant with the pavement design models

The software programs presented in this paper have the role of explaining the evolution of the cost analysis for construction works. Due to the great variety and quantity of information necessary to make the analysis this computer software have the purpose to facilitate the work for the analysis, to take into considerations different alternatives, to access new funding opportunities and to take optimal investment decisions.

High-rise buildings, pipelines, highways, railroads and long bridges are construction projects characterized by activities that are repeated sequentially at different locations, sections, units, or construction sites. These particular types of construction projects are considered high risk making the management of resources and partial delivery times a very important issue. The paper **Available Scheduling Software for Linear Repetitive Construction Projects** by **Cristina Cosma**, reviews the existent scheduling software available on the American and European market in an attempt to enhance knowledge of commercially available applications in the specific area of Linear Scheduling. Why is important that? Because for the case of pipeline, highways or railroad projects the repetition is the result of the geometrical layout of the project which is also characterized by linearity. All these projects are referred to as either linear, or repetitive or linear-repetitive construction projects. The linear repetitive construction projects usually require large amounts of resources which are used in a sequential manner. Projects of this type are considered high risk. The scheduling techniques that are being most used for

construction projects are the Bar Chart and the Network Diagrams (Critical Path Method - CPM). and Linear Scheduling Method. The market for linear scheduling software has been on the rise constantly and aggressively for the past two decades. From prototype software developed as a result of academic research, the market has advanced today to offering high performing, highly visual, user friendly software which can satisfy the diversity of construction management needs of linear repetitive construction projects.

References:

- [1]. Saeed Khorram, Modeling of light Non-aqueous phase liquids Spreading and Migration to fate of oil and Locate the Source,
- [2]. Saeed Khorram, Numerical Simulation of Wave Transformation in the Fars Gulf.
- [3]. Iulia Brîndușa Ciobanu, Computational modeling development for radionuclide decay
- [4]. Ioan Pavaloi, Florin Rotaru, Cristina Nita Dan Diaconu, IITGEN System - Mesh Generation and Analysis System for 2D Surfaces
- [5]. Victoria E. Roșca, Vitor M.A. Leitão, Numerical implementation of meshless methods for beam problems
- [6]. Amos Dufka, Problems with determination of degradation level of reinforced elements from fire affected constructions
- [7]. Dan Diaconu, Ioan Pavaloi, Using WinFidias System for Temperature Distribution Computing
- [8]. Huseyin Bilgin, Hasan Kaplan and Salih Yilmaz, Seismic Assessment of Existing R.C. Public Buildings in Turkey
- [9]. Doina Stefan, Gabriela Covatariu The seismic force development related to romanian designing codes
- [10]. Nicuta Alina Mihaela, Computational Approaches for Life Cycle Cost Analysis
- [11]. Cristina Cosma Available Scheduling Software for Linear Repetitive Construction Projects by

Computational Modeling In Civil Buildings

Irina Baran¹

Computational science and engineering (CSE) is a rapidly growing multidisciplinary area with connections to the sciences, engineering, mathematics, and computer science. CSE focuses on the development of problem-solving methodologies and robust tools for the solution of scientific and engineering problems. The ever increasing complexity of engineering problems has enormous demands on the computational tools available to engineers. Today, modeling computational tools are needed to analyze new projects with sophisticated high performance materials used in civil engineering structures.

Using computational modeling, it can be predicted the evolution of a process, starting not from the studied system, but from its analytic model, adapted to the computer implementation. Assuming different initial and border conditions, it can be obtained variations of the investigated parameters that can be used in the same manner as the information get on an experimental base.

The numerical modeling is very useful for the study of phenomena that are difficult to reproduce in laboratories. Sometimes the experimental studies involve not only huge expenses, but also a big risk. The study of building behaviour in laboratory conditions means important expenses, and the variations domain of oneness is quite limited, giving insufficient data for the phenomena characterization.

For these reasons the numerical modeling is more and more required.

In some cases, taking over some information resulted from experimental tests, this kind of modeling can study the real behaviour of buildings structures.

All the activities involved in the construction sector are today strongly influenced by the exceptional development of technologies and information science. The necessity of a sustainable development of the built environment, the decreasing risk of loosing human and material values, have been become of a global importance.

All the presented papers are underlying the research focus on the increasingly sophisticated simulations and modeling frameworks, supported by complementary experimental testing, to asses and predict the performance of civil engineering structures and materials.

This strong emphasis on modeling links of several inter-related research themes which aim to consolidate and enhance the research standing.

¹ “Gh. Asachi” Technical University of Iasi, Civil Engineering and Building Services Faculty

The paper entitled **Computer Simulations for Physics Laboratory [1]** (authors Irina Radinschi² and Cristian Damoc³) presents new computational technologies used for the implementation of the computer simulations of physics phenomena. These are powerful tools for learning physics concepts and developing skills of measurement and analysis.

The purpose of this paper is to present a physics simulation elaborated in Adobe Flash CS3 program and which is designated for the study of virtual evolution of the laws of photoelectric effect. Two important laws are verified, the current voltage curve, which is given by the dependence between the photoelectric current intensity I_f and the voltage U , $I_f = f(U)_{E=const.}$ for constant values of the illuminance E , and the dependence between the photoelectric current intensity I_f and the illuminance E , $I_f = f(E)_{U=const.}$ at constant values of the voltage U .

The application is developed to simulate the values obtained using the laboratory apparatus. The computer simulation is a copy of the real device and can be used at the same time with the experiment, and gives the possibility of making a comparative study between experiment and simulation. It can be also used as a checking tool of the results yielded by experimental work.

The goal is to allow students to use computer simulations as a method of discovery in physics. The students have in this way an open access to the virtual labs and simulations, and can work with a comparative mode of learning: experiments and software applications.

Adrian Doloca⁴, Oana Țănculescu⁴ present in the paper **Epiqr energy – A New Software For the Evaluation of Thermal Energy Consumption in Buildings[2]** a new software instrument that can be used by civil engineers and architects to estimate the necessary thermal energy for heating and hot water preparation for different scenarios: new building, refurbishment/modernization of an existing building, evaluation of an existing building for selling or renting,

The epiqr energy software is a useful tool for the design of the new buildings as well as for the modernisation of existing buildings which are required to meet the present energy conservation standards. It meets the most recent German and European standards to which the Romanian standards also tend. It is flexible and user-friendly

² Department of Physics, “Gh. Asachi” Technical University, Iasi

³ Faculty of Automatic Control and Computer Science, “Gh. Asachi” Technical University, Iasi

⁴ Department of Mathematics and Informatics, University of Medicine and Pharmacy “Gr.T. Popa” Iasi

The software has the following applications:

1. energy audit;
2. energy passport generation for new buildings or existing buildings in case of selling or renting;
3. testing the existing buildings if they comply with the current energy consumption standards;
4. optimization of a building energy performance, in the design phase, by analysing various solutions;
5. evaluation of energy conservation measures applied on existing buildings;
6. evaluation of the necessary energy resources at the national level by calculating energy consumption for representative buildings.

The paper **Building Projects Control by Software Products**[3], (authors Mária Kozlovská⁵, Lukáš Sabol⁵) deals with building projects risks issue from point of individual partners of project. Construction project presents a very difficult and extensive system of construction processes. Today, the preparation phase and management skills of construction participants are more important than ever. The whole construction project is very complex because of:

- the great number of construction participants,
- opposite purpose of construction participants (related to time and cost especially),
- complicated legislation and contracts between construction participants,
- frequent changes in construction plan by construction participants,
- construction participants are involved into other projects (with other construction participants).

Increased complexity of buildings and market demands calls for more integrated software tools, which create background with unitary source of information and data about structural elements and constructions. The software background with these demands is 3D information model, which can be linked with facility management and virtual building software tools.

These software tools are using BIM technology (Building Information Modeling). BIM can be used to demonstrate the entire building life cycle including the processes of construction and facility operation. Quantities and shared properties of materials can easily be extracted. Scopes of work can be isolated and defined.

In present time, the available technology can be specifics like switching between 3D technologies to 5D technologies. The Vico Software Virtual Construction™ product line and services address exactly these challenges. Using Virtual Construction technology, building owners, general constructors, and construction managers improve project predictability, reduce risk, manage costs, and optimize

⁵ Technical University of Kosice, Faculty of Civil Engineering, Slovakia

schedules on large, complex building projects. The Virtual Construction Software suite is a highly integrated 5D solution designed specifically to bring the benefits of BIM to construction companies.

The Vico software Virtual Construction product line consists of six integrated modules: Constructor 2008, Estimator 2008, Control 2008, 5D Presenter 2008, Cost Manager 2008, Change Manager 2008. Each of modules covers different issue in construction process.

Ion Anghel⁶, Popa Constantin⁶ and Pavel Alecsandru⁷ present the paper entitled Application of computer modeling in civil fire safety engineering. Glass breakage in fire [4].

The work analyses the propagation of fire to the upper floors of a building, because of the window glass breakage in the fire origin compartment.

The moment for glass breakage is estimated by using the Berkeley Algorithm for Breaking Window Glass in a Compartment Fire (BREAK1) computer program. The initiation, development and spread of the fire are simulated by using the Fire Dynamics Simulator (FDS) computer program.

Both programs are created by The National Institute of Standards and Technology (NIST-USA), and used together can be very helpful in providing fire safety specialists with valuable information about the spread of the fire, particularly for the high-rise buildings. To estimate the collapse of the structural elements (as window breakage) means a very important step in a real fire situation modeling and also a step in taking the necessary measures to minimize loss of human lives and material damage.

The article **Modeling and simulation of ventilation in fire emergency situations** [5] (authors Popa Constantin⁸, Ion Anghel⁸ and Panaitescu Valeriu⁹) treats the problem of ventilation in fires and a modern technique to keep the evacuation hallways and stairwells free of smoke and hot gases resulted from fires.

Fire Dynamics Simulator (FDS) is a computer program designed by the specialists at National Institute for Standards and Technology (NIST) in U.S.A., and is used by fire researchers all over the world, to simulate the development and all involved characteristics of fires, with given primary conditions (fire enclosure, fuel, wind). The program offers information about the temperature, concentration of gases and visibility in the compartments of the simulation.

⁶Fire Officers Faculty, "A.I.Cuza" Police Academy, Bucharest, Romania

⁷Petroleum Gas University, Ploiești, Romania

⁸Fire Officers Faculty, "Alexandru Ioan Cuza" Police Academy, Bucharest, Romania

⁹Energetic Faculty, Universitatea „Politehnica”, Bucharest, Romania

Two simulations were made, both of them on the same building, with the same conditions. The only difference is that in the first - which will be called standard simulation – no PPV was used; the second, PPV simulation, is the same as the first one, with PPV acting in the stair shaft, pressuring it. There are analyzed: the levels of carbon monoxide, level of smoke, pressure into the shaft, temperatures, visibility. The information and simulations proved that when a fan is used to pressurize a stair shaft, that space which have a greater pressure than the enclosure directly connected with the fire, do not permit the smoke and hot gases to permeate in large quantities into the shaft.

People Presence Stochastic Model for Building Energy Simulations [6] presented by Roman Musil¹⁰, presents an universal probability model of presence user inside buildings. This model will serve for people behaviour influence assessment on total yearly energy need. The user presence profile approximating the real behavior can help to improve energy calculation results and simultaneously the profile serves like first stage for modeling next energy loads which depend on people presence (hot and cold water consumption profiles , using lightings and electric appliances profiles, natural ventilation profile, pollutant production profile (heat gain, CO₂ production), heat and cooling system control profile – users interventions into system).

Model was created like universal which will generate user profile presence for one person after input presence of typical building and its processing. If we have more than one person in the interior then the algorithm will calculate so often how many times people is in the interior and total result will sum.

A new kind of building material is studied by Dalibor Beneš¹¹ in his work called **Masonry mortar development based on fluid fly ashes [7]**. The author investigated the potential of fluid fly ashes utilization as hydraulic bonding material in preparation of dry mortar mixtures and the presumed potential hydraulic capacities of fluid fly ashes that have been theoretically assumed on the basis of its chemical-mineralogical composition. Problems of hydraulic binder was solving not only in laboratory environment but also in real conditions for development dry mortar mixture. There were studied the following characteristics: the workability, compressive strength and tensile strength, the water consumption, plasticity, setting time and spreading for close masonry. The chosen granulometry was in agreement with the grading curve according to Bolomey.

¹⁰ Department of Environmental and Building Services Engineering, Czech Technical University in Prague

¹¹ Institute of Building Materials and Components , Faculty of Civil Engineering, Brno University of Technology, Czech Republic

Another topic is the preservation of building structures of historical monuments.

Jerzy Szolomicki¹², investigated different numerical techniques for the analysis of historical masonry structures. The paper is called **Different numerical methods using for analysis of historical masonry structures [8]**.

The following approaches are taken into account:

- standard FEM modeling method, based on concept of homogenized material and smeared cracking,
- FEM with discontinuous elements which are used for modelling vertical and horizontal mortar joints,
- discrete element modelling.

It was presented an overview of numerical methods with their specific theoretical aspects that can have practical usefulness in analysis of behaviour of historical masonry structures.

In spite of the specific limitations of each model, all three methods are able to correctly grasp the global behaviour of analyzed masonry structures.

The paper **The elastic-plastic load-carrying capacity of thin-walled steel members with quasi-homogenous and hybrid cross-sections [9]** (authors: Pavol Juhás¹³, Mohamad Al Ali¹³, Zuzana Kokoruďová¹³) presents fundamental information about realized experimental-theoretical research of the load-carrying capacity of thin-walled compressed steel members with quasi-homogenous and hybrid cross-sections. The load-carrying capacity of such members is influenced by the local web buckling subjected in the elastic-plastic region. The aim of this research has been oriented on the elastic-plastic post-critical behavior of thin web and its interaction with compact flanges.

Are presented the experimental program, tested members and their geometrical parameters and material properties and the comparison of theoretical and experimental limit loads.

References

1. Irina Radinschi, Cristian Damoc - Computer Simulations for Physics Laboratory
2. Adrian Doloca, Oana Țănculescu- epiqr energy – A New Software For the Evaluation of Thermal Energy Consumption in Buildings
3. Mária Kozlovská, Lukáš Sabol, Building Projects Control by Software Products

¹² Department of Civil Engineering, Wrocław University of Technology, Wrocław, Poland

¹³ Institute of Structural Engineering, Technical University of Košice, Košice, Slovakia

4. Ion Anghel, Popa Constantin and Pavel Alecsandru - Application of computer modeling in civil fire safety engineering. Glass breakage in fire
5. Popa Constantin, Ion Anghel and Panaitescu Valeriu - Modeling and simulation of ventilation in fire emergency situations
6. Roman Musil- People Presence Stochastic Model for Building Energy Simulations
7. Dalibor Beneš - Masonry mortar development based on fluid fly ashes
8. Jerzy Szolomicki - Different numerical methods using for analysis of historical masonry structures
9. Pavol Juhás, Mohamad Al Ali, Zuzana Kokoruďová - The elastic-plastic load-carrying capacity of thin-walled steel members with quasi-homogenous and hybrid cross-sections

Advanced Computer Based Structural Design

Octavian Rosca¹, Mihai Budescu²

Summary

During the last decade, the state-of-the art in Earthquake Engineering Design and Structural Analysis made important advances towards a more rational design. The computer performances paid respect to the Moore's law i.e. the present computer power increased dramatically. More sophisticated and refined analysis are carried out.

The Computational Civil Engineering 2008 international symposium gathered a number of scientific papers that emphasis the present stage of the researches in the field. This paper depicts the approaches and achievements reflected in the proceedings of the above mentioned symposium

A nice tradition regarding computation in Civil Engineering is already established.

The diversity of work together with the diversity of countries, universities and other institutions implied in Computational Civil Engineering symposiums lead to the conclusion that the field is strong and needed.

KEYWORDS: Civil Engineering, computers, research, education, computation in engineering and science.

1. INTRODUCTION

Since 2003 the international symposium Computational Civil Engineering is organized each year in Iași, Romania, at the Faculty of Civil Engineering and Installations. It is organized in several sections; one is the Earthquake Engineering section.

Complex applications were presented. Our world recorded earthquake databases, geotechnical engineering, the structural behaviour and shaking table tests made possible a significant shift from force based design approaches to the displacement based design methods.

The papers dealt with computational models, seismic dissipators, the influence of the damping ratios on the earthquake response, database-assisted seismic analysis of

¹ Sen. Lect., Technical University of Iasi, Romania, e-mail: victor_rosca@yahoo.com

² Prof., Technical University of Iasi, Romania, e-mail: vesper@telebit.ro

tall buildings, intelligent control systems, analysis with the Robot Millenium software etc.

2 COMPUTER AIDED STRUCTURAL DESIGN

Horia A. Barbat³ and a team from Technical University of Catalonia, Barcelona, Spain and University of Chile; Santiago, Chile develops a computational model for buildings with energy dissipators subjected to seismic action [1].

The poor performance of many framed RC structures in recent strong earthquakes has alerted about the need of improving their seismic behaviour especially when they are designed according to obsolete seismic codes. Sometimes, RC buildings show a low level of structural damping, important second order effects and low ductility of the connecting joints, among other defects.

These characteristics allow proposing the use of energy dissipating devices for improving their seismic behaviour, controlling their lateral displacements, providing additional damping and ductility. In this work, the nonlinear dynamic response of RC buildings with energy dissipating devices is studied using advanced computational techniques. A fully geometric and constitutive nonlinear model for the description of the dynamic behaviour of framed structures is used. The model proposed for the structures and the dissipating devices is based on the geometrically exact formulation for beams which considers finite deformation and finite strains. The equations of motion of the system are expressed in terms of sectional forces and generalized strains and the dynamic problem is solved using the displacement based method formulated in the finite element framework. An appropriated version of Newmark's integration scheme is used in updating the kinematics variables in a classical Newton type iterative scheme. Each material point of the cross section is assumed to be composed of several simple materials with their own constitutive laws developed in terms of the material description of the First Piola Kirchhoff stress vector.

Appropriated constitutive laws for concrete and for steel reinforcements are provided. The simple mixing theory is used to treat the resulting composite. A specific finite element based on the beam theory is proposed for modeling the energy dissipating devices. Several constitutive descriptions in terms of force and displacements are provided for the dissipators. Special attention is paid to the development of local and global damage indices capable of describing the residual strength of the buildings. Finally, several numerical tests are carried out to validate

³ A.H. Barbat, P. Mata, S. Oller, J.C. Vielma, Technical University of Catalonia, UPC Edificio C1, Campus Nord, Gran Capit' a s/n. 08034 Barcelona, Spain.

R. Boroschek, University of Chile; Department of Civil Engineering 837-0449 Santiago, Chile.

the ability of the model to reproduce the nonlinear seismic response of RC buildings with energy dissipating devices.

Conventional seismic design practice permits designing reinforced concrete (RC) structures for forces lower than those expected from the elastic response on the premise that the structural design assures significant structural ductility. Frequently, the dissipative zones are located near the beam-column joints and, due to cyclic inelastic incursions during earthquakes, several structural members can suffer a great amount of damage. In the last decades, new techniques based on adding devices to the buildings with the main objective of dissipating the energy exerted by the earthquake and alleviating the ductility demand on primary structural elements have improved the seismic behaviour of the structures.

The purpose is to control the seismic response of the buildings by means of a set of dissipating devices. In the case of *passive energy dissipating devices* (EDD) an important part of the energy input is dissipated without the need of an external energy supply.

Several works about seismic control with passive EDDs are available. The design methods proposed for RC structures are mainly based on supposing that the behaviour of the bare structure remains elastic, while the energy dissipation relies on the control system. However, experimental and theoretical evidence show that inelastic behavior can also occur in the structural elements during severe earthquakes. In order to perform a precise dynamic nonlinear analysis of passively controlled buildings sophisticated numerical tools became necessary.

Considering that most of the elements in RC buildings are columns and beams, one dimensional formulations for structural elements appear as a solution combining both numerical precision and reasonable computational costs. An additional refinement is obtained considering an arbitrary distribution of materials on the beam cross section, and in this case, the constitutive relationship at cross sectional level is deduced by integration. Formulations considering both, constitutive and geometric nonlinearity are rather scarce; most of the geometrically nonlinear models are limited to the elastic case and the inelasticity has been restricted mainly to plasticity. From the numerical point of view, EDDs usually have been described in a global sense by means of force–displacement or moment–curvature relationships which intend to capture appropriately the energy dissipating capacity of the devices .

In this work, a fully geometric and constitutive nonlinear formulation for beam elements is developed. A fiber–like approach is used for representing arbitrary distributions of composite materials on the plane beam cross sections. EDDs are considered as beam elements without rotational degrees of freedom. Thermodynamically consistent constitutive laws are provided for steel, concrete and EDDs. The mixing rule is employed for the treatment of the resulting composite. A brief description of the damage indices capable of estimate the

remaining load carrying capacity of the buildings is also given. Finally, the numerical simulation of the seismic behaviour of a precast RC structure with EDDs is presented.

Horatiu Mociran⁴ and Alexandra Stan carried out a study regarding the influence of damping ratios on earthquake response of steel frame structures [2].

The comparison was performed by the means of the seismic performance indices of a five story steel frame building with three different damping ratios (5%, 20% and 30%) and two structural systems (moment frame and viscously damped frame). A novel approach for earthquake hazard mitigation is the use of viscous dampers. The objective of this approach is to dissipate earthquake-induced energy in devices designed especially for this purpose, and to eliminate or minimize energy dissipation demand and inelastic action in primary structural members. The non-dimensional performance indices considered for the models are: Peak Drift ratio, Pick Base Shear and Peak Level Acceleration.

Conventionally, structures have been designed to resist natural hazards through a combination of strength, deformability, and energy absorption. These structures may deform well beyond the elastic limit, for example, in a severe earthquake. They may remain intact only due to their ability to deform inelastically, as this deformation results in increased flexibility and energy dissipation. Unfortunately, this deformation also results in local damage to the structure, as the structure itself must absorb much of the earthquake input energy.

The level of damping in a conventional elastic structure is very low, and hence the amount of energy dissipated during transient disturbances is also very low. The concept of supplemental dampers added to a structure assumes that much of the energy input to the structure will be absorbed by supplemental devices. An ideal damper will be able to reduce both stress and deflection in the structure.

The moment frame structure is situated in Iași and was designed according to Romanian seismic code P100-1/2006. The structure was then modified by addition of fluid viscous dampers to improve the seismic performance, with no attempt made to redesign the main frame elements.

The seismic performance of these structures was studied using nonlinear response-history analysis. Three artificial earthquakes of Vrancea type, that matched P100-1/2006 Provisions response spectrum were used for analysis.

The seismic performance indices show that these viscous dampers when incorporated into the structure reduce the earthquake response significantly in proportion to the amount of damping supplied in these devices.

⁴Horatiu Alin Mociran, Alexandra Denisa Stan, Faculty of Civil Engineering, Technical University, Cluj-Napoca, 400027, Romania

Mihail Iancovici ⁵and Cristian Gavrilesu are introducing the database-assisted analysis concept and the advantages of using it in the practical seismic design of large scale structures in [3].

The integrated seismic performance analysis system is an unitary format that allows (1) performing the seismic response analysis, energy balance-based analysis, fragility and seismic risk analyses, by using the time series of real/scaled/simulated earthquake ground motions and the induced effects (stresses, efforts, strains, displacements, velocities, accelerations, forces, energies), (2) the design of the structural elements and connections in a straightforward and transparent manner and (3) getting higher performance structures, safer and cost effective. This format becomes much more important in the case of irregular structures, having plan and elevation complex shape, in which the main directions of motion are not obvious.

It is investigated the applicability of such procedure that makes it possible to estimate the earthquake-induced effects in tall buildings, at a higher level of automation and transparency. Seismic response analyses of a 60 story typical building subjected to long predominant period ground motions are conducted and the main results are emphasized.

While some of the input ground motion components are usually neglected, the actual format allows the use of large number of full sets of accelerograms.

Ideally, a structural system must have equal performance to earthquake ground motions from all possible directions, resulting a uniformly exposed to risk structure. For a class of structures however, e.g. having non-uniform plan and elevation mass and stiffness distributions, the main directions of motion are not obvious. In order to cover all the structural cases, an incremental directivity of ground motion is considered.

In a 3D modal superposition method any number of vibration modes can be considered. The induced effects are expressed as time-series. There is no need to consider static load combinations.

The design of structural elements and connections is done in a straightforward and transparent manner, directly from the time-histories of efforts; there is no more need of making use of various rules for maxima superposition (e.g. “30% “ rule, SRSS, CQC, CQC3 etc.). The design is made by applying given interaction formulas (e.g. AISC-LRFD, EC3 etc.).

⁵ Mihail Iancovici, Department of Mechanics, Statics and Dynamics of Structures, Technical University of Civil Engineering (UTCB), Bucharest, 020396, Romania
National Center for Seismic Risk Reduction (NCSRR), Bucharest, 021652, Romania
Cristian Gavrilesu, Kohn Pedersen Fox Architects (KPF), 13 Langley St., Covent Garden, London, UK

The use of complete sections databases allows the design with an improved level of automation. The distribution of material can be more efficient and economical.

This analysis format represents the decision support for structural type changing, of incorporating various seismic energy dissipation devices and techniques (active, semi-active, passive and hybrid) and for the assessment of the structural optimization need and effectiveness, as a higher analysis level.

The integrated performance analysis system deals directly with different classes of uncertainties in input ground motion and structural behavior. The use of a large number of data allows a full probabilistic assessment of structural performance, an appropriate approach from the point-of-view of implementing the performance concept.

Ludovic Kopenetz⁶ and Ferdinand-Zsongor Gobesz are dealing with the expert study of bearing structures, using intelligent control systems based on fuzzy logic.

The existing bearing structures must insure the carrying capacity for the actual loads, transferring them safely through the foundation into the ground. Considering that the structural design of new facilities, while still insuring the global quality of the existing buildings, issues many random features, the practicability of an accurate damage evaluation is representing a genuine hazard.

Cutting back the level of this hazard beyond a certain threshold is technically and economically not justified.

The condition of a structure depends on the degree of its vulnerability as well as on its actual damage ratio, in situ. The degree of vulnerability expresses the composing manner of the structure, through the available cross-sectional strength at the moment of the assessment. The damage ratio depends on the nature and both on the amount and on the location of physical failures in the whole structure.

Considering that the “Conclusions” chapter of an expert study contains decisions which, due to the multitude of uncertainties, can be qualitatively altered by the participation of a human factor, a methodology is proposed for the handling of the uncertain aspects, applying intelligent control and fuzzy logic.

The use of fuzzy logic based decisions during an expert study allows an accurate assessment of the bearing structure’s technical condition and the implementation of instant measures in order to insure safety when the assessed construction shows dangerous failures.

⁶ Ludovic Kopenetz, Department of Structural Mechanics, Technical University of Cluj-Napoca, Cluj-Napoca, 400020, Romania

Ferdinand-Zsongor Gobesz, Department of Structural Mechanics, Technical University of Cluj-Napoca, Cluj-Napoca, 400020, Romania

It should be noticed that, by the involvement of fuzzy logic concepts, the fundamental issues of the expert study of structures remain valid, just the viewpoint of information processing changes.

The question that follows after the performed research is, “if the implementation of intelligent control systems based on fuzzy logic has a future?”

As in the majority of situations, an answer to this question is very hard to be given. Most likely, the experts will use in the future, more and more, expert systems in comprehensive combination with in situ monitoring, testing labs and integrated real time software based on case studies (namely “case based reasoning”), neural networks and genetic algorithms.

As for the near future, the use of permanently monitoring systems in sure conjunction with fuzzy control concepts, in case of highly important buildings, can be predicted.

A team conducted by Meisam Safari Gorji⁷ from the School of Civil Engineering, College of Engineering, University of Tehran, Iran presents a paperwork concerning the seismic assessment and strengthening of intermediate moment resisting concrete frames.

The objective of this study was to investigate the seismic evaluation and strengthening of Intermediate Moment Resisting Concrete Frames (IMRCF) designed according to the Iranian concrete code of practice (ABA) and Iranian Seismic Code (Standard No. 2800).

This type of RC frames is excessively used in Iran while their vulnerability in earthquake prone area and their performance level is not clearly known for designers.

Several intermediate moment resisting concrete frames have been selected and subjected to seismic evaluation according to the Iranian Guidelines for the Seismic Rehabilitation of Existing Buildings.

In this study, to determine the target point of frames, the Capacity Spectrum Method (CSM) has been used.

This article presents an analytical investigation of the effects of different strengthening methods on the seismic performance of the Intermediate Moment Resisting Concrete Frames (IMRCF) using rational displacement-based analytical method (nonlinear static pushover analysis) based on realistic and efficient

7 Meisam Safari Gorji, School of Civil Engineering, College of Engineering, University of Tehran, Tehran, Iran.

Masoud Taribakhsh, Department of Civil and Environmental Engineering, Amirkabir University of Technology, Tehran, Iran.

Amirhossein Gandomi, Department of Civil Engineering, Tafresh University, Tafresh, Iran.

computational models of the structural components. On the basis of results, several conclusions can be drawn.

Assessment of the performance levels of the frames structural elements according to the Iranian guidelines shows that some of the beams and columns were seismically deficient in terms of life safety.

The frames including four spans have a better performance as compared with the frames having three spans.

Comparison between the three strengthening strategies, shows that the most increase in the lateral strength were related to using steel bracing system.

With regards to the performance levels of the structural elements in strengthened frames, the best strengthening system was adding shear wall.

By utilizing reinforced concrete infill to strengthen the frame, the performance level of the frame has been improved significantly. In this case, the Immediate Occupancy (IO) performance level was reached and the relative displacement corresponding to the performance point decreased significantly owing to the increase in lateral stiffness of the strengthened frame.

In the strengthened frame with steel bracing system, the compressive bracings buckle rapidly. In order to prevent the buckling of braces, if stronger braces were used, the failure mechanism may transferred to columns and beams owing to the increase in axial load of columns as well as the increase in shear forces of beams and columns. In this case study, in order to improve the performance level up to the Immediate Occupancy, only adding bracing is not sufficient but also some of the structural element should be strengthened along with adding steel bracings to resist the increase of forces in these structural elements.

The analyses results show that ordinary masonry infill can increase the lateral strength of the frames and improve the performance level of the system to some extent.

Mihai Nedelcu⁸ from TU of Cluj-Napoca, Romania, presented a seismic analysis using Robot Millennium software.

The paper presents the modeling and structural analysis of a complex structure under seismic loads using the Robot Millennium software package. In order to test the output results, the author chose a building already designed in the documentation [6].

The above mentioned documentation was created as a guideline for applying the design standard P100-1/2006. The objective of the paper was to show the Robot

⁸ Mihai Nedelcu, Department of Structural Mechanics , Technical University of Cluj-Napoca, 400020, Romania

Millennium instruments used for modelling this type of structures, also the various modelling ways for the same structure highlighting the most convenient one.

The results accuracy of the analysis was compared with the output given by the ETABS software.

For the seismic analysis, the structure is considered fixed at the ground floor base. Using Robot Millennium v.20.1, the author modeled the structure using bars for columns/beams and panels for slabs/ R.C. walls. After the mesh generation (even with large finite elements) the great number of equations (of order 10^5) led to a significant slowing down of the analysis. As a good alternative the Rigid Links additional attribute can be used instead of panels for the slabs modeling. By introducing the Membrane rigid link, the user can connect the nodes of each floor according to any DOF, in this case the X,Y displacements and the RZ rotation. And so the slab effect as a rigid body is fully covered. At the same time the beams have to be modeled as T-section, taking into account the corresponding slab rigidity. A slab width of $3x_{hp}$ (the slab thickness) was taken on each side for the interior beams and of $2x_{hp}$ on each side for the marginal beams. Having no slab finite elements reduces considerably the analysis time with absolutely no damage to the results.

The conclusions are that the Robot Millennium software package gives us a reliable and elegant alternative for seismic analysis. Its features fully cover the demands of P100-2006. However, careful examination of its tools has to be done in order to choose the optimal modeling strategy.

3 CONCLUSIONS

Since 2003, the Computational Civil Engineering symposiums held every year in Iaşi, Romania, at the Faculty of Civil Engineering and Installations.

A continuous evolution of the scientific paper works is noticed. The quality and the level is high, therefore the symposium attended its major goals.

A larger participation is expected for the following years, thus offering a good opportunity for the scientific exchanges.

References

1. A.H. Barbat, P. Mata, S. Oller, R. Boroschek and J.C. Vielma, *Computational model for buildings with energy dissipators subjected to seismic action*, Civil Engineering, Proceedings of the International Symposium "Computational Civil Engineering 2008", Editura Societăţii Academice "Matei-Teiu Botez", Iaşi, 2008, ISBN 978-973-8955-14.
2. Horatiu Alin Mociran, Alexandra Denisa Stan, *The influence of damping ratios on earthquake response of steel frame structures*, *idem*.

3. Mihail Iancovici, Cristian Gavrilescu, *Database-assisted seismic analysis of tall buildings subjected to long predominant period Vrancea earthquakes, idem.*
4. Ludovic Kopenetz, Ferdinand-Zsongor Gobesz, *Expert Study of Bearing Structures, Using Intelligent Control Systems Based on Fuzzy Logic, idem.*
5. Meisam Safari Gorji, Masoud Taribakhsh and Amirhossein Gandomi, *Seismic Assessment and Strengthening of Intermediate Moment Resisting Concrete Frames, idem.*
6. Mihai Nedelcu, *Seismic analysis using Robot Millennium, idem.*

Concrete and Reinforced Concrete Structures

Marinela Bărbuța¹ and Daniel Lepădatu²

*2Concrete structure, Building material, Technology and Management Department, Technical
University "Gh. Asachi", Iasi, Romania*

1Civil Engineering Department, Technical University "Gh. Asachi", Iasi, Romania

1. INTRODUCTION

Today in Romania there are great housing facilities. A part is represented by old constructions, that were affected in time by seismic actions (1940,1977, 1986 and 1990) and they must be consolidated. In time, to constructions can appear degradations as a consequence of material aging, chemical attack, soil sliding, fires, explosions, floods, etc. The structures which are in use require more attention in the fields of preservation and rehabilitation for satisfying ecological, resistant and durability conditions and for ensuring secure service life.

Near the rehabilitation of constructions, new buildings costs require a diversification of construction materials, with improved performances which can satisfy the new requirements of sustainability and durability.

The concrete is probably the most widely and extensively used building material in the world. Maintaining its competitiveness implies more ways: improving the properties of cement concrete by realizing high strength concrete or high and ultra high performance concrete or by developing new special concretes for specific using domains such as: hydraulic concretes, marine and offshore concretes, concrete resistant to chemical aggressiveness, etc. Another way supposes the development of new types of concretes, for example: reactive powder concretes, compact reinforced concrete, polymer concrete, lightweight high strength concretes, etc.

Since every property related to the strength and durability development in concrete is a time-dependent process, one needs to choose concrete material constituents in such way that will foster synergic interaction with time.

The use of high strength concrete is becoming more common in the construction industry because its advantages compared with conventional concrete. A big number of international researches are now in progress for obtaining fundamental information to help spread the application domain of high strength concrete. Because for realizing high strength concretes are implied many factors (aggregate, cement, admixture and addition) the correspondence between them must be carefully analyzed having in view the local possibilities and needs.

In the last 40 years the application of polymer on concrete has significantly progressed. Although Polymer-Modified Concrete (PMC) and Polymer Concrete (PC) came into use in the 1950s, only in the 1970s, after Polymer-Impregnated Concrete (PIC) was developed the PC materials were received fairly publicity in concrete industry. The use domain of PC in time was extended from pre-cast components for buildings, bridges panel, waste components, transportation components to repair of structural members, waterproofing, anticorrosive and decorative finishes, overlay of pavements, etc. The PC occurred and developed in construction industry due to its advantages compared with the Portland cement concrete, such as: quick setting characteristics, high mechanical strength, chemical resistance and wear resistance. In the composition of polymeric concrete are used the same components: aggregates and the binder that for polymeric concrete is a resin that reacts with a hardener and bind together the aggregates. The limits of polymer concrete include: cost, toxicity, small and inflammability.

Continuous increase in global prices of important raw materials have a negative impact on the economy and for that it is necessary to look for maximum possible savings in these raw materials. A lot of researches have been made for fully use all kinds of industrial by-products and wastes such as: slag, fly ash, silica fume, construction waste, glass, PETS, etc. In our country there are produced great amounts of waste materials as by-products of iron and steel production: blast-furnace slag as by product of iron production and steel slag as by-product of steel production. Both kinds of slag are suitable for road building purposes. Steel slag has not been used for building purpose so far. Today this material is used in road building for bituminous mixtures for road pavement. In particular, this material could be suitable for wear layer for urban and rural roads.

Ashes are waste which result from coal combustion process in the thermoelectric stations. According to many factors (the physical nature, the chemical-mineralogical coal composition, combustion systems etc.) variable quantities of ash are obtained, which represents about 25-40% from the amount of burned fuel. The importance of this waste use is proven also by the large number of research works in the world.

Another by-product is silica fume (SUF) resulted from the ferro-silicon manufacturing process. It is used for improving the performances of cement concrete.

The construction waste is another material used in construction. This type of waste can be reuse as a recycled aggregate in buildings or roads. Unfortunately there are not regulations considering qualification and standard requirements for recycled aggregate and they were considered as any natural aggregate.

The papers included in the Conference present the results of studies on concrete as building material and on the reinforced concrete structures.

2. SECTION CONTENTS

2.1. In the paper “*Study of durability prediction of concrete structures using computer’s software*” the authors present the EUCON software used for prediction of concrete service life, focused on the basic deterioration phenomena of reinforced concrete, such as carbonation and chloride penetration that initiate the reinforcing bars corrosion. The EUCON software was developed at Patras Science Park S.A. Greece.

First, the essential parameters that characterize a concrete composition (mixture proportions) are selected, and this is the main source on which all other concrete characteristics depend. Thereafter, the main chemical and volumetric characteristics of concrete are calculated (chemical composition of hydrated cementations materials, porosity and related characteristics) and this is also another source to receive more information. Based on the selected mixture proportions (cement type and strength class, cement content, water-cement ratio, air content, aggregate type, type and activity of additions, etc.), the compressive strength class of concrete is further estimated.

For each significant deterioration mechanism, according to the specific environment where the structure would be found, an appropriate proven predictive model is used. Concrete carbonation and chloride penetration are the most common causes for reinforcement corrosion onset, and for further concrete deterioration. The service life of the structure found in these environments, which cause either carbonation or chloride penetration, is calculated. The degree of deterioration from a possible chemical attack (future development) is also estimated, either as a reduction in the effective concrete section (in the case of acid or biological attack) or as a reduction in strength of the affected concrete (in the case of sulphate or alkali attack). Finally, cost and environmental aspects regarding concrete composition are analyzed.

The software offers the possibility of investigating the efficiency of various protection measures, such as waterproof sealants, cement-lime mortar coatings, inhibitors, etc. Using these software packages, an optimum concrete design can be achieved by estimating reliably the concrete strength, durability and production cost.

2.2. In the paper “*Aggregates Types Impact on Features of Fresh and Hardened Concrete Using Gypsum Free Cement*” the authors present the results of experimental tests on concrete using gypsum free cement, realized with some types of aggregates.

Experiment works were done focused on detection of aggregates mineralogical and chemical compositions impact on fresh concrete using gypsum free cement starting point of setting and its strength values.

Diverse types of greywacke and coarse aggregates with respect to mineralogical composition or in view of the origin (extracted or crushed) were used.

The analyzed results of experimental works have confirmed that:

- That aggregates, especially the greywacke and its mineralogical composition, have an influence on starting point of fresh concrete using gypsum free cement setting;
- Using of limestone and dolomites for concrete fabrication is not recommended; upon selection of greywacke, the exploited aggregates should be preferred over the crushed ones; it is recommendable to use exploited sands with high ratio of quartz grains; sands with high ratio of feldspars are not convenient;
- The types of coarse aggregates have no significant impact on hardened concrete strength parameters. Differences for the tested types of aggregates, especially those regarding bending strength, are caused among others by inconvenient form index of grains. Therefore it is necessary to have in mind this parameter as well, when selecting the aggregates for concretes using gypsum free cement;
- No dolomite and limestone aggregates are recommendable for fabrication of concretes using gypsum free cement.

2.3. This paper “*Glass addition influence on cement-bound composite materials’ strength characteristics*” deals with the brief summary research which is concerned a utilization of secondary raw materials in cement-bound composites problems. A recycled screen and monitor panel glass was used as the secondary raw material.

In the preamble of the paper is stated short developments retrieval of selected authors, who are engaged in the themes involved. Next subchapter then continues to a certain extent their science findings, whereas main care is paid a partial compensation of cement by secondary raw material.

Following paper section is focused on experimental research. Generally, fourth part of cement in test specimens was replaced by fine glass powder. Below there are stated some computational methods, which are cohering with some physical and mechanical properties determination.

2.3.1 Recycled glass in cement-bound composites as an aggregate

The up to now research works how to utilize recycled glass (RG) have aimed at two main ways. A partial or full replacement coarse or fine aggregate by RG have been examined in the first case. Particularly physic-mechanical and micro structural material characteristic and next an appropriate rise of so much important alkali-silica reaction (ASR) were investigated on test specimens (Figure 1).

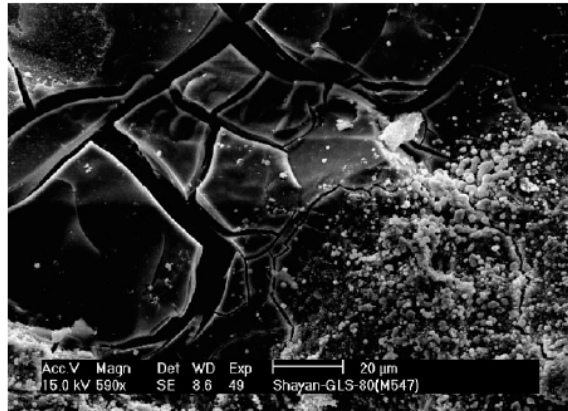


Figure 1. Site ASR gel formation in concrete and the composition of the gel

2.3.2 Recycled glass in cement-bound composites as a pozzolanic material

A second featured way how to utilize RG for production of cement-bound composites results from its chemical composition, which in principle similar (silica content) to aforementioned fly ash.

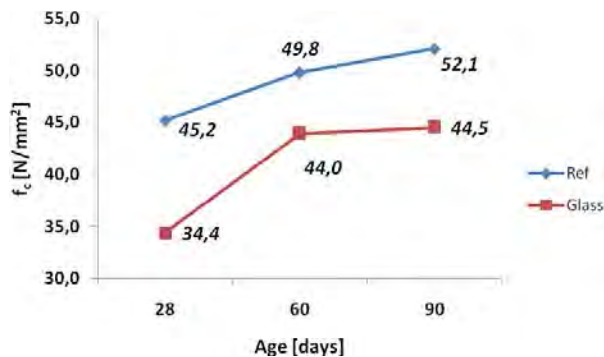


Figure 2. Compressive strength development of Ref and Glass samples comparison

By the research and its evaluation in the paper a positive influence of partial cement binder replacement by CRT glass on strength characteristics. Replacement of 25 % is advantageous in light of environmental and economical aspects. Conclusion and evaluation of the article would be served as groundwork for another research in the field of glass secondary raw materials applied in cement-bound composites. Above all an attention would be paid to appropriate ASR (alkali-silica reaction) inception, durability characteristics, workability of fresh batch, microstructure (DTA, RTG, Chemical analysis) etc.

2.3.4 Conclusion

On the basis of aforementioned it is possible to claim, that cement partial replacement by recycled CRT glass is practicable and even for certain aspects convenient.

2.4. The paper “*Slab stiffness influence in design of reinforced concrete frame system*” summarizes and analyses the basic requirements associated with initial conceptual design and hypothesis of reinforced concrete structural frames that are included in Eurocode 8, Eurocode 2 (EC8, EC2), SR EN 1992-1, P100/2006 into an easily understandable synopsis accompanied with one numerical model and pictures. One of the principal hypotheses is stiffness slab and the product EI which has influence on the model analyze and the structure behavior.

Reinforced concrete structural frames have multiple advantages. Many buildings have this kind of structure. In analyze and design of these structures is necessary little completion. Software models give the response of structures. The response can be correct or incorrect, that’s depend on how the hypothesis is made.

The model of the building shall adequately represent the distribution of stiffness and mass in it so that all significant deformation shapes and inertia forces are properly accounted for under the seismic action considered. In the case of non-linear analysis, the model shall also adequately represent the distribution of strength. The model should also account for the contribution of joint regions to the deformability of the building, e.g. the end zones in beams or columns of frame type structures. Non-structural elements, which may influence the response of the primary seismic structure, should also be accounted for.

After the models analyze observes that the value of bending moment on column is increasing while the modulus of elasticity is reduced. On beams, the modification of product EI makes that the value of bending moment to reduce.

This knowledge is important because in reality the structure behavior is affected by the concrete condition, and that must be provided in simulation model. Because the

slab and beam pull together is necessary that the slab have same stiffness like beam.

2.5. In order to perform an assessment, the classical linear elastic methods are not appropriate, and the structure engineers had to resort to non-linear techniques, such as the static «pushover» analysis. This pushover analysis is a relatively simple way of exploring a structure's design. The pushover analysis consists in pushing the mathematical model of a structure, imposing a displacement in order to plan the sequence of the damage in the inelastic field and to detect the weak links.

In a pushover analysis, a nonlinear inelastic model is being subjected to a lateral load until a moving target is reached or the model is destroyed. The displacement of the target represents the maximum displacement that could take place during the seismic calculation. The control knot or the displacement of the target is set at the centre of the terrace's level mass. Various forms of lateral load can be considered a uniform charge, a modal charge or any other form defined by the analyst. The model of the structure must be developed starting from the law-bending moments of the elements.

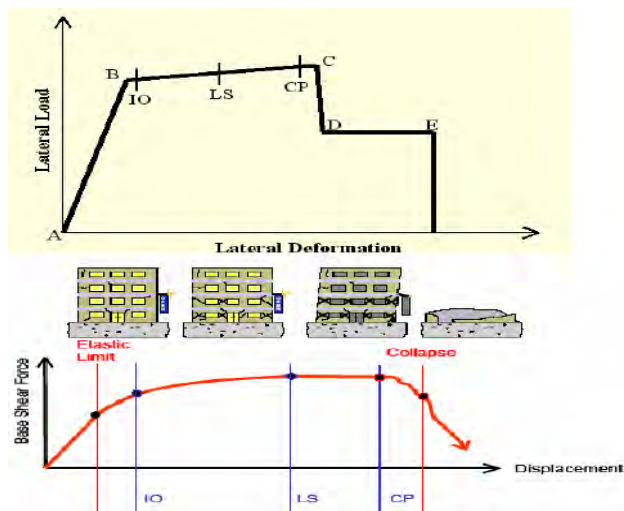


Figure 3. Capacity curve "CC" can be achieved for all kinds of buildings

The application example given in the article "*Pushover analysis of reinforced concrete structures (Damage theory)*" refers to a reinforced concrete structure from a seismic area in Algeria.

This analysis can be used for performing an assessment of the actual seismic behavior of the existent buildings. Particularly when it comes to the seismic renovation of the reinforced concrete structures existing in the areas with high seismicity – and this is a topic of high interest – the vulnerable structures must be identified and an acceptable protection level must be established.

The pushover analysis is a powerful and extremely useful tool, able to allow structure engineers to seek several patterns for comfort of the existing buildings and to study new structures that will behave in an appropriate manner during future earthquakes. The results obtained from a pushover analysis in terms of demand, capacity and plastic hinge offers an overview on the physical behavior of the structure.

2.6. New types of polymer concrete with silica fume have specific requirements, in contrast to conventional concrete; these are susceptible in case of changing technological factors (especially of the mix). They require a new optimization approach in issues of concrete mix design. On the other hand, in the conditions of market economy there is a wide range, that to achieve maximal economy, and at the same time to provide maximally good mechanical characteristics for this new type of concrete.

The aim of this paper “**Optimal mix design of polymer concrete using generalized reduced gradient algorithm**” is the optimization of mix proportion of polymer concrete with silica fume content by using the statistical techniques. The experimental studies were realized on polymer concrete prepared with epoxy resin, silica fume in different dosages and aggregates of two sorts. The experimental mix combinations were designed based on the mixture design of experiments concept for the minimum content of resin. The predicted values of mechanical characteristics were theoretically determined and they were compared with experimentally results using Response Surface Methodology (RSM). The effect of each variable on the response was analyzed by this advanced method. The optimization method includes two phases. The first involve the objective function prediction using mixture design of experiments and response surface method, while the second is an optimization process using a Generalized Reduced Gradient algorithm. The optimum combination of the input mix parameters design is given for the best values of compressive strength or adherence stress.

References

1. Ioan Paul Voda, Nicolae Florea and Vasile Iacob. Study of durability prediction of concrete structures using computer's software
2. Jiří Brožovský, Jiří Brožovský, Jr. and J. Bydžovský. Aggregates Types Impact on Features of Fresh and Hardened Concrete Using Gypsum Free Cement
3. George Țăranu, Mihai Budescu. Slab stiffness influence in design of reinforced concrete frame system
4. Tomáš Melichar. Glass addition influence on cement-bound composite materials' strength characteristics
5. Salim Sadi . Pushover analysis of reinforced concrete structures (Damage theory)
6. Daniel Lepadatu, Marinela Barbuta. Optimal mix design of polymer concrete using generalized reduced gradient algorithm

Soft Computing in Transportation and Civil Engineering

Radu Andrei, Constantin Ionescu, Alina Nicuta

*Department of Civil Engineering
Technical University “Gheorghe Asachi” Iasi*

The world of soft computing provides powerful tools for civil engineers to carry out various numerical simulation studies. Some of them are knowledge driven methods, such as Fuzzy Logic and Probabilistic Reasoning approaches. Others are data driven methods, like Artificial Neural Networks and Evolutionary Computing approaches. These methods independently, and in hybrid forms, are successfully applied in the following various fields of civil engineering: Structural Engineering - Structural analysis, design, diagnostics and control problems, Structural material behaviour modelling, Environmental engineering Geo-technical engineering- Liquefaction potential assessment, piles design, Transportation engineering - Bridge management systems, Pavement management systems, Pavement behavior models, Construction process engineering, etc.

Environmental Engineering, Structural Engineering and Transportation are specific fields where the most of methods used for solving optimization problems are based on experience, experiments and specific models. The present work outlines some specific subjects addressed by various specialists from transportation and other civil engineering fields to this new edition of **International Symposium on Computational Civil Engineering**.

From these significant number of papers, dedicated to solving various problems in the field of railway, road and bridge engineering, a first one entitled: „**The Comparison of the Dynamic Parameters of the Rail Fastening Vossloh W 14 and Pandrol FC**”, drafted by Jaroslav Smutny and his collaborators from Czech Republic, deals with the analysis and comparison of the dynamic parameters of the rail fastening used in a standard way in the trunk line of the high-speed lanes of the Czech Rail. The paper also includes the description and recommendations of the methods of measurement and a suitable mathematical apparatus for the evaluation of the measured parameters.

A second paper, drafted by author Voichița Roib from Civil Engineering Faculty, Cluj-Napoca, Romania is proposing a „**Management Program for Urban Traffic Road**“, presenting the methodology of implementing a traffic management program, in Cluj-Napoca city.. This program is using a new technology for the collection, organization and transmission of information related to the infrastructure and traffic status. The results obtained by the application of this Management Program have a special importance by providing road users and decision makers with valuable information concerning traffic conditions.

With their paper : „**Simplified Inventory for Road Culverts and Bridges** „, the authors Claudiu Romanescu , Cristina Romanescu and Rodian Scinteie from Romanian Centre for Road Engineering Studies & Informatics-CESTRIN, are proposing a new software system capable to provide more efficiently, information of the technical condition of bridges . This paper presents the Simplified Inventory for Road Culverts and Bridges (SIRCUB) program that wishes to be an answer to specialist’s basic requests, delivering data related to structure identification, geometrical and material characteristics and a brief set of functional information. The authors are stressing that this software is available to all users having usual database software (MS Access) and may constitute the basis for further developments to include data about technical condition, a basic intervention prioritization of bridges, etc. SIRCUB is very flexible program , allowing displaying data of selected structures, modifications of records, and also modifications of the graphical user interface to permit more information to be viewed and assessed.

The same group of authors : Cristina Romanescu, Claudiu Romanescu and Rodian Scînteie from CESTRIN Bucharest are further presenting in their paper entitled : “**Analysis of repair works assignment to create the BMS works database**” the main futures and capabilities of a repair works database in Romania. To create this database Romanian experience was considered and comparison has been made toward other systems like Pontis - American bridge management system and Gepeto - French bridge administration software belonging to GETEC Company. This bridge management system STELA-R developed at CESTRIN for CNADNR, stores inventory and inspection information of the bridges situated on the Romanian national road network in a relational database that supports a set of analysis procedures used in evaluating the needs of each structure. The Romanian Bridge Management process starts with the building of a relational database that includes inventory data and inspection information. The system STELA-R uses a group of elements at inspection level data as follows: superstructure - main elements; superstructure - elements that sustain the deck; substructure elements; channel and road approaches elements; carriageway elements. Bridge inventory and inspection data are managed using the STELA-R Inspection Module. It consists of a set of relational tables and user graphical interface for creating new records, entering new inspection data, modifying existing ones and eventually erasing the obsolete data. Through field inspections CESTRIN personnel quantifies the technical condition of structures. All defects and degradation are pointed out, evaluated and for each of them one or more intervention works are attached, works that could be maintenance, repair, rehabilitation or replacement of elements or groups of elements. Works are assigned to defects in the Analysis Module.

The next series of papers, presented to this Symposium, are focussing with specific applications of soft computing in other fields of civil engineering.: such as Structural Engineering , Environmental Engineering , Construction Process Engineering, etc.

Addressing such issues, the author , Renáta Bašková, from Technical University of Košice, with her paper „**Automation of building process time structure models**“ is proposing some models for the analyses of building process time structure and their specific parameters. The particular network analyses model and its mathematical mechanism are behind the software , dedicated for building scheduling. The mathematical links classifying of network process method allow new views toward the possibilities of particular software to satisfy the requirements, which are risen during a creating and improving building schedule modeling in the premanufacturing, manufacturing and realization of a specific process.

The following two papers are addressing various ways of solving environmental problems such as protection of people from radiation or the influence of people behavior on the total energy need in a specific working space.

Thus, the paper : “**Gamma Radiation Shielding**” drafted by Czech authors David Procházka and Dalibor Beneš from the Brno Institute of Building Materials and Components , deals with the shielding of gamma and X-ray radiation for the protection of people who are often confronted with this problem in hospitals, nuclear plants or in departments or laboratories for non-destructive testing. These radiations are in greater doses harmful for the man and it is necessary to protect adequately persons working in these locations., the material propose for the shield construction being the barite.

In his paper :”**People Behavior Influence for Total Yearly Energy Need in one Person Office Room**”, the author Roman Musil from the Department of Environmental and Building Services Engineering, Czech Technical University in Prague, presents a practical application probability model of presence user into energy simulations. User presence probability model in one office room is processed like a set of Matlab scripts. Model works on base empiric probability functions and pseudo-random numbers and ensures a non-repetitive one generated profile from each other like it is in real life. By help of the multiple simulations in energy simulation tool will be determined the energy need dispersion in dependence on user human factor presence (and other direct activities depending on user presence) in office. These simulations will be compared with currently used static profile for office facilities.

Finally, in their work entitled : „ **Methods for estimation of horizontal loads that act of formworks**“, the authors : Eugen Pamfil , Vasile Iacob and Ioan Paul Voda , from Technical University „ Gh. Asachi“ Iasi, are presenting a comparative study regarding three standardized European methods for estimation

on horizontal loads that act on formworks. Here are some of the main conclusions, drawn by the authors:

- In evaluation of the maximum pressure on the vertical formworks are interfering many influence factors, and it is difficult to translate this factors in mathematical relations, to describe accurately the physical phenomenon;
- The resulted values for the maximum pressure, measured through different methods, are totally different, from very small values (methods CIB-CIRIA) to very big values (C140-86, DIN 18202/18218); the maximum pressure values are influenced by the concreting speed in every method of evaluation presented. Sometimes, through computations results maximum pressures higher than the hydrostatic pressure, it is in contradiction with the real situations.
- In evaluation and grouping of horizontal loads that act on the vertical formworks must be observed the technical prescription that exists in every country, the requirements of legal technical settlements must be applied correctly and with judgment.

Selected References :

- Instructiuni pentru stabilirea starii tehnice a unui pod, indicative AND 522-2006 (in Romanian).
 Scinteie, R., Baze de date si algoritmi pentru cai de comunicatie, 2003 (in Romanian).
 RNDr. Vojtěch Ullmann: Nuclear and Radiation Physics (online), (in Czech).
 Ivan Štoll: Physics of the Micro-world, Prometheus, Praha, (in Czech).
 Pavel Schmid et al.: Quality Control, Cerm, Brno 2001 (in Czech)
 Measured presence data 2007. Netherlands: TU Delft, Faculty of Technology, Department of Architecture
 Smutný J., Pazdera L. New techniques in analysis of dynamic parameters rail fastening, *InSight, The Journal of The British Institute of Non-Destructive Testing*, Vol. 46, No 10, October, 2004, pp. 612-615, ISSN 13542575
 Smutný J., Pazdera L., *Time frequency analyses of real signals*, 2003
 Banciu, D., Hrin, R., Mihai, G., Eșanu, A., Alexandrescu, M., Anghel, L. *Sisteme Inteligente de Transport - ghid pentru utilizatori și dezvoltatori*, Ed. Tehnică, București, 2003. (in Romanian)
 AND 557-1999. *Instrucțiunile pentru efectuarea înregistrării circulației rutiere pe drumurile publice.* (in Romanian)
 *** Normativ pentru executarea lucrărilor din beton și beton armat, indicativ C 140/86, Buletinul Construcțiilor vol. 12, ICCPDC București, 1986
 Trelea, A., Giușcă, N., Pamfil, E., *Tehnologia și mecanizarea lucrărilor de construcții civile, industriale și agricole*, vol. 1, 2, Institutul Politehnic Iași, Iași, 1988.
 Domșa, J., Ionescu, A., *Utilaje, echipamente tehnologice și procedee performante de betonare*, Editura Oficiului de informare documentară pentru industria construcțiilor de mașini, București, 1994.

Trends in soil improvement to accommodate constructions of high class importance in urban restrictive zones

Irina Lungu

Department of Roads, Railways, Bridges and Foundations, Technical University "Gh. Asachi", Iasi, 700050, Romania

Summary

Development projects nowadays face important infrastructure issues related to specific site conditions that reflect in a tremendous increase of soil improvement techniques. At the same time strong restrictions regarding safety and comfort developed the last decades related to both transportation infrastructures and buildings.

Research is therefore oriented to assess with high accuracy the construction effect when soil improvement is involved, to model and predict the soil/structure interaction after ground treatment. When ground treatment is not answering the safety requirements during both construction and service time period, deep foundation systems are usually considered the appropriate solution.

The continuous evolution in computer software opened various applications to predict future behavior of soils after being applied a treatment technique. Thus evolutionary algorithms with artificial neural networks and fuzzy logic become relevant in prediction of nonlinearities that so far limit considerably the conventional computing methods.

Energy consumption for heating the indoor space is more and more a relevant issue related to building design and hence, alternative energy sources are explored in terms of availability, application technology and thermal behavior according to appropriate models and methods for the design process. Monitoring the applied solutions is always beneficial in terms of a better calibration of the existing calculation methods and also to focus on improving the technical solution to cover more efficiently the required zone.

Viscoplastic fluids that are so common in construction field require an efficient flow control so that the processing safety of these materials when being fluid is maintained and controlled at high rate.

KEYWORDS: soil improvement, stabilized soil, viscoplastic fluids, retaining structures, alternative energy

1. INTRODUCTION

The deposits of loose granular and soft cohesive soils, of natural occurrence or as earth fills on the site of future constructions require technical solutions for the improvement of their properties in order to satisfy the structural design requirements related to bearing capacity and stability during service [1].

These soils display a positive reaction to the improvement of their mechanical properties as consequence of either the controlled inducing of some dynamic energy, with or without adding materials, or by injection, mixing or reinforcing techniques. Thus, the end result is a densification of the subsoil materials at various depths, classically divided into surface and deep soil improvement techniques.

One soil improvement concept is implemented in practice by various techniques with different effects reflected on the design methods applied on the infrastructure. The technology developed in such a way that the installation effect is both stress and strain controlled when applied and cost effective in terms of time and overall investment compared to some deep foundation solutions.

Surface compaction and deep compaction usually induce a significantly increase of the soil moduli and hence a strong decrease of settlements when compared with the ones generated in the initial soil conditions. The most efficient techniques in deep improvement are related to stone/sand columns by vibro compaction, vibro replacement, lime columns, deep dry mixing columns, compaction grouting – for urban zones and for large secluded areas, dynamic compaction proved to be efficient to induce dynamic compaction as well.

2. TRENDS IN GEOTECHNICAL DESIGN OF VARIOUS CONSTRUCTIONS

Soil improvement for transportation infrastructure often requires only a soil improvement over a small depth. Stabilizers used to induce such ground treatment solutions have been extensively studied to obtain the most cost efficient solution for a given situation. The paper with the title “Soft computing based approaches for lime-microsilica stabilized clayey soils” by Moradi, M., Alavi, A.H., Pashabavandpour, M.A., Gandomi, A.H., Askarinejad, A. [7] from Iran and Switzerland refers to the stabilization process of soft soils with various stabilizers. The special interest developed in this research is focused on the prediction of the resulted ground treatment based on new computer software developed on specific evolutionary algorithms that related to artificial neural networks can develop an accurate calculation of the unconfined compressive strength. Laboratory tests and

calibration on the initial model reflects the benefit of this research project, very well documented on the three case studies presented in the paper.

When soil improvement no longer represents the best technical solution to provide the safety requirements during both construction and service time period, deep foundation solution as pile foundations are applied and hence, research projects to predict as accurately as possible the construction behavior are always of interest. “The seismic soil-structure interaction effect for pile-raft systems” reflects the theoretical approach in modelling the construction behavior during an earthquake motion as Romania is strongly oriented on seismic protection design of all constructions [9].

The horizontal displacement is presented at the pile head level when considering the interaction of both raft and soil with the torsion effect present during an earthquake event. Results can be used in design practice to reach a more accurate prediction of the construction behavior during severe earthquake motion.

The paper “Modeling lateral earth pressure on concrete retaining wall” written by Alexandra Stan and Horatiu Mociran [8] relates in an efficient manner the classical solution to solve a local failure of soil on an imposed ground level difference. Whether earth pressure is working in an active, passive or at rest state is related to the direction and value of the wall displacement related to the supported soil if any. Conventional retaining structures, reinforced concrete walls are cost effective in specific situations and should be used as stability solution of the site.

The ground although mainly regarded as the construction support or as a potential construction material is also an energy source more unconventional considered than others. Papers as “The theoretic base simulation and calculation of boreholes”, “The soil Thermal analysis in the neighbor of ground source heat exchanger of the heat pump”, and “The thermal behavior of the water to water heat pump” all written by Helena Křišíková from the Czech Republic reflect this concept and develop knowledge for the thermal design of buildings using an alternative energy source by ground source heat exchangers [4], [5], [6].

Measurements performed to assess the soil regeneration capacity in temperature accumulation during summer are useful to select the best technical solution in terms of thermal design of the indoor space. The soil thermal analysis based on the data base created from measurements of sensors is important in order to realistically correlate climatic conditions with the soil profile over a specific construction site.

The thermal behavior of a single-family house designed with the ground heat as the energy source is presented in order to assess all factors influencing the system efficiency and thus potentially considering a larger use of this research projects for the future of building design.

Viscoplastic fluids that are so familiar to the construction process such as bentonite, slurries, fresh concrete, ceramic past and molten polymers develop a flow control issue that have various solutions, one of them is being presented in the paper “Numerical solution for unsteady Couette flow of viscoplastic fluids” by Irene Daprà and Giambattista Scarpi from Italy [2].

In order to bridge the difficulties to solve problems developed during unsteady motion for fluids, the author examined different procedures of the start-up and cessation of flow of a viscoelastic fluid using a regularized constitutive equation based on the error function. The rheological characteristic of such fluids is very important on the obtained results and thus numerical experiments within the research reached a convenient value to be implemented in the finite difference method.

Ecologic accidents along water streams as well as flooding events imposed on extensive research projects related to discharge on the water level, the celerity and dispersion of waves with respect to the time dependent biomass on the river bed. Numerical model applied in realistic simulation of the hydraulic characteristics of a water stream/river system is an interesting approach to limit the extensive and costly measurements otherwise needed to provide an efficient water management.

The paper “Computational aspects of river hydraulics” by De Doncker L., Troch P., Verhoeven R., Desmet N., Buis K., Meire P. [2], refers to a calibration aspect of the Manning coefficient with respect to measurements performed since 1997 over the downstream part of the river Aa, in the region of Antwerp, Belgium. The ‘Femme’ (flexible environment for mathematically modeling the environment) is used as an application on the ecological time dependent process.

The ecosystem modelling with the implementation of a one dimensional hydrodynamic model for surface water flow is the important achievement of this research when related to the variation of the Manning coefficient with the vegetation variously developed on the river bed.

3. CONCLUSIONS

All papers reflect an extensive research generated by various interests to obtain cost efficient solutions in construction design and performance. All these contributions to the benefit of society at large are appreciated.

Although solutions have been given, important issues related to geotechnical engineering are still open to consider better solutions and thus, researchers will continue their work.

References

1. Lungu, I., Stanciu, A., Boti, N., “*Probleme Speciale de Geotehnica si Fundatii*”, Junimea Publishing House, Iasi, Romania, 2002, (in Romanian language).
2. Dapra, I. and Scarpi G., Numerical solution for unsteady Couette flow of viscoplastic fluids, “*Computational Civil Engineering 2008*”, International Symposium Iasi, Romania, 2008.
3. De Doncker, L., Troch, P., Verhoeven, R., Desmet, N., Buis, K., Meire, P., Computational aspects of river hydraulics, “*Computational Civil Engineering 2008*”, International Symposium Iasi, Romania, 2008.
4. Křišíková, H., The theoretic base for simulation and calculation of boreholes, “*Computational Civil Engineering 2008*”, International Symposium Iasi, Romania, 2008.
5. Křišíková, H., The soil thermal analysis in the neighbor of ground source heat exchanger of the heat pump, “*Computational Civil Engineering 2008*”, International Symposium Iasi, Romania, 2008.
6. Křišíková, H., The thermal behavior of the water to water heat pump, “*Computational Civil Engineering 2008*”, International Symposium Iasi, Romania, 2008.
7. Moradi, M., Alavi, A.H., Pashabavandpour, M.A., Gandomi, A.H., Askarinejad, A., Soft computing based approaches for lime-microsilica stabilized clayey soils, “*Computational Civil Engineering 2008*”, International Symposium Iasi, Romania, 2008.
8. Stan, A. and Mociran, H., Modelling lateral earth pressure on concrete walls, “*Computational Civil Engineering 2008*”, International Symposium Iasi, Romania, 2008.
9. Ungureanu, N., Vrabie, M., Teodoru, I.B., The Seismic soil-structure interaction effect for piled raft systems, “*Computational Civil Engineering 2008*”, International Symposium Iasi, Romania, 2008.

Dynamic And Seismic Analysis Of Some Structures

Doina Stefan¹, Violeta-Elena Chitan²

¹"Gh. Asachi" Technical University of Iași, România

²"Gh. Asachi" Technical University of Iași, România

Summary

Defining Computational Civil Engineering as an independent domain is very complex task considering its very generous and wide domain.

A group of three enthusiasts from Romania decided to organize a small symposium that latter repeated and may become a tradition that is a platform for impressive researches and a chance for researchers to integrate more in the scientific Civil Engineering community.

An important aspect of the Computational Civil Engineering is given by the general fact that the computational power is exponentially growing with time at comparatively same price. This leads to new perspectives and findings through computational analysis and simulations therefore to a highly dynamic field.

This domain is mainly one of support and a development environment for the other Civil Engineering sub-domains. It is very probably that there is no Civil Engineering specialist who can escape the influence imposed by the use of computers and numerical methods specific to Civil Engineering.

The above ideas are excellent shown by the works presented during the International Symposium "Computational Civil Engineering". In what follows it is intended to make a short review of the domain reflected by these works.

KEYWORDS: civil engineering, computers, research, computer aided design, education, databases, computation in engineering and science.

1. INTRODUCTION

Structural analysis represents an issue which was, is, and will be under scrutiny. The wide range of structures and building materials leads to various way in tackling structural computing.

There have been sent and accepted for publishing to section Structural Analysis of Structures of International Conference for Computational Civil Engineering a

number of seven papers, papers which deal with various aspects of high rise buildings, cable structures and railway turnout structures.

2. DEVELOPMENTS AND TRENDS

The complexity of structural analysis of high rise structures arises as a consequence of the non – linear behavior of these mechanical systems. The execution methods for the resistance structure of high rise buildings are based on: steel, masonry, reinforced concrete, pre-stressed reinforced concrete and combinations of these structural materials.

*The most difficult phases of the structural analysis are the establishment of the approximate mathematical model and the interpretation of the results. Using advanced investigation methods and concepts from system theory, in the paper “**Structural Analysis of High Rise Building Structures**”, the authors present the problematic aspects of structural analysis.*

The main characteristic of all tall structures or high rise structures is that they have large horizontal and vertical geometric dimensions. In order to satisfy the strength and stability conditions imposed by the static and especially by the dynamic actions, these structures need special attention from the designers.

The aspects presented by the authors help in substantiation of the design codes for high rise buildings, which are being currently developed. The accuracy of the results of a static and dynamic structural analysis depends on the matching of the mathematical models for the entire structure and on the correct establishment of the stress hypotheses.

The parameters of the structural behavior are: displacements, speeds, accelerations and specific deformations. The study of the tall civil structures comprises conception, design and execution of the construction work for buildings with a large number of floors, in the light of the new European and international codes. Besides the rigorous approach aspects, a series of practical structural analysis facts are presented in the paper.

The aspects presented by **Ludovic Kopenetz** and **Alexandru Cătărig** help in substantiation of the design codes for high rise buildings, which are being currently developed.

The study of the dynamical response of cable structures and cable stayed systems started back in the 70’s – 80’s.

In the 1990’s new papers and books appeared on the subject, which compare the theoretical results with the experimental results obtained in the 1970’s.

Ferencz Lazar-Mand and **Dragos Florin Lisman** presents in the paper “*Practical Aspects about Linear Dynamic Analysis of Cable Structures*”, aspects about frequency and pulsation computation of pretensioned cable structures.

The eigenvalues and the eigenvectors were computed using the QR method from the IMSL library. The modeling of the mass matrix and of the stiffness matrix is of great importance. For the stiffness matrix modeling, an approach similar to the one described by P. Krishna is used, except the fact that the non-linear, residual terms are not taken into account.

The authors analyzed two types of structures. The Jensen’s planar cable - beam is the first structure. The frequencies were computed for three cases of concentrated masses. The second structure is the Aden Airways building hyperbolic paraboloid. There are computed the pulsations in the case of lumped masses (masses resulting from the proper weight of the cables). The results obtained are compared with the theoretical results obtained by other authors, respectively with the experimentally obtained results.

The authors **Banut V.** and **Teodorescu M.-E.** in their paper “*Stability Plane Structures Analysis Program by Correction Functions*”, present a method of classical stability analysis transforming – by using characteristic equation – in a eigenvalues and eigenvectors problem, using correction functions in elements stiffness evaluation, respectively structures.

Stability plane structures analysis using classical formulation implies iteration solving of stability equation–witch represents unknown coefficients determinant from displacement method.

Strength structures designing or checking suppose elements flexibility considering by introducing compression axial force effect act on unitary efforts values in the most stressed transversal section. The element that introduces this effect is effective length, according to witch slinness coefficient is obtained. Effective length of a compressed element is obtained from a stability analysis.

In stability issue classical formulation – having as base Euler’s theory- the characteristic equation is obtained, being a determinant that is solved by iterations. This determinant’s elements represents structure stiffness to the possible displacements of the nodes, corrected with some correction functions–functions introducing geometrical nonlinear effect, produced by the axial force.

Finite element method appearance and perfectionist analysis instruments allowed elaboration of matrix method for stability analysis. It is possible that the solving by iterations of characteristic equation representing stability condition in case of using correction functions to be transformed into an eigenvalues and eigenvectors problem.

The special program STAFCO was made. It allows the calculus of critical forces and the effective lengths for strongly compressed bars.

Teodorescu M.-E. and Topala Cristina-Alexandra describe in “The Detection Of Singular Points In The Stability Analysis Of Structures”, a methodology for detection of the singular points in the stability analysis of structures.

Depending of the history of loading, the stiffness of the structure may be softening or stiffening, the equilibrium path may be stable or unstable and the structure itself may be on a stage of loading or unloading. All such phenomena are typified by the occurrence of singular points (limit points and bifurcation points) which tend to bring us numerical difficulties in the solution process.

The finite element method is an important tool for the analysis of non-linear problems, such as geometrical and material non-linear behaviour of solids and structures. For tracing the entire load deflection path is necessary an automatically incremental-iterative procedure using control parameters for guiding the direction of the loading and also the presence of the singular points. The control parameter is computed in the predictor phase and characterized the equilibrium position of the structure and the degree of non-linearity.

The number of negative pivots (NPV) is inefficient for structures, which present multiple bifurcation points. This control parameter can be used to determine the nature of singular points.

The current stiffness parameter (CSP) is used for determine the nature of singular points (limit or bifurcation) and is not suitable for application to problems involving snap-back.

The general stiffness parameter (GSP) can predict the occurrence of limit points; it serves as a good indicator for changing the direction of loading.

Using an original program for 3D – truss structures, there are presented two numerical examples. The results obtained are much closed with the results given by others authors.

The strengthening of steel members under loading by means of additional parts is connected with many problems. Welding effects and high temperatures during the welding process cause a temporary local reduction of heated area. This problem becomes complicated thereby that these members rapidly get to the elastic-plastic zone. The displacement of the original centroid caused by temporary local reduction of heated cross-sectional area creates an additional moments.

Mohamad Al Ali’s article “The Simulation of Weakening of Steel Columns` Cross-Sections Caused by Welding When Strengthening Under Load“, deals with simulation of the cross-sectional weakening of steel columns during the welding process and brings out some comparing with experimental results. The paper presents also the actual state of this problem, some explanations for welding

stress formation and creation of additional moments and deformations when the strengthening is realized under loading. There are also presented some recommendations for calculation and appraisal process.

Higher carrying capacity obtained by the experiment is a result of the interaction between favorable and unfavorable effects of the several imperfections. With increasing load the results of the simulating calculation show a lower carrying capacity in average 10%. At the strengthening of steel member under loading, three-stage theory has to be considered.

The severity of analytical solution is residing in the complexity of identification of actual stress' pattern, which incessantly changes during welding process of new parts to original cross-section until finishing of strengthening process and sequential loading.

The vibration is affected by the weight on the axle, the speed of the railway vehicles, the arrangement of axles, their spring mounting and the spring mounting of the coach body and also the quality of the running surface of the wheel tyre. The vibration of the superstructure is particularly affected by its quality, by operational technical conditions, by climatic phenomena and above all by the dynamic loading due to the wheelsets of the railway vehicles.

The subject paper made by **Jaroslav Smutny, Lubos Pazdera, Ivo Moll and Miroslav Bajer** in „*The Analysis of Dynamic Effects in Turnout Structures by the Method of Quadratic Time and Frequency Invariant Transformations*” is focused on the analysis of dynamic parameters of turnout structures. The paper also deals with the comparison of the parameters measured in the turnout provided with the spring movable frog and with their comparison with the fixed crossing frog. It is also include the description of the methods of measurement and a suitable mathematical apparatus for the evaluation of the parameters measured.

It was described an experimental analysis of dynamic effects in turnout structures focused on the comparison of the turnout provided with the spring crossing movable frog (SCMF) with the standard turnout structure with a fixed frog point (FFP).

Based upon the analyses made, the springing of the whole system may be recommended by inserting rail pads, which could decelerate the process of the disintegration of the gravel bench under the sleeper heads in the turnout provided with the fixed frog point.

The measured and also the calculated values show sufficient accuracy and informative capabilities. Within the framework of the frequency analysis, the Welch method proved to be very reliable. This method, together with time frequency procedures, offers a comprehensive view on the dynamic behaviour of the turnout structures.

For the most part it may be stated that the advantage of the turnout provided with the spring crossing movable frog point will fully reveal at speeds higher than $160\text{km}\cdot\text{h}^{-1}$. Up to this speed, both investigated structures are almost comparable.

“The Seismic Force Development Related To Romanian Designing Codes” by **Doina Stefan** and **Gabriela Covatariu** presents the seismic calculus researches in the past 50 years, which are based on experimental recordings and are led to changes in the building design standards.

Major changes were made in estimating the dynamic amplification coefficient β , which is established in relation to the spectral composition of the seismic movements generated by the Vrancea source and in relation with the dimensionless coefficient ψ , which accounts for the ductility of the structure.

„Minimum Weight Buildings Design Best Evaluation Using Inequalities Method Automatic Evaluation Program” by **Cosmina Geanina Adam**, **Iulian Gabriel Mihai** presents the principles and use of an automatic evaluation program for minimum weight buildings design, based on inequalities method.

References

1. Lee, L.T., Collins, J.D., *Engineering Risk Management for Structures*, Journal of the Structural Division, ASCE 103, No. ST9.
2. ***, EUROCODE 8, Part 1.4., *Design Provisions for Earthquake Resistance of Structures. General Rules, Strengthening and Repair of Buildings*, 1998.
3. ***, Cod de Proiectare Seismică, Partea 1, *Prevederi de Proiectare pentru Clădiri*, indicative P100 – 1/2006. (in Romanian)
4. ***, *Normativ pentru Proiectarea Antiseismică a Construcțiilor de Locuințe, Social – Culturale, Agrozootehnice și Industriale, Indicativ P100 – 92*. (in Romanian)
5. Kopenetz, L.G., Ionescu, A., *Lightweight Roof for Dwellings*, IAHS, International Journal for Housing and its Application, vol. 9, No. 3, pg. 213 – 220, Miami, Florida, U.S.A. 1985.
6. Cătărig, Al., Kopenetz, L. G., *Time Surveillance and in Situ Testing by Dynamic Methods of Steel Structures*, The 6th Conference on Steel Structures, Timișoara, Romania, 1991.
7. Bârsan, G.M., Kopenetz, L.G., Alexa, P., *Analiza Dinamică a Structurilor cu Reazeme Depărtate*, Lucrările SNIC, Sibiu, Romania, 1984. (in Romanian)
8. Cătărig, Al., Kopenetz L.G., Alexa, P., *Nonlinear Analysis of Static and Dynamic Stability of Metallic Chimneys*, International Journal Thin – Walled Structures - 20, Elsevier Applied Science Publishers, England, 1994, (also in Romanian at) U.T. Press, Cluj – Napoca, 1998.
9. Borș, I., Bârsan, G.M., Alexa, P., Kopenetz, L.G., *The Laplace Transforms in Dynamics Analysis of Guyed Steel Structures*, A VI-a Conferință de Construcții Metalice, vol.2, pg.306 – 314, Timișoara, Romania, 1991.
10. Chisăliță, A., *Numerical Analysis*, Universitatea Tehnică din Cluj Napoca, 2002.
11. Chisăliță, A., *Program NELSAS – Manual de utilizare*, Universitatea Tehnică din Cluj Napoca, 2007. (romanian)
12. Chisăliță, A., 2007. *Metode numerice*, Curs Școala Doctorală, U.T.C.N., <ftp://ftp.utcluj.ro/users/chisalita/> (romanian)
13. Krishna, P., *Cable – suspended roofs*, McGraw-Hill Inc., 1978.

14. Kwan, A. S. K., *A simple technique for calculating natural frequencies of geometrically nonlinear prestressed cable structures*, Computers and Structures, 1998, vol. 74, pp. 41-50.
15. Smith, B.T., J.M. Boyle, J.J. Dongarra, B.S. Garbow, Y. Ikebe, V.C. Klema, C.B. Moler, *Matrix Eigensystem Routines – EISPACK Guide*, Springer-Verlag, New York, 1976.
16. Volokh, K. Yu., Vilnay, O., Averbuh, I., *Dynamics of cable structures*, Journal of Structural Engineering, 2003, ASCE, Vol. 129, No. 2, pp. 175-180.
17. “Compaq Fortran – Language Reference Manual”, Compaq Computer Corporation, 1999.
18. “Compaq Visual Fortran Language Reference Manual”, 2001, ftp://ftp.compaq.com/pub/products/fortran/vf/docs/cvf_lref.pdf
19. “Compaq Visual Fortran Programmer’s Guide”, 2001, ftp://ftp.compaq.com/pub/products/fortran/vf/docs/cvf_pg.pdf
20. “IMSL Libraries Reference”, Compaq Visual Fortran Help, 2001
21. Chisalita A. *Finite deformation analysis of cable networks*. ASCE J Engng Mech., 1984 in Kwan, A. S. K., 1998. *A simple technique for calculating natural frequencies of geometrically nonlinear prestressed cable structures*, Computers and Structures, 74, 41-50.
22. Geshwinder LF, West HH. *Parametric investigations of vibrating cable networks*. ASCE J Struct Div., 1979 in Kwan, A. S. K., 1998. *A simple technique for calculating natural frequencies of geometrically nonlinear prestressed cable structures*, Computers and Structures, 74, 41-50.
23. Jensen JJ. *Eine Statische und Dynamische Untersuchung der Seil und Membrantragwerke*, Report No 70 – 1, Norwegian Institute of Technology, University of Trondheim, 1970 in Kwan, A. S. K., 1998. *A simple technique for calculating natural frequencies of geometrically nonlinear prestressed cable structures*, Computers and Structures, 74, 41-50.
24. Banut, V. , *Stabilitatea structurilor elastice*, Ed. Academiei RSR, 1975
25. Banut, V. , *Calculul neliniar al structurilor*, Ed. Tehnica, 1981
26. Banut, V. , *Calculul de ordinul II si de stabilitate ale elementelor si structurilor de rezistenta*, Ed. Conspres, 2005
27. Banut, V. , Teodorescu, M.E., *Calculul de ordinul II si de stabilitate. Aplicatii rezolvate*, Ed. MatrixRom, 2007
28. Barsan, G.M., *Dinamica si Stabilitatea Constructiilor*, Ed. Didactica si Pedagogica, 1979
29. Rautu, S., Bergman, M., *Stabilitatea statica a structurilor elastice*, Ed. Ministerului Invatamantului si Culturii, 1960
30. Scarlat, A., *Stabilitatea si calculul de ordinul II al structurilor*, Ed. Didactica si Pedagogica, 1969
31. Timoshenko, P.S., Gere, M.J., *Teoria stabilitatii elastice*, Ed. Tehnica, 1967
32. B.G.Bergan, G. Horrigmoe, B. Krakeland and T.H. Soreide -Solution techniques for non-linear finite element problems, *Int. J.Numer. Methods Eng.*, 12, 1677-1696, (1978)
33. Clarke, M.J., Hancock, G.J. - *A study of incremental-iterative strategies for non-linear analysis*. *Int. J. Num. Meth. & Engng.*, 29, 1365-1391 (1990)
34. Crisfield, M.A. - *Non-linear Finite Element Analysis of Solids and Structures*, Vol.1 Essentials, John Wiley&Sons 1991, Vol.2 Advanced topics, John Wiley&Sons 1997
35. Fujii,F., Perez, B.G., Choong, K.K. - *Selection of the control parameter in displacement incrementation*. *Comput. & Struct.*, 42, 167-174 (1992)
36. Healey, T.J. – *A group – theoretic approach to computational bifurcation problems with symmetry*. *Comp. Meth. Appl. Mech. & Eng.*, 67, 257-295 (1984)
37. Teodorescu, M.E. - *Studiu comparativ al metodelor pentru determinarea solutiilor in calculul neliniar al structurilor* Teza de doctorat, 1999
38. Masubuchi, K., *Analysis of welded structures*, PERGAMON PRESS, USA, 1980.
39. Tokuzawa, N., Horikawa, K., Mechanical behaviors of structural members welded under loading, *Transaction of JWRI*, Vol.10, No. 1, Welding Research Institute, Osaka – Japan, 1981.
40. Suzuki, H., Horikawa, K., *Experimental study of the reshape of a plate girder under loading*, *Transaction of JWRI*, Vol.14, No. 1, Welding Research Institute, Osaka – Japan, 1985.
41. Masubuchi, K., *Joint evaluation and quality control*, PERGAMON PRESS, USA, 1990.

42. Hunersen, G., Haensch, H., Augustyn, J., *Repair welding under load*, Welding in the world, VOL.28, No. 9/10, P. 174-182, 1990.
43. Marzouk, H., Mohan, S., Strengthening of wide – flange columns under load, *CAN. J. CIV. ENG.*, Vol.17, P. 835-843, 1990.
44. Al Ali, M., *The influence of welding process on strengthening of centrally compressed steel members under loading*, PhD. dissertation work, Košice – Slovak Rpublic, 2005.
45. Smutný J., Pazdera L. *New techniques in analysis of dynamic parameters rail fastening*, InSight, The Journal of The British Institute of Non-Destructive Testing, Vol. 46, No 10, October, 2004, pp. 612-615, ISSN 13542575
46. Melcer, J, Kucharova, D, *Mechanical properties of rubber pads under static and dynamic load*, International Conference on Materials Science and Engineering, BRAMAT 2003, Romania, Brasov, 3/2003, University of Brasov, 2003, pp 18-314.
47. Smutný J., Pazdera L., *Time frequency analyses of real signals*, 2003
48. Cohen L. *Time-frequency distributions - a review*, Proc. IEEE, Vol. 77 No. 7, 941-981, 1989
49. ***Conditioned Standards for Civil and Industrial Constructions Design in Seismic Regions - P13-63
50. ***Standards for Civil and Industrial Constructions Design in Seismic Regions - P13-70
51. ***The Antiseismic Standards for Design of Civil, Socio-Cultural, Agrozootechnical and Industrial Constructions P 100-78
52. ***The Antiseismic Standards for Design of Civil, Socio-Cultural, Agrozootechnical and Industrial Constructions - P100-92
53. ***Seismic Projection Code - part I – Building Design Provisions, P100-1/2006
54. Amariei C., Mihai G. I - *Minimum Weight Buildings Design Using Inequalities Method*, *Civil Engineering* -International Symposium „Computational Civil Engineering 2007”, „Matei-Teiu Botez” Academic Society Publishing House, Iași, 2007
55. Mihăilă N. – *Introduction to linear programming*, EDP, Bucharest, 1970
56. Logofătu D., – *Fundamental algorithms in Java*, Polirom Publishing House, 2007

Computational model for buildings with energy dissipators subjected to seismic action

A.H. Barbat¹, P. Mata¹, S. Oller¹, R. Boroschek² and J.C. Vielma¹

1 Technical University of Catalonia, UPC
Edificio C1, Campus Nord, Gran Capit' a s/n. 08034 Barcelona, Spain.
2 University of Chile; Department of Civil Engineering
837-0449 Santiago, Chile.

Summary

The poor performance of many framed RC structures in recent strong earthquakes has alerted about the need of improving their seismic behavior especially when they are designed according to obsolete seismic codes. Sometimes, RC buildings show a low level of structural damping, important second order effects and low ductility of the connecting joints, among other defects.

These characteristics allow proposing the use of energy dissipating devices for improving their seismic behavior, controlling their lateral displacements, providing additional damping and ductility. In this work, the nonlinear dynamic response of RC buildings with energy dissipating devices is studied using advanced computational techniques. A fully geometric and constitutive

nonlinear model for the description of the dynamic behavior of framed structures is used. The model proposed for the structures and the dissipating devices is based on the geometrically exact formulation for beams which considers finite deformation and finite strains. The equations of motion of the system are expressed in terms of sectional forces and generalized strains and the dynamic problem is solved using the displacement based method formulated in the finite element framework. An appropriated version of Newmark's integration scheme is used in updating the kinematics variables in a classical Newton type iterative scheme. Each material point of the cross section is assumed to be composed of several simple materials with their own constitutive laws developed in terms of the material description of the First Piola Kirchhoff stress vector.

Appropriated constitutive laws for concrete and for steel reinforcements are provided. The simple mixing theory is used to treat the resulting composite. A specific finite element based on the beam theory is proposed for modeling the energy dissipating devices. Several constitutive descriptions in terms of force and displacements are provided for the dissipators. Special attention is paid to the development of local and global damage indices capable of describing the residual strength of the buildings. Finally, several numerical tests are carried out to validate the ability of the model to reproduce the nonlinear seismic response of RC buildings with energy dissipating devices.

KEYWORDS: Geometric nonlinearity, nonlinear analysis, beam model, composites, reinforced concrete structures, damage index, mixing theory.

1. INTRODUCTION

Conventional seismic design practice permits designing reinforced concrete (RC) structures for forces lower than those expected from the elastic response on the premise that the structural design assures significant structural ductility [6]. Frequently, the dissipative zones are located near the beam-column joints and, due to cyclic inelastic incursions during earthquakes, several structural members can suffer a great amount of damage.

In the last decades, new techniques based on adding devices to the buildings with the main objective of dissipating the energy exerted by the earthquake and alleviating the ductility demand on primary structural elements have improved the seismic behavior of the structures [25]. The purpose is to control the seismic response of the buildings by means of a set of dissipating devices. In the case of *passive energy dissipating devices* (EDD) an important part of the energy input is dissipated without the need of an external energy supply.

Several works about seismic control with passive EDDs are available; for example, in reference [4] the response of structures equipped with viscoelastic and viscous devices is compared; in reference [8] an approximated method is used to carry out a comparative study considering metallic and viscous devices. Aiken [1] presents the contribution of the extra energy dissipation due to EDDs as an *equivalent damping* added to the linear bare structure. A critical review of reduction factors and design force levels can be consulted in [10]. A method for the preliminary design of passively controlled buildings is presented in reference [3]. The design methods proposed for RC structures are mainly based on supposing that the behavior of the bare structure remains elastic, while the energy dissipation relies on the control system. However, experimental and theoretical evidence show that inelastic behavior can also occur in the structural elements during severe earthquakes [20]. In order to perform a precise dynamic nonlinear analysis of passively controlled buildings sophisticated numerical tools became necessary [14].

Considering that most of the elements in RC buildings are columns and beams, one dimensional formulations for structural elements appear as a solution combining both numerical precision and reasonable computational costs [11]. An additional refinement is obtained considering an arbitrary distribution of materials on the beam cross section [18], and in this case, the constitutive relationship at cross sectional level is deduced by integration. Formulations considering both, constitutive and geometric nonlinearity are rather scarce; most of the geometrically nonlinear models are limited to the elastic case [7, 21] and the inelasticity has been restricted mainly to plasticity [24]. Recently, Mata *et.al.* [11, 12] have extended the geometrically exact formulation for beams due to Reissner-Simo [19, 21, 23] to an

arbitrary distribution of composite materials on the cross sections for the static and dynamic cases.

From the numerical point of view, EDDs usually have been described in a global sense by means of force–displacement or moment–curvature relationships [25] which intend to capture appropriately the energy dissipating capacity of the devices [13].

In this work, a fully geometric and constitutive nonlinear formulation for beam elements is developed. A fiber–like approach is used for representing arbitrary distributions of composite materials on the plane beam cross sections. EDDs are considered as beam elements without rotational degrees of freedom. Thermodynamically consistent constitutive laws are provided for steel, concrete and EDDs. The mixing rule is employed for the treatment of the resulting composite. A brief description of the damage indices capable of estimate the remaining load carrying capacity of the buildings is also given. Finally, the numerical simulation of the seismic behaviour of a precast RC structure with EDDs is presented.

2. FINITE DEFORMATION FORMULATION FOR STRUCTURAL ELEMENTS

2.1. Beam model

The original geometrically exact formulation for beams due to Simo and Vu Quoc [21, 22] is expanded here for considering an intermediate curved reference configuration according to [7]. Let $\{\hat{E}_i\}$ and $\{\hat{e}_i\}$ be the spatially fixed *material* and *spatial* frames¹, respectively. The straight reference beam is defined by the curve $\hat{\varphi}_{00} = S\hat{E}_1$, with $S \in [0, L]$ its arch–length coordinate. Beam cross sections are described by means of the coordinates ξ_β directed along $\{\hat{E}_\beta\}$. The curved reference beam is defined by means of the spatially fixed curve given by $\hat{\varphi}_0 = \sum_i \varphi_{0i}(S)\hat{e}_i \in \mathbb{R}^3$. Each point on this curve has rigidly attached an orthogonal local frame $\hat{t}_{0i}(S) = \Lambda_0 \hat{E}_i \in \mathbb{R}$, where $\Lambda_0 \in SO(3)$ is the orientation tensor². The planes of the cross sections are normal to the vector tangent to the reference curve³, *i.e.* $\hat{\varphi}_{0,S} = \hat{t}_{01}(S)$. The position vector of a material point on the curved reference beam is $\hat{x}_0 = \hat{\varphi}_0 + \sum_\beta \Lambda_0 \xi_\beta \hat{E}_{0\beta}$.

The motion deforms points on the curved reference beam from $\hat{\phi}_0(S)$ to $\hat{\phi}(S, t)$ (at time t) and the local orientation frame is simultaneously rotated together with the beam cross section, from $\Lambda_0(S)$ to $\Lambda(S, t)$ by means of the *incremental rotation tensor* as $\Lambda = \Lambda_n \Lambda_0 \in SO(3)$. In general, \hat{t}_1 does not coincides with $\hat{\phi}_{,s}$ because of the shearing [21]. The position vector of a material point on the current beam is

$$\hat{x}(S, \xi_\beta, t) = \hat{\phi}(S, t) + \sum_\beta \xi_\beta \hat{t}_\beta(S, t) = \hat{\phi} + \sum_\beta \Lambda \xi_\beta \hat{E}_\beta$$

Eq. (1) implies that the current beam configuration is determined by $(\hat{\phi}, \Lambda)$. The deformation gradients of the curved reference beam and of the current beam referred to the straight beam are denoted by \mathbf{F}_0 and \mathbf{F} , respectively. The deformation gradient $\mathbf{F}_n := \mathbf{F}\mathbf{F}_0^{-1}$ is responsible for the development of strains and can be expressed as [9, 11]

$$\mathbf{F}_n = \mathbf{F}\mathbf{F}_0^{-1} = \frac{1}{|\mathbf{F}_0|} \left[\hat{\phi}_{,s} - \hat{t}_1 + \tilde{\omega}_n \sum_\beta \xi_\beta \hat{t}_\beta \right] \otimes \hat{t}_{01} + \Lambda_n$$

where $|\mathbf{F}_0|$ is the determinant of \mathbf{F}_0 and $\tilde{\omega}_n \equiv \Lambda_{n,s} \Lambda_n^T$ is the curvature tensor relative to the curved reference beam. In Eq. (2) the term defined as $\hat{\gamma}_n = \hat{\phi}_{,s} - \hat{t}_1$ corresponds to the reduced strain measure of shearing and elongation [9, 21] with material description given by $\hat{\Gamma} = \Lambda^T \hat{\gamma}$.

The material representation of \mathbf{F}_n is obtained as $\mathbf{F}_n^m = \Lambda^T \mathbf{F}_n \Lambda_0$. It is possible to construct the strain tensor $\varepsilon_n = \mathbf{F}_n - \Lambda_n$, which conjugated to the asymmetric *First Piola Kirchhoff* (FPK) stress tensor $\mathbf{P} = \hat{P}_i \otimes \hat{t}_{0i}$ referred to the curved¹ reference beam [21]. The spatial strain vector acting on the current beam cross section is obtained as $\hat{\varepsilon}_n = \varepsilon_n t_{0i}$ and the spatial *stress resultant* \hat{n} and *stress couple* \hat{m} vectors can be estimated from \hat{P}_1 according to

$$\hat{n}(S) = \int_A \hat{P}_1 dA; \quad \hat{m}(S) = \int_A (\hat{x} - \hat{\phi}) \times \hat{P}_1 dA$$

¹ The indices i and β range over $\{1,2,3\}$ and $\{2,3\}$, respectively.

² The symbol $SO(3)$ is used to denote the finite rotation manifold [21, 22].

³ The symbol $(\bullet)_{,x}$ is used to denote partial differentiation of (\bullet) with respect to x .

The material form of $\hat{P}_j, \hat{\varepsilon}_n, \hat{n}$ and \hat{m} are obtained as $\hat{\varepsilon}_n = \Lambda^T \hat{\varepsilon}_n \hat{P}_j^m = \Lambda^T \hat{P}_j$, $\hat{m}^m = \Lambda^T \hat{n}$ and $\hat{m}^m = \Lambda^T \hat{m}$, respectively. An objective measure of the *strain rate* vector \hat{s}_n acting on any material point can be deduced using the definition of the Lie derivative

operator $\left[\begin{array}{c} \nabla \\ \bullet \end{array} \right]$ [11, 12] as follows:

$$\hat{s}_n = \left[\begin{array}{c} \nabla \\ \hat{\varepsilon}_n \end{array} \right] = \left[\begin{array}{c} \nabla \\ \hat{\gamma}_n \end{array} \right] + \left[\begin{array}{c} \nabla \\ \hat{\omega}_n \end{array} \right] \sum_{\beta} \zeta_{\beta} \hat{t}_{\beta} = \dot{\hat{\phi}}_{,s} - \tilde{v}_n \hat{\phi}_{,s} + \tilde{v}_{n,s} \sum_{\beta} \zeta_{\beta} \hat{t}_{\beta}$$

where $\tilde{v}_n \equiv \dot{\Lambda}_n \Lambda_n^T$ is the current *spin* or angular velocity of the beam cross section with respect to the curved reference beam. The material form of Eq. (4) is $\hat{S}_n = \Lambda^T \hat{s}_n$.

The classical form of the *equations of motion of the Cosserat beam* for the static case are

$$\begin{aligned} \hat{n}_{,s} + \hat{n}_p &= \mathbf{A}_{\rho 0} \ddot{\hat{\phi}} + \underbrace{\hat{\alpha}_n \mathbf{S}_{\rho 0} + \tilde{v}_n \tilde{v}_n \mathbf{S}_{\rho 0}}_{D_1} \\ \hat{m}_{,s} + \hat{\phi}_{,s} \times \hat{n} + \hat{m}_p &= \mathbf{l}_{\rho 0} \hat{\alpha}_n + \tilde{v}_n \mathbf{l}_{\rho 0} \hat{v}_n + \underbrace{\mathbf{S}_{\rho 0} \times \ddot{\hat{\phi}}}_{D_2} \end{aligned}$$

where \hat{n}_p and \hat{m}_p are the external *body force* and *body moment* per unit of reference length at time t , $\mathbf{A}_{\rho 0}$, $\hat{\mathbf{S}}_{\rho 0}$ and $\mathbf{l}_{\rho 0}$ are the cross sectional mass density, the first mass moment density and the second mass moment density per unit of length of the curved reference beam, respectively; their explicit expressions can be consulted in references [9, 22]. $\tilde{\alpha}_n \equiv \ddot{\Lambda}_n \Lambda_n^T - \tilde{v}_n^2$ is the angular acceleration of the beam cross section and \hat{v}_n and $\hat{\alpha}_n$ are the axial vectors of \tilde{v}_n and $\tilde{\alpha}_n$, respectively. For most of the practical cases, the terms D_1 and D_2 can be neglected.

Considering a kinematically admissible variation⁴ $h \equiv (\delta\hat{\phi}, \delta\hat{\theta})$ of the pair $(\hat{\phi}, \Lambda)$ [22], taking the dot product with Eqs. (5a) and (5b), integrating over the length of the curved reference beam and integrating by parts, we obtain the nonlinear functional $G(\hat{\phi}, \Lambda, h)$ corresponding to the *weak form of the balance equations* [7, 22]

$$\begin{aligned} \mathbf{G}(\hat{\phi}, \Lambda, h) &= \int_L \left[(\delta\hat{\phi}_{,s} - \delta\hat{\theta} \times \hat{\phi}_{,s}) \cdot \hat{n} + \delta\hat{\theta}_{,s} \cdot \hat{m} \right] dS \\ &+ \int_L \left[\delta\hat{\phi} \cdot \mathbf{A}_{\rho 0} \ddot{\hat{\phi}} + \delta\hat{\theta} \cdot (\mathbf{l}_{\rho 0} \hat{\alpha}_n + \hat{v}_n \mathbf{l}_{\rho 0} \hat{v}_n) \right] dS \\ &- \int_L \left[\delta\hat{\phi} \cdot \hat{n}_p + \delta\hat{\theta} \cdot \hat{m}_p \right] dS - \left(\delta\hat{\phi} \cdot \hat{n} + \delta\hat{\theta} \cdot \hat{m} \right) \Big|_0^L = 0 \end{aligned}$$

The terms $(\delta\hat{\varphi}_{,s} - \delta\hat{\theta} \times \hat{\varphi}_{,s})$ and $\delta\hat{\theta}_{,s}$ appearing in Eq. (6) correspond to the co-rotated variations of the reduced strain measures $\hat{\gamma}_n$ and $\hat{\omega}_n$ in spatial description.

2.2. Energy dissipating devices

The finite deformation model for EDDs is obtained from the beam model releasing the rotational

degrees of freedom and supposing that all the mechanical behavior of the device is described in terms of the evolution of a unique material point in the middle of the resulting bar.

The current position of a point in the EDD bar is obtained from Eq. (1) and considering that $\xi_\beta = 0$ as $\hat{x}(S, t) = \hat{\varphi}(S, t)$. Supposing that the current orientation of the EDD bar of initial length L^* is given by the tensor $\Lambda^*(t)$, ($\Lambda^*_{,s} = 0, \dot{\Lambda}^* \neq 0$), the spatial position of the *dissipative point* in the EDD is obtained as $\hat{\varphi}(L^*/2, t)$ where $L^*/2$ is the arch-length coordinate of the middle point in the bar element and the axial strain and the axial strain rate in the dissipative point are obtained from Eqs. (2) and (4) as

$$\hat{\Gamma}_1(t) = \{(\Lambda^{*T} \hat{\varphi}_{,s}) \cdot \hat{E}_1\} \Big|_{(L^*/2,t)} - 1$$

$$\dot{\hat{\Gamma}}_1(t) = \{(\Lambda^{*T} (\dot{\hat{\varphi}}_{,s} - \tilde{\nu}_n \hat{\varphi}_{,s})) \cdot \hat{E}_1\} \Big|_{(L^*/2,t)} \approx \frac{d}{dt} \hat{\Gamma}_1(t) \Big|_{(L^*/2,t)}$$

Finally, the contribution of the EDD bar to the functional of Eq. (6), written in the material description, is given by

$$\mathbf{G}_{\text{EDD}} = \int_{L^*} n_1^m \delta\hat{\Gamma}_1 dS + \{(\Lambda^{*T} \delta\hat{\varphi})^T [\mathbf{M}]_d (\Lambda^{*T} \ddot{\hat{\varphi}})\} \Big|_{(L^*/2,t)}$$

where it was assumed that $I_{\rho 0} \approx 0$, *i.e.* the contribution of the EDDs to the rotational mass of the system is negligible and $[\mathbf{M}]_d$ is the EDD's *translational inertia* matrix. The term $\delta\hat{\Gamma}_1 = (\Lambda^{*T} (\delta\hat{\varphi}_{,s} - \delta\hat{\theta} \times \hat{\varphi}_{,s})) \cdot \hat{E}_1$ corresponds to the material form of the variation of the axial strain in the EDD.

3. CONSTITUTIVE MODELS

In this work, material points on the cross sections are considered as formed by a *composite material* corresponding to a homogeneous mixture of different simple *components*, each of them with its own constitutive law. The resulting behavior is obtained by means of the *mixing theory*. Two kinds of nonlinear constitutive models for simple materials are used:

the *damage* and *plasticity* models. The constitutive models are formulated in terms of the material form of the FPK stress and strain vectors, \hat{P}_1^m and $\hat{\varepsilon}_n$, respectively [11, 12].

3.1. Degrading materials: damage model

The progress of the damage is based on the evolution of the scalar damage parameter $d \in [0, 1]$ [15]. Starting from an appropriated form of the free energy density and considering the fulfillment of the Clasius–Plank inequality and applying the Coleman’s principle [11] the following constitutive relation in material form is obtained:

$$\hat{P}_1^m = (1-d)\mathbf{C}^{me}\hat{\varepsilon}_n = \mathbf{C}^{ms}\hat{\varepsilon}_n = (1-d)\hat{P}_{01}^m$$

where \mathbf{C}^{me} and $\mathbf{C}^{ms} = (1-d)\mathbf{C}^{me}$ is the *secant constitutive tensor*. Eq. (9) shows that the FPK stress vector is obtained from its elastic counterpart by multiplying it by the factor $(1-d)$.

The damage yield criterion \mathbf{F} [2, 5] is defined as a function of the undamaged elastic free energy density and written in terms of the components of the material form of the undamaged principal stresses, \hat{P}_{p0}^m , as

$$\mathbf{F} = \mathbf{P} - f_c = [1 + r(n-1)]\sqrt{\sum_{i=1}^3 (P_{p0i}^m)^2} - f_c \leq 0$$

where \mathbf{P} is the equivalent stress, r and n are given in function of the tension and compression strengths f_c and f_t and the parts of the free energy density developed when the tension, $(\Psi_t^0)_L$, or compression, $(\Psi_c^0)_L$, limits are reached and are defined as

$$\begin{aligned} (\Psi_{t,c}^0)_L &= \sum_{i=1}^3 \frac{\langle \pm P_{p0i}^m \rangle \varepsilon_{ni}}{2\rho_0}, \quad \Psi_L^0 = (\Psi_t^0)_L + (\Psi_c^0)_L \\ f_t &= (2\rho\Psi_t^0 E_0)_L^{\frac{1}{2}}, \quad f_c = (2\rho\Psi_c^0 E_0)_L^{\frac{1}{2}}, \quad n = \frac{f_c}{f_t}, \quad r = \frac{\sum_{i=1}^3 \langle P_{p0i}^m \rangle}{\sum_{i=1}^3 |P_{p0i}^m|} \end{aligned}$$

A more general expression equivalent to that given in Eq. (10a) [2] is given by

$$\bar{\mathbf{F}} = \mathbf{G}(\mathbf{P}) - \mathbf{G}(f_c), \quad \mathbf{G}(\mathbf{X}) = 1 - \frac{\bar{\mathbf{G}}(\mathbf{X})}{\mathbf{X}} = 1 - \frac{\mathbf{X}^*}{\mathbf{X}} e^{k(1-\frac{\mathbf{X}^*}{\mathbf{X}})}$$

where the term $\bar{\mathbf{G}}(\mathbf{X})$ gives the initial yield stress for certain value of the scalar parameter $\mathbf{X} = \mathbf{X}^*$ and for $\mathbf{X} \rightarrow \infty$ the final strength is zero. The parameter \cdot is calibrated to

obtain an amount of dissipated energy equal to the specific fracture energy of the material $g_f^d = G_f^d / l_c$; where G_f^d is the tensile fracture energy and l_c is the characteristic length of the fractured domain. The evolution law for the internal damage variable d is given by

$$\dot{d} = \dot{\mu} \frac{\partial \bar{F}}{\partial \mathbf{P}} = \dot{\mu} \frac{\partial \mathbf{G}}{\partial \mathbf{P}}$$

where $\dot{\mu} = \dot{\mathbf{P}} \geq 0$ is the *damage consistency* parameter [11]. Finally, the Kuhn-Thucker relations: (a) $\dot{\mu} \geq 0$, (b) $\bar{F} \leq 0$, (c) $\dot{\mu} \bar{F} = 0$ have to be employed to derive the unloading–reloading conditions *i.e.* if $\bar{F} < 0$ the condition (c) imposes $\dot{\mu} = 0$; on the contrary, if $\dot{\mu} > 0$ then $\bar{F} = 0$.

3.1.1. Viscosity

The rate dependent behavior is considered by using the Maxwell model. The FPK stress vector $\hat{\mathbf{P}}_1^{mt}$ is obtained as the sum of a rate independent part $\hat{\mathbf{P}}_1^m$, Eq. (9), and a viscous component $\hat{\mathbf{P}}_1^{mv}$ as

$$\hat{\mathbf{P}}_1^{mt} = \hat{\mathbf{P}}_1^m + \hat{\mathbf{P}}_1^{mv} = \mathbf{C}^{mv} \hat{\boldsymbol{\varepsilon}}_n + \eta^{sm} \hat{\mathbf{S}}_n = (1-d) \mathbf{C}^{me} \left(\hat{\boldsymbol{\varepsilon}}_n + \frac{\eta}{E_0} \hat{\mathbf{S}}_n \right)$$

where $\eta^{sm} = \eta / E_0 \mathbf{C}^{ms}$ is the *secant viscous* constitutive tensor, $\mathbf{C}^{mv} = (1-d) \mathbf{C}^{me}$, and the parameter η is the viscosity. The linearized increment of the FPK stress vector (material and co–rotated forms) are calculated as

$$\Delta \hat{\mathbf{P}}_1^{mt} = \mathbf{C}^{mv} \Delta \hat{\boldsymbol{\varepsilon}}_n + \eta^{sm} \Delta \hat{\mathbf{S}}_n, \quad \Delta[\hat{\mathbf{P}}_1^t] = \mathbf{C}^{sv} \Delta[\hat{\boldsymbol{\varepsilon}}_n] + \eta^{ss} \Delta[\hat{\mathbf{S}}_n]$$

where $\mathbf{C}^{sv} = \Lambda \mathbf{C}^{mv} \Lambda^T$ and $\eta^{ss} = \Lambda \eta^{sm} \Lambda^T$. The explicit form of the terms $\Delta \hat{\mathbf{S}}_n$ and $\Delta[\hat{\mathbf{S}}_n]^\nabla$ and the material description of the tangent constitutive tensor \mathbf{C}^{mv} can be consulted in reference [12].

3.2. Plastic materials

In the case of materials which can undergo non–reversible deformations the plasticity model formulated in the material configuration is used for predicting their mechanical response. Assuming small elastic, finite plastic deformations, an appropriated form of the free energy density and analogous procedures as those for the damage model we have

$$\hat{\mathbf{P}}_1^m = \rho_0 \frac{\partial \Psi(\hat{\boldsymbol{\varepsilon}}_n^e, k_p)}{\partial \hat{\boldsymbol{\varepsilon}}_n^e} = \mathbf{C}^{ms} (\hat{\boldsymbol{\varepsilon}}_n - \hat{\boldsymbol{\varepsilon}}_n^P) = \mathbf{C}^{me} \hat{\boldsymbol{\varepsilon}}_n^e$$

where the $\hat{\boldsymbol{\varepsilon}}_n^e$ is the elastic strain calculated subtracting the plastic strain $\hat{\boldsymbol{\varepsilon}}_n^P$ from the total strain $\hat{\boldsymbol{\varepsilon}}_n$ and ρ_0 is the density in the material configuration.

Both, the yield function, \mathbf{F}_p , and plastic potential function, \mathbf{G}_p are formulated in terms of the FPK stress vector $\hat{\mathbf{P}}_1^m$ and the plastic damage internal variable k_p as

$$\mathbf{F}_p(\hat{\mathbf{P}}_1^m, k_p) = \mathbf{P}_p(\hat{\mathbf{P}}_1^m) - f_p(\hat{\mathbf{P}}_1^m, k_p) = 0, \quad \mathbf{G}_p(\hat{\mathbf{P}}_1^m, k_p) = \mathbf{K}$$

where $\mathbf{P}_p(\hat{\mathbf{P}}_1^m)$ is the equivalent stress, which is compared with the *hardening* function $f_p(\hat{\mathbf{P}}_1^m, k_p)$ and \mathbf{K} is a constant value [16]. In this work, k_p constitutes a measure of the energy dissipated during the plastic process and it is defined [17] as

$$g_f^p = \frac{G_f^p}{l_c} = \int_{t=0}^{\infty} \hat{\mathbf{P}}_1^m \cdot \dot{\boldsymbol{\varepsilon}}_n^P dt, \quad 0 \leq [k_p = \frac{1}{g_f^p} \int_{t=0}^t \hat{\mathbf{P}}_1^m \cdot \boldsymbol{\varepsilon}_n^P dt] \leq 1$$

where G_f^p is the specific plastic fracture energy of the material in tension and l_c is the length of the fractured domain defined in analogous manner as for the damage model. The integral term in Eq. (17) corresponds to the energy dissipated by means of plastic work. The flow rules for the internal variables $\hat{\boldsymbol{\varepsilon}}_n^P$ and k_p are defined as

$$\dot{\boldsymbol{\varepsilon}}_n^P = \dot{\lambda} \frac{\partial \mathbf{G}_p}{\partial \hat{\mathbf{P}}_1^m}, \quad \dot{k}_p = \dot{\lambda} \mathcal{H}(\hat{\mathbf{P}}_1^m, k_p, G_f^p) \cdot \frac{\partial \mathbf{G}_p}{\partial \hat{\mathbf{P}}_1^m} = \mathcal{H}(\hat{\mathbf{P}}_1^m, k_p, G_f^p) \cdot \dot{\boldsymbol{\varepsilon}}_n^P$$

where $\dot{\lambda}$ is the plastic consistency parameter and \mathcal{H} is the following *hardening* vector [16]. In what regards the hardening function of Eq. (16), the following evolution equation has been proposed:

$$f_p(\hat{\mathbf{P}}_1^m, k_p) = r\sigma(k_p) + (1-r)\sigma_c(k_p)$$

where r has been defined in Eq. (10c) and the scalar functions $\sigma(k_p)$ and $\sigma_c(k_p)$ describe the evolution of the yielding threshold in uniaxial tension and compression tests, respectively. As it is a standard practice in plasticity, the loading/unloading conditions are derived in the standard form from the Kuhn-Tucker relations formulated for problems with unilateral restrictions, *i.e.*, (a) $\dot{\lambda} \geq 0$, (b) $\mathbf{F}_p \leq 0$ and (c) $\dot{\lambda} \mathbf{F}_p = 0$. Explicit expressions of $\dot{\lambda}$ and of the material form of the tangent constitutive tensor can be reviewed in references [11, 16, 17].

3.3. Mixing theory for composites

Each material point on the beam cross section is treated as a composite material according to the *mixing theory* [16]. Supposing N different components coexisting in a generic material point subjected to the same material strain $\hat{\varepsilon}_n$, we have the following closing equation: $\hat{\varepsilon}_n \equiv (\hat{\varepsilon}_n)_1 = \dots = (\hat{\varepsilon}_n)_q = \dots = (\hat{\varepsilon}_n)_N$, which imposes the strain compatibility between components. The free energy density of the composite, $\overline{\Psi}$, is obtained as the weighted sum of the free energy densities of the N components. The weighting factors correspond to the quotient between the volume of the q^{th} component, V_q , and the total volume, V , such that $\sum_q k_p = 1$.

The material form of the FPK stress vector \hat{P}_1^{mt} for the composite, including the participation of rate dependent effects, is obtained in analogous way as for simple materials *i.e.*

$$\hat{P}_1^{mt} \equiv \sum_q^N k_q (\hat{P}_1^m + \hat{P}_1^{mv})_q = \sum_q^N k_p \left[(1-d) \mathbf{C}^{me} \left(\hat{\varepsilon}_n + \frac{\eta}{E_0} \hat{S}_n \right) \right]_q$$

where $(\hat{P}_1^m)_q$ and $(\hat{P}_1^{mv})_q$ correspond the strain and rate dependent stresses of each one of the N components. The material form of the secant and tangent constitutive tensors for the composite, $\overline{\mathbf{C}}^{ms}$ and $\overline{\mathbf{C}}^{mt}$, are obtained in an analogous manner [16].

3.4. Constitutive relations for EDDs

The constitutive law proposed for EDDs is based on a previous work of the authors [13] which provides a versatile strain–stress relationship with the following general form:

$$\overline{P}^m(\varepsilon_1, \dot{\varepsilon}_1, t) = \overline{P}_1^m(\varepsilon_1, t) + \overline{P}_2^m(\dot{\varepsilon}_1, t)$$

where \overline{P}^m is the average stress in the EDD, ε_1 the strain level, t the time, $\dot{\varepsilon}_1$ the strain rate, \overline{P}_1^m and \overline{P}_2^m are the strain dependent and rate dependent parts of the stress, respectively. The model uncouples the total stress in viscous and non-viscous components, which correspond to a viscous dashpot device acting in parallel with a nonlinear hysteretic spring. The purely viscous component does not requires to be a linear function of the strain rate. Additionally, hardening, and variable elastic modulus can be reproduced [13].

4. NUMERICAL IMPLEMENTATION

In order to obtain a numerical solution, the linearized form of Eq. (6) is written as

$$\mathbf{L} [\mathbf{G}(\hat{\varphi}_*, \Lambda_*, h)] = \mathbf{G}(\hat{\varphi}_*, \Lambda_*, h) + D\mathbf{G}(\hat{\varphi}_*, \Lambda_*, h) \cdot p$$

where $\mathbf{L} [\mathbf{G}(\hat{\varphi}_*, \Lambda_*, h)]$ is the linear part of the functional $\mathbf{G}(\hat{\varphi}, \Lambda, h)$ at the configuration $(\hat{\varphi}, \Lambda) = (\hat{\varphi}_*, \Lambda_*)$ and $p \equiv (\Delta \hat{\varphi}, \Delta \hat{\theta})$ is an admissible variation. The term $\mathbf{G}(\hat{\varphi}_*, \Lambda_*, h)$ supplies the *unbalanced force* and it is composed by the contributions of the inertial, external and internal terms; and $D\mathbf{G}(\hat{\varphi}_*, \Lambda_*, h) \cdot p$, gives the *tangential stiffness* [22].

The linearization of the inertial and external components, $D\mathbf{G}_{\text{ine}} \cdot p$ and $D\mathbf{G}_{\text{ext}} \cdot p$ give the inertial and load dependent parts of the tangential stiffness, \mathbf{K}_{I^*} and \mathbf{K}_{P^*} , respectively, and it can be consulted in [22, 23]. The linearization of the internal term is calculated as

$$D\mathbf{G}_{\text{int}} \cdot p = \underbrace{\int_{[0,L]} h^T [\mathbf{B}_*]^T [\mathbf{C}_*^{st} [\mathbf{B}_*]] p dS}_{\mathbf{K}_{\text{M}^*}} + \underbrace{\int_L h^T \cdot [\mathbf{B}_*]^T \left[\begin{smallmatrix} \cdot & st \\ \cdot & \cdot \end{smallmatrix} \right] [\mathbf{V}_*] p dS}_{\mathbf{K}_{\text{V}^*}} + \underbrace{\int_{[0,L]} h^T ([\tilde{\mathbf{n}}_{S^*}] - [\mathbf{B}_*]^T [\tilde{\mathbf{F}}_*]) p}_{\mathbf{K}_{\text{G}^*}}$$

where the operators $[\mathbf{C}_*^{st}]$, $[n_{S^*}]$, $[\mathbf{B}_*]$, $\left[\begin{smallmatrix} \cdot & st \\ \cdot & \cdot \end{smallmatrix} \right]$, $[\mathbf{V}_*]$ and $[\tilde{\mathbf{F}}_*]$ can be consulted in references [9, 11,12, 22]. The linearized terms \mathbf{K}_{G^*} , \mathbf{K}_{M^*} and \mathbf{K}_{V^*} , evaluated at the configuration $(\hat{\varphi}_*, \Lambda_*)$, give the *geometric*, *material* and *viscous* parts of the tangent stiffness, which allows to rewrite Eq. (22) as

$$\mathbf{L} [\mathbf{G}_*] = \mathbf{G}_* + \mathbf{K}_{\text{I}^*} + \mathbf{K}_{\text{M}^*} + \mathbf{K}_{\text{V}^*} + \mathbf{K}_{\text{G}^*} + \mathbf{K}_{\text{P}^*}$$

The solution of the discrete form of Eq. (25) by using the FE method follows identical procedures as those described in [22] for an iterative Newton-Rapson integration scheme and it will not be included here.

5 DAMAGE INDICES

A measure of the damage level of a material point can be obtained as the ratio of the existing stress level to its elastic counter part. Following this idea, it is possible to define

the fictitious damage variable \check{D} as [2]

$$\sum_{i=1}^3 |P_{li}^m| = \left(1 - \check{D}\right) \sum_{i=1}^3 |P_{li0}^m| \rightarrow \check{D} = 1 - \frac{\sum_{i=1}^3 |P_{li}^m|}{\sum_{i=1}^3 |P_{li0}^m|}$$

where $|P_{li}^m|$ and $|P_{li0}^m|$ are the absolute values of the components of the existing and elastic stress vectors, respectively. Initially, the material remains elastic and $\check{D} = 0$, but when all the energy of the material has been dissipated $|P_{li}^m| \rightarrow 0$ and $\check{D} \rightarrow 1$. Eq. (26) can be extended to consider elements or even the whole structure by means of integrating over a finite volume as explained in reference [11].

6 NUMERICAL EXAMPLES

6.1 Seismic response of a precast RC building with EDDs

The nonlinear seismic response of a typical precast RC industrial building shown in Figure 1 is studied. The building has a bay width of 24 m and 12 m of inter-axes length. The story height is 12 m. The compression limit of the concrete is 35 MPa with an elastic modulus of 290.000 MPa. It has been assumed a Poisson coefficient of 0.2. The ultimate tensile stress for the steel is 510 MPa. This figure also shows some details of the steel reinforcement of the cross sections. The dimensions of the columns are 60x60 cm². The beam has an initial high of 60 cm on the supports and 160 cm in the middle of the span. The permanent loads considered are 1050 N/m² and the weight of upper half of the closing walls with 432,000 N. The input acceleration corresponds to the N-S component of the EL Centro 1940 earthquake.

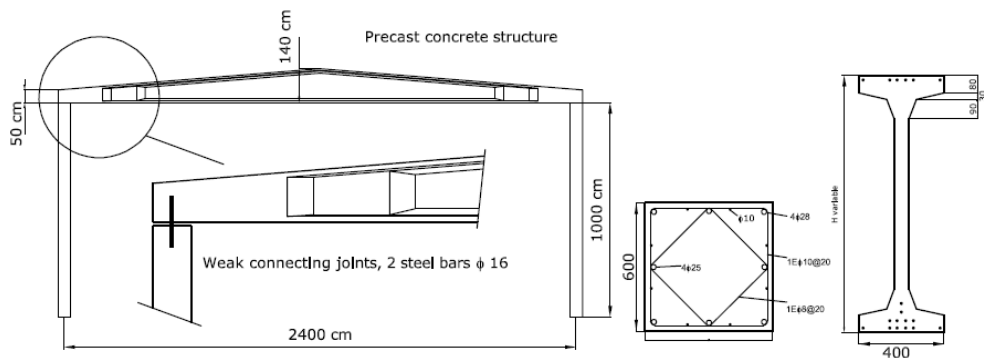


Figure 1: Description of the structure.

The half part of the building is meshed using 4 quadratic elements with two Gauss integration points for the resulting beam and column. The EED element was calibrated for reproducing a plastic dissipative mechanism. The properties of the device were: a yielding force of 150.000 N for a displacement of 1.5 mm.

The results of the numerical simulations allow seeing that the employment of plastic EDDs contributes to improve the seismic behavior of the structure. Figure 2a shows the hysteretic cycles obtained from the lateral displacement of the upper beam–column joint and the horizontal reaction (base shear) in the columns for the structure with and without devices. It is possible to appreciate that the non–controlled structure (bare frame) presents greater lateral displacements and more structural damage. Figure 2b shows the hysteretic cycles obtained in the EDD, evidencing that part of the dissipated energy is concentrated in the controlling devices, as expected.

Figure 3 shows the time history response of the horizontal displacement of the upper beam– column joint. A reduction of approximately 40 % is obtained for the maximum lateral displacement when compared with the bare frame. A possible explanation for the limited effectiveness of the EDD is that the devices only contribute to increase the ductility of the beam–column joint without alleviating the base shear demand on the columns due to the dimensions of the device and its location in the structure.

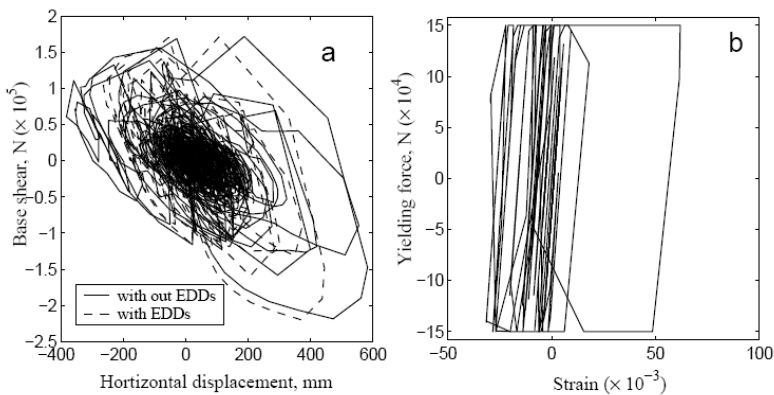


Figure 2: a: base shear–displacement relationship. b: Hysteretic cycles in the EDD.

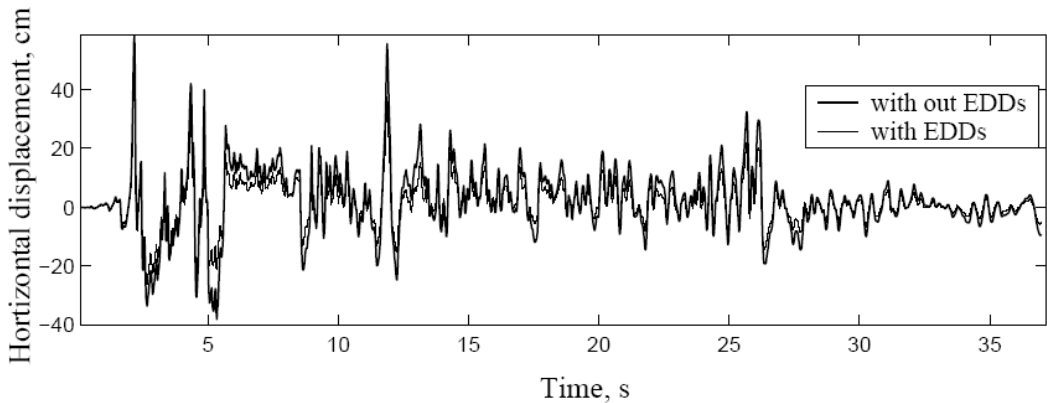


Figure 3: Time history of the top horizontal displacement.

7 CONCLUSIONS

In this work, a geometrically exact formulation for initially curved beams has been extended to consider arbitrary distributions of composite materials on the cross sections in the seismic case. The consistent linearization of the weak form of the momentum balance equations considers the constitutive nonlinearity with rate dependent effects. The resulting model is implemented in a displacement based FEM code. An iterative Newton-Rapson scheme is used for the solution of the discrete version of the linearized problem. A specific element for EDD is developed, based on the beam model but releasing the rotational degrees of freedom. Each material point of the cross section is assumed to be composed of several simple materials with their own constitutive laws. The mixing rule is used to describe the resulting composite. Viscosity is included at constitutive level by means of a Maxwell model. Beam cross sections are meshed into a grid of quadrilaterals corresponding to fibers directed along the beam axis. Two additional integration loops are required at cross sectional level in each integration point to obtain the reduced quantities. Local and global damage indices have been developed based on the ratio between the visco elastic and nonlinear stresses. The present formulation is validated by means of a numerical example: the study of the seismic response of a RC precast structure with EDDs.

Acknowledgement

This research was partially supported by the European Commission, CEE-FP6 Project FP6-

50544(GOCE) "Risk Mitigation for Earthquakes and Landslides (LESSLOSS)", by the Spanish Government (Ministerio de Educación y Ciencia), project BIA2003-08700-C03-02 "Numerical simulation of the seismic behavior of structures with energy dissipation devices", project MAT2003-09768-C03-02 "Delamination of reinforced matrix composites (DECOMAR)" project BIA2005-06952 "Study of composite materials for design, reinforcement and retrofit of civil engineering structures (RECOMP)" by the Spanish Government (Ministerio de Fomento) "Numerical simulation methodology for the reinforced concrete behavior structures reinforced with composite materials". All this support is gratefully acknowledged.

References

1. Ian Aiken. Passive energy dissipation hardware and applications. *Proceedings, Lo Angeles County and Seasc Symposium on Passive Energy Dissipation Systems for New and Existing Buildings*, Los Angeles, July 1996;
2. A.H. Barbat, S. Oller, A. Hanganu, E. Oñate. Viscous damage model for Timoshenko beam structures. *International Journal for Solids and Structures*, 1997; 34(30):3953–3976.
3. J.J. Connor, A.Wada, M. Iwata, Y.H. Huang. Damage-controlled structures. I: Preliminary design methodology for seismically active regions. *Journal of Structural Engineering*, 1997; 123(4):423–431.
4. Yaomin Fu, Kazuhiko Kasai. Comparative study of frames using viscoelastic and viscous dampers. *Journal fo Structural Engineering*, 1998; 124(5):513–522.
5. A.D. Hanganu, E. Oñate, A.H. Barbat. Finite element methodology for local/global damage evaluation in civil engineering structures. *Computers and Structures*, 2002; 80:1667–1687.
6. Robert D. Hanson, Ian D. Aiken, Douglas K. Nims, Philip J. Richter, Robert E. Batchman. State of the art and state of the practice in seismic engineering dissipation. *Proceedings, ATC-17-1. Seminar on seismic isolation, passive energy dissipation and active control. Applied Technology Council, San Francisco, California*, March 1993;
7. A. Ibrahimbegović. On finite element implementation of geometrically nonlinear Reissners beam theory: three-dimensional curved beam elements. *Computer Methods in Applied Mechanics and Engineering*, 1995; 122:11–26.
8. Kasuhiko Kasai, Yaomin Fu, Atsushi Watanabe. Passive control systems for seismic damage mitigation. *Journal of Structural Engineering*, 1998; 124(5):501–512.
9. R.K. Kapania, J. Li. On a geometrically exact curved/twisted beam theory under rigid cross-section assumption. *Computational Mechanics*, 2003; 30:428–443.
10. Y.Y. Lin, K.C. Chang. Study on damping reduction factors for buildings under earthquake ground motions. *Journal of Structural Engineering, JEE*, 2003; 129(2):206–214. 11 A.H. Barbat, S. Oller, P. Mata A. and J.C. Vielma P.
11. P. Mata A, S. Oller, A.H. Barbat. Static analysis of beam structures under nonlinear geometric and constitutive behavior. *Computer Methods in Applied Mechanic and Engineering*, 2006; (Submitted).
12. P. Mata A, S. Oller, A.H. Barbat. Dynamic analysis of beam structures considering geometric and constitutive nonlinearity. *Computer Methods in Applied Mechanic and Engineering*, 2006; (Submitted).

13. Pablo Mata A, Rubén Boroschek K, Alex H. Barbat, Sergio Oller. High damping rubber model for energy dissipating devices. *Journal of Earthquake Engineering, JEE*, 2006; (Accepted).
14. P. Mata A, S. Oller, A.H. Barbat, R. Boroschek. Numerical code for seismic analysis of structures incorporating energy dissipating devices. *First European Conference on Earthquake Engineering and Seismology, ECEES*, Geneva, Switzerland, 3-8 September 2006.
15. Oliver J., Cervera M., Oller S., Lubliner J. Isotropic damage models and smeared crack analysis of concrete. *Proceedings 2nd ICCAADCS, Zell Am See, Austria, Pineridge Press*, 1990; 2:945–958.
16. S. Oller, E. Oñate, J. Miquel, S. Botello. A plastic damage constitutive model for composites materials. *International Journal of Solids and Structures*, 1996; 33(17):2501–2518.
17. S. Oller, E. Oñate, J. Miquel, Mixing anisotropic formulation for the analysis of composites, *Communications in Numerical Methods in Engineering*. 12 (1996) 471–482.
18. Phani Kumar V.V. Nukala, Donal W. White. A mixed finite element for three-dimensional nonlinear analysis of steel frames. *Computer Methods in Applied Mechanics and Engineering*, 2004; 193(5):2507–2545.
19. E. Reissner. On one-dimensional large-displacement finite-strain beam theory. *Studies in Applied Mathematics*, 1973; LII, 287–95.
20. K.L. Shen, T.T Soong. Design of energy dissipation devices based on concept of damage control. *Journal of Structural Engineering*, 2005; 122(1):76–82.
21. J.C. Simo. A finite strain beam formulation. The three-dimensional dynamic problem. Part I. *Computer Methods in Applied Mechanics and Engineering*, 1985; 49:55–70.
22. J.C. Simo, L. Vu-Quoc. A three-dimensional finite-strain rod model. Part II: Computational aspects. *Computer Methods in Applied Mechanics and Engineering*, 1986; 58:79–116.
23. J.C. Simo, L. Vu-Quoc. On the dynamics in space of rods undergoing large motions – A geometrically exact approach. *Computer Methods in Applied Mechanics and Engineering*, 1988; 66:125–161.
24. J.C. Simo, Keith D. Hjelmstad, Robert L. Taylor. Numerical formulations of elastoviscoplastic response of beams accounting for the effect of shear. *Computer Methods in Applied Mechanics and Engineering*, 1984; 42:301–330.
25. T.T. Soong, G.F. Dargush. *Passive Energy Dissipation Systems in Structural Engineering*, 1997; John Wiley & Sons Ltd.

Minimum weight buildings design best evaluation using inequalities method automatic evaluation program

Cosmina Geanina Adam¹, Iulian Gabriel Mihai ²

¹Hydrotechnics Department, “Ovidius” University, Constanta, 900524, Romania
²S.C. EdilConst S.A. Campina, Prahova, 105600 Romania,

Summary:

We shall present the principles and use of an automatic evaluation program for minimum weight buildings design, based on inequalities method.

KEYWORDS: best design, automatic evaluation, minimum weight, inequalities method, linear programming.

1. GENERAL ISSUES

For an engineer, “doing one’s best” should be a permanent objective when conceiving a building, when measuring an installation, etc. The expression is relative, according to the budget, security and other limitations, whose level will be the object of previous and often subsequent decisions.

In the technical problems, the possible alternatives often represent a continuum and an exhaustive enumeration of possibilities cannot be conceived. This is the reason why we must find an algorithm that provides the best performance as possible, which is a method of determining the way to the best solution among all the possible ones.

The optimization may be defined as the science of determining “the best” solutions to certain problems that are mathematically defined, which are often models of the physical reality. It involves the study of the optimization for certain problems, determining the solution using algorithmic methods, the study of the structures of these methods and the computer checking of the methods having experimental data and real data. The automatic evaluation program that is being presented in this paper offers the values of the plastic moments of the pillars and beams sections, of the critical sections moments and the value of weight function (the function of the objective). The mathematical method that represents the basis of making the

evaluation program is part of the linear programming methods and is called the simplex method.

The language in which the evaluation program was carried out is named JAVA.

Java is more than a new language; it is a new approach of computer science. The hopes invested in this language are very big and only the future may confirm if it will become a “lingua franca” of XXI century computers. Though it borrows many aspects from the languages C and C++, the Java language gets rid of many unessential features of them, for example structures, overloading the operators, multiple heritage, etc.

The Java language allows the programmer to create a special type of programs, called applets, which may be included in Web pages. When the user views the Web page that includes an applet, the machine to which he is connected transmits the applet to the user and the user navigator will perform the applet (it is supposed that the machine, which the user is working on, is provided with a Java switch). We shall limit ourselves to mentioning that the applets may include graphics, animation, sound, games, etc.

2. THE PROGRAM USE

For an easier understanding, the presentation will be performed by using an example of evaluation such as:

The value of the minimum weight function will be determined, the values of the plastic moments of the pillars and beams sections and the values of the moments from the critical sections of the bar for the frame in figure 1.

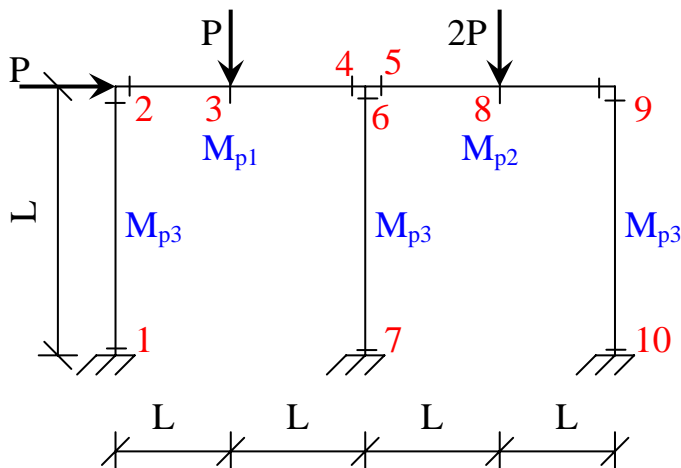


Fig.1

Numerical data: $P=3; L=3$

The plastic moments on the beams and pillars will be marked as follows:

$$M_{p1}=x_1; M_{p2}=x_2; M_{p3}=x_3;$$

The moments from the critical sections will be marked as follows:

$$M_4=x_4; M_5=x_5; M_6=x_6; M_7=x_7; M_8=x_8; M_9=x_9; M_{10}=x_{10}; M_{11}=x_{11}; M_{12}=x_{12}; M_{13}=x_{13};$$

There will be written:

I.) The static balance relationships using the mechanic virtual work principle:

a) bar balance:

$$x_{12}+2x_{13}+x_4=P \cdot L=3 \cdot 3=9 \quad (1)$$

$$x_5+2x_8+x_9=2P \cdot L=2 \cdot 3 \cdot 3=18 \quad (2)$$

b) movement balance:

$$x_{11}+x_{12}+x_7+x_6+x_9+x_{10}=P \cdot L=3 \cdot 3=9 \quad (3)$$

c) knot balance:

$$x_4+x_5+x_6=0 \quad (4)$$

II.) Plastic flow conditions:

$$\begin{aligned} -x_3 \leq x_{11} \leq x_3; -x_3 \leq x_{12} \leq x_3; -x_1 \leq x_{12} \leq x_1; -x_1 \leq x_{13} \leq x_1; -x_1 \leq x_4 \leq x_1; -x_2 \leq x_5 \leq x_2; \\ -x_3 \leq x_6 \leq x_3; -x_3 \leq x_7 \leq x_3; -x_2 \leq x_8 \leq x_2; -x_2 \leq x_9 \leq x_2; -x_3 \leq x_9 \leq x_3; -x_3 \leq x_{10} \leq x_3 \end{aligned} \quad (5)$$

The program imposes that inequalities (5) to be transformed into equalities, according to the following model:

Example:

$$-\varepsilon \leq x \leq \varepsilon \text{ that is } |x| \leq \varepsilon$$

$$\text{So } x_{11}=|x_{11}| \leq x_3, \text{ that is } x_3-x_{11} \geq 0 \text{ or } x_{11}-x_3 \leq 0$$

To transform the relationship $x_{11}-x_3 \leq 0$ into an equality an aleatory variable will be added: $x_{11}-x_3+x_{14}=0$

As a consequence, the transformation of relationships (5) from inequalities into equalities is performed by adding an aleatory variable to each inequality. Thus, the relations (5) are included into the following pattern:

$$\begin{aligned} x_{11}-x_3+x_{14}=0; x_{12}-x_3+x_{15}=0; x_{12}-x_1+x_{16}=0; x_{13}-x_1+x_{17}=0; x_4-x_1+x_{18}=0 \\ x_5-x_2+x_{19}=0; x_6-x_3+x_{20}=0; x_7-x_3+x_{21}=0; x_8-x_2+x_{22}=0; x_9-x_2+x_{23}=0 \quad (6) \\ x_9-x_3+x_{24}=0; x_{10}-x_3+x_{25}=0 \end{aligned}$$

The function of the objective (the function of weight) has the following expression:

$$X = \sum_{i=1}^n l_i \cdot M_{pi} \quad (7)$$

For the example taken into consideration, the function of weight is the following:

$$X=2L \cdot M_{p1}+2L \cdot M_{p2}+L \cdot M_{p3}+L \cdot M_{p3}+L \cdot M_{p3}=6 \cdot x_1+6 \cdot x_2+9 \cdot x_3$$

The relations (1), (2), (3), (4) and (7) form a mathematical model that will be solved using the elaborated evaluation program.

The program development will be performed in the following steps:

The „Simplex Solution” folder is copied from the CD. The „Java” program is installed by double click on the file „j2sdk-1_4_2_15-windows-i586-p”. Then, from the „Update Java” the file „jre-6u2-windows-i586-p1” is installed.

Observation: The program was performed in Net Beans 5.5.1.

Enter folder „build” → „classes” and then double click on the file „test HTML Document” and the next page will appear:



Click on „**Problemă nouă**” (New Problem) and the following page will appear:

Introduceti urmatoarele valori

Numarul de Constrangeri:
 > 2

Numarul de Variabile:
 > 2

Java Applet Window

start classes My Pictures Microsoft Word - Cu... Untitled 1 - Microsof... Introduceti urmatoa... EN 18:22

- For the option called “number of restrictions”, we shall introduce the number of equations of the model. In the following example we have the equations (1), (2), (3), (4) and (6), that is **16 equations**.
- For the option called „number of variables” we shall introduce the number of variables from the equations (1), (2), (3), (4) and (6), that is **25**.
- Click on “continue” and the following page will appear:

Introduceti Problema de Programare Linialar

Minimizare ▾

Conditii:

<input type="text" value="x1+"/>	<input type="text" value="x2+"/>	<input type="text" value="x3+"/>	<input type="text" value="x4+"/>	<input type="text" value="x5+"/>	<input type="text" value="x6+"/>	<input type="text" value="x7+"/>	<input type="text" value="x8+"/>	<input type="text" value="x9+"/>	<input type="text" value="x10+"/>	<input type="text" value="x11+"/>	<input type="text" value="x12+"/>	<input type="text" value="x13+"/>	<input type="text" value="x14+"/>	<input type="text" value="x15+"/>	<input type="text" value="x16+"/>	<input type="text" value="x17+"/>	<input type="text" value="x18+"/>	<input type="text" value="x19+"/>	<input type="text" value="x20+"/>	<input type="text" value="x21+"/>	<input type="text" value="x22+"/>	<input type="text" value="x23+"/>	<input type="text" value="x24+"/>	<input type="text" value="x25+"/>	<input type="button" value="=<"/>
<input type="text" value="x1+"/>	<input type="text" value="x2+"/>	<input type="text" value="x3+"/>	<input type="text" value="x4+"/>	<input type="text" value="x5+"/>	<input type="text" value="x6+"/>	<input type="text" value="x7+"/>	<input type="text" value="x8+"/>	<input type="text" value="x9+"/>	<input type="text" value="x10+"/>	<input type="text" value="x11+"/>	<input type="text" value="x12+"/>	<input type="text" value="x13+"/>	<input type="text" value="x14+"/>	<input type="text" value="x15+"/>	<input type="text" value="x16+"/>	<input type="text" value="x17+"/>	<input type="text" value="x18+"/>	<input type="text" value="x19+"/>	<input type="text" value="x20+"/>	<input type="text" value="x21+"/>	<input type="text" value="x22+"/>	<input type="text" value="x23+"/>	<input type="text" value="x24+"/>	<input type="text" value="x25+"/>	<input type="button" value="=<"/>
<input type="text" value="x1+"/>	<input type="text" value="x2+"/>	<input type="text" value="x3+"/>	<input type="text" value="x4+"/>	<input type="text" value="x5+"/>	<input type="text" value="x6+"/>	<input type="text" value="x7+"/>	<input type="text" value="x8+"/>	<input type="text" value="x9+"/>	<input type="text" value="x10+"/>	<input type="text" value="x11+"/>	<input type="text" value="x12+"/>	<input type="text" value="x13+"/>	<input type="text" value="x14+"/>	<input type="text" value="x15+"/>	<input type="text" value="x16+"/>	<input type="text" value="x17+"/>	<input type="text" value="x18+"/>	<input type="text" value="x19+"/>	<input type="text" value="x20+"/>	<input type="text" value="x21+"/>	<input type="text" value="x22+"/>	<input type="text" value="x23+"/>	<input type="text" value="x24+"/>	<input type="text" value="x25+"/>	<input type="button" value="=<"/>
<input type="text" value="x1+"/>	<input type="text" value="x2+"/>	<input type="text" value="x3+"/>	<input type="text" value="x4+"/>	<input type="text" value="x5+"/>	<input type="text" value="x6+"/>	<input type="text" value="x7+"/>	<input type="text" value="x8+"/>	<input type="text" value="x9+"/>	<input type="text" value="x10+"/>	<input type="text" value="x11+"/>	<input type="text" value="x12+"/>	<input type="text" value="x13+"/>	<input type="text" value="x14+"/>	<input type="text" value="x15+"/>	<input type="text" value="x16+"/>	<input type="text" value="x17+"/>	<input type="text" value="x18+"/>	<input type="text" value="x19+"/>	<input type="text" value="x20+"/>	<input type="text" value="x21+"/>	<input type="text" value="x22+"/>	<input type="text" value="x23+"/>	<input type="text" value="x24+"/>	<input type="text" value="x25+"/>	<input type="button" value="=<"/>
<input type="text" value="x1+"/>	<input type="text" value="x2+"/>	<input type="text" value="x3+"/>	<input type="text" value="x4+"/>	<input type="text" value="x5+"/>	<input type="text" value="x6+"/>	<input type="text" value="x7+"/>	<input type="text" value="x8+"/>	<input type="text" value="x9+"/>	<input type="text" value="x10+"/>	<input type="text" value="x11+"/>	<input type="text" value="x12+"/>	<input type="text" value="x13+"/>	<input type="text" value="x14+"/>	<input type="text" value="x15+"/>	<input type="text" value="x16+"/>	<input type="text" value="x17+"/>	<input type="text" value="x18+"/>	<input type="text" value="x19+"/>	<input type="text" value="x20+"/>	<input type="text" value="x21+"/>	<input type="text" value="x22+"/>	<input type="text" value="x23+"/>	<input type="text" value="x24+"/>	<input type="text" value="x25+"/>	<input type="button" value="=<"/>
<input type="text" value="x1+"/>	<input type="text" value="x2+"/>	<input type="text" value="x3+"/>	<input type="text" value="x4+"/>	<input type="text" value="x5+"/>	<input type="text" value="x6+"/>	<input type="text" value="x7+"/>	<input type="text" value="x8+"/>	<input type="text" value="x9+"/>	<input type="text" value="x10+"/>	<input type="text" value="x11+"/>	<input type="text" value="x12+"/>	<input type="text" value="x13+"/>	<input type="text" value="x14+"/>	<input type="text" value="x15+"/>	<input type="text" value="x16+"/>	<input type="text" value="x17+"/>	<input type="text" value="x18+"/>	<input type="text" value="x19+"/>	<input type="text" value="x20+"/>	<input type="text" value="x21+"/>	<input type="text" value="x22+"/>	<input type="text" value="x23+"/>	<input type="text" value="x24+"/>	<input type="text" value="x25+"/>	<input type="button" value="=<"/>
<input type="text" value="x1+"/>	<input type="text" value="x2+"/>	<input type="text" value="x3+"/>	<input type="text" value="x4+"/>	<input type="text" value="x5+"/>	<input type="text" value="x6+"/>	<input type="text" value="x7+"/>	<input type="text" value="x8+"/>	<input type="text" value="x9+"/>	<input type="text" value="x10+"/>	<input type="text" value="x11+"/>	<input type="text" value="x12+"/>	<input type="text" value="x13+"/>	<input type="text" value="x14+"/>	<input type="text" value="x15+"/>	<input type="text" value="x16+"/>	<input type="text" value="x17+"/>	<input type="text" value="x18+"/>	<input type="text" value="x19+"/>	<input type="text" value="x20+"/>	<input type="text" value="x21+"/>	<input type="text" value="x22+"/>	<input type="text" value="x23+"/>	<input type="text" value="x24+"/>	<input type="text" value="x25+"/>	<input type="button" value="=<"/>
<input type="text" value="x1+"/>	<input type="text" value="x2+"/>	<input type="text" value="x3+"/>	<input type="text" value="x4+"/>	<input type="text" value="x5+"/>	<input type="text" value="x6+"/>	<input type="text" value="x7+"/>	<input type="text" value="x8+"/>	<input type="text" value="x9+"/>	<input type="text" value="x10+"/>	<input type="text" value="x11+"/>	<input type="text" value="x12+"/>	<input type="text" value="x13+"/>	<input type="text" value="x14+"/>	<input type="text" value="x15+"/>	<input type="text" value="x16+"/>	<input type="text" value="x17+"/>	<input type="text" value="x18+"/>	<input type="text" value="x19+"/>	<input type="text" value="x20+"/>	<input type="text" value="x21+"/>	<input type="text" value="x22+"/>	<input type="text" value="x23+"/>	<input type="text" value="x24+"/>	<input type="text" value="x25+"/>	<input type="button" value="=<"/>
<input type="text" value="x1+"/>	<input type="text" value="x2+"/>	<input type="text" value="x3+"/>	<input type="text" value="x4+"/>	<input type="text" value="x5+"/>	<input type="text" value="x6+"/>	<input type="text" value="x7+"/>	<input type="text" value="x8+"/>	<input type="text" value="x9+"/>	<input type="text" value="x10+"/>	<input type="text" value="x11+"/>	<input type="text" value="x12+"/>	<input type="text" value="x13+"/>	<input type="text" value="x14+"/>	<input type="text" value="x15+"/>	<input type="text" value="x16+"/>	<input type="text" value="x17+"/>	<input type="text" value="x18+"/>	<input type="text" value="x19+"/>	<input type="text" value="x20+"/>	<input type="text" value="x21+"/>	<input type="text" value="x22+"/>	<input type="text" value="x23+"/>	<input type="text" value="x24+"/>	<input type="text" value="x25+"/>	<input type="button" value="=<"/>
<input type="text" value="x1+"/>	<input type="text" value="x2+"/>	<input type="text" value="x3+"/>	<input type="text" value="x4+"/>	<input type="text" value="x5+"/>	<input type="text" value="x6+"/>	<input type="text" value="x7+"/>	<input type="text" value="x8+"/>	<input type="text" value="x9+"/>	<input type="text" value="x10+"/>	<input type="text" value="x11+"/>	<input type="text" value="x12+"/>	<input type="text" value="x13+"/>	<input type="text" value="x14+"/>	<input type="text" value="x15+"/>	<input type="text" value="x16+"/>	<input type="text" value="x17+"/>	<input type="text" value="x18+"/>	<input type="text" value="x19+"/>	<input type="text" value="x20+"/>	<input type="text" value="x21+"/>	<input type="text" value="x22+"/>	<input type="text" value="x23+"/>	<input type="text" value="x24+"/>	<input type="text" value="x25+"/>	<input type="button" value="=<"/>
<input type="text" value="x1+"/>	<input type="text" value="x2+"/>	<input type="text" value="x3+"/>	<input type="text" value="x4+"/>	<input type="text" value="x5+"/>	<input type="text" value="x6+"/>	<input type="text" value="x7+"/>	<input type="text" value="x8+"/>	<input type="text" value="x9+"/>	<input type="text" value="x10+"/>	<input type="text" value="x11+"/>	<input type="text" value="x12+"/>	<input type="text" value="x13+"/>	<input type="text" value="x14+"/>	<input type="text" value="x15+"/>	<input type="text" value="x16+"/>	<input type="text" value="x17+"/>	<input type="text" value="x18+"/>	<input type="text" value="x19+"/>	<input type="text" value="x20+"/>	<input type="text" value="x21+"/>	<input type="text" value="x22+"/>	<input type="text" value="x23+"/>	<input type="text" value="x24+"/>	<input type="text" value="x25+"/>	<input type="button" value="=<"/>
<input type="text" value="x1+"/>	<input type="text" value="x2+"/>	<input type="text" value="x3+"/>	<input type="text" value="x4+"/>	<input type="text" value="x5+"/>	<input type="text" value="x6+"/>	<input type="text" value="x7+"/>	<input type="text" value="x8+"/>	<input type="text" value="x9+"/>	<input type="text" value="x10+"/>	<input type="text" value="x11+"/>	<input type="text" value="x12+"/>	<input type="text" value="x13+"/>	<input type="text" value="x14+"/>	<input type="text" value="x15+"/>	<input type="text" value="x16+"/>	<input type="text" value="x17+"/>	<input type="text" value="x18+"/>	<input type="text" value="x19+"/>	<input type="text" value="x20+"/>	<input type="text" value="x21+"/>	<input type="text" value="x22+"/>	<input type="text" value="x23+"/>	<input type="text" value="x24+"/>	<input type="text" value="x25+"/>	<input type="button" value="=<"/>

>= 0

Apasati preprocesare pentru a incepe.

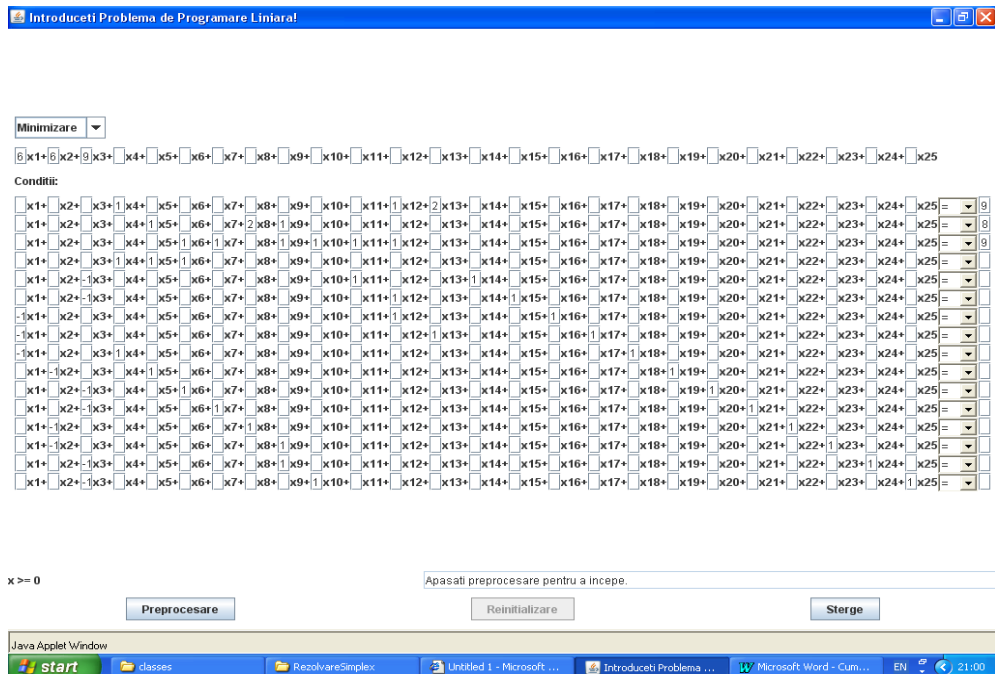
Java Applet Window

start classes RezolvareSimplex Untitled 1 - Microsoft... Introduceti Problema... Microsoft Word - Cum... RO 20:04

- Select “Minimization” (if it is not selected) because we are interested in the minimum of the objective function. (The program can find out the maximum of the objective function, too).

In the first line, we introduce the coefficient of the objective function, that is 6 for x_1 , 6 for x_2 and 9 for x_3 .

- For the option called “conditions” there will appear the 16 equations from the system formed of equations (1), (2), (3), (4) and (6). For each unknown x , we shall introduce the coefficients of the equations (1), (2), (3), (4) and (6), starting with the first line that corresponds to the first equation and the free terms in the right box. If the free term is 0 it will not be introduced. Before the box containing the free term we shall select “=”.
- After introducing the coefficients of the unknown and the free terms we shall obtain the following page:



Click on “Preprocessing” and the following page will appear:

Rezolvare Simplex

Problema de Minimizare
 $0.0 \cdot x1 + 0.0 \cdot x2 + 9.0 \cdot x3 + 0.0 \cdot x4 + 0.0 \cdot x5 + 0.0 \cdot x6 + 0.0 \cdot x7 + 0.0 \cdot x8 + 0.0 \cdot x9 + 0.0 \cdot x10 + 0.0 \cdot x11 + 0.0 \cdot x12 + 0.0 \cdot x13 + 0.0 \cdot x14 + 0.0 \cdot x15 + 0.0 \cdot x16 + 0.0 \cdot x17 + 0.0 \cdot x18 + 0.0 \cdot x19 + 0.0 \cdot x20 + 0.0 \cdot x21 + 0.0 \cdot x22 + 0.0 \cdot x23$

Problema preprocesata de Minimizare

x	vb	pb	Matricea Et
x1= 3.40000001	0.12500003	3.0	0.0 0.0 0.0 1.00000000 0.00000000 0.00000000 0.00000000
x2= 0.1	0.12499998	3.0	0.0 0.0 0.0 0.00000000 1.00000000 0.00000000 0.00000000
x3= 1.0	0.25	0.59999999	0.0 0.0 0.0 0.00000000 0.00000000 1.00000000 0.00000000
x4= 0.0	0.0	3.0	0.0 0.0 0.0 1.00000000 0.00000000 0.00000000 0.00000000
x7= 1.0	0.25	-0.59999999	0.0 0.0 0.0 -1.00000000 0.00000000 0.00000000 0.00000000
x8= 0.1	-0.125	-1.0	0.0 0.0 0.0 1.00000000 0.00000000 0.00000000 0.00000000
x9= 1.0	0.25	0.0	-7.000 0.0 0.0 0.00000000 0.00000000 0.00000000 0.00000000
x10= 1.0	0.25	0.0	1.000 0.0 0.0 0.00000000 0.00000000 0.00000000 0.00000000
x12= 1.0	0.25	0.0	1.000 0.0 0.0 0.00000000 0.00000000 0.00000000 0.00000000
x13= 1.0	-0.125	0.0	0.0 1.000 0.0 0.00000000 0.00000000 0.00000000 0.00000000
x14= 1.0	1.25	0.0	0.0 0.0 1.000 0.00000000 0.00000000 0.00000000 0.00000000
x15= 1.0	-0.37500003	-0.59999999	0.0 0.0 0.0 1.000 0.0 0.00000000 0.00000000 0.00000000
x16= 3.0	-0.12500001	-0.0	0.0 1.000 0.0 0.000 0.0 0.00000000 0.00000000 0.00000000
x19= 0.1	0.12499998	0.0	0.0 1.000 0.0 0.000 0.0 0.00000000 0.00000000 0.00000000
x20= 1.0	0.25	-3.0	0.0 0.0 1.000 0.000 0.0 0.00000000 0.00000000 0.00000000
x23= 0.29999997	0.37499994	0.0	0.0 0.0 0.0 1.000 0.000 0.000 0.000 0.000 0.000 0.000

Valoarea obiectiv curenta: 06.4

Legenda culori: Variabile de baza Variabile surpluse



Double click several times on the option called “Perform repetition” and the values of the unknown will appear that is of the moments and the value of the objective function, respectively the following page:

Rezolvare Simplex

Problema de Minimizare
 $0.0 \cdot x1 + 0.0 \cdot x2 + 9.0 \cdot x3 + 0.0 \cdot x4 + 0.0 \cdot x5 + 0.0 \cdot x6 + 0.0 \cdot x7 + 0.0 \cdot x8 + 0.0 \cdot x9 + 0.0 \cdot x10 + 0.0 \cdot x11 + 0.0 \cdot x12 + 0.0 \cdot x13 + 0.0 \cdot x14 + 0.0 \cdot x15 + 0.0 \cdot x16 + 0.0 \cdot x17 + 0.0 \cdot x18 + 0.0 \cdot x19 + 0.0 \cdot x20 + 0.0 \cdot x21 + 0.0 \cdot x22 + 0.0 \cdot x23$

Problema preprocesata de Minimizare

x	vb	pb	Matricea Et
x1= 3.40000001	0.12500003	3.0	0.0 0.0 0.0 1.00000000 0.00000000 0.00000000 0.00000000
x2= 0.1	0.12499998	3.0	0.0 0.0 0.0 0.00000000 1.00000000 0.00000000 0.00000000
x3= 1.0	0.25	0.59999999	0.0 0.0 0.0 0.00000000 0.00000000 1.00000000 0.00000000
x4= 0.0	0.0	3.0	0.0 0.0 0.0 1.00000000 0.00000000 0.00000000 0.00000000
x7= 1.0	0.25	-0.59999999	0.0 0.0 0.0 -1.00000000 0.00000000 0.00000000 0.00000000
x8= 0.1	-0.125	-1.0	0.0 0.0 0.0 1.00000000 0.00000000 0.00000000 0.00000000
x9= 1.0	0.25	0.0	-7.000 0.0 0.0 0.00000000 0.00000000 0.00000000 0.00000000
x10= 1.0	0.25	0.0	1.000 0.0 0.0 0.00000000 0.00000000 0.00000000 0.00000000
x12= 1.0	0.25	0.0	1.000 0.0 0.0 0.00000000 0.00000000 0.00000000 0.00000000
x13= 1.0	-0.125	0.0	0.0 1.000 0.0 0.00000000 0.00000000 0.00000000 0.00000000
x14= 1.0	1.25	0.0	0.0 0.0 1.000 0.00000000 0.00000000 0.00000000 0.00000000
x15= 1.0	-0.37500003	-0.59999999	0.0 0.0 0.0 1.000 0.0 0.00000000 0.00000000 0.00000000
x16= 3.0	-0.12500001	-0.0	0.0 1.000 0.0 0.000 0.0 0.00000000 0.00000000 0.00000000
x19= 0.1	0.12499998	0.0	0.0 1.000 0.0 0.000 0.0 0.00000000 0.00000000 0.00000000
x20= 1.0	0.25	-3.0	0.0 0.0 1.000 0.000 0.0 0.00000000 0.00000000 0.00000000
x23= 0.29999997	0.37499994	0.0	0.0 0.0 0.0 1.000 0.000 0.000 0.000 0.000 0.000 0.000

Valoarea obiectiv curenta: 06.4

Legenda culori: Variabile de baza Variabile surpluse



The results obtained:

$$x_1 = M_{p1} = 3.6; \quad x_2 = M_{p2} = 8.1; \quad x_3 = M_{p3} = 1.8; \quad x_4 = M_{p4} = 0;$$

$$x_5 = M_{p5} = 0;$$

$$x_6 = M_{p6} = 0; \quad x_7 = M_{p7} = 1.8; \quad x_8 = M_{p8} = 8.1; \quad x_9 = M_{p9} = 1.8;$$

$$x_{10} = M_{p10} = 1.8$$

$$x_{11} = M_{p11} = 0; \quad x_{12} = M_{p12} = 1.8; \quad x_{13} = M_{p13} = 3.6; \quad x_{14} = M_{p14} = 0;$$

$$x_{15} = M_{p15} = 0$$

$$x_{16} = M_{p16} = 1.8; \quad x_{17} = M_{p17} = 0; \quad x_{18} = M_{p18} = 3.6; \quad x_{19} = M_{p19} = 8.1;$$

$$x_{20} = M_{p20} = 1.8; \quad x_{21} = M_{p21} = 0; \quad x_{22} = M_{p22} = 0; \quad x_{23} = M_{p23} = 6.29$$

and the weight function value: $X=86.4$

For checking we shall proceed in the following manner:

1. We shall replace the values of the plastic moments x_1, x_2, x_3 in the expression of the objective function: $6 \cdot x_1 + 6 \cdot x_2 + 9x_3 = 6 \cdot 3.6 + 6 \cdot 8.1 + 9 \cdot 1.8 = 86.4$ so the value obtained by calculation.
2. We shall introduce into the relations (1), (2), (3), (4) and (6) the values of the unknown found and we must obtain the free term in the respective relation.

Bibliography:

1. Amariei Constantin, Mihai Gabriel Iulian- Minimum Weight Buildings Design Using Inequalities Method, Civil Engineering - International Symposium „Computational Civil Engineering 2007”, „Matei-Teiu Botez” Academic Society Publishing House, Iași, 2007
2. Mihăilă N. – Introduction to linear programming, Didactical and Pedagogical Publishing House, Bucharest, 1970
3. Doina Logofătu – Fundamental algorithms in Java, Polirom Publishing House, 2007

Application of computer modeling in civil fire safety engineering. Glass breakage in fire

Ion Anghel¹, Popa Constantin² and Pavel Alecsandru³

¹Fire Officers Faculty, “A.I.Cuza” Police Academy, Bucharest, 014031, Romania

²Fire Officers Faculty, “A.I. Cuza” Police Academy, Bucharest, 014031, Romania

³Petroleum Gas University, Ploiești, 021918, Romania

Summary

The work analyses the propagation of fire to the upper floors of a building, because of the window glass breakage in the fire origin compartment.

The moment for glass breakage is estimated by using the Berkeley Algorithm for Breaking Window Glass in a Compartment Fire (BREAK1) computer program. The initiation, development and spread of the fire are simulated by using the Fire Dynamics Simulator (FDS) computer program.

Both programs are created by The National Institute of Standards and Technology (NIST-USA), and used together can be very helpful in providing fire safety specialists with valuable information about the spread of the fire, particularly for the high-rise buildings.

KEYWORDS: glass breaking, BREAK1, FDS, fire growth, fire spread.

1. INTRODUCTION

In the special literature related to fires, the spread of fire is defined as the occurrence of ignition of nearby exposed items. The objective of building compartmenting is to contain a fire inside the compartment of fire origin.

Spread can occur in two ways: either within the compartment of fire origin only or, of course beyond the compartment of fire origin. Spread within the compartment of fire origin is defined as the ignition of neighboring items inside the same compartment of origin. Spread outside the compartment of fire origin is assumed if an item outside of this compartment is ignited and initiates fire growth in adjacent compartments.

As we all know, in multi-storey buildings, the fire can spread from one floor to another; this situation is undesirable and the fire safety design should consider spread of fire from floor-to-floor, which can occur through: failure of floor or ceiling fire separations, concealed spaces, service ducts and shafts, stairways and external openings. Exterior windows (see figure 1) and openings are the main

means of fire spread in multi-storey buildings, especially when easy-to-ignite materials are nearby. That’s why the present article deals with the spread of fire through exterior windows.[6]

Ventilation is one of most important factors that influence the fire safety in buildings. Fire ventilation can take place via open doors, building leakages, air-conditioning and via window openings provided that the glass closing the window opening has been broken. As windows constitute the largest openings in buildings, especially in many modern buildings with virtually fully glazed facades, the most important problem in fire sciences is when this glass breaks, creating a natural ventilation opening.

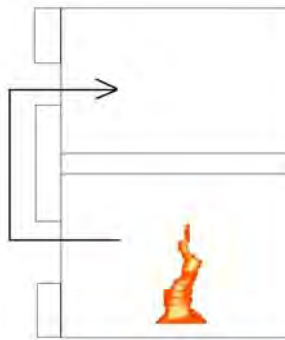


Figure 1. Schematic view of the spread of fire from one floor to another through exterior windows

2. SPREAD OF FIRE OUTSIDE A FIRE COMPARTMENT

2.1. Factors affecting fire spread

The factors influencing spread of fire beyond the compartment of fire origin include:

- fire intensity;
- fire load in the compartment of fire origin;
- fire resistance of barriers;
- installed fire suppression systems;
- fire dampers and air-handling systems;
- concealed spaces such as ceiling voids, spaces with hollow construction, under floors and under exterior cladding through which hot gases may spread

- undetected (easy preheat and ignition of internal combustibles at weak points);
- large open spaces with high ceilings (atriums and malls) where fires are likely to be fuel-controlled (spread occurs due to direct radiation from fires);
 - access to vertical shafts such as stairways, elevator shafts and large service ducts.

2.2. Routes of fire spread

Fire spread beyond the compartment of fire origin is generally caused by excessive heat exposure and the formation of openings in the compartment boundaries. The following is a list of potential routes of fire spread that may exist or may be created by a fire in an usual fire compartment:

- existing openings (e.g., open doors, open windows, open roofs, etc.);
- formation of openings as a result of glass breakage and glazing;
- formation of openings as a result of deterioration of the compartment barriers from structural failure, formation of cracks or local excessive temperature rise on the unexposed face through heat conduction.

Openings that are created as a result of a fire should be considered in fire safety design, because they can change the development of a fire, e.g., change to the ventilation inside the fire compartment. The designer must, therefore, consider all possible openings that could be created as the fire develops and grows. The most probable reasons for fire spread should be determined. This includes the existing openings such as open doors and windows and the openings created due to glass breakage and/or barrier deterioration. For barriers, fire resistance time can be used to evaluate the deterioration of the assembly including the formation of holes.

3. MODELING FIRE SPREAD USING COMPUTATIONAL FLUID DYNAMICS

The FDS code is a computational fluid dynamics model for simulation of fire-driven fluid flow developed by the National Institute of Standards and Technology (NIST). [2]

FDS solves numerically a form of the Navier-Stokes equations appropriate for low speed, thermally-driven flow with an emphasis on smoke and heat transport from fires. The core algorithm is an explicit predictor-corrector scheme, second order accurate in space and time. Turbulence is treated by means of the Smagorinsky form of Large Eddy Simulation (LES).[2]

Two types of combustion models have been implemented in the FDS code. The choice depends on the resolution of the underlying grid. However, in an LES calculation where the grid is not fine enough to resolve the diffusion of fuel and oxygen, a mixture fraction-based combustion model is used.

In the numerical algorithm implementing the mixture fraction model, the local heat release rate is computed by first locating the flame sheet, then computing the local heat release rate per unit area, and finally distributing the energy to the grid cells cut by the flame sheet. In this way, the genuinely, infinitely thin flame sheet is smeared out over the width of one grid cell, consistent with all other gas phase quantities. [3]

The physical limitation of the mixture fraction approach to modeling combustion is the assumption that fuel and oxygen burn instantaneously when mixed

3.1. Glass breakage in fires

Due to the importance of understanding the performance of window glass in fire, this issue has been addressed in many outstanding research endeavors, including theoretical studies (e.g. Keski-Rahkonen 1988, Keski-Rahkonen 1991, Joshi & Pagni 1990-1994, Pagni, Cuzzillo & Pagni 1998) and experimental studies (Richardson & Oleszkiewicz 1987, Skelly et al. 1991, Joshi & Pagni 1994, Hassani et al. 1994-1996, Shields et al. 1997/1998, Mowrer 1998, Anon. 1999, Harada et al. 2000, Shields et al. 2001-2002).[4]

The studies carried out by Joshi and Pagni have been implemented as a computer program BREAK1 (Joshi & Pagni 1991) which is a Fortran program enabling to calculate the occurrence of the first fire-induced fracture and fallout of the glass pane. BREAK1 is freely available at the NIST Internet site. The results calculated with BREAK1 have been found to agree well with experimental data.

3.2. Description of computer program BREAK1

Following the suggestion by Pagni [1], we model the glass fallout as an event which takes place after a certain number of glass cracking have occurred. The sequence of the glass cracking is determined so that the next cracking is deemed to take place when the glass temperature has risen on an average by an amount of ΔT_g (figure 2).[4]

The average glass temperature rise ΔT_g forms the basis of the modeling of the glass cracking following the first crack: it is assumed that there will be a cracking of the glass pane always when the average glass temperature has increased by an amount of ΔT_g after the preceding cracking.

When the glass pane has shattered for the first time, its response to heating changes is almost unpredictable due to the influence on the first cracking on the system. One implication of this greatly increased uncertainty is that for practical purposes it seems quite unnecessary to model the system response to heating at the high level of sophistication afforded by the BREAK1 code, but a less rigorous but computationally simpler approach suffices.

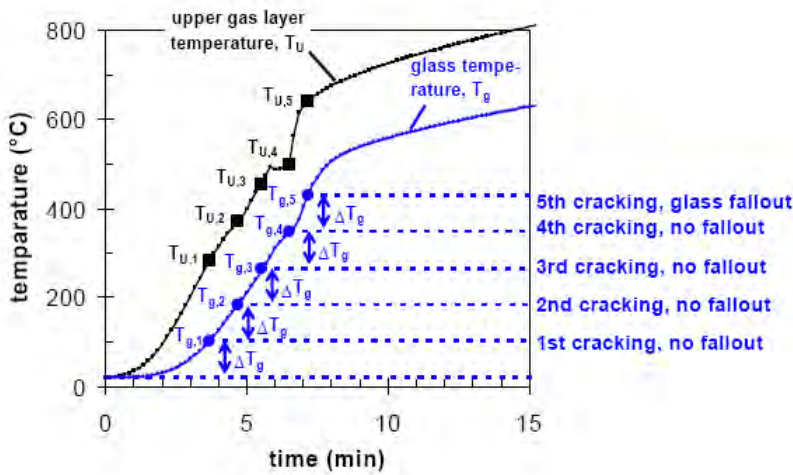


Figure 2. Glass fracture and fallout as a series of cracking occur, when glass temperature rises by an amount of ΔT_g

3.3. Physical, thermal and mechanical properties of glass

We consider the window as slab of soda-lime float glass. Below we first describe the relevant thermal and mechanical properties as well as the heat transfer characteristics with their variability characterized by suitable statistical distribution. [4]

The density of the glass, ρ , is modeled according to the data given by Pagni: $\rho = (2500 \pm 100) \text{ kg m}^{-3}$.

The specific heat c_p varies between $750 \text{ JK}^{-1}\text{kg}^{-1}$ and $950 \text{ JK}^{-1}\text{kg}^{-1}$ and the thermal conductivity k varies between $0,7 \text{ WK}^{-1}\text{m}^{-1}$ and $1,4 \text{ WK}^{-1}\text{m}^{-1}$. Thermal diffusivity α is determined by the three above mentioned quantities via the relation $\alpha = k/(\rho c_p)$. In the temperature range $0 \dots 300 \text{ }^\circ\text{C}$, the thermal coefficient of linear expansion β has a value $(9,0 \pm 0,5) \cdot 10^{-6} \text{ K}^{-1}$.

The modulus of rupture or breaking stress σ_t has a value $\sigma_t = (48 \pm 1,5)$ MPa, in function of different glass thicknesses ($L = 2 \dots 8$ mm). The Young modulus of the glass is treated as a deterministic parameter with value equal to $E = 72$ GPa.

3.3. Glass-breaking study using BREAK1

In the first part of the research one used the informatics program BREAK1 to calculate the moment in time when the window glass is breaking, in a compartment, as a result of the occurrence of a fire.

The fire compartment is considered to be a room in an office building (see figure 3), with $3\text{m} \times 3\text{m} \times 3\text{m}$ dimensions. The walls, the ceiling and the floor are made from concrete; the room has a door with $2\text{m} \times 0,8\text{m}$ dimensions, and also a window of $1\text{m} \times 1,2\text{m}$, both of them in the “closed” position, at the time of the simulation. The fire load density in the room is considered to be 511 MJ/m^2 , and the heat release rate (HRR) 250 KW/m^2 , according to the destination of the room [7].

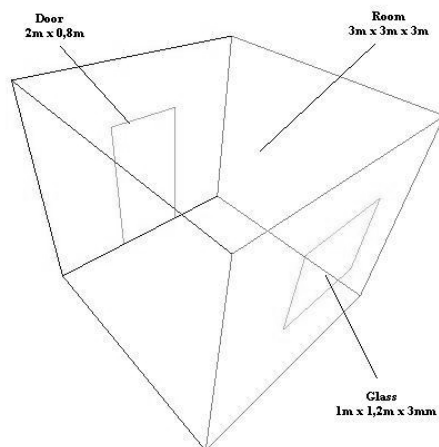


Figure 3. The geometry of the fire origin compartment

3.5. Discussion of BREAK1 Study Results

After the BREAK1 program calculated the given situation, the first window glass cracked in the 64th second - counted from the initiation of the flame - a medium speed development fire in the compartment considered in figure 3 (speed of fire growth medium, $t_a = 300\text{s}$ - necessary time to reach a total Heat Release Rate of 1 MW -, HRR 250 KW/m^2) [5,6]. The temperature of the hot gases from the compartment reaches $160 - 220^\circ\text{C}$. The complete breakage of the window,

therefore natural ventilation, occurs at 87,6 seconds from the initiation of the flame in the fire origin compartment.

4. FIRE SPREAD STUDY USING FDS

In the second part of the research, the information resulted from the use of BREAK1, were used to give the data for a Fire Dynamics Simulator (FDS) numerical modeling. This way, one used FDS to implement the geometry of the compartment and the limit conditions (glass breakage time) in FDS, to mathematical modeling of the initiation, development and spread of the fire in the same compartment – the fire origin room, as well as at the upper floor room, just on top of the first one (see figure 4). Because BREAK1 can not calculate the action of the fire over the structural elements from the second floor (window glass cracking), a thermocouple is implemented on the outside part of the window, and when it gives a 175 °C temperature (Kim and Taber (1989) stated that critical temperatures on the exposed side of glazing were 150 to 175°C for plain glass and 350°C for both heat strengthened and tempered glass.), the program removes the window, considering it completely cracked; therefore, a simple hole remains instead of it.

All these simulations are made in a computational domain with a dimension of 14 meters wide, 18 meters long and 18 meters high. Total number of cells in which are made hydrodynamics calculus is 412 176 (104 976 for the whole computational domain, and in order the results to be more precise, in the area of the two offices involved; a thicker network of 307 200 cells was disposed).

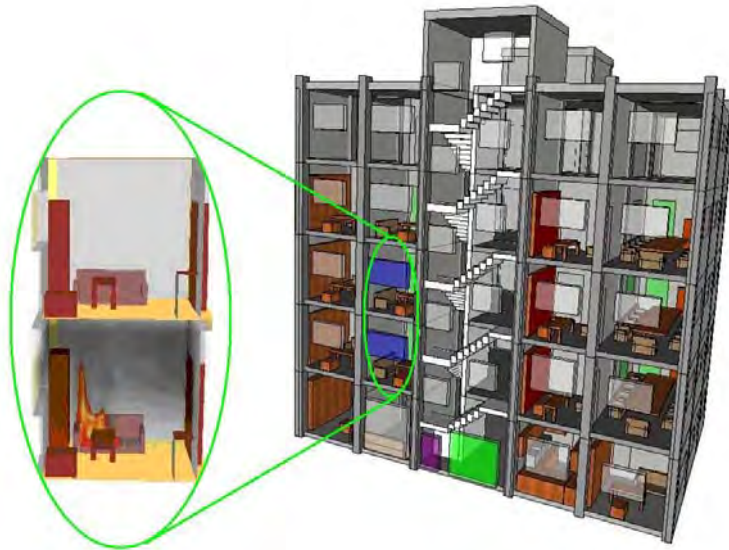


Figure 4. General view of the office building to emphasize the area where simulations take place.

The fire is supposed to occur on the couch in the 1st floor office (figure 4); the ambient temperature is 20 °C and the total time of the simulation is 600 seconds. The simulation was conducted on a computer having the following configuration: 2400 MHz, Intel Core 2 Duo processor with 1024 MB DDRAM memory; the computer made 77887 reiterations in 36,15 hours.

4.1. Discussion of FDS Study Results

In figure 5 is highlighted the temperatures field in the moment just before the glass breakage (simulation time 87 seconds) and the moment of the breakage of the fire origin compartment window glass (86,7 seconds). Also one can observe the movement of the fire effluents movement outside the fire compartment. Good accordance can be seen between the burning gases temperature value predicted by BREAK1 (a zone fire model), and the temperature given by the FDS (a field fire model) numerical simulations.

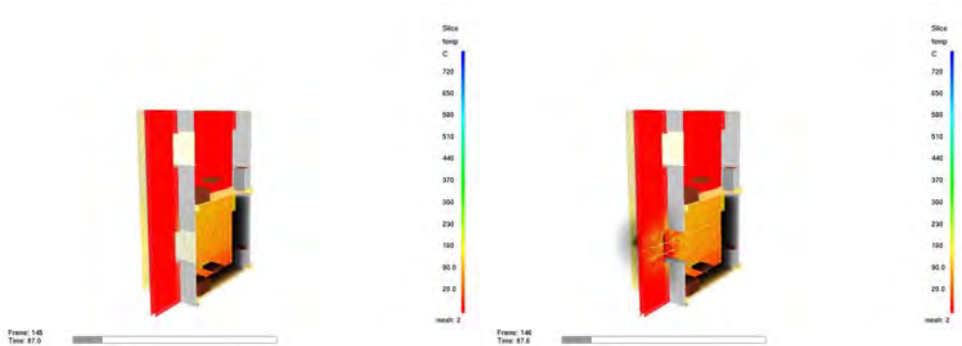


Figure 5. Images with the moment before and after the breakage of the first floor office window

An important role in the development of a fire is reserved to ventilation. The breakage of the window, from the fire hotbed room, creates a cold fresh air current, which reaches the room, through the lower part of the opening, forcing this way the fire effluents to get out of the room using the upper part of the window hole, affecting the environment.

The displacement of the smoke and hot gases on the horizontal and vertical direction, can be explained because of the expansion of gases that are heated, and the draught which is created during the fire.

The 6th figure shows the influence of creating an opening in the fired compartment, influence on the future development of the fire (intensification of the burning, because of the plus contribution of oxygen) and also the figure shows the value of the hot gases and flames temperature on the side of the building in the surrounding of the second floor office window.

One can see also the important rising of the temperature value in the fired compartment from almost 160 °C (figure 5) to 300°C (figure 6).

Figure 7 emphasizes the temperatures field in the moment precursory to the breakage of the second floor window (simulation time 171,6 seconds) and also in the moment when the glass breaks (simulation time 172,2 seconds).

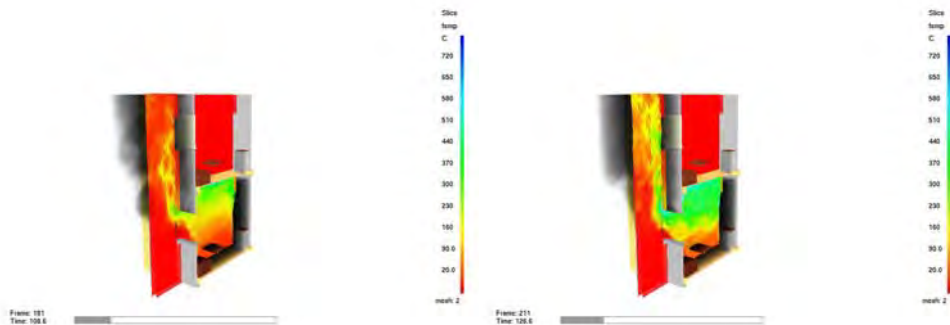


Figure 6. Intensification of the burning as a result of the first floor office window

The simulation of the glass breakage is analytically made by recording the temperature with a thermocouple positioned on the opposite side of the window. The future evolution of the fire do not lead to the lighting of the combustible materials situated in the second floor office, in the simulation conditions (null wind speed); only the effluents of the fire (mainly smoke and hot gases) passes through the enclosure, with the expected negative consequences.

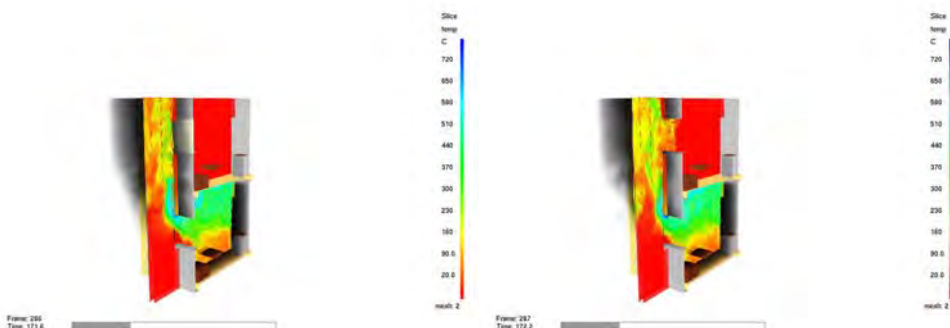


Figure 7. The breakage of the second floor office window

5. CONCLUSIONS

In many fires all around the globe, peoples perished just because a window cracked due to temperature, allowing the fire to spread to upper floors. That's why is very important to predict this moment in the development of a building fire, therefore take the necessary measures to minimize loss of human lives and material damage.

As resulted from the research above, apparition of a sudden opening in a building structure has a major influence on the future development of a fire. Therefore, an implementation of a FDS routine which would calculate the collapse of the structural elements (as window breakage) is a very necessary step in a real fire situation modeling.

References

1. Pagni, P. J.- *Thermal Glass Breakage* - International Association for Fire Safety Science, p. 3-22, 2003.
2. McGrattan K. B. - *Fire Dynamics Simulator (Version 4) Technical Reference Guide*, NIST Special Publication 1018, Fire Research Division, Building and Fire Research Laboratory in cooperation with VTT Building and Transport, Finland , NIST, 2006.
3. Anghel I., Darie E. și Flucuș I. - *Simularea numerică a unui incendiu într-o clădire cu structură ușoară* - The IXth Scientific Communications Session with international participation of “Al. I. Cuza” Police Academy – Fire Officers Faculty, p. 101-108, București, 2006.
4. Hietaniemi, Jukka - *Probabilistic simulation of glass fracture and fallout in fire* - VTT Building and Transport, Finland , 2005.
5. ***ISO/TR 13387- 2 - *Fire safety engineering. Part 2: Design fire scenarios and design fires*, p. 6-7, 1999.
6. ***ISO/TR 13387-6 *Fire safety engineering -- Part 6: Structural response and fire spread beyond the enclosure of origin*, p. 10-11, 1999.
7. ***Eurocod 1: *Acțiuni asupra structurilor Partea 1-2: Acțiuni generale-Acțiuni asupra structurilor expuse la foc*, p. 43-44, 2004.

Stability plane structures analysis program by correction functions

Banut Valeriu, Teodorescu Mircea-Eugen

Department of Mechanics, Static and Dynamic of Structures, Technical University of Civil Engineering, Bucharest, 38RO-020396, Romania

Summary

Stability plane structures analysis using classical formulation implies iteration solving of stability equation – witch represents unknown coefficients determinant from displacement method (as usually used method). For developed structures manual solving becomes practical impossible.

For surmounting of this difficulty, in the present paper is described a way for skipping iterative solving of a determinant and replacing of this with an eigenvalue and eigenvector problem for a symmetric matrix.

Expression of this eigenvalues and eigenvectors problem is

$$|K_E - \lambda K_F| = 0$$

where K_E represents elastic stiffness matrix and K_F is the matrix witch contains geometrical nonlinearity effect, express by using correction functions.

For practical applications it was made an analysis program, called STAFCO, with witch two examples where solved.

KEYWORDS: stability, program, correction functions,

1. INTRODUCTION

Strength structures designing or checking suppose elements flexibility considering by introducing compression axial force effect act on unitary efforts values in the most stressed transversal section. The element that introduces this effect is effective length, according to witch slinness coefficient is obtained. Effective length of a compressed element is obtained from a stability analysis. If for isolated bars effective length is known, in structures case a general method is necessary to be use – for example displacements method – in classical formulation or matrix formulation.

In stability issue classical formulation – having as base Euler’s theory- the characteristic equation is obtained, being a determinant that is solved by iterations. This determinant’s elements represents structure stiffness to the possible displacements of the nodes, corrected with some correction functions- functions introducing geometrical nonlinear effect, produced by the axial force. Determinant iterative solving suppose a big amount of time and in big structures case becomes practical impossible. Because of this reason, in structures design are considered approximate values of effective length, fact that leads to wrong results – smaller or bigger according the stresses values.

Finite element method appearance and perfectionist analysis instruments allowed elaboration of matrix method for stability analysis [1], [2].

In this paper is presented a method of classical stability analysis transforming – by using characteristic equation – in a eigenvalues and eigenvectors problem, using correction functions in elements stiffness evaluation, respectively structures.

2. BEAM STIFFNESS MATRIX USING CORRECTION FUNCTIONS

Elements stiffness for stability analysis are obtained from elastic linear analysis stiffness corrected with correction functions, witch introduce axial forces effect. This correction functions are presented in different stability analysis papers, older [5], [6], [7], [8] or newer [1], [2], [3]. Correction functions expressions are presented in Appendix 1.

Stiffness matrixes of bars with different connections to the ends are following:

- beam with rigid conexions at the ends

$$k_F = \begin{bmatrix} \frac{EA}{L} & 0 & 0 & -\frac{EA}{L} & 0 & 0 \\ 0 & \frac{12EI}{L^3} \eta_2(v) & \frac{6EI}{L^2} \varphi_4(v) & 0 & -\frac{12EI}{L^3} \eta_2(v) & \frac{6EI}{L^2} \varphi_4(v) \\ 0 & \frac{6EI}{L^2} \varphi_4(v) & \frac{4EI}{L} \varphi_2(v) & 0 & -\frac{6EI}{L^2} \varphi_4(v) & \frac{2EI}{L} \varphi_3(v) \\ -\frac{EA}{L} & 0 & 0 & \frac{EA}{L} & 0 & 0 \\ 0 & -\frac{12EI}{L^3} \eta_2(v) & -\frac{6EI}{L^2} \varphi_4(v) & 0 & \frac{12EI}{L^3} \eta_2(v) & -\frac{6EI}{L^2} \varphi_4(v) \\ 0 & \frac{6EI}{L^2} \varphi_4(v) & \frac{2EI}{L} \varphi_3(v) & 0 & -\frac{6EI}{L^2} \varphi_4(v) & \frac{4EI}{L} \varphi_2(v) \end{bmatrix} \quad (1)$$

where $v = L\sqrt{\frac{N}{EI}}$ is the axial load parameter

- fixed end – hinged end beam

$$k_F = \begin{bmatrix} \frac{EA}{L} & 0 & 0 & -\frac{EA}{L} & 0 & 0 \\ 0 & \frac{3EI}{L^3} \eta_1(v) & \frac{3EI}{L^2} \varphi_1(v) & 0 & -\frac{3EI}{L^3} \eta_1(v) & 0 \\ 0 & \frac{3EI}{L^2} \varphi_1(v) & \frac{3EI}{L} \varphi_1(v) & 0 & -\frac{3EI}{L^2} \varphi_1(v) & 0 \\ -\frac{EA}{L} & 0 & 0 & \frac{EA}{L} & 0 & 0 \\ 0 & -\frac{3EI}{L^3} \eta_1(v) & -\frac{3EI}{L^2} \varphi_1(v) & 0 & \frac{3EI}{L^3} \eta_1(v) & 0 \\ 0 & 0 & 0 & 0 & 0 & 0 \end{bmatrix} \quad (2)$$

- hinged end – fixed end beam

$$k_F = \begin{bmatrix} \frac{EA}{L} & 0 & 0 & -\frac{EA}{L} & 0 & 0 \\ 0 & \frac{3EI}{L^3} \eta_1(v) & 0 & 0 & -\frac{3EI}{L^3} \eta_1(v) & \frac{3EI}{L^2} \varphi_1(v) \\ 0 & 0 & 0 & 0 & 0 & 0 \\ -\frac{EA}{L} & 0 & 0 & \frac{EA}{L} & 0 & 0 \\ 0 & -\frac{3EI}{L^3} \eta_1(v) & 0 & 0 & \frac{3EI}{L^3} \eta_1(v) & -\frac{3EI}{L^2} \varphi_1(v) \\ 0 & \frac{3EI}{L^2} \varphi_1(v) & 0 & 0 & -\frac{3EI}{L^2} \varphi_1(v) & \frac{3EI}{L} \varphi_1(v) \end{bmatrix} \quad (3)$$

-double hinged beam

$$k_F = \begin{bmatrix} \frac{EA}{L} & 0 & 0 & -\frac{EA}{L} & 0 & 0 \\ 0 & \frac{EI}{L^3} v^2 & 0 & 0 & -\frac{EI}{L^3} v^2 & 0 \\ 0 & 0 & 0 & 0 & 0 & 0 \\ -\frac{EA}{L} & 0 & 0 & \frac{EA}{L} & 0 & 0 \\ 0 & -\frac{EI}{L^3} v^2 & 0 & 0 & \frac{EI}{L^3} v^2 & 0 \\ 0 & 0 & 0 & 0 & 0 & 0 \end{bmatrix} \quad (4)$$

3. STABILITY EQUATION

Stability equation, in Euler's theory conditions, where forces are growing depending on a single parameter, is obtained from the condition that for a small growing of forces, displacements should have very big values, theoretically infinitely big. Theoretically this situation corresponds to the condition that structure stiffness is equal to zero.

Instantaneous equilibrium condition is:

$$\Delta P = K_T \cdot \Delta U \quad (5)$$

from where

$$\Delta U = [K_T]^{-1} \cdot \Delta P \quad (6)$$

Instability phenomena – nonlinear displacements growing for small forces variation – is mathematically express by the condition

$$|K_T| = 0 \quad (7)$$

or considering tangent stiffness matrix form, expression (7) becomes

$$|K_E - \lambda K_G| = 0 \quad (8)$$

where K_E represents elastic stiffness matrix, and K_G is geometric stiffness matrix, witch introduce nonlinear geometric effect.

Matrixes K_E and K_G are obtained from elements stiffness matrix implantation, meaning k_E si k_G , this heaving defined signification for structure.

In case of correction functions using, the geometric stiffness matrix at the element level is obtained by

$$k_G = k_E - k_F \quad (9)$$

where k_F has the expression (1) – (4).

4. ANALYSIS PROGRAM

For bringing out the expression (8) to an eigenvalues and eigenvectors problem are necessary some transformations like [1],[2]:

- elimination of rows and columns containing only null elements, from matrix K_G (induced by introducing of restrains conditions and those existing in rows and columns 1 and 3 of matrix K_G)

- stability matrix determination in symmetric form $S = L^T \cdot K_E^{-1} \cdot L$ where $L^T \cdot L$ represents the decomposition of K_G matrix
- final expression of the eigenvalues problem

$$|S - \omega| = 0 \quad (10)$$

where $\omega = \frac{1}{\lambda}$

The program, called STAFCO, is using powers method for eigenvalues and eigenvectors calculus, which gives the biggest eigenvalue ω , respectively the smallest value λ , of the critical multiplier, this corresponding to the stability equilibrium loss condition.

The elements given by the program are:

- critical multiplier value,
- eigenvector associated (stability loss proper shape),
- effective lengths of the compressed bars, corresponding to the first mode of stability loss.

The program gives at request other consecutive eigenvalues, but these have only theoretical importance.

Observation: Theoretically, the effective length, determined from Euler's formula, is equal with infinite for axial uncharged forces ($N=0$). For avoiding possible confusions in case of obtaining of exaggerates effective length, program does not calculate effective length for axial uncharged bars or with axial forces under a minimum value considered.

5. NUMERICAL EXAMPLES

5.1. Example 1

For the cantilever beam from figure 1,a is requested to determinate the critical force and the effective length. The input data are : $E=0.21 \times 10^8$ kN/m², $A=0.24$ m², $I=0.72 \times 10^{-2}$ m⁴. The bar was divided in two equal finite elements (fig. 1,b).

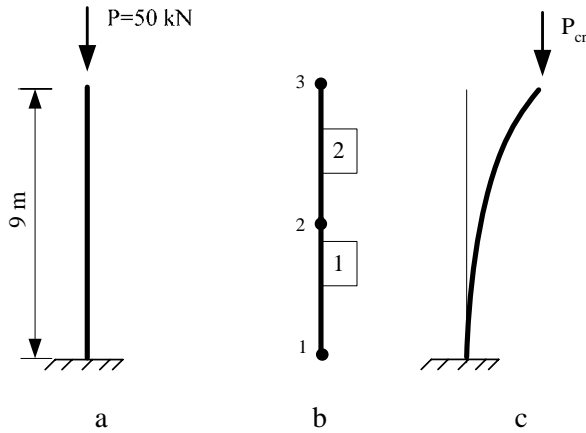


Figure 1

The first eigenvalue obtained is $\lambda_1 = 92.161$, this leading to the critical force $P_{cr} = \lambda_{cr} \cdot P = 92.161 \cdot 50 = 4608.05 \text{ kN}$ and the effective length is $\ell_f = 17.99 \text{ m}$. The stability loss shape is presented in figure 1,c.

Exact values calculated with Euler's formula are $P_{cr} = \frac{\pi^2 EI}{4\ell^2} = 4605.82 \text{ kN}$ and $\ell_f = 2 \cdot \ell = 18.00 \text{ m}$. The differences are under 1‰ is observed.

5.2. Exemple 2

For the structure depicted in figure 2,a is request to determinate critical multiplier and effective lengths of the compressed columns. Following geometrical and material characteristics are considered: $E=0.21 \times 10^8 \text{ kN/m}^2$, $A=0.036 \text{ m}^2$, $I=0.10 \times 10^{-2} \text{ m}^4$. Each bar was considered an element.

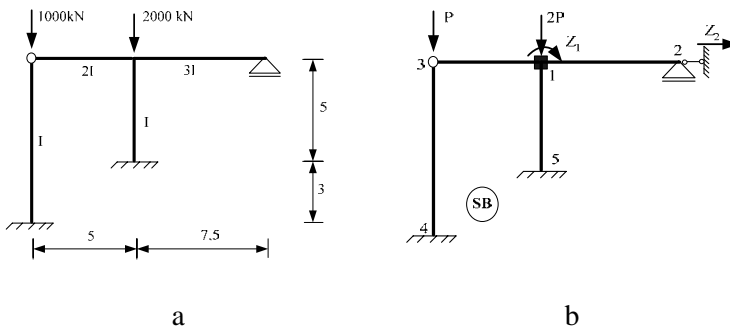


Figure 2

Critical multiplier of the axial forces using STAFCO program is 2.894, and the effective lengths of the compressed columns are:

- for fixed end – hinge end column $\ell_{f,1} = 8.488 m$

- for double fixed end column $\ell_{f,2} = 6,002 m$.

The stability analysis by displacements method (by hand) is guided on the primary system from figure 2,b.

Characteristic equation is

$$D = \begin{vmatrix} r_{11} & r_{12} \\ r_{21} & r_{22} \end{vmatrix} = 0$$

where r_{ij} represents structure stiffness on the unknowns directions (Z_1 and Z_2).

After iterative solving, critical multiplier value of axial forces is 2,94 [4]. A value bigger with 1,50% than the one given in automate analysis is obtained, because in manual analysis the axial deflection of beams is not counted. The output data are presented in Appendix 2.

6. CONCLUSIONS

Theoretically, it is possible that the solving by iterations of characteristic equation representing stability condition in case of using correction functions to be transformed into an eigenvalues and eigenvectors problem.

The program made in this purpose, allows the calculus of critical forces and the effective lengths for strongly compressed bars.

References

1. Banut, V. , *Stabilitatea structurilor elastice*, Ed. Academiei RSR, 1975
2. Banut, V. , *Calculul nelinier al structurilor*, Ed. Tehnica, 1981
3. Banut, V. , *Calculul de ordinul II si de stabilitate ale elementelor si structurilor de rezistenta*, Ed. Conpress, 2005
4. Banut, V. , Teodorescu, M.E., *Calculul de ordinul II si de stabilitate. Aplicatii rezolvate*, Ed. MatrixRom, 2007
5. Barsan, G.M., *Dinamica si Stabilitatea Constructiilor*, Ed. Didactica si Pedagogica, 1979
6. Rautu, S., Bergman, M., *Stabilitatea statica a structurilor elastice*, Ed. Ministerului Invatamantului si Culturii, 1960
7. Scarlat, A., *Stabilitatea si calculul de ordinul II al structurilor*, Ed. Didactica si Pedagogica, 1969
8. Timoshenko, P.S., Gere, M.J., *Teoria stabilitatii elastice*, Ed. Tehnica, 1967

Appendix 1

The expressions of correction functions used in the paper are:

$$\varphi_1(v) = \frac{v^2 \tan v}{3(\tan v - v)};$$

$$\varphi_2(v) = \frac{v \cdot (\tan v - v)}{4 \tan v \cdot \left(2 \tan \frac{v}{2} - v\right)};$$

$$\varphi_3(v) = \frac{v \cdot (v - \sin v)}{2 \sin v \cdot \left(2 \tan \frac{v}{2} - v\right)};$$

$$\varphi_4(v) = \frac{v^2 \cdot \tan \frac{v}{2}}{6 \left(2 \tan \frac{v}{2} - v\right)};$$

$$\eta_1(v) = \varphi_1(v) - \frac{v^2}{3};$$

$$\eta_2(v) = \varphi_4(v) - \frac{v^2}{12}$$

wher $v = L \sqrt{\frac{N}{EI}}$ represents the axial load parameter

Appendix 2

PROBLEMA 1 Exemplul 2

NUMARUL DE FORME PROPRII DE FLAMBAJ NVP= 1

COORDONATELE NODURILOR DIMENSIUNEA MATRICEI N= 15

NODUL(1)	X= 0.00000E+00	Y= 0.00000E+00
NODUL(2)	X= 0.00000E+00	Y= 0.80000E+01
NODUL(3)	X= 0.50000E+01	Y= 0.30000E+01
NODUL(4)	X= 0.50000E+01	Y= 0.80000E+01
NODUL(5)	X= 0.12500E+02	Y= 0.80000E+01

CARACTERISTICELE ELEMENTELOR

NEL	NO1	COD	NO2	COD	E	S	AI
1	1	1	2	0	0.21000E+08	0.36000E-01	0.10000E-02
2	3	1	4	1	0.21000E+08	0.36000E-01	0.10000E-02
3	2	0	4	1	0.21000E+08	0.72000E-01	0.20000E-02
4	4	1	5	0	0.21000E+08	0.10800E+00	0.30000E-02

CONDITII DE REZEMARE

IDIR	NODURI BLOCATE									
1	1	3	0	0	0	0	0	0	0	0
2	1	3	5	0	0	0	0	0	0	0
3	1	3	0	0	0	0	0	0	0	0

FORTE AXIALE IN ELEMENTE

NEL	EFORT AXIAL
1	0.10000E+04
2	0.20000E+04
3	0.00000E+00
4	0.00000E+00

MODURI DE FLAMBAJ SI MULTIPLICATORI CRITICI

1 ILEA MOD

=====

IT = 4

MULTIPLICATOR CRITIC = 0.28766E+01

NODUL	X	Y	TE
1	0.00000E+00	0.00000E+00	0.00000E+00
2	0.10000E+01	0.37220E-02	0.00000E+00
3	0.00000E+00	0.00000E+00	0.00000E+00
4	0.99896E+00	-0.75329E-03	-0.70682E-01
5	0.99896E+00	0.00000E+00	0.00000E+00

ELEMENT LUNGIMEA DE FLAMBAJ

1	0.84883E+01
2	0.60021E+01

Automation of building process time structure models

Renáta Bašková

*PhD., Department of Construction Technology
Technical University of Košice, Faculty of Civil Engineering
e-mail: renata.baskova@tuke.sk*

Summary

A determining element of building management system, which allows modeling of data in time, is a building schedule. In the paper are present the models analyze of building process time structure and elements parameters analyze of these models. The particular network analyze model and its mathematical mechanism are behind software for building scheduling. The mathematical links classifying of network process method allow new view at possibilities of particular software to satisfying requirements, which are risen during a creating and improving building schedule modeling in the pre-manufacturing, manufacturing and realization phase of invested process. For development of new one or improvement already existed software for building schedule automatized modeling is necessary not only clear and entire requirement specifications to software, but also theoretical basis of process network analyses adjusting for the building process conditions.

KEYWORDS: modeling, building schedule, networks analyses methods, software

1. INTRODUCTION

Most of the building companies are aimed about integrated information management system, processed by computers in the all its part. The main principle of this integration is a saving of all primary, processing dates about particular building objects into suitable organized databases and permanent showing of these dates into calendar time. A determining element of building management system, which allows modelling of data in time, is a building schedule. Therefore is necessary to have the building schedule computational processing as the most reliable model of objective building process course models.

2. METHODOLOGY

The methods of network analysis are the main tool for processing of building schedule by computers. Particular methods allow a mathematical project modelling by networks. The medium of building production, in the network, is becoming

an operation, i. e. building process at the different level of aggregation. A network topology describes a way of mutual activities connection at the model. The classical methods of network analyse have general application, but during their using are rising the building process mathematical modelling inaccuracies, which markedly decrease a quality of final model, i. e. building schedule. (1) (8) (9)

The process relativities have their particularities in building industry. Network topology of building model should represent real technological and organizational relativities of particular building processes. During the time course modelling of building by computers in the network topology is possible to define just these links among processes, which are mathematical defined by particular method of the computer software. Equally, the modelling of internal time, technological and also spatial structure of building processes is possible just in the dimensions, which are provided by particular computer software.

2.1. Time structure models of building process

The various abstract models are used for time structure expression of building process:

- verbal (time structure is defined by parameters description and their time assessment),
- mathematically (time structure is described by mathematical expressions),
- graphic models (time structure is defined by graphical representation).
- Generally, all these three model types are used together and are each other completed for better visualise and understanding and higher informative ability.
- For the graphical visualise of processes time course and their parameters in the building practise are used (4) (7):
- Gantt diagram – line graphic schedule,
- time-spatial graph,
- histogram – cumulative graph of building-up sources using,
- network – arc or node defined network model.

The graphical model of building is always completed by description and mathematical term. Also, the network analyses of building processes and their combinations, which is in generally a mathematical methods summary of projects modelling by networks and is using the combination of all three abstract model types. The network is a base, which is completed by entered or calculated of time parameters, or by description of particular process. The given mathematical mechanism is suitable for assessment of graph elements (nodes, arcs) parameters.

Between individual graphical drawing model ways of building course is always close connection. The outputs, which are obtained by network analyses methods, are mostly graphically interpreted by Gantt diagram. On the second hand is common, that this line graphic schedule is completed by graphical drawing of taken mathematical bonds among processes.

2.2. Elements of time course building model

In generally, the elements of time course building model in the building projects are:

- **Particular activities – processes.**, which are necessary for achievement of projects goals, an activity is realization of classified element or its parts, which are realized by one capacity unit on one place in continuous time,
- **Process configurations** – configuration of activities, which are focused to the goal achievement, process configuration is ordered group of processes,
- **Milestones** – in advance clearly defined requirements and specifications for project course,
- **Connections and relativities between processes or process and milestone** – mutual technical, technological, organizational and logical connections between activities, processes, process configurations and milestones (when relativity is expressed by mathematical way, that means a bond between processes or process and milestone)

The bond means mathematical expression of mutual relativities between processes, their configurations and milestones. The time bond between two points in time (events) of processes or milestones is expressed by mathematical term. The first point is referred to previous process/milestone „i“, the second point of bond is referred to process/milestone „j“, which follows previous process/milestone.

2.3. Time parameters of building process or milestone

Among the time parameters of building process belong (4) (7):

- t_i - process duration i ,
- tRo_i - process development date i ,
- tUs_i - process consolidation date i ,
- tZu_i - process reduction date i ,
- tPr_i - process technological interval duration i ,
- tOd_i - defferment process duration i .

Next, among processes time parameters belong terms (non-calendar or calendar), terms of start TZ_i or term of finish TK_i i -process, or its part, or milestone term Tm . At the network analyses are parameters, which are expressed events terms, neatly classified into the earliest events terms defined by „forward calculation“ and the latest events terms defined by „ahead calculation“, necessary the earliest or the latest term or fixed necessary term:

- NT - necessary date (defined by real or relatively calendar date),
- ZM_i - the earliest start of activity i date,
- KM_i - the earliest finish of activity i date,
- ZP_i - the latest start of activity i date,
- KP_i - the latest finish of activity i date.

A time parameters assessment (in the chosen units of measures) of building process can be defined by constant (by estimation, calculation, stochastic,

deterministic) or as an average parameter, which is dependent on a valuation of other parameters in particular process or else processes.

2.4. Connections and relativities between processes

During the planning, the particular processes are jointed (organized) in the process configuration so that in the realization time first one makes a building preparedness by its activities necessary for second one. At the same time, they do not destroy a result of own activity each other. The process order in the configuration is defined on the connections base among processes. Between two processes can be:

- **Connection of dependency** – a start of process course is directly relative by previous process finish (or its part).
- **Connection of partial dependency** – production space or process course is influenced by continuance or result product of another process.
- **Connection of independency** – course and result products are irrelevant each other.

The connection of dependency between two processes can rise as a result their technological and organization relativity:

- **Technological relative connection** – is, when previous process make next working queue
- **Organization relative connection** – is, when processes use the same working equipments and labour power.

The terms process **relativity** and **bond** between processes are sometimes changed in literature (4) (7) (10). The process relativity is technological or organization matter and is followed from building process structure. The term – “bond between processes” relates with network analyses. It is mathematically expressed mutual technical, technological, organization or logical relativity between activities, processes and their configurations and milestones. During the computer processing of schedules by software, which done on base of network analyses (3) (5) (6) is necessary the process relativity express by mathematical bonds.

2.5. Mathematical bonds in network analyses methods

The base for automated modelling of time project course is always particular network analyses method. During the modelling of building time course by computer is possible to define in the network topology technological or organization process relativities only by these mathematical bonds, which are defined in the particular network analyses method and its mathematical mechanism.

2.5.1. *Types of bonds in network analysis method*

In Types of connection define, which time parameters of two jointed processes/milestones are in the calculation directly considered, specially for „forwards calculation” and also for „aback calculation“. Each type of connections is characteristic also way of definition and time assessment of distance.

The mathematical bond between processes/milestones is possible to divide into:

- Simple bonds – these bonds express the connection between one event of previous process and one event of next process. There are connections: finish-start (K–Z), start-start (Z–Z), finish-finish (Z–Z) and the bonds, which are derived from them, such partial start-start ČZ-Z and partial finish-finish ČK-K. The definition of necessary the earliest date (NT) belongs among simple bonds too.
- Double bonds – allow by one mathematical mechanism to express the connection between two events (also one) of previous process and between two events (or one) of next process. They are the mathematical connections of two simple bonds. Their elementary representative is critical approach bond (KP), and it's derived construction-technological (STV) and line (PRV) bond.
- Cyclic bonds – these bonds express a feedback between event of next process/milestone and event of previous process/milestone. That is the bond, which has a given particular maximal possible value of time distance „b“ (where $b \neq \infty$). Eventually, it can be a double bond between events of two processes, where first bond has given a maximal possible time distance and second one has a maximal accepted time distance. The elementary representative of cyclic bond is a definition of the latest or stably necessary date (NT). There belongs a stably process connection (PP) without the interruption possibility of working teams (or with given maximal possible interruption) between two processes i. e. finish work of one process and start work of another process.

The cyclic bond can be cause of conflict of dates during the network calculation. The conflict of dates is a situation, when the calculated dates of event activities in the network modelling are in conflict with specific requirements of process time course. The next problem is that an enclosed cycle can generate at mathematical calculation of dates during give a cycle bond, i. e. number of calculation iterations is unlimited and that gives out a logical mistake in network model. It follows necessity of opened cycle using with limited number of calculation iterations.

2.5.2. *Time parameters of bonds between processes*

Among time parameters of bonds belong (1) (8) (9):

- Minimal (the shortest possible) time distance „a“ of two events,
- Maximal (the longest accepted) time distance „b“ of two events,

- These time parameters of processes/milestones, which value time affects a calculation of events time distance jointed by bond. It can use different or equivalent processes parameters for terms forwards or aback calculation of particular bond type.

A time distance size „a“ also „b“ of two events is express in the particular time measure. For individual connection types have time distance these values:

- minimal time distance „a“:
- $a < 0$, $a = 0$, $a > 0$, when „a“ is not given, $a=0$
- maximal time distance „b“: $b < 0$, $b = 0$, $b > 0$, when „b“ is not given, $b = \infty$.

The time distance value can be given for each bond type followed:

- defined by particular number (given constant) in time measure,
- defined by mathematical term, where time distance is a function of particular process parameters (previous or next process). When is time distance value derived from particular processes parameters value, mostly is necessary to give out a factor k (in % or as an index number). The value of factor k can be followed:
 - from time parameters of previous process,
 - from time parameters of next process,
 - from time parameters of previous also next process,
 - as a rate of minimal working queue on the working place a. o.

defined by mathematical term, where time distance is a function of given constant and particular processes parameters (previous or next process).

2.6. Working operation at building time course of modelling

Among working operations, which are necessary to do during the creation, debugger and updating of building schedule belong:

- setting a process bill of quantities,
- definition of process duration,
- definition of process requirements for building sources
- relativity organizational allowance of processes (milestones),
- definition of processes (milestones) starts and finishes necessary dates,
- processes summarization or decomposition,
- processes aggregation and desegregations,
- processes connection are interruption,
- summarization, equalizing or planning of building sources e. i.

Each of these modelling operations of building schedule demand special approaches. The result model of building schedule is used as documentation for preparation and organization requirements and process management of building product realization. The difficultness of individual operation or possibility of individual operation automated performing during schedule computer processing,

is depended on using software ability. The creation of models and documentation can be quicker and higher quality by using an integrated connection inputs and outputs of various systems.

A process position concerning at time axle is depicted following process specific relativity during building schedule processing in Gantt diagram or time spatial graph. The main question for planner is: "When can particular process start concerning already scheduled (realized) processes?" The time parameters changes of any process cause that the schedule can be unrealistic and it is necessary to do it again. According as schedule actualization is able to allow all processes relativity, which was in a previous time model, is dependent of the planner special ability. The implementation of these changes into schedule can be equally complicate as its primary draft.

2.7. Automated modeling of building process time structure

Some computers programs allow mathematical connection of parameters processes calculation, but not allow entry process relativity by mathematical bonds (e. g. MS-Excel). The process position in time is defined by fixed location on time axel. This result model of building schedule has "static" character, e. i. time process parameters are stably definite and the change of them is not possible to automated change in schedule model creation, debugging and using.

The schedule "static" model, which is not set for automated debugging or actualization, is possible to create by each software, which is using the mathematical bond. Its creation is quicker, less complicated and there are necessary less planer specific abilities than in creation of "dynamic" model. There is not so important that using mathematical bond real allows for example internal time structure of building process after any process parameters change. The using bond can have constantly given time distances. The processes relativities are possible to define for example only by simple bond, or by necessary dates. In this case, all processes dates have to be real planned and allow all specific requirements for particular building schedule. In time schedule processing by computers, the mathematical definition of mutual processes time position is using only for recording of source requirement or creation of necessary processes documentation.

When a building model is designed for optimal plan debugging, for plan actualization in time realization or for various building simulation, is necessary to use such software (network analyses method), which allows correct definition of mutual processes position in time during any parameters change of model elements. For example, when the software uses bonds with constantly given time distances only, in time of processes parameters changes is necessary rethink given time distance bond value too.

Some software allows the using only limited number of bond types. On the figure 1 is example building schedule, which is made in MS-Project program (3) (5) and processes bonds definitions, where double connections are omitted. In this case, here can start up a necessity of change the time distance value and change of used bond type among processes. The process debugging becomes expertly difficult and slow by this way.

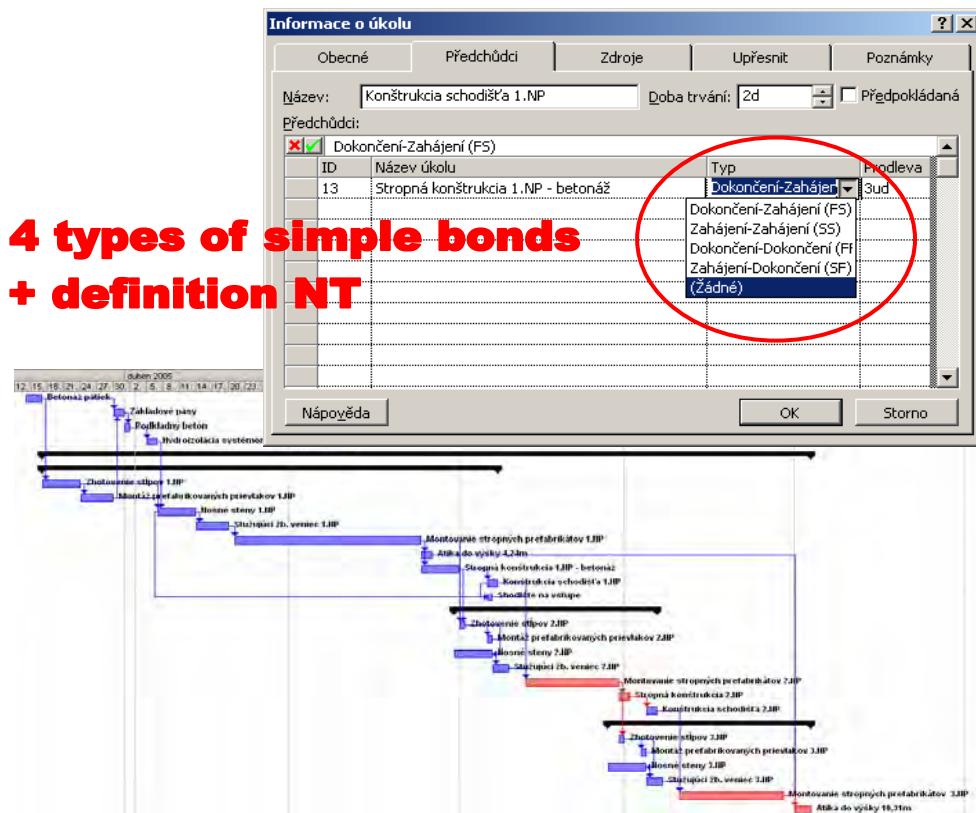


Figure 1: Building schedule and bonds in MS-Project program

When a computer program allows a definition of mutual technological and organizational relativities among processes by suitable mathematical bonds, the result schedule debugging is not too difficult. On the figure 2 is example of building schedule made by Contec program (6), which for example for the definition technological process relativity uses STV bond. This bond allows consecutive the automated plan debugging without the ignored relation of relativity

risk among processes. This program allows in the created schedule by gradual simulations, the revision of different options and finding out the optimal result for previous given limited specification and given criteria.

On the second hand, the software like this can demand the higher requirements at modeller expertness or can have the difficult process parameters entry and their assessment.

A particular network analysis method is behind each computer program for building schedule. The program ability discharge of users requirements, which are made in time of building schedule model creation and debugging in the pre-manufacturing, manufacturing and realization phase of invested process, is depend to mathematical mechanism.

A software development for automation of building process modeling is not in final phase. The completed requests specification at software, which will be a result of real necessity of their users is only first one, but very important step on this way to progress.

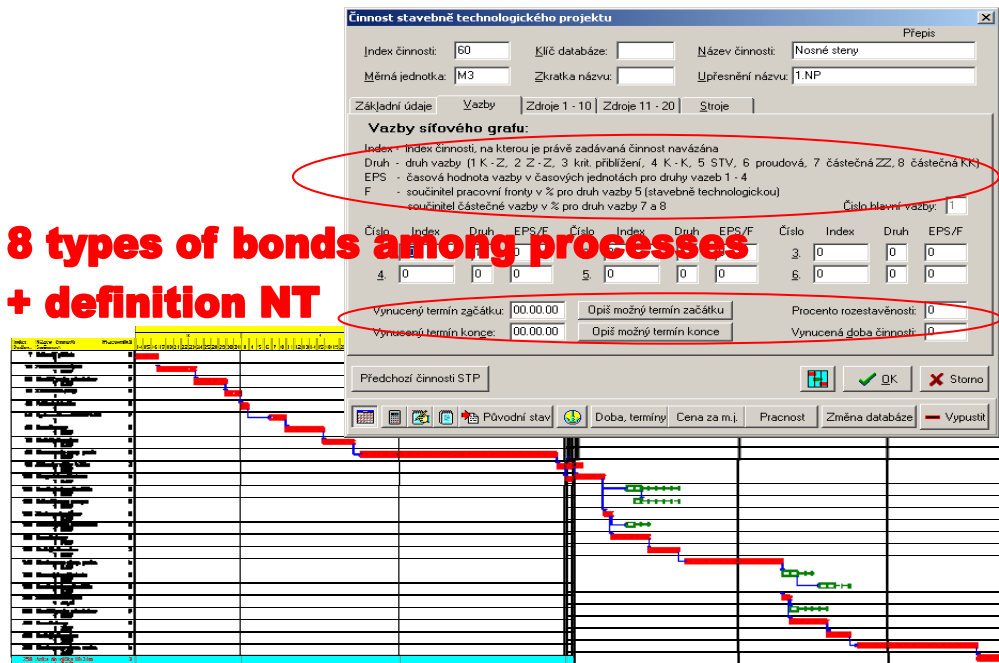


Figure 2: Building schedule and bonds in Contec program

3. CONCLUSIONS

Nowadays, the difficultness of schedule creation, manually or by computer in particular software background is relatively high. All mathematical schedule models, which are created by particular network analyses methods, do not allow a saving of schedule reality in time of its time parameters changes or different limits (necessary dates or disposable amount for particular sources e. i.). When a computer program, following some of network analyses methods, allows a suitable definition by mathematical connection of mutual technological and organizational relativities among processes, their debugging or implementation of changes into schedule result in time building, it has not to be so difficult.

For automated modelling purposes of building schedule is necessary not only clear and completed request specification at software, but also an adjusting of process network analyses theoretical information at building process condition. The computer programs for creation of building schedule should be made by this way, instead the mathematical connections entry allow directly operation entry among processes. The programs for building schedule modelling should allow an inputs and outputs integration of different individual information systems, as are production plan of constructions, budget, safety and protection health at work. Finally, the programs for building schedule modelling should allow automated debugging of schedule in time building condition change, or more options simulation and creation of schedule for multi-criteria assessment and a selection optimal option.

Acknowledgements

The article is the part of the projects **AV 4/0008/07 Risks research arising from building process acceleration solution** and **VEGA nr. 1/0689/08 Management of building structures parameters interactions.**

References

1. Bašková, R.: Modelovanie procesov výstavby: Ekonomicko-matematické metódy – časť I. (Lineárna optimalizácia a sieťová analýza). 1. vydanie. Košice: TU v Košiciach - SvF, 2004. 150 str. ISBN 80-8073-188-8.
2. Bašková, R.: Models Management in Building Project. In: KIP- Quality-Innovation-Prosperity VII/2, Q-Project PLUS Ltd., Košice, 2003. Pages 1-11. ISSN 1335-1745.
3. Bašková, R.: Computational modeling of building process time behaviour In: Proceedings of the International Symposium „Computational Civil Engineering 2006“, Iasi, Romania, May 26. Iasi: Editura Societății Academice „Matei Botez“, 2006. ISBN (10) 973-7962-89-3, ISBN (13) 978-973-7962-89-8, s.226-237
4. CA-SuperProject 3.0. Bratislava: Data System Soft, s.r.o., 2003
5. Fickuliak, I. a kol.: Výstavba objektov a stavieb. Bratislava: Vydavateľstvo STU Bratislava, 2004. ISBN 80-227-2167-0

6. Hyndrák, K.: Vytváříme projekty v programu MS-Project 2000. Praha: Computer Press, 2002. ISBN 80-7226-329-3
7. Jarský, Č.: Automatizovaná příprava a řízení realizace staveb. CONTEC, Kralupy nad Vltavou, 2000
8. Jarský, Č. a kol.: Technologie staveb II – příprava a realizace staveb. Brno: AN CERM s.r.o., 2003. ISBN80-7204-282-3
9. Trávník, I. a Vlach, J. Siet'ová analýza. 1.vyd. Bratislava: Vydavateľstvo Alfa, 1974. ISBN 63-057-74
10. Unčovský, L.: Modely siet'ovej analýzy. 1.vyd. Bratislava: Vydavateľstvo Alfa, 1991. ISBN 80-05-00812-0.
11. Hulínová, Z.: The decision-making process in the selection of optimum building technologies. In: International Conference on Developments in Building Technology. Bratislava, 1996, p.51-57.

Masonry mortar development based on fluid fly ashes

Dalibor Beneš¹

¹ Institute of Building Materials and Components, Faculty of Civil Engineering, Brno University of Technology, 602 00 Brno, Czech Republic

Summary

This work was expected to examine the potentialities of fluid fly ashes utilization as hydraulic bonding material in preparation of dry mortar mixtures or more precisely to examine presumed potential hydraulic capacities of fluid fly ashes that have been theoretically assumed on the basis of its chemical-mineralogical composition. Problems hydraulic binder was solving not only in laboratory environment but especially in conditions real development dry mortar mixture.

KEYWORDS: masonry mortar, fluid fly ash, hydraulic binder, dry mortar mixture

1. INTRODUCTION

Purposes work was solving problems utilize fluid fly-ash to preparation mixed hydraulic binder in the concrete mortar type hydraulic binder with addition fluid fly-ash. This mixed hydraulic binder with assembling then from fluid fly-ash and lime hydrate. In previous period was inquest that mixture which contain higher share fly-ash mark higher fort respectively you which have higher share lime hydrate embody major plasticity. Both these characteristics it is satisfactory fort and plasticity then mixed hydraulic binder and fluid fly-ash directly predetermination hereto to serve as binder dry mortar mixture. From they with acts above all about masonry mortar that are relatively unpretentious on fort but from views application quality must have sufficient plasticity.

Pursuant above-mentioned was experimental work orientation on mixture for masonry mortar with utilize develop mixed hydraulic binder. In frames hereof development was emphasis laying above all on optimal dosage both component mixed hydraulic binder. Like basis for optimization watch parameter be of service evaluation technological and application quality develop dry mortar mixture.

2. PROPOSAL COMPOSITION

Basic prescriptions were designed so that with loom from:

- 12 % mixed hydraulic binder
- 88% crushed sand

Like referential specimen masonry mortar was proposed mixture:

- 9% Portland cement 42,5 R
- 3% lime hydrate
- 88 % crushed sand

Development masonry mortar proceed with mixed hydraulic binder with current fluid fly-ash and lime hydrate in mutual structural conditions from 1:1,25 till up 1:0,625. Was establishment that hydraulic binder in mentioned structural purview embody bonding power on principle based on behavior fluid fly-ash like pozzolana.

2. INPUT RAW MATERIALS

In the concrete with mixed hydraulic binder fanfold from fluid fly-ash from locality coal power station Hodonin (Czech Republic) and lime hydrate CL 90. Chemist fluid fly-ash show in tablet 1 and lime hydrate tablet 2. Mixed hydraulic binder was designed in quadruplet variant dosage fluid fly-ash namely :

- one massic part filter fly-ash plus 1,25 massic part lime hydrate further in text sample " 1,25 F"
- one massic part filter fly-ash plus 1 massic part lime hydrate further in text sample " 1F "
- one massic part filter fly-ash plus 0,83 massic lots lime hydrate further in text sample " 0,83 F"
- one massic part filter fly-ash plus 0,625 massic lots lime hydrate further in text sample " 0,625 F"

Table 1. : Chemical analysis fluid fly – ash

Oxide	SO ₃	P ₂ O ₅	SiO ₂	MnO	Fe ₂ O ₃	MgO	Al ₂ O ₃	TiO ₂	CaO	Na ₂ O	K ₂ O
%	7,84	0,341	31,6	0,103	6,64	3,72	17	0,541	29,4	0,326	1,17

Table 2. : Chemical analysis lime hydrate CL 90

Oxide	CaO	MgO ₃	SiO ₂	Fe ₂ O ₃	Al ₂ O ₃	SO ₃	CO ₂	H ₂ O	CaO
%	7,84	0,341	31,6	0,103	6,64	3,72	17	0,541	29,4

3. WORK FLOW

According to designed prescriptions was first fit exhibits through homogenize of all input component in quantity 25 kg. From technological quality was in this case following:

- workability freshly mortar
- compressive strength and tensile strength up 3 as far as 28 days

From application properties were following:

- real consumption batch waters
- plasticity
- setting time
- spreading for close masonry

4. EVALUATION RESULT

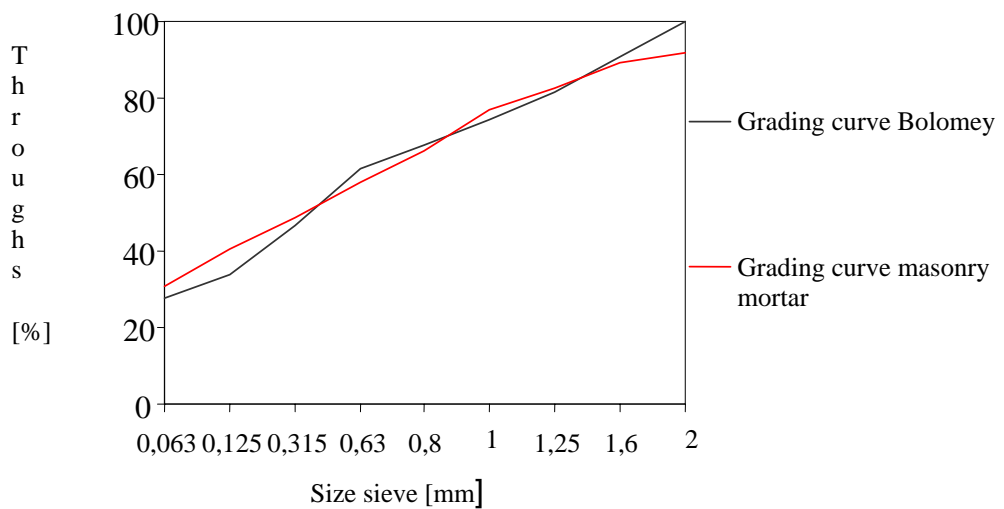
They are here state result sieve analysis table 3 and granularity using aggregate which is in very draw the balance agreement with grading curve according to Bolomey. Show in here result application and technological quality checking masonry mortar. Table 4 shows in comparison grading curve masonry mortar with ideal fission according to Bolomey.

Table 3. Sieve analysis used fraction and content single component

Sieve	Fraction 0-0,7 mm	Fraction 0,7-1,2mm	Fraction 1,2-2 mm	Fraction 2-4 mm	Component	Content component [%]
4	100,0	100	100	100	Binder	12
2	100,0	100	99,2	20		
1,6	100,0	100	90,8	10	Fraction sand 0 - 0,7 mm	40
1,25	100,0	100	55,6	5,8		
1	100,0	99,8	23,6	5,6	Fraction sand 0,7-1,2 mm	20
0,8	100,0	67,2	2,4	5,2		
0,6	91,4	28,8	0,8	0	Fraction sand 1,2 - 2mm	18
0,315	70,5	1,4	0,4	0		
0,125	46,4	0,6	0,2	0	Fraction sand 2 -4 mm	10
0,063	100,0	0,2	0	0		

Table 4. Comparison grading curve masonry mortar with ideal fission according to Bolomey

Sieve [mm]	Masonry mortar		Fission according to Bolomey	
	Scrap on sieve [%]	Troughs [%]	Scrap on sieve [%]	Troughs [%]
2	25,3	74,8	9,3	100
1,6	7,8	67,0	9,1	90,7
1,25	9,4	57,6	7,4	81,6
1	7,1	50,5	6,6	74,2
0,8	22,8	27,8	6,2	67,6
0,6	17,1	10,6	14,5	61,4
0,315	9,6	1,0	12,9	46,9
0,125	0,5	0,5	6,4	34
0,063	0,3	0,3	27,6	27,6



Technological properties

Table 5: Technological properties masonry mortar

Composition binder/ trace properties	Mark specimen				
	REF	1,25 F	1 F	0,83 F	0,625F
Portland cement 42,5 R [%]	9	0	0	0	0
Lime hydrate CL 90 [%]	3	6,5	5	5,5	4,5
Fluid fly - ash [%]	0	5,5	6	6,5	7,5
W* [-]	0,21	0,28	0,25	0,25	0,24
Compressive Strenght [MPa]					
3 days	1,7	0,3	0,4	0,4	0,6
7 days	2,4	0,8	1,1	1,2	1,3
14 days	3	2	2,4	2,6	2,8
28 days	3,1	2,6	2,7	3,1	3,8
tensile Strenght [MPa]					
3 days	0,9	0,4	0,4	0,5	0,4
7 days	1	0,6	0,7	0,6	1
14 days	1,5	1,2	1,2	1,2	1,6
28 days	1,6	1,6	1,3	1,4	1,4
Density [kg/m3]					
3 days	2030	2040	2030	2040	2050
7 days	2010	2000	1950	1900	2020
14 days	2000	1950	1930	1900	2010
28 days	1990	1950	1930	1900	2000

* $w = \frac{V}{SMS}$ SMS – weight dry mortar mixture V – weight water

Application properties

Table 7: Application properties masonry mortar

Composition binder/ trace properties	Mark specimen				
	REF	1,25 F	1 F	0,83 F	0,625F
Portland cement 42,5 R [%]	9	0	0	0	0
Lime hydrate CL 90 [%]	3	6,5	5	5,5	4,5
Fluid fly - ash [%]	0	5,5	6	6,5	7,5
Quantity water*	0,25	0,27	0,26	0,26	0,26
Period stiffen [min]	0 : 3	0 : 6	0 : 3	0 : 3	0 : 3
Spreading	good	great	good	good	good

* $w = \frac{V}{SMS}$ SMS – weight dry mortar mixture V – weight water

5. CONCLUSION

Like binder masonry mortar was using mixed hydraulic lime binder extensive ratio spacing dosage both his starting component. Technological characteristics exhibits ready according to these proposal without problem meeting on class masonry mortar M 2,5 therewith that enhancement fort show out sample with binder 0,625F. Adjustment granulometry was carried base Bolomey fission under participation quadruplet choice faction. Thanks changes of granulometric constitution used sand reach the expressive improvement application quality mortar without of that, he should with worsen properties technological. Adjustment granulometry with quite in principle influence spreading exhibits masonry mortar. Thanks addition enhancement quantity dusty share with that is prevent separation connective suspension and thereby with mortar state very well as far as fine triturate on basis masonry. In fine it is possible state that mature mixed hydraulic binder presents out of problem compensation classical lime - cement binder near industrial production dry mortar mixture which fetch not only economic favored for producer but advance also lower current ecological loading.

ACKNOWLEDGEMENTS

The work was supported by the MSM 0021630511 plan: Progressive Building Materials with Utilization of Secondary Raw Materials and GACR 103/06/1829 project.

References

1. ČSN EN 1015-3 Methods of test for mortar for masonry - Part 3: Determination of consistence of fresh mortar (by flow table).
2. ČSN 196-1 Methods of cement testing – part 1: Determination of strength.
3. VAVŘÍN F. : Mortary , Brno University of Technology, Praha 1980 (in Czech).

Seismic Assessment of Existing R.C. Public Buildings in Turkey – An Overview with a Case Study

Huseyin Bilgin¹, Hasan Kaplan¹ and Salih Yilmaz²

¹Civil Engineering Department, Epoka University, Tirana, Albania

²Civil Engineering Department, Pamukkale University, Denizli, Turkey.

Summary

The recent devastating earthquakes have exposed the vulnerability of the existing public buildings in Turkey. A great part of these reinforced concrete buildings has been designed considering earlier codes when seismic loads were not required or the design was at lower level of seismic loads of what is currently specified. In Turkey, template designs developed by the General Directorate of Construction Affairs are used for many of the buildings intended for governmental services (administrative centers, hospitals, schools, etc.) as prevalent practice to save on architectural fees and ensure quality control. The need for evaluating the seismic adequacy of these public buildings has come into focus following the enormous loss of life and property during the recent earthquakes.

This paper aims to evaluate the seismic performance of a public building with the selected template design in Turkey considering the nonlinear behavior of reinforced concrete members. For the building addressed in this paper, material properties are based on field investigation on government public buildings in western part of Turkey. Seismic performance evaluation will be carried out in accordance with the recently published Turkish Earthquake Code-2007 that has many similarities with FEMA 356 guidelines.

Capacity curves of investigated building will be determined by nonlinear static analysis. The effects of material quality on seismic performance of this public building will be investigated. In conclusion, different possible deficiencies and solutions to improve template design building will be discussed. This study gives an in depth sight into to the rehabilitation of public buildings in Turkey.

KEYWORDS: Nonlinear static analysis; Public building; Reinforced concrete; Seismic Code; Seismic performance evaluation.

1. INTRODUCTION

Considerable losses of life and properties have taken place as a result of the destruction caused by the earthquakes that have happened in Turkey during the past two decades. A large number of existing buildings in Turkey and other developing countries, built according to design codes of the 70s, shows that many of them behave poorly and have insufficient seismic safety. Particularly, damages that occurred on public buildings are more serious and irreparable compared to the damage that occurred on residential buildings. The damages that occurred to the public buildings in Erzincan earthquake of March 13, 1992; Adana-Ceyhan earthquake of June 27 1998; Marmara Earthquake of November 12, 1999 and Bingöl earthquake of May 1, 2003 [1-5] made it clear that these buildings, which are built mostly of reinforced concrete, need to be examined and retrofitted rapidly and effectively if necessary.

The projects and the construction of existing public buildings that were built before 1998 were constructed in accordance with the regulations TBC-1984 [6] and TEC-1975 [7] which were in effect at that time. In general, public buildings designed without seismic considerations have significant deficiencies, such as discontinuity of positive moment reinforcement in beams and wide spacing of transverse shear reinforcement. However, the earthquake and the construction regulations underwent significant changes with revisions made in 1998, 2000 and 2007 [8-9-10]. The strengthening of existing public buildings in conjunction with new contract specifications, thereby reducing losses of life and property to a minimum in case of an earthquake has become one of the most important issues on the agenda of Turkish Government [11]. In addition, a number of major earthquakes during last two decades in Turkey have underscored the importance of mitigation to reduce seismic risk.

Seismic retrofit of existing structures is one method to reduce the risk to vulnerable structures. Recently, a significant amount of research has been devoted to the study of various retrofit techniques to enhance the seismic performance of RC structures. However, few studies have been conducted to assess the seismic performance of representative concrete structures in Turkey using the criteria of Turkish Earthquake Code-2007 (TEC-2007) [10].

The objectives of this study are to evaluate the seismic performance of a typical 1990s RC public (hospital) building in Turkey using TEC-2007 which has many similarities with FEMA-356 [12], performance criteria and determine the various seismic retrofit techniques. Both the TEC-2007 global level and member level limits were assessed for three performance levels. In order to compute global structural parameters, such as stiffness, strength and deformation capacity; pushover analysis was conducted for the case hospital building. The results of the pushover analysis were investigated according to TEC-2007 requirements for

evaluating the seismic response of this building. Finally, different possible retrofitting solutions able to improve the seismic behaviour of non-seismically designed public buildings have been discussed.

2. PUBLIC BUILDINGS IN TURKEY

2.1. Template Designs

In Turkey, template designs developed by the Ministry of Public Works are used in all provinces for many of the buildings intended for governmental services (administrative centers, health clinics, hospitals, schools etc.) as common practice to save on architectural fees and ensure quality control. For that reason, these are the buildings must be dealt with firstly. Although the used projects display minor differences from province to province, they were similar architecturally.

For example, for the school buildings a revolutionary step was taken in 1997 when the 5-year mandatory education was extended to 8 years. This transformation led to the emergence of a need for new spaces. Attempts were made to solve these problems by adapting the exiting primary schools to the 8-year ones through some physical changes or by constructing new school buildings, efforts that still continue. The most preferred method for the adaptation of existing buildings is the addition of floors.

The general and the common properties of public buildings are as follows:

- The load bearing system of these buildings is composed of reinforced concrete column and beam system.
- These buildings are constructed in accordance with TEC-1975 and TBC-1984.
- There is less or no reinforced concrete shear wall in the load bearing system to resist lateral loads and impart rigidity to the building.
- Mostly, the column members of structural frame are located on the exterior axes.

2.2. Seismic Performance of Public Buildings in Turkey

Substantial damages have occurred in recent earthquakes, which led to serious doubts as to the seismic performance of public buildings [1-5]. The damages that occur in public buildings are caused by the following reasons:

- Beams stronger than columns (in terms of moment capacities),
- Compression strength of concrete is very low (7-16 MPa),
- Insufficient stirrup spacing in column and beam joints,
- Plain and improper reinforcement bars,

- The fact that the hooks of stirrups have a 90° in angle,
- Insufficient column sections,
- Lack of shear walls,
- The fact that vertical load bearing elements are unidirectional.

2.3. Description of the Case Study Building

Hospitals likewise the other buildings intended for governmental services are generally constructed by applying template designs developed by the Ministry of Public Works. Therefore, a considerable number of buildings have the same template designs in different parts of Turkey.

A field survey was carried out in Sparta and Denizli to select the most common type of hospital buildings. These cities are located in a seismically active part of Turkey. According to the survey, a most common type of template design (TD-11276) for hospital buildings was selected to represent these public buildings in medium-sized cities. It is, of course, impossible to reflect all the template RC public building features of the building stock of the country with only a selected template design. However, it can be assured that the selected building should have some general properties representative of these types.

This is a four-story hospital building with a plan area of 560 square meters at the base. All floor slabs are reinforced concrete with a thickness of 0.22 m. The story heights are 3.2 m for each story. There exists no exact data about the roofing and the masonry partitions of the building. From the architectural drawing plotted at the time of construction, reasonable values are assumed for both in dead load and other calculations, considering probable changes made during the construction.

The building has a typical structural system, which consists of reinforced concrete frames with masonry infill walls of hollow clay brick units. The structural system is free of shear walls since usage of vertical elements with depth/width ratio greater than five (given by TEC-1975) is not widely preferred in construction practice concerning the overall building stock. There are no structural irregularities such as soft story, weak story, heavy overhangs, great eccentricities between mass and stiffness centers and etc. One of the possible deficiencies for this building designed per TEC-1975 [7] is the strong beam-weak column behavior as it is not regarded by that code. Fig. 1-2 provides a typical floor plan and 3-D view of this case study structure respectively.

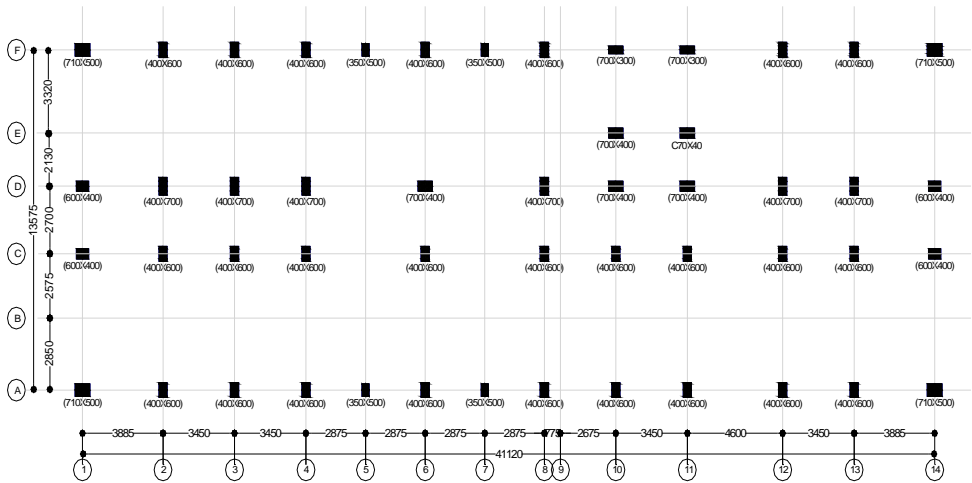


Figure 1. Typical structural floor plan view of the TD-11276 building

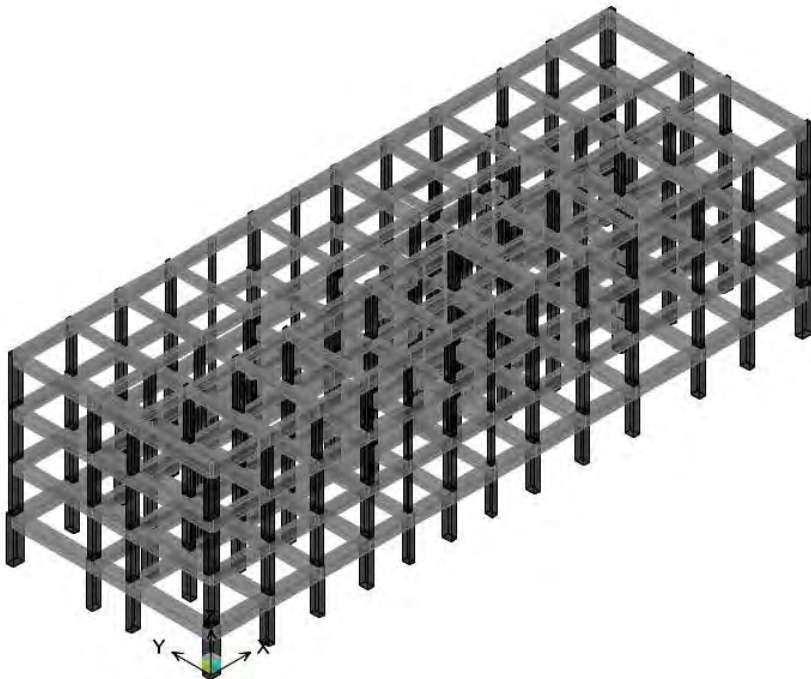


Figure 2. Three dimensional view of the TD-11276 building

3. MODELLING OF THE CASE STUDY BUILDING

3.1. Analytical Modelling of the Case Study Building

For modelling and the analysis of the case study building, the computer program SAP2000NL [13] was employed. This is a general-purpose structural analysis program for performing static and dynamic finite element analyses of structures. In this study, Nonlinear Version 8.2.3 of the program was used. Description of the modelling details is provided below.

This building was modelled as three dimensional frame system formed by beams and columns. Frame type elements having zero mass were used for the definition of all elements in order to control total mass of the building. The representation of beam-column joints was realized by assigning rigid end offsets at the ends of the elements. The joints connecting the base columns to the foundation were restrained for all degrees of freedom assuming an infinitely rigid foundation. All joints at a floor level were constrained to move as a planar diaphragm in order to prevent in—plane membrane deformations. No slabs were defined; instead, slab weights were distributed to side beams as dead loads. Weights of the beams, columns, walls and the roofs were also assigned as distributed dead loads on beams. Another load case was defined to introduce live loads on beams. Masses assigned to the stories were calculated using these dead and live load values. The calculation of these masses, live loads and dead loads were made according to Turkish Standards for Reinforced Concrete, TBC-2000 [9], Turkish Standards for Design Loads, TS498 [10] and TEC-1975 [11].

For nonlinear analysis of the case building, as-built material properties determined from field investigation and experiment were taken into account. Material properties considered in his study were determined based on field study on 98 public buildings. Figure 3. plots the distribution of the expected concrete strength of these public buildings. According to test results, two types of strength values, 10, 16 MPa were taken into consideration to represent typical concrete strength values for this building.

Experimental study on sampled buildings indicated that the buildings constructed per pre-modern code had Grade 220 MPa reinforcement for both longitudinal and transverse reinforcement. The yield strength of both longitudinal and transverse reinforcement is taken as 220 MPa. Strain-hardening of longitudinal reinforcement has been taken into account and the ultimate strength of the reinforcement is taken as 330 MPa. Although there were extreme cases where transverse reinforcement spacing was 370 mm, the observed transverse reinforcement spacing ranged between 150 and 250 mm. Hence, two spacing values are considered as 150 and 250 mm to reflect ductile and non-ductile detailing, respectively. In this study,

“poor” construction quality term is used for the buildings with 10 MPa concrete strength and 250 mm transverse reinforcement spacing while “average” construction quality refers to the buildings with 16 MPa concrete strength and 150 mm transverse reinforcement spacing.

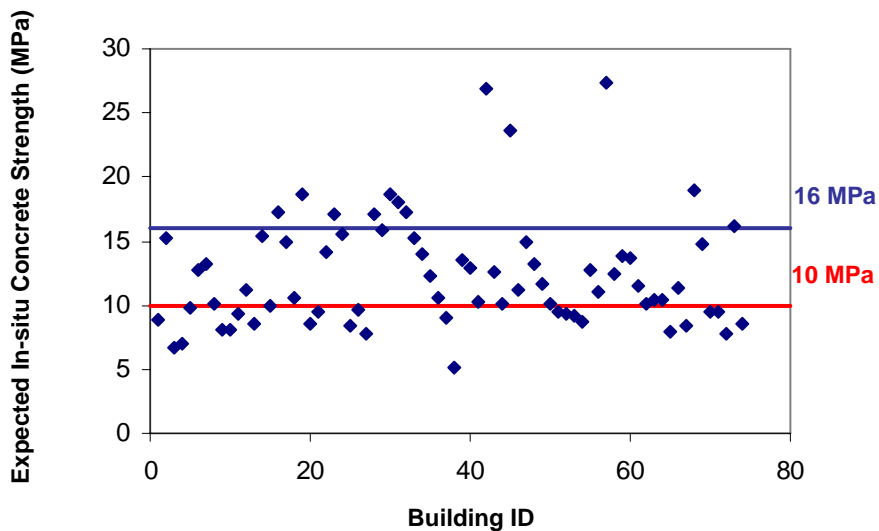


Figure 3. Expected in-situ concrete strength distribution of the school buildings

3.2. Determination of Nonlinear Parameters of Beam – Column Elements

Member size and reinforcements in the template design were used to model the sample building for nonlinear analysis. No simplifications are made for the reinforcements of members; like rounding-off or grouping members ones with close reinforcement amount. All members are modelled as given in the template design.

Three-dimensional model of the case study building is created in SAP2000 to carry out nonlinear static analysis. The structural modelling is carried out with the beam and column elements, considering the nonlinear behaviour concentrated in plastic hinges at both ends of beams and columns. SAP2000 provides default or the user-defined hinge properties options to model nonlinear behaviour of components. Inel and Ozmen [15] studied possible differences on the results of pushover analysis by implementing default and user-defined nonlinear component properties. They observed that although the model with default hinge properties seemed to provide reasonable displacement capacity for the well-confined case, the displacement

capacity estimate was quite high compared to that of the poorly-confined case. Thus, this study implements user-defined hinge properties.

The definition of user-defined hinge properties requires moment-curvature relationships for beams and columns and axial force moment capacity data for the columns are necessary for the SAP2000 input as nonlinear properties of elements (Fig. 4).

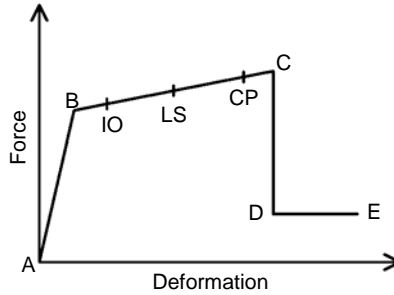


Figure 4. Typical Force Deformation Relationship

Mander model was used for unconfined and confined concrete while typical steel stress-strain model with strain hardening for steel [16] was implemented in moment-curvature analyses. The points B and C on Fig. 4 are related to yield and ultimate curvatures. The point B is obtained from SAP2000 using approximate component initial effective stiffness values as per ATC-40 [17]; $0.5EI$ and $0.70EI$ for beams and columns, respectively. In this study, the ultimate curvature is defined as the smallest of the curvatures corresponding to (1) a reduced moment equal to 80% of maximum moment, determined from the moment-curvature analysis, (2) the extreme compression fiber reaching the ultimate concrete compressive strain as determined using the simple relation provided by Priestley et al. [18], given in Eqs. 1, and (3) the longitudinal steel reaching a tensile strain of 50% of ultimate strain capacity that corresponds to the monotonic fracture strain. Ultimate concrete compressive strain (ϵ_{cu}) is given as

$$\epsilon_{cu} = 0.004 + \frac{1.4\rho_s f_{yh} \epsilon_{su}}{f_{cc}} \quad (1)$$

where ϵ_{su} is the steel strain at maximum tensile stress, ρ_s is the volumetric ratio of confining steel, f_{yh} is the yield strength of transverse reinforcement, and f_{cc} is the peak confined concrete compressive strength.

The input required for SAP2000 is moment-rotation relationship instead of moment-curvature. Also, moment rotation data have been reduced to five-point input that brings some inevitable simplifications. Plastic hinge length is used to obtain ultimate rotation values from the ultimate curvatures. Several plastic hinge

lengths have been proposed in the literature (Priestley et al. 1996 [18]; Park and Paulay 1975 [19]; Fardis and Biskinis 2003 [20]). Plastic hinge length definition given in Eq. 3 which is proposed by Priestley et al. [18] is used in this study.

$$L_p = 0.08L + 0.022f_{ye}d_{bl} \geq 0.044f_{ye}d_{bl} \quad (2)$$

In Eq. 2, L_p is the plastic hinge length, L is the distance from the critical section of the plastic hinge to the point of contra-flexure, f_{ye} and d_{bl} are the expected yield strength and the diameter of longitudinal reinforcement.

Following the calculation of the ultimate rotation capacity of an element, acceptance criteria are represented defined as labeled IO, LS, and CP on Fig. 2. IO, LS, and CP stand for Immediate Occupancy, Life Safety, and Collapse Prevention, respectively. This study defines these three points corresponding to 10%, 60%, and 90% use of plastic hinge deformation capacity.

In existing reinforced concrete buildings, especially with low concrete strength and insufficient amount of transverse steel, shear failures of members should be taken into consideration. For this purpose, shear hinges were introduced for beams and columns. Because of brittle failure of concrete in shear, no ductility was considered for this type of hinges. Shear hinge properties were defined such that when the shear force in the member reaches its shear strength, member immediately fails. The shear strength of each member (V_r) is calculated according to TBC-2000 [9].

$$V_r = 0.182bd\sqrt{f_c} \left(1 + 0.07 \frac{N}{A_c} \right) + \frac{A_{sh}f_{yh}d}{s} \quad (3)$$

In Eq. 3, b is section width, d is effective section depth, f_c is concrete compressive strength, N is compression force on section, A_c is area of section, A_{sh} , f_{yh} and s are area, yield strength and spacing of transverse reinforcement.

4. EVALUATION METHODOLOGY

4.1. Nonlinear Static Procedure (Pushover Analysis)

The pushover analysis consists of the application of gravity loads and a representative lateral load pattern. The applied lateral forces were proportional to the product of mass and the first mode shape amplitude at each story level under consideration. P-Delta effects were taken into account.

In the capacity curve plots, shear strength coefficient that is the base shear normalized by building seismic weight is on the vertical axis, while global displacement drift that is lateral displacement of building at the roof level

normalized by building height is on the horizontal axis. Capacity curves of the building considered in this study was obtained for different concrete strength and transverse reinforcement spacing mentioned in previous section; two concrete strength and two transverse reinforcement spacing values were taken into account (Fig. 5). The notation in figures and tables corresponds to concrete strength in MPa and transverse reinforcement spacing in mm. For example, the C10-s150 means that the building with 10 MPa concrete strength (C10) and 150 mm transverse reinforcement spacing (s150).

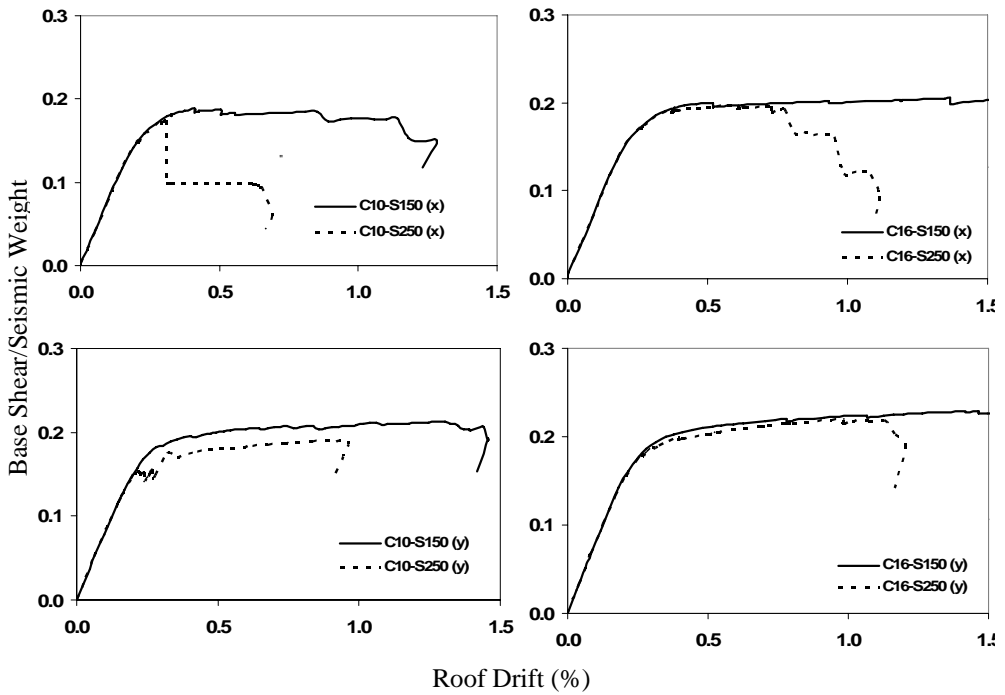


Figure 5. Capacity curves of the building TD-11276 for different concrete strength and transverse reinforcement spacing obtained by pushover analysis.

The effect of transverse reinforcement spacing on displacement capacity is obvious in longitudinal direction as seen in Fig. 5-6. Considerably small displacement capacity for 250 mm transverse reinforcement spacing is as cause of shear failure of the columns. Since the amount of transverse reinforcement is not enough to prevent shear failure and to provide ductile flexural response either, such brittle behaviour occurs. For the 150 mm spacing case, the effect of concrete strength is only limited to poor concrete case (10 MPa), having smaller displacement at significant lateral strength loss compared to the 16 MPa concrete strength.

Two extreme cases were considered in order to have a more accurate understanding in the boundaries of behavior for the case study building with the considered template design. The first one represents the buildings in poor condition having poor concrete quality (10 MPa) with non-ductile detailing (250 mm transverse reinforcement spacing). The second one refers to the buildings in average condition having average concrete quality (16 MPa) with ductile detailing (150 mm transverse reinforcement spacing). Capacity curves corresponding to poor and average conditions are illustrated in Figs. 6 for longitudinal (x) and transverse (y) directions.

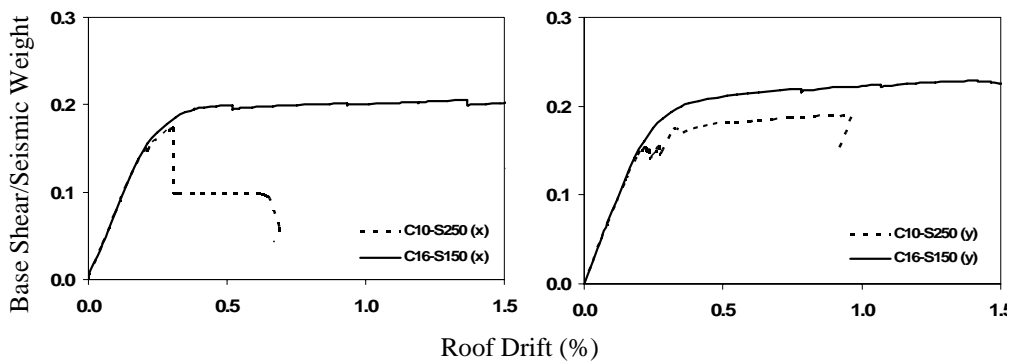


Figure 6. Capacity curves of the building TD-11276 for different concrete strength and transverse reinforcement spacing obtained by pushover analysis.

Evaluation of the capacity curves for the investigated building points out that: (1) Concrete quality and detailing has significant role in both displacement and lateral strength capacity of buildings. (2) Although the difference of poor (C10 and s250) and average (C16 and s150) conditions on lateral strength capacity is limited, the difference in displacement capacity is noteworthy. The displacement capacity for average condition is more than twice of that for poor condition. (3) The effect of concrete strength is limited.

4.2. Capacity Assessment

Capacity assessment of the investigated case study buildings is performed using recently published TEC-2007. Three performance levels, immediate occupancy (IO), life safety (LS), and collapse prevention (CP) are considered as specified in this code and several other international guidelines such as FEMA-356 [12], ATC-40 [17], and FEMA-440 [21]. Criteria given in the code for three performance levels are listed in Table 1.

Table 1. Performance levels and criteria provided in Turkish Earthquake Code-2007

Performance Level	Performance Criteria
Immediate Occupancy (IO)	<ol style="list-style-type: none"> 1. There shall not be any beams beyond LS. 2. There shall not be any column or shear walls beyond IO level. 3. The ratio of beams in IO-LS region shall not exceed 10% in any story. 4. Story drift ratio shall not exceed 0.8% in any story.
Life Safety (LS)	<ol style="list-style-type: none"> 1. The ratio of beams in LS-CP region shall not exceed 20% in any story. 2. In any story, the shear carried by columns or shear walls in LS-CP region shall not exceed 20% of story shear. This ratio can be taken as 40% for roof story. 3. In any story, the shear carried by columns or shear walls yielded at both ends shall not exceed 30% of story shear. 4. Story drift ratio shall not exceed 2% in any story. 5. There shall not be any columns or shear walls beyond CP.
Collapse Prevention (CP)	<ol style="list-style-type: none"> 1. The ratio of beams beyond CP region shall not exceed 20% in any story. 2. In any story, the shear carried by columns or shear walls beyond CP region shall not exceed 20% of story shear. This ratio can be taken as 40% for roof story. 3. In any story, the shear carried by columns or shear walls yielded at both ends shall not exceed 30% of story shear. 4. Story drift ratio shall not exceed 3% in any story.

Pushover analysis data and criteria of Table 1 were used to determine global displacement drift ratio (defined as lateral displacement at roof level divided by building height) of each building corresponding to the performance levels considered. Table 2 lists global displacement drift ratios of the building. Small displacement capacities at LS and CP performance levels are remarkable for the building with poor concrete quality and less amount of transverse reinforcement due to shear failures in columns.

Table 2. Global displacement drift capacities (%) of the investigated building obtained from capacity curves for considered performance levels

Material Quality	X-direction			Y-direction		
	IO	LS	CP	IO	LS	CP
	$\Delta_{roof}/H_{building}$	$\Delta_{roof}/H_{building}$	$\Delta_{roof}/H_{building}$	$\Delta_{roof}/H_{building}$	$\Delta_{roof}/H_{building}$	$\Delta_{roof}/H_{building}$
C10-S150	0.27	0.33	0.84	0.26	0.28	1.32
C10-S250	0.17	0.27	0.30	0.11	0.22	0.95
C16-S150	0.34	0.54	1.51	0.28	0.47	1.44
C16-S250	0.24	0.36	0.76	0.20	0.26	1.11

The displacement capacity values are solely not meaningful themselves. They need to be compared with demand values. According to Turkish Earthquake Code, hospital buildings are expected to satisfy IO and LS performance levels under design and extreme earthquakes, corresponding to 10% and 2% probability of

exceedance in 50 years, respectively. Response spectrum for the design and extreme earthquake is plotted in Fig.7 for high seismicity region and soil class Z3 that is similar to class C soil of FEMA-356. Displacement demand estimates and capacities corresponding to IO and LS performance levels are compared in order to see whether the hospital building has adequate capacity.

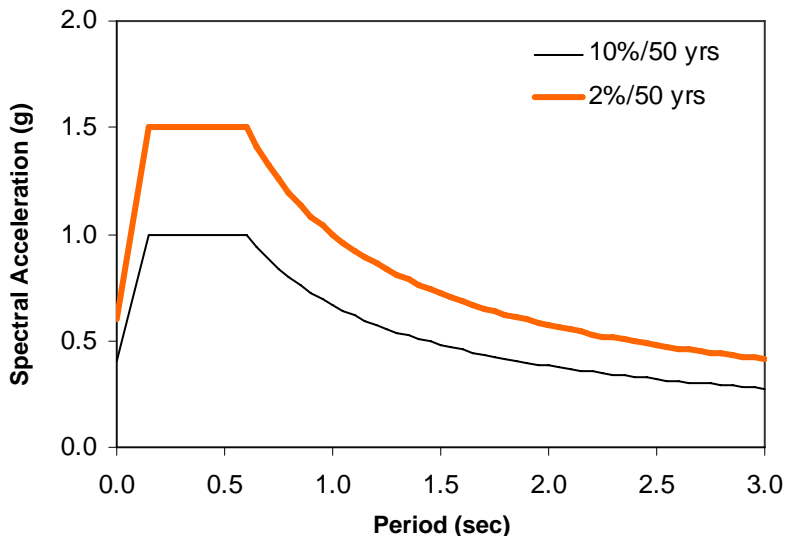


Figure 7. Response spectrum for design and extreme earthquake events provided in TEC-2007

Displacement demand estimates were obtained (Table 3) using the “equivalent” SDOF idealization of the building response as described in TEC-2007 that is similar to ATC-40.

Table 2. Global demand drift ratios (%) of the investigated building according to TEC-2007

X-direction		Y-direction	
IO	LS	IO	LS
$\Delta_{\text{roof}}/H_{\text{building}}$	$\Delta_{\text{roof}}/H_{\text{building}}$	$\Delta_{\text{roof}}/H_{\text{building}}$	$\Delta_{\text{roof}}/H_{\text{building}}$
0.93	1.40	0.93	1.40

However, the case study building constructed per TEC-1975 is far from satisfying the performance requirements of recently published code. The obvious trend between poor and average cases supports the enhancement in the building performance as the concrete quality and transverse reinforcement amount increases.

The capacity curves of template design are revisited to identify possible deficiencies and their solutions. Each pushover curve is carefully examined at LS and CP performance levels. Longitudinal direction has considerably small displacement capacity, especially for 250 mm transverse reinforcement spacing. Shear failures in columns are observed. Additional shear walls definitely take earthquake effects and reduce the burden of columns. Moreover, critical columns need to be enhanced for shear failures.

3. CONCLUSIONS

This study evaluated seismic capacity of a typical hospital building with the selected template design constructed per pre-modern code in Turkey considering nonlinear behavior of reinforced concrete components. Selection of template designed building and material properties were based on field investigation on public buildings in several cities in western part of Turkey. Capacity curves of investigated buildings were determined by pushover analyses conducted in two principal directions. Seismic performance evaluation was carried out in accordance with recently published Turkish Earthquake Code (2007) which has similarities with FEMA-356 guidelines. Deficiencies and possible solutions to improve the capacity of this case study building are discussed. The observations and findings of the current study are briefly summarized as following;

- Evaluation of laboratory and Schmidt hammer test results obtained from 98 buildings identifies that the expected concrete strength ranges between 5.1 and 27.4 MPa while the concrete strength of most buildings is within 10 and 16 MPa ranges. Hence, two strength values, 10 and 16 MPa, were considered in this study to represent typical concrete strength values of existing hospital buildings constructed per pre-modern code.
- Field investigation on sampled buildings indicated that the buildings constructed before the modern code had Grade 220 MPa reinforcement for both longitudinal and transverse reinforcement. Although there were extreme cases where transverse reinforcement spacing was 370 mm, the observed transverse reinforcement spacing ranged between 150 and 250 mm. Hence, two spacing values are considered as 150 and 250 mm to reflect ductile and non-ductile detailing, respectively.
- Evaluation of the capacity curves for the investigated buildings points out that concrete quality and detailing has significant role in displacement and lateral strength capacity of buildings either in both directions. Although the difference of poor (C10 and s250) and average (C16 and s150) conditions on lateral strength capacity is limited, the difference in displacement capacity is

noteworthy. The displacement capacity for average condition is more than twice of that of the poor condition.

- Shear failures of columns are common problems for poor concrete and low amount of transverse reinforcement, resulting in brittle failure for existing hospital buildings.
- The observed public building damages during the past earthquakes in Turkey support the analytical results obtained in this study; the reports from past earthquakes pointed out poor material quality and inadequate transverse reinforcement spacing within potential plastic hinge regions causing shear failures of columns. Shear failures observed in pushover analyses for the poor condition (C10s250) are clear indicators of such failures and a potential risk in existing hospitals for future earthquakes.
- According to Turkish Earthquake Code, hospital buildings are expected to satisfy IO and LS performance levels under design and extreme earthquakes, corresponding to 10% and 2% probability of exceedance in 50 years, respectively. The existing hospital building is far from satisfying the expected performance levels, suggesting that urgent planning and response need to be initiated.
- As material quality gets better, performance of buildings improves. The displacement capacities obtained for different performance levels evidently indicate that concrete quality and transverse reinforcement spacing have limited effect on IO level while amount of transverse reinforcement plays an important role in seismic performance of buildings for LS and CP levels.
- Amount of transverse reinforcement is a significant parameter in seismic performance of the buildings. This study shows that as the amount of transverse reinforcement increases the displacement capacity increases as well and therefore the sustained damage decreases.
- Adding of shear walls increases lateral load capacity and decreases displacement demands significantly. Thus, existing deficiencies in frame elements are less pronounced and poor construction quality in buildings is somehow compensated [5].

References

1. Erzincan after 1992 Erzincan, Turkey earthquake, *Erzincan Office of Governorship, Turkey*; ISBN: 975-94987-1-5 (In Turkish).
2. Adalier K., Aydingun O., Structural engineering aspects of the June 27, 1998 Adana–Ceyhan (Turkey) earthquake, *Engineering Structures*, vol. 23, pp. 343-355, 2001
3. Sezer H, Whittaker AS, Elwood KJ, Mosalam KM. Performance of reinforced concrete buildings during the August 17, 1999 Kocaeli, Turkey earthquake, and seismic design and construction practise in Turkey. *Engineering Structures Journal* 2003;25(1):104–14.
4. Dogangun A. Performance of reinforced concrete buildings during the May 1, 2003 Bingol Earthquake in Turkey. *Engineering Structures Journal*, 2004;26(6):841–56.

5. Bilgin, H. Seismic Performance Evaluation of Public Buildings Using Non-Linear Analysis Procedures and Solution Methods, Ph.D. Thesis, Pamukkale University, August 2007, Denizli, Turkey (in Turkish).
6. TBC-1984. Requirements for design and construction of reinforced concrete structures. Ankara, Turkey: TSE; 1984.
7. Turkish Earthquake Code (TEC-1975). Regulations on structures constructed in disaster regions. Ankara, Turkey: Ministry of Public Works and Settlement; 1975 (in Turkish).
8. Ministry of Public Works and Settlement, Turkish Earthquake Code-1998. *Specifications for structures to be built in disaster areas*. Ankara, Turkey (in Turkish), 1998
9. TBC-500 (2000). Requirements for design and construction of reinforced concrete structures. Ankara: TSE; 2000.
10. Turkish Earthquake Code (TEC-2007). Regulations on structures constructed in disaster regions. Ankara: *Ministry of Public Works And Settlement*; 2007.
11. <http://www.meb.gov.tr/duyurular/duyurular2006/projeler/>.
12. FEMA-356, 2000. Prestandard and Commentary for the Seismic Rehabilitation of Buildings, *American Society of Civil Engineers (ASCE)*, Reston, VA.
13. CSI, SAP2000 V-8. Integrated finite element analysis and design of structures basic analysis reference manual; Berkeley, California (USA); *Computers and Structures Inc.*
14. Turkish Standart Institute, 1997, TS-498 – Design Loads for Buildings.
15. Inel M. and Ozmen H. B. Effect of plastic hinge properties in nonlinear analysis of reinforced concrete buildings, *Engineering Structures*, 2006, Vol. 28, No.11, 1494-1502
16. Mander J. B. *Seismic design of bridge piers*. Research Report 84-2. Christchurch (New Zealand): Department of civil engineering, University of Canterbury; February 1984
17. Applied Technology Council, ATC-40. *Seismic evaluation and retrofit of concrete buildings*, Vols. 1 and 2. California, 1996.
18. Priestley M. J. N., Seible F., Calvi G. M. S. *Seismic design and retrofit of bridges*. New York, John Wiley & Sons, 1996
19. Park R. and Paulay T. *Reinforced concrete structures*. New York: John Wiley & Sons; 1975.
20. Fardis M.N. and Biskinis D. E. Deformation of RC members, as controlled by flexure or shear. In: *Proceedings of the international symposium honoring Shunsuke Otani on performance-based engineering for earthquake resistant reinforced concrete structures*. The University of Tokyo, Tokyo (Japan), September 8-9, 2003.
21. Federal Emergency Management Agency, FEMA-440. Improvement of nonlinear static seismic analysis procedures. Washington (D.C); 2005.

Aggregates Types Impact on Features of Fresh and Hardened Concrete Using Gypsum Free Cement

Jiří Brožovský¹, Jiří Brožovský¹, Jr.² and Jiří Bydžovský³

^{1,3} *Institute of Building Materials and Components, Faculty of Civil Engineering, Brno University of Technology, 602 00 Brno, Czech Republic*

² *Department of Building Mechanics, Faculty of Civil Engineering, VSB-Technical University of Ostrava, 708 33 Ostrava, Czech Republic*

Summary

The paper deals with peaces of knowledge regarding the impact of mineralogical and chemical compositions of fine and coarse aggregates on features of concretes using gypsum free Portland cement. Mineralogical and chemical compositions of fine aggregates (greywacke) effect on starting point of fresh concrete setting was proved, the aggregates types influence on strength values were of no great significance.

KEYWORDS: gypsum free cement, aggregates, mineralogical composition, chemical composition, initial setting time, flexural strength, compressive strength, fresh concrete, hardened concrete.

1. INTRODUCTION

The works [2, 3] give results of concrete using gypsum free cements (GFC) research, showing that aggregates mixed into cement matrix cause an earlier fresh concrete using gypsum free cement starting point of setting in comparison with starting point of setting detected on cement paste. Consequently, this phenomenon had a negative influence on concreting; in some cases, concrete put into a structure hardened before compacting. Analyses of this phenomenon have indicated a possible cause thereof connected with aggregates types worked into the concrete. Therefore, experiment works were done, focused on detection of aggregates mineralogical and chemical compositions impact on fresh concrete using gypsum free cement starting point of setting and its strength values.

Diverse types of greywacke and coarse aggregates with respect to mineralogical composition or in view of the origin (extracted or crushed) were used. The paper shows pieces of knowledge ascertained.

2. COMPOSITES USING GYPSUM FREE CEMENT, STARTING POINT OF SETTING

Measuring results evaluation of cement paste, standard mortar for determination of cement strength values and fresh concrete has shown that fresh concrete starting point of setting is substantially shorter than the same of cement paste. Gypsum free cement period of hardening being very short in comparison with gypsum Portland cements (15-40 minutes from starting point of setting) has not been evaluated; in case of cement pastes, standard mortars and fresh concretes, the period of hardening is even shorter. Upon these grounds, starting point of setting is the decisive parameter for workable treatment of fresh concrete.

Figure 1 shows starting point of setting alterations for cement paste, standard mortar and fresh concrete. The cement paste starting point of setting was taken as a 100 % value.

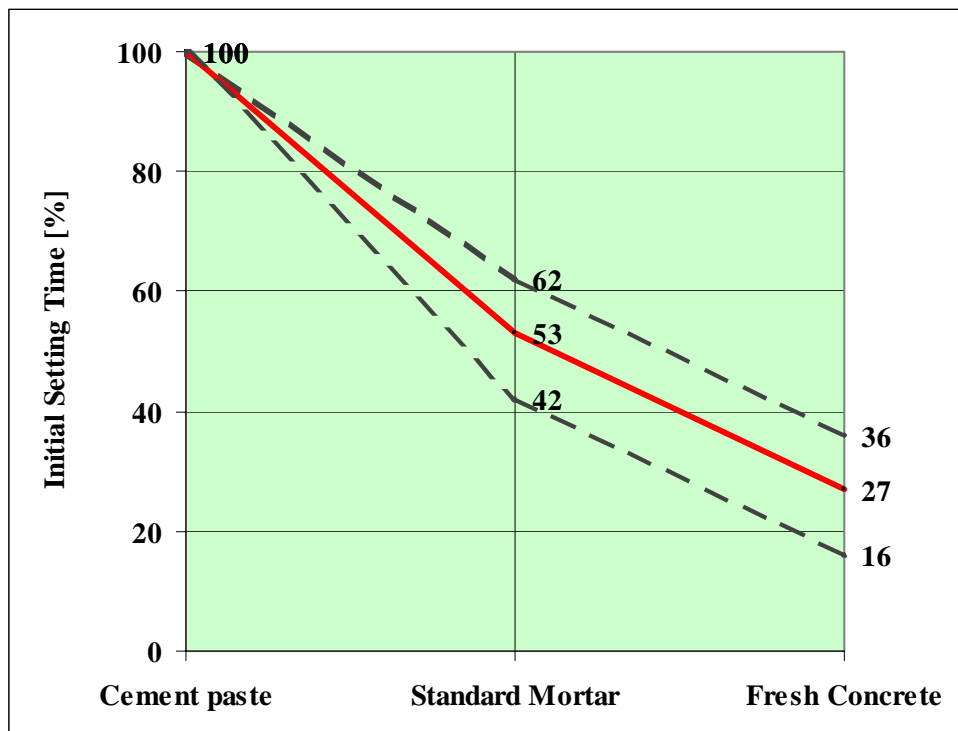


Figure 1. Starting Point of Setting Alterations for Cement Paste, Standard Mortar and Fresh Concrete Using GFC

3. TRACING OF AGGREGATES TYPES EFFECT ON GFC USING CONCRETES

10 diverse mix compounds with various combinations of greywacke and coarse aggregates (see Tab. 3) were prepared for testing. Starting points of setting and strength values of concrete mixtures (baby squares $0.04 \times 0.04 \times 0.16$ m) aged 1, 3 and 28 days were tested.

3.1. Characteristics of Aggregates

Variables in Concrete Using GFC:

- a) Greywacke (exploited and crushed)
- b) Coarse aggregates (crushed and exploited)

With regard to diversified geological origin of rocks used for concrete fabrication and owing to the great number of exploitation localities, only the characteristic aggregates types were chosen for testing.

a) Greywacke (fraction 0/4 mm)

Aggregates types of diverse quality were tested:

- Exploited aggregates with high ratio of quartz grains (> 75 %) from localities of Ostrožská Nová Ves (ONV), Tovačov (To) a Provozdín (Pr)
- Exploited aggregates with high ratio of feldspars (30-50 %) from the locality of Bratčice (Br)
- Crushed aggregates, neutral - granodiorite from the locality of Olbramovice (Ol).

b) Coarse Aggregates (fraction 4/8 mm)

Selection of coarse aggregates was based on general rock assortment according to SiO_2 ratio (ČSN 721001). Generally, the rocks have been divided into 3 categories: - sour, neutral, alkaline rocks. The types selected for testing are stated in Table 1.

Table 1: Types of Coarse Aggregates

AGREGATES	SOUR	NEUTRAL	ALKALINE
SiO_2 RATIO	> 65 %	52-65 %	< 52 %
CRASHED	GRANITE Ořechov PORFYR Klecany (Kl)	(Or) GRANODIORITE Olbramovice (Ol) GREYWACKE Jakubčovice (Ja); ca 30 % of feldspars	LIMESTONE Lažánky (La)

AGREGATES	SOUR	NEUTRAL	ALKALINE
SiO ₂ RATIO	> 65 %	52-65 %	< 52 %
EXPLOITED	Gravel with high ratio of quartz grains (Tovačov-To)	Note: Abbreviations in round brackets will be used for designation of localities in the text below.	

Mineralogical and chemical composition of the used aggregates is stated in Tables No. 2 and 3.

Table 2: Chemical Composition of Coarse Aggregates (Fraction 4-8)

CRUSHED AGGREGATES				EXPL. AGGR.
COMPONENTS [% dens.]	GRANITE <i>Ořechov</i>	GRANODIORITE <i>Olbramovice</i>	LIMESTONE <i>Lažánky</i>	HIGH RATIO OF FELDSPARS <i>Bratčice</i>
Lost by annealing				

Table 3: Mineralogical Composition of Greywacke (Fraction 0-4)

AGGREGATES EXPLOITED From Localities			
COMPONENTS [% dens.]	OSTROŽSKÁ NOVÁ VES	PROVODÍN	BRATČICE
Quartz	70-80	80-90	15-25
Feldspars	4-12	---	30-50
Gneiss	---	---	15-30
Aphibolite	---	---	5-10
Greywacke	---	---	---
Quartzite	4-8	2-10	---

3.2. Concrete Composition and Test Results

Basic Concrete Composition [kg/m³]

GFC : 500 kg

Fraction 0 - 4 : 790 kg

Fraction 4 - 8 : 960 kg

Cement-Water Ratio : 0.33

The test results are shown in Table 3 and Figures 2-4.

Table 3: Test Results for Tracing of Aggregates Mineralogical and Chemical Compositions Effects on Physical and Mechanical Characteristics of Fresh and Hardened Concrete Using GFC

NAME OF MIXTURE		K 1	K 2	K 3	K 4	K 5	K 6	K 7	K 8	K 9	K 10
GREYWACKE (0 - 4)		ONV	ON V	ON V	ON V	ON V	ON V	To	OL	Pr	Br
		TK	TK	TK	TK	TK	TK	TK	DG)	TK	TZi
COARSE AGGREGATES (4 - 8)		Or	Ja	To	Kl	La	Ol	Ol	Ol	Ol	OL
		DŽ	DDr	TK	DPo	DV	DG	DG	DG	DG	DG
Initial Setting Time of Fresh Concrete [hrs : min]		0:54	0:51	0:55	0:47	0:42	0:54	0:51	0:42	0:55	0:38
f_t [MPa]	1 day	6,55	7,42	5,75	8,00	8,13	7,13	6,99	6,99	7,10	7,23
	3 days	8,11	9,18	7,63	9,38	10,9	9,50	8,74	8,87	9,63	9,44
	28 days	8,98	9,60	8,12	10,1	11,3	9,20	9,38	8,84	9,14	8,91
$f_{c,cu}$ [MPa]	1 day	47,5	44,8	45,4	44,1	45,9	47,8	49,8	48,1	44,9	44,3
	3 days	52,2	51,5	52,2	49,9	52,5	56,7	53,8	52,1	46,9	52,1
	28 days	69,5	59,4	71,6	64,6	60,8	74,8	71,8	64,4	72,9	58,7

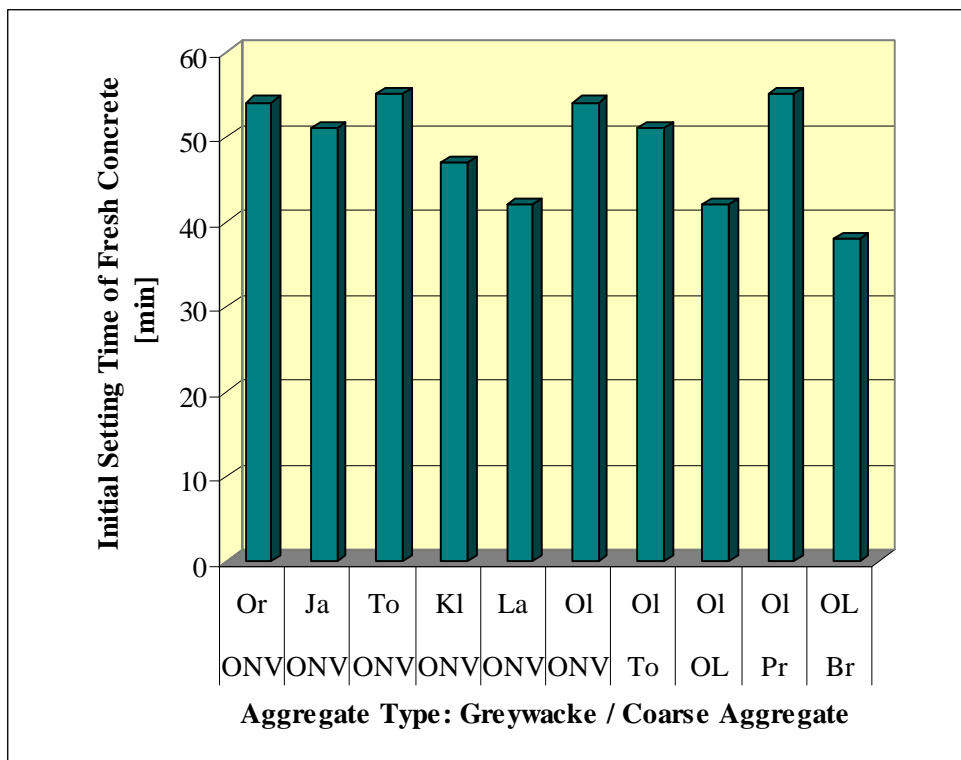


Figure 2. Impact of Aggregate Type on Fresh Concrete Initial Setting Time

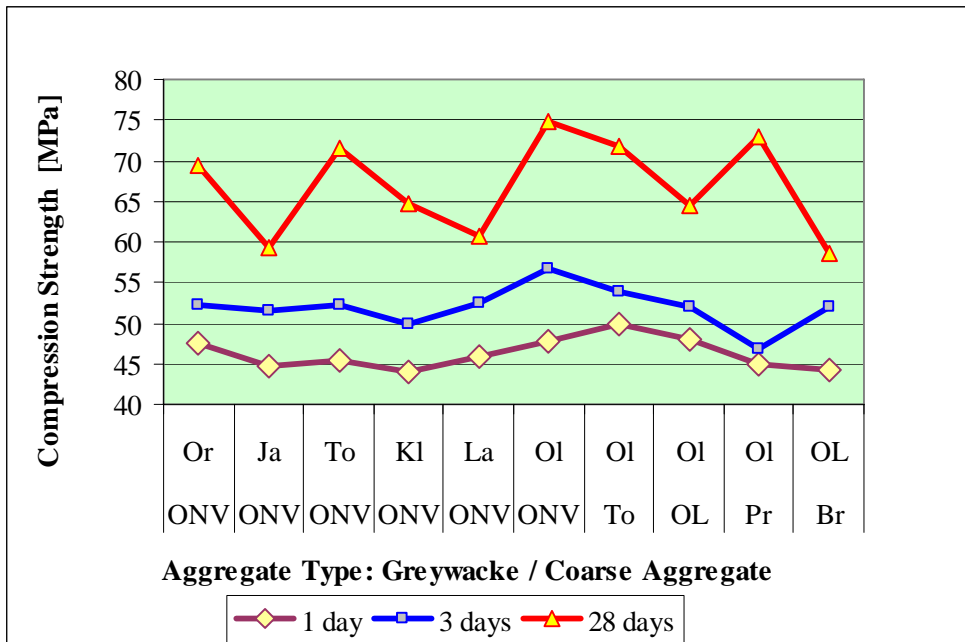


Figure 3. Impact of Aggregate Type on Compression Strength of Hardened Concrete

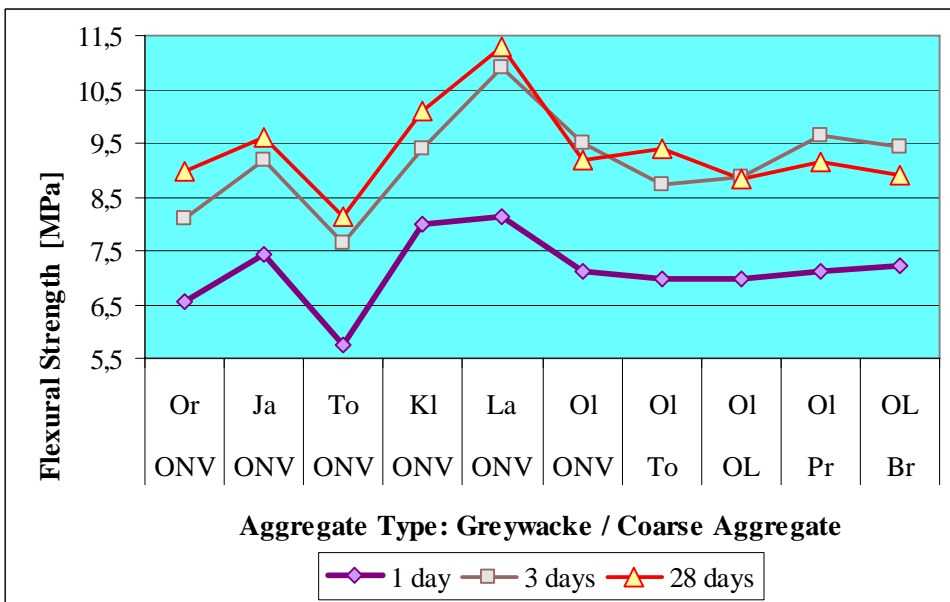


Figure 4. Impact of Aggregate Type on Flexural Strength of Hardened Concrete

4. CONCLUSION

The analysed results of experimental works focused on tracing of greywacke and coarse aggregates mineralogical and chemical composition impact on features of fresh and hardened concrete using gypsum free cement have confirmed :

- That aggregates, especially the greywacke and its mineralogical composition, have an influence on starting point of fresh concrete using gypsum free cement setting;
- Using of limestone and dolomites for concrete fabrication is not recommended; upon selection of greywacke, the exploited aggregates should be preferred over the crushed ones; it is recommendable to use exploited sands with high ratio of quartz grains; sands with high ratio of feldspars are not convenient;
- The types of coarse aggregates have no significant impact on hardened concrete strength parameters. Differences for the tested types of aggregates, especially those regarding bending strength, are caused among others by inconvenient form index of grains. Therefore it is necessary to have in mind this parameter as well, when selecting the aggregates for concretes using gypsum free cement;
- No dolomite and limestone aggregates are recommendable for fabrication of concretes using gypsum free cement.

ACKNOWLEDGEMENTS

The work was supported by by the MSM 0021630511 plan: Progressive Building Materials with Utilization of Secondary Raw Materials and their Impact on Structures Durability and MPO FT-TA3/148 project Research and development of surface Diagnostic of roads and highways. Project of maintenance and reconstruction for roads administrators in the Czech Republic.

References

1. Drochytka R.: et al. Progressive Building Materials with Utilization of Secondary Raw Materials and their Impact on Structures Durability. but, *Final report of the project VVZ CEZ MSM: 0021630511, Brno 2007.* Brozovsky J.: Subtask 3 (in Czech).
2. Brozovsky, J. Investigation of the utilization and preparation of concretes with highly early strength values, Military academy Brno, 1994, (in Czech),
3. Brozovsky, J. Concrete with gypsum-less cement- research results and experience of utilization in practice. *In : the 1st Conference on Concrete and Reinforced Concrete, Moscow, Russia, 2001 (in Russian)*
4. Brozovsky, J., Brozovsky, J. jr. : Concrete with gypsum free cement – basic characteristics *In : The Intenational Symposium on Non – Traditional Cement & Concrete, Brno, Czech Republic, 2002*

Available Scheduling Software for Linear Repetitive Construction Projects

Cristina Cosma

Civil, Construction & Environment, Wentworth Institute of Technology, Boston, MA, 02115, USA

Summary

Linear repetitive construction projects like pipelines, highways and railroads are characterized by activities that are repeated sequentially at different locations, sections, units, or construction sites.

These particular types of construction projects are considered high risk making the management of resources and partial delivery times a very important issue. In order to achieve significant reductions in project times a broader, more comprehensive approach to the problem is needed principally during the planning and scheduling phases.

Despite the fact that at present the Bar Chart and the Critical Path Method (CPM) scheduling techniques are being most used for construction projects a continuously growing awareness of the fact that the traditional network is not the best tool for the planning of linear projects and the shortcomings of bar charts in today's complex world has led to a resurgence of interest in Linear Scheduling Method (LSM) to assist in planning these particular projects.

One of the main obstacles in using LSM (as reported by contractors) is the lack of user friendly software to support scheduling linear construction projects. US available software for example are more a graphical tool than a planning tool forcing the American planners to use software available for CPM and Bar Charts like Primavera and Microsoft Project.

The paper reviews the existent scheduling software available on the American and European market in an attempt to enhance knowledge of commercially available applications in the specific area of Linear Scheduling.

KEYWORDS: DYNAProjectTM, Linear Repetitive Construction Projects, Linear Scheduling Software, Vico Software ControlTM, TILOS.

1. INTRODUCTION

High-rise buildings, pipelines, highways, railroads and long bridges are construction projects characterized by activities that are repeated sequentially at different locations, sections, units, or construction sites. For the case of pipeline, highways or railroad projects the repetition is the result of the geometrical layout of the project which is also characterized by linearity. All these projects are referred to as either linear, or repetitive or linear-repetitive construction projects.

The linear repetitive construction projects usually require large amounts of resources which are used in a sequential manner. Projects of this type are considered high risk, due to unforeseen natural causes, potential involvement in legal disputes, unpredicted weather conditions, etc., which can cause delays in overall project completion and cost overruns, thus making the management of resources and partial delivery times a very important issue [8].

Particularly for highway construction and maintenance projects applications of procedures to improve project planning, scheduling, and control can provide many benefits. Improved organization of the construction process usually reduces overall cost, increases construction safety, and shortens the project duration. For new highway construction, a shorter duration increases public safety by allowing a needed highway to open earlier. For highway rehabilitation and reconstruction projects, benefits of shorter construction duration include reduced traffic delay and associated costs, fewer collisions and injuries associated with construction-related accidents, and lower capital costs for maintenance of traffic (MOT).

In order to achieve significant reductions in highway construction project times a broader, more comprehensive approach to the problem is needed than looking for marginal improvements in existing techniques. Re-conceptualization of the problem during the planning phase, for example, might lead to alternative approaches to construction that could yield greater benefits in terms of reduced delay and disruption than could be achieved through typical approaches to minimizing contractor lane occupancy. Although project time reductions can be achieved in each of the project activities, the primary benefits will be realized during construction.

Despite the fact that at present the Bar Chart and the Critical Path Method (CPM) scheduling techniques are being most used for construction projects a continuously growing awareness of the fact that the traditional network is not the best tool for the planning of linear projects and the shortcomings of bar charts in today's complex world has led to a resurgence of interest in Linear Scheduling Method (LSM) to assist in planning these particular projects.

2. CONSTRUCTION PROJECT SCHEDULING METHODS

The scheduling techniques that are being most used for construction projects are the Bar Chart and the Network Diagrams (Critical Path Method - CPM).

2.1. Bar Charts/Gantt Charts

Developed in the 1910's by Henry Gantt, Bar Charts (also called Gantt Charts) are the easiest and most widely used form of scheduling in construction management.

A typical Bar Chart is a list of activities with the start, duration and finish of each activity shown as a bar plotted to a time scale (Figure 1). The level of detail of the activities depends on the intended use of the schedule. The links between an activity and its preceding activities which have to be complete before this activity can start can be easily shown creating the so called linked Bar Charts. The bar charts are also useful for calculating the resources required for the project.

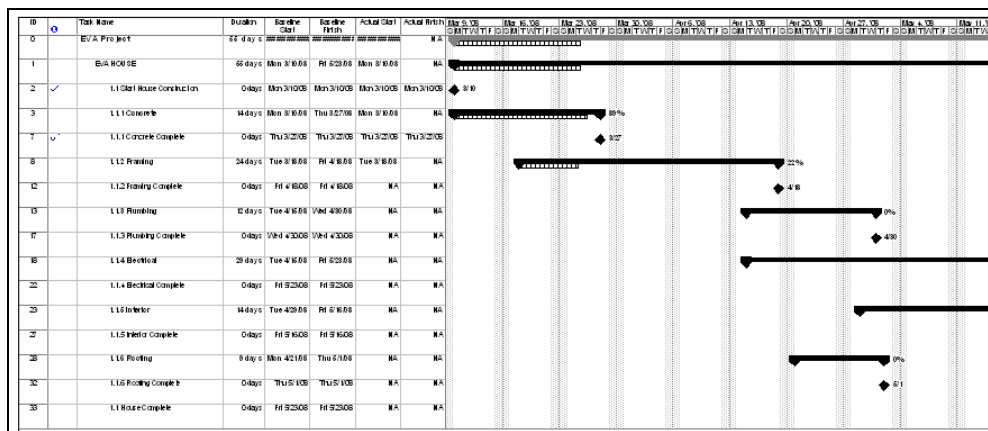


Figure 1 Bar Chart Built in Microsoft Project

The major advantage of a Bar Chart is its simplicity and ease of understanding. The major disadvantage of a Bar Chart is that the interrelationships of the activities are not shown. One other significant shortcoming of a Bar Chart is that it usually lacks detail. Activities are defined in broad categories with little or no breakdown by station, by span, and so on, highly necessary particularly for highway construction projects.

Because of these shortcomings, it is difficult to identify and/or forecast delays or potential problems, to change sequence in response to problems, and to accurately measure progress during the execution of a broadly defined activity.

2.2. Network Diagrams / CPM

The CPM Network Diagrams were developed in 1950’s by DuPont and are the most used scheduling technique by the construction industry, particularly by large and medium size companies. CPM is used to some degree by 99% of the ENR Top 400 contractors [9].

CPM schedules are a graphical representation of the construction activities either by arrow, called Activity on Arrow Diagrams or AOA (Figure 2), or by node, named Activity on Node Diagrams or AON (Figure 3).

The CPM diagram also depicts activities’ sequence, logic, and relationships. The actual CPM then calculates the critical path, or the path of activities which if delayed will delay the overall completion of the project. The paths of activities that are not critical have discrete amounts of float or slack time that allow the construction manager to recognize how much slippage can be tolerated before affecting project progress.

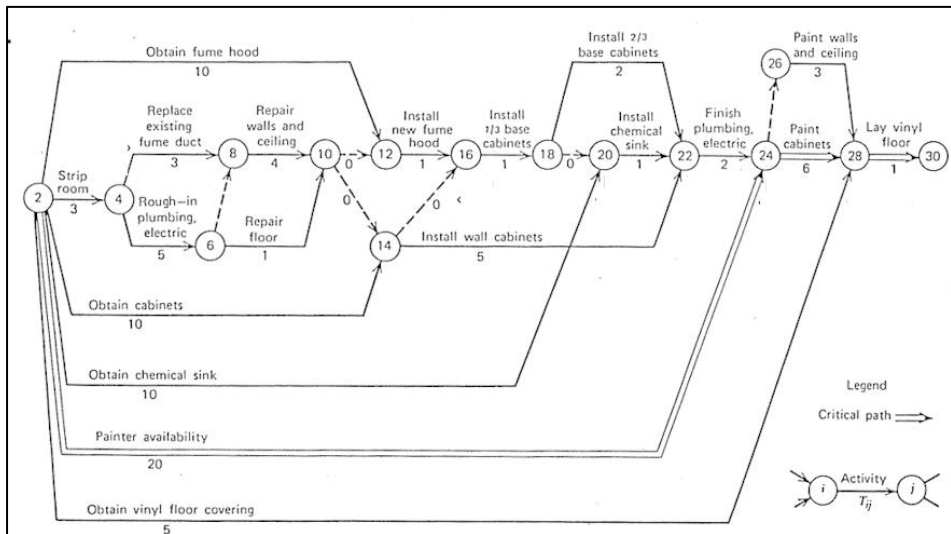


Figure 2 Network Diagram for a Laboratory Rehabilitation Project (AOA)

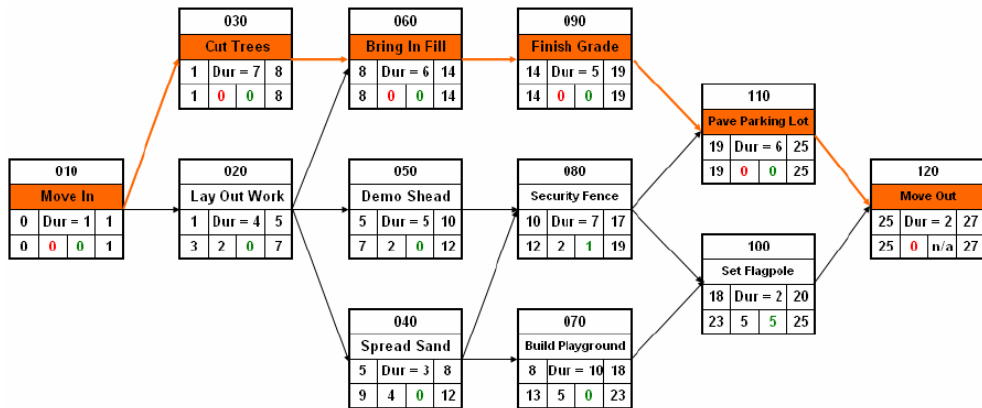


Figure 3 CPM Diagram for a Children Playground Project (AON)

CPM can be used for many different applications through the life cycle of a construction project and is used in all phases of construction from design development through operation and maintenance of projects.

The main project areas where CPM is used are:

- Detailed planning before the start of construction;
- Periodic control of work after the start of construction;
- Design development and during the estimating and bidding phase;
- Operation and maintenance of projects;
- Other areas: sales presentations, proposals, forensic, and claims analysis.

CPM usage has largely increased due to the introduction of personal computers. The main software packages available for developing CPM schedules include: Primavera, Sure Track, Microsoft Project, Open Plan, and Artemis. These software packages allow rapid calculations of the scheduling information, project and resource management and control, and numerous options for creating graphic output reports [5].

Despite their extensive use network methods have a number of shortcomings, particularly when used in scheduling linear repetitive construction projects [1]:

- Do not guarantee continuity of work in time;
- Difficult to implement multiple crew strategies;
- Do not provide an efficient structure for representing repetitive tasks;
- No consideration of the location of work.

2.3. Linear Scheduling Method (LSM)

An awareness of the fact that the traditional network diagram is not the best tool for the planning of linear projects and the shortcomings of bar charts in today's

complex world has led to a resurgence of interest in techniques to assist in planning these particular types of projects [12]. The techniques that have been developed are generally referred to as Linear Scheduling Method(s) (LSM) were introduced at Goodyear Tire and Rubber Company in 1941 and fully utilized during World War II in the defense industry [2].

The major benefit of the LSM is that it provides production rate and duration information in the form of an easily interpreted graphical format. Linear scheduling provides a simple diagram which shows both the location and the time at which a given crew will be performing a construction operation (Figure 3).

This graphical technique for scheduling enhances visualization and results in a better understanding of the project. LSM plots for a linear construction projects can be easily constructed can show at a glance what is wrong with the progress of project, and allows for the detection of potential future bottlenecks.

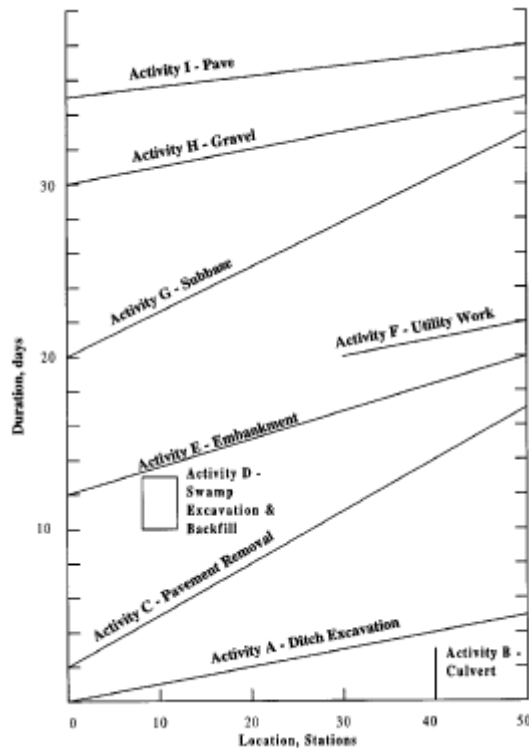


Figure 3 LSM for a Road Project [11]

Although the LSM can be used to aid in the planning and control of any type of project it is better suited for application to repetitive projects as opposed to non-repetitive projects. A limitation of this method is that it assumes that production

rates are linear, assumption that may be erroneous due to the stochastic nature of construction processes.

The Linear Scheduling Method (LSM) is also known under various names as follow:

- Line-of-Balance (LOB)
- Time-velocity diagram
- Repetitive scheduling method (RSM)
- Time-space scheduling method (TSSM)
- Time-location planning technique
- Time-distance planning
- Time-chainage planning
- French diagram
- March chart.

3. SCHEDULING SOFTWARE FOR LINEAR CONSTRUCTION PROJECTS

3.1 US Software

Not much software is commercially available in the United States (US) to support scheduling linear construction projects by using Linear Scheduling Methods. The programs that are available are more a graphical tool than a planning tool. Therefore, the American planners in linear construction projects are mostly using software available for CPM and Bar Charts.

Research has focused lately on developing software for linear scheduling. However, there are some major errors in the programs developed, which if solved will offer a powerful tool for planning and scheduling linear projects.

Not taking into consideration the site constraints, improper design of time and location axes, not considering the productivity rate of activities, lack of resource scheduling options, etc. are some of the major flaws observed on the software studied.

3.1.1. TransCon XPosition

TransCon XPosition is a linear scheduling software developed by TransCon Consulting, Ltd., (1997), a Richmond, Virginia based firm. This software is compatible with any computer that has Windows 95 or Windows NT operating systems.

The TransCon is more a drawing software because the user has to know for each activity, the start and the finish dates together with the start and finish locations (Figure 4). By using TransCon Xposition, it is possible to print or plot the schedule to any printing device supported by Windows 95. The user can also print the tabular activity data to be included with the schedule.

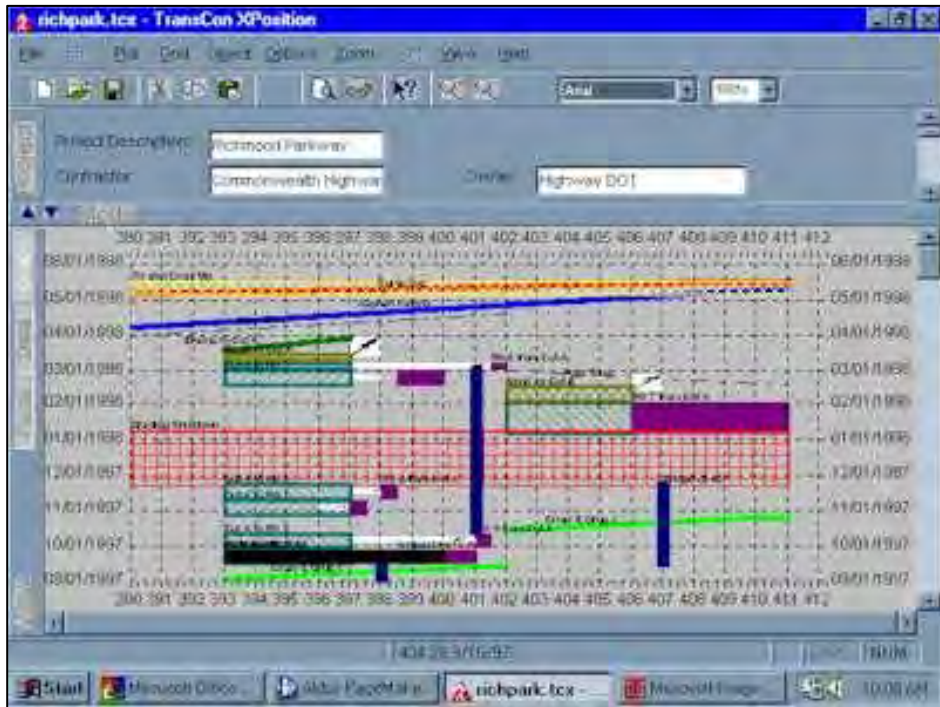


Figure 4 TransCon Xposition Output

3.1.2. Linear Construction Project Manager (LCPM V1.0)

LCPM V1.0 is a prototype of a planning and scheduling software for linear construction projects such as highways and pipelines. The software was developed as a tool to assist in performing the calculations required in using the Linear Construction Planning Model (LCPM), which is a model proposed by Sameh Monir El-Sayegh in his PhD. dissertation for planning and scheduling linear construction projects.

LCPM was developed using Microsoft Access 2.0. In order to ease the reference, storing and sorting capabilities and also the ability to link to other existing company’s information, a database structure is used to develop this prototype.

3.1.3. Florida Linear Scheduling Program (FLSP)

Florida Linear Scheduling Program (FLSP) is also a prototype software for planning and scheduling linear construction projects developed by a group of graduate students within the Department of Civil and Coastal Engineering at University of Florida [7].

FLSP has two functions: the first function is scheduling a specific linear construction project by using the Linear Scheduling Method and the second function is to perform resource management. The software has a user-friendly interface. Minimal knowledge of computers is needed to use FLSP. The output (Figure 5) capabilities of FLSP v1.0 are:

- Linear Schedule Graph
- Resource Histogram
- S-Curves

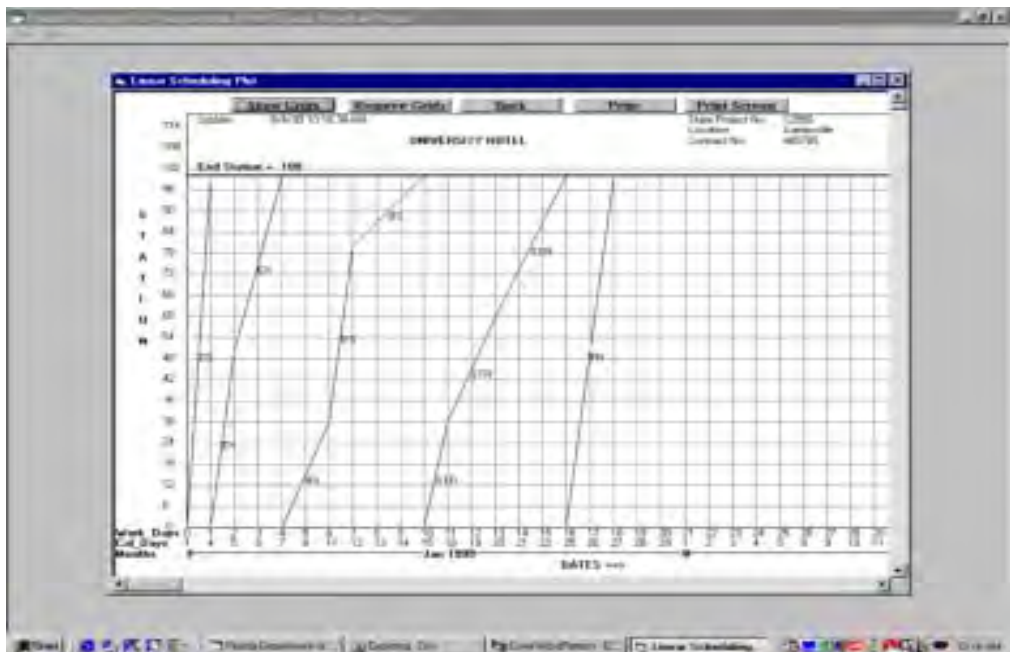


Figure 5 FLSP Screen

3.1.4. Purdue University Linear Scheduling Software (PULSS)

PULSS is also a prototype software developed within a Computer Aided Design (CAD) environment which allows the user to visually create linear schedules and calculate the controlling activity path (CAP – the equivalent of the Critical Path from CPM) [6].

One of the limitations of PULSS is that it cannot calculate the controlling activity path (CAP) if there is a time period where there is no activity being executed in the project. A second shortcoming of PULSS is that all activities are considered continuous for the CAP calculation.

3.1.5. LSCEDULER

El-Rayes developed in 2001 an object-oriented model for scheduling repetitive construction projects. LSCEDULER is implemented as a WINDOWS application that supports user-friendly interface, including menus, dialog boxes, and windows. LSCEDULER can be applied to perform regular scheduling as well as optimized scheduling. In optimized scheduling the model can assist in identifying an optimum crew utilization option for each repetitive activity in the project that provides a minimum duration or cost for the scheduled repetitive construction projects. LSCEDULER also integrates repetitive and non-repetitive activities [4].

The LSCEDULER model is implemented using C++ programming language that supports object-oriented modeling. The user interface of LSCEDULER incorporates menus, a tool bar, a status bar, dialog boxes, and multiple document interface windows (Figure 6). To perform scheduling calculations in LSCEDULER, the user needs to provide necessary input data at the project level and at the activity level including activity relationships.

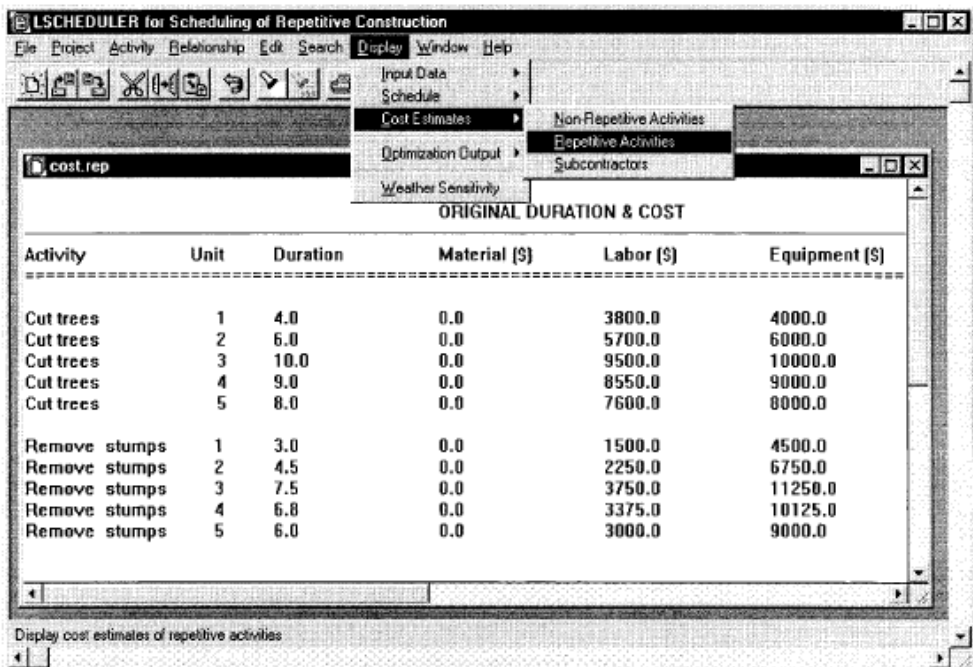


Figure 6 LSCEDULER Windows Application [4]

3.1.5. *Vico Software Control™ 2008*

Vico Software Control™ 2008 (marketed by Vico Software Inc., a Colorado based company) is a location-based scheduling program, which empowers rapid schedule creation for construction projects, developing clear and intuitive schedules (Figure 7).

At the basic level, the resultant project plan is able to control the flow of work production to further empower productivity improvements in production. Project management is improved with the innovative control and risk management of projects in progress.

The software is modular, with a growing range of additional functions. The current list of components includes:

- The Design mode;
- Risk simulation;
- Procurement;
- The Controlling mode;
- Micro management (must have The Controlling mode);
- Costs;
- Logistics (needs procurement);
- Quality & Prerequisites.

The Vico Software Control™ 2008 standard package includes Schedule Planning, Project Control, Procurement, and Risk Management. Advanced features include Micromanagement, Costs, and even Logistics and Quality [16].

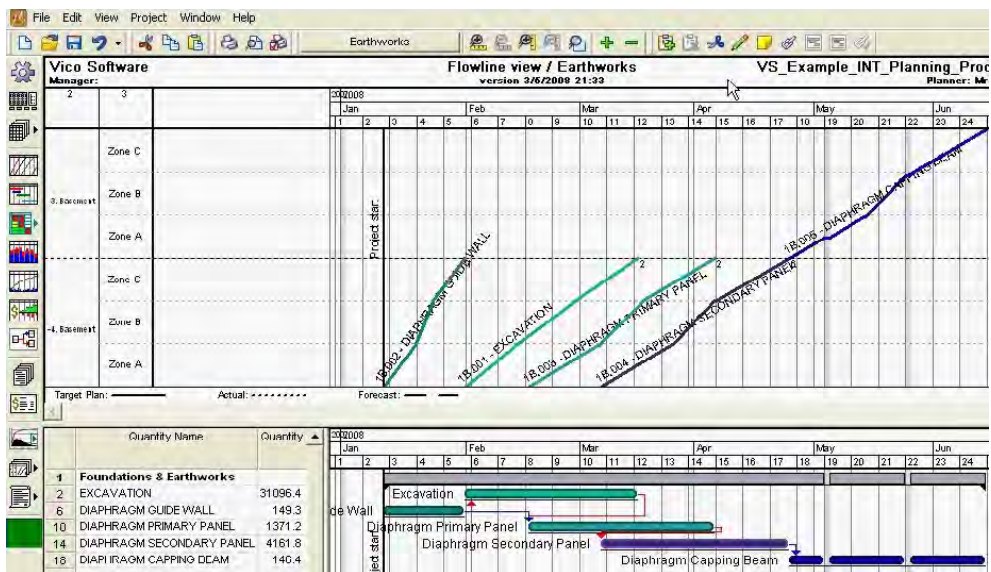


Figure 7 Vico Software Control™ 2008, Flowline & Bar Chart View

3.2 EU Software

In terms of scheduling software available for linear construction projects the European market seems to be a step ahead the American market. For the last ten years several high performing software that facilitates planning, scheduling and project control based on a time-location system have been developed and successfully implemented in many EU countries. The leaders in this area are Finland, UK, and Germany.

3.2.1. DynaProject™ /Control™

As a result of two decades of research and development, a comprehensive LOB based planning, scheduling and control system, has been developed and implemented among the main contractors in Finland [13]. The various functions of this planning, scheduling and control system were integrated in a commercial software package, originally named DynaProject™ (called Control™ in later versions) which empowers the Finnish LOB based system.

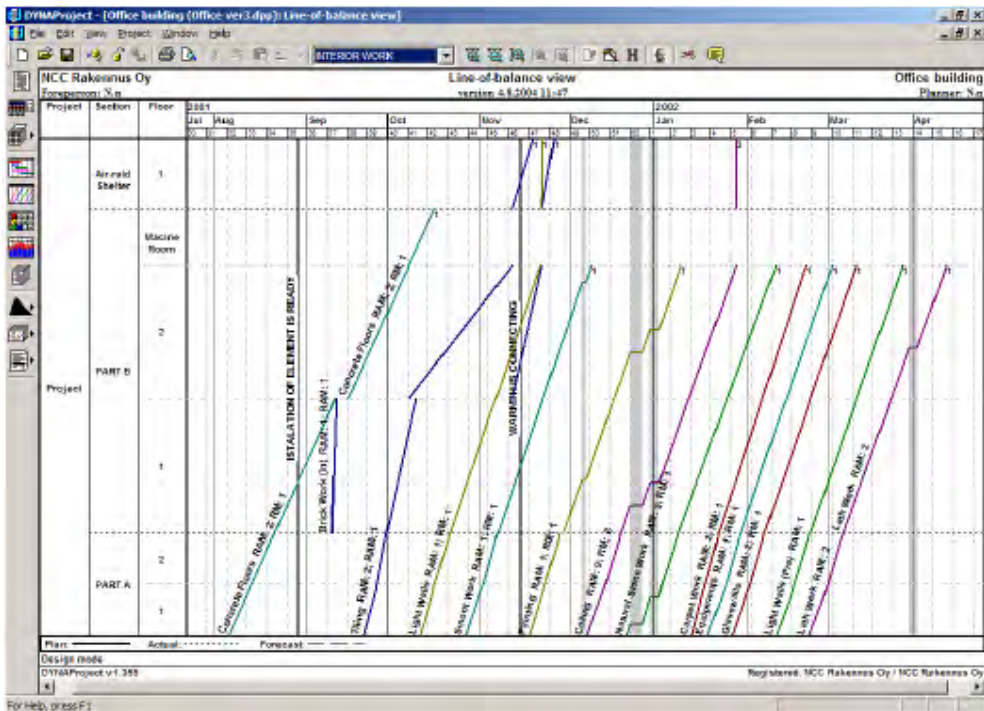


Figure 8 DYNAPROJECT Application

3.2.2. DynaRoad

The DynaRoad software has been in use since 2001. The technology is an innovative combination of years of construction research at Helsinki University of Technology, modern software and optimization technologies, and industrial customer-oriented development [3]. DynaRoad Schedule module combines mass haul plans with a resource based schedule with the help of automatic planning aid. The software uses a powerful Time-Distance View to complete construction plans.

The main key features of DynaRoad Schedule module are:

- Time-distance (Time-chainage) charts displaying multiple road lines
- Gantt view
- Automatic optimization tools
- Resource graphs
- Text reports on planned mass flow, work flow, and resource usage

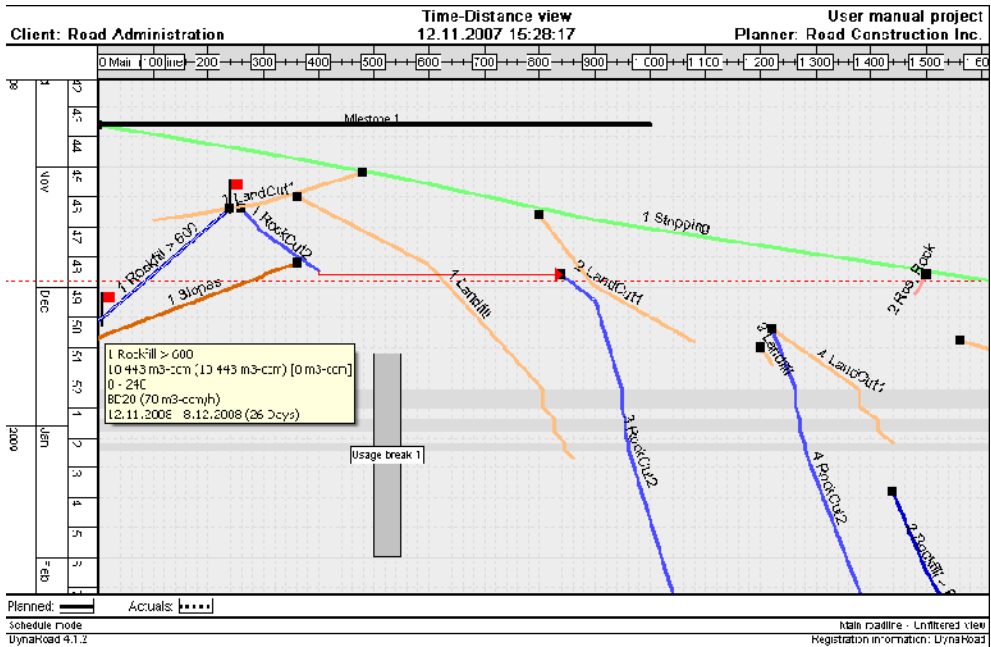


Figure 9 DynaRoad Application

3.2.3. LinearPlus Time Chainage Charts Software

LinearPlus was developed by PCF, a UK based company as an extension to another planning and scheduling software (QEI Exec) for TransManche Link, the group set up to construct the Channel Tunnel.

LinearPlus enables planners to create and modify Time Chainage Charts which are commonly used on linear construction projects because they display activities against both time and distance. One of the main benefits of this software is the fact it assists the management of work in confined spaces where typically only one operation can be performed at a time. Diagrams can be annotated with a wide variety of graphics, including site plans or custom symbols imported from CAD systems [10].

The system needs for LinearPlus are PC running Windows NT, 2000 or XP with at least 256Mb RAM and 30Mb free disk space.

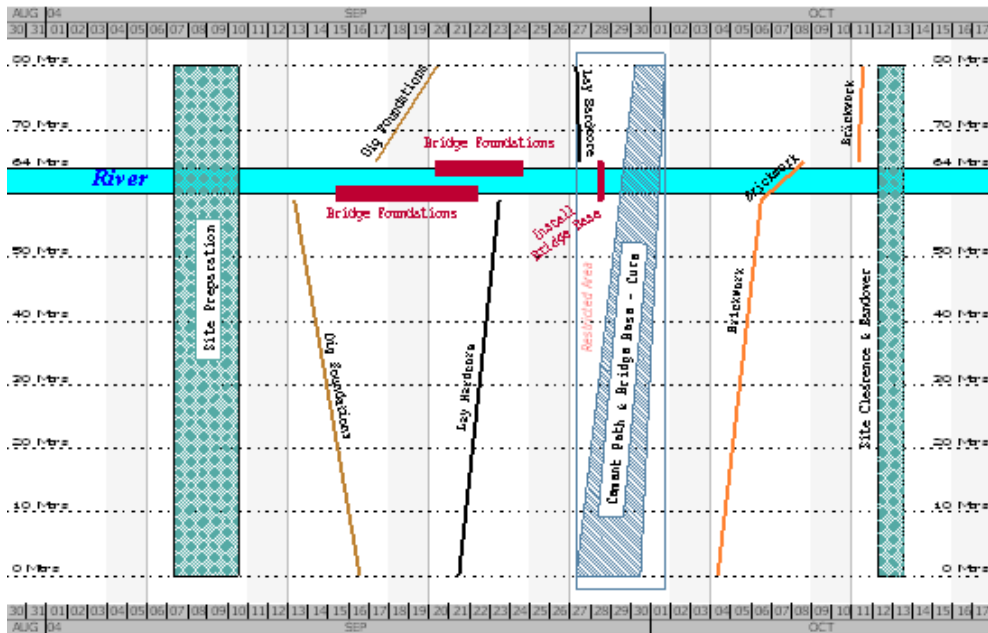


Figure 10 LinearPlus - Time Chainage Diagram

3.2.4. TILOS

TILOS is also a time-location planning software for managing linear construction projects developed by Asta Development GmbH, Asta Development plc’s partner company, based in Karlsruhe Germany. The first version of TILOS was launched in 1998.

TILOS visually displays project plans in terms of both time and distance by connecting the geographical information with the schedule enabling planners to clearly see the status of a construction project in terms of what needs to be done on each location and by when.

TILOS also combines the features of a drawing program with a project management system (including scheduling, resource and cost management). TILOS can exchange data with other scheduling systems including Microsoft Project, Primavera/P3, and Microsoft Excel [15].



Figure 11 TILOS Example of Road & Bridge Project

3.2.5. Spider Project

Spider Project is developed by Spider Management Technologies, a Russian company. The first version of Spider Project was released in 1992. Construction of Olympic Village for the International Youth Games in Moscow is particularly famous among the projects performed using Spider Project [14].

The software has features that cover all areas of construction management from resource constrained scheduling to risk analysis and simulation. The software provides a large variety of output graphics tailored to most users' needs (Gantt Charts, WBS, Network Diagrams and Linear Diagrams).

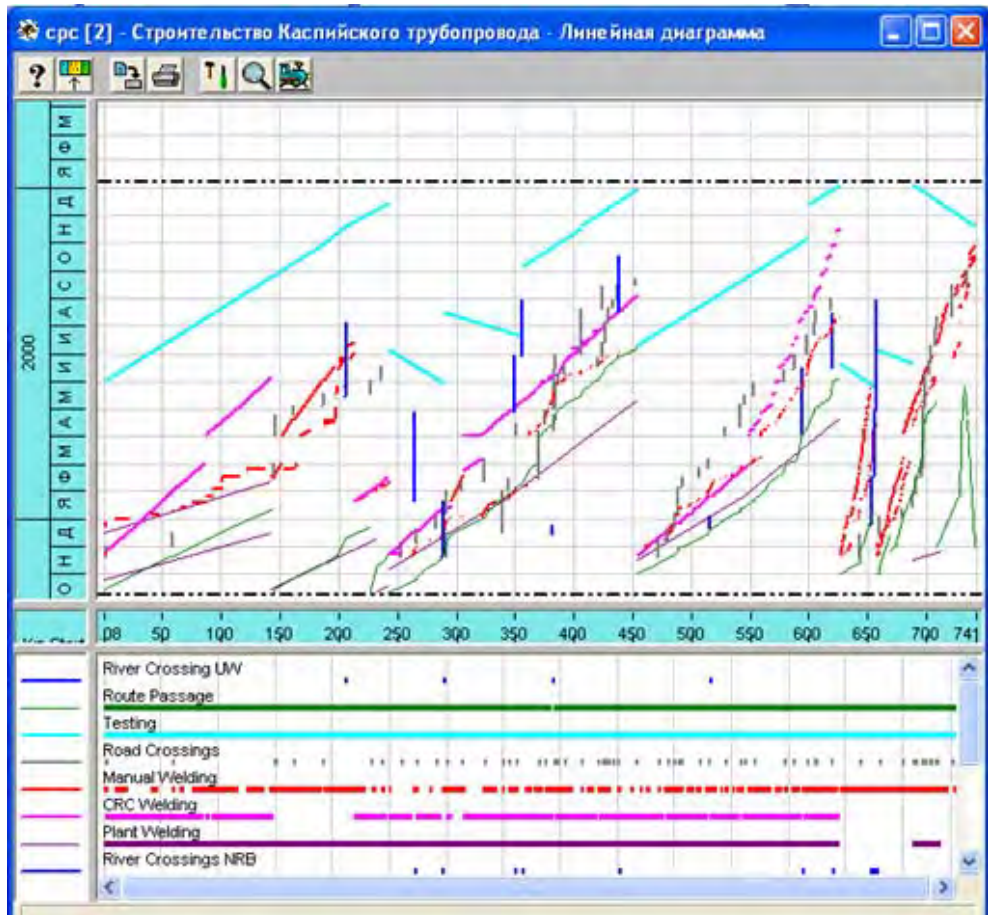


Figure 12 Spider Project Linear Diagram

3. CONCLUSIONS

The market for linear scheduling software has been on the rise constantly and aggressively for the past two decades. From prototype software developed as a result of academic research, the market has advanced today to offering high performing, highly visual, user friendly software which can satisfy the diversity of construction management needs of linear repetitive construction projects.

As the construction industry is moving from 2D CAD to 3D BIM, linear scheduling software can offer support and assistance to this trend. More training and knowledge transfer is needed to prepare the 21st century schedulers.

References

1. Adeli, H., Neural Network Computing Model for Highway Construction Project Scheduling and Management, *Ohio State University, Columbus; Ohio Department of Transportation; Federal Highway Administration*, 1999.
2. Defense Contract Management Agency, Line of Balance, <http://guidebook.dcmamail>.
3. DynaRoad Ltd., <http://www.dynaroad.fi>, 2006.
4. El-Rayes, K., Object-Oriented Model for Repetitive Construction Scheduling, *Journal of Construction Engineering and Management*, ASCE, Volume 127, Issue 3, pp. 199-205, 2001.
5. Handa, V.K., Barcia, R.M., Linear Scheduling Using Optimal Control Theory, *Journal of Construction Engineering and Management*, ASCE, vol. 112, no. 13, pp. 387-393, 1986
6. Harmelink, D., Yamin, R., Development and Applications of Linear Scheduling Techniques to Highway Construction Projects, <http://docs.lib.purdue.edu/jtrp/53>, 2001.
7. Herbsman, Z.H., Application of Linear Scheduling in the FDOT Construction Operation, WPI # 0510851, *University of Florida, Florida Department of Transportation*, 1999.
8. Ipsilandis, P.G., Multiobjective Linear Programming Model for Scheduling Linear Repetitive Projects, *Journal of Construction Engineering and Management*, ASCE, vol. 133, Issue 6, pp.417-424, 2007.
9. Kelleher, A.H., An Investigation of the Expanding Role of the Critical Path Method by ENR's Top 400 Contractors, *Master of Science in Civil Engineering Theses*, Blacksburg, Virginia, 2004.
10. LinearPlus Product Brochure, <http://www.pcfltd.co.uk/index.html>, 2006.
11. Mattila, K.G., Park, A., Comparison of Linear Scheduling Model and Repetitive Scheduling Method, *Journal of Construction Engineering and Management*, ASCE, vol. 129, Issue 1, pp.56-64, 2003.
12. Oberlender, G.D., Ahmed, S.A., Duffy, G.A., Linear Scheduling of Highway Construction Projects, *OTC Project No. 25*, 2005.
13. Seppänen, O., Alto, E., A Case Study of Line-of-Balance based Schedule and Control System, *Proceedings IGLC-13*, Sydney, Australia, pp.271-279, 2005.
14. Spider Project Presentation, <http://www.spiderproject.ru>, 2008.
15. TILOS Brochure, <http://www.astadev.com/software/tilos>, 2008
16. Vico Software™ Control 2008 Brochure, <http://www.vicosoftware.com>, 2008.

Cristina COSMA

PhD, EIT

Assistant Professor

cosmac@wit.edu

Department: Civil, Construction & Environment

<http://www.wit.edu/prospective/academics/overview.html>

Institution: Wentworth Institute of Technology

<http://www.wit.edu/index.php>

550 Huntington Ave

Boston, MA, 02115, USA

Numerical solution for unsteady Couette flow of viscoplastic fluids

Irene Daprà¹, Giambattista Scarpi¹

¹*DISTART, University of Bologna, 40136, Italy*

Summary

Many fluids which are of interest in engineering, as bentonite, slurries, fresh concrete, ceramic past, molten polymers, behave as Bingham fluids, i.e. fluids which present a yield stress. This paper investigates numerically the unsteady motion between two coaxial cylinders when the internal one rotates about its axis. The constitutive law of the fluid presents a discontinuity for zero shear rate, which introduces severe difficulties in solving any problem of unsteady motion, both analytically and numerically. A suitable way to avoid the obstacle is to regularize the constitutive equation using a smooth function to approximate the Bingham law: in this paper the suggested law is based on the error function. Different procedures of start-up and cessation of flow are examined numerically using an implicit finite difference method

KEYWORDS: Unsteady flow, viscoplastic fluids, viscosity regularisation, Couette flow.

1. INTRODUCTION

Viscoplastic fluids begin to move if a shear stress greater than a critical value (the so-called yield stress) is applied. After yielding, the rheological behavior is that of a Newtonian fluids, while in the unyielded region the materials behave as a solid body. The discontinuity at zero shear rate in the constitutive equation proposed by Bingham introduces severe difficulties even for computational solution of unsteady flows, whereas no analytical solution in closed form exists. To avoid the obstacle, *Glowinski* (1984) suggested to regularize the constitutive law: the discontinuous function can be replaced by a continuous one, which, when a given parameter tends to an assigned limit, usually zero or infinity, tends (at least in the sense of distributions theory) to the true Bingham law. Several models for regularization have been proposed in literature; one of the most used is that of *Papanastasiou* (1987). An interesting analysis of advantages and disadvantages of continuous models with exhaustive literature is given by *Frigaard & Nouar* (2005) and an important review on the numerical simulation of viscoplastic flow by *Dean et al.* (2005). Characteristic of a Bingham fluid is the fact that its stopping time is finite, whereas Newtonian fluids and generally fluids without yield stress need an infinite

time to stop. *Glowinski* (1974) and *Huilgol et al.* (2002) give a theoretical upper bound for the stopping time in pipe and plane flow. *Chatzimina et al.* (2005) study numerically the cessation of the plane and Poiseuille flow of a Bingham fluid using the Papanastasiou model, comparing the numerical results with the theoretical predictions. *Daprà & Scarpi* (2005) give an analytical solution to the start-up problem in a circular pipe; *Arefev* (2008) investigates theoretically the steady Couette flow of a viscoplastic fluid with a hydrolubricant on the inner cylinder.

This paper investigates numerically the start-up and the cessation of a Bingham plastic between two coaxial cylinders: the internal one rotates, the external is fixed. This geometrical outline is used for example in drilling, where viscoplastic fluids such as bentonite or montmorillonite cool the drill and reduce wear. The radius of the external cylinder is supposed less than a critical value, depending on Bingham number, so that the shear stress is everywhere greater of the yield stress and then the whole fluid between the cylinders moves. The constitutive law of the material is regularized with a rheological model based on the error function.

2. STEADY FLOW

A given incompressible viscoplastic fluid fills the gap between two coaxial circular cylinders: the internal one, whose radius is R_i , rotates whereas the external is fixed. Using cylindrical coordinates r, θ, z , the z axis being the cylinder axis, and supposing a laminar axisymmetric flow, the momentum equation can be written as

$$\frac{\partial \tau}{\partial r} + 2\frac{\tau}{r} = \rho r \frac{\partial \omega}{\partial t} \quad (1)$$

where τ is the shear stress, ρ the fluid density, ω the angular velocity and t the time.

The stress-strain equation for a Bingham fluid can be written as

$$\tau = \tau_0 \frac{\dot{\gamma}}{|\dot{\gamma}|} + \mu \dot{\gamma} \quad (2)$$

where τ_0 is the yield stress, $\dot{\gamma} = r \frac{\partial \omega}{\partial r}$ the shear rate and μ the viscosity.

The steady solution of (1) can be written as

$$\tau = \frac{c}{2\pi r^2} \quad (3)$$

where c is the torque applied to the rotating cylinder: the fluid moves if $|c| > 2\pi\tau_0 R_i^2$. If the radius R_e of the external cylinder is greater than $R_0 = \sqrt{\frac{|c|}{2\pi\tau_0}}$

the fluid is at rest for $R_0 \leq r \leq R_e$ and the flow is independent from the existence of the external wall: in this case, the solution is the same as if the internal cylinder rotates in an infinite mass of fluid. In this paper R_e is supposed to be less than R_0 .

By steady flow the angular velocity is

$$\omega(r) = a + \frac{b}{r^2} + \frac{\tau_0}{\mu} \ln \frac{r}{R_i} \quad (4)$$

where

$$a = \omega_1 - \left(\omega_1 + \frac{\tau_0}{\mu} \ln \frac{R_e}{R_i} \right) \frac{R_e^2}{R_e^2 - R_i^2} \quad (5)$$

$$b = \left(\omega_1 + \frac{\tau_0}{\mu} \ln \frac{R_e}{R_i} \right) \frac{R_e^2 R_i^2}{R_e^2 - R_i^2} \quad (6)$$

ω_1 being the angular velocity of the internal cylinder.

As usually, the Bingham number is defined, $Bn = \tau_0 R_i / \mu V$, where V is the mean velocity of the fluid. Being $q = \int_{R_i}^{R_e} r\omega(r)dr$ the discharge for unit length,

$$V = \frac{q}{R_e - R_i} = (R_e + R_i) \left(\frac{a}{2} - \frac{\tau_0}{4\mu} \right) + \frac{1}{R_e - R_i} \left(b + \frac{R_e^2 \tau_0}{2\mu} \right) \ln \frac{R_e}{R_i} \quad (7)$$

The Bingham number depends thus on the rheological parameters of the fluid and on the flow geometry. Introducing the dimensionless quantities $\eta = r/R_i$, $\eta_e = R_e/R_i$, $\eta_0 = R_0/R_i$, $\theta = \tau R_i / \mu V$, $\dot{\gamma} = \dot{\gamma} R_i / V$, $C = c / \mu V R_i$, $T = t\mu / \rho R_i^2$, $\Omega = \omega R_i / V$, $\Omega_1 = \omega_1 R_i / V$, $Q = q / V R_i$ equation (1) becomes

$$\frac{\partial \theta}{\partial \eta} + 2 \frac{\theta}{\eta} = \eta \frac{\partial \Omega}{\partial T} \quad (8)$$

If

$$Bn \leq Bn_{\max} = \frac{2(\eta_e - 1)}{(\eta_e^2 + 1) \ln \eta_e - \eta_e^2 + 1} \quad (9)$$

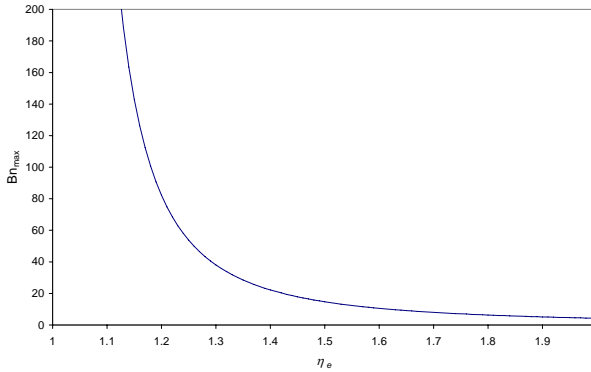


Figure 1 Relation between the external radius η_e and Bn_{max}

the motion concerns the whole fluid between the cylinders (Fig. 1) and the steady angular velocity Ω can be written as

$$\Omega(\eta) = A + \frac{B}{\eta^2} + Bn \ln \eta \tag{10}$$

where

$$A = -\frac{1}{\eta_e^2 - 1} (\Omega_1 + \eta_e^2 Bn \ln \eta_e) \tag{11}$$

$$B = \frac{\eta_e^2}{\eta_e^2 - 1} (\Omega_1 + Bn \ln \eta_e) \tag{12}$$

The dimensionless discharge becomes

$$Q = \frac{q}{VR_i} = \frac{V(R_e - R_i)}{VR_i} = \eta_e - 1 = \int_1^{\eta_e} \eta \Omega d\eta \tag{13}$$

Eq. (13) allows to correlate the angular velocity of the cylinder and the Bingham number (Fig. 2):

$$\Omega_1 = \frac{\eta_e - 1 - Bn \left[\frac{\eta_e^2}{\eta_e^2 - 1} (\ln \eta_e)^2 - \frac{\eta_e^2}{4} + \frac{1}{4} \right]}{\frac{\eta_e^2}{\eta_e^2 - 1} \ln \eta_e - \frac{1}{2}} \tag{14}$$

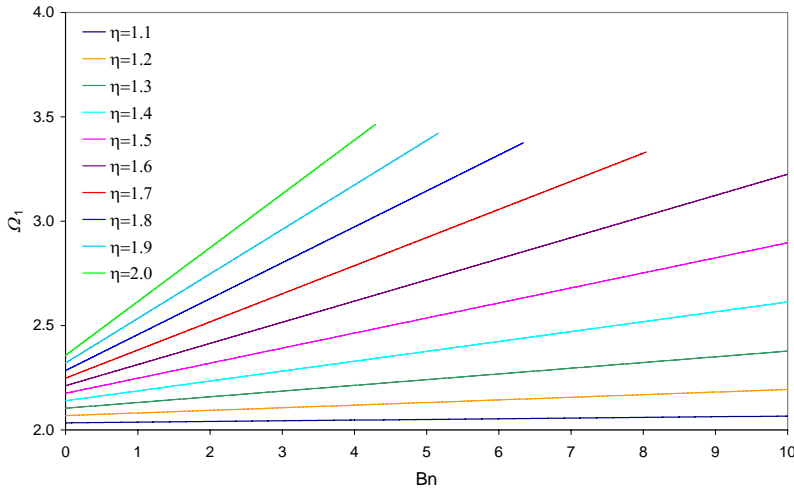


Figure 2. Angular velocity of the internal cylinder versus Bn for some values of η_e

The applied dimensionless torque C is

$$C = 2\pi\theta = 2\pi \left(-Bn + \eta \left. \frac{d\Omega}{d\eta} \right|_{\eta=1} \right) = -\frac{4\pi\eta_e^2}{\eta_e^2 - 1} (\Omega_1 + Bn \ln \eta_e) \quad (15)$$

3. UNSTEADY FLOW

The constitutive equation of Bingham fluids contains a singularity for $\dot{\gamma} = 0$ which can be overcome substituting the rheological law (2) with a suitable continuous function. A well fitting relation, continuous and infinitely derivable everywhere, is

$$\tau = \mu \dot{\gamma} + \tau_0 \operatorname{erf} (k \dot{\gamma}) \quad (16)$$

or, in dimensionless form

$$\theta = \dot{\gamma} + Bn \operatorname{erf} (K \dot{\gamma}) \quad (17)$$

where $K = \frac{kV}{R_i}$ and $\operatorname{erf} (x) = \frac{2}{\sqrt{\pi}} \int_0^x e^{-t^2} dt$.

If $K \rightarrow \infty$ eq. (16) tends to (2).

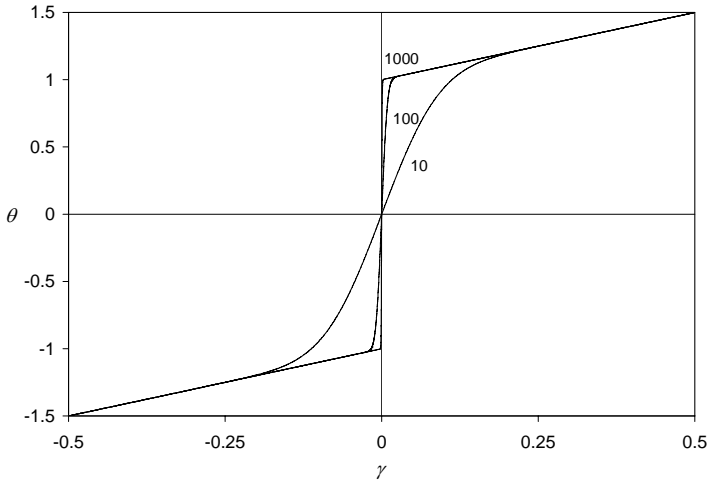


Figure 3. Regularized constitutive law

The rheological law (17) is plotted in Fig. 3 for $K = 10; 100; 1000$ and $Bn = 1$. Equation (8) becomes

$$\left[1 + \frac{2Bn}{\sqrt{\pi}} \exp\left(-K^2 \eta^2 \left(\frac{\partial \Omega}{\partial \eta}\right)^2\right) \right] \eta \frac{\partial^2 \Omega}{\partial \eta^2} + \left[3 + \frac{2Bn}{\sqrt{\pi}} \exp\left(-K^2 \eta^2 \left(\frac{\partial \Omega}{\partial \eta}\right)^2\right) \right] \frac{\partial \Omega}{\partial \eta} + \frac{2Bn}{\eta} \operatorname{erf}\left(K \eta \frac{\partial \Omega}{\partial \eta}\right) = \eta \frac{\partial \Omega}{\partial T} \quad (18)$$

which, with suitable initial and boundary conditions can be solved numerically.

3.1 Start-up flow

For a given Bingham number, two different procedures of start-up are examined:

a) The internal cylinder suddenly rotates with a fixed constant angular velocity Ω_1 which corresponds to an applied asymptotic torque C which can be evaluated using (14) and (15). Initial and boundary conditions associated to (18) are

$$\Omega(\eta, T) = 0 \quad 1 \leq \eta \leq \eta_e \quad T \leq 0; \quad \Omega(1, T) = \Omega_1 \quad T > 0; \quad \Omega(\eta_e, T) = 0 \quad \forall T$$

b) A constant torque $C > 2\pi Bn$ is suddenly applied to the cylindrical shaft. Initial and boundary conditions associated to (18) are

$$\Omega(\eta, T) = 0 \quad 1 \leq \eta \leq \eta_e \quad T \leq 0; \quad \Omega(\eta_e, T) = 0 \quad \forall T$$

$$\left. \frac{\partial \Omega}{\partial \eta} \right|_{\eta=1} = Bn - \frac{2\eta_e^2}{\eta_e^2 - 1} (\Omega_1 + Bn \ln \eta_e) \quad T > 0.$$

3.2 Cessation of flow

Although a Bingham fluid requires an infinite time to reach a permanent flow, it is supposed that the initial conditions are given by the steady solution (10):

For a given Bn , two possible ways for the cessation of flow are examined:

a) The shaft is suddely stopped

$$\Omega(1, T) = 0 \quad T > 0; \quad \Omega(\eta_e, T) = 0 \quad \forall T$$

b) The applied torque is suddenly removed, neglecting shafts inertia

$$\left. \frac{\partial \Omega}{\partial \eta} \right|_{\eta=1} = 0 \quad T > 0; \quad \Omega(\eta_e, T) = 0 \quad \forall T$$

4. NUMERICAL RESULTS

Equation (18) with appropriate initial and boundary conditions has been solved numerically using an implicit finite differences method. The considered values for Bingham number are $Bn = 1; 3; 5; 10$. The radius of the external cylinder has been fixed as $R_e = 1.5R_i$, i.e. $\eta_e = 1.5$. The maximum Bingham number which allows the whole fluid to move is $Bn_{\max} = 14.76$. An uniform spatial grid with step $\Delta\eta = 10^{-4}$ has been adopted. The time step suitable to avoid numerical instability is $\Delta T = 10^{-8}$ for the start-up and $\Delta T = 0.5 \cdot 10^{-8}$ for the cessation of flow. Numerical experiments indicated $K = 1000$ as a correct value of the parameter K in order to obtain valid results. For lower values the regularized equation does not sufficiently approximate the behavior of a Bingham fluid; if $K > 1000$ the numerical procedure needs smaller spatial and time steps, but the results are nearly the same. The steady theoretical velocity profiles and that obtained with the numerical solution differ less than 1%.

4.1. Start-up

For both start-up procedures the angular velocity as function of time has been evaluated at $\eta = 1.1$, which is representative of the behavior of the fluid. The two following results have been obtained:

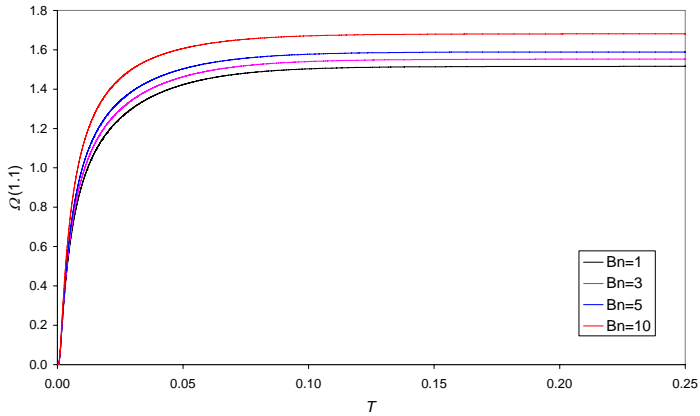


Figure 4. a): Angular velocity at $\eta=1.1$ versus time

a) Fig. 4 shows the angular velocity for $Bn=1;3;5;10$ as function of time. The corresponding values of the angular velocity of the shaft are $\Omega_1 = 2.248; 2.392; 2.536; 2.897$. The flow tends to the steady condition more rapidly the greater Bn is (theoretically the steady state is reached in an infinite time). Fig 5 shows the asymptotic angular velocity profile for the same Bingham numbers. For $Bn=10$, Fig. 6 illustrates the angular velocity profiles at some instants; at $T=0.25$ the fluid has almost reached the steady state.

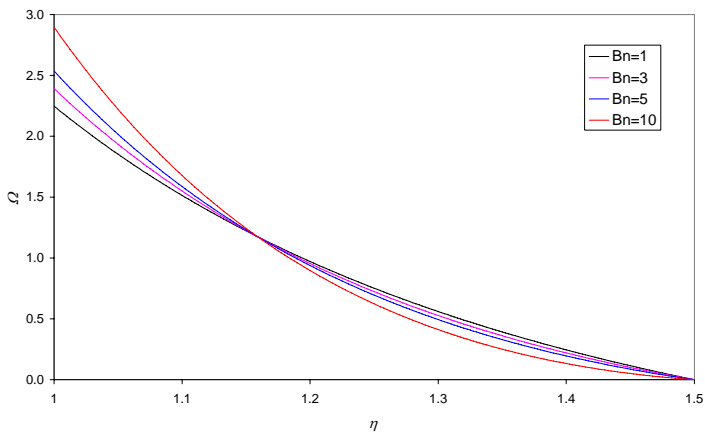


Figure 5. Asymptotic angular velocity

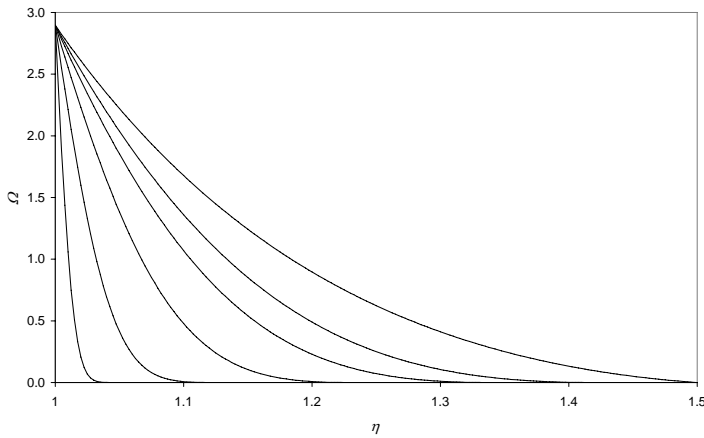


Figure 6. a): Angular velocity profiles at $T=6.25 \cdot 10^{-5}$; $6.25 \cdot 10^{-4}$; $3.125 \cdot 10^{-3}$; $9.375 \cdot 10^{-3}$; $1.875 \cdot 10^{-3}$; 0.25

b) Fig. 7 shows the angular velocity for $Bn=1; 3; 5; 10$ versus time. The corresponding values of the applied torque are $C = 60.01; 81.62; 103.22; 157.24$. The asymptotic profiles are obviously the same of case a). The steady state is reached more slowly than in case a). For $Bn=10$, Fig. 8 illustrates the angular velocity profiles at some instants; anyway, as $T = 0.5$ the fluid has almost reached the steady state.

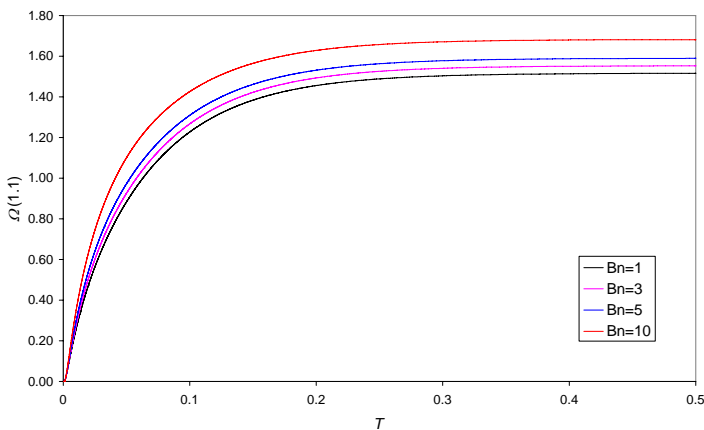


Figure 7. b): Angular velocity at $\eta=1.1$ versus time

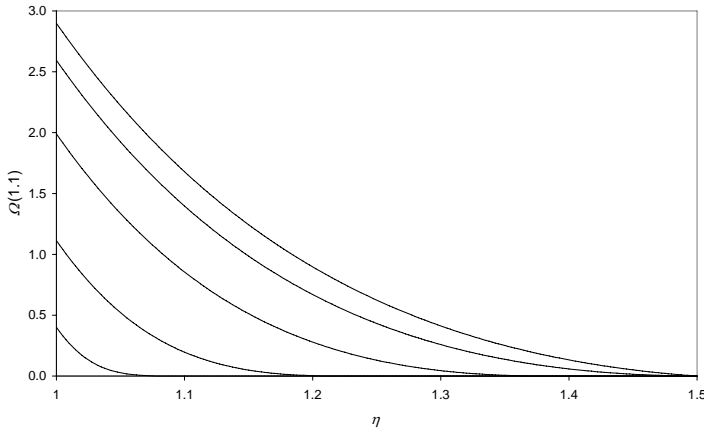


Figure 8. b): Angular velocity profiles at $T=6.25 \cdot 10^{-4}$; $6.25 \cdot 10^{-3}$; $3.125 \cdot 10^{-2}$; $9.375 \cdot 10^{-2}$; 0.5

4.2. Cessation of flow

Unlike Newtonian fluids and generally fluids without yield stress, which need an infinite time to stop, Bingham fluids require a finite stopping time T_s . *Glowinski* (1974) and *Huilgol et al.* (2002) gave a theoretical upper bound for T_s for pipe and plane flow. The angular velocity as function of time has been evaluated at $\eta = 1.2$ for the procedure a), whereas $\eta = 1.01$ is a more representative value for the procedure b).

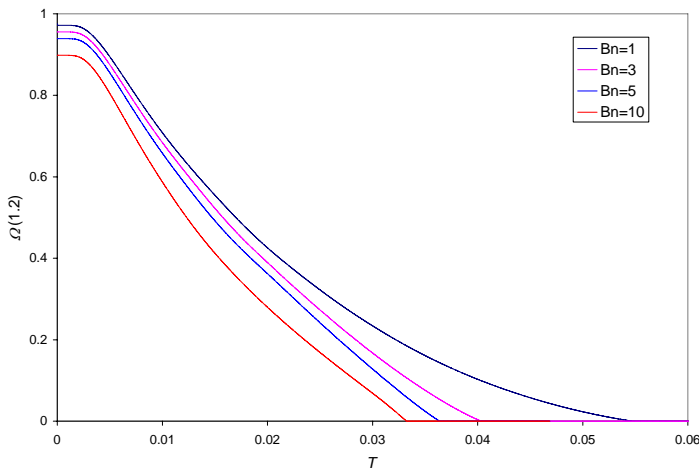


Figure 9. a): Angular velocity at $\eta = 1.2$ versus time

The following results have been obtained:

a) Fig. 9 shows the angular velocity $\Omega(1.2)$ for $Bn=1; 2; 3; 10$. As expected, Ω decreases the more rapidly the greater Bn is. Fig. 10 shows for $Bn=10$ the velocity profile at some instants. The flat region, where $\dot{\gamma} \approx 0$ becomes larger for increasing time.

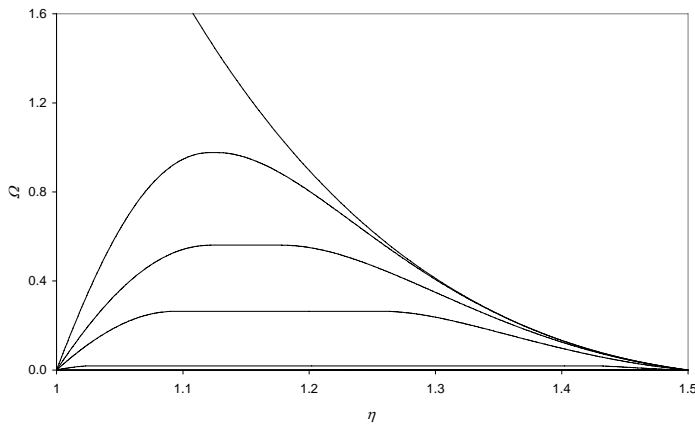


Figure 10. a): Angular velocity profiles at $T=0; 1.875 \cdot 10^{-3}; 3.75 \cdot 10^{-3}; 7.5 \cdot 10^{-3}; 1.5 \cdot 10^{-2}$

b) Fig. 11 shows $\Omega(1.01)$ for $Bn=1; 2; 3; 10$. As expected, Ω decreases the more rapidly the greater Bn is. Fig. 12 shows for $Bn=10$ the velocity profile at some instants. The time required to stop is significantly greater than in case a).

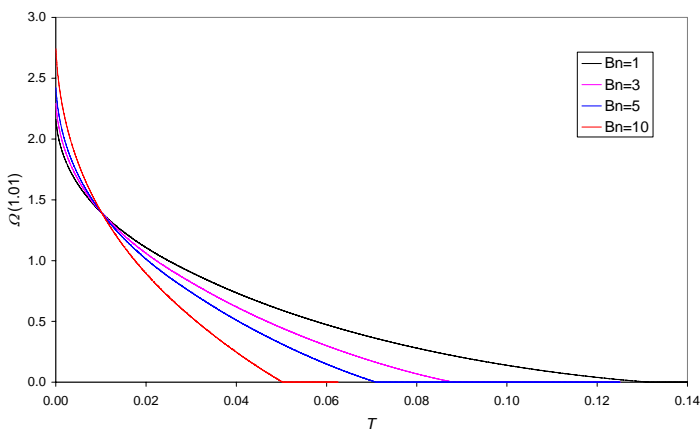


Figure 11. b): Angular velocity at $\eta=1.01$ versus time

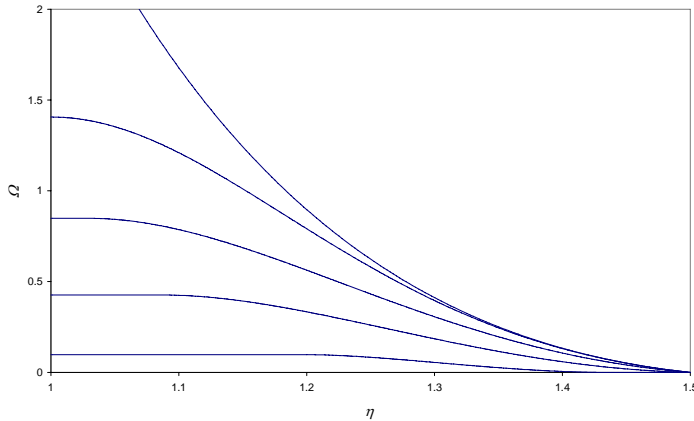


Figure 12. b): Angular velocity profiles at $T=0; 0.01; 0.02; 0.03; 0.04$;

5. CONCLUSIONS

The start-up problem and the cessation of flow of a viscoplastic fluid between two coaxial rotating cylinders have been analysed numerically. The momentum equation has been written using a regularized constitutive equation proposed by the authors, based on the error function. The computation has been carried out via an implicit finite differences method. A uniform grid with spatial step 10^{-4} and time step 10^{-8} for the start-up and $0.5 \cdot 10^{-8}$ for the cessation of flow have been adopted. Numerical experiments indicated that the value $K=1000$ for the rheological parameter K allows to obtain consistent results. In particular, the obtained results confirm that Bingham fluids require a finite time for stopping, unlike Newtonian fluids or generally fluids without yield stress.

References

1. Aref'ef, N.N., Free circular viscoplastic fluid flow with a hydrolubricant layer in the gap between coaxial cylinders, *Fluid Dynamics* 2008, (43) 1, 77-85.
2. Chatzimina, M., Georgiou, G.C., Argyropaidas, I., Mitsoulis, E. & Huilgol, R.R. Cessation of Couette and Poiseuille flows of a Bingham plastic and finite stopping times, *J. Non-Newtonian Fluid Mech.* 2005, (129), 117-127.
3. Daprà, I., Scarpi, G, Start-up flow of a Bingham fluid in a pipe, *Meccanica*, 2005, (40), 49-63.
4. Dean, E.J., Glowinski, R. & Guidoboni, G. On the numerical simulation of Bingham visco-plastic flow: Old and new results, , *J. Non-Newtonian Fluid Mech.* 2005, (142), 36-62.
5. Frigaard, I.A., Nouar, C. On the usage of viscosity regularisation methods for visco-plastic fluid flow computation, *J. Non-Newtonian Fluid Mech.* 2005, (127), 1-26.
6. Glowinski, R. Numerical methods for nonlinear variational problems, Springer-Verlag, New York, 1984.

7. Glowinski, R. Sur l'écoulement d'un fluide de Bingham dans une conduite cylindrique, *J. de Méc.* 1974, 13, 601-621.
8. Huilgol, R.R., Mena, B. & Piau, J.M. Finite stopping time problems and rheometry of Bingham fluids, *J. Non-Newtonian Fluid Mech.* 2002, (102), 97-107.
9. Papanastasiou, T.C. Flows of materials with yield, *J. Rheol.* 1987, 31 (5), 385-404.

Computational Aspects of River Hydraulics.

L. De Doncker¹, P. Troch¹, R. Verhoeven¹,
N. Desmet², K. Buis², P. Meire²

¹*Hydraulics Laboratory, Ghent University, Ghent, 9000, Belgium*

²*Ecosystem Management Research Group, University of Antwerp, Wilrijk, 2610, Belgium*

Summary

Research of river systems is expanding enormously. Therefore, the amount of needed measurements is also increasing rapidly. To limit this effort, computer modelling is an interesting tool. The environment 'Femme' ('a flexible environment for mathematically modelling the environment') is used to model ecological processes as the transport of nutrients and pollutants. Here, the hydraulic part, which is incorporated and based on the Saint-Venant equations, is used to check the influence of river roughness (expressed by the Manning coefficient) on discharges and water levels.

It is shown that the Manning coefficient of a specific river is influenced by the discharge and the amount of vegetation in the river. The variation of biomass over the year includes also a seasonal variation of the Manning coefficient. Next to good numerical approximation of the physical processes in rivers by good calibration, three sensitivity analysis are carried out.

First, the influence of the discharge on the water level is checked and in general, discharges are more sensitive to variations than water levels and are preferred as upstream boundary condition. Second, the influence of discharge and Manning coefficient on celerity and dispersion of waves is studied. Celerity and dispersion are larger when Manning coefficient or discharge is increasing. Third, it is shown that higher Manning coefficients can cause larger back watereffects and can consequently cause flood problems.

As a conclusion, the calibration of the Manning coefficient in any numerical model is indicated as very important to come to accurate results and realistic simulation of the hydraulic characteristics of the river.

KEYWORDS: ecosystem modelling, Manning coefficient, flood routing, vegetated rivers.

1. INTRODUCTION

Numerical modelling is an important discipline in the study of river hydraulics. Next to measurements, this branch of computer engineering is giving plenty of information regarding to water management. Measurement of velocities, discharges and water levels is fundamental in data collection of the river system, but in longer terms, predictions of inundations are required and numerical models are introduced in this science.

A large database is the first step in the study of river systems, it allows to get feeling with the field and to set up a model. Furthermore, the model can be calibrated and validated, using the dataset.

2. STUDY AREA

Focus of the study is the downstream part of the river Aa (Fig. 1), this is the stretch between weir 3 and weir 4, a distance of 1.4 km, near the village of Poederlee. In this area the interaction between groundwater, surface water and vegetation will be studied. Regular measurements of discharge and water level allow to gather data to calibrate the model. The catchment basin of the river Aa is situated in the region of Antwerp and is hydrographical part of the Nete basin. More than 40 % of the water in the Nete basin is going to the river Aa, which is although an important river. The river Aa flows into in the Kleine Nete near the city of Grobbendonk. The origin of the river Aa is found near the communities of Merksplas and Turnhout and is streaming through Turnhout, Gierle, Gielen, Poederlee and Vorselaar. The river Aa has a total length of 36.8 km and the drainage area is about 23,700 ha.

Hydraulic data as water levels and discharges are necessary, but also topographical data of the river bed and banks has to be collected. While carrying out velocity measurements in the river, the water depth and consequently, the bottom profile is registered. However, this is not sufficient to collect a useful topographical data set. Therefore, the study area of the river Aa is monitored in more detail. The stretch covers 1.4 km and every 50 m, a section is surveyed. So a set of 30 sections is available containing detailed information on the different cross sections and the bottom slope of the river. The cross sections are irregular due to the meandering aspect of the river. The average bottom slope (from upstream to downstream) is 0.0002 m/m. The monitoring results date from 1997.



Figure 1: The river Aa

2. MODEL CALIBRATION

2.1 Equations and Manning Coefficient

Using a numerical model to describe the river processes asks for model calibration. The measured discharges and water levels are used for the calculation of the roughness coefficient of the stretch, making use of the Bresse equation and the Manning equation. In general, hydraulic models for surface flow are based on the Saint-Venant equations for one dimensional unsteady open channel flow (Chow et al. 1988). These equations (continuity equation and momentum equation) are the one dimensional simplification of the Navier Stokes equations, which describe water flow in three dimensions. Starting from the values of the discharge and the water levels, the Saint-Venant equations allow for the calibration of the roughness of the bottom expressed by the roughness coefficient or friction factor.

Here, this roughness is represented by the Manning coefficient n and is calculated from the energy slope. For steady flow, the momentum equation is known as the Bresse equation (Eq. 1). In steady state conditions and assuming uniform flow, the energy slope is equal to the bottom slope and discharge, water levels and Manning coefficient are linked directly by Manning's equation (Chow et al. 1988). The roughness coefficient is determined out of the measurements. Channel flow is also connected with the hydraulic and geometric characteristics of the channel.

$$\frac{dh}{ds} = \frac{S_0 - S_f}{\sqrt{(1 - S_0^2) - \frac{Q^2 B}{gA^3}}} \quad (1)$$

$$S_f = \frac{fPQ^2}{8gA^3} \quad (2)$$

The Manning coefficient n is easily linked to the Bresse equation and the expression for the energy slope S_f (Eq. 2) by the roughness coefficient of Darcy-Weisbach f (Eq.3):

$$f[-] = \frac{8gn^2}{R^{1/3}} \quad (3)$$

$$n[m^{-1/3}s] = \frac{S_f^{1/2} R^{2/3}}{U} = \frac{S_f^{1/2} A^{5/3}}{QP^{2/3}} \quad (4)$$

with Q = discharge [m^3/s], U = average velocity [m/s], A = wetted cross section [m^2], B = channel width [m], P = wetted perimeter [m], R = hydraulic radius [m], g = gravity [m/s^2], S_f = energy slope [m/m], S_0 = bottom slope [m/m], h [m] = water height, s [m] = distance along the channel, n = Manning coefficient [$m^{-1/3}s$] and f = roughness coefficient of Darcy-Weisbach [-].

Although, the Manning coefficient can be used as calibration parameter. This roughness coefficient includes factors as the bed material and average grain size, the surface irregularities of the channel, channel bed forms, erosion and depositional characteristics, meandering tendencies, channel obstruction, geometry changes between channel sections and vegetation along the bankline in the channel (Dyhouse et al., 2003). The variable vegetational influence over the year is studied in the following.

2.2 Manning coefficient

So, the Manning coefficient is determined as more than only a calibration parameter, it is linked to the physical processes in the river.

The Manning coefficient can be seen as a constant value, which is a good and easy choice for the modeling of one short event (e.g. the simulation of discharge and water levels over a couple hours). Although, this is already doubtful due to the

relation between discharge and Manning coefficient. So, a constant Manning coefficient is an accurate value for baseflow simulations.

Longer events and peak flows have to be simulated using a variable Manning coefficient. The relation between Manning coefficient, discharge and biomass is plotted in Figure 2 and Figure 3 (De Doncker et al., 2007). In the following, it is shown that the Manning coefficient is an important parameter which has to be determined as accurate as possible to avoid wrong estimations and calculations of discharge and water level.

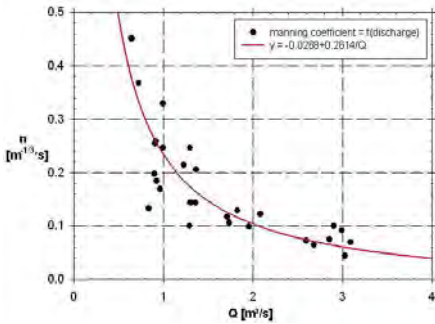


Figure 1: Correlation between discharge and Manning coefficient in the river Aa from September 04 to May 07.

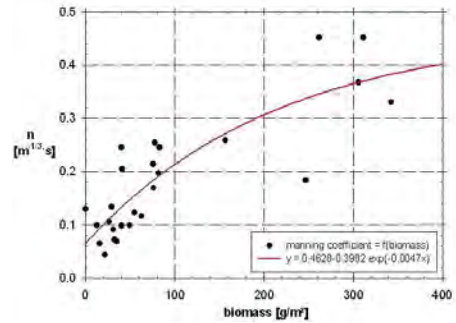


Figure 3: Calculated Manning coefficient and measured biomass in the period from September 04 to March 06 in the river Aa

The relation proposed in Fig. 3 is a good approximation of the measured values but Fig. 5 indicates next to the exponential also a sigmoidal approximation.

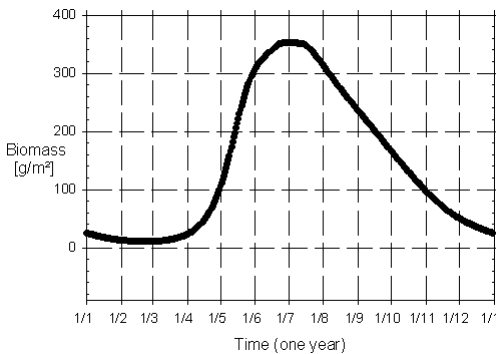


Figure 4: Variation of the amount of biomass over the year

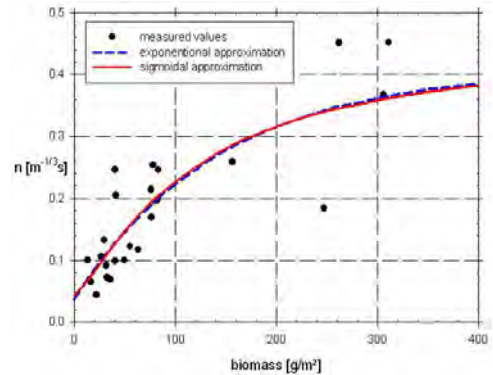


Figure 5: Correlation between biomass and Manning coefficient in the river Aa from September 04 to May 07 (exponential and sigmoidal correlation)

The Manning coefficient is calculated using Eq. 4 and the measured data. A numerical curve is fit on these values. Different possibilities are tested. Here, it was

clear that not only the mathematical accurateness is important, but also the physical interpretation. A well known relation is the exponential one (Fig. 3), the trend gives the most accurate correspondence between the continuous numerical curve and the values calculated out of the measurement. A sigmoid curve however, allows to follow the physical processes. First of all, no numerical instabilities occur, due to the fluent curve, while for the exponential trend the Manning coefficient for very low and very high amount of biomass is set on a fixed constant value and build in the model with a switch function.

Further, it can be seen that for low biomass, the Manning coefficient is determined by other characteristics as the river bed, the hydraulic characteristics, etc. Then, the resistance is increasing with increasing amount of vegetation. And, for very high values of the biomass, macrophytes are gathered in a patch and obstruction of the flow decreases again.

3. MODEL SENSITIVITY

3.1 Introduction

‘Femme’ or ‘a flexible environment for mathematically modelling the environment’ is developed by NIOO (Netherlands Institute of Ecology) (Soetaert et al. (2004)). ‘Femme’ is a modelling environment for the development and application of ecological time dependent processes by use of numerical integration in the time of differential equations. The program is written in Fortran.

‘Femme’ consists of a wide range of numerical calculations and model manipulations (as integration functions, forcing functions, linking to observed data, calibration possibilities, etc.). These technical possibilities allow the user to focus on the scientific part of the model and detailed research of the model without the confrontation with real program linked problems.

‘Femme’ is focused on ecosystem modelling, is open source (no black box) and exists of a modular hierarchical structure (implementation of different models next to each other). What was missing up till now was the implementation of a hydrodynamic surface water model to couple ecology and surface water in each timestep. For the study of the interaction of ecological processes and flow in the river, a realistic modelling of the surface water flow is necessary. Here, the implementation of a one dimensional hydrodynamic model for surface water flow in ‘Femme’ is reported.

With this ‘Femme’ model, some calculations are carried out. As a first verification of the model, a stretch of a river is modelled. The wave, measured upstream, has a

given hydrograph $Q(t)$. The hydrograph is derived from a gamma function. The resulting hydrograph at the downstream boundary is calculated next to the water levels over the stretch. The total length of the channel is 5000 m. The channel is rectangular, has a bottom width of 12 m and a bottom level of 8.89 m.

3.2 Influence of discharge on water level

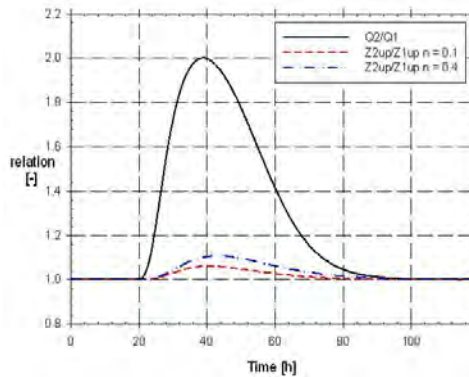


Figure 6: Influence of discharge on water level

In Fig. 6 the impact of the discharge on the water level is checked if the discharge increases. Two different hydrographs are chosen, $Q_1(t)$ and $Q_2(t)$. The relation between the basic hydrograph $Q_1(t)$ and the increased discharge $Q_2(t)$ is plotted and shows a peak value of 2. The impact on the water level, however, is much smaller and varies with varying Manning coefficient. For $n = 0.1 \text{ m}^{-1/3} \text{ s}$, the relation is 1.06, while for $n = 0.4 \text{ m}^{-1/3} \text{ s}$, the relation is 1.10. The impact on the water level is higher for a higher Manning coefficient. In general, discharges are much more sensitive to changes than water levels and therefore, upstream hydrograph values are preferred above water levels as a boundary condition.

3.3 Influence of discharge and Manning coefficient on celerity and dispersion of waves

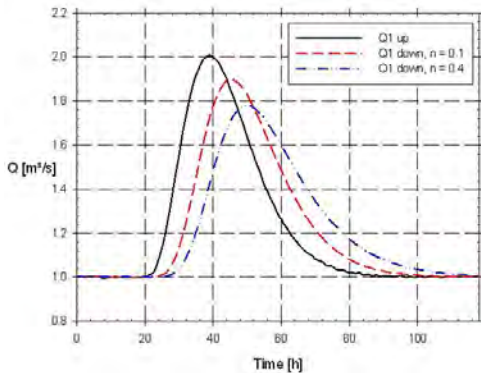


Figure 7: Influence of discharge $Q_1(t)$ and Manning coefficient on celerity and dispersion of waves

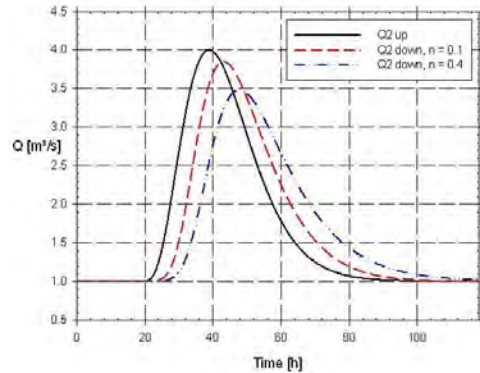


Figure 8: Influence of discharge $Q_2(t)$ and Manning coefficient on celerity and dispersion of waves

Figure 7 and Figure 8 show results for different hydrographs $Q_1(t)$ and $Q_2(t)$ with relation as mentioned in Fig. 6. The upstream hydrograph is a fixed boundary condition and the downstream discharge values are mentioned for comparison (Table 1). For both values of the discharge, it seems that the wave celerity (velocity by which a disturbance travels along the flow path) and the dispersion (tendency of the disturbance to disperse longitudinally if it travels downstream) (Chow, 1959) is larger for higher Manning coefficients (higher roughness). Furthermore, the wave celerity is larger when the discharge increases. This is according the continuity equation, agrees with larger celerities in streams with larger water levels (Verhoeven, 2006) and corresponds with the larger backwater effect for larger roughness coefficients. Not only the larger dispersion is an effect of the larger Manning coefficient but also the slower decrease of the wave is due to the higher resistance.

Table 1. Comparison of celerity and dispersion for different discharge and Manning coefficient

	Q_{up}	$Q_{down} (n = 0.1)$	$Q_{down} (n = 0.4)$
Q1	2	1.898 m	1.779 m
Q2	4	3.844 m	3.481 m
Q1	0	6 h	4 h
Q2	0	11 h	9 h

3.4 Influence of discharge and Manning coefficient on water levels

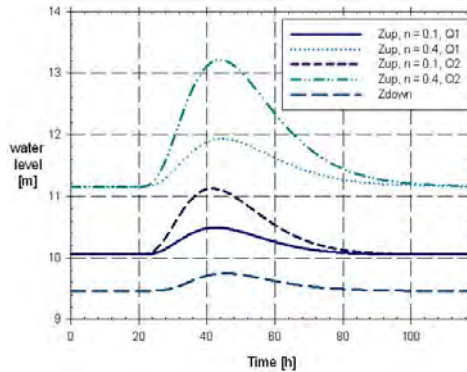


Figure 9: Influence of discharge and Manning coefficient on water levels

Fig. 9 depicts the back water effect which is higher for higher Manning coefficients and higher. It can be seen that peak flows (higher discharge) in summer situations (more vegetation and although higher resistance described by a higher Manning coefficient) can cause dangerous situations. When the height of the dikes is rather low, inundations will occur.

4. CONCLUSIONS

The importance of numerical modeling is well known. River research is based on data collection, but predictions and studies of inundations and floods ask for hydraulic software. The Femme environment allows modelling of ecological processes. It is shown that the hydraulic model can come up with quick and accurate results. Attention is paid to the importance of the Manning coefficient. This parameter is used as a calibration coefficient, taking into account the physical properties of the river processes.

Acknowledgements

This research is funded by the FWO (Fund for Scientific Research) - Flanders (G.0306.04). It is part of the multidisciplinary research project 'A fundamental study on exchange processes in river ecosystems' (University of Antwerp, Vrije Universiteit Brussel, Ghent University, 2004 - 2007). The overall objective is to study the physical and biological exchange processes in margins and inundation areas of water courses and how their interactions determine the exchange of water, dissolved compounds and particulate matter.

Thanks to Mr. Martin Van Daele and Mr. Stefaan Bliki for their assistance with the discharge measurements.

References

1. Abbott, M. B. et al., *Unsteady Flow in Open Channels*, Vol. 1, Ed. by Mahmood, K. and Yevjevich, V., 1975.
2. Buis, K., Anibas, C., Banasiak, R., De Doncker, L., Desmet, N., Gerard, M., Van Belleghem, S., Batelaan, O., Troch, P., Verhoeven, R. and Meire, P., *A multidisciplinary study on exchange processes in river ecosystems*, W3M, Wetlands: Monitoring, Modelling, Management, 22 – 25 September, Wierzba, Poland, 2005.
3. Cunge, J., Holly, F. and Verwey, A., *Practical aspects of computational river hydraulics*, Pitman Advanced Publishing Program, London, 1980.
4. Chow, V.T., *Open Channel Hydraulics*, McGraw-Hill, New York 1959.
5. Chow, V.T., Maidment, D. R., Mays, L.W., *Applied Hydrology*, McGraw-Hill, New York 1988.
6. De Doncker, L., Troch, P., Verhoeven, R., *Influence of aquatic weed growth on the flow resistance of the river Aa*, 6th FirW PhD Symposium, 30th November 2005, Ghent University, Belgium.
7. Soetaert, K., de Clippele, V., Herman, P., 'Femme', a flexible environment for numerically modeling the environment, Manual, NIOO-CEME, Yerseke, The Netherlands.
8. Verhoeven, R., Water beheer en waterbeheersing, course for civil engineers, part C: 'Afvoer en berging van water', 2006.

epiqr energy – A New Software For the Evaluation of Thermal Energy Consumption in Buildings

Adrian Doloca, Oana Țănculescu

Department of Mathematics and Informatics, University of Medicine and Pharmacy “Gr.T. Popa”,
Iași, 700115, Romania

Summary

The paper presents a new software instrument developed in cooperation with CalCon G.m.b.H. Germany for the evaluation of thermal energy consumption in residential buildings. It can be used by civil engineers and architects to calculate the necessary thermal energy for heating and warm water preparation for different scenarios: new building, refurbishment/modernization of an existing building, evaluation of an existing building for selling or renting, etc. The software is Windows compatible, was written in VB.NET and has the capability of working with Access Databases as well as with MS-SQL Databases. It has a user-friendly interface (presently only in German), it is easy to install and operate. The main functions of the program are: testing the existing buildings if they comply with the current energy consumption standards; optimization of a building energy performance, in the design phase, by analysing various solutions; evaluation of energy conservation measures applied on existing buildings; evaluation of the necessary energy resources at the national level by calculating energy consumption for representative buildings. A very important function is the generation of energy passports, resulting in a PDF file which is then printed out and signed by the issuer. The calculation of the energy consumption is based on German and European standards which will be adopted also in Romania and uses the simplified methods.

KEYWORDS: thermal energy consumption, energy passport, residential building.

1. INTRODUCTION

The building sector accounts globally for approx. 40% of the primary energy use in Europe, including Romania. As a consequence, it has an important contribution to the CO₂ discharges and to the economic balance at the country level but also at each building owner. Now, a series of laws and technical codes stipulate the necessity to establish the specific final energy consumption and to cut down this indicator from 200-250 Kwh/m²·a to about 75-120 Kwh/m²·a, if the energy is obtained from fossil fuels [1, 2, 3].

The building sector therefore stands in great need of practical instruments for energy consumption analysis to be used by the architects and civil engineers working for the:

- thermal rehabilitation of the old residential buildings, schools, hospitals, etc.;
- new building design.

The aim of our action, together with CalCon (an establishment of the Institute for Building Physics in Holzkirchen, Germany) was to develop a user friendly software adapted to the last requirements of technical codes in Germany and Romania.

2. EPIQR ENERGY SPECIFICATIONS

epiqr energy calculates the final and primary energy necessary for residential buildings based on the simplified methods described in the norms DINV-4108-6 and DINV-4701-10 [4],[5] (Figure 1).

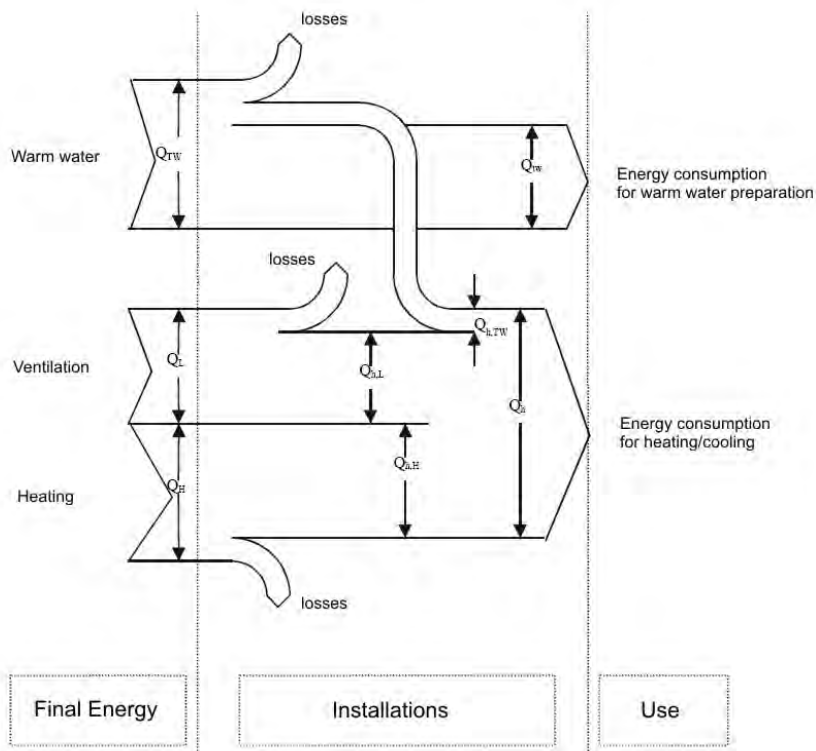


Figure 1. Energy flow for calculating consumption related to heating, ventilation and warm water preparation

For assessing the energy efficiency of a building, two approaches are used:

1. calculation of the necessary energy based on physical description of the building (envelope, installations, etc.);
2. calculation based on real fuel consumption over periods of one year.

The software has the following applications:

1. energy audit;
2. energy passport generation for new buildings or existing buildings in case of selling or renting;
3. testing the existing buildings if they comply with the current energy consumption standards;
4. optimization of a building energy performance, in the design phase, by analysing various solutions;
5. evaluation of energy conservation measures applied on existing buildings;
6. evaluation of the necessary energy resources at the national level by calculating energy consumption for representative buildings.

epiqr energy uses two databases:

- the catalogue database – contains fix information (constants) that describe transmission coefficients for different types of building elements, efficiency coefficients for installations, climatic data, etc. ([6],[7]);
- the project databases – contains information that is building dependant and is input by the user, for example: facade area, heated volume of the building, type of the heating system, ventilation system, etc.

3. EPIQR ENERGY OPERATION

The software is project oriented which means it is building oriented. The data input, the computation and the output of the results are building based and are independent from one building to another.

In the case of calculation of the necessary energy based on physical description, the input of the building data is done in several windows: general information, envelope description, ventilation, heating system, warm water production. For calculation based on real fuel consumption, the consumption over three periods must be input and they will be averaged to produce the final result (Figure 2).

Furthermore, an overview is displayed at first showing which information is complete (green bubble), which is partial (yellow bubble) and which requires input (red bubble) (Figure 3, a).

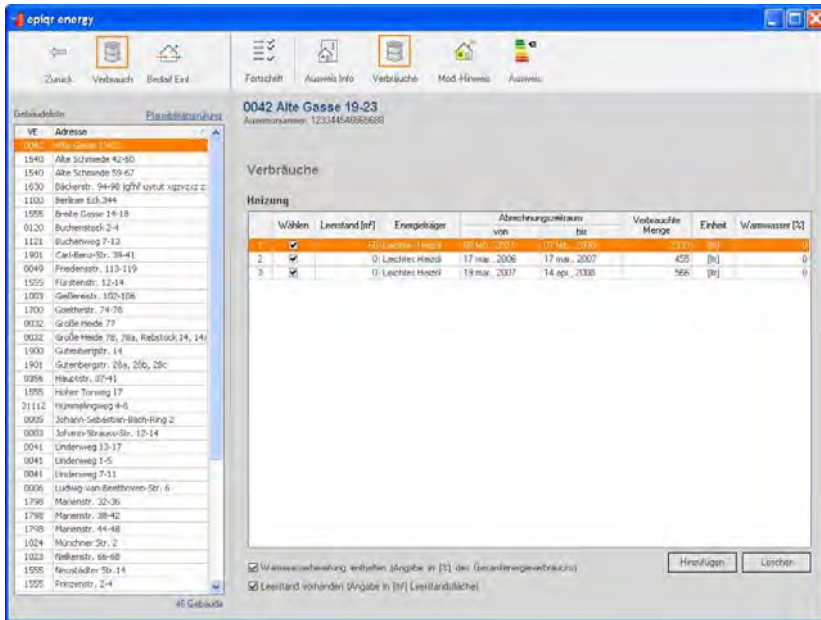


Figure 2. Data input for consumption based calculation

The general information section (Figure 3, b) contains a reference number, reason for passport generation, person that made the data acquisition, location of the building but also some geometrical data like heated volume, number of apartments, etc.

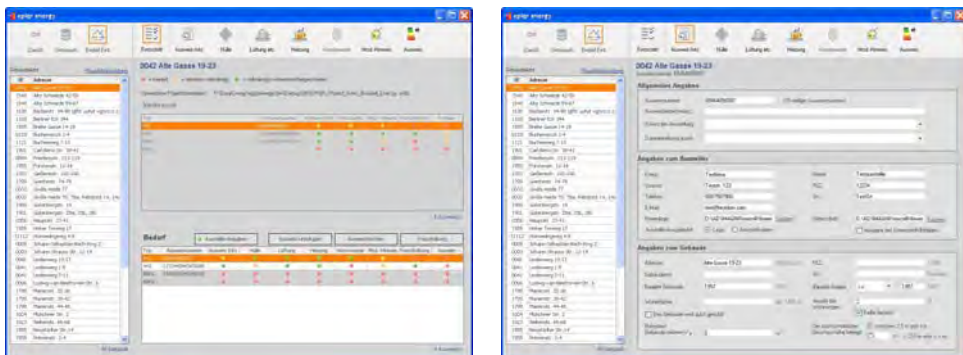


Figure 3. (a) Overview of the data input, (b) General information

The next section (Figure 4) collects the physical data in terms of surfaces of different building elements that make up the building envelope: roof, facade, floors, and windows. Areas and percentage of extra insulated elements are given.

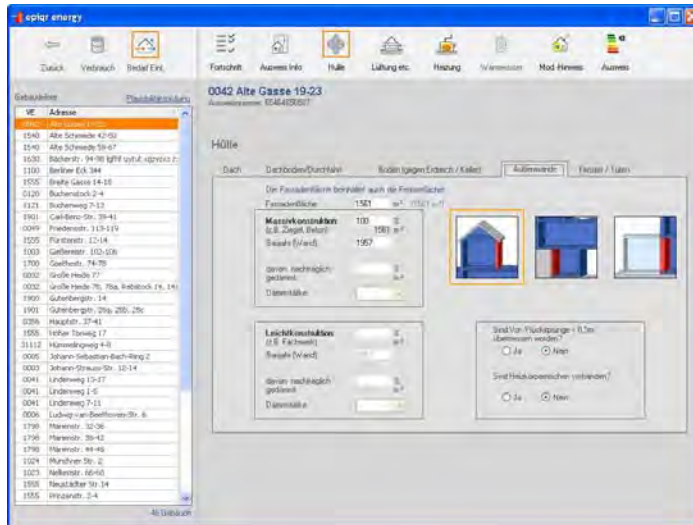


Figure 4. Envelope data

Figure 5 shows the module that describes the heating system. One can choose between predefined combination of heating and warm water production system or detailed description of the heating and warm water installations.

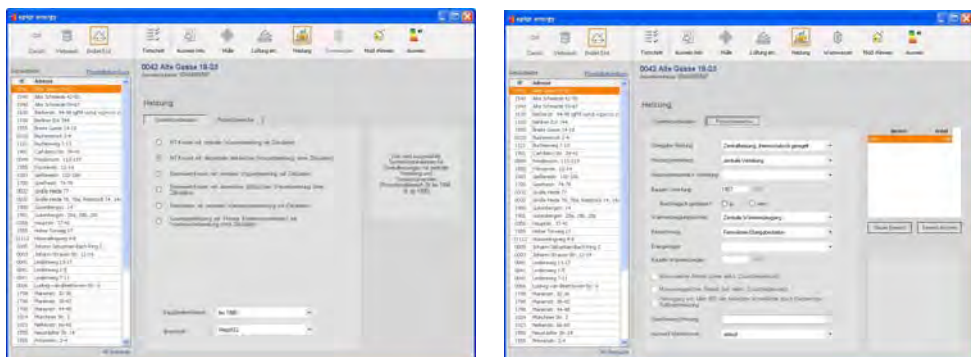


Figure 5. Heating system

The results page (Figure 6) displays the calculated final and primary energy and the specific transmission heat loss. They are given both in numeric form and graphical form by means of a color bar with colors ranging from green (energy efficient building) to red (energy inefficient building). From this page, the energy passport can be generated, using an external software module available from DENA (Deutsche Energie-Agentur) [8]. The passport is generated in the form of a PDF file ready to be printed out and signed (Figure 7).

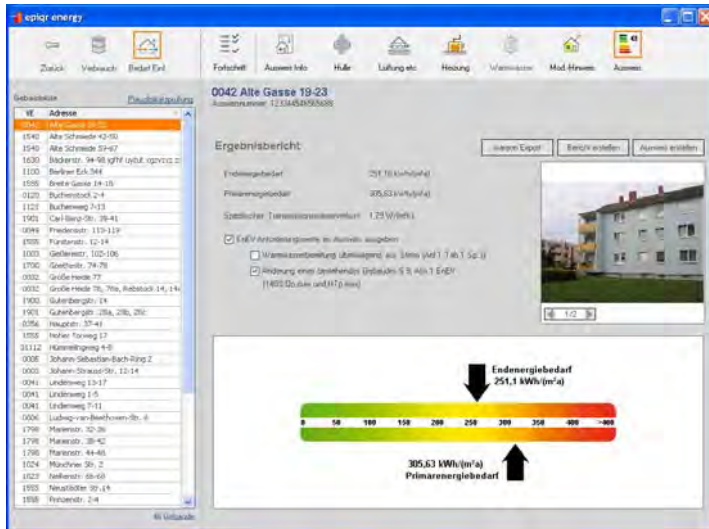


Figure 6. Results

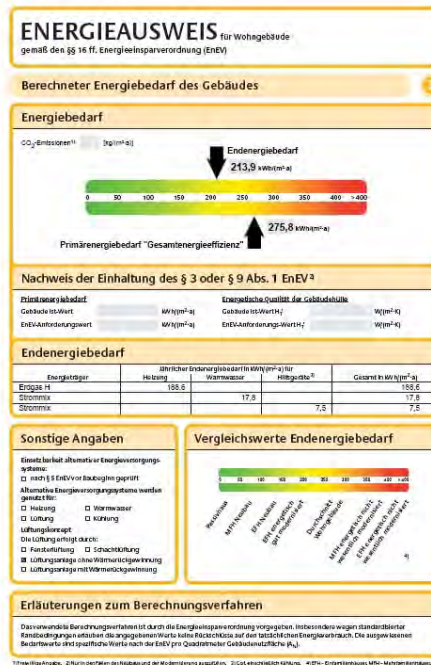


Figure 6. Energy passport

3. CONCLUSIONS

The epiqr energy software is a useful tool for the design of the new buildings as well as for the modernisation of existing buildings which are required to meet the present energy conservation standards. It meets the most recent German and European standards to which the Romanian standards also tend. It is flexible and user-friendly at the same time and is compatible with all Windows operating systems beginning with Windows 2000.

References

1. Arndt, H., *Wärme- und Feuchteschutz in der Praxis*, Verlag für Bauwesen, Berlin, 1996;
2. Radu, A., et. al., Satisfacerea exigentelor de izolare termica si conservare a energiei in constructii, Editura "Societatii Academice Matei-Teiu Botez", Iasi, 2003;
3. Norme românești: N-C-107/1-3, NP47,48,49;
4. DIN 4108-6 Wärmeschutz und Energie-Einsparung in Gebäuden, June 2003;
5. DIN 4701-10 Energetische Bewertung heiz- und raumluftechnischer Anlagen, August 2003;
6. Bundesministerium für Verkehr, Bau und Stadtentwicklung – Bekanntmachung: Regeln für Energieverbrauchskennwerte im Wohngebäudebestand, June 2007;
7. Bundesministerium für Verkehr, Bau und Stadtentwicklung – Bekanntmachung: Regeln zur Datenaufnahme und Datenverwendung im Wohngebäudebestand;
8. Deutsche Energie-Agentur Website energy passport generation download: <http://www.zukunft-haus.info/de/planer-handwerker/energieausweis/ausstellerbereich/software/dena-formularapplikation.html>

Problems with determination of degradation level of reinforced elements from fire affected constructions

Amos Dufka¹

¹ Institute of Building Materials and Components, Faculty of Civil Engineering, Brno University of Technology, 602 00 Brno, Czech Republic

Summary

Degradation of material as a consequence of synergistic action occurs at the fire affected reinforced concrete constructions of both physical (temperature shocks, expansion pressures of water steam etc.), and physically chemical mechanisms (decomposition of cement swage, modification changes in aggregate etc.). With regard to these facts it is obvious that correct judgement of state respectively measure of disruption of constructions interfered this way makes demands on measure of tests and analysis realised in the frame of constructional technical research. The article presented treats problems of diagnostic procedures indispensable for valuable judgement of state of fire-affected constructions.

KEYWORDS: degradation level of reinforced elements, fire, extreme temperatures, physical and physically chemical mechanisms, diagnostic procedures, state of fire-affected constructions.

1. INTRODUCTION

Fire is one of the factors that might be the cause of considerable failure on constructional objects and in extreme cases they might cause the collapse of the whole construction. It is possible to state generally that extreme temperatures connected with the outbreak of fire degraded building materials by contribution of both physical (expansion pressures of water steam, linear respectively volume changes etc.), and physically chemical principles (degradation of material swage, modification changes etc.). This synergy of negative mechanisms will be applied understandably in case of fire affected reinforced concrete constructions.

The fact that reinforced concrete elements are degraded in case of fire by contribution of different principles must be naturally taken into account while choosing diagnostic methods respectively while putting together the conception of constructional technical research whose aim is to judge succinctly the state of building respectively measure of damage caused by fire.

This article is focused on problems with choosing diagnostic procedures that are required for correct judgement of state of reinforced concrete constructions. It is possible to state that these problems (i.e. problems of diagnostic of reinforced concrete constructions affected by fire) are a scientific field that is somehow neglected nowadays by expert public.

One of the key aspects which is indispensable to accept while choosing diagnostic procedures whose aim is to judge the state of constructions affected by fire is taking into account the mechanisms that cause degradation of reinforced concrete. In this chapter, attention is drawn on principles of degradation of reinforced concrete.

2. THE PRINCIPLES OF DEGRADATION OF REINFORCED CONCRETE CONSTRUCTIONS IN ACTION OF EXTREME TEMPERATURES

We can summarise the negative effects in consequence of which failures may occur after the outbreak of fire, possibly entire loss of load-bearing capacity by the following:

Rapid growth in temperature occurs at the outbreak of fire, that is, the surface of construction is exposed to considerable changes of temperature. The speed of growing temperature of construction depends primarily on intensity of fire and character of construction. Destruction of concrete is a consequence of such shocking temperature stress when breaking of the surface concrete layers in thickness up to several centimetres occurs. This kind of failure is called as so-called "blasting of concrete" (spalling). The consequence of this type of failure is among others the fact that the top layer of concrete above the reinforcement was weakened; eventually the reinforcement is exposed to direct action of fire. A considerable heating of reinforcement occurs, accompanied by loss of its bastion, which can threaten in principle the structural analysis of the whole construction.

From the point of view of decrease of physically mechanical parameters of concrete on a basis of Portland cement, which occur as a result of action of higher temperature, the processes that occur in microstructure of cement swage have crucial importance. Mainly these facts are important:

The dehydrating of calciumhydrosilicates respectively calciumhydroaluminates occurs at temperatures up to c. 400°C. These reactions are to a certain extent reversible. The phases stated above do not create as a rule major binder component of cement stone.

The dissociation of portlandite in cement stone happens in the interval of temperatures 460 until 560°C. Portlandite is one of the materials that significantly affect binder capabilities of cement stone.

Modification change of silica that as a rule creates the majority part of concrete aggregate (gravel) occurs in temperature of concrete 573°C. Change of β silica to modification γ that happens at the temperature stated is accompanied by significant volume changes and is therefore a cause of genesis of considerable expansion pressures in the structure of concrete.

The decomposition of compact-grained calcium carbonate (that is, vaterite and aragonite) occurs in approximate range of temperatures 700-820°C. The dissociation of large-grained calcium carbonate (mainly calcite) occurs in the interval of temperatures c. 820-940°C. The modification of calcium carbonate belongs to phases that considerably influence adhesive force of cement swage.

It is obvious from the above stated that decrease of mechanical features of concrete exposed to extreme temperatures created by fire is caused by synergic action both physical principles (i.e. destruction as a consequence of “temperature shock”) and physically chemical processes that proceed in microstructure of concrete (i.e. decomposition of concrete swage, modification changes in gravel etc.). From the point of view of load-bearing capacity the changes in features of reinforcement respectively decrease of mechanical bond are very important.

Another aspect that can further increase the development of degradation of constructions evaluated is chilling during fire fighting.

3. DIAGNOSTICS OF FIRE AFFECTED CONSTRUCTIONS

In the previous text the fact was stated that mechanisms, which cause the development of degradation on reinforced constructions affected by fire, are not trivial. This reality understandably determines the fact that if the state respectively measure of degradation on reinforced construction affected by fire has to be judged correctly, a complex approach to this problem is indispensable.

A complex of activities whose aim is to judge succinctly the state of fire affected construction respectively judge the measure of degradation on reinforced constructions by extreme temperatures, can be designated as constructional technical research. Methodological approaches applied in the frame of diagnostics of constructions affected by fire, must be understandably adapted to character and state of construction. The following text is looking at the problems.

Visual inspection is a source of initial information about the extent of damage caused by fire and measure of disturbance of individual construction elements. In

the frame of visual inspection, the whole state of construction is evaluated primarily, that is, an inquiry is made if some of the elements collapsed, deviation from column is then watched in vertical elements, deflexion was watched in roof girders etc. (gained knowledge this way can be specified geodetically). Furthermore, in the frame of visual inspection, attention is directed on judgement on state of surface of individual elements (destruction of surface layers, presence of breaks etc.), disturbance of decking above reinforcement is watched, measure of bare reinforced steel etc. Gained knowledge in visual inspection enables us to gain source information about damage caused by fire that, understandably, must be completed and expanded in a considerable way for correct judgement of state of construction.

To judge succinctly the state of reinforced constructional elements, in the frame of constructional technical research, determinations are made whose aim is to monitor physically mechanical (that is, especially bastion) and physically chemical (i.e. especially the state of cement swage) parameters of concrete.

Physically mechanical parameters of concrete:

- Determination of compression strength – destructively on core holes (ČSN EN 12390-3) eventually non-destructively (for instance, ČSN 73 1373),
- Determination of bastion of concrete in simple tension (ČSN 73 1318),
- Determination of tensile strength of surface concrete layers (ČSN 73 1318),
- Determination of elongation modulus (ČSN 731371).

Physically chemical analysis

The aim of physically chemical determinations is to judge the state respectively measure of disturbance of cement swage of concrete, eventually to analyse the state of aggregate in concrete. It is possible to use these analyses in advantage for discovering of these facts:

- X-ray diffraction analysis (RTG analysis) – qualitative analysis whose aim is to determine mineralogical composition of swage, eventually aggregate. The procedure of this analysis is defined by methodological approach of VUT FAST in Brno, no. 30-33/1,
- Differential thermal analysis (DTA analysis) – quantitative analysis. Its aim is to quantify especially the volume of phases that create concrete swage. The procedure of this analysis is defined by methodological approach of VUT FAST in Brno, no. 30-33/1.

Another phenomenon that is also monitored in the frame of research of fire-affected constructions is the features of reinforced steel (tensile strength, characteristic strength).

The places for realisation of making tests respectively places of offtake of core holes are chosen as a rule the way that both the localities in which visual inspection proved obvious intensive affection of evaluated elements by fire would be involved and the places in which this disruption is not visible by visual inspection. The aspect applied when judging the state of concrete in separate elements is then comparison of characteristics monitored determined on samples taken in places markedly affected by fire and from constructions in which the traces of action of fire were not obvious.

Another criterion that can be taken into account when judging the state of constructions researched is comparison of features of concrete evaluated with facts declared by project documentation (mainly with declared concrete grade of bastion etc.).

4. THE PROBLEMS THAT COMPLICATE THE INTERPRETATION OF GAINED KNOWLEDGE

Problems of judging of the state of reinforced constructions affected by fire require a complex approach. While judging the state of real constructions, the facts can occur that can significantly complicate the interpretation of gained knowledge in the frame of constructional technical research. The best way will be to document this statement by experience and examples that were gained while evaluating of state of reinforced concrete constructions affected by fire.

We made a constructional technical research of one storey prefabricated reinforced concrete hall, created by prefabricated columns, beams and bearers, membrane roofing was then created by reinforced concrete TT panels. This hall was affected by fire.

Gained knowledge at visual inspection stated the fact that most of constructional elements of this hall (that is, columns, bearers and membrane roofing) was quite markedly struck by action of temperatures emerging during fire. A collapse of joining balks and membrane roofing occurred in some parts of the hall. Some of the joining balks did not collapse entirely, but their deflexion was considerable. There were a lot of cracks on joining balks. In some localities, decking of concrete on joining balks was entirely destructed and reinforcement was disclosed. Membrane roofing was also struck by significant failures. In localities where joining balks collapsed, a collapse of membrane roofing occurred understandably. There were places on columns in which traces of fire were striking, that is, it

concerns mainly destruction of decking above the reinforcement. Presence of cracks was also identified on columns. Some of the columns deviated from perpendicular, which could be seen already in visual inspection.

Gained knowledge in visual inspection were naturally completed by a complex of determination both physically mechanical and physically chemical characterisations of concrete. It is possible to summarize this knowledge by the following:

It was found that bastion characterisation of concrete evaluated range in very wide interval.

In localities where intense action of fire was obvious, tensile strength of surface layers was significantly in decrease and in some cases it actually equalled zero.

A rather different situation was found in case of compressive strength. In some elements in which evident traces after massive action of fire were detected by visual inspection, from the point of view of compression strength concrete corresponded with facts noted by project documentation. On the contrary, in some cases the compression strength of concrete was lower than concrete grade of bastion declared by project documentation. From the point of view of judgement of state of separate constructional elements the fact that in some cases decomposition of elements occurred during offtake of core holes was important too. Destruction of core holes was caused by presence of cracks in concrete. In the majority of cases these were cracks that on the surface of construction were only hair cracking, whereas in concrete, which creates the „inner mass“ of the element, their opening was wider. The decomposition of core holes during offtake occurred in some cases as well as when core holes were taken from components in which traces of action of fire were not visible in visual inspection.

The samples of concrete were put through physically chemical determinations that enable them to analyse their composition for judgement of measure of degradation. One of the aspects that was taken into account in evaluation of results of physically chemical analyses was comparison of gained knowledge for separate samples with results of analyses made on sample that was taken off collapsed joining balk, i.e. element that was very strongly affected by fire. It was stated that cement swage is very intensely degraded by action of high temperatures in samples taken off collapsed joining balks. Cement swage of these samples was practically wholly decomposed including phases of calcium carbonate. The modifications of calcium carbonate (calcite, vaterite, aragonite) are minerals that decompose in relatively high temperatures (c. 800 to 950°C). In this case the results of physically chemical analyses proved very intense destruction of cement swage and this fact entirely corresponded with very low bastion of concrete that was found. Intense development of degradation on cement swage by high temperatures was found as well in some other constructional elements. Generally, it can be stated that elements, in which the decomposition of cement swage was found, this fact was

accompanied by decrease (and as a rule very considerable) of bastion characterisation of concrete.

Indeed, the results of physically chemical analyses in some of the elements evaluated indicate a relatively low measure of degradation on cement swage by high temperatures, which did not respond to the results of physically mechanical determinations, when a considerable decrease of bastion parameters of concrete was found. This disproportion between gained knowledge by physically chemical analyses and results of tests of bastion characterisation of concrete can be justified by these principles respectively by their synergy:

- In consequence of “temperature shocks” emerging at the outbreak of fire respectively even while putting it out conditions for development and propagation of cracks are created in the structure of concrete. The cracks can also develop as a consequence of cumulation of water steam in the structure of concrete (spalling). The development of cracks can occur even in relatively low temperatures. These cracks do not result in significant changes in mineralogical composition of cement swage.
- The changes happening in aggregate, which creates filler in concrete, also take part in lowering of mechanical parameters of concrete. Aggregate with relatively high volume of silica was used in this case. Modification changes occur in increase of temperatures in this material (change of β silica to modification γ) accompanied by volume changes. However, these processes are reversible, that is, after lowering of temperature silica in modification β dominates absolutely again in the structure of concrete. It is obvious from the stated above that detection whether modification changes in concrete filler occurred as a consequence of fire is (with regard to reversibility of these changes) relatively difficult.
- In action of high temperatures on cement swage decomposition reactions of phases that create this swage occur. It is mainly the decomposition of, for instance, calciumhydrosilicates, ettringite, portlandite, phases of calcium carbonate etc. It was proved that some of these decomposition reactions are reversible in real time horizon. As an example of this fact, we can state repeated creation of portlandite in cement paste exposed in temperatures that go beyond the temperature of dissociation of portlandite.

5. CONCLUSION

This article treats diagnostic processes whose aim is to judge succinctly the state of reinforced concrete constructions struck by fire and especially securing the data for static judgement of constructions evaluated.

Generally, it can be stated that while monitoring the state of constructions struck by fire, de facto analogical characteristics are watched, as in case of constructional technical research of objects exploited in “common” conditions. Thus both physically mechanical parameters of concrete are watched (especially its bastion characterisation) and physically chemical analyses are made (with an aim to judge the state of cement swage) and the state of steel reinforcement is monitored as well. It is indispensable to respect mechanisms that caused destruction of reinforced concrete constructions evaluated (i.e. the fact that synergy of physical and physically chemical principles is the cause of creation of failures) for relevant interpretation of gained knowledge by a complex of these tests.

On the basis of knowledge found at evaluating of state of reinforced concrete constructions struck by fire, it is possible to state that one of the phenomenon which significantly takes a share in many cases on intense decrease of bastion characterisation of concrete, is creation and development of cracks. The creation of cracks is determined mainly by physical principles (as for instance, changes in temperature by shock, expansion pressure by water steam).

Another piece of knowledge which was gained in the frame of diagnostic procedures realised on fire affected constructions, is the fact that the quantity which very precisely describes measure of interference on reinforced concrete element by extreme temperatures, is tensile strength of surface layers of concrete.

Generally, it is possible to state that action of extreme temperatures significantly decreases tensile strength of concrete than compression strength is. This fact is caused by creation of microscopic cracks in cement swage, by creation of defects in the interface of swage – grains of aggregate etc. It is obvious that tensile strength of surface layers is a quantity which describes mainly the state respectively measure of disturbance in full the surface of element evaluated. We recommend unambiguously expanding the results of statement of tensile strength of surface layers of concrete by carrying out tests of concrete tensile strength (tests on core holes) for a more complex judgement of state of constructional elements.

Physically chemical analyses whose results in an effective way complete the gained knowledge by physically mechanical tests are an integral part of complex of analyses realised in research of reinforced concrete constructions struck by fire. It is possible to specify more closely the temperature at which separate elements were exposed and thus formulate an assumption about change of bastion parameters of

concrete on a basis of determination of mineralogical composition of cement swage in concrete etc.

Acknowledgements

The work was supported by by the MSM 0021630511 plan: Progressive Building Materials with Utilization of Secondary Raw Materials and their Impact on Structures Durability and MPO FT-TA3/148 project Research and development of surface Diagnostic of roads and highways. Project of maintenance and reconstruction for roads administrators in the Czech Republic.

References

- [1] E.L. Gluekler, Local thermal and structural behavior of concrete at elevated temperatures. In: *Transaction of the 5th International Conference on Structural Mechanics in Reactor Technology vol. A*, International Congress Center Berlin, Berlin, Germany (1979), pp. 13–17 H8/4
- [2] H.L. Malhotra, The effect of temperature on the compressive strength of concrete. *Mag. Conc. Res.* 18 23 (1956), pp. 85–94
- [3] Matoušek, M., Drochytka, R.: *Atmosférická koroze betonů*, (The atmospheric corrosion of concrete), IKAS Praha 1998,

Database-assisted seismic analysis of tall buildings subjected to long predominant period Vrancea earthquakes

Mihail Iancovici^{1,2}, Cristian Gavrilesco³

¹*Department of Mechanics, Statics and Dynamics of Structures, Technical University of Civil Engineering (UTCB), Bucharest, 020396, Romania*

²*National Center for Seismic Risk Reduction (NCSRR), Bucharest, 021652, Romania*

³*Kohn Pedersen Fox Architects (KPF), 13 Langley St., Covent Garden, London, UK*

Summary

Facing the new economic environment and public needs, there is an exploratory concern to develop modern tall building structures in Romania. The seismic hazard generated from the Vrancea source is the major concern for the practitioners, especially due to medium-soft soil conditions in the Bucharest-city. Tall buildings therefore might have the highest exposure to significant damage as well as economical and human losses.

The integrated seismic performance analysis system is an unitary format that allows (1) performing the seismic response analysis, energy balance-based analysis, fragility and seismic risk analyses, by using the time series of real/scaled/simulated earthquake ground motions and the induced effects (stresses, efforts, strains, displacements, velocities, accelerations, forces, energies), (2) the design of the structural elements and connections in a straightforward and transparent manner and (3) getting higher performance structures, safer and cost effective. This format becomes much more important in the case of irregular structures, having plan and elevation complex shape, in which the main directions of motion are not obvious.

The paper investigates the applicability of such procedure that makes it possible to estimate the earthquake-induced effects in tall buildings, at a higher level of automation and transparency. Seismic response analyses of a 60 story typical building subjected to long predominant period ground motions are conducted and the main results are emphasized.

KEYWORDS: tall building, database, bi-directional input ground motion, interaction formula, risk

1. INTRODUCTION

Achieving modern business and residential infrastructure in Romania is necessary especially in the capital-city Bucharest. The increasing interest of business community and population- according to the new financial environment, to use building structures located in dense urban areas, exposed to multi-hazard natural/artificial sources (repeated strong ground motions, wind, blast, impact, fire etc.), would lead to the completion of tall buildings having high performance, safer and cost effective.

The seismic hazard generated from the Vrancea source in Bucharest is the major concern for practitioners, especially due to medium-soft soil conditions. Tall buildings might have the highest exposure to significant damage as well as economical and human losses.

The modern Romanian construction practice is represented by medium-rise buildings (10~12 stories). The design practice, as well as the construction technology and execution work of high-rise complex structures is well behind other developed, seismic prone countries practice (U.S., Japan, China etc).

The structural analysis methods and procedures have considerably improved due to increasingly computational capabilities.

The objective of the paper is to introduce the database-assisted analysis concept and the advantages of using it in the practical seismic design of large scale structures.

2. TALL BUILDINGS: OVERVIEW AND CURRENT SEISMIC DESIGN PRACTICE

Tall buildings are symbols of cities, the certainty of economic growth, of the force and image of a civilization. In the last centuries, more than in any other historical period, important structures were built mainly due to the modern technology development. What is happening nowadays in the world it is unique and has no precedent.

Dozens of modern cities are erected like over the night in China and India. In the Middle East there is a frenzy of constructions. In Dubai, Qatar, Kuwait, an ocean of cranes is erecting towers, as higher as sophisticated. New airports, museums, stadiums, public spaces and complex transportation and telecommunication networks are continuously developing.

After years of stand-by in its own self-satisfactory historical conditions, Europe is cosmetizing its appearance with the most interesting concepts and urban developments known up to now.

United States is a model of the continuously changes in urban planning. Thus shortly after Chicago's supremacy in the battle over the sky, New York City takes the major role and produces one of the most innovative and beautiful tall buildings: *Woolworth Building* (arch. Cass Gilbert, 1913)- the tallest building in the world at that time, *Rockefeller Center* (arch. Raymond Hood, 1940), *Chrysler Building* (arch. William Van Alen, 1930)- a 319 m height famous art deco architectural example, *Empire State Building* (arch. Shreve, Lamb and Harmon, 1931)- the symbol of New York, 102 stories and 381 m height, for 41 years the tallest building in the world.

Today, from one to another side, the world is passing through the same phenomenal economic transformation. Naturally Romania must has not be out of this process, by seriously taking the initiative to develop super-tall buildings, integrated in modern urban developments.

The history of tall buildings in Romania begins in 1800, when the *Coltea Tower* ($H=50$ m) has been built and was destroyed by the strong earthquake of October 26, 1802 ($M_w=8.1$). In the modern era, the tallest reinforced concrete *Carlton Building* (14 stories) collapsed during the November 10, 1940 earthquake ($M_w=7.6$) and about 30 medium-rise buildings were destroyed at the March 4th, 1977 earthquake ($M_w=7.4$).

These important events have drawn the attention on the low accuracy level in reproducing real behavior of medium-tall buildings through standard design provisions. A summary of tall buildings built prior 2008 is given in figure 1 and table 1 (Iancovici, 2007).



Figure 1. Tall buildings in Bucharest, 2008

Table 1. Summary of tall buildings in Bucharest, 2008

No.	Building	Construction yr.	Height, m	Structure
1	Free Press Building	1957	104	reinforced
2	Tower Center	2007	100	steel
3	BRD Tower	2001	87	reinforced
4	The Parliament Palace	1986	86	reinforced
5	Bucharest Financial	1997	83	reinforced
6	The Intercontinental	1970	77	reinforced
7	Millennium Business	2006	72	steel
8	Charles de Gaulle Plaza	2006	70	steel

While currently the tallest building in Romania still is the *Free Press Building* (1975) in Bucharest, the world tallest building is the *Taipei 101* from Taiwan (101 stories, 508 m, including the telecommunication system), about five times the height of the tallest building in Romania. However *Burj of Dubai Building* is expected to be in 2008 the tallest building ever built (~940 m).

Due to the lack of design and construction practice of tall buildings (>180m), there is no enough evidence on how these structures will perform under strong ground motions in the Bucharest soil condition and other exposed cities to seismic hazard.

The seismic design standards do not provide details about the analysis and design of tall buildings. The standard structural design is done in terms of static equivalent seismic loads, obtained from the absolute acceleration response spectra. Little guidance is provided on using time series of ground motions-either recorded or artificially generated, structural 3D modeling etc.; full analyses procedures in the *time-domain* are not yet available in a standardized manner while the time-history analysis tool is mostly used for structural behavior checking purposes.

The *structural seismic performance concept* (SEAOC, 1995) consists of tuning the structural and the earthquake ground motion properties in order to obtain a predictable behavior associated to various pre-defined limit states (no damage, minor damage, serviceability, reparability, safety) with a higher level of accuracy, making use of vulnerability and risk analyses.

In the *Romanian seismic design standard P100-2006* (EC 8 format), a single level of performance is stated. This addresses to the ultimate limit state (i.e. life safety) and the prescribed peak acceleration of ground (*PGA*) is related to a 100 years mean return interval (*MRI*), having 10% probability of exceedance. Any other performance level is not explicitly stated yet.

For tall buildings however, the current analysis procedure may lead to an inappropriate performance, resulting in highly exposed to seismic risk structures. The response spectrum method approach has no the capacity to accurately

reproduce the high flexibility effect, structural mass and stiffness dissymmetry effect, damping distribution effect, geometric and physical nonlinear behavior, stability loss, the effect of non-structural elements interaction, of soil-structure interaction etc.

Therefore, a higher level of structural analysis and design format is needed, in order to more accurately predict the seismic performance, primarily using the large computational capabilities.

3. DATABASE-ASSISTED ANALYSIS AND DESIGN OF TALL BUILDINGS

Beginning with the *Moment distribution method* (Cross, 1930), continuing with the *Indeterminate coefficients method* (Filipescu, 1935), the *Direct stiffness matrix method* (Turner, 1958) and the effective computational algorithms based on the *finite element technique* (Courant, 1942; Clough, 1960), the structural analysis methods and procedures has considerably improved due to increasingly computational capabilities.

The integrated seismic structural performance analysis uses the concept called *database-assisted analysis and design*. Initially developed for the analysis and design of structures subjected to wind (Whalen et al., 2000; Simiu et al., 2003; Iancovici et al., 2003), the concept can be adopted successfully for the earthquake ground motion case.

This is an unitary structural performance analysis format that allows (1) performing the seismic response analysis, energy balance-based, fragility and seismic risk analyses, using the time series of ground motion and the induced effects (stresses, efforts, strains, displacements, velocities, accelerations, forces, energies), (2) the design of structural elements and connections in a straightforward and transparent manner and (3) getting higher performance structures, safer and cost effective.

While some of the input ground motion components are usually neglected, the actual format allows the use of large number of full sets of accelerograms.

Ideally, a structural system must have equal performance to earthquake ground motions from all possible directions, resulting a uniformly exposed to risk structure. For a class of structures however, e.g. having non-uniform plan and elevation mass and stiffness distributions, the main directions of motion are not obvious. In order to cover all the structural cases, an incremental directivity of ground motion is considered (Iancovici et al., 2006).

In a *3D modal superposition method* any number of vibration modes can be considered. The induced effects are expressed as time-series. There is no need to consider static load combinations.

The design of structural elements and connections is done in a straightforward and transparent manner, directly from the time-histories of efforts; there is no more need of making use of various rules for maxima superposition (e.g. “30% “ rule, SRSS, CQC, CQC3 etc.). The design is made by applying given interaction formulas (e.g. AISC-LRFD, EC3 etc.).

The use of complete sections databases allows the design with an improved level of automation. The distribution of material can be more efficient and economical.

This analysis format represents the decision support for structural type changing, of incorporating various seismic energy dissipation devices and techniques (active, semi-active, passive and hybrid) and for the assessment of the structural optimization need and effectiveness, as a higher analysis level.

The *integrated performance analysis system* deals directly with different classes of uncertainties in input ground motion and structural behavior. The use of a large number of data allows a full probabilistic assessment of structural performance, an appropriate approach from the point-of-view of implementing the performance concept.

This analysis format requires the use of:

- (a) *Input ground motion database*,

By using a large number of time-series of ground acceleration components, either recorded or artificially generated. The input motion is fully described through amplitude, frequency and phase content, duration, power and energy content, in both *time* and *frequency* domains.

The amount of significant records, from the structural point-of-view, provided by the two seismic observation networks in Romania (INCERC, about 166 accelerometers installed in free field, in boreholes and buildings, about 55 in Bucharest; INFP-18 seismic stations) is relatively small but offers important information for the synthetic accelerograms simulation. These can be obtained by realistically scaling/simulating a large number of sets of accelerograms or series of accelerograms (called “pulse trains”, Iancovici *et al.*, 2006) using available techniques (Gasparini *et al.*, 1976; Abrahamson, 2006).

Vertical and rotational component of the ground motion- mostly induced due to the non-synchronism of the spatial motion, can be simulated using similar techniques.

Such valuable information can be efficiently stored and represented using the GIS technology in the form of user-friendly databases.

(b) Structural systems models database,

Regarding the overall model, either a simplified one or a full FEM model.

The structural systems may be defined in terms of “classes”, consisting of dual systems: (i) moment resisting frames with braces – dedicated to medium heights range, (ii) central core and perimeter frames – dedicated to high-rise buildings and (iii) hybrid systems. The materials are usually high-strength reinforced concrete (60-120 MPa) and steel (800-1000 MPa). The constitutive laws of the structural elements are either analytical or experimental-based.

The effects of mass and stiffness plan and elevation dissymmetry can be primarily reproduced by the vibration modes correlation. One of the modes correlation descriptors is given by (Der Kiureghian, 1980)

$$\rho_{jk} = \frac{8\sqrt{\xi_j \xi_k} (\beta_{jk} \xi_j + \xi_k) \beta_{jk}^{3/2}}{(1 - \beta_{jk}^2)^2 + 4\xi_j \xi_k \beta_{jk} (1 + \beta_{jk}^2) + 4(\xi_j^2 + \xi_k^2) \beta_{jk}^2} \quad (1)$$

where,

ξ_j, ξ_k are the damping ratios corresponding to the vibration modes j and k , β_{jk} is the ratio of the natural circular frequencies of the j^{th} and k^{th} vibration modes.

The results of experimental tests on actual buildings damping properties, revealed the dependency of damping ratio by the natural vibration frequency and amplitude. Assigning a specific value of modal damping ratios can be made using various proposed empirical relationships (Jeary, 1986; Lagomarsino, 1993), code proposals or experimental databases (e.g. *Japanese Damping Database*). The experimental databases however allow a higher level of accuracy in assigning the damping characteristic.

By given knowledge on the site conditions, on the initial structural system and the pre-defined performance levels, the analysis and design will provide realistic solutions for the structural system (fig. 2).

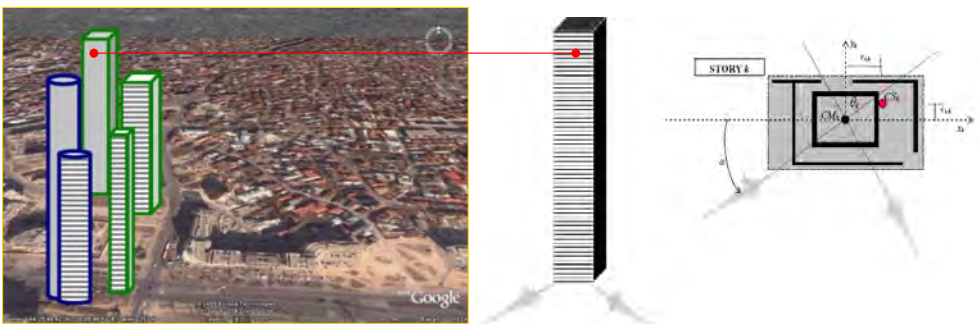


Figure 2. Tall building and typical story plan

Case study: in order to illustrate the applicability of the concept, a standard tall building is considered (fig. 2).

The building is a 60 stories reinforced concrete structure and has a typical story plan shown in the fig. 2. The plan dimensions are $L_x=30m$, $L_y=18m$ and the total height, $H=180m$.

For the sake of clarity, the model is assumed linear-elastic, having equal floor stiffness eccentricity in both directions -10% of radius of gyration, and 3 DOF/floor. A Rayleigh proportional damping model is used, the damping ratio for the first two translational vibration modes was assumed as 5%.

Using firstly a 30° directionality increment orthogonal accelerograms components, recorded on March 4th, 1977 at the INCERC Bucharest site, in all structural elements are obtained the instantaneous induced effects (stresses, efforts, strains, displacements, velocities, accelerations, forces, energies) expressed vectorial in the form

$$E_{e,k,s,\alpha}(t) = f(e, k, s, \alpha, t) \tag{2}$$

where e is the structural element, k - the story, s is the set of input motion components associated to a certain mean return interval of the earthquake ground motion, α is the directionality angle of the ground motion set and t is time variable.

The structural eigendynamics is summarized in table 2, through the natural periods and the modal correlation coefficients (eq. 1) for the first 12 vibration modes.

Table 2: Vibration modes correlation coefficients, ρ_{jk}

Mode	1	2	3	4	5	6	7	8	9	10	11	12	Tn,s
1	1.000	0.958	0.033	0.012	0.012	0.009	0.009	0.008	0.008	0.008	0.007	0.007	3.991
2	0.958	1.000	0.036	0.013	0.013	0.009	0.009	0.009	0.008	0.008	0.008	0.008	3.908
3	0.033	0.036	1.000	0.066	0.062	0.028	0.027	0.026	0.022	0.022	0.020	0.020	2.260
4	0.012	0.013	0.066	1.000	0.984	0.141	0.134	0.123	0.078	0.076	0.063	0.062	1.344
5	0.012	0.013	0.062	0.984	1.000	0.154	0.146	0.133	0.083	0.081	0.066	0.065	1.316
6	0.009	0.009	0.028	0.141	0.154	1.000	0.993	0.951	0.445	0.421	0.264	0.256	0.807
7	0.009	0.009	0.027	0.134	0.146	0.993	1.000	0.980	0.482	0.455	0.282	0.274	0.790
8	0.008	0.009	0.026	0.123	0.133	0.951	0.980	1.000	0.555	0.523	0.319	0.309	0.761
9	0.008	0.008	0.022	0.078	0.083	0.445	0.482	0.555	1.000	0.996	0.739	0.715	0.577
10	0.008	0.008	0.022	0.076	0.081	0.421	0.455	0.523	0.996	1.000	0.777	0.753	0.565
11	0.007	0.008	0.020	0.063	0.066	0.264	0.282	0.319	0.739	0.777	1.000	0.999	0.457
12	0.007	0.008	0.020	0.062	0.065	0.256	0.274	0.309	0.715	0.753	0.999	1.000	0.449

Considering the induced effects (2) in terms of shear forces, the time-histories in the x - and y - directions, corresponding to the 30° directivity angle of the input ground motions, in a column at the 10th floor, are given in the fig. 3.

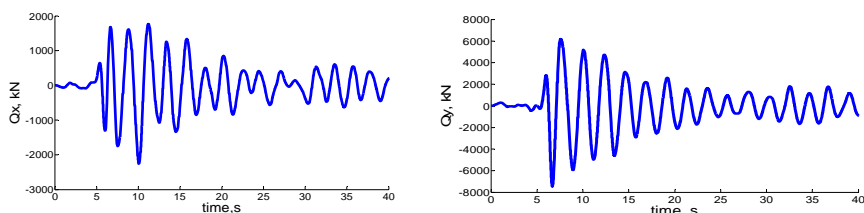


Figure 3. Time-histories of shears in the x - and y - directions in a typical column

In a similar way, all the time-histories of the induced effects (2) are obtained (efforts, displacements, velocities, accelerations, forces, energies).

The peaks of the base shear forces in the x - and y - directions in the same column are computed for all 12 directions of the input ground motion. Design values are obtained by practitioners and myriad standard structural analysis software, using common statistical peaks combination rules, e.g. *30% rule*, *SRSS rule* etc.

On the other hand, the time-history of the resultant shear force can be obtained by vectorial composition of time-instant of shears in the x - and y - directions. This is called the „exact approach”.

The analysis results are presented in the table 3.

Table 3: Design base shear forces in a typical column

Direction,deg.	QmaxX,kN	QmaxY, kN	Q30%	QSRSS	Qvect	Q30%/Qvect	QSRSS/Qvect
0	3463.646	11020.443	6769.779	10156.192	11193.529	0.60	0.91
30	2904.752	7811.405	5248.174	8158.876	8186.598	0.64	1.00
60	3260.544	10032.798	6270.383	10457.000	10152.069	0.62	1.03
90	3154.546	9260.352	5932.651	9782.908	9696.268	0.61	1.01
120	2939.764	8435.801	5470.505	8474.973	8526.183	0.64	0.99
150	3455.964	10523.778	6613.097	10650.323	10827.347	0.61	0.98
180	2732.178	7115.233	4866.748	7466.496	7326.798	0.66	1.02
210	3689.449	11319.372	7085.260	11905.469	11576.779	0.61	1.03
240	2685.088	6671.562	4686.557	7191.623	6897.677	0.68	1.04
270	3631.555	11369.439	7042.387	10240.517	11573.102	0.61	0.88
300	2784.443	7330.900	4983.713	7317.737	7505.929	0.66	0.97
330	3403.330	10670.601	6604.510	11161.437	10822.063	0.61	1.03

One can be observed that while for some directions the standard combination rules give severe un-conservative results, for others are providing conservative results. The underestimation using *30% rule* goes up to 40% for this case.

The distribution of the peaks design shear forces in a column on the building height, are presented in the table 4, for the 30° directivity angle, due to space limit, shown only for the first 25 stories.

Table 4: De sign shear forces in a typical column, on the building height, 30° directivity

Story	QmaxX,kN	QmaxY, kN	Q30%	QSRSS	Qvect	Q30%/Qvect	QSRSS/Qvect
1	2904.75	7811.41	5248.17	8158.88	8186.60	0.64	1.00
2	2844.20	7765.46	5173.84	7921.92	8002.48	0.65	0.99
3	2780.74	7761.44	5109.17	7695.02	7991.07	0.64	0.96
4	2714.36	7748.34	5038.87	7482.00	7971.25	0.63	0.94
5	2645.02	7725.10	4962.55	7284.30	7941.74	0.62	0.92
6	2572.87	7691.02	4880.17	7098.97	7901.69	0.62	0.90
7	2497.99	7645.61	4791.67	6923.05	7850.50	0.61	0.88
8	2420.61	7588.60	4697.19	6754.68	7787.75	0.60	0.87
9	2340.91	7519.99	4596.90	6592.17	7713.48	0.60	0.85
10	2259.19	7439.85	4491.14	6434.43	7627.64	0.59	0.84
11	2175.64	7348.46	4380.18	6280.59	7530.34	0.58	0.83
12	2090.55	7246.05	4264.36	6129.71	7422.07	0.57	0.83
13	2004.16	7133.06	4144.08	5980.78	7303.15	0.57	0.82
14	1916.71	7009.98	4019.71	5838.28	7173.99	0.56	0.81
15	1828.48	6877.36	3891.68	5697.00	7035.17	0.55	0.81
16	1739.69	6735.81	3760.44	5555.53	6887.37	0.55	0.81
17	1650.61	6585.87	3626.37	5413.95	6731.01	0.54	0.80
18	1561.49	6428.24	3489.97	5272.59	6566.97	0.53	0.80
19	1472.58	6263.57	3351.66	5131.93	6395.70	0.52	0.80
20	1384.18	6092.56	3211.95	4992.58	6218.14	0.52	0.80
21	1296.50	5915.81	3071.25	4855.23	6034.85	0.51	0.80
22	1209.85	5734.20	2930.11	4720.60	5846.54	0.50	0.81
23	1140.32	5548.26	2804.79	4589.34	5653.88	0.50	0.81
24	1083.23	5358.71	2690.84	4462.00	5457.48	0.49	0.82
25	1024.32	5166.13	2574.16	4339.04	5258.25	0.49	0.83

In this case too, the *SRSS rule* gives better estimation of the maximum design shear forces, but the „exact approach” has to be used for analysis and design.

Usually the seismic performance limit states are basically controlled through demand peaks of drift ratios for all the input directions considered, in the *x*- and *y*-directions (fig. 4).

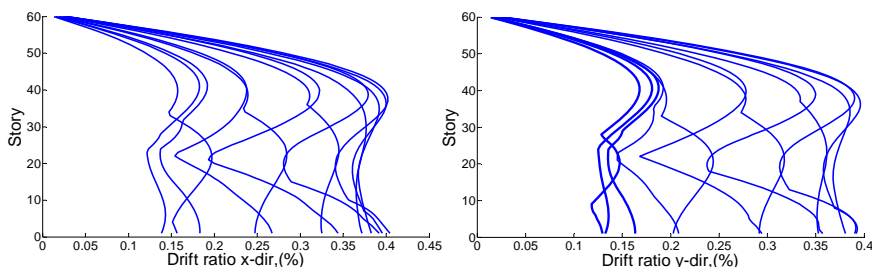


Figure 4. Peaks of drift ratios in the *x*- and *y*- directions, 12 input directions

There are a very limited number of records that can serve for the analysis format. Therefore a large number of artificial strong ground motion accelerograms were generated, with the aim of realistically reproduce similar amplitude, frequency content and duration as the real ones, recorded in Bucharest on soft soil conditions.

Artificial ground motions were simulated using the procedure described by Gasparini *et al.*(1976), who's response spectra match the 5% damped elastic acceleration response spectra, given in the Romanian seismic design code P100-2006 (fig.6).

A set of 10 synthetic bi-directional accelerograms having peak ground accelerations of 0.24g, associated to 100 years *MRI*, low predominant frequencies and small frequency bandwidth (Cartwright & Longuet-Higgins) were obtained and used in analyses. Typical orthogonal artificial accelerograms are presented in the fig.5.

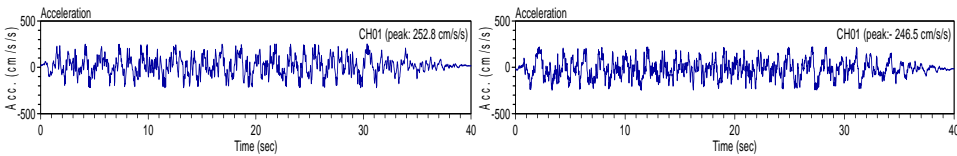


Figure 5. Typical bi-directional artificial input ground motion accelerograms

For the considered input set, the code-based and the computed normalized acceleration spectra and the corresponding normalized power spectral density functions (*PSD*) as well, are shown in the fig. 6.

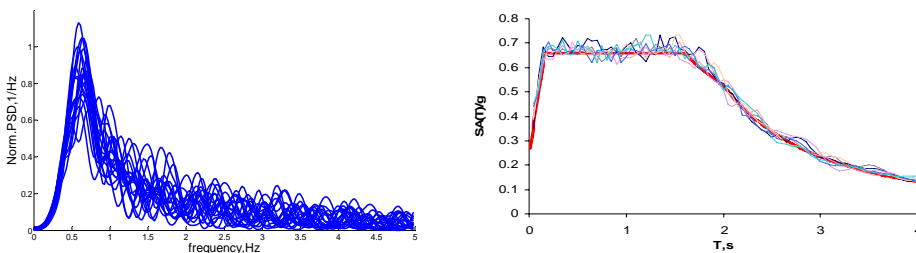


Figure 6. P100-2006 code spectra compatible accelerograms and corresponding normalized PSD functions, 10 sets of artificial accelerograms, PGA = 0.24g, MRI = 100 years

Using same technique, synthetic accelerograms corresponding to various hazard levels can be obtained. For instance for Bucharest, P100-2006 code provides a *PGA* value of 0.36g for ground motions having 475 years *MRI*.

For the generated sets of input ground motion corresponding to 30° directionality angle, the drift ratios in the *x*- and *y*- directions are represented in the fig. 7.

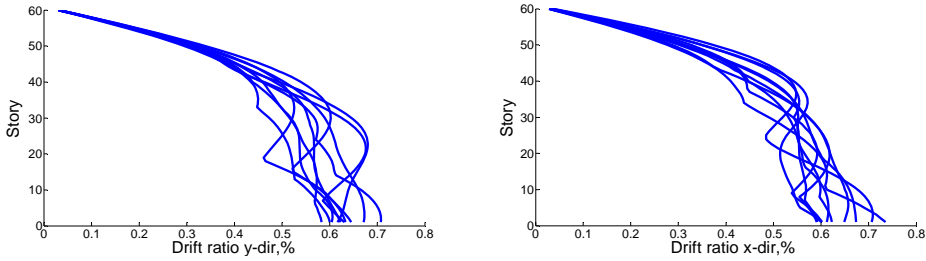


Figure 7. Drift ratios in x- and y-directions, 10 sets of bi-directional artificial accelerograms, PGA = 0.24g, MRI = 100 years

Large databases of input ground motions allow statistical analyses for high reliability design and associated risk analyses.

3.1. Structural design facts

The time-histories of the induced-efforts (axial forces, shear forces and bending moments) are used in design equations. For instance, for a steel column subjected to large axial load in *Load and Resistance Factor Design*, the following interaction formula has to be fulfilled

$$\frac{N_{e,k,s,\alpha}(t)}{\phi N_{ne}} + \frac{8}{9} \left(\frac{M_{x_{e,k,s,\alpha}}(t)}{\phi_b M_{nex}} + \frac{M_{y_{e,k,s,\alpha}}(t)}{\phi_b M_{ney}} \right) \leq 1 \quad (3)$$

In the eq. 3, N_{ne} , M_{nex} , and M_{ney} are the nominal axial and flexural strengths of member e , ϕ and ϕ_b are the axial and flexural resistance factors (AISC, 2001), and the quantities in the numerators are the time-instant axial load and bending moments due to ground motion from direction α .

Similar formula is provided in the Eurocode 3 (section 6).

The structural design is done in a straightforward manner, directly from the time-series of the induced effects, by using the full capabilities of the dynamic analysis procedure and computational tool.

4. CONCLUSIONS

The *integrated performance analysis system* consists of a considerable amount of modeling and data processing effort. This is highly supported by large computational capabilities. The approach has clear advantages and represents a higher level, modern and effective tool for practitioners.

The analysis format removes the needs of the current analysis model simplification (e.g. neglecting some degrees of freedom, sub-structuring etc.), the use of the maxima superposition rules.

It was shown that this approach provides a higher accuracy in estimating the structural demand, resulting safer and cost effective structures.

The *integrated performance analysis system* needs further developments by adding full design module as well as integrated seismic vulnerability and risk evaluation modules.

References

1. Abrahamson, N.A., 2006. *Selecting and scaling accelerograms for dynamic analysis*.
2. Gasparini, D.A., Vanmarcke, E.H., *Simulated Earthquake Motions Compatible With Prescribed Response Spectra*, Department of Civil Engineering, Research Report R76-4, Massachusetts Institute of Technology, Cambridge, Massachusetts, 1976
3. Iancovici, M., Kaminosono, T., *Seismic energy distribution in one-story irregular structures under bi-directional ground motion*. First European Conference on Earthquake Engineering and Seismology ECEES 2006, September 3-8, Geneva, Switzerland
4. Iancovici M, Riley MA, Sadek F, and Simiu E., *Wind effects on high-rise buildings: database-assisted design versus the high-frequency force-balance technique*. In: Proc. 11th Int. Conf. on Wind Engineering, Lubbock, TX, 2003.
5. Whalen T, Sadek F, and Simiu E., *Database-assisted design for wind: basic concepts and software development*. Journal of Wind Engineering and Industrial Aerodynamics 2002; 90:1349-1368.
6. Eurocode 3-*Design of Steel Structures 1993-1-1*, 2005
7. *Manual of steel construction: load and resistance factor design*. 3rd Edition, American Institute of Steel Construction (AISC), Chicago, IL, 2001.
8. *Romanian Seismic Design Code P100/2006*, Ministry of Transport, Construction and Tourism, Romania, 2006

The elastic-plastic load-carrying capacity of thin-walled steel members with quasi-homogenous and hybrid cross-sections

Pavol Juhás, Mohamad Al Ali, Zuzana Kokoruďová

Institute of Structural Engineering, Technical University of Košice, Košice, 04200, Slovakia

Summary

The paper presents fundamental information about realized experimental-theoretical research of the load-carrying capacity of thin-walled compressed steel members with quasi-homogenous and hybrid cross-sections. The load-carrying capacity of such members is influenced by the local web buckling subjected in the elastic-plastic region. The research joins on previous research of the first author [1, 2]. The aim of this research has been oriented on the elastic-plastic post-critical behavior of thin web and its interaction with compact flanges.

The experimental program, tested members and their geometrical parameters and material properties are evident from Tables 1, 2 and Figures 1 and 2. The test arrangement and failures of the tested members are illustrated on Figures 3 and 4. Some experimental results and comparisons are presented on the Figures 5, 6, 7, 8 and in Table 3. The theoretical limit loads of the tested members and their comparison contains Table 4. The comparison of theoretical and experimental limit loads is done in Table 5 and on Figures 9.

The results of presented research affirm and expand the knowledge of the previous research about the elastic-plastic behavior and load-carrying capacity of the thin-walled compression members with quasi-homogenous and hybrid cross-sections.

KEYWORDS: compressed steel member, hybrid cross-section, elastic-plastic loading, post-critical behavior, local and global buckling, buckling load-carrying capacity.

1. INTRODUCTION

The continued effort for economic design of steel structures leads to decrease their weight by shape and material optimization through the using of thin webs, high-strength steels and their effective combination with usual structural steels. The efficiency of high-strength steels using and their combination with usual structural steels is evident in the case of members – beams mostly subjected to bending loading. But from the complex optimization analyses follow, that the using of high-strength steels and their combination with usual structural steels can be advantage also in the case of members – columns mostly subjected to compression loading, mainly in the case of thin-walled members.

The paper presents basic information about realized experimental-theoretical research of the elastic-plastic load-carrying capacity of thin-walled compressed steel members with quasi-homogenous and combined cross-sections. This research has been distinctively oriented on the investigation and analyses of post-critical behavior of slender and ultra-slender member webs and their interaction with flanges in the process of their loading and failure [1- 8].

2. THE EXPERIMENTAL RESEARCH PROGRAM AND TESTED MEMBERS

The realized experimental research program included the testing of 24 welded compression steel model members having quasi-homogenous and combined I cross-sections with different dimensions, advisable elected to show, in decisive extent, the elastic-plastic post-critical effect of the slender webs and their interaction with flanges in process of their loading, transformation and failure. Table 1 presents the total research program, designed geometrical dimensions and materials of the individual test members and groups. Scheme of the test members is illustrated in Figure 1. The basic geometrical and material characteristics of the individual test members groups are presented in Table 2.

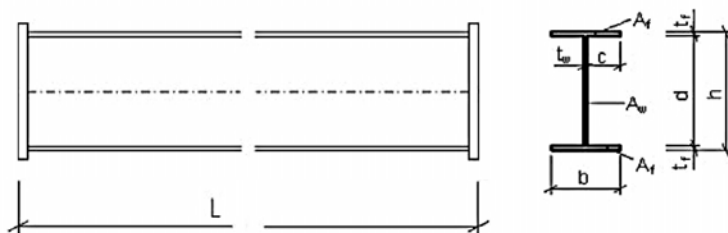


Figure 1. Scheme of the test members

Table 1. The total research program, geometrical dimensions and materials of the test members

Test members			Geometrical dimensions [mm]						Steels	
M.G.	C.G.	marking	<i>L</i>	<i>h</i>	<i>b</i>	<i>t_f</i>	<i>d</i>	<i>t_w</i>	flanges	webs
A	1	AS11, AS12, AS13	250	112	60		100			
	2	AS21, AS22, AS23	500	212	90	6	200	2	S235	S235
	3	AS31, AS32, AS33	750	312	120		300			
	4	AS41, AS42, AS43	1000	412	150		400			
B	1	BS11, BS12, BS13	250	112	60		100			
	2	BS21, BS22, BS23	500	212	90	6	200	2	S355	S235
	3	BS31, BS32, BS33	750	312	120		300			
	4	BS41, BS42, BS43	1000	412	150		400			

All test members are divided into 2 material groups (M.G.: A, B) and 4 cross-sectional groups (C.G.: 1, 2, 3 and 4). The materials group A is created by members with homogenous cross-section made from steel S235 and group B is created by members with combined cross-section made from steel S355 (flanges) and S235 (webs). The individual cross-sectional groups have different dimensions, but first of all they have different web slenderness β_w . It is apparently, that the members are thin-walled at the compression loading. At the same time, according to local stability aspects, the flange dimensions are designed to be compact (slenderness β_f), when subjected to the elastic region of loading. At last, according to the global stability aspects and dimensions of the individual cross-sectional groups, the lengths of members *L* are designed to be quasi-compact (slenderness $\lambda_y, \lambda_z, \lambda_z > \lambda_y$). The ratios γ give an evident characteristic of the economic efficiency of designed cross-sections – Table 2.

Table 2. Basic geometrical and material characteristics of the test members

Members		Geometrical characteristics					Material characteristics
M.G.	C.G.	$\lambda_y = L/i_y$	$\lambda_z = L/i_z$	$\beta_f = c/t_f$	$\beta_w = d/t_w$	$\gamma = A_w/A$	$m_y = f_{yf}/f_{yw}$
A	1	5.03	16.02	4.83	50.0	0.217	1.000
	2	5.01	20.80	7.33	100.0	0.270	
	3	4.99	23.02	9.83	150.0	0.294	
	4	4.98	24.28	12.33	200.0	0.308	
B	1	5.03	16.02	4.83	50.0	0.217	1.511
	2	5.01	20.80	7.33	100.0	0.270	
	3	4.99	23.02	9.83	150.0	0.294	
	4	4.98	24.28	12.33	200.0	0.308	

The flanges of all members were made out from 2 sheets, 6 mm thick (steel S235 and S355) and the webs from 2 sheets, 2 mm thick (steel S235). Three material specimens were taken from each of the used sheet to make normative shaped test specimens. The test specimens underwent a tension tests to find out the stress-strain diagrams and the actual material characteristics.

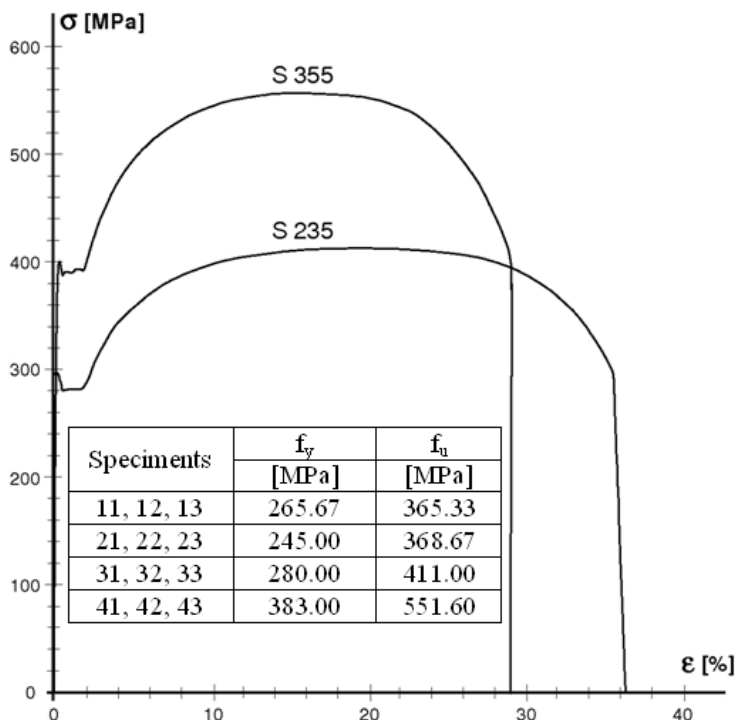


Figure 2. Characteristic stress-strain diagrams and determined material characteristics

Characteristic stress-strain diagrams are illustrated in Figure 2, where the average values of determined yield stresses f_y and limit tensile strength f_u are presented, too. Mentioned yield stresses f_y and ultimate tensile strength f_u were assigned to the relevant flanges and webs of the individual members.

For the consistent evaluation and analyses of the experimental knowledge and results, it is also necessary to know the real geometrical dimensions of the test members. Therefore the detailed dimension measuring of the all members was done before test. The dimensions of cross-sections: height h , width b , thicknesses of flanges t_f and webs t_w was measured on the top, middle and bottom of each member. The average values of measured dimensions are considered as actual.

Figure 2 shows the good quality of test members' steels and required material characteristics. The determined yield stresses of flanges f_{yf} and webs f_{yw} are higher than the normative values. Also in the case of materials group A members with designed homogenous cross-sections, the determined flanges yield stress values were higher than the webs yield stresses, $f_{yf} > f_{yw}$. It means, that they are also material combined ($m_y = 1.054$, event. 1.143). In the case of materials group B it is categorical go about members with material combined cross-sections ($m_y = 1.442$,

event. 1.563). In the case of all test specimens a good material ductility was found, too ($A_5 > 29\%$).

3. METHODOLOGY AND CONTENT OF THE TESTS

The tests of members were realized at the Bearing structures laboratory of the TU Košice by hydraulic loading machine. The general layout of the tests is illustrated in Figure 3.

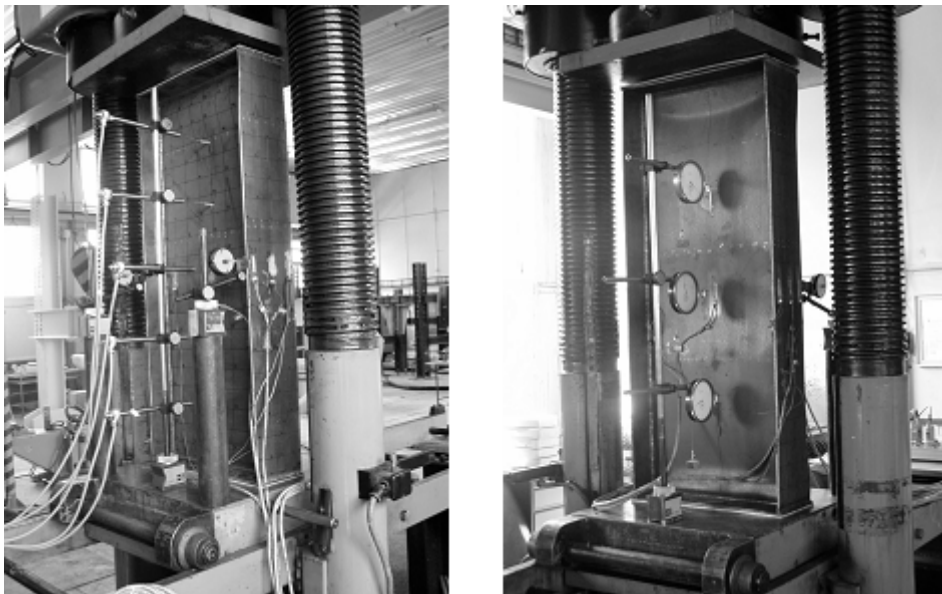


Figure 3. General layout of the test, measurement of strains ϵ , deflections of the web w and buckling of the members v

The tests have had to bring out detailed investigation about transformation, failure and ultimate load-carrying capacity of the test members, in consider of the individual geometrical and material parameters.

In accordance with research target, the emphasis has been imposed on the elastic-plastic post-critical behavior of the slender webs and their interaction with flanges. In context with that, the initial shape deflections of members, mainly the initial buckling of slender webs are significant for the experimental results valuation and connected theoretical analyses. Therefore, the initial buckling of the all member webs on previously drawn raster by means of inductive sensors were finding out before testing start. During consecutive programmed overloading of test members,

the strains ε in the middle cross-section were measured. Measurement was realized in 12 places, double-faced on the web in 6 places and also on the flanges in 6 places. The resistance tensiometers were used to measurement the strains ε by means of measuring apparatus Hottinger Balwin UPM 60 connected to computer for direct evaluation. According to member's length, the deflections of web w were measured in 3 or more places elected in the characteristic positions. The web deflections w were measured using inductive sensors connected to computer and also using mechanic gauges. In the case of members with ultra-slender webs (AS41 ~ AS43 and BS41 ~ BS43), the global buckling was also investigated in the middle cross-section on the edges of flanges. The member's global buckling v was measured by means of mechanic gauges. The measurement of strains ε , lateral deflections of the web w and global buckling v of the members are illustrated in Figure 3.

The members during the test were consecutively overloaded and released. The member overloading was regulated close to its behavior, measured values of strains ε and deflections of the web w . The test continued up to total failure, defined by the beginning of consecutive, continuous increasing of strains ε and deflections of the web w . Figure 4 illustrates the total failure of members AS21, AS22 and AS23 by local buckling of their webs and flanges.

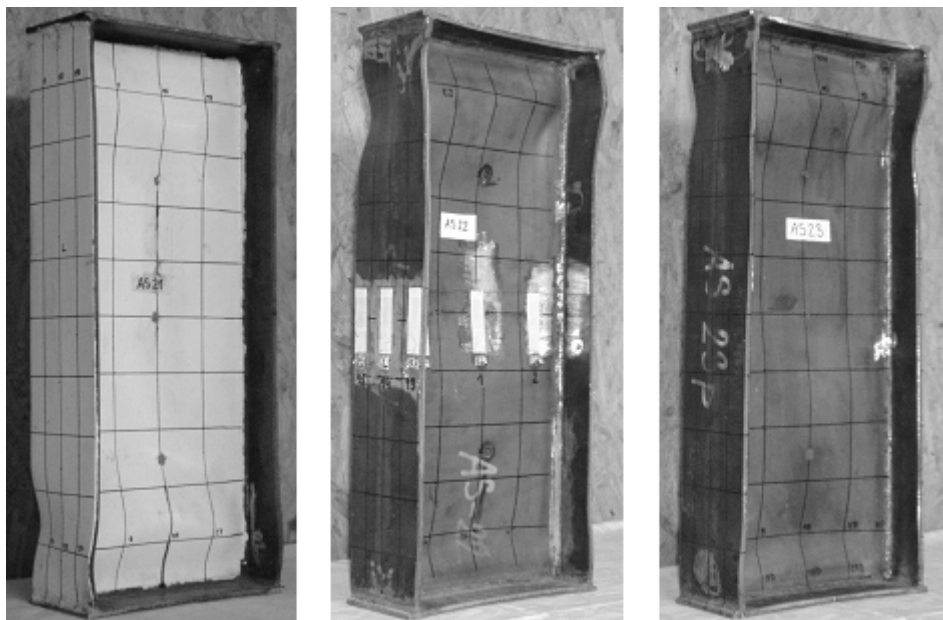


Figure 4. The total failure of members AS21, AS22 and AS23 by local buckling of their webs and flanges

4. EXPERIMENTAL RESULTS

According to the mentioned methodology the experimental tests of all members were done. The initial and final webs buckling shapes along of the some selected test members are illustrated in Figures 5 and 6.

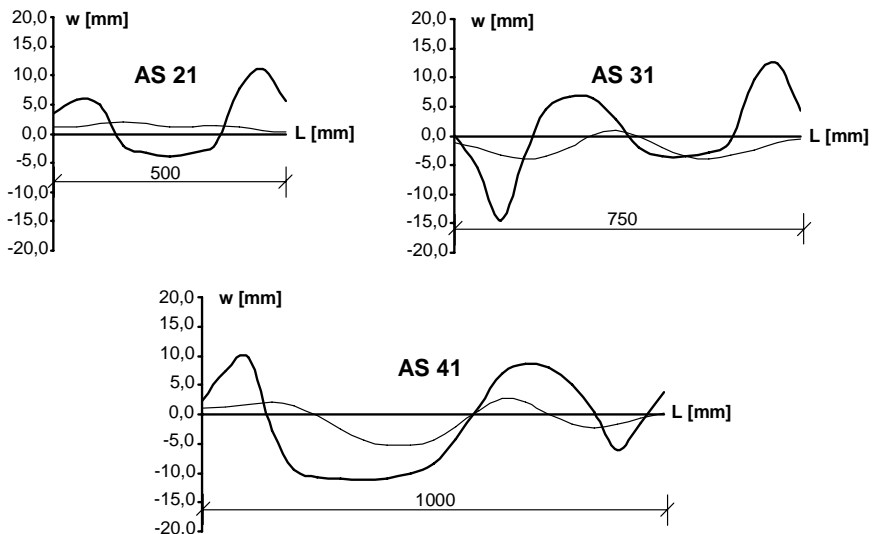


Figure 5: Initial and final webs buckling shapes along of members AS 21, AS 31 and AS41
 ——— initial shape, ——— final shape

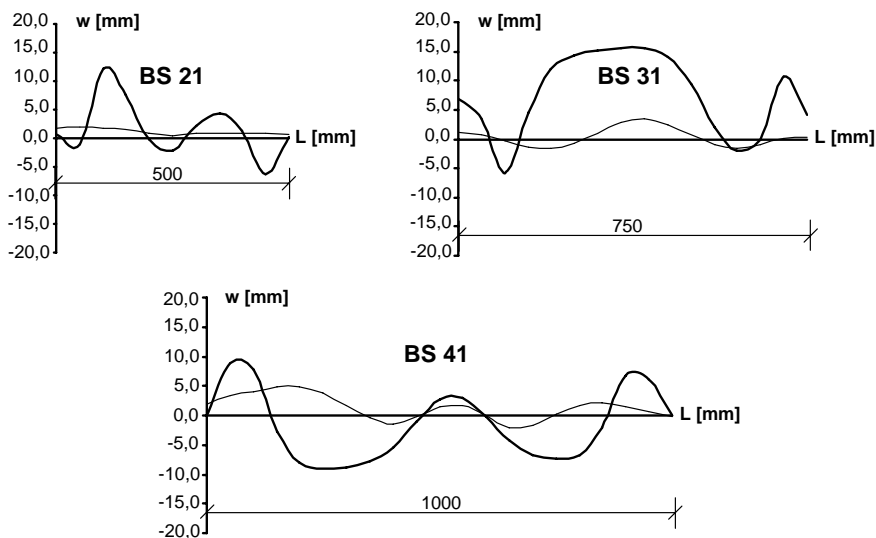


Figure 6: Initial and final webs buckling shapes along of members BS 21, BS 31 and BS41
 ——— initial shape, ——— final shape

Table 3 explains the overall behavior of all tested members and also presents the experimental ultimate limit loads. In dependence on the sequential load increasing the deflections w and the strains ε of the tested members were recorded.

Table 3. The test results – transformation, failure and the experimental ultimate loads of tested members

Member	Transformation and failure	$w_{0,max}$ [mm]	Halfwave number	$N_{u,exp}$ [kN]
AS11	» Original state:	-	3	278.0
AS12	The initial web buckling in different amplitudes	-	4	275.0
AS13	(w_0) and shapes, depending on the web	-	4	280.0
BS11	slenderness β_w .	-	4	357.0
BS12	» Transformation:	-	4	363.0
BS13	The primary local web buckling and	-	4	357.0
AS21	consecutive local buckling and warping of the	2.05	3	357.0
AS22	flanges, in dependence of web slenderness β_w	2.26	4	373.0
AS23	and its initial buckling shapes.	4.19	4	359.0
BS21	The consecutive changes and formation of new	2.02	5	466.0
BS22	web's buckling shapes. Consecutive impression	3.31	4	492.0
BS23	of frontal (ending) plates into webs at the ends	5.33	5	482.0
AS31	of members.	-3.99	4	447.0
AS32	» Failure:	4.66	3	432.0
AS33	The webs and flanges are buckled along the	2.90	3	442.0
BS31	members, buckling of the webs into multiple	3.41	4	565.0
BS32	configurations of half-waves, different lengths	4.73	4	577.5
BS33	of the several web's half-waves buckling,	3.32	4	562.5
AS41	reduction of web's half-wave buckling lengths	-5.35	4	490.0
AS42	at the ending parts members.	5.31	4	512.5
AS43	The local buckling and warping of the flanges,	-4.19	5	480.0
BS41	depending on web's buckling.	4.92	5	657.5
BS42	The impression of frontal (ending) plates into	4.27	3	590.0
BS43	webs at the ends of members.	-3.76	4	625.5
AS43	The distinct impression of flanges into			
BS41	member's cross-section was not manifested,			
BS42	neither at the most slender webs ($\beta_{w,max} = 200$).			
BS43	The total buckling was not manifested, neither			
	at the most slender members ($\lambda_{z,max} = 24.28$).			

Figure 7 illustrates the topographical form of the initial and final web’s buckling shapes of member AS31. Figure 8 presents the relations $N - w$ and $N - \varepsilon$ of the members BS23 and BS22.

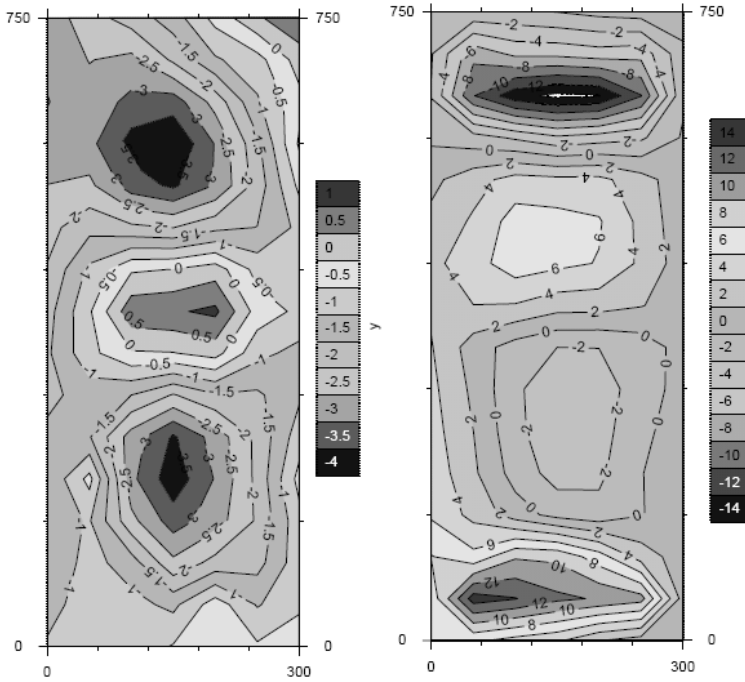


Figure 7. Initial and final topographical form of web’s buckling shapes of member AS31

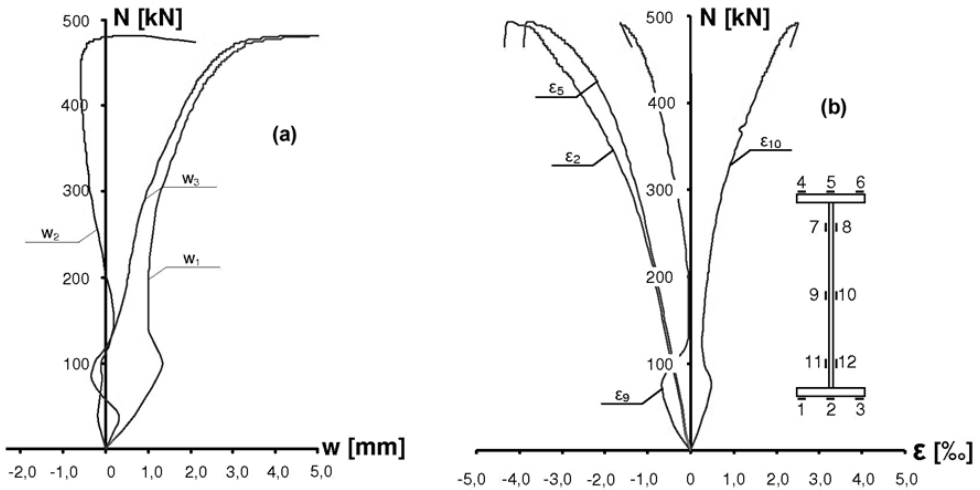


Figure 8. Web deflections w in the middle and quarters of member BS 23 (a), the web and flanges strains ε of member BS 22 (b)

The experimental knowledge and results presented in Table 3 and Figures 5, 6, 7 and 8 mention very clearly on complicity and variable elastic-plastic behavior of the individual test members during loading. But the experimental limit loads of the individual test members within the geometrical and material groups are relatively equivalent.

5. THEORETICAL LIMIT LOADS AND THEIR COMPARISON

According to the calculation procedures and formulae of the first author the theoretical limit loads of all test members were determined as following [3]:

N_{el}	limit elastic load of member definite by attaining the web yield stress f_{vw} ,
N_{pl}	limit plastic load of member definite by attaining the flanges yield stress f_{yf} ,
$N_{ul,el}$	limit elastic post-critical load of member definite by attaining the yield stress f_{vw} in the outer fibers of cross-sectional web,
$N_{ul,ep}$	limit elastic-plastic post-critical load of member definite by attaining the ultimate strain $\varepsilon_u = \varepsilon_{yf}$ in the outer fibers of cross-sectional web,
$N_{u,y}, N_{u,z}$	limit buckling load of member according to axis y and z considering the elastic-plastic post-critical behavior of the web.

Table 4 presents the relevant theoretical values of the individual members' limit loads and their comparison. All limit loads were calculated according to real – measured dimensions and determined yield stresses of their flanges and webs.

The ratios of elastic-plastic post-critical limit loads and full plastic limit loads $N_{ul,ep} / N_{pl}$ indicate at the negative effect of the web buckling on global load-carrying capacity of the tested members, with increasing of the web slenderness β the ratios decrease.

The ratios of elastic-plastic post-critical limit loads and the elastic post-critical limit loads $N_{ul,ep} / N_{ul,el}$ indicate at the positive effect of the web plasticity behavior on local load-carrying capacity of the tested members, with increasing of the flange yield stress the ratios increase.

The ratios of elastic-plastic post-critical limit loads and the global buckling loads $N_{ul,ep} / N_{u,z}$ indicate at the certain small possibility of the lateral torsional buckling of the tested members during loading, but it depends on their real support conditions.

Table 4. Theoretical limit loads and their comparison [kN]

Member	N_{el}	N_{pl}	$N_{ul,el}$	$N_{ul,ep}$	$N_{u,z}$	$N_{u,y}$	$\frac{N_{ul,ep}}{N_{pl}}$	$\frac{N_{ul,ep}}{N_{ul,el}}$	$\frac{N_{ul,ep}}{N_{u,z}}$
AS11	249.9	260.2	249.9	260.2	260.2	260.2			
AS12	251.3	261.8	251.3	261.8	261.8	261.8	1.000	1.042	1.000
AS13	249.9	260.3	249.9	260.3	260.3	260.3			
AS21	377.6	416.7	322.8	360.9	356.1	360.9			
AS22	377.1	415.6	321.9	359.2	354.3	359.2	0.865	1.117	1.014
AS23	376.0	414.4	320.9	358.2	353.3	358.2			
AS31	540.2	560.3	424.5	444.8	435.6	444.8			
AS32	542.8	563.0	426.8	447.2	438.1	447.2	0.794	1.048	1.021
AS33	549.7	570.0	432.2	452.7	443.4	452.7			
AS41	651.5	713.8	491.0	552.0	539.1	552.0			
AS42	653.9	716.6	493.9	555.4	542.0	555.4	0.775	1.124	1.024
AS43	654.6	717.4	494.6	556.2	542.8	556.2			
BS11	253.6	339.8	253.6	339.8	335.5	339.8			
BS12	261.6	350.6	261.6	350.6	346.5	350.6	1.000	1.341	1.012
BS13	257.0	345.1	257.0	345.1	341.0	345.1			
BS21	376.4	527.8	321.2	469.2	454.9	469.2			
BS22	376.0	527.3	320.9	468.7	454.7	468.7	0.888	1.460	1.031
BS23	370.1	517.9	314.9	459.2	445.7	459.2			
BS31	544.6	711.3	429.2	592.8	569.9	592.8			
BS32	549.0	716.6	432.6	597.2	574.3	597.2	0.834	1.381	1.040
BS33	546.1	713.5	430.7	595.0	572.2	595.0			
BS41	643.0	888.2	486.7	691.8	659.5	691.8			
BS42	654.7	902.1	494.4	709.2	676.1	709.2	0.780	1.425	1.049
BS43	650.9	896.2	490.5	695.7	663.0	695.7			

6. COMPARISON OF THEORETICAL AND EXPERIMENTAL LIMIT LOADS

The numerical comparison of the theoretical limit loads $N_{ul,ep}$, $N_{u,z}$ and experimental limit loads $N_{u,exp}$ for the individual test members and member groups is done in Table 5. Their graphic evaluation and comparison is presented in Figure 9.

In general, the buckling limit loads of the tested members $N_{u,z}$ have the smallest values. However, these limit loads are very close to the elastic-plastic post-critical limit loads $N_{ul,ep}$. But when the real boundary conditions of members are considered in accordance with arrangement of the loading machine, the elastic-plastic post-critical behavior and interaction between thin webs and flanges may appear in conclusive rate. All of the tested members were failure by means of the local failure of flanges in consequence of webs' local deflection in multiple half-waves

with different shapes. The conclusive buckling of web and flanges was mainly concentrated in the ending areas of members – obviously because of concentrated loading transfer.

Table 5: Comparison of the theoretical and experimental limit loads

Member	$N_{u,lep}$	$N_{u,z}$	$N_{u,exp}$	$N_{u,exp}/N_{u,lep}$	$N_{u,exp}/N_{u,z}$
AS11	260.2	260.2	278.0	1.068	1.068
AS12	261.8	261.8	275.0	1.050	1.065
AS13	260.3	260.3	280.0	1.076	1.076
AS21	360.9	356.1	357.0	0.989	1.003
AS22	359.2	354.3	3730	1.038	1.010
AS23	358.2	353.3	359.0	1.002	1.016
AS31	444.8	435.6	447.0	1.005	1.026
AS32	447.2	438.1	432.0	0.966	0.982
AS33	452.7	443.4	442.0	0.976	0.997
AS41	552.0	539.1	490.0	0.888	0.909
AS42	555.4	542.0	512.5	0.923	0.891
AS43	556.2	542.8	480.0	0.863	0.884
BS11	339.8	335.5	357.0	1.051	1.064
BS12	350.6	346.5	363.0	1.035	1.040
BS13	345.1	341.0	357.0	1.034	1.047
BS21	469.2	454.9	466.0	0.993	1.024
BS22	468.7	454.7	492.0	1.050	1.031
BS23	459.2	445.7	482.0	1.050	1.081
BS31	592.8	569.9	565.0	0.953	0.991
BS32	597.2	574.3	577.5	0.967	0.955
BS33	595.0	572.2	562.5	0.945	0.983
BS41	691.8	659.5	657.5	0.950	0.997
BS42	709.2	676.1	590.0	0.832	0.873
BS43	695.7	663.0	625.0	0.898	0.943

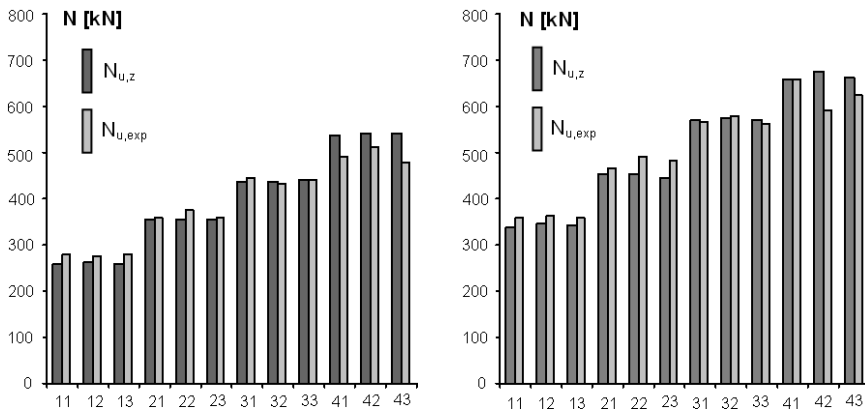


Figure 9: The comparing of theoretical and experimental capacities of members, material group A (left), material group B (right)

Very good consonance can be found from the comparison of the determined experimental limit loads $N_{u,exp}$ and the theoretical limit loads $N_{ul,ep}$ or $N_{u,z}$, if the web slenderness of the tested members $\beta_w \leq 150$. However, in the case of members with web slenderness $\beta_w = 200$ (AS41 ~ AS43 and BS41 ~ BS43) more significant differences were registered between evaluated theoretical and experimental limit loads.

The results mention very clearly the effect of the local buckling and interaction of the member web and flanges subjected to compression. This effect is very significant first of all in the places of the direct transmission of the loading to compressed members.

7. CONCLUSIONS

- The results of presented research affirm and expand the knowledge of the previous research about the elastic-plastic behavior and load-carrying capacity of the thin-walled compression members with quasi-homogenous and combined cross-sections.
- Elastic-plastic post-critical load-carrying capacity of compression members depends in a large scale on the initial web buckling shapes and their consecutive formation and changes during the loading process.
- Post-critical load-carrying capacity of the thin-walled compression members increases by increasing the number of buckling waves during the elastic-plastic and plastic stage of the loading.
- Thin webs with slenderness $\beta_w \leq 150$ (A), event. $\beta_w \leq 100$ (B) prove a sufficient support of compression members' flanges. Theoretical limit loads $N_{ul,ep}$ and $N_{u,z}$ are in a good consonance with the obtained experimental limit loads $N_{u,exp}$.
- In the case of members with webs' slenderness $\beta = 200$, the influence of non-sufficient support of compression flanges by ultra thin web was also manifested here. This effect was significant near the members' ending which can be caused by local transfer of loading to the flanges and web. In the case of these members, theoretical local load-carrying capacity $N_{ul,ep}$ and global buckling load-carrying capacity $N_{u,z}$ are a bit less than the elastic-plastic load-carrying capacity $N_{u,exp}$ determined by experiments.

Acknowledgements

The research was partially founded by Scientific Grant Agency of the Ministry for Education SR and the Slovak Academy of Sciences No. 1/4220/07. The author would like to acknowledge with thanks the financial support.

References

1. Juhás, P., Kriváček, J., Investigation of Thin-Walled Compressed Combined Steel Elements. *Building Research Journal* 41, No. 4/2, p.871-907, 1993.
2. Juhás, P., Thin-walled hybrid compressed elements. *Publications of the University of Miskolc, Series C: Mechanical Engineering*. Vol. 47, p. 123-129, 1997.
3. Juhás, P., Load-carrying capacity of hybrid compressed steel elements. In: *Proceedings of the 2nd European Conference of Steel Structures, Vol. 2, EUROSTEEL'99*. CTU Praha, p. 697-700, 1999.
4. Juhás, P., Juhásová, E., Load-Carrying Capacity of Hybrid Compressed Steel Elements. In: *Proceedings of Annual Technical Session and Meeting*. SSRC, Memphis – USA, p.75-88, 2000.
5. Juhás, P., Buckling Load-Carrying Capacity of Steel Hybrid Thin-Walled Compressed Members. *Selected Scientific Papers – Journal of Civil Engineering* 1, p. 7-27, 2006.
6. Juhás, P., Kokoruďová, Z., Al Ali, M., Investigation of Elastic-Plastic Load-Carrying Capacity of Thin-Walled Compressed Steel Elements. In: *Proceedings of the 8th Scientific Conference of the TU - Civil Engineering Faculty Košice*. Civil Engineering Faculty, Košice, p. 99-106, 2007.
7. Juhás, P., Al Ali, M., Kokoruďová, Z., Experimental Investigation of Elastic-Plastic Carrying Capacity of Thin-Walled Compressed Steel Members. In: *Proceedings of Czech – Slovak Conference Experiment'07*. AP CERM, Ltd., Brno - Czech Republic, p. 139-146, 2007.
8. Kriváček, J., The knowledge from Experiment – Basis for numerical Simulation of Thin-Walled Steel Structures' behavior. In: *Proceedings of Czech – Slovak Conference Experiment'07*. AP CERM, Ltd., Brno - Czech Republic, p. 229-234, 2007.

Numerical Simulation of Wave Transformation in the Fars Gulf

Saeed Khorram¹

¹Civil Engineering, EMU, Famagusta, (392), North Cyprus

Summary

A numerical model has been developed for the simulation of wave transformations that is applicable to irregular bottom topographies. Model is based on nonlinear parabolic mild slope equation and could simulate wave shoaling, refraction, diffraction together. The numerical model has been solved by Mac Cormack Method with using Point Gauss Seidel Iteration Method. Wave phase gradient of Ebersole (1985) has been used to determine local wave number in the model. The model is applicable to arbitrary varying bottom topographies. Unidirectional waves are considered for the numerical model. It is a reliable tool to simulate wave shoaling, refraction and diffraction. Model predictions are compared with the physical experiment over semicircular shoaling area. Model has been applied to Fars Gulf located on the Mediterranean Sea Coast of Iran which has an industrially important role for Iran since a great industrial harbour and oil pipelines are located.

KEYWORD: Sea wave, refraction, diffraction, wave shoaling, Numerical Simulation

1. INTRODUCTION

Berkhoff (1972) solved the wave propagation from deep water to shallow water under combined refraction and diffraction effect with an elliptical equation. This equation is called as mild slope equation in the literature.

$$\frac{\partial}{\partial x}(CC_g \frac{\partial \tilde{\phi}}{\partial x}) + \frac{\partial}{\partial y}(CC_g \frac{\partial \tilde{\phi}}{\partial y}) + w^2 \frac{C_g}{C} \tilde{\phi} = 0 \quad (1.1)$$

C is the wave celerity, C_g is the group velocity, w is angular frequency, $\tilde{\phi}$ is two dimensional complex potential function. It is assumed that the bottom topography has a mild slope for this equation. It is to say $|\nabla h|/kh \ll 1$ where h , k , ∇ are water depth, wave number, horizontal gradient operator, respectively. This elliptical mild slope equation includes combined refraction-diffraction, shoaling and reflection effects.

Radder (1979) recommended parabolic approach because of complexity of solving elliptical mild slope equation. Elliptical mild slope equation is reduced to Helmholtz equation and parabolic equation is obtained after this reduction. Parabolic equation is applicable to the short waves over irregular bathymetries in large coastal areas if reflection is negligible.

Kirby and Dalrymple (1983) solved parabolic equation for the combined refraction-diffraction of Stokes waves by mildly varying topography. In this approach, only unidirectional waves and forward scattered components arising from interaction with structures or inhomogenities of the domain are considered. This parabolic equation is obtained by a WKB- type expansion for the velocity potential. That represents a wave travelling in a prespecified direction.

Dalrymple et al. (1984) developed a parabolic model to simulate combined refraction- diffraction phenomena including dissipation of wave energy. They focused on the nature of the localized energy dissipation. A shadow region of low wave energy exists due to the region of localized dissipation.

Kirby (1986) developed rational approximations based on minimax principles to overcome small angle incidence limits in the parabolic equation.

In this study, parabolic equation proposed by Kirby and Dalrymple (1983) is solved as the governing equation including both refraction and diffraction effects. This equation amplitude order, therefore it is simpler to solve than the potential order equations. This nonlinear equation gives approximate results with the general elliptic mild slope equation and it overcomes small angle incidence restriction of the linear parabolic equation. Furthermore, the definition of wave number recommended by Ebersole (1985) is used in this study. Ebersole (1985), developed an alternative equation that expresses the propagation of linear waves over mild sloping bathymetry and also defined wave number as a function wave phase derivative.

2. THEORY

Yue and Mei (1980) obtained a parabolic equation that described the propagation of weakly nonlinear Stokes waves in a specified direction over constant depth. This nonlinear Schrödinger equation is given below.

$$2iA_x + \frac{1}{k} A_{yy} - K'|A|^2 A = 0 \quad (2.1)$$

A is complex amplitude; x is the principal direction of propagation. k referred wave number.

$$K' = k^3 \left(\frac{C}{C_g} \right) D \tag{2.2}$$

$$D = \frac{\cosh 4kh + 8 - 2 \tanh^2 kh}{8 \sinh^4 kh} \tag{2.3}$$

Equation (2.1) is applicable to the bathymetry with a constant depth. Kirby and Dalrymple (1983) proposed a more general formulation suitable for slow but arbitrary depth variations. Nonlinear effects are important when waves are focused by topographic variations. The inclusion on nonlinearity enhances the lateral spread of energy away from regions with high waves.

$$2ikCC_g A_x + 2k(k - k_0)(CC_g)A + i(kCC_g)_x A + (CC_g A_y)_y - k(CC_g)K'|A|^2 A = 0 \tag{2.4}$$

- k : Wave number (1/m)
- C : Wave celerity (m/sec)
- C_g : Group velocity (m/sec)
- k_0 : Wave number in deep water (1/m)
- A : Wave amplitude (m)

Subscripts x and y define the first derivatives in x and y direction, respectively.

Derivation of governing equation that is solved in this study can be found below where k_0 is the initial wave number at deep water.

Ebersole (1985) showed the relationship between wave number and phase function with the equation below where s is wave phase function and H is wave amplitude in the equation (2.5).

$$|\nabla s|^2 = k^2 + \frac{1}{H} \left[\frac{\partial^2 H}{\partial x^2} + \frac{\partial^2 H}{\partial y^2} + \frac{1}{CC_g} \left(\frac{\partial H}{\partial x} \frac{\partial CC_g}{\partial x} + \frac{\partial H}{\partial y} \frac{\partial CC_g}{\partial y} \right) \right] \tag{2.5}$$

In this study, equations (2.4) and (2.5) are used to solve the propagation of travelling waves from deep water to shallow water in a prespecified direction over slowly arbitrary bottom topography under combined refraction-diffraction effects.

3. NUMERICAL MODEL

MacCormack method is applied to equation (2.4) using Point Gauss Seidel iteration method. MacCormack method is a multistep method. Firstly, forward finite difference approximations are used to obtain the predictor and then backward finite difference approximations are applied to the governing equation to find the corrector. This method gives more realistic results than the other methods since it

assures static stability. Point Gauss Seidel Iteration provides to reach the convergence more rapidly because the current variables of dependent variable are used to compute the neighbouring points as soon as they are available.

4. APPLICATION TO SEMICIRCULAR SHOALING AREA

Whalin (1971) tested wave refraction and diffraction phenomena over a semicircular shoaling area. The model topography was determined with the equations below and shown in Figure 1.

$$h(x, y) = 0.4572 \quad (0 \leq x \leq 10.67 - G(y)) \tag{4.1}$$

$$h(x, y) = 0.4572 + \frac{1}{25}(10.67 - G(y) - x) \quad (10.67 - G(y) \leq x \leq 18.29 - G(y)) \tag{4.2}$$

$$h(x, y) = 0.1524 \quad (18.29 - G(y) \leq x \leq 21.34) \tag{4.3}$$

$$G(y) = [y(6.096 - y)]^{1/2} \quad (0 \leq y \leq 6.096) \tag{4.4}$$

In these equations, x and y are in meters.

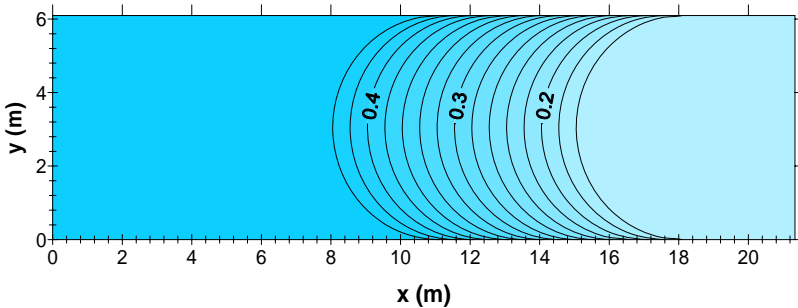


Figure 1: Tank bathymetry (h(m))

The bathymetry is symmetric to the centerline $y=3.048\text{m}$. Model topography shoals from 0.4572m to 0.1524m .

The wave amplitude distribution along the centerline for the wave approaching normally with the wave period $T=2\text{sec}$ has been shown in Figure 2 where the consistency between numerical and physical results can be observed. Diffraction effects become an important role after the distance of 15m in x direction and a caustic region occurs so the linear theory fails in that region. With the use of parabolic mild slope equation, this problem has been overcome.

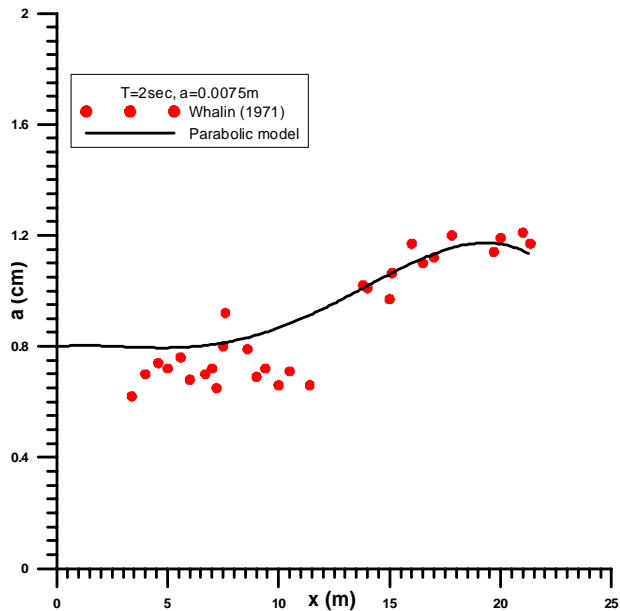


Figure 2: Wave amplitude (cm) along x-axis ($y=3.048\text{m}$, $T=2\text{ sec.}$, $a=0.0075\text{m}$, $\theta = 0^0$)

5. APPLICATION TO FARS GULF

Fars Gulf is located in the Mediterranean Coasts of Iran. Fars Gulf coast has a great harbour and oil pipelines therefore it is important from the coastal engineering point of view. The dominant wave direction is SSW. Significant wave period $T=9.02\text{sec}$ and significant wave height $H_s=5.46\text{m}$ for the return period $t=50$ years. In this study, a part of Fars Gulf coast has been numerically modeled. In Figure 3, the bathymetry has been given. Depths are in meters. In Figure 4, the predicted wave height distribution has been shown. The wave heights are in meters, too.

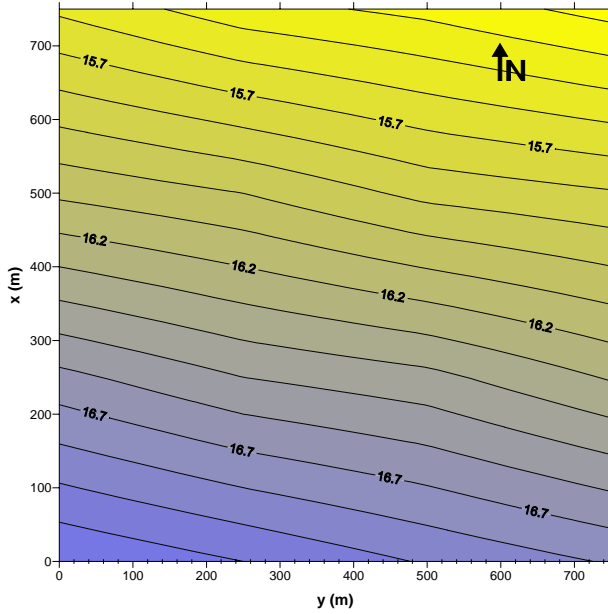


Figure 3: Bathymetry of Fars Gulf Coastal Region (Depths are in meters.)

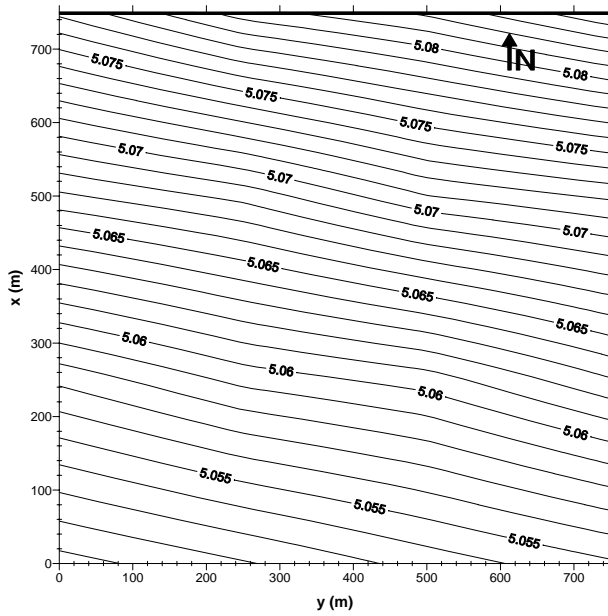


Figure 4: Wave height distribution (Wave heights are in meters.)

6. CONCLUSIONS

A numerical model that simulates the propagation of waves from deep water to shallow water under shoaling, refraction and diffraction effects has been presented. Nonlinear effects have been included in the solution. Mac Cormack method is applied to the governing model equation using Point Gauss Seidel Iteration method. The nonlinear parabolic model has been used in this study so as to overcome caustics problems of the linear theory. The use of wave phase gradient provides more accurate results to obtain the local wave number. The model can be successfully used over arbitrary bathymetries in the prespecified direction.

References

1. Berkhoff, J. C. W., (1972), ‘Computation of Combined Refraction-Diffraction’, Proceedings, 13th International Conference on Coastal Engineering, ASCE, 1, 472-490
2. Booij, N., (1983), ‘A Note on the Accuracy of the Mild Slope Equation’, Coastal Engineering, 7, 191-203
3. Dalrymple, R.A., Kirby, J.T., Hwang, P.A., (1984), Wave Diffraction due to Areas of Energy Dissipation, Journal of Waterway, Port, Coastal and Ocean Engineering, 110 (1), 67-79
4. Ebersole, B. A., (1985), ‘Refraction-Diffraction Model For Linear Water Waves’, Journal of Waterway, Port, Coastal and Ocean Engineering, 111 (6), 939-953
5. Hsu, T-W., Wen, C-C., (2001a), On Radiation Boundary Conditions and Wave Transformation Across the Surf Zone, China Ocean Engineering, 15 (3), 395-406
6. Hsu, T-W., Wen, C-C., (2001b), A Parabolic Equation Extended to Account for Rapidly Varying Topography, Ocean Engineering, 28, 1479-1498
7. Isobe, M., (1987), A Parabolic Equation Model for Transformation of Irregular Waves due to Refraction, Diffraction and Breaking, Coastal Engineering in Japan, 30 (1), 33-47
8. Kadomtsev, B.B., Petviashvili, V.I., (1970), On the Stability of Solitary Waves in Weakly dispersing media, Sov. Phys. Dokl., 15, 539-541
9. Kirby, J.T., (1986), Rational Approximations in the Parabolic Equation Method for Water Waves, Coastal Engineering, 10, 355-378
10. Kirby, J.T., (1988), Parabolic Wave Computations in Non- Orthogonal Coordinate Systems, Journal of Waterway, Port, Coastal and Ocean Engineering, 114 (6), 673-685
11. Kirby, J.T., Dalrymple, R.A., (1983), ‘A parabolic equation for the combined refraction-diffraction of Stokes waves by mildly varying topography’, Journal of Fluid Mechanics, 136, 453-456
12. Li, B., (1994), An Evolution Equation for Water Waves, Coastal Engineering, 23, 227-242
13. Liu, P. L.-F., Yoon, S.B., Kirby, J.T., (1985), Nonlinear Refraction- Diffraction of Waves in Shallow Water, Journal of Fluid Mechanics, 153, 185-201
14. Mordane, S., Mangoub, G., Maroihi, K.L., Chagdali, M., (2004), A Parabolic Equation Based on a Rational Quadratic Approximation for Surface Gravity Wave Propagation, Coastal Engineering, Vol. 50, pp. 85-95
15. Radder, A.C., (1979), ‘On the Parabolic Equation Method for Water-Wave Propagation’, Journal of Fluid Mechanics, 95, 159-176
16. Whalin, R.W., (1971), The limit of application of linear wave refraction theory in convergence zone, U.S. Army Corps of Engineers Waterways Experiment. Station, Vicksburg, Report No. H-71-3
17. Yue, D.K. -P, Mei C.C., (1980), ‘Forward diffraction of Stokes waves by a thin wedge’, Journal of Fluid Mechanics, Vol. 99, pp. 33-52

Modeling of light Non-aqueous phase liquids Spreading and Migration to fate of oil and Locate the Source, case study in Estahban

Saeed Khorram¹

¹*Civil Engineering, EMU, Famagusta, (392), North Cyprus*

Summary

A common problem associated with oil refineries is the subsurface contamination resulted from leaking of light non-aqueous phase liquids (LNAPL), released from storage tanks and underground facilities. In this paper, LNAPL transport on the water table is modeled numerically to simulate the extent of current oil contamination plumes over the groundwater and to investigate the future fate of the contamination by finding possible suitable locations for their treatment. The model assumes a sharp interface between the LNAPL and groundwater that takes into account the groundwater velocity and pertinent soil parameters. Spreading and migration of LNAPL mounds with time are predicted using the sharp interface model and current leak conditions that are simulated by applying an “error evaluation” procedure. Analyses are carried out considering presence and absence of the leaking sources. The results show that, migration is relatively small. Consequently, sources of contamination are expected to be located in the proximity of points with maximum LNAPL thickness. Results also indicate that, the size and volume of LNAPL mounds are estimated more realistically compared to geostatistical analysis.

KEYWORDS: LNAPL; sharp interface; groundwater; spreading; leak

1. INTRODUCTION

Petroleum liquids are part of our modern lives. Their uses include fuels, lubricants and raw materials of manufactured products. Non-aqueous phase liquids (NAPLs) are hydrocarbons that exist as a separate and immiscible phase when in contact with water and/or air. Non-aqueous phase liquids are typically classified as either light non-aqueous phase liquids (LNAPLs) which have densities less than that of water, or dense non-aqueous phase liquids (DNAPLs) which have densities greater than that of water. Contamination due to non-aqueous phase liquids (NAPL) has emerged lately as a major environmental problem. The major concern caused by NAPLs is due to NAPLs persistence and their ability to contaminate large volumes of soil and groundwater. An estimated 1.8 million underground storage tanks are in use in the United States. EPA estimates are that 280,000 tanks are leaking; of

which more than 20% are discharging their contents directly into the ground water [1]. In other countries with numerous oil refineries including various underground storage tanks like Iran the situation is not better.

When a LNAPL leaks above an unconfined aquifer, the NAPL migrates through the unsaturated zone as a separate phase under the dominant influence of gravity, leaving residual droplets in the unsaturated zone. Once it reaches the water table, the LNAPL forms a free-product mound floating on the water table. Then the LNAPL spreads laterally and moves in the direction of decreasing hydraulic gradient, leaving residual LNAPL droplets. Valuable works are cited in [2-4].

2. THEORETICAL FRAMEWORK

The mass balance equation of the NAPL phase in a porous medium is the starting point to develop a governing equation in terms of oil thickness, in order to simulate areal spreading and migration of LNAPL mound with ambient groundwater flow. The mass balance equation can be expressed as:

$$\nabla \cdot \rho_o q_o + \frac{\partial(\rho_o S_o n)}{\partial t} = 0 \tag{1}$$

where ρ_o is the density of the NAPL phase; q_o is the specific discharge of the NAPL phase; S_o is the degree of saturation of NAPL phase; t is the time component; and n is the porosity of medium.

The governing equation describing spreading and migration of LNAPL mound with ambient groundwater flow in terms of NAPL thickness is developed by averaging Equation (1) along the vertical in the NAPL lens and rearranging as given in [5]:

$$\frac{k_{or} K_o L_o (\rho_w - \rho_o)}{n \rho_w (S_{oo} - S_{OUN})} \nabla^2 L - \frac{q_w K_{or} K_o}{K_w n (S_{oo} - S_{OUN})} \nabla L = \frac{\partial L}{\partial t} \pm \frac{Q_o}{n (S_{oo} - S_{OUN})} \delta(x - \xi) \delta(y - \xi) \tag{2}$$

where ρ_o is the density of the water; K_w, K_o are the hydraulic conductivities of the NAPL and water phases respectively; K_{or} is relative permeability of the NAPL phase; S_{oo} and S_{oun} are saturation degrees of mobile NAPL and residual NAPL, respectively; L is the floating NAPL thickness on the water table defined as;

$L(x, y, z) = h(x, y, t) - \eta(x, y)$ under steady state groundwater flow conditions (h is the elevation of the mound surface and η is the elevation of the groundwater from a specific datum); L_o is a reference thickness of the NAPL mound defined as the volume of oil per unit area of aquifer divided by porosity. q_w is the specific discharge of water; Q_o is the rate of leaking/pumping at the point (ξ, ζ) ; and δ denotes the Dirac delta function used to represent point sources.

Two different states of displacement for NAPL phase is considered in the unsaturated zone. The LNAPL migration on the water table shows two distinct surface areas between the LNAPL phase and the air phase: some portion of the surface is in imbibition, and another portion is in drainage [6]. The LNAPL surface in drainage leaves residual NAPL, because the NAPL phase is displaced by the air phase on the surface. The LNAPL surface in imbibition does not leave residual NAPL because this portion displaces the air phase in the pores. Therefore, with a continuous source, S_{oin} in equation (2) becomes zero because all of the surface areas are in imbibition. In the absence of a continuous source, part of the surface area is in the drainage state and the value of S_{oin} becomes the value of residual saturation.

3 NUMERICAL SOLUTION

The governing partial differential equation is solved numerically using a finite difference technique of 2-D governing equation through classical Implicit, Alternate Direction Implicit (ADI), or explicit finite difference methods. Explicit methods are conditionally stable; therefore, for given values of horizontal and vertical space intervals (Δx & Δy) stability condition places a limitation on the time step Δt . Therefore, explicit methods are restricted to minor steps and this limitation requires a large amount of computational time to solve the transport equation. On the contrary, implicit methods are unconditionally stable; however, in order to solve the resulting simultaneous linear algebraic equations high-capacity computers are required. In this research, 'Hopscotch Method' presented was adopted [7]. The method works by solving every other node explicitly, then solving the nodes in-between using an implicit scheme.

4. COMPUTER PROGRAMS

A computer program was developed to incorporate the above-mentioned algorithm in order to simulate the migration and spreading of LNAPL mounds. Computer

program was developed in “MATLAB” environment. Two computer programs were developed: Program #1: Solves the governing differential equation assuming a continuous LNAPL source with a prescribed discharge value to predict LNAPL spreading and migration in the solution domain with time. Program #2: Solves the governing differential equation in the absence of a continuous LNAPL source. This program is capable of simulating migration and spreading of LNAPL mound on an ambient groundwater surface by taking into account the residual mass loss, which is left behind in the pores.

5. CASE STUDIED

5.1. Site Description

Estahban oil Refinery with the annual capacity of 2 million tons of oil products was designed and constructed in the early 1970s. The refinery started operating by the Iranian engineers and experts in 1973. Main products include gas-oil, bitumen, motor gasoline, fuel oil, kerosene, LPG (liquid petroleum gas), and sulfur. The refinery site is located approximately 15 kilometers northeast of Estahban and it has occupied an area of 2.3 square kilometers. The geology at the site is composed of fine sand with varying amounts of silt and gravel. Depth to groundwater ranges from 0.5 to 13 meters with an average of 5 meters. Local direction of groundwater flow is from south-west toward northeast of the refinery site. The preliminary investigations revealed that the industrial activities have led to subsurface environmental contamination, particularly groundwater contamination there were 24 pre-existing boreholes that had been drilled in order to lower the groundwater table. Since the monitoring stations had been installed for a different task and some of them were destroyed in the course of time, the existing network was augmented. By the beginning of this research 35 monitoring stations were available and in operation. LNAPL thickness measured in these boreholes was used to calibrate the model.

5.2. Meshing the solution domain

Definition of the solution domain includes determination of location and dimensions of the domain shape of the domain, grid spacing, direction and location of the local axis of coordinates. Location and dimensions of the domain are determined according to dimensions and location of the significant LNAPL mound. Grid spacing ($\Delta x, \Delta y$) is limited to the accuracy of calculation. Direction and location of local axis of coordinates of the solution domain should satisfy the following conditions:

- Positive x-direction of local axis must coincide with the ambient ground water flow direction.
- Origin of the local coordinate system must coincide with the center of LNAPL source.

A rectangular solution domain was chosen for this study.

5.3. Boundary and Initial Conditions

It is assumed that the meshing domain is large enough compared to the contaminated zone and hence gradient of LNAPL are zero at both boundaries. For modeling fresh leaks, the initial thickness of LNAPL is zero. However, for the case of modeling spreading and migration of an existing LNAPL, an estimation or direct thickness measurement of the current LNAPL thickness is essential. The so-called apparent thickness of LNAPL was measured using an electro-optical interface meter with accuracy of 1 mm.

6. MODEL PARAMETERS

Parameters involved in the sharp interface model may be divided into three categories:(1) geotechnical parameters which describe subsurface characteristics of the site; (2) hydro-geological parameters which contain detailed information on multi-phase flow of existing fluids in the porous medium; and (3) leakage parameters. Summary of model parameters for the case studied is presented in Table 1. Figure (2) shows groundwater flow direction and head contours at the site using geostatistical interpolation. Site investigations and measurements of LNAPL thickness at the site concluded that 8 of 36 available monitoring stations had immiscible LNAPL phase. Two distinct LNAPL mounds were identified through geostatistical interpolation, which their details presented in Table 2. As clear from Table 2, mound #1 covered a larger area with a much superior apparent LNAPL thickness. Figure (3) shows the location & distribution of the corresponding LNAPL mounds.

7. MODEL RESULTS

Results obtained using sharp interface model for the case studied, are discussed in two different parts:

A- Speculation of previous history and pattern of leaks,

B- Prediction of future LNAPL plumes spreading and migration with time:

B-1: spreading and migration of current LNAPL mounds considering a continuous leaking source.

B-2: spreading and migration of LNAPL mounds with no leaking source

Table 1. Parameters used in simulation.

Parameter	Symbol	Value	unit
porosity	n	0.35	***
Darcy velocity	q_w	0.01 (mound#1) 0.018 (mound#2)	m / d
Hydraulic conductivity of water	k_w	0.432	m / d
Hydraulic conductivity of oil	k_o	0.173	m / d
NAPL saturation in NAPL lens	S_{oo}	0.8	***
Residual water saturation	S_{ow}	0.2	***
Residual NAPL saturation	S_{ow}	0	***
water density	ρ_w	1000	kg / m^3
NAPL density	ρ_o	780	kg / m^3
NAPL relative permeability	k_{or}	0.6	***
NAPL source flow rate	Q_o	0.35 (mound#1) 0.022 (mound#2)	m^3 / d
Radius of source	r	50 (mound#1) 70 (mound#2)	m

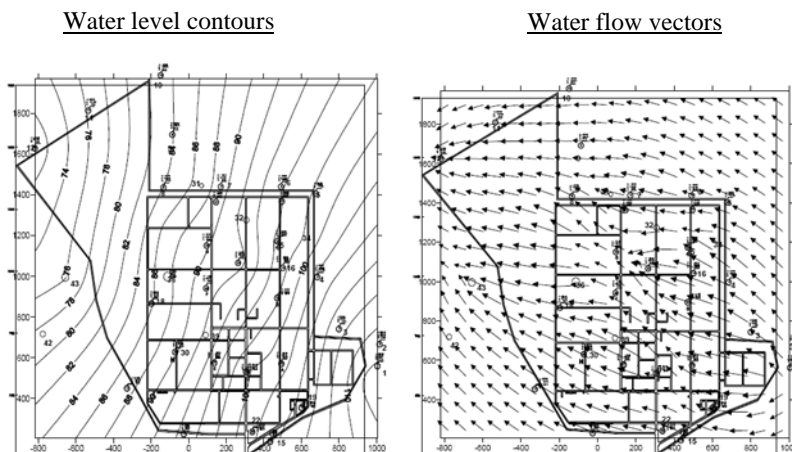


Figure 2. Head contours and velocity vectors of groundwater flow at the site

Table 2. Details of recognized LNAPL mounds obtained using data interpolation.

Max apparent thickness (mm)	Area of mound (m ²)	Estimated volume of LNAPL (m ³)
1840	221000	2810
50	110885	115

8. CONCLUSION

Sharp interface modeling was employed to screen current condition of leak and to predict the consequences of spreading and migration of LNAPL mounds at a refinery site. Geotechnical and hydro-geological parameters were estimated based on laboratory experiments and empirical relationships. Two different scenarios were considered in this study: (1) simulation of history and pattern of the leaks; and (2) prediction of further spreading and migration of LNAPL mounds both in presence and absence of continuous LNAPL source.

LNAPL mounds were simulated and duration and pattern of leaks leading to the existing condition were estimated. According to model results, further migration of LNAPL mounds was small. Consequently, sources of LNAPL contamination were expected to be located in the proximity of maximum LNAPL thicknesses for each mound. This fact helped locating possible source of leakage at the site. The insignificant migration of mounds was due to low groundwater velocity and low hydraulic conductivity of porous medium (which is a result of topographical condition and soil type resting beneath the studying area). According to simulation, results it was summarized that for a given volume of free product released into a permeable soil (e.g., sand, gravel), the plume will tend to be flat and relatively broad in extent. The same volume of free product if released into less permeable soil (e.g., silt, very fine sand), will form a thicker plume (especially near the point of release) and the spread will not be as broad. Based on the trends observed through migration of contaminant any location in the downstream of the migrating LNAPL mounds could be identified as possible suitable locations for their treatment.

References

- [1] El-Kadi, A.I., "Applicability of sharp-interface models for NAPL transport: 1. Infiltration", *Ground Water*, 1992, 30(6), pp. 849-856.
- [2] Corapcioglu, M. Y., Lingam, R., Kambham, K. K. R., and Pandey, S., "Multiphase contaminants in natural permeable media: Various modeling approaches, in *Migration and Fate of Pollutants in Soils and Subsoils*, edited by D. Petrozelli and F. G. Helfferich, Springer-Verlag, New York, 1993, pp. 191-220.

- [3] Corapcioglu, M.Y., Tuncay, K., Lingam, R., Kambham, K.K.R., “Analytical expressions to estimate the free product recovery in oil-contaminated aquifers”. *Water Resour. Res.*, 1994, 30 (12), pp. 3301–3311.
- [4] El-Kadi, A.I., “Applicability of sharp-interface models for NAPL transport: 2. spreading of an LNAPL”, *Ground Water*, 1994, 32(5), pp. 784-795.
- [5] Corapcioglu, M.Y., Tuncay, K., Ceylan, B.K., “Oil mound spreading and migration with ambient groundwater flow in coarse porous media”, *Water Resour. Res.*, 1996, 32 (5), pp. 1290-1308.
- [6] Kim, J., Corapcioglu, M.Y., “Sharp interface modeling of LNAPL spreading and migration on the water table”, *Environ. Eng. Sci.*, 18 (6), pp. 359– 367.
- [7] Gourlay, A.R., Mcguire, G.R., “General hopscotch algorithm for the numerical solution of partial differential equations”, *J. Inst. Math. Appl.*, 1971, 7, pp. 216-227.
- [8] Abdul, A.S., Kia, S.F., and Gibson, T.L., “Limitations of monitoring wells for the detection and quantification of petroleum products in soils and aquifers”, *Ground Water Monit. Rev.*, 1989, 9(2), pp. 90-99.
- [9] Noye, J., “Numerical Solutions of Partial Differential Equations”, Part one, North- Holland Publishing Company, Proceedings of the 1981 conference on the numerical solutions for partial differential equations, Melbourne University, Australia, 1982, pp. 15-87.

Structural Analysis of High Rise Building Structures

Ludovic Kopenetz¹, Alexandru Cătărig¹

¹Dep. of Structural Mechanics, Technical Univ. of Cluj - Napoca, Cluj - Napoca, 400020, Romania

Summary

The main characteristic of all tall structures or high rise structures is that they have large horizontal and vertical geometric dimensions.

These structures need special attention from the designers in order to satisfy the strength and stability conditions imposed by the static and especially by the dynamic actions.

Usually, the parameters of the structural behavior are: displacements, speeds, accelerations and specific deformations.

The accuracy of the results of a static and dynamic structural analysis depends on both on the matching of the mathematical models for the entire structure and on the correct establishment of the stress hypotheses.

The establishment of the approximate mathematical model and the interpretation of the results are the most difficult phases of the structural analysis.

In the paper, the authors present the problematic aspects of structural analysis using advanced investigation methods and concepts from system theory.

KEYWORDS: high rise structures, structural analysis, practical structural analysis.

1. INTRODUCTION

The study of the tall civil structures comprises conception, design and execution of the construction work for buildings with a large number of floors, in the light of the new European (EUROCODE) and international codes.

The conception of bearing structure is tightly connected to the adopted solution for the execution of the construction work, (Fig.1). The execution methods for the resistance structure of high rise buildings, are based on: steel, masonry, reinforced concrete, pre-stressed reinforced concrete and combinations of these structural materials (the so called mixed solutions: steel – concrete, concrete – masonry, steel – masonry).



Figure 1. Hige rise building structures

Besides the safe undertaking of the permanents actions, the structural conception will track the variable actions, especially the actions with dynamic effect like wind and earthquakes. Another important aspect to take into account is the necessity to create a stable behavior of the building to actions caused by exceptional situations (e.g. fire, explosions, impact between the building and aircrafts, caused either by human error or terrorist attacks). As a result, it is very important to use a structure type which can help avoid the chain collapse of the building, even in the situation when some of the structural elements or parts of the building are accidentally destroyed.

2. STRUCTURAL CONCEPTION

Conceptual design is based on official national and international codes. During this activity detection, thru scientific calculation of the possible differences between the ideal (project) and the in situ situation is performed. The in situ situation is based on effective forces, execution tolerances and structural materials with real quality.

Taking into account that nowadays 99% of the design activity is computer aided design, a new decisive necessity arises: the control of the order of magnitude of the results. It is well known that the results of an automated computation depend both on the physical modeling and on the quality of the computation program that is used. Thus, cases of tall buildings recomputed several times with the same modeling error and computation error, are known. (because of the mathematical model implemented in the program). For the mitigation of this major uncertainty danger and for the pre – dimensioning of the structure, engineering structural analysis methods are still necessary.

In Europe and in the U.S.A., the computation of tall structures is performed by using the semi probabilistic method of threshold conditions, namely conditions when the conceived and executed structure does not comply with the maximum bearing capacity and with normal exploitation.

The final threshold conditions of the maximum bearing capacity in the case of high rise buildings comprise the following criteria

- strength threshold condition;
- final stability threshold condition (buckling through bending, torsion, bending – torsion, halation);
- final balance threshold condition (through displacement, sliding, turnover, support lifting, etc.);
- fatigue threshold condition.

The threshold condition of normal exploitation is connected to phenomena that can cause the disruption the normal utilization of the high rise building. These types of phenomena are:

- large displacements and elastic deformations;
- oscillations of the bearing structure.

3. ORGANIZATION OF TALL STRUCTURES

In essence, tall structures are spatial systems that are composed of the following structural elements:

- poles, structural walls (vertical diaphragms), vertical wind bracings;
- girder, floors, rigid slabs in the floors plane, horizontal wind bracings;
- “radier”, pilot or isolated foundations.

Using these structural elements, the following structural schemes can be executed:

- rigid frames on both directions;
- wind bracing frames on both directions;
- core or cores and peripheral poles;
- tube, tube in tube and multiple tubes.

The bearing structure is chosen taking into account the following aspects:

- usage of the building (offices, hotel, flats, etc.);
- shape, dimension and the degree of occupancy of the available ground area;
- climatic and seismic area;
- geotechnical conditions;
- financial conditions;
- structural materials and the execution and assembling techniques;
- H/B ratio (H – height of the building, B – the minimum planar dimension);
- outer cover type (exterior closing) and the type of installation systems used(heating, electrical, air conditioning, water, sewage, signaling, elevator systems, etc.).

Taking into account that the bearing structure represents approx. 10-15% of the final cost, it is very important to perform a correct analysis for choosing the optimal type of structure.

The horizontal and vertical shape of the tall structure is correlated both with the purpose (usage) of the building and with the good behavior under the action of wind and seism. In order to address the seismic action, when choosing the shape, the following aspects have to be taken into account:

- the achievement of a planar symmetry, thus the ideal choices are circular, square, rectangular shapes;
- the vertical bearing structure will be conceived with rigidities almost equal after the symmetry axes;
- for the H/B ratio a value smaller than 4 is recommended;
- for the buildings, that are placed in seismic areas with $a_g \gg 0.20g$, the planar dimension will not be greater that 35 – 50m (for avoiding the effects of out of phase excitations);
- the gaps in the floors (horizontal slabs) should not be more that 15 – 20% of the floor surface area;
- elevators and the stair cases should be grouped in centers (cores) (preferably, at most 2 centers);
- in the case of the irregular levels, inter space division should be used, in order to obtain regular compact shapes (the width of the inter spaces will be chosen in order to avoid collisions between buildings during the oscillations caused by seismic activity).

4. STRUCTURAL ANALYSIS

4.1. General Aspects

The bearing structures used for high rise buildings are characterized by slenderness, thus they need special attention from the designers in order to satisfy the strength and stability conditions for static and especially for dynamic loads. The parameters that characterize the dynamic behavior are usually: displacements, speeds, accelerations and specific deformations.

The purpose of the special measures from dynamic loads, stipulated in the project, is to stop the phenomena of degradation of the structure. These measures are taken in order to maintain the equilibrium of the structural assembly. The purpose is for the bearing structure to maintain its shape, namely to be stable from the point of view of the strength, through static and dynamic loads. This implies such an assembly of the structural elements and a fastening of the building to the foundation soil or to other constructions, to get near EUCLID's model hypothesis. This means that the structure should be an assembly of well controlled displacements, with values below the ones stipulated in the design codes. As it can be noticed, in these cases, besides the strength criterion (which is implicitly fulfilled) another stricter criterion emerges: the flexibility limitation criterion.

The crucial aspects of the structural analysis are closely related to the overtaking of the horizontal forces created by wind and seism. An effect of the action of the wind is the emergence of displacements and horizontal oscillations that have a magnitude that depends on the bending stiffness of the bearing structure.

The bending stiffness of the bearing structure will be chosen in such a way that the horizontal displacement caused by the action of the wind is not bigger than $H/300 - H/600$ (H – height of the building). The proper frequency has to be different than the frequency of the gusts of wind. The overtaking of the seismic forces can be realized in the following ways:

- without energy dissipation, namely the hysteresis effects are neglected and the behavior factor is $q=1$; in this case the computation of the stresses is performed using global elastic structural analysis, based on the linear relationship between deformations and strains;
- with energy dissipation, in this case the hysteresis effects from plastic deformations and local veiling are taken into account, thus the behavior factor is $q > 1$.

Lately, there is a large number of solutions based on ductile steel plate walls (DSPW) for the overtaking of horizontal loads, besides the use of centric or eccentric steel wind bracings and reinforced concrete structural walls.

4.2. Fundamentals of Static and Dynamic Structural Analysis

The decision on the mathematical model with a finite number of degrees of freedom has to be done in order not to modify the physical behavior of the building.

A very difficult problem is the modeling of the structural discontinuities. These structural discontinuities, gaps and partially open or open interspaces, and even constructive interspaces, can lead in certain conditions to the collapse of the structure. The mechanic effect of the structural discontinuities depends on the relationship between status of the loads and the emergence and dispersion of these discontinuities.

High rise structures behave more or less non-linear because of the following reasons:

- first of all, because of the non – linear behavior of the material from which the structure is made of (this fact influences the behavior of the structures when the operation (exploatare) loads are exceeded, thus the theories that suggest the evaluation of the limit (threshold) load have to be taken into account);
- second, because of the “large” deformations which are common to high rise structures;
- finally, because of the influence of the axial effort on the bending rigidity of the bars; it is well know that the tension axial effort increases the rigidity while the compressing axial effort diminishes the rigidity; although this phenomenon can be seen as a sub case of the previous reason, it deserves a great deal of attention because in some cases it can supply information regarding the limit load (e.g. balance bifurcation); the exceeding of the limit load can cause the loss of the structures stability, which continues to behave elastically.

In the case of a high rise structure, which is a system with a non – linear behavior, the balance of the dynamic forces is practically identical with the balance equation for systems with linear behavior.

Thus the equation is

$$F_d = F_e + F_i + F_a \quad (1)$$

where:

- F_d – exterior dynamic disturbance forces (time functions);
- F_e – elastic forces caused by the deformed structural elements;
- F_i – inertia forces;
- F_a – damping forces.

In the case of high rise buildings, based on the non – linearity degree there exist several methods for resolving equation (1). Thus in many cases it is not allowed to

apply the principle of the superposition of effects. There has to be performed an analysis for each load hypothesis (Fig.2).

In the case of the structures with a slight non – linearity, a general formulation is based on a step by step integration method, similar to the one for linear structures. In this case, the approximate mass, damping and rigidity matrices are computed for the time interval taken into consideration. The inertial, damping and elastic forces are determined at the end of the time step.

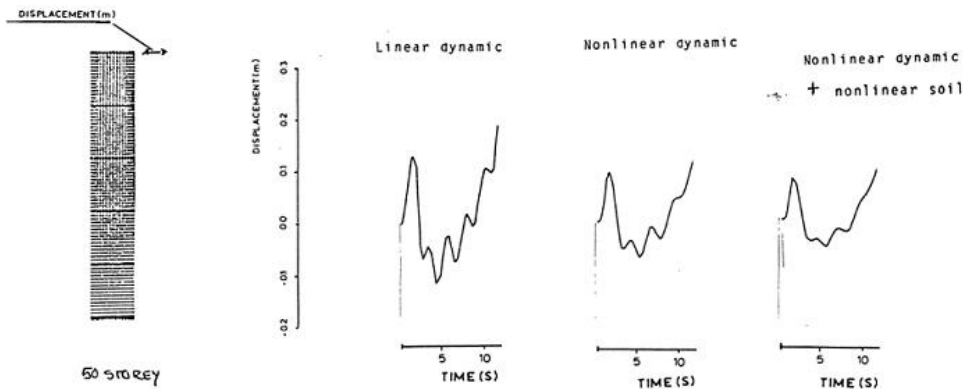


Figure 2. Dynamic analysis of 50 storey high rice building

In the case of the structures with a strong non – linearity, an iterative computation will be used during the time step. For solving the problems of dynamic analysis in the case of high rise structures, three methods are usually used:

- modal superposition method;
- direct numerical integration method;
- integration with transformation method.

In the past, the modal superposition method was rarely used, because the method is more desirable than the implicit integration methods, just when the bandwidth of the system matrices grows and when less proper shapes are required.

Direct integration methods are well known and researched in the linear domain, but relatively less is known about their use in the solving of the problems created by non – linear dynamics. Thus, the Newmark and Wilson methods lose their unconditional stable behavior if an incremental formulation is used for non – linear oscillations (through balancing iteration at each step).

4.3. Practical Dynamic Analysis

Dynamic analysis can be realized either using the deterministic or probabilistic method. One of the first aspects of the analysis refers to the compressed elements

of high rise buildings, taking into account that there exists the danger of stability loss of the initial balance form. The stability loss is the result of reaching critical stresses which cause either balance bifurcation (1st order imbalance) or balance divergence (2nd order imbalance). In the case of the existing high rise structures, it has to be taken into account that they were designed in between 1900 – 1970, based on the linear structure concept, characterized through a response (effort, displacements) which is directly proportional with loads; that is the influence of deformations and displacements over the geometry and efforts was not taken into account.

A special situation appears in the study of the seism influence. The use of an acceleration graph is recommended, where an excitation in the form of supports movement exists. The supports movements caused by seismic activity are described using the three components of translational acceleration. For the response of high rise building with slight non – linearity the method of superposition of individual responses is permitted. The individual responses are computed separately for each component acting simultaneously all the parts of the structure’s foundation.

In the cases of very big structures (with more than 6000 freedom degrees) it is admitted to apply Ritz’s reduction method in the form of the subspace iteration method. The following hypotheses are highlighted:

1. In addition to the ground’s translation movements, the supports will be subject to rotation movements. Taking into account that there is no information about measurements regarding the magnitude and the character of the rotation components of the ground, this effect is considered just as an order of magnitude, where the rotation movements were hypothetically deduced from the translation components;
2. An aspect that is generally not taken into account when defining the effective developed forces in a high rise building by an earthquake is that the ground movements at the basis of a structure are influenced by the proper movements of the structure. The movements introduced at the basis of a structure can be different from the free field movements, which could be observed in the absence of the structure. This interaction between the foundation ground and the structure, in other words its effect is less important if the foundation ground is a hard ground and the building is flexible (e.g. high rise buildings made of steel). In this case the high rise building can transmit to the ground just a small amount of energy and the free field movement is an adequate measure for the displacements of the foundation. In the case when the structure is heavy and rigid (e.g. historical buildings, monuments, high rise buildings made of masonry and reinforced concrete) and when there are supports in a soft foundation soil, a considerable amount of energy will pass from the structure to the foundation soil and movements at the basis can considerably differ from the free field conditions.

3. The simultaneous acting on all the parts of the structure's foundation caused by seismic excitations implies neglecting the rotation movements, namely the foundation ground or the foundation rock is considered rigid. Note: In the case of high rise structures with distant supports (more than 50 – 70 m) can bring in significant errors.

Professional computing applications use different numerical methods in order to reduce the high amount of numerical computation needed to obtain the eigenvalues and eigenvectors. Thus, for subspace iteration usually a single determinant load hypothesis is considered, which is used to determine the smallest eigenvalue. This operation is repeated using different evaluation and elimination techniques. A basic task for the structure engineer, during dynamical analysis, is to be sure that all the frequencies are determined, namely to verify that none of the important frequencies were lost. For this reason, the authors recommend the study of the Sturm sequence.

The activity of practical structural analysis frequently implies the use of graphical modeling both for data input and for the interpretation (reading) of the computed results. The selection and the presentation of information for graphical modeling have a critical importance during computer aided static and dynamical analysis.

The surveying of the primary coordinates at existing constructions can be made through geodetical and photogrammetric methods. For smaller high rise structures, no higher than a few tens of meters, closed photogrammetry is sufficient. Closed photogrammetry is a special application of photogrammetry that has the advantage of a higher accuracy and the possibility to perform measurements with no contact to the construction. The accuracy of the measurements can get as close to 0.1 – 5 mm for the Rolleiflex S166 family of devices. Surfaces and curves can be represented in the implicit, explicit or parametric form. For digital processing the parametric representation is the most used.

For the computer aided survey of high rise buildings where the architectural composing elements and the structure exhibit a lot of prominences and tips (vertex), it is very advantageous to use cubic spline functions.

4.4. Existing High Rise Structures

Structural interventions are needed for controlling the dynamic parameters, in the case of the existing high rise structures that were built before the 1970'ties. These rehabilitation interventions at existing high rise buildings are performed in order to keep up the structures to the technical demands of nowadays regarding strength and stability to static, dynamic and seismic forces. In compliance with national and international regulations, these structural interventions in the case of light structures can be made only after a structural expert study.

The correctness of the results of a dynamical analysis depends on the adaptation of the mathematical models for the entire structure and on the establishment of the dynamical load hypotheses. Similar to general structures, high rise structures have an infinity of degrees of dynamical freedom. The choice for the approximate mathematical model and the interpretation of the results are considered the most difficult phases of the dynamical analysis.

3. CONCLUSIONS

The complexity of structural analysis of high rise structures arises as a consequence of the non – linear behavior of these mechanical systems. Basically it has three classical sources: physical, geometrical and physical – geometrical non – linearity.

The structural analysis of high rise buildings entirely depends on the used mathematical models.

The aspects presented by the authors help in substantiation of the design codes for high rise buildings, which are being currently developed.

Besides the rigorous approach aspects, a series of practical structural analysis facts are presented in the paper.

References

1. Lee, L.T., Collins, J.D., *Engineering Risk Management for Structures*, Journal of the Structural Division, ASCE 103, No. ST9.
2. ***, EUROCODE 8, Part 1.4., *Design Provisions for Earthquake Resistance of Structures. General Rules, Strengthening and Repair of Buildings*, 1998.
3. ***, Cod de Proiectare Seismică, Partea 1, *Prevederi de Proiectare pentru Clădiri*, indicative P100 – 1/2006. (in Romanian)
4. ***, Normativ pentru Proiectarea Antiseismică a Construcțiilor de Locuințe, Social – Culturale, Agrozootehnice și Industriale, Indicativ P100 – 92. (in Romanian)
5. Kopenetz, L.G., Ionescu, A., *Lightweight Roof for Dwellings*, IAHS, International Journal for Housing and its Application, vol. 9, No. 3, pg. 213 – 220, Miami, Florida, U.S.A. 1985.
6. Cătărig, Al., Kopenetz, L. G., *Time Surveillance and in Situ Testing by Dynamic Methods of Steel Structures*, The 6th Conference on Steel Structures, Timișoara, Romania, 1991.
7. Bârsan, G.M., Kopenetz, L.G., Alexa, P., *Analiza Dinamică a Structurilor cu Reazăme Depărtate*, Lucrările SNIC, Sibiu, Romania, 1984. (in Romanian)
8. Cătărig, Al., Kopenetz L.G., Alexa, P., *Nonlinear Analysis of Static and Dynamic Stability of Metallic Chimneys*, *International Journal Thin – Walled Structures - 20*, Elsevier Applied Science Publishers, England, 1994, (also in Romanian at) U.T. Press, Cluj – Napoca, 1998.
9. Borș, I., Bârsan, G.M., Alexa, P., Kopenetz, L.G., *The Laplace Transforms in Dynamics Analysis of Guyed Steel Structures*, A VI-a Conferință de Construcții Metalice, vol.2, pg.306 – 314, Timișoara, Romania, 1991.

Expert Study of Bearing Structures, Using Intelligent Control Systems Based on Fuzzy Logic

Ludovic Kopenetz and Ferdinand-Zsongor Gobesz
*Department of Structural Mechanics, Technical University of Cluj-Napoca,
Cluj-Napoca, 400020, Romania*

Summary

The expert study of bearing structures arise highly complex problems due to the multiple random variables which are interfering.

The generalized interpretation of bearing structures as information carrying technological systems is claiming more and more pregnant the issue of the priority of decisions within expert study and assessment tasks.

In this sense, fuzzy logic based reasoning can be applied with success in case of tall and large structures, where the human factor (the expert) has the fundamental role in the matter of the decision concept.

The paper discusses some aspects concerning the introduction of fuzzy reasoning for the expert study of structures which are exhibiting a certain wear and damage ratio, by using degradation functions and dynamic identification concepts of structures. Finally, the safety assessment of a complex structure is illustrated briefly, using a rule driven inference engine.

KEYWORDS: building, structure, assessment, expert study, fuzzy logic.

1. INTRODUCTION

The existence of a considerable stock of buildings (in both urban and rural areas) which need to be kept in use over time, raises new and complex issues for the art of constructions, mainly due to three reasons:

- approx. 60–70% of the national territory has high seismic risk;
- the needs for built-up areas are rising;
- a proper safety level should be well-kept, respecting the actual standards and regulations.

The existing bearing structures must insure the carrying capacity for the actual loads, transferring them safely through the foundation into the ground. Considering that the structural design of new facilities, while still insuring the global quality of

the existing buildings, issues many random features, the practicability of an accurate damage evaluation is representing a genuine hazard.

Cutting back the level of this hazard beyond a certain threshold is technically and economically not justified.

The condition of a structure depends on the degree of its vulnerability as well as on its actual damage ratio, in situ. The degree of vulnerability expresses the composing manner of the structure, through the available cross-sectional strength at the moment of the assessment. The damage ratio depends on the nature and both on the amount and on the location of physical failures in the whole structure.

Considering that the “Conclusions” chapter of an expert study contains decisions which, due to the multitude of uncertainties, can be qualitatively altered by the participation of a human factor, a methodology is proposed for the handling of the uncertain aspects, applying intelligent control and fuzzy logic [1], [2], [3], [4].

2. STRUCTURE IDENTIFICATION

The expert study of a construction is based mainly on the identification of an actual bearing structure which exists in situ.

The structure identification activity is a logical process, in order to develop a mathematical model for the existing physical system. The process is based on the feedback provided by the system to a known input, while collecting, processing, interpreting a vast amount of data (signals, information) [5], [6], [7].

The classification of the information is based on the following criteria:

- the nature of the investigated system;
- the aim of the identification;
- the type of working data.

The input can have several kinds: static or dynamic forces, imposed displacements, impulses etc.; while the output can be consisting of: displacements, velocities, accelerations, deformations of the actuated physical structure [8], [9].

The mathematical model obtained through the identification process must produce the same output like the physical system, when the same input is applied.

Generally, the identification process of a system has three parts:

- ascertainment of the model’s shape and of the system parameters;
- appraisal and selection of the identification criteria;
- selection of the algorithms which will modify the parameters.

3. IN SITU ASSESSMENT

3.1. Geometrical survey – scan and collecting uncertain data

For these tasks laser scanners, interior and exterior hologram techniques are used lately. The mapping of primary coordinates can be done by geodetic and photogrammetric methods. In case of large structures aerial photogrammetry can be useful.

It is very important to notice if the structure is stand-alone or bonded to the neighboring buildings. In case of bonded structures (building assemblies), the nature and geometry of the gaps must be specified. At large constructions the inner (subsidence, thermal and seismic) gaps must be specified too.

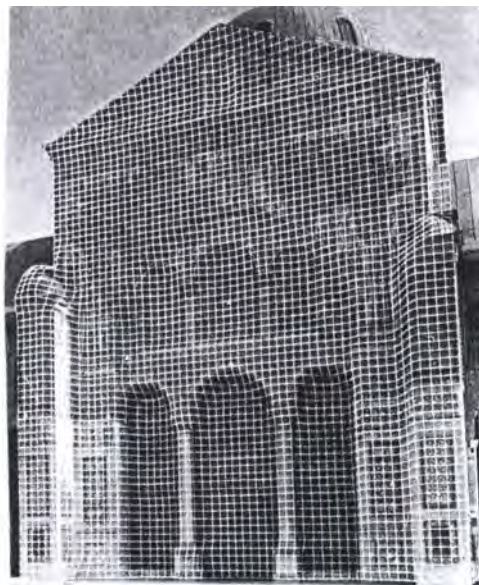


Figure 1. Sample photogrammetric image of a building.

The main uncertainties of a bearing structure are:

- supports, connections between the load-carrying parts, the foundations;
- actual displacements, deformations of the horizontal and vertical structural elements;
- the kind and magnitude of damage, related to:
 - the position and type of the fissures, cracks;
 - the peeling, crumbling and corrosion of the concrete;
 - the position, type, number and corrosion of the reinforcements;
 - the degree of alkalinity of the concrete etc.

The arrangement of these degradations will be made with the help of some template files (in the current study, files named as “*vertical_fissures*”, “*horizontal_fissures*”, “*oblique_fissures*” etc. were used), and creating a set of attributes corresponding to the revealed damages and tagging these attributes.

3.2. Site conditions

The hydro-geotechnical and geodynamical conditions are very important for the surveying input data set.

The major concern by expert study is the establishing of the severe seismic stroke direction which is particular for the site. In this sense, it can be noticed that in Bucharest’s area the severe seismic stroke direction is identical to the straight line connecting the city with the Vrancea region, namely corresponding to a 27° angle direction from North.

Considering the fact that the probability for the occurrence of a severe earthquake during the lifetime of a structure is low; the following combinations are usually adopted for structural analysis:

- a site characteristic “standard” earthquake, causing insignificant damage to the building (so called “damage limitation requirements”);
- the strongest possible earthquake for the given site, in order to assess the structural safety of the building by accepting major structural damage, but nevertheless avoiding collapse and loss of human lives (so called “no collapse requirements”).

3.3. Measurements for the appraisal of the dynamic parameters

In order to appraise the dynamic parameters, the persistent micro-seismic disturbance of the ground and small intensity pulses can be used as excitation [10].

The research equipment is including the following components:

- seismic transducers;
- filtering and amplifier systems;
- recording systems;
- Fourier analyzer.

It should not be forgotten that the accuracy of measurements depends very much upon the characteristics (precision, acuity, sensitivity, instability, hysteresis etc.) of the equipment used for appraisal.

The identification of the basic frequency is made from the representation of the self-correlation function, computed with the help of the Fourier spectrum. With the help of the basic frequency, the total stiffness (K_x , K_y , and K_θ) can be established.

4. STRUCTURAL ANALYSIS WITH RESPECT TO THE PERTAINING UNCERTAINTIES

The accuracy of the results from an expert study depends mainly on the appraisal of the mathematical models (for the structure as well as for the foundation ground and for the selection of the load combinations).

4.1. The analysis of the structural assembly

The existing bearing structures must insure the carrying capacity for all actual loads, transferring in safe conditions the stresses to the foundation ground [11], [12].

Following this idea, it is presumed that the structure must keep its shape, namely it must be stable from the point of view of strength. This is implying such a construction (joining) manner of the composing structural parts, and such a binding of the structure to the ground, in which way, considering the hypothesis of the Euclid model (perfectly rigid behavior of the material), the structure would represent an assembly of beams, slabs, geometrically invariable diaphragms.

For the study of these aspects, a detailed cinematic analysis of the structure and of its connections is required, with respect to the typology, topology and geometry of the construction, in order to avoid the mechanism or pseudo-mechanism character in case of an initially critical assembly or as a consequence to alteration caused by operating conditions (weakening, destruction of some joints; demolition of bearing walls or partition walls etc.).

During the analysis of the structure assembly, the orientation of the effective structural stiffness (existent in situ) will be specified according to the severe seismic stroke direction, knowing that the ideal case is when the maximal stiffness of the construction is found on this direction [13].

4.2. The analysis of displacements, deformations

The structural materials are suffering deformations under the action of stresses provoked by loads. In this sense, the flexibility of the floor slabs in their bridging plane is very important.

The hypothesis, that slabs are rigid in their plane (namely “rigid floor diaphragms”), is generally accepted in case of buildings with regular shapes in plan, with regularly positioned walls without leaping stiffness from a story to another. In some cases this hypothesis cannot be accepted, even if the floor construction (made from reinforced concrete or steel) apparently matches the concept of rigid floor diaphragm. Such issues appear at long and narrow

constructions, buildings with irregular shape in plan, or with walls positioned regularly but with stiffness leaps vertically [14].

For the practical analysis of these aspects, in a first approach, the method proposed by the engineer M. Mironescu (Bucharest) can be applied, considering the following steps:

- the assignation of equivalent static loads for the primary mode, assuming rigid floor diaphragms;
- reckoning the slab’s deformations caused by these loads, adjusting the relative level stiffness of the vertical structural parts;
- the redistribution of lateral forces taken up by vertical elements, related to their adjusted stiffness;
- the computing of the stresses in the floor slabs after the load redistribution.

Displacements and deformations are occurring also at the free joints of the structure (the joints which are not tied to the ground). Generally, for a large class of structures these displacements are very small in comparison to the geometrical dimensions of the structural elements. If these displacements are large, a limitation of them is imposed (below the maximal values allowed by the standards) through effective strengthening solution proposals, assuring this way the proper operating conditions of the building (namely “performance requirements”). In such cases the strength criterion (which usually is implicitly fulfilled) is no more sufficient, being replaced with much severe ones (namely “compliance criteria”).

4.3. The assessment of the flexibility

This assessment will be done in all cases. In the case of flexible structures with compressed elements, there is a danger of loosing the balanced initial shape by reaching so called “critical” stresses, which are causing either balance bifurcation (first-order instability), or balance divergence (second-order instability).

Considering that the majority of the existing structures were designed based on the “linear structure” concept, characterized by a response (expressed as displacements and stresses) which is directly proportional to the loads, the influences of the deformations on the geometry and on the stresses was neglected.

In the case of flexible structures, these aspects need a more sophisticated analysis in order to determine if there are any consequences resulting from the non-linear behavior.

4.4. Dynamic analysis

The structural analysis can be performed either in deterministic or in probabilistic (nondeterministic) way. For a deterministic approach, “modal response spectrum

analysis” or “time history analysis” is recommended. The creation of the dynamic model and the interpretation of the results are the most critical phases of the dynamic analysis.

Considering that the physical structure has infinite dynamical freedom degrees, the selection of the mathematical model with a finite number of freedom degrees has to be done in such manner in which the physico-mechanical properties of the structure should not be altered.

During this analysis, an accelerogram is used, from which results the excitation in the form of the movement of the supports. The movement of the supports caused by an earthquake is expressed by using the three components of the translational acceleration. The structural response to this input is usually computed by overlaying the separately computed responses for each component considered acting simultaneously on all parts of the structure’s foundation. For this, the following facts are noticed:

- In the reality, beside the translational movement of the ground the supports will suffer rotations too. Considering the lack of data about measurements concerning the magnitude and the character of the rotational motion components of the ground, this effect is taken into account only as magnitude, the rotational motions being hypothetically deducted from the translational motion components.
- The simultaneous actuation by seismic excitations of all parts of the structure’s foundation, assumes the neglecting of the rotational motions, namely considering the ground or the foundation rock to be rigid. This hypothesis can cause significant errors in case of large, wide-span structures with remotely supports (over 100–150 m).
- A generally disregarded factor is, when defining the effective forces which are developed inside a structure during an earthquake, that the ground movements at the bottom of the structure can be influenced by the structure’s self motion. In other terms, the inducted motions at the bottom of a structure can be different from the free-field motions, which could be observed in the absence of a structure. This interaction between the ground and the structure, namely its effect, is insignificant as importance if the foundation ground is hard soil and if the building is flexible (for example a tall building). In this case, the structure can transfer just a small amount of energy to the ground and the free-field motion is an adequate measure for the displacements of the foundation. In the case of heavy and rigid structures (e.g. historical monuments, buildings with brick masonry or stonework structure etc.) placed on a soft soil, a considerable amount of energy will be transferred from the structure to the foundation ground and thus the motions from the base can noticeably differ from the free-field conditions.

As it can be noticed, smaller or bigger uncertainties appear everywhere.

5. MODELING OF THE UNCERTAINTIES

Looking at as to an informational system, the characteristic of a real structural system is uncertainty.

In case of load-carrying structural systems, the uncertainties can have multiple originating causes (hydro-geotechnical conditions, ambient temperature, physical sub- and superstructure, effective cross-sectional strengths etc.) which are usually hard to be identified.

With the growth of the structural dimensions and complexity, these uncertainties are exponentially amplified. Any hierarchical classification of the practically usable information depends on the character of the expert study.

The uncertainties can be classified in two main groups:

- uncertainties with inaccurate (vague) information;
- uncertainties with doubtful (uncertain) information.

As it can be seen, the main issue appears from the necessity of quantification of this inaccurate information.

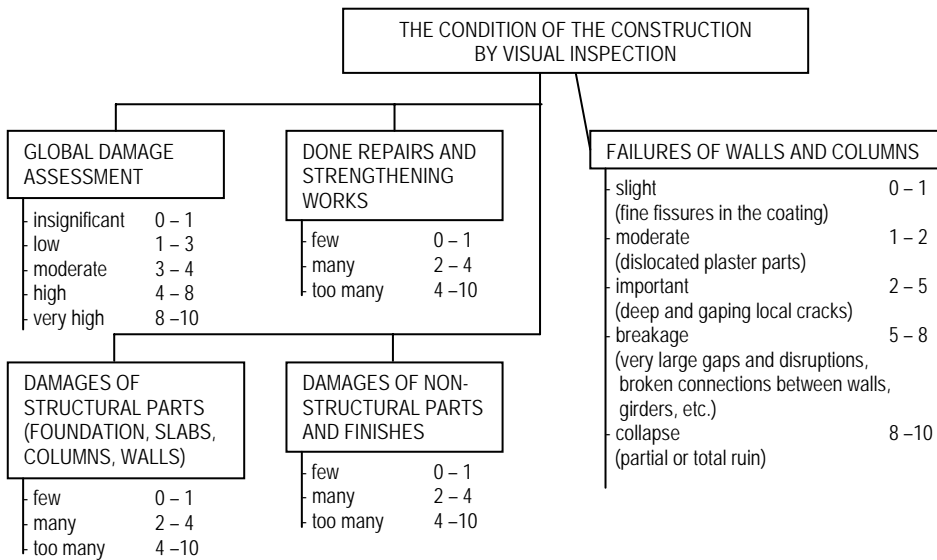


Figure 2. Sample diagram for structural assessment through visual inspection.

For the management of the uncertainties with inaccurate information, fuzzy logic or vague logic is used. In this sense, the ambiguous inaccurate terms are represented by using fuzzy sets with linguistic (or pseudo-linguistic) descriptions.

Generally, the model is expressed through fuzzy implications, bearing an “antecedent and subsequent” form relationship, namely:

$$\begin{array}{l} \text{if} \quad (\text{decisive condition model "A"}) \\ \text{then} (\text{decided condition model "A"}). \end{array}$$

In this way, the *model* “A” is defined if the fuzzy values associated to the fuzzy variables are specified.

In order to operate with uncertainties, having doubtful (uncertain) information, the *CF* “certitude factor” (also known as “confidence factor”) is used, which is usually a numerical value between 0.00 (*absolutely false*) and 1.00 (*absolutely true*).

In Figure 2 a sample diagram is illustrated, namely a slice from a practical tool used for visual inspection during the fuzzy logic based expert study of a bearing structure.

6. CONCLUSIONS

Although the expert study of existing built-up structures implies all the best of the art and science of structural engineering, the number and amplitude of uncertainties is even so distinctly great. In the paper, a quantification of these uncertainties was attempted to be made, by the implementation of intelligent control systems based on fuzzy logic.

The use of fuzzy logic based decisions during an expert study allows:

- an accurate assessment of the bearing structure’s technical condition;
- implementation of instant measures in order to insure safety when the assessed construction shows dangerous failures.

It should be noticed that, by the involvement of fuzzy logic concepts, the fundamental issues of the expert study of structures remain valid, just the viewpoint of information processing changes.

The question that follows after the performed research is, “if the implementation of intelligent control systems based on fuzzy logic has a future?”

As in the majority of situations, an answer to this question is very hard to be given. Most likely, the experts will use in the future, more and more, expert systems in comprehensive combination with in situ monitoring, testing labs and integrated real time software based on case studies (namely “case based reasoning”), neural networks and genetic algorithms.

As for the near future, the use of permanently monitoring systems in sure conjunction with fuzzy control concepts, in case of highly important buildings, can be predicted.

References

1. Bothe, H.H., *Fuzzy Logic*, Springer Verlag, New York, London, 1994.
2. Kandel, A., *Fuzzy Techniques in Pattern Recognition*, John Wiley and Sons, New York, 1986.
3. Dubois, D., Prade, H., *Fuzzy sets and systems: Theory and Applications*, Academic Press, London, 1980.
4. Bocklisch, S. F., *Prozessanalyse mit unscharfen Verfahren*, VEB Verlag Technik, Berlin, 1987.
5. Bandemer, H., Gottwald, S., *Einführung in Fuzzy Methoden*, Akademie Verlag, Berlin, 1990.
6. Cătărig, A., Kopenetz L., Time surveillance and in situ testing by dynamic methods of steel structures, *The 6th Conference of Steel Structures*, Timișoara, Romania, 1991.
7. Lee, L.T., Collins, J.D., Engineering Risk Management for Structures, *Journal of the Structural Division*, ASCE 103, No. ST9, September 1977, pp. 1739-1756.
8. Bârsan, G.M., Kopenetz, L.G., Alexa, P., Analiza dinamică a structurilor cu reazeme depărtate, *Lucrările SNIC*, Sibiu, Romania, 1984. (in Romanian)
9. Cătărig, A., Kopenetz, L.G., Alexa, P., Nonlinear Analysis of Static and Dynamic Stability of Metallic Chimneys, *International Journal of Thin-Walled Structures*, Nr.20, Elsevier Applied Science Publishers, England, 1994.
10. Borș, I., Bârsan, G.M., Alexa, P., Kopenetz, L.G., The Laplace Transforms in Dynamics Analysis of Guyed Steel Structures, *The 6th Conference of Steel Structures*, Timișoara, Romania, vol.2, 1991, pp. 305-314.
11. Kopenetz, L.G., Cătărig, A., Reabilitarea structurilor de construcții cu materiale textile, *Lucrările Conferinței Naționale CisC-2000*, Iași, Romania, 2000. (in Romanian)
12. Kopenetz, L.G., Cătărig, A., Țeserea pământului cu metodă nouă de consolidare, *Congres Național de Drumuri și Poduri din România*, București, Romania, 2006. (in Romanian)
13. Bârsan, G.M., Kopenetz, L.G., Alexa, P., Calculul distanței admisibile între structura de construcție și zona cu focar de explozie posibil în condițiile exploatărilor miniere, *Buletinul științific al I.P.C.-N.*, Cluj-Napoca, Romania, Nr.30, 1987, pp. 35-40. (in Romanian)
14. Gobesz, F., Kopenetz, L.G., Platforme de foraj marin ancorate cu cabluri, *Lucrările SNIC V*, Sibiu, Romania, 1986, pp. 322-329. (in Romanian)

Building projects control by software products

Mária Kozlovská, Assoc. Prof. PhD¹, Lukáš Sabol, Ing.¹

¹Technical University of Kosice, Faculty of Civil Engineering, Slovakia

Summary

The paper deals with building projects risks issue from point of individual partners of project. The newest trends in field of software products will be analyzed. These software products support a building projection following more complex information about construction elements. This way of projection allows a simulation of building costs parameters and building schedule parameters already in the stage of constructional model. Only this approach in project preparation provides a minimize of needed projects actualization in building course, risk minimize of next building and successful and effective building completion, following planning building parameters.

KEYWORDS: building, project, software support

1. INTRODUCTION

The ability for prediction of all parts of construction project, has hardly improved over past seventy years. In fact, the situation has gotten dramatically worse. According to The Economist magazine, 30% of the construction process is rework, and 60% of labor effort is wasted. There is also a 10% loss due to wasted materials. Current technologies for managing the construction process are proving inadequate for addressing the increased complexity of buildings and the incessant market demand for shorter timescales. Today's technologies for managing the construction process are not very effective.

2. THE BUILDING PROJECT SPECIFIKATION

Construction project presents a very difficult and extensive system of construction processes. Nowadays, the emphasis is on the preparation phase and management skills of construction participants more than ever. Whole construction project is very complex and complicated according to:

- the great number of construction participants,
- opposite purpose of construction participants (related to time and cost especially),

- complicated legislation and contracts between construction participants,
- frequent changes in construction plan by construction participants,
- construction participants are involved into other projects (with other construction participants).

From point of management activities system, the building industry specifications are expressed in the design phase and in the invested action of realization phase as well. Specific characteristics of building production are involved not only those contracts, where is the realization of whole building. But also where the contract object is a subdelivery of building works or the contracts directly from investors and is related to just a particular building works group. The specific characteristics of building projects are divided into individual preparation and realization building phases:

From point of product providing – construction product providing:

- the building providing is financially, organizationally and time difficult,
- liable to approval procedure before building beginning and after its finishing as well,
- the more customers are „lays“ – they are not satisfied with time of building preparation and realization, and price as well,

In the phase of product design – building preparation:

- the design and the building-up process are made according individual order,
- more suppliers – designer are interested in building design,
- each project design has to go through the individual approval procedure before the building-up process beginning,
- the project design can be changed also during the building realization.

In the phase of product performance – building realization:

- the construction is special, unrepeatable and unique product,
- the construction has preknown customer (investor),
- more suppliers are interested in building realization,
- more subjects (sub suppliers) are participated in building realization,
- the construction has a stabile character – people, machines, articles „follow“ the product,
- the building making requests a lot of workers – their number and professions,
- the main building works (ground works, foundation, processes of bearing structure) realization) are exposed to climatic effects, it follows the interruption of building realization mainly in winter months,
- manufacturing capacity of enterprises are often needed at several buildings (contracts) at the same time,
- the relative long time of building production – realization,
- the building regulations has to realize before product using.

From point of product - building utilization:

- the construction can be used for that purpose, which is permitted for,
- the relatively long guaranty time for provided building works,
- long time of using,
- necessity of regular maintenance,
- reparations, modernization, reconstruction.

The one of the traditional classification of activities, which are connected with building-up is made from point of individual building participants. These participants are defined in various laws and regulations as persons, who are responsible for particular activities of building process. Among the main participants of building processes belong:

- **investor** – as a person, who are invested the financial resources (for purpose of profit, public or other benefits),
- **contractor** – as a person, who is the building realize for and who is responsible for its preparation, realization and giving into utilization according a law,
- **customer (user)** – as a person, who will use the result of project, (in some cases is contractor, investor and users of building the same person),
- **suppliers** – as persons or subjects, who are contracted to some admission in the frame of preparation and realization activities which are connected with building-up. There are belong:
 - **designer** – as a person, who are provided for investor following his conceptions and requirements (specifications) the building design (he is responsible for it according the law) and all requirements, which are connected with project documentation processing for area and administrative procedure for all professions (water, heating, gas, power line, ...) and operative complex documentation,
 - **main (general) supplier of building works** – as a person, who is responsible for building performance (organization, management, coordination of building works and other activities at building site) according law,
 - **subsuppliers (of main supplier, generally)** – as persons, who are provided the specialistic works or works, which the main supplier do not have needed capacity for,
 - **engineering supplier** – as a person, who is provided the project and building works as well (by own capacity, but more frequently by subdeliveries) – so called supplier engineering, or person, who is provided the investor matter (permission arrange, suppliers selection, making contracts, ...) – so called investor engineering,
 - **building products suppliers** and all goods connected with building as well,
 - **technological equipment suppliers** of building and technological completes

- and other suppliers from various institutions, who give the references, expert opinions, metering and testing to individual building activities, when it is necessary.

The professional organisations are more intensive started in building market, except the traditional participants of building process. These organisations are aimed at project management, developers or facility management. These participants make the presumption for more effective utilization of building projects management forms, which expect using of latter and more integrated software backgrounds.

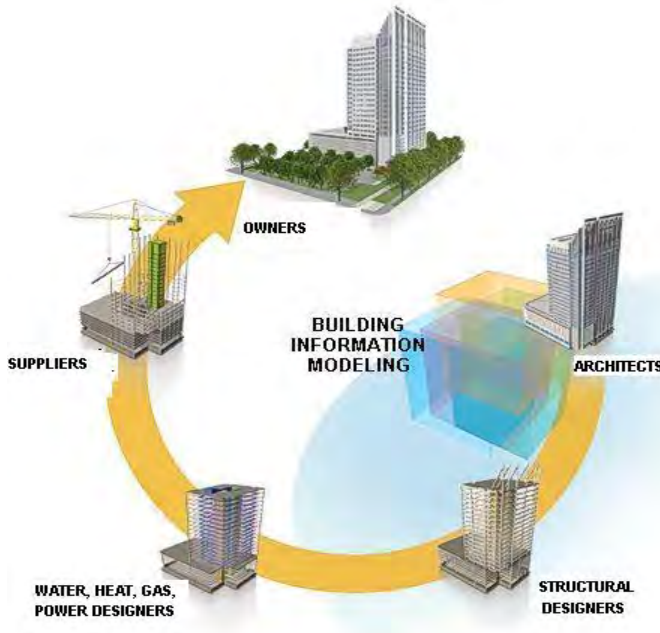
3. CONSTRUCTION PARTICIPANTS SOFTWARE BACKGROUNDS

For the beginning period of using computer aid design is specific, that each construction participants used different software tools (foundation engineering, stress analysis, distribution of water, electricity, estimating, schedule, ...). After a short time some software tools were integrated into complex software tools (stress analysis + construction part + professions, estimate + schedule). As a starting point of computer aid design, we can set computer aid design in two dimensions (2D), using software tools such as AutoCAD, Micro Station, Nemetchek.

Increased complexity of buildings and market demands calls for more integrated software tools, which create background with unitary source of information and data about structural elements and constructions. The software background with these demands is 3D information model, which can be linked with facility management and virtual building software tools.

Nowdays is characteristics in changing software tools from 2D systems to 3D systems (Allplan, ArchiCAD, Autodesk Revit). These software tools are using BIM technology (Building Information Modeling). BIM can be used to demonstrate the entire building life cycle including the processes of construction and facility operation. Quantities and shared properties of materials can easily be extracted. Scopes of work can be isolated and defined. Systems, assemblies, and sequences are able to be shown in a relative scale with the entire facility or group of facilities. The first implementation of BIM was under the Virtual Building concept by Graphisoft's ArchiCAD. ArchiCAD provides the potential for a virtual information model to be handed from design team (architects, surveyors, consulting engineers, and others) to contractor and subcontractors and then to the owner, each adding their own additional discipline-specific knowledge and tracking of changes to the single model. The Virtual Building approach also means

that you can make changes at any time maintaining the integrity of documents, without risking costly errors or costing you productivity.



Pic.1 BIM Technology efficiency

Virtual Building represents a central database of 3D model data. From this can be extracted all the information needed to completely describe design - complete plans, sections and elevations, architectural and construction details, bills of quantities window/door/finish schedules, renderings, animations and virtual reality scenes. That means while you're designing, ArchiCAD is creating all the project documentation so there's little repetitive and tedious drafting work. Comprehensive schedules and bills of materials are available for builders and sub-contractors, as well as drawings of scale-sensitive details. Builders can plan tasks, create time-based animations and document any phase of a building's construction or demolition. And developers can use the photo-realistic renderings for a sales brochure. ArchiCAD stores all the information about the building in a central database; changes made in one view are updated in all others, including floor plans, sections/elevations, 3D models and bills of material [3].

According to long time dominance 2D computer aided design, switching into 3D computer aided design is very slow. But nowadays technology is much more

developed. In present time, the available technology can be specific like switching between 3D technologies to 5D technologies. The Vico Software Virtual Construction™ product line and services address exactly these challenges. Using Virtual Construction technology, building owners, general constructors, and construction managers improve project predictability, reduce risk, manage costs, and optimize schedules on large, complex building projects. The Virtual Construction Software suite is a highly integrated 5D solution designed specifically to bring the benefits of BIM to construction companies. . The software synchronizes the 3D virtual construction model, estimating and scheduling data and helps construction firms determine how best to construct buildings. The Virtual Construction suite covers project constructability, estimating, cost management, schedule planning, procurement, and change management processes. Using Virtual Construction, improve project predictability, optimize the schedule, reduce risk, and manage project cost.

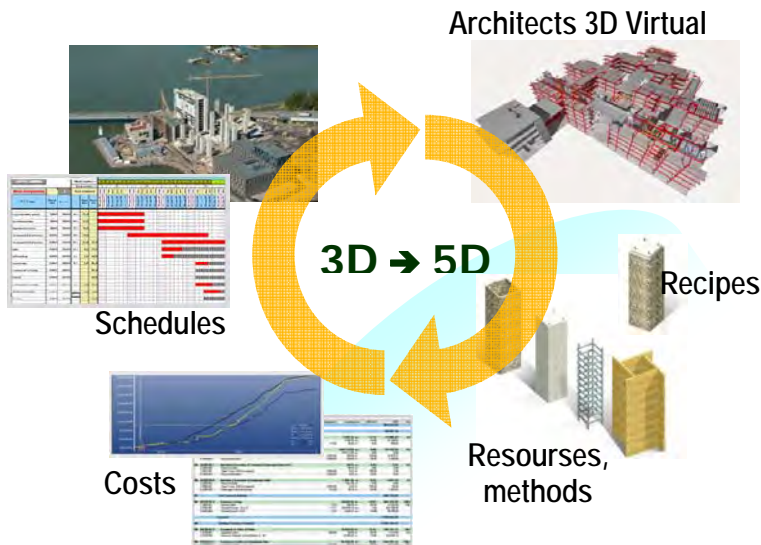
4. 5D TECHNOLOGIES – CHALLENGE FOR COMPLEX CONSTRUCTION PROCESS MANAGEMENT

The Vico software Virtual Construction product line consists of six integrated modules: Constructor 2008, Estimator 2008, Control 2008, 5D Presenter 2008, Cost Manager 2008, Change Manager 2008. Each of modules covers different issue in construction process.

- Vico Software Constructor™ is a dedicated construction modeling application that enables the creation and analysis of highly detailed Virtual Construction™ models. Constructor 2008 helps to solve constructability and coordination issues between disciplines, improve team communication and integrate design, cost and scheduling data. Vico Constructor modeling tools cover architectural, structural and MEP modeling, allowing to create a true Virtual Building model of project. Serving as the hub of the Virtual Construction suite, Constructor enables swift and highly accurate model-based quantity takeoff and schedule information. This data is efficiently handled by Vico Estimator™ to generate cost estimates and by Vico Control™ to create project schedules. The synchronized data can be analyzed and project progress simulated using Vico Software 5D Presenter™. The integrated Vico Software solution helps building owners and general contractors reduce risk, manage cost and shorten project schedules.
- Vico Software Estimator™ 2008 is a unique 3D model based estimating system. By using quantities extracted from Vico Software Constructor™ 3D models, highly accurate estimates can be created in less time. The “what you see is what you estimate” approach reduces inaccuracies and risks and helps

you identify and communicate the relations between quantities, costs and locations.

- Vico Software Control is a unique location-based construction management system. Incorporating locations, estimated quantities and productivity rates in Control's Flowline™ view yields clear, accurate and feasible, yet significantly compressed, schedules. As a construction management system Vico Control enables What-If analyses, provides forecasts based on actual production rates, and analyzes resource usage. Control's Risk Analysis tool improves schedule predictability, and delivers optimized schedule planning.



Pic.2 From 3D to 5D evolution

- A powerful management and communication tool, Vico Software's 5D Presenter can be used by the entire project team to view model data, schedules and cost information along with an interactive and realistic 3D view. This advanced tool gives the construction team a unified and interactive 5D view of a project's progress. Equipped with Earned Value Analysis capability, 5D Presenter 2008 enhances the project management team's ability to track project progress and related costs by revealing the correlation between the budgeted/actual cost and the scheduled/actual work performed.
- Vico Software Cost Manager 2008 gives you the tightest possible control over your project's budget. With this straightforward visual monitoring system, you can easily grasp and communicate project cost variances, and compare them to targeted costs. Cost Manager's unique graphic interface provides a color-coded macro-level view of project costs. This clear picture immediately

allows you to analyze variances, and track them to individual project elements.

- Vico Software Change Manager 2008 automates the process of checking for drawing revisions across construction drawing sets. Building projects generate frequent revisions to hundreds or thousands of drawing files. Identifying and responding to these changes is time-consuming, and missing even a single change could have costly consequences. Vico Software Change Manager reduces risk and improves productivity by identifying these changes, providing workflow control for assigning tasks, and tracking the progress of the entire project team

5. CONCLUSION

Instead of finish allow me a few people voices, which work with this 5D technology.

By simulating before building, we really eliminate many of the surprises that happen on a construction project. These surprises all too often cost money. (Jim Bedrick AIA VP, Virtual Construction & Design Webcor Builders, USA)

In a project of this size, we used to have a full – time estimator and 10 other people extracting quantities from drawings. With Vico’s Virtual Construction suite, one man works with the model and feeds the whole organization faster and more accurately. With Vico Software Virtual Construction technology, quantities stem directly from models. This makes schedules more realistic than ever before. (Erno Aalto, On-Site Engineer, The Palmberg Group, Finland)

5D modeling is the direction of the future. It would make everybody's life easier. That's the way to go! (Walid Shihayed, Chief Estimator CW Driver, USA)

In terms of cost savings, over the long term we are certainly targeting a 5-10% cost reduction as the result of the Virtual Construction technology. (Pierre Puyrigaud, Pre-production Director Applecross, UK)

After running Vico Software Change Manager on one project, we found that only 30% of the changes were clouded by architects and engineers. Without Change Manager, this would have resulted in a dramatic cost escalation. (Darrell Griffith, Director of Business Development, Control Air North, Inc, USA)

Acknowledgements

The article is the issue of the projects AV 4/0008/07 Risks research arising from building process acceleration solution, VEGA 1/0689/08 Management of building structures parameters interaction and AV 4/2018/08 Intelligent constructional elements database for building works scheduling and evaluation.

References

1. <http://www.cegra.cz/112-produkty-software-archicad-11.aspx>
2. Sabol L.: Possibilities of application BIM technology in software ArchiCAD by building participants. In: JUNIORSTAV 2007 – doctoral study conference, Brno, 2007.
3. <http://www.graphisoft.com/>
4. http://www.vicosoftware.com/Products/Products_Overview/tabid/46257/Default.aspx
5. ArchiCAD 10 Reference Guide
6. Designing evolution. In: Eurostav, vol.14, No. 4, 2008, ISSN 1335-1249

The theoretic base for simulation and calculation of boreholes

Helena Kříšáková¹

¹Department of environmental and building services engineering, Czech Technical University in Prague, Prague, 166 29, Czech Republic

Summary

Nowadays, when the big requirement for saving energy and ecological operations of heating and cooling systems is in need, there is a big tendency for using the alternatives sources of the energy. The ground source heat exchangers introduce a very interesting and important alternative source of energy which has a very good possibility for using not only in residential buildings in future.

The borehole is advantageous for layout of the ground temperature on its surface. With rising dept under the terrain the temperature of soil grows up. When the system of borehole is simulated, the minimal dept of the borehole can be determined to ensure the building energy demand.

This article introduces the theoretic method for simulation and calculation of boreholes with the possible influences to the system.

KEYWORDS: The simulation of boreholes, borehole, the energy savings, alternative energy, source of energy, alternative sources

1. INTRODUCTION

The ground source heat exchangers introduce a very interesting and important alternative source of energy which has a very good possibility for using not only in residential buildings in future.

The borehole is advantageous for layout of the ground temperature on its surface. With the rising dept under the terrain the temperature of soil grows up. When the system of borehole is simulated, the minimal dept of the borehole can be determined to ensure the building energy demand.

2. THE THEORETIC BASE OF THE MODEL [1], [2], [3], [4]

The heat transfer from the place with the higher, to the place with lower temperature is called heat transmission. There can be specified three types of heat transmission:

- conducting
- convection
- radiation

In the majority of real cases all three types of heat transmission are applied. In theoretical research always is necessary to determine which type of heat transmission can be reached in the system.

The combination of conducting and convection heat transmission is supposed in the borehole system.

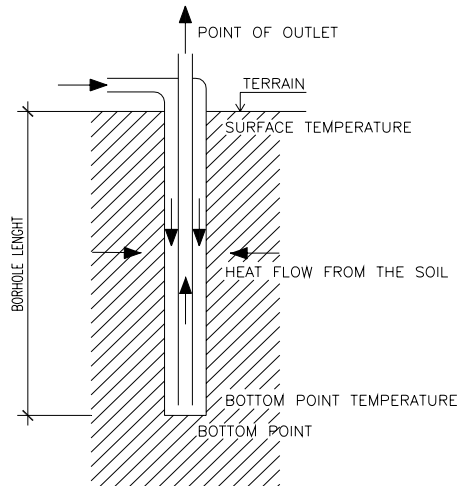


Figure 1. The system of borehole

In general, the process of heat conducting evokes the change of temperature in the space and in the time as well. The field of temperature is than described with the function:

$$t = f(x, y, z, \tau)$$

t – temperature [$^{\circ}\text{C}$]

x, y, z – coordinate [m]

τ = time

The field of temperature is entire set of all points' temperatures in supposed area in each moment on the time. There can be distinguished the field of temperature:

- Stationary - $t = f(x, y, z)$ – only the function of coordinates
- Non-stationary - $t = f(x, y, z, \tau)$ – with the dependence on the time

In the scalar field of temperatures, determined by the equation $t = f(x, y, z, \tau)$, can be defined the isothermal areas – the places with the same temperature. At bidirectional solution the isothermal areas will change to isothermal lines, which are connecting the points with the same temperature.

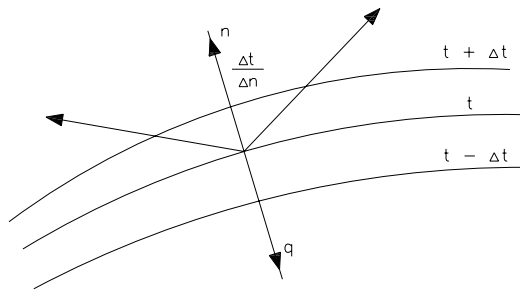


Figure 2. Isothermals, the temperature gradient

2.1. The influence of conducting

The temperatures in the system are changing in all directions, which are cutting through the isothermals. The highest thermal change on the length unit is in the normal direction n to isothermals. The growth of temperature in normal direction is determined by the temperature gradient – the vector perpendicular to isothermal, routed to the side of rising temperature.

The value of temperature gradient is:

$$\text{grad}t = \frac{\partial t}{\partial n} = \frac{\partial t}{\partial x} + \frac{\partial t}{\partial y} + \frac{\partial t}{\partial z} \quad [Km^{-2}]$$

The condition for heat transmission is unsteady temperatures lay out in the solved system. The heat transferred within the time unit is called heat flow (P). The heat flow passing through the area unit is described like a density of heat flow (q).

Than is obtained the next equation:

$$dP = q \cdot dS \quad [W]$$

q – density of heat flow $[Wm^{-2}]$

The density of heat flow dependence on temperature gradient is given by the first Fourier law. The density of heat flow is direct proportional to temperature gradient.

$$q = -\lambda \text{ grad } t \text{ [W/m}^2\text{]}$$

λ - coefficient of thermal conductivity [$\text{Wm}^{-1}\text{K}^{-1}$]

The vector q and temperature gradient t are lying on the same line, but with opposite directions. Heat is always handed over from the warmer to the colder parts of the system.

The vector q numerical value is:

$$q = -\lambda \cdot \text{grad} t = -\lambda \cdot \left(\frac{\partial t}{\partial x} + \frac{\partial t}{\partial y} + \frac{\partial t}{\partial z} \right) \text{ [Wm}^{-2}\text{]}$$

Heat dQ , which passes through the isothermal area can be determined from the equation:

$$dQ = q \cdot dS \cdot d\tau \text{ [J]}$$

The definiteness conditions

In the problems, where the heat transmission is solved, the physical conditions are given by the coefficient of thermal conductivity λ , specific thermal capacity c_p , density ρ and the internal sources boundlessness q_v .

The unit proportion and form are characterized by the geometrical conditions, which are usually adjusted to be able to replace this unit with the simplest form as possible.

The initial condition describes the temperature layout in the system on the process beginning – in the time τ_0 .

The mutual thermal operations between the ambient and the system surface are given by the surface conditions. In the majority of cases it is necessary to involve the internal and external surfaces, which are dividing solved, from the other system. Usually, there are four types of surface conditions:

- First type of surface condition – describes the temperature layout t_p on the unit surface P as a function of time and coordinates

$$t = f(x, y, z, \tau) \text{ [}^\circ\text{C]}$$

- Second type of surface condition – describes the density of heat flow layout on the surface of the unit as a function of the time

$$q = f(x, y, z, \tau) \text{ [Wm}^{-2}\text{]}$$

with the harmony with the Fourier law

$$q = -\lambda \cdot \text{grad}t = -\lambda \cdot \left(\frac{\partial t}{\partial n}\right)_p \text{ [Wm}^{-2}\text{]}$$

n – normal to the surface P

- Third type of surface condition – is used, when the ambient temperature and the coefficient of heat transfer is known.

$$q = \alpha_c (t_p - t_{ok}) = -\lambda \cdot \left(\frac{\partial t}{\partial n}\right)_p \text{ [Wm}^{-2}\text{]}$$

When je $t_p < t_{ok}$, from the previous $q < 0$. For calculations is normally used Fourier condition in the form:

$$q = -\alpha_c (t_p - t_{ok}) \text{ [Wm}^{-2}\text{]}$$

- Fourth type of surface condition – describes the heat exchange on the system surface with the principles of heat transmission. The solved system is supposed to have ideal contact with the other system, so their surfaces have the same temperature. On this presumption is based next equation:

$$\lambda_1 \left(\frac{\partial t_1}{\partial n}\right)_p = \lambda_2 \left(\frac{\partial t_2}{\partial n}\right)_p \text{ [Wm}^{-2}\text{]}$$

The field of temperature on the cylindrical systems is solved like on the plane systems, only with re-writing previous equations to cylindrical axis.

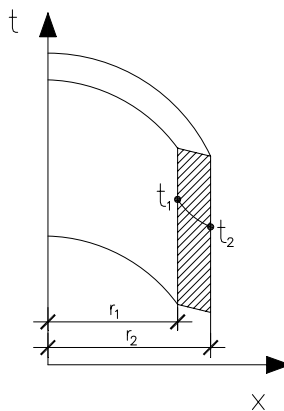


Figure 3. scheme of heat conduction through the cylindrical wall

The temperature gradient in the cylinder axis direction is zero and the field of temperature is constant on the cylinder perimeter.

Then is possible to write:

$$\frac{d^2 t_1}{dr^2} + \frac{1}{r} \cdot \frac{dt}{dr} = 0 \quad [Km^{-2}]$$

By solving the integrals and determination of integral constants is possible to write:

$$t = t_1 - (t_1 - t_2) \cdot \left(\frac{\ln(r/r_1)}{\ln(r_2/r_1)} \right) \quad [^{\circ}C]$$

In case of planner systems the temperature is the only function of the coordinates, at the cylindric systems we obtain the logarithmic dependence.

For not to express the dependence $q=f(r)$, for cylindrical units the heat flow P is usually used.

Than it is possible to write:

$$P = -\lambda \cdot \frac{dt}{dr} \cdot S = -\lambda \cdot \frac{dt}{dr} \cdot 2 \cdot \pi \cdot l \quad [W]$$

For random point in the layer can be deduced:

$$t = t_1 - \frac{q_l}{\pi} \left[\sum_{i=1}^{k-1} \frac{1}{2 \cdot \pi \cdot \lambda} \cdot \ln \frac{r_{i+1}}{r_i} + \frac{1}{2 \cdot \lambda_k} \cdot \ln \frac{r}{r_k} \right] \quad [^{\circ}C]$$

2.1. The influence of the water convection

The next factor which is necessary to mention in frame of borehole calculation is water convection. The heat is handed over from the cylindric wall surface to the circulation water. This heat transmission is described by the continuity equation, dynamic balance equation and the energetic equation.

In majority of cases, there is necessary to idealize these equations for solving in bidirectional space.

$$\frac{\partial w_x}{\partial x} + \frac{\partial w_y}{\partial y} = 0 \quad [s^{-1}]$$

$$w_x \frac{\partial w_x}{\partial x} + w_y \frac{\partial w_x}{\partial y} = \nu \left(\frac{\partial^2 w_x}{\partial x^2} + \frac{\partial^2 w_x}{\partial y^2} \right) \quad [ms^{-2}]$$

$$w_x \frac{\partial w_y}{\partial x} + w_y \frac{\partial w_y}{\partial y} = \nu \left(\frac{\partial^2 w_y}{\partial x^2} + \frac{\partial^2 w_y}{\partial y^2} \right) \quad [ms^{-2}]$$

$$w_x \frac{\partial T}{\partial x} + w_y \frac{\partial T}{\partial y} = a \left(\frac{\partial^2 T}{\partial x^2} + \frac{\partial^2 T}{\partial y^2} \right) \quad [Ks^{-1}]$$

When we only know the conditions on the system surface, in majority of cases the surface temperature T_s and heat flow q , the calculation can be simplified.

It is frequently to want to get the coefficient of heat transmission values.

$$\alpha = \frac{q_s}{T_s - T_f} \quad [Wm^2K^{-1}]$$

3. CONCLUSION

The alternative sources of energy utilization will be more frequent in future. When the simulation of ground conditions and its influence to the heating system is made it is possible to obtain big savings in the initial and operation building costs. The system and each physical factor description can optimize the heating and cooling system.

References

1. Rédr, M., Příhoda, M., *Základy tepelné techniky*, Nakladatelství technické literatury, Praha 1, 1991, ISBN 80-03-00366-0. (in Czech)
2. Nožička, J., *Základy termomechaniky*, Vydavatelství ČVUT, Praha 6, 2001, ISBN 80-01-02409-1. (in Czech)
3. Pečeňa, Z., Súkup, J., *Termomechanika a hydraulika*, Alfa-vydavateľstvo technickej a ekonomickej literatury, Bratislava , 1986, (in Slovak)
4. Sazima, M., *Sdílení tepla*, Praha, 1993, ISBN 80-03-00675-9. (in Czech)

The soil thermal analysis in the neighbor of ground source heat exchanger of the heat pump

Helena Křišíková¹

¹Department of environmental and building services engineering, Czech Technical University in Prague, Prague, 166 29, Czech Republic

Summary

The aim of this article is thermal behavior of ground source heat exchanger during the one year measured period. It represents soil temperature dependences on the depth under the terrain during the time. The ground source heat exchangers introduce a very interesting and important alternative source of energy which has a very good possibility for using not only in residential buildings in future.

In the article, daily, monthly and annual dependences of soil temperatures from particular sensors, placed in the system of ground source heat exchanger are analyzed.

Generally known rule that with the growing depth under the terrain the temperature of soil is less influenced by the weather conditions with the measured dates is validated. At the same time stands up the question, to which depth the soil is able to regenerate itself and when it cannot be revive by reason of big depth under the terrain.

Than it is necessary to consider the local conditions if it is better to use ground source heat exchanger or to make a borehole.

KEYWORDS: The ground source heat exchangers, temperature dependences, alternative energy, source of energy, alternative sources, the thermal behavior

1. INTRODUCTION

Nowadays, when the big requirement for saving energy is in need, there is a tendency to use natural and alternative sources of energy. The heat exchangers have a very good potential for using in residential housing and in large buildings as well in future. This article deals with soil thermal behavior in the neighbor of ground heat exchanger of the ground to water heat pump. The measurements are from one year period – from February to December 2007.

2. THE MEASURED SYSTEM DESCRIPTION

The measurements were made from February 2007 to December 2007 during all days in the interval one minute. This system is installed in the family house with overall heat loss aprox. 12kW. The energy demand for heating and hot water is covered by the ground to water heat pump. R404a is used in the ground heat exchanger like a cooling medium.

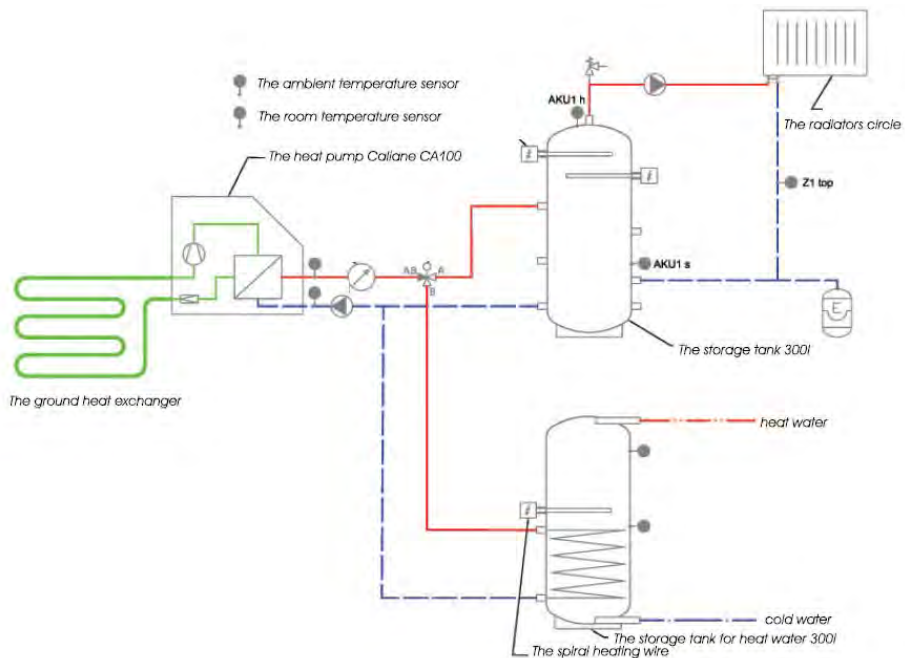


Figure 1. The system connection in the family house

For the measurements the DS18B20 sensors were utilized (Dallas Semiconductor producer). These sensors work with thermal range -55°C to $+125^{\circ}\text{C}$, with the accuracy $\pm 0,5^{\circ}\text{C}$ for 10°C to $+85^{\circ}\text{C}$.

15 sensors are placed in the different depth under the terrain, which are scanning the soil and piping temperature – viz. figure 2.

The AKU2h sensor is situated in 1,1m under the terrain and is screened from the ground exchanger by the polystyrene board to prevent the influence from piping to the soil.

The ground register is placed in the 1,1m under the terrain and is made from 5 piping loops. From the previous geological enquiry, the clay, cohesive and medium dry soil was found out.

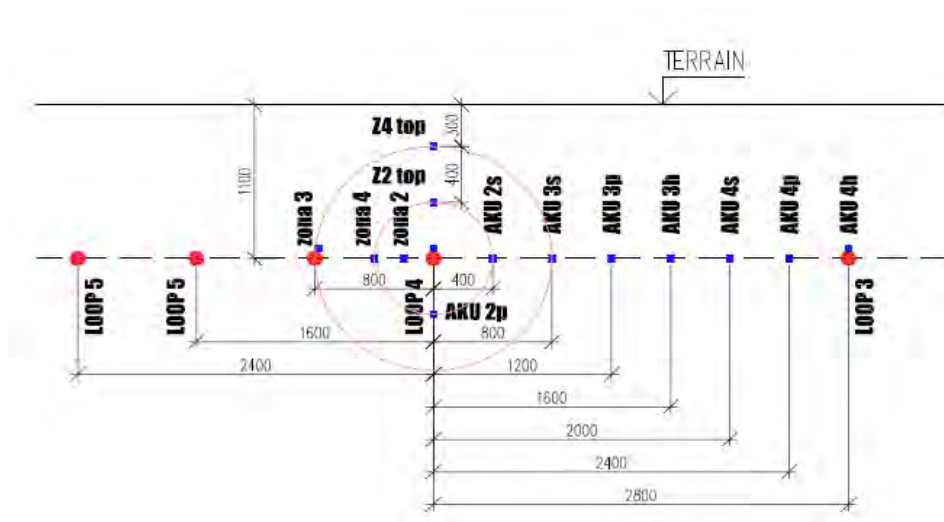


Figure 2. The situation of the used sensors

3. DATAS PROCESSING [1], [2], [3], [4]

Regarding to a large number of dates, from the ambient temperature, the coldest and the warmest month was determined. The coldest month in 2007 was December, the warmest one was June. As in the June the dates are not totally complete for next comparisons the July was studied.

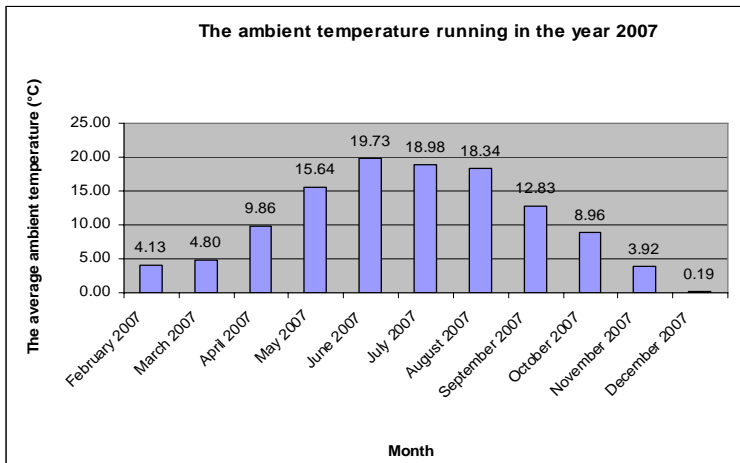


Figure 3. The average ambient temperatures in 2007

The next chart shows the temperature process in the soil during the reference day in the month (the 15 of July and the 15 of December). The data are taken from the sensors z4top, z2top and aku2h in these days. For the same level under the terrain, the temperature running is during the day almost constant. In July the warmest temperature can be observed in the depth 0,3m under the terrain, the most constant than in 1,1m under the terrain (aku2h sensor – screened sensor by the polystyrene board). In the December the highest temperature has the soil 1,1m under the terrain (the aku 2h sensor), the soil 0,3m and 0,7m under the terrain is more influenced by the weather conditions.

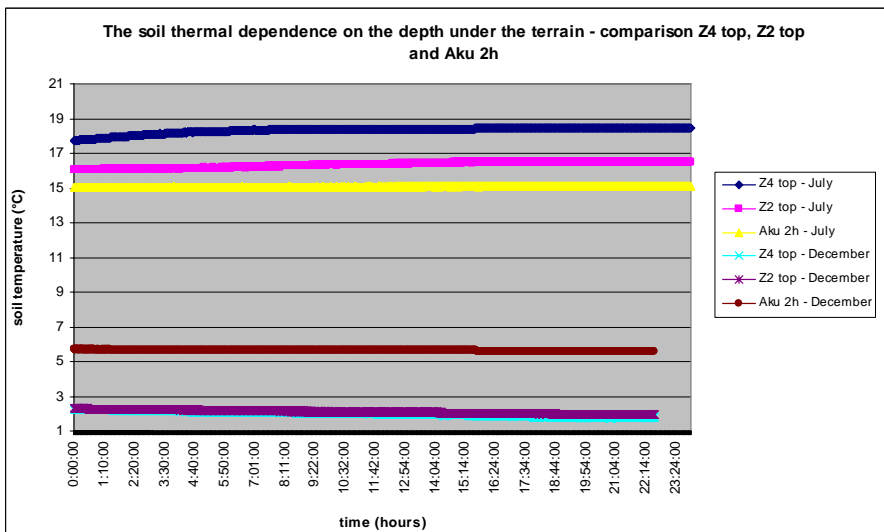


Figure 4. The soil dependence on the depth under the terrain

Table 1. The daily average values of soil temperature in dependence on the depth under the terrain

	sensor Z2 top (°C)	sensor Z4 top (°C)	sensor Aku 2h (°C)	sensor Aku 2p (°C)
July 2007	16.33	18.32	15.07	14.85
December 2007	2.09	1.99	5.62	3.94

The soil daily running temperature in the dependence of the depth under the terrain and the sensor position, in the next charges is shown. The daily process of the temperature is based on the aku 2h and z4top sensors measurements. The temperature differences on the beginning and in the end of measured interval (24 hours) are almost negligible. From the sensor aku 2h in the day 14.07.2007 the difference is 0,04°C, for the day 15.07.2007 than 0,02°C. For the same days from the sensor z4 top these differences are higher and it is 1,13°C for the day 14.07.2007 and 0,73°C for 15.07.2007.

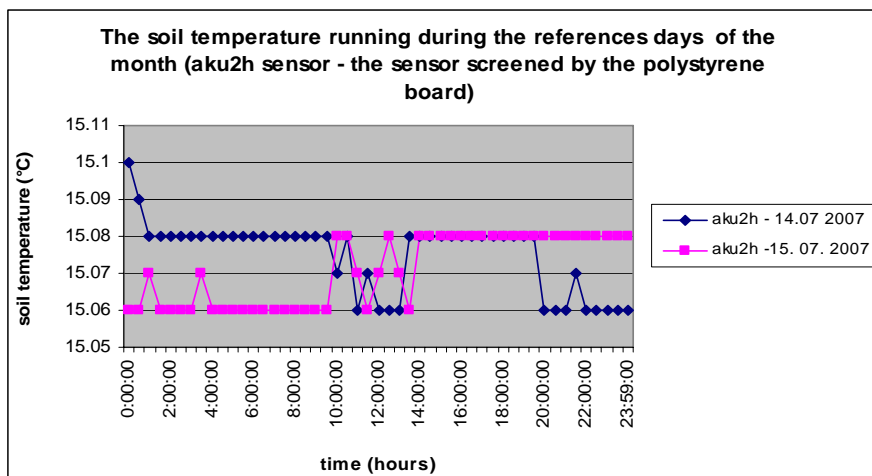


Figure 5. The soil thermal dependence on the depth under the terrain from aku 2h sensor

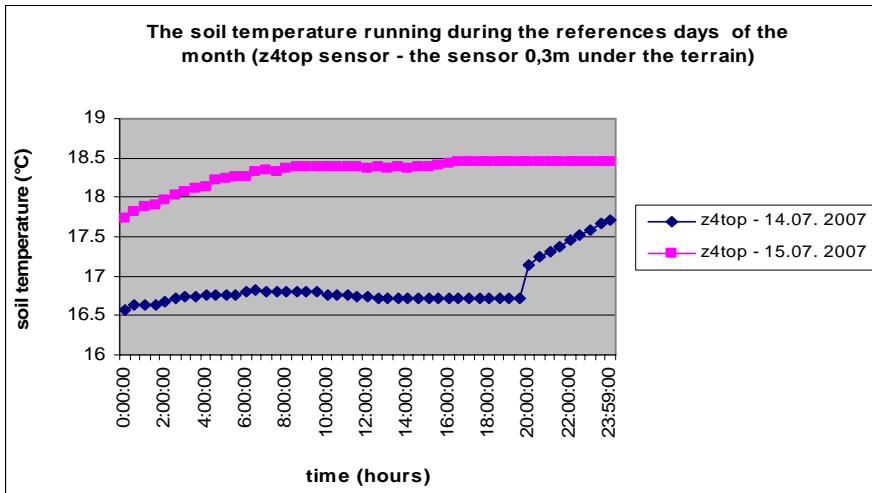


Figure 6. The soil thermal dependence on the depth under the terrain from z4 top sensor

How can be seen from these measured dates the most stable is the soil in the depth 1,5m under the terrain, because in this depth the soil is not so influent by the weather conditions.

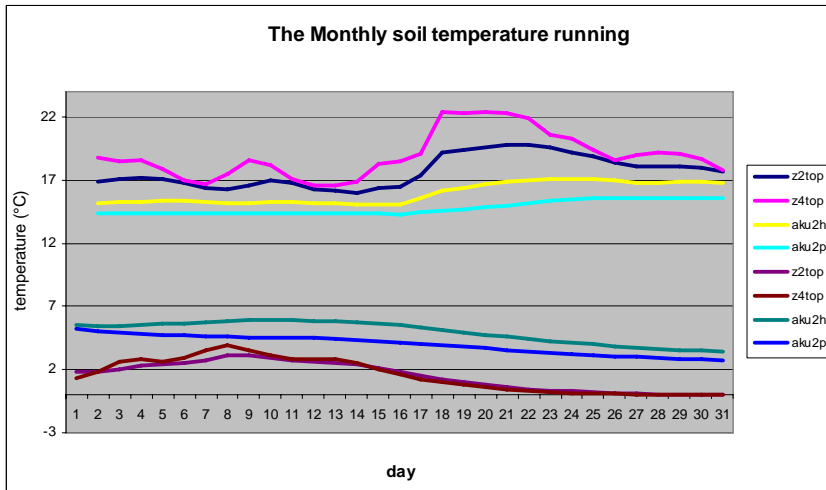


Figure 7. The monthly soil thermal dependences in June and in December

From the figure 7 can be seen the differences in the temperature divergence. The difference from the sensor z4 top is in frame 5°C, from aku 2p it makes the difference 1,5°C in the June. In the December, there can be observed the highest divergence in temperature from the 0,3m level under the terrain and it makes 4°C.

The figure 8 shows the comparison between the soil thermal dependences during the June and December 2007. The differences can be seen from the chart.

The maximal thermal differences in the month values during the year is between the dept 0,3m and 1,5m under the terrain, and it makes 5,91°C.

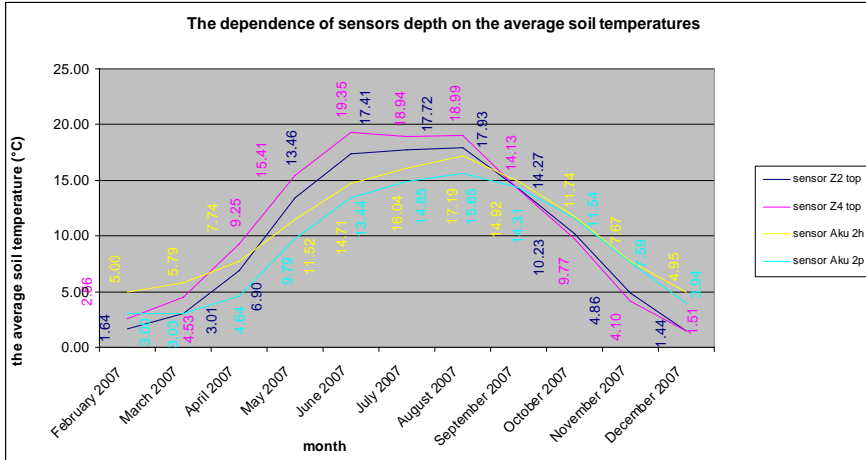


Figure 8. The year dependence of sensors position on the depth under the terrain

The soil temperature is influent by the ground heat exchanger piping with the cooling medium inside. From the next charge can be seen that this temperature is impressed only to the 0,4m length from this piping. In the higher distance from the ground register the soil temperature differences are almost negligible.

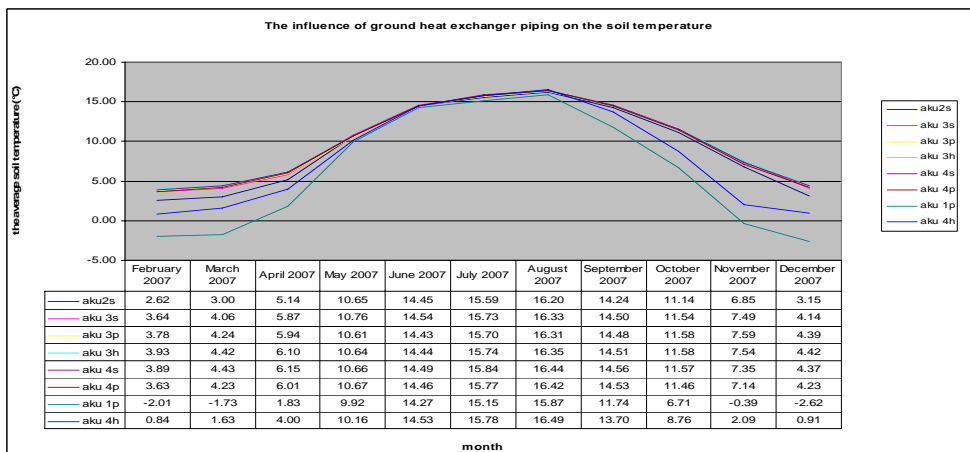


Figure 9. The influence of register piping to the soil temperature

4. CONCLUSION

From the previous dates follows the soil thermal dependences on the depth under the terrain. The generally known rule, that with the growing depth under the terrain the soil thermal dependence is less influent by the weather conditions is by the previous dates confirmed.

In the same time there is a question about the soil ability to revive itself. To which dept the soil can be during the summer regenerated. Than it is necessary to look over the climate conditions if it is better to make the ground heat exchanger or to prefer a borehole.

The special thanks are given to the company Regulus s.r.o, Do Koutů 1897/3, Prague 4 – Komořany, with its help was the measured dates obtained.

References

1. Rédr, M., Příhoda, M., *Základy tepelné techniky*, Nakladatelství technické literatury, Praha 1, 1991, ISBN 80-03-00366-0. (in Czech)
2. Nožička, J., *Základy termomechaniky*, Vydavatelství ČVUT, Praha 6, 2001, ISBN 80-01-02409-1. (in Czech)
3. Pečeňa, Z., Súkup, J., *Termomechanika a hydraulika*, Alfa-vydavateľstvo technickej a ekonomickej literatury, Bratislava , 1986, (in Slovak)
4. Sazima, M., *Sdílení tepla*, Praha, 1993, ISBN 80-03-00675-9. (in Czech)

The thermal behavior of the water to water heat pump

Helena Křišíková¹

¹*Department of environmental and building services engineering, Czech Technical University in Prague, Prague, 166 29, Czech Republic*

Summary

This article deals with the thermal processes in frame of the ground to water heat pump. The system is really running in the single-family house with total heat losses cca. 15kW.

The source of energy for the house is a borehole with the water like a circulation medium.

The particular temperature dependences are described in the four years measured period.

KEYWORDS: heat pumps, borehole, thermal behavior, the energy savings, alternative energy, source of energy,

1. INTRODUCTION

Nowadays, there is a big tendency to use the natural sources of energy for heating and cooling in buildings. In the article, the thermal runnings are analyzed in the frame of ground to water heat pump. The heat pump is installed in a single family house with overall heat loss approximately 15kW. It is a two floor family house, which contains six living rooms, two bathrooms, kitchen and dinning room.

2. THE MEASURED SYSTEM DESCRIPTION

For central heating water, hot water and heating the swimming pool water the ground to water heat pump is used. Like another source of energy the solar collectors are installed. The ground plans are shown on the picture 1 and 2.

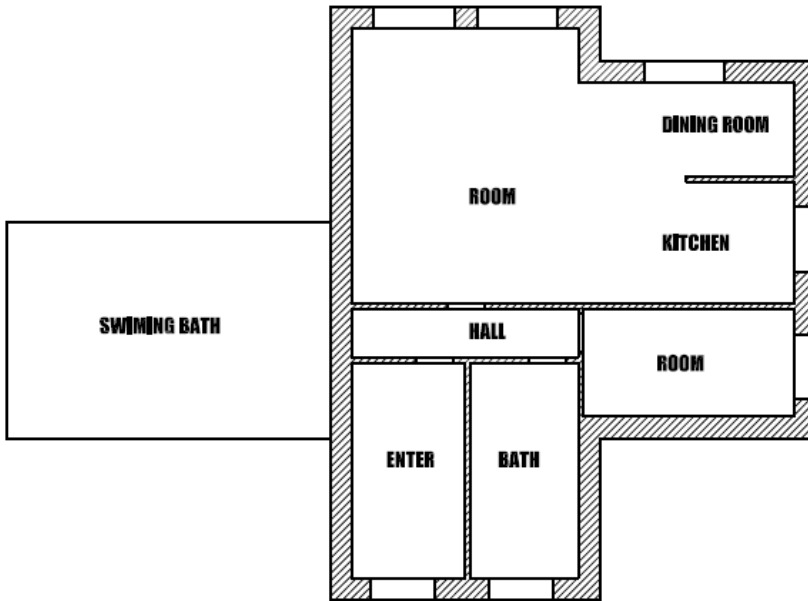


Figure 1. The ground floor of the family house

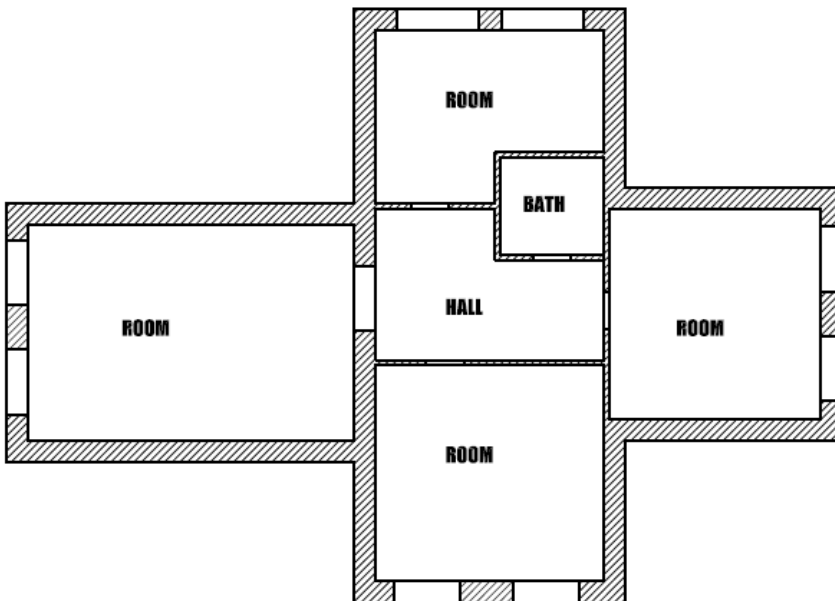


Figure 2. The second floor of the family house

The situation of particular sensors, in picture 3 is shown. The temperatures in the borehole, the water inlet to evaporator and condenser, water outlet from evaporator and condenser, inlet temperature to compressor, water temperature in storage tank and in the solar collectors and the operation of water pumps were measured.

The measured values were obtained from April 2004 to January 2008. The measurements were made in each day in these years in the 6 seconds interval.

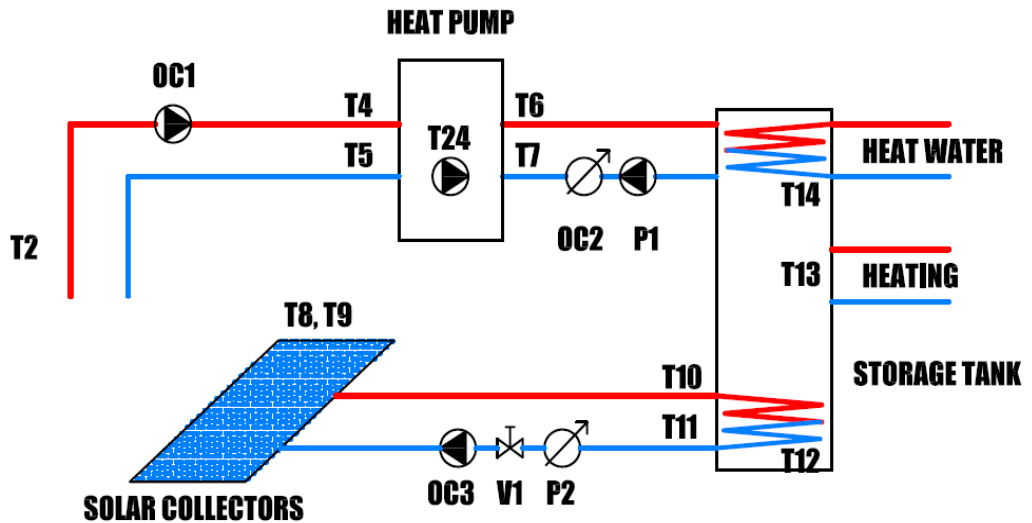


Figure 3. The system connection

3. DATAS PROCESSING [1], [2], [3], [4]

The processed dates are from the measured period from April 2004 to January 2008. The temperature running in the heat pump borehole shows the chart 4. This temperature running is from the whole measured period.

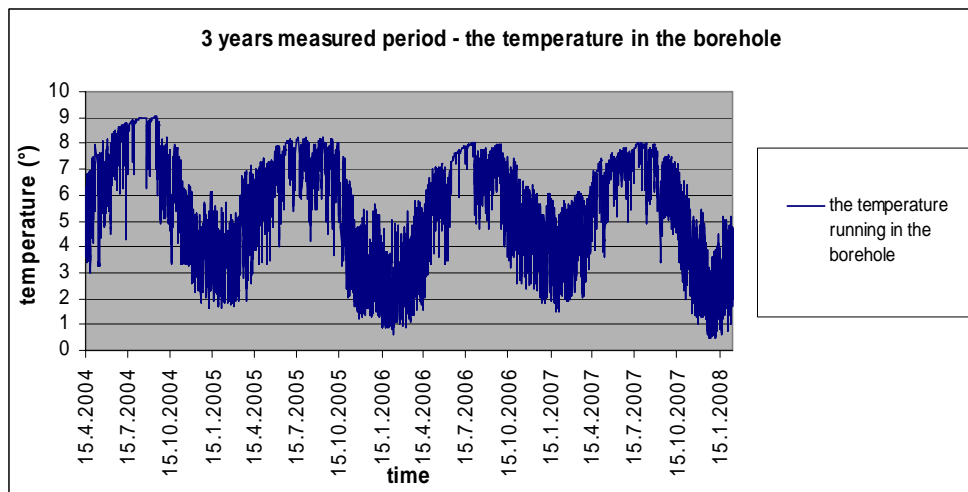


Figure 4. The temperature running in the borehole

The average month values from the years 2004 to 2007 represents the chart 5. The soil in the neighbor of the borehole is not overtired and it is able to hand over almost the constant amount of heat in the following years.

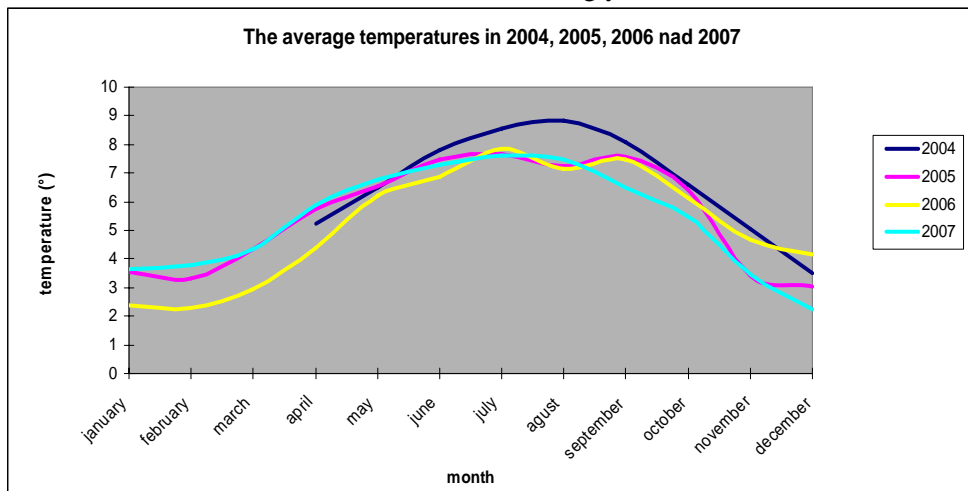


Figure 5. The average month temperatures in 2004, 2005, 2006 and 2007

The thermal differences in frame of the borehole in the December of 2005, 2006 and 2007 are shown in the following graph. The maximal thermal divergence in the December in the measured years is 4,95°C – for December 2007.

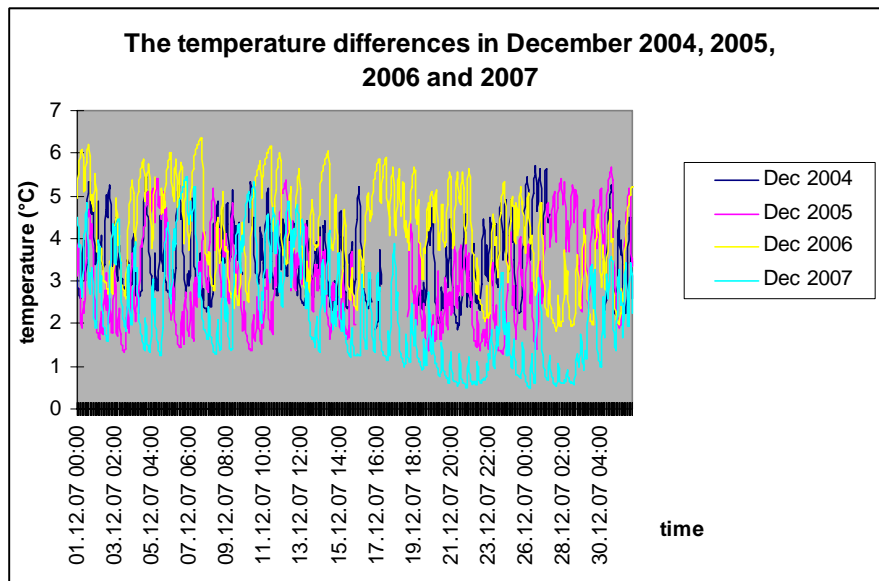


Figure 6. The temperature differences in December 2004 – 2007

The average December's minimal and maximal borehole temperature values are in the next table.

Table 1. The minimal and maximal temperatures in the borehole in Decembers

	December 2004	December 2005	December 2006	December 2007
Max. temp. (°C)	5.695	5.674	6.37	5.441
Min. temp. (°C)	1.851	1.288	1.825	0.485

The temperature running in frame of the borehole in the warmest month – June – is shown in the chart 7. It is the temperature from the Junes from measured years 2004 to 2007. The soil temperature in June is warmer of 4,48°C in max. value, 2,58°C in average value than in the December.

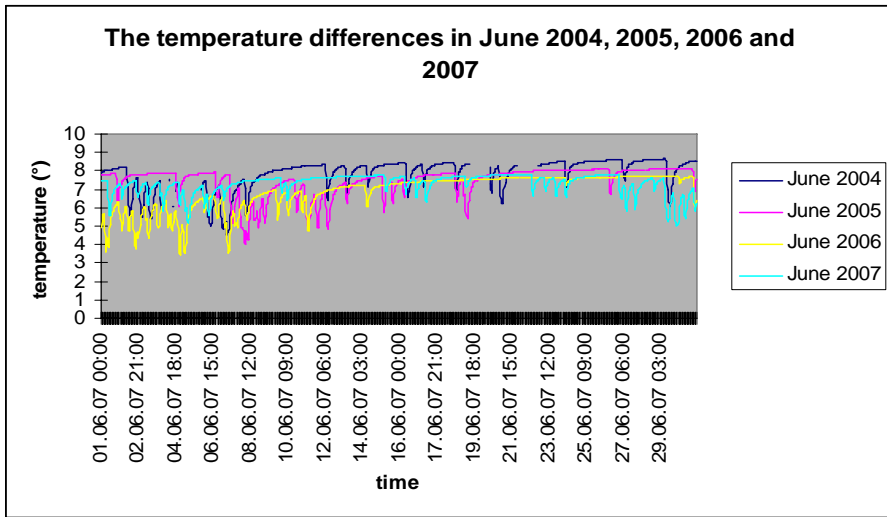


Figure 7. The temperature differences in June 2004 – 2007

	June 2004	June 2005	June 2006	June 2007
Max. temp. (°C)	8.655	8.138	7.723	7.810
Min. temp. (°C)	4.488	4.002	3.479	4.966

The water inlet temperature to evaporator of the heat pumps is copying the temperature running in the borehole. Before entering the evaporator, the water from the borehole gets warmer on its layout and makes the difference between the temperature in the measured place in the borehole and the inlet to evaporator.

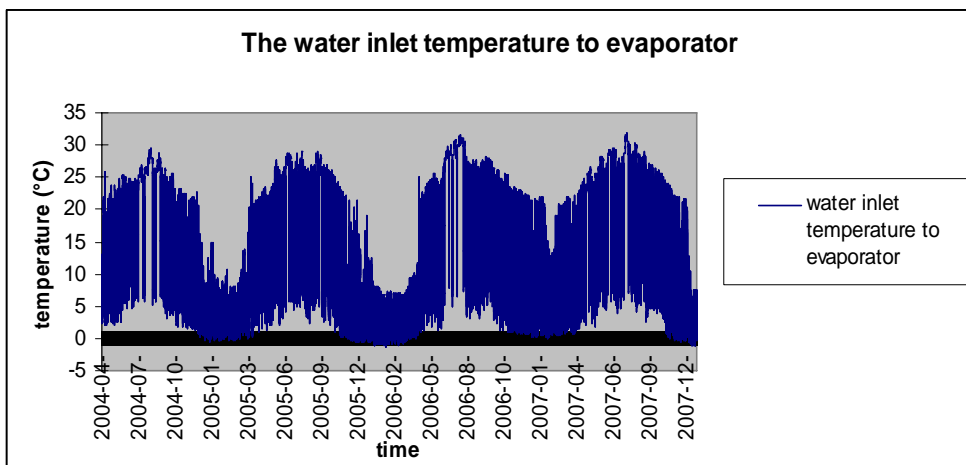


Figure 8. The water inlet temperature to heat pump evaporator

4. CONCLUSION

From the previous dates can be seen, that by the heat extraction from the soil it is not overtired and it is able to hand over almost the same amount of heat in the following years of heat pump operation. The borehole gives sufficient heat store which is needed for heat pump operation and building energy demand. It is not as influent by the weather conditions as can be observed in the square ground heat exchanger.

References

1. Rédr, M., Příhoda, M., *Základy tepelné techniky*, Nakladatelství technické literatury, Praha 1, 1991, ISBN 80-03-00366-0. (in Czech)
2. Nožička, J., *Základy termomechaniky*, Vydavatelství ČVUT, Praha 6, 2001, ISBN 80-01-02409-1. (in Czech)
3. Pečeňa, Z., Súkup, J., *Termomechanika a hydraulika*, Alfa-vydavateľstvo technickej a ekonomickej literatury, Bratislava , 1986, (in Slovak)
4. Sazima, M., *Sdílení tepla*, Praha, 1993, ISBN 80-03-00675-9. (in Czech)

The analysis of the liquid-filled cylindrical tank’s wall flexibility

Ciprian Lamatic¹, Nicolae Ungureanu² and Mihai Vrabie³

¹Department of Structural Mechanics, Faculty of Civil Engineering and Building Services, Iasi,
700050, Romania

² Department of Structural Mechanics, Faculty of Civil Engineering and Building Services, Iasi,
700050, Romania

³ Department of Structural Mechanics, Faculty of Civil Engineering and Building Services, Iasi,
700050, Romania

Summary

The studies consider metallic or composite vertical cylindrical tanks, which exhibits sensitiveness regarding the walls stability. The main objective of the investigation is the analysis of those situations in which the action is generated by the earthquakes and the stress state in the walls is generated by the coupled effects of the horizontal and vertical acceleration and the loading’s alternation. Another goal is the study of the likely cases which may led to the appearance of the critical stress in the walls and the effects of the wall’s flexibility and seated way’s at the base of the tanks .

KEYWORDS: cylindrical tank, seismic excitation, vertical acceleration, axial loads, stability.

1. CONSIDERATIONS REGARDING THE STABILITY OF TANKS

Metallic tanks, which have the walls thickness dimensioned from the strength condition, must have their stability checked. It is observed that the loss of their structural stability can be produced for other load combinations, others than the ones adequate to strength’s calculus. Significantly is the fact that, for the stability analysis, the seismic effects generated by the vertical components of earthquake acceleration are important.

The walls of liquid storage tanks are subjected to uniform compression came from static and dynamic axial symmetrically effects, like the ones due to vertical acceleration and an nonuniform pressure generated by the horizontal action of earthquake.

For the stability of tank's shell, the internal forces from tangent plan are important, especially axial forces directed after generatrix, but in a more refined analysis the sliding forces and respectively those circumferential, are considered.

Theoretical and experimental researches [4, 5, 7, 14, 17, 18, 19, 28] attest that for an analysis exactly enough for shell's stability, membrane state effects from cylindrical shell are those who determine the phenomenon.

A circular cylindrical shell subjected to a uniform axial pressure can loose the stability through axial symmetrical buckling, semi-waves forming in generatrix directions (fig.1.a), or diamante shape buckling through building-up bi-directional semi-waves: in generatrix directions and circumferential (fig. 1.b.)

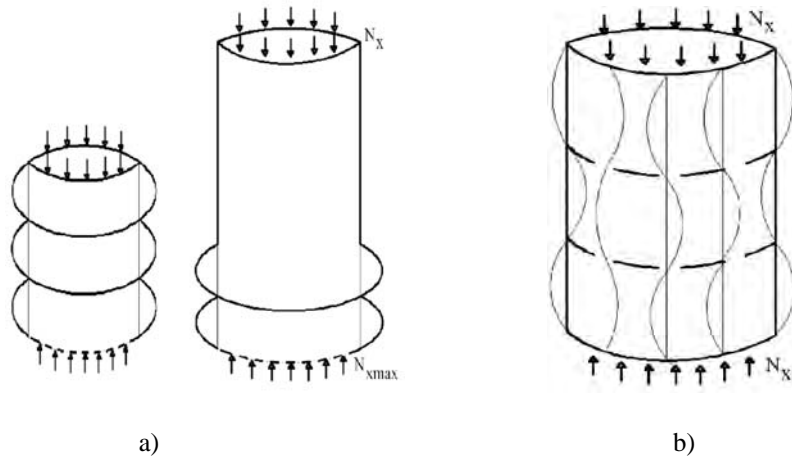


Figure 1. Shapes of stability loss for cylindrical tanks

In the case of tanks, we can meet both situations, but obviously, under a specific mode, because axial compression is a variable effort in generatrix direction. Loss of stability remains axial symmetrical, but it is focusing in the zones of maximum axial force, in the case of vertical tanks this being the base rule.

If the wall's thickness is variable (in case of metallic tanks this variation on height is stepped), more zones of stability loss may appear, mainly focused at thickness alteration.

Although in seismic designing, actions are of two kinds, static and dynamic, stability calculus of tanks is performed trough quasi-static method. Complex researches regarding dynamic effects are done in papers [4, 14, 20, 22] and the conclusions of those studies certifies the sufficiency, especially for designing, of quasi-static analysis.

Stability loss through buckling given by membrane internal forces can be caused by the bending global effects generated by liquid vibration due to horizontal acceleration.

In relation to considered reference system (x axis in generatrix direction), important compression forces are N_x , which come from roof's structural elements, from hydrostatic and hydrodynamic pressures generated by vertical and horizontal acceleration, last one having two components, one due to convective movement of liquid and one due to impulsive movement of liquid and structure. The impulsive component results from the rigid translation with ground's acceleration and from wall's deformation due to its flexibility, which involves impulse mass of liquid, the acceleration being height variable.

Impulse and convection horizontal actions have as effect a rotational moment (overturning) taking as reference the own axis of the tank's horizontal section, normal to the earthquake excitation's direction. This moment produce axial forces N_x , nonuniform distributed on section, with maximum values in the main plan of vibration. Hydrodynamic pressures give rise of sliding forces $N_{\theta x}$ in cylindrical shell, which may significantly influence the critic loadings. A special role comes to circumferential efforts N_{θ} , when they are of tension concur at instability phenomena attenuation. The positive influence of N_{θ} is, in general, variable, both in real time and as position. The variations $N_x, N_{\theta x}, N_{\theta}$ forces along circumference lead to local and non-symmetrical instability phenomena. Often, different influence of N_{θ} force on circumference concurs at tendency of instability symmetric shape.

2. WALL'S INSTABILITY SHAPES

Instability phenomena in the case of tanks is included in instability process of thin shells.

Instability, as a function of material's behavior, so of physics laws, can be:

- a) elastic instability, which represent the loss of original shape stability in elastic deformation domain;
- b) non-elastic instability, meaning the loss of stability after the emergence of non-elastic or elastoplastic or viscous deformations.

The appearance of non-elastic deformations and stresses can take place before the instability phenomenon and/or as a consequence of that.

An important role in producing the instability phenomenon has the imperfections which appear in these structures. In designing process is conceived a structure that can be named as an ideal one. After beginning the construction, real structure is obtained. Two structures built after the same project never will be identical, because of execution imperfections.

Two kinds of imperfections may occur:

- a) geometric imperfections, represented by the deviations from the designed surface as a result of building and tracing errors;
- b) structural imperfections, which come from eccentricity, material non-homogeneity, initial stresses, effects of the temperature.

Experimental researches [18, 19], but also theoretical [13, 14, 22, 29, 30], mark that imperfections, deviations from the ideal structure, lead to critical load modifications, concordant to the loss of stability.

2.1. Elastic instability

In the case of metallic thin shells, in particular in the case of tanks, because of the small thickness of walls, most of times the loss of stability take place in elastic domain.

Loss of stability take place trough bifurcation process, meaning the transition from the original stable shape of equilibrium to a new deformed shape. Bifurcation take place at the meeting point of two load-displacement curves: a) primary load-displacement curve belonging to small deformation and idealized shape equilibrium, b) secondary curve, belonging to finite displacement (average or large); this curve represent load-displacement relation in post-critical domain. The common point of those two curves is bifurcation point. What is described above are schematically represented in figure 2.

At the bifurcation, an indifferent, limit non-stable or critical equilibrium is realized. This may be characterized from energetic point of view. Thus, if Π is total potential energy function, first variation of this energy is canceled $\delta\Pi = 0$, and if $\delta^2\Pi = 0$, the equilibrium is instable.

From the designing codes perspective, critical equilibrium, which corresponds to critical loading and associated critical stress state, is important.

Trough bifurcation it may carry over on a secondary curve, also stable, but with a modified load-displacement law (stable bifurcation) or a secondary curve evolving to failure (labile bifurcation). Bifurcation can be symmetrical or non-symmetrical.

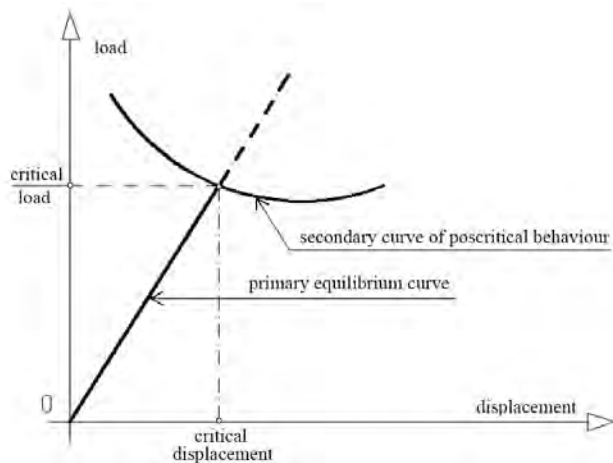


Figure 2. Load-displacement curves

2.2. Non-elastic instability

There are two different situations:

- a) elastoplastic material with variable tangentially stiffness (fig 3.a)
- b) ideal elastoplastic material (fig 3.b.)

High quality steels, aluminum and his alloys can be included in the first category described by a) model, while soft steel, copper alloys, some plastic or composite materials are included in the second category described by b) model.

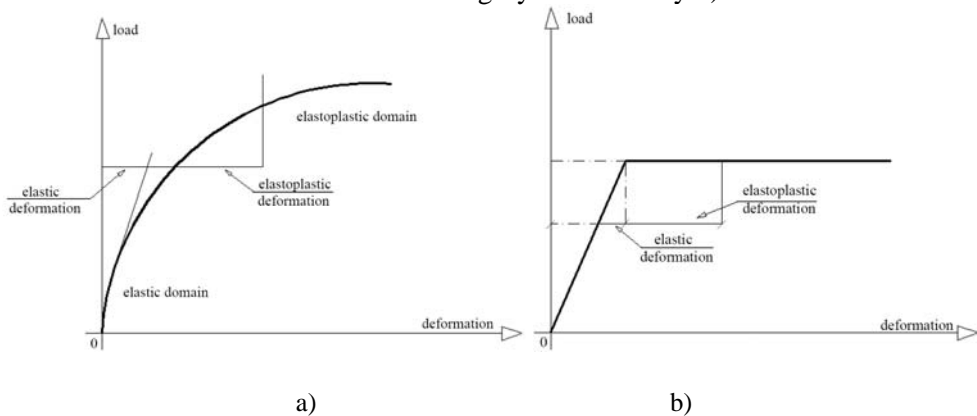


Figure 3. Load-deformation (stress-strain) curves

First consequence of exceeding elastic domain is reducing of the material stiffness, implicitly the one of element or structure.

The stiffness of linear elastic materials is constant. For non-linear behavior materials, elastic tangential stiffness is defined and for non-elastic materials loading tangential stiffness is defined.

If the loss of stability takes place by a stable bifurcation, loading may increase but with another load-deformation law. In the case of unstable bifurcation, stable post-critical states with controlled deformation may exist, conditioned by decrease of loading; in opposite case failure by buckling appears.

3. PRACTICAL STABILITY CALCULATION OF TANKS

The vertical component of earthquake's action, being axisymmetrical, does not produce overturning moment, but his influence on pressure and structural stability may be important so to take into account in calculation.

The pressures generated by vertical acceleration can diminish hydrodynamic pressures on walls without altering the overturning moment and so axial force N_x in generatrix direction.

Structural stability issue of tanks, especially of those metallic ones, has very much practical concern for appreciating the safety level of the structure and failure risk, respectively. Tank's stability represent a stability problem of shell's, with specific characteristics of this structural systems, especially from the loading point of view.

Instability phenomenon met in the case of tanks was experimentally and theoretically analyzed in many papers, from which the most significant are [1...8, 10, 15, 20, 21]. Still, the results of these researches are limited and insufficient, many of the aspects regarding instability, especially from putting in the action point of view, or have no answer or much complex techniques are proposed.

Next, a ordering and a development of instability practically calculation methods (buckling analysis) are presented.

Pressure superposition is made in order to be obvious the first instability mode (buckling) and yielding zone from tank's walls, both situations being very important for tank failure risk evaluation. The observations on failure at the earthquake action of some metallic tanks shows that superposition by spectral seismic response method is not sufficient for a real assessment of the risk.

Some aspects are distinguishing:

- i) it is possible that, at some point, dynamic pressure due to horizontal acceleration and minimal dynamic pressure given by vertical acceleration to be temporarily one and the same.
- ii) is possible simultaneous apparition of maximal pressure generated both by horizontal acceleration and the vertical one, which may cause elastoplastic buckling.

These cases differ from superposition trough spectral seismic response method. So it is absolutely necessary to take into consideration superposition trough scalar addition or subtraction of pressures.

In metallic tank’s case, the most probably failure mode is loss of stability. It yields that a quasi-statically analysis is needed, taking into consideration the compressive stress in shell’s generatrix direction, given by the overturning moment (generally bending around horizontal axis, normal to the direction of earthquake excitation). Quasi-statically way is indicated because natural frequencies corresponding to vibration modes, similar to buckling modes, are very high.

As it was shown above, for stability calculation of tanks, much importance is accorded to loading combinations, static and dynamic pressures given by horizontal or vertical acceleration.

If in practical design real recorded earthquakes are used, these standard recordings being made on N-S, E-V directions, hydrodynamic pressures at horizontal actions can be vectorial composed, prior determined for each recording direction.

The groupings of pressures for instability analysis can be done in many ways, the number of most unfavorable being three.

First case is the one discussed in the paper and is conform to the next pressure superposition:

$$p = p_{st} + p_{Hd} - p_{vd} \tag{1}$$

where:

p = design pressure;

p_{st} =hydrostatic pressure;

p_{Hd} =hydrodynamic pressure due to horizontal acceleration;

p_{vd} = hydrodynamic pressure due to vertical acceleration.

This superposition leads, in generally, to an elastic buckling in the case of moderately heigh tanks ($1.0 \leq H / R \leq 4.0$), the most practically used.

Stabilizer effect of internal pressures is reduced by dynamic pressure diminution due to earthquake vertical acceleration. Tanks are regarded as medium compressed cylinders at which critical axial force (mostly generated by the overturning moment who produce N_x membrane force) is determined by the next equation:

$$N_{cr} = \frac{E}{[3 \cdot (1 - \nu^2)]^{1/2}} \frac{h^2}{R} = \gamma_1 \frac{Eh^2}{R} \tag{2}$$

where γ_1 depends on material trough ν ; for different values of ν , γ_1 is given in table 1

$$\gamma_1 = \frac{1}{[3 \cdot (1 - \nu^2)]^{1/2}} \tag{3}$$

Table 1. Values of γ_1 function of Poisson's ratio, ν

ν	0.2	0.25	0.3	0.35	0.4
γ_1	0.589	0.596	0.605	0.616	0.623

To take into account the imperfections, deflection from theoretical calculation model, ground support and some local plastic effects, next equation is used:

$$N_{cr} = \gamma \gamma_1 \frac{Eh^2}{R} \tag{4}$$

where γ is represented in figure 4, function of R/h.

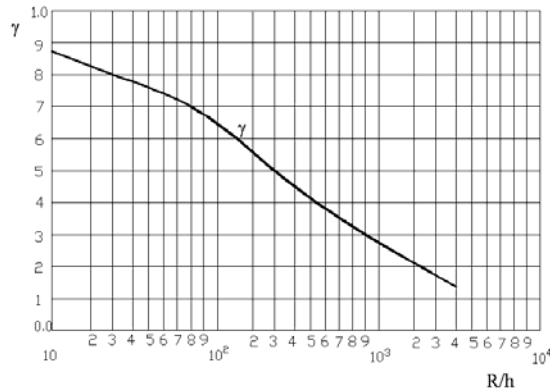


Figure 4. Variation of γ with R/h

To take into account stabilizer effect of previous pressures next revised equation can be used:

$$N_{xcr} = C_c \frac{Eh^2}{R} \tag{5}$$

which corresponds critical stress

$$\sigma_{cr} = C_c E \frac{h}{R} \tag{6}$$

where

$$C_c = \gamma_1 + \Delta C_c \tag{7}$$

For tanks with $R/h > 700$, corrective factor, ΔC_c , is given in figure 5, in which P is internal pressure [2, 10, 11].

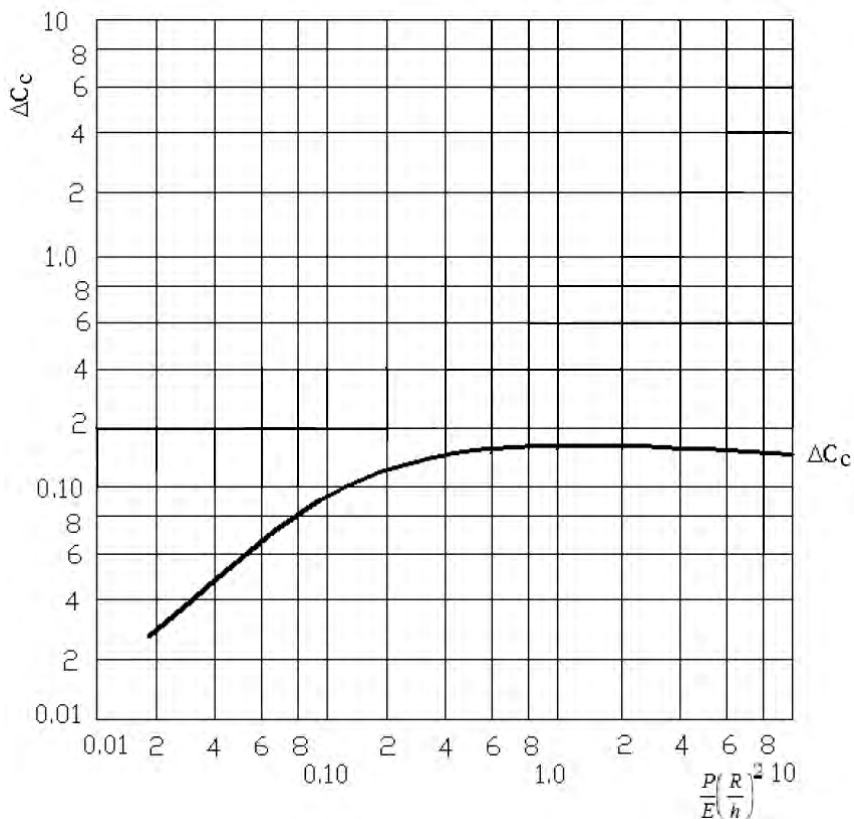


Figure 5. Variation of factor ΔC_c

3. CONCLUDING REMARKS

For stability design is used N_{Xcr} which depends of equivalent exterior action, resulted from coupled effective actions to which adequately safety coefficients are applied.

Non-elastic instability at continuous increasing of the loading may be assimilated with the same phenomenon in elastic domain, where the tangential stiffness is introduced. But, the major difficulty is that to establish tangential stiffness in bifurcation point. Practically, it may be used specific iterative techniques, witch will be presented in another paper.

References

1. Auli, W. , Rammerstorfer, F.G., On the Dynamic instability of Shell Structures - Criteria and Algorithms, *Finite Element Method for Plate and shell Structures*, T.J.R. Hughes and E. Hilton (Eds.), Vol. 2, Pineridge press, Swansea, U.K.,1986.Achkire, Y., Preumont, A., Active tendon control of cable-stayed bridges, *Earthquake Engineering and Structural Dynamics*, vol. 25, 1996.
2. Baker, H.E., Kovalevski, L., Rish, L.F., *Structural Analysis of Shells*, Mc Graw Hill Book Company, N.Y., St. Louis, San Francisco, London, 1972.Magaña, M.E. and Rodellar, J., Nonlinear decentralized active tendon of cable-stayed bridges, *Journal of Structural Control*, vol. 5, 1998.
3. Batdorf, S.B., *A Simplified Method of Elastic - Stability Analysis for Thin Cylindrical Shells*, NASA, 1974.
4. * * * *Buckling of Thin - Walled Circular Cylinders*, NASA, 1968.
5. Chiba, M., Tani, J., Yamaki, N., Dynamic Stability of Liquid. Filled Cylindrical Shells Partially Submerged or Filled with Liquid, *Journal of Sound andf Vibration*, Vol. 113(1), 1987.
6. Esslinger, M., Geier, B., Buckling and Postbuckling Behaviour of Thin - Walled Circular Cylinders, *Internat. Colloq. on Progress or Shell Structures*, IASS, Madrid, sept - oct 1969.
7. Fischer, D.F., Rammerstorfer, G.F., Stability of Liquid Storage Tank under Earthquake Excitation, *7th WCEE, San Francisco*, 1984.
8. Flugge, W.J., *Stress in Shells Springer*, 1973.
9. Furiş, D., *Contribuții la calculul rezervoarelor*, Teză de doctorat, ICB, 1979.
10. Gerard, G., Becker, H., *Handbook of Structural Stability*, Part III, Buckling of Curved Plates and Shells, NASA, 1957.
11. Gerard, G., *Handbook of Structural Stability*, supplement to Part III, Buckling of curved Plates and Shells, NASA, 1959.
12. Haroun, M.A., and Badawi, H.S., Seismic Behavior of Unanchored Ground Based Cylindrical Tanks, *Proceedings of the 9th WCEE*, vol. VI, Tokyo - Kyoto, Japan, 1988.
13. Hutchinson, J.M., Amagigo, C.J., Imperfection - Sensitivity of Eccentrically Stiffened Cylindrical Shells, *AIAA Journal*, 5.3.1967.
14. Hutchinson, J.M., Koiter, W.T., *Post - Buckling Theory*, Appl. Mech. review, 12, 1970.
15. Ivan, M., *Încărcare critică de bifurcare a cilindrului circular supus la compresiune uniformă*, Hidrotehnica 1979.
16. Luft, R.W., Vertical Accelerations in Prestressed Concrete Tanks, *Journal of Structural Engineering*, ASCE, vol. 110, 1984.
17. Rotter, J.M., and Seide, P., On the Design of Unstiffened Shells Subjected to an Axial Load and Internal Pressure, *Proceedings of the ECCS Colloquium on Stability on Plate and Shells Structures*, Ghent University, 1987.

18. Tani, J., Chiba, M., Experimental Study on the Dynamic Stability of Nuclear Entainment Vessels Under Horizontal Excitation, *Proceedings of the 8th SMIRT*, vol. K20/6, 1985.
19. Clough, R.W., Niwa, A., *Static Tilt Tests of a Tall Cylindrical Liquid Storage Tanks*, Report No UBC/EERC-79/06, University of California, Berkeley, 1979.
20. Fischer, D.F., Rammerstorfer, G.F., Scharf, K., *Earthquake Resistant Design of Anchored and Unanchored Liquid Storage Tanks under Three – Dimensional Earthquake Excitation*, Structural Dynamics – Recent Advances – Springer Verlag, Heidelberg, 1980.
21. Rammerstorfer, G.F., Scharf, D.F., A Proposal for the Earthquake Resistant Design of Tanks Results from the Austrian Research Project, *proceedings of the 9th WCEE*, vol. VI, Tokyo – Kyoto, Japan, 1988.
22. Scharf, K., Rammerstorfer, F.G., Fischer, F.D., *Elastic Plastic stability Analysis of Earthquake Loaded Tanks, Nichtlineare Berechnungen im Konstruktiven Ingenieurban Berichte zum Schlußkolloquium des gleichnamigen DFG, Schwerpunkt programms am 2/3 Marz 1989 in Hannover* Springer - Verlag, Berlin, Heidelberg, New York, London, Paris, 1989.
23. Ungureanu, N., Negoită, Al., *Rezervoare, Aplicații ale ingineriei seismice*, Editura Tehnică București, 1990.
24. Ungureanu, N., Strat, L., Vrabie, M., Bending Effects in Liquid Storage Tanks with Stepwise Variable Wall Thickness, *Proceedings of the 17th Congress Committee Yugoslav Society of Mechanics*, Belgrad, 1986.
25. Veletsos, S.A., Tang, Yu., Tang T.H., Dynamic Response of Flexibly Supported Liquid Storage Tanks, *Journal of Struct. Eng.ASCE*, Vol. 118, NO.1, 1992.
26. * * * *Cercetări teoretice și experimentale privind comportarea la acțiuni seismice a rezervoarelor cu pereți flexibili*, Contract 6869/1993, Faza 2/1993, Faza 3/1994, Universitatea Tehnică Iași. Facultatea de Construcții și Arhitectură, Catedra de Mecanica Construcțiilor, Beneficiar ÎNCERC Filiala Iași.
27. Spanos, P.D., Koh, A.S., and Roesset, J.M., Seismic Uplifting of Structures on Flexible Foundation, *Proceedings of the 8th ECEE*, 1986.
28. Kim, S. E, Kim, C. S., Buckling strength of the cylindrical shell and tank subjected to axially compressive loads, *Thin-Walled Structures*, Volume 40, Issue 4, April 2002, Pages 329-353.
29. Winterstetter, Th. A., Schmidt, H., Stability of circular cylindrical steel shells under combined loading, *Thin-Walled Structures*, Volume 40, Issue 10, October 2002, Pages 893-910.
30. Tafreshi, A., Bailey, C. G., Instability of imperfect composite cylindrical shells under combined loading, *Composite Structures*, Volume 80, Issue 1, September 2007, Pages 49-64.

Practical Aspects about Linear Dynamic Analysis of Cable Structures

Ferencz Lazar-Mand¹, Dragoș Florin Lișman²

¹*Dep. of Structural Mechanics, Technical Univ. of Cluj – Napoca, Cluj – Napoca, 400020, Romania*

²*Dep. of Structural Mechanics, Technical Univ. of Cluj – Napoca, Cluj – Napoca, 400020, Romania*

Abstract

In the paper, the authors present a series of aspects about frequency and pulsation computation of pretensioned cable structures. Both mass modeling and stiffness matrix modeling are discussed. For the stiffness matrix modeling, an approach similar to the one described by P. Krishna is used, except the fact that the non-linear, residual terms are not taken into account.

At the end of the paper, the theoretical computer results of two case studies are compared with the results obtained by other authors and with the results obtained experimentally.

1. INTRODUCTION

The study of the dynamical response of cable structures and cable stayed systems started back in the 1970's – 1980's. In the 1990's new papers and books appeared on the subject, which compare the theoretical results with the experimental results obtained in the 1970's.

Through a structure's dynamic analysis, it is understood the analysis of the structure that is subject to dynamical efforts. Although the response of a structure to a static or dynamic effort is non – linear, nevertheless linear analysis is an important study subject today.

One of the few researchers that were concerned with the problem of determining the frequencies / pulsations and the eigenvibration mode shapes is A. S. K. Kwan, in his paper from 1998.

In the present paper two structures are analyzed. The first structure is Jensen's planar cable - beam. The frequencies were computed for three cases of concentrated masses. The results obtained are compared with the theoretical results obtained by other authors, respectively with the experimentally obtained results.

The second structure is the *Aden Airways building* hyperbolic paraboloid. The pulsations in the case of lumped masses are computed (masses resulting from the proper weight of the cables). The results obtained are compared to the results obtained by other authors.

2. COMPUTATION OF FREQUENCIES AND VIBRATION MODE SHAPES

The equations that describe the free and undamped vibrations of a system with N freedom degrees are:

$$M\ddot{u} + Ku = 0 \tag{1}$$

, where M is the mass or inertial matrix of the system and K is the stiffness matrix of the system. The frequencies and the vibration mode shapes are determined by solving the generalized eigenvalues problem:

$$(K - \lambda M)x = 0 \tag{2}$$

, where: $\lambda = \omega^2$, and K and M are positive and symmetric matrices (K is the stiffness matrix, M is the inertia or mass matrix and ω is the pulsation).

3. MASS MODELING AND ELASTIC MODELING

3.1. Mass model

The chosen mass model (in the studied cases), is the concentrated mass model. The mass matrix has the order $s = (NN - NNFIX)*DOF$ and it is a matrix where the mass elements are on the main diagonal, all the other elements being equal to zero (this is the simplest case of mass models).

$$M = \begin{bmatrix} m_1 & 0 & 0 & 0 \\ 0 & m_2 & 0 & 0 \\ 0 & 0 & \dots & 0 \\ 0 & 0 & 0 & m_s \end{bmatrix} \tag{3}$$

The computation of R in the case when M is diagonal.

$$S = S^T = \begin{bmatrix} \sqrt{m_1} & 0 & 0 & 0 \\ 0 & \sqrt{m_2} & 0 & 0 \\ 0 & 0 & \dots & 0 \\ 0 & 0 & 0 & \sqrt{m_s} \end{bmatrix} \tag{4}$$

$$S^{T^{-1}} = S^{-T} = \begin{bmatrix} \frac{1}{\sqrt{m_1}} & 0 & 0 & 0 \\ 0 & \frac{1}{\sqrt{m_2}} & 0 & 0 \\ 0 & 0 & \dots & 0 \\ 0 & 0 & 0 & \frac{1}{\sqrt{m_s}} \end{bmatrix} \quad (5)$$

Taking into account that matrix M is positive definite, the generalized problem can be transformed into the standard problem for a symmetric matrix, as in the following [1]:

Cholesky decomposition of M is performed:

$$M = S^T S \quad (6)$$

, where S is an upper triangular matrix (also, lower triangular decomposition can be used). Thus, (2) written as:

$$Kx = \lambda Mx \quad (7)$$

becomes:

$$Kx = \lambda S^T Sx$$

and is written again as:

$$KS^{-1}(Sx) = \lambda S^T(Sx).$$

Denote

$$y = Sx \quad (8)$$

The previous equation becomes:

$$KS^{-1}y = \lambda S^T y.$$

multiply to the left by

$$(S^T)^{-1} = (S^{-1})^T = S^{-T}$$

(the last equality is a notation), we obtain

$$S^{-T}KS^{-1}y = \lambda Iy \quad (9)$$

Now R is defined as:

$$R = S^{-T} \cdot K \cdot S^{-1} \quad (10)$$

R is a symmetric and positive definite matrix. Problem (2) is cast to the standard problem for matrix R, namely:

$$(R - \lambda I)y = 0 \tag{11}$$

Problems (2) and (11) have the same eigenvalues. After solving (11) for λ and y , the eigenvectors of the original problem (2) are given by:

$$x = S^{-1}y \tag{12}$$

The r_{ij} element is given by:

$$r_{ij} = \begin{bmatrix} \dots & \frac{1}{\sqrt{m_i}} & \dots \end{bmatrix} \cdot \begin{bmatrix} \dots & \dots & \dots \\ \dots & k_{ij} & \dots \\ \dots & \dots & \dots \end{bmatrix} \cdot \begin{bmatrix} \vdots \\ \frac{1}{\sqrt{m_j}} \\ \vdots \end{bmatrix} = \tag{13}$$

$$= \begin{bmatrix} 0 & \dots & \frac{1}{\sqrt{m_i}} & \dots & 0 \end{bmatrix} \cdot \begin{bmatrix} k_{1j} & \frac{1}{\sqrt{m_j}} \\ \vdots & \vdots \\ k_{ij} & \frac{1}{\sqrt{m_j}} \\ \vdots & \vdots \\ k_{nj} & \frac{1}{\sqrt{m_j}} \end{bmatrix} = \frac{1}{\sqrt{m_i}} \cdot \left(k_{ij} \cdot \frac{1}{\sqrt{m_j}} \right)$$

$$= \frac{k_{ij}}{\sqrt{m_i} \cdot \sqrt{m_j}}$$

3.2. Stiffness matrix – structure and computation

The elements of the stiffness matrix are computed using a method similar to the one presented in [4]. The structure of the stiffness matrix is exemplified in [7], in the case of a planar cable – beam (6 joints – 12 degrees of freedom).

This can be naturally generalized to structures with 3 degrees of freedom / joint.

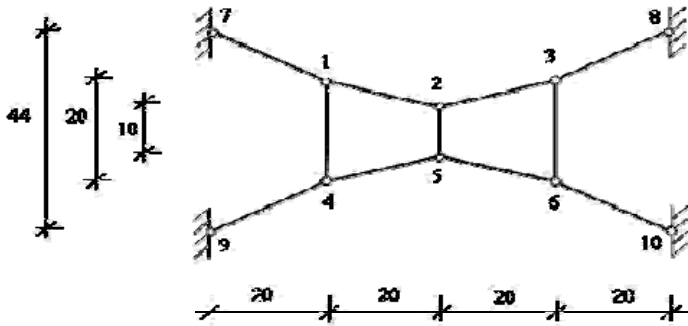


Figure 1. Planar Cable - Beam

3.2.1. The structure of the stiffness matrix

	u_1	v_1	u_2	v_2	u_3	v_3	u_4	v_4	u_5	v_5	u_6	v_6		
K=	x_1	$-A_{xx}^1$	$-A_{xy}^1$	A_{xx}^{12}	A_{xy}^{12}	0	0	A_{xx}^{14}	A_{xy}^{14}	0	0	0	1	
	y_1	$-A_{xy}^1$	$-A_{yy}^1$	A_{xy}^{12}	A_{yy}^{12}	0	0	A_{xy}^{14}	A_{yy}^{14}	0	0	0	2	
	x_2	A_{xx}^{21}	A_{xy}^{21}	$-A_{xx}^{22}$	$-A_{xy}^{22}$	A_{xx}^{23}	A_{xy}^{23}	0	0	A_{xx}^{25}	A_{xy}^{25}	0	0	3
	y_2	A_{xy}^{21}	A_{yy}^{21}	$-A_{xy}^{22}$	$-A_{yy}^{22}$	A_{xy}^{23}	A_{yy}^{23}	0	0	A_{xy}^{25}	A_{yy}^{25}	0	0	4
	x_3	0	0	A_{xx}^{32}	A_{xy}^{32}	$-A_{xx}^{33}$	$-A_{xy}^{33}$	0	0	0	0	A_{xx}^{36}	A_{xy}^{36}	5
	y_3	0	0	A_{xy}^{32}	A_{yy}^{32}	$-A_{xy}^{33}$	$-A_{yy}^{33}$	0	0	0	0	A_{xy}^{36}	A_{yy}^{36}	6
	x_4	A_{xx}^{41}	A_{xy}^{41}	0	0	0	0	$-A_{xx}^{44}$	$-A_{xy}^{44}$	A_{xx}^{45}	A_{xy}^{45}	0	0	7
	y_4	A_{xy}^{41}	A_{yy}^{41}	0	0	0	0	$-A_{xy}^{44}$	$-A_{yy}^{44}$	A_{xy}^{45}	A_{yy}^{45}	0	0	8
	x_5	0	0	A_{xx}^{52}	A_{xy}^{52}	0	0	A_{xx}^{54}	A_{xy}^{54}	$-A_{xx}^{55}$	$-A_{xy}^{55}$	A_{xx}^{56}	A_{xy}^{56}	9
	y_5	0	0	A_{xy}^{52}	A_{yy}^{52}	0	0	A_{xy}^{54}	A_{yy}^{54}	$-A_{xy}^{55}$	$-A_{yy}^{55}$	A_{xy}^{56}	A_{yy}^{56}	10
	x_6	0	0	0	0	A_{xx}^{63}	A_{xy}^{63}	0	0	A_{xx}^{65}	A_{xy}^{65}	$-A_{xx}^{66}$	$-A_{xy}^{66}$	11
	y_6	0	0	0	0	A_{xy}^{63}	A_{yy}^{63}	0	0	A_{xy}^{65}	A_{yy}^{65}	$-A_{xy}^{66}$	$-A_{yy}^{66}$	12

3.2.2. *Computation formulae*

The computation of the elements of the matrix can be performed in the following way:

$$A_{xx}^1 = A_{xx}^{1,7} + A_{xx}^{1,2} + A_{xx}^{1,4} \tag{14}$$

$$A_{xy}^1 = A_{xy}^{1,7} + A_{xy}^{1,2} + A_{xy}^{1,4}$$

$$A_{yx}^1 = A_{xy}^1$$

$$A_{yy}^1 = A_{yy}^{1,7} + A_{yy}^{1,2} + A_{yy}^{1,4}$$

These matrices represent the sub matrices of A, described on the previous page. In this example, the first matrix, which has the elements with index 1, represents the first “box” of the stiffness matrix. The xx index, points out the fact that the computation is performed with $(x_p - x_q)^2$, where p and q are the initial / final joints. Indices 1,7 for example, indicate the connection between joint 1 and 7 (in this case joint 7 represents the support joint). Indices 1,2 indicate the connection of joint 1 with joint 2, etc..

Index xy refers to the computation with $(x_p - x_q) \cdot (y_p - y_q)$, respectively index yy refers to the computation with $(y_p - y_q)^2$. Obviously, in the situation of 3 degrees of freedom, sub matrices of 3 x 3 are used, and the z coordinates will be considered, too.

The joint balance equations are similar to the one written by P. Krishna in [4], the only difference being that the non – linear, residual terms are neglected.

$$KU = -P + R \tag{15}$$

The linear equations are written in the following way:

$$KU = -P \tag{16}$$

The notation $A = K (U^0)$ was used, where U^0 defines the equilibrium state under the weight of the masses. The formulae that define the elements of the sub matrices of K are [2]:

$$A_{xx}^{i,j} = \frac{1}{l_{i,j}} [F_i + (EA_i - F_i) \cdot (\theta_x^i)^2] \tag{17}$$

$$A_{yy}^{i,j} = \frac{1}{l_{i,j}} [F_i + (EA_i - F_i) \cdot (\theta_y^i)^2]$$

$$A_{xx}^{i,j} = \frac{(EA_i - F_i)}{l_{i,j}} \cdot (\theta_x^i) \cdot (\theta_y^j)$$

,where:

$$l_{i,j} = l_{q,p} \tag{18}$$

$$l_{q,p} = \sqrt{(x_q - x_p)^2 + (y_q - y_p)^2 + (z_q - z_p)^2}$$

The directing cosines θ_d^i (d = x, y, z) are computed using the coordinates of the joints in the balance position (the displaced position).

F – pretensioning force

E –Young’s Module

A – area

θ – directing cosines

l – length of the elements.

$$\theta_{q,p}^0 = \left(\frac{x_q^0 - x_p^0}{l_{q,p}^0}, \frac{y_q^0 - y_p^0}{l_{q,p}^0}, \frac{z_q^0 - z_p^0}{l_{q,p}^0} \right) \tag{19}$$

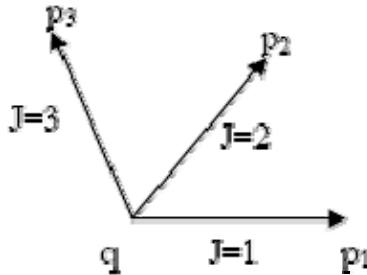


Figure 2. Joint “q” connected to joints p₁ – p₃, on the directed edges j = 1,3

The stiffness matrix is composed of sub matrices (of 2 x 2 or 3 x 3 elements, generally DOF x DOF). These sub matrices will be denoted with II (number of the sub matrix on lines), respectively JJ (number of the sub matrix on columns). The big matrix is composed of i (number of lines in the matrix), respectively j (number of columns in the matrix). There exist integer indices like L1, respectively L2, too.

All these values are used for the correct positioning of the elements of the matrix. A good example found in [7] is the planar cable - beam presented in Figure 1:

DOF – number of degrees of freedom = 2

Let $i = 11$, then $II = 6$ and $L1 = 1$

$j = 6$ then $JJ = 3$ and $L2 = 2$

In the previous example the authors presented the element on line 11, sub matrix 6, column 6, sub matrix 3, hence it is about “box” 6/3 with the position of line $L1 = 1$ and column $L2 = 2$, namely the element $A_{xy}^{6,3}$.

3.2.3. Determination of the equilibrium state (under the load of the mass)

For the input data, the coordinates of the structure were used, based on the equilibrium state (displaced), computed using NELSAS application [2]. The static non – linear computation:

$$f(U_0) = G \quad (20)$$

For the computation of the frequencies / pulsations a program was written using the FORTRAN programming language [8], [9], [10]. The program is composed of:

- main program, where the read of the input data, the write of the output data in several output files and the calling of the subroutines are performed;
- STIFF subroutine, which computes the structure’s stiffness matrix based on the equations (17);
- MASS subroutine, which computes the mass matrix of the structure.

As a numerical method, the QR method was chosen, which uses the EVCRG subroutine from the IMSL library [11]. EVCRG computes the eigenvalues and the eigenvectors of a real matrix. The matrix is first balanced. Orthogonal similarity transformations are used to reduce the balanced matrix to a real upper Hessenberg matrix. The implicit double – shifted QR algorithm is used to compute the eigenvalues and eigenvectors of the Hessenberg matrix. The balancing routine is based on the EISPACK routine BALANC. The reduction routine is based on the EISPACK routines ORTHES and ORTRAN. The QR algorithm routine is based on the EISPACK routine HQR2. Smith et al. developed the EISPACK routines in 1976 [6].

4. CASE STUDIES

4.1. Structures

The example in Figure 3 is presented in [5] and it is a model for a planar cable – beam. The geometrical data and the pretensioning are given in the figure. The cable (upper and lower) have $EA = 190.314 \text{ N}$, and the upright beams have $EA = 103.005 \text{ N}$.

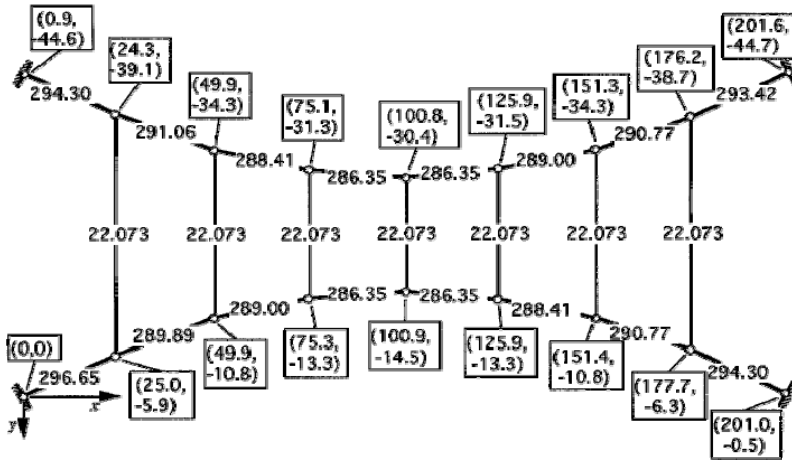


Figure 3. Jensen's planar cable beam

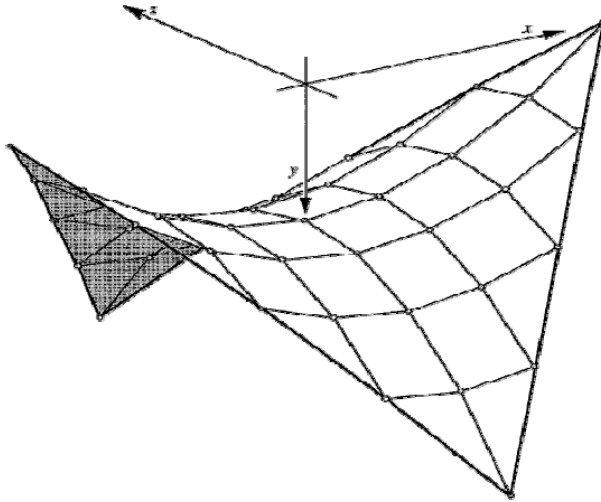


Figure 4. The Aden Airways hyperbolic paraboloid

In the example in Figure 4 a hyperbolic paraboloid is described, *Aden Airways building* which has planar dimensions of 35.052 x 35.052 m. This hyperbolic paraboloid has the following equation (coordinates are given in meters):

$$y = \frac{5.334}{17.526^2} \cdot z^2 - \frac{3.81}{17.526^2} \cdot x^2 \quad (21)$$

The structure is composed of seven equidistant cables, which have the same $EA = 210.312 \text{ MN}$, and density $\rho = 10.0 \text{ kg/m}$. The horizontal components of the pretensioning forces are equal to 200.17 kN (on the x direction) and 142.97 kN (on the z direction). The structure has 25 displaceable joints and 75 degrees of freedom.

4.2. Comparative results

The example with the planar cable beam presented in Figure 3 is a model on which Jensen performed experiments with different values for masses, obtaining different frequencies. These values are compared to the values obtained theoretically, both by Jensen and Kwan and Chisăliță. The results were obtained for 3 cases of concentrated masses in joints. In Table 1, one can observe the cases of mass distribution:

Table 1. Cases of mass distribution

	Case A	Case B	Case C
Mass on upper joints (kg)	0.03	0.01	0.50
Mass on lower joints (kg)	1.00	0.50	0.50

In Table 2, the frequencies are presented, according to the cases of mass distribution, and compared to the values obtained by other authors.

Table 2. Comparison of the proper frequencies

Case A				
Nr. crt.	Experiment (Jensen) ⁽¹⁴⁾	Theoretic (Chisăliță)	Theoretic (Kwan)	Present study
1	5.7	5.698	5.683	4.203
2	8.1	7.999	8.009	5.813
3	10.9	10.423	10.402	7.579
...
28		1558.5	1557.5	1550.6

Case B				
Nr. crt.	Experiment (Jensen) ⁽¹⁴⁾	Theoretic (Chisăliță)	Theoretic (Kwan)	Present study
1	7.50	8.077	8.077	5.94
2	11.1	11.354	11.382	8.229
3	14.5	14.785	14.781	10.737
...
28			2697.7	2685.56

Case C			
Nr. crt.	Theoretic (Chisăliță)	Theoretic (Kwan)	Present study
1	5.773	5.768	5.768
2	8.131	8.124	8.126
3	10.593	10.569	10.569
...
28	382.10	382.16	382.17

In the case of the Aden Airways hyperbolic paraboloid, the equivalent lumped mass resulting from the proper weight of the cable was taken into account. Based on these values the pulsations were computed. In Table 3, a comparison between the results obtained in this paper and the results obtained by other others is presented.

Table 3. Comparison of the pulsations (in rad/s)

Nr. crt.	Geshwinder and West, lumped ⁽¹³⁾	Chisăliță, Lumped ⁽¹²⁾	Kwan, lumped	Present study, lumped
1	32.87	32.892	32.890	32.098
2	39.18	39.209	39.203	38.304
3	39.89	39.916	39.909	38.825
...
75	1436	1435.893	1435.896	1441.949

5. CONCLUSIONS

In this paper, a method for computing the mass matrix and the structure of the stiffness matrix is presented. In the final section of the paper, a comparison between the values obtained for two pretensioned cable structures by other authors and the values obtained during the authors study is performed. It can be observed that the frequencies, respectively the pulsations obtained in this paper have close values to the ones obtained by other authors, using linear methods of computation. The eigenvalues and the eigenvectors were computed using the QR method from the IMSL library. The modeling of the mass matrix and of the stiffness matrix is of great importance. It is obvious that a linear analysis is necessary even in the cases when the structure behaves non – linear.

References

1. Chisăliță, A., *Numerical Analysis*, Universitatea Tehnică din Cluj Napoca, 2002.
2. Chisăliță, A., *Program NELAS – Manual de utilizare*, Universitatea Tehnică din Cluj Napoca, 2007. (romanian)
3. Chisăliță, A., 2007. *Metode numerice*, Curs Școala Doctorală, U.T.C.N., <ftp://ftp.utcluj.ro/users/chisalita/> (romanian)
4. Krishna, P., *Cable – suspended roofs*, McGraw-Hill Inc., 1978.
5. Kwan, A. S. K., *A simple technique for calculating natural frequencies of geometrically nonlinear prestressed cable structures*, Computers and Structures, 1998, vol. 74, pp. 41-50.
6. Smith, B.T., J.M. Boyle, J.J. Dongarra, B.S. Garbow, Y. Ikebe, V.C. Klema, C.B. Moler, *Matrix Eigensystem Routines – EISPACK Guide*, Springer-Verlag, New York, 1976.
7. Volokh, K. Yu., Vilnay, O., Averbuh, I., *Dynamics of cable structures*, Journal of Structural Engineering, 2003, ASCE, Vol. 129, No. 2, pp. 175-180.
8. “Compaq Fortran – Language Reference Manual”, Compaq Computer Corporation, 1999.
9. “Compaq Visual Fortran Language Reference Manual”, 2001, ftp://ftp.compaq.com/pub/products/fortran/vf/docs/cvf_lref.pdf
10. “Compaq Visual Fortran Programmer’s Guide”, 2001, ftp://ftp.compaq.com/pub/products/fortran/vf/docs/cvf_pg.pdf
11. “IMSL Libraries Reference”, Compaq Visual Fortran Help, 2001
12. Chisalita A. *Finite deformation analysis of cable networks*. ASCE J Engng Mech., 1984 in Kwan, A. S. K., 1998. *A simple technique for calculating natural frequencies of geometrically nonlinear prestressed cable structures*, Computers and Structures, 74, 41-50.

13. Geshwinder LF, West HH. *Parametric investigations of vibrating cable networks*. ASCE J Struct Div., 1979 in Kwan, A. S. K., 1998. *A simple technique for calculating natural frequencies of geometrically nonlinear prestressed cable structures*, Computers and Structures, 74, 41-50.
14. Jensen JJ. *Eine Statische und Dynamische Untersuchung der Seil und Membrantragwerke*, Report No 70 – 1, Norwegian Institute of Technology, University of Trondheim, 1970 in Kwan, A. S. K., 1998. *A simple technique for calculating natural frequencies of geometrically nonlinear prestressed cable structures*, Computers and Structures, 74, 41-50.

Optimal mix design of polymer concrete using generalized reduced gradient algorithm

Daniel Lepădatu¹ and Marinela Bărbuța²

¹Civil Engineering Department, Technical University “Gh. Asachi”, Iasi, Romania

²Concrete structure, Building material, Technology and Management Department, Technical University “Gh. Asachi”, Iasi, Romania

Summary

New types of polymer concrete with silica fume have specific requirements, in contrast to conventional concrete; these are susceptible in case of changing technological factors (especially of the mix). They require a new optimization approach in issues of concrete mix design. On the other hand, in the conditions of market economy there is a wide range, that to achieve maximal economy, and at the same time to provide maximally good mechanical characteristics for this new type of concrete. The aim of this paper is the optimization of mix proportion of polymer concrete with silica fume content by using the statistical techniques. The experimental studies were realized on polymer concrete prepared with epoxy resin, silica fume in different dosages and aggregates of two sorts. The experimental mix combinations were designed based on the mixture design of experiments concept for the minimum content of resin. The predicted values of mechanical characteristics were theoretically determined and they were compared with experimentally results using Response Surface Methodology (RSM). The effect of each variable on the response was analyzed by this advanced method. The optimization method includes two phases. The first involve the objective function prediction using mixture design of experiments and response surface method, while the second is an optimization process using a Generalized Reduced Gradient algorithm. The optimum combination of the input mix parameters design is given for the best values of compressive strength or adherence stress.

KEYWORDS: optimization, polymer concrete, silica fume, response surface methodology, generalized reduced gradient algorithm

1. INTRODUCTION

Among the modern building materials the polymer concrete occupies an important place in construction industry because its large domain of utilization such as: making various pre-cast products, repair of structures, waterproofing, overlay of pavements, bridge deck, floors [1]. Polymer can be used as a single binder –and the

composite in this case is called polymer concrete (PC) or can be incorporated in the cement paste and in this case the composite is called Polymer Modified Concrete (PMC). In the case of PC the polymer is the matrix of the composite and it must bind all the aggregates. The final properties and the curing behavior of polymer concrete depend on the selection and the content of resin, type and dosage of aggregates and filler [2]. To optimize the composite mixture and the properties of polymer concrete the statistical analyze is presented in this paper. Mechanical characteristics of polymer concrete such as: compressive strength or adherence stress, based on epoxy resin, silica fume and aggregates was optimized.

2. EXPERIMENTAL PROGRAM

The materials used were: epoxy resin, silica fume (SUF) and crushed aggregates of two grades 0-4 mm (Sort I) and 4-8 mm (Sort II). The epoxy resin in combination with the hardener forms the binder of the polymer concrete. The silica fume is a by-product that results from ferrosilicon production. The aggregates were obtained from river stone by crushing.

Polymer concrete of different compositions as is given in Table 1 was prepared by mixing required quantities of epoxy resin firstly with aggregates, than with the filler (SUF) was added slowly in a mechanical mixer. Than was the casting of specimens (prism of 210x70x70 mm sides were prepared - Figure 1) for determining the mechanical characteristics such as: Compressive Strength (CS) and Adherence Stress (AS).



Figure 1. Test samples of PC

Table 1. Mixture design combinations for polymer concrete

Mixture	Epoxy resin (%)	SUF (%)	Aggregate Sort I (%)	Aggregate Sort II (%)
PC1	18.8	6.48	37.4	37.4
PC2	12.4	12.8	37.4	37.4
PC3	12.4	6.4	43.8	37.4
PC4	12.4	6.4	37.4	43.8
PC5	15.6	9.6	37.4	37.4
PC6	15.6	6.4	40.6	37.4
PC7	15.6	6.4	37.4	40.6
PC8	12.4	9.6	40.6	37.4
PC9	12.4	9.6	37.4	40.6
PC10	12.4	6.4	40.6	40.6
PC11	16.4	7.2	38.2	38.2
PC12	13.2	10.4	38.2	38.2
PC13	13.2	7.2	41.4	38.2
PC14	13.2	7.2	38.2	41.4
PC15	14.0	8.0	39	39.0

3. MIXTURE DESIGN OF EXPERIMENT AND RESPONSE SURFACE METHODOLOGY

3.1. Mixture design of experiment

Research in many disciplines frequently involves blending two or more ingredients together. The design factors in a mixture experiment [3-5] are the proportions of the components of a blend, and the response variables vary as a function of these proportions making the total and not actual quality of each component. The total amount of the mixture is normally fixed in a mixture experiment and the component settings are proportions of the total amount. The component proportions in a mixture experiment cannot vary independently as in factorial experiments since they are constrained to sum to a constant (1 or 100% for standard design). Imposing such constraint on the component proportions complicates the design and the analysis of mixture experiments. Although the best-known constraint in a mixture experiment is to set the sum of the components to one (100%) additional constraints such as imposing a maximum or minimum value on each mixture component may also apply.

In the mixture design approach the total of amount of the input variables was fixed and constrained to sum 100. For each statistical combination, all properties of interest were measured and empirical models for each property as function of the input variables were determined from regression analysis. The advantage of the mixture approach is that the experimental region of interest is more naturally defined. To simplify calculation and analysis, the actual variables ranges were transformed to dimensionless coded variables with a range 0 and 1. Intermediate values were also translated similarly. Those variables were codified using the following formula:

$$Pseudo = (R_i - L_i)/(1 - L) \quad (1)$$

where:

$R_i = A_i / \sum A_i$, L_i is the lower constraint in real value, L is the sum of lower constraint in real value, A is the actual value, and A_i is the total of actual values.

3.2. Response Surface Methodology

Response Surface Methodology (RSM) provides an approximate relationship between a true response y and p design variables, which is based on the observed data from the process or system [6-10]. The response is generally obtained from real experiments or computer simulations, and the true response y is the expected response. Thus, real experiments are performed in this paper. We suppose that the true response y can be written as:

$$y = F(x_1, x_2, \dots, x_p) \quad (2)$$

where the variables x_1, x_2, \dots, x_k are expressed in natural units of a measurement. So they are called "natural variables". Usually, the approximating function, F , of the true response, y , is chosen to be either a first-order or a second-order polynomial model, which is based on a Taylor series expansion. In this study, the second-order model given

$$y = \beta_0 + \sum_{i=1}^k \beta_i x_i + \sum_{i=1}^k \beta_{ii} x_i^2 + \sum_{i=1}^k \sum_{j=1, j \neq i}^k \beta_{ij} x_i x_j + e \quad (3)$$

where: β_0 , β_i , β_{ij} and β_{ijk} are called regression coefficients, and e represent the noise or the error observed in the response y [11]. In order to more accurately predict the response, the second-order model is used to fit a curvature response. From the above approximating function, the estimated response Y_i at the n^{th} data point can be written in matrix form as:

$$y = X \cdot \beta + \varepsilon \tag{4}$$

In equation 5, X is a matrix of model terms evaluated at the data points. The regression coefficients of the predictive model are estimated by the method of the least squares using the general formulation as:

$$\beta = (X^T \cdot X)^{-1} \cdot X^T \tag{5}$$

where: X^T is the transpose of the matrix X .

The second-order polynomial relation with special cubic interactions can approximate the mathematical relationship between the independent variables x_i and the response Y :

$$Y = \beta_0 + \sum_{j=1}^p \beta_j x_j + \sum_{j=1}^p \beta_{jj} x_j^2 + \sum_{i < j} \beta_{ij} x_i x_j + \sum_{i < j} \sum_{\substack{k=1 \\ k \neq i, j}}^p \beta_{ijk} x_i x_j x_k + \varepsilon \tag{6}$$

where: β_i are linear coefficients, β_{ii} are quadratic coefficients, β_{ij} are cross-product coefficients, β_{ijk} are the special cubic coefficients and ε is the random error which includes measurement error on the response and is inherent in the process or system. These coefficients are unknown coefficients usually estimated to minimize the sum of the squares of the error term, which is a process known as regression.

4. OPTIMIZATION PROCEDURE

The general formation of a conventional optimization is expressed as follows:

$$\text{Maximize: } f(x) \quad (7)$$

$$\text{Subjected to: } hi(x) = 0, i = 1, p \quad (8)$$

$$gj(x) \leq 0, j = 1, m \quad (9)$$

$$x_L \leq x_k \leq x_U, k = 1, m, \quad (10)$$

where: $f(x)$ is the objective function, $hi(x)$ is the equality constraint function, p is the number of constraints, $gj(x)$ is the inequality constraint function, x_L , x_U are the lower bound and the upper bound of the design variables and m is the number of constraints. From the limitation of the interval constraint, the range of design variables are limited by their lower and upper bounds, respectively A_{min} , A_{max} , B_{min} , B_{max} , C_{min} , C_{max} , D_{min} and D_{max} .

$$A_{min} \leq A \leq A_{max} \quad B_{min} \leq B \leq B_{max} \quad (11)$$

$$C_{min} \leq C \leq C_{max} \quad D_{min} \leq D \leq D_{max} \quad (12)$$

Generalized Reduced Gradient method, which is one of the optimization algorithms (9), has been commonly used to minimize the objective function that satisfies the constraints of this paper.

The range of design variables are limited by their lower and upper bounds, presented in the Table 2. The proposed method solves an optimizing problem through the application of non-linear mathematical programming to an estimated solution space using the objective function obtained by RSM method. The proposed method actually consists of two main processes. The first involves the prediction of the objective function while the second is an optimization process.

In the present work, the optimization computation is carried out with a GRG algorithm using a Microsoft Excel Worksheet. In the first phase, polynomial models are generated with the available design of experiments data. In the second phase the optimizer uses the objective function during the search for the optimum until the final converged solution is obtained.

5. RESULTS AND DISCUSSIONS

Out of number of factors identified by their simplified notation (A, B, C and D), the following ones were considered to be most important and necessary to control:

1. Epoxy resin (A),
2. Silica fume (B),
3. Aggregate sort I, 0-4 (C),
4. Aggregate sort II, 4-8 (D).

The input variables, range chosen for the study, their coded value, and mixture design combination are given in Tables 2 and 3.

Table 2. Range of variables and their coded form

Sample	Variable	Lower limit		Upper limit	
		Coded value	%	Coded value	%
1	A	0	0.124	1	0.188
2	B	0	0.064	1	0.128
3	C	0	0.374	1	0.438
4	D	0	0.374	1	0.438

Each polymer concrete mixture was used for casting specimens that were tested under identical conditions, according to European Standard [12]. Compressive CS and AS at 14 days were determined experimentally, adopting standard techniques [12] for all combinations given in Table 3. Table 4 summarizes mixture design and their experimental responses – CS and AS for each polymer concrete combination based on the concept of design of experiments. Mixture designs (1-10 runs) are sometimes augmented by adding interior points (11-15 runs). A center points will be added to the design data (Table 4) with 5 runs making 15 runs total. This addition will change the design from simplex-lattice to simplex-centroid design.

Table 3. Mixture design combination for Polymer Concrete

Combination reference	A(%)	B(%)	C(%)	D(%)
1	18.8	6.48	37.4	37.4
2	12.4	12.8	37.4	37.4
3	12.4	6.4	43.8	37.4
4	12.4	6.4	37.4	43.8
5	15.6	9.6	37.4	37.4
6	15.6	6.4	40.6	37.4
7	15.6	6.4	37.4	40.6
8	12.4	9.6	40.6	37.4
9	12.4	9.6	37.4	40.6
10	12.4	6.4	40.6	40.6
11	16.4	7.2	38.2	38.2
12	13.2	10.4	38.2	38.2
13	13.2	7.2	41.4	38.2
14	13.2	7.2	38.2	41.4
15	14.0	8.0	39	39,0

The experimentally studied response based on the results observed at the 14-days was analyzed statistically used Statistica software. In Table 4, each individual response (CS, AS) can be predicted by the regression equation, which expresses the relationship between the input variables and the concerned response.

Table 4. Experimental and predicted value for mixture design combinations of PC

Combination reference	CS		AS	
	Y _{predicted}	Y _{experimental}	Y _{predicted}	Y _{experimental}
1	57,97	59,20	6,99	7,27
2	58,92	58,79	5,02	5,18
3	60,32	59,59	5,36	5,67
4	58,08	57,61	6,45	6,57
5	63,99	64,08	8,23	8,45
6	59,18	58,62	9,90	10,25
7	43,76	43,47	8,84	9,01
8	47,81	45,95	7,31	7,56
9	56,80	55,21	7,60	7,66
10	57,99	55,62	8,89	9,06
11	61,31	58,80	7,35	5,87
12	60,43	63,20	6,52	5,47
13	59,88	65,32	7,34	5,77
14	53,24	57,61	8,78	7,96
15	61,15	57,75	7,32	10,15

For example the regression equation for CS can be predicted by the following equation:

$$Y_{CS} = 518.12A + 980.85B + 110.801C - 81.43D - 14.27AB - 1.69AC - 28.23AD - 0.166BC - 0.1184BD - 0.014CD + 2.184ABC \quad (13)$$

The coefficients of the individual variable in this equation give a measure of the effect of variable on the predicted response. For variable having coefficient of large magnitudes, even a marginal increment will give a significant change in the response. However ever, for variables having coefficients of lower magnitudes, even a large increase will result in only a small change in the response. Thus significant and less significant variable can be identified from the equation. The above equations are based on the special cubic model, because this model fitted well with the experimental data.

A standard statistical technique to carry it out is the analysis of variance (ANOVA) [5-6], it is routinely used to provide a measure of confidence. ANOVA results for 14-days strength are shown in Table 5. By this way we can observe the importance of interaction effect of the three leading factors (ABC), which is expressed by the coefficient R-sqr – 0.999876 (Table 5). This coefficient shows an adequate fit for the predictive response surface model of CS.

ANOVA for each model (Tables 5-6) gives the sum of squares and degrees of freedom for the model terms from which mean squares values of the individual model terms are calculated.

Table 5. Summary of ANOVA for CS

	SS Effect	df Effect	MS Effect	SS Error	df Error	MS Error	F	p	R-Sqr
Linear	10.4285	3	3.4761	228.504	11	20.77316	0.16734	0.916175	0.043646
Quadratic	155.595	6	25.932	72.9095	5	14.58191	1.778405	0.272058	0.694854
Special									
Cubic	72.8799	4	18.219	0.02963	1	0.02963	614.9242	0.030235	0.999876
Total									
Adjusted	238.933	14	17.066						

The lack-of-fit test compares the residual error to the pure error from replication and gives F-values for all the models. The F-values must be lower if a particular model is to be significant. From the F-test, it was fund that only the model passed the F-test.

Table 6. Summary of ANOVA for AS

	SS Effect	df Effect	MS Effect	SS Error	df Error	MS Error	F	p	R-Sqr
Linear	22,571	3	7,523	257,428	11	23,4026	0,321495	0,809785	0,080612
Quadratic	212,247	6	35,37	45,181	5	9,036204	3,914762	0,077884	0,838639
Special									
Cubic	38,5143	4	9,628	6,666	1	6,666667	1,444288	0,547853	0,97619
Total									
Adjusted	280	14	20						

Analysis for the both responses that were studied clearly shows that the cubic modulation is adequate for this study and is explained by the fact that only by interaction of three factors (is a case of a mixture) we have a modulation corresponding to the physic phenomenon.

Pareto charts obtained from the statistical analysis are presented in Figures 2 and 3, and they show the importance order of the variables.

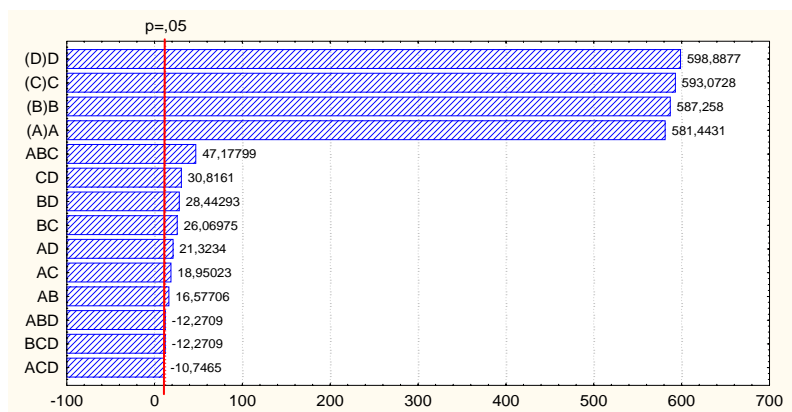


Figure 2. Pareto charts of standardized effect of CS

Also it can observe that for two responses that are analyzed there are not significant effects in interaction of factors (AS) and for the other response (CS) almost all second interactions among factors are important. It must remark that for these responses also there are important interactions of third degree (ABC interaction for CS – Figure 2).

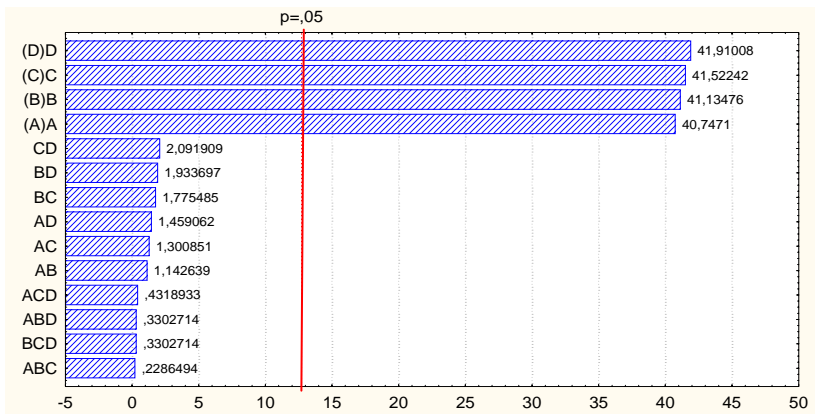
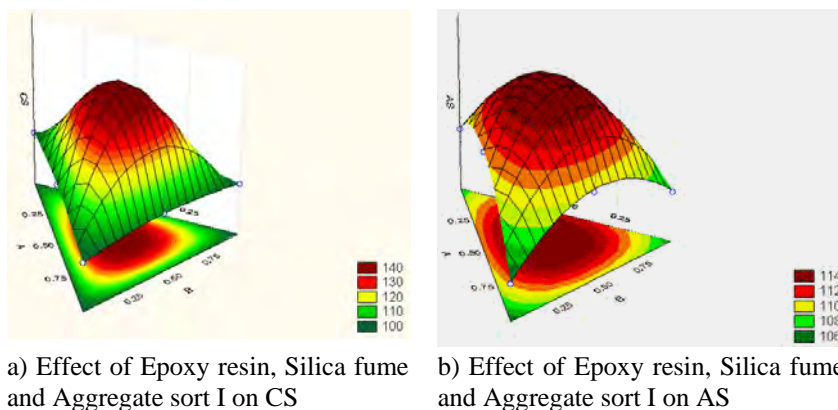


Figure 3. Pareto charts of standardized effect of AS

Analyzing these charts it can conclude that for all two responses the factors that were studied have a very important influence. For example analysis of variance of CS and AS gives the non-linear response surface for two responses (Figures 4 a, b) with the significant cubic interactions, only for CS: ABC - epoxy resin (A), silica fume (B) and crushed aggregates sort I (C) - Figure 4 a). The results from the designed experiment indicate that the factors have very significant effects. The all second-order interactions have an important role. The special cubic interaction ABC has very significant effects and all others cubic interactions have very weak effects whereas the other interactions are barely noticeable at all. As a consequence, those interaction effects can be neglected.



a) Effect of Epoxy resin, Silica fume and Aggregate sort I on CS

b) Effect of Epoxy resin, Silica fume and Aggregate sort I on AS

Figure 4. Responses surfaces.

Analysis of variance (ANOVA) and the responses surfaces for desirability effects of variables interactions show significant non-linear effects (all the response surfaces are curved - Figure 5) for CS of PC for example, that means that are not

enough known the influences of each factor on the behavior of this type of PC and on the contact elements.

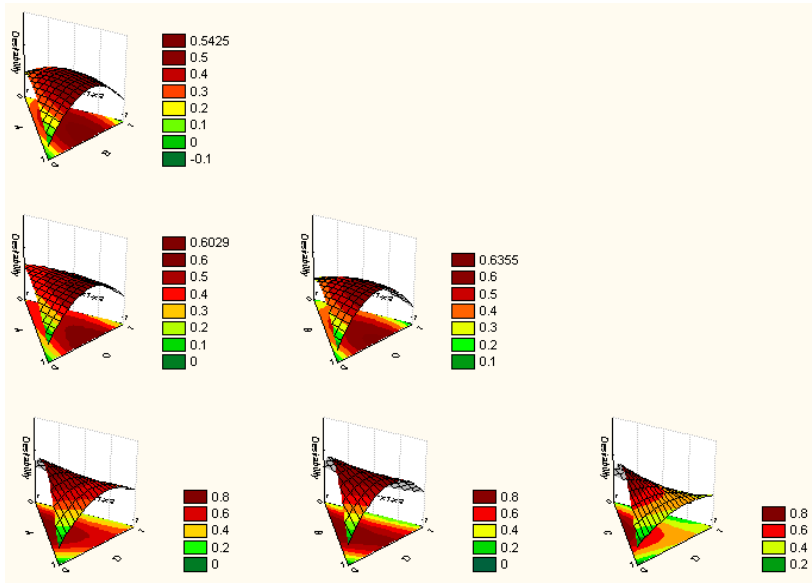


Figure 5. Response surface for desirability effects of variables interactions

The application of the first phase of the optimization approach RSM yielded the following regression equation, which is an empirical relationship between the STS and the four factors (Equation 13).

The second phase consists of resolving the optimization problem expressed by:

$$\text{Maximize: } Y_{STS}(A,B,C,D) \text{ and } Y_{FS}(A,B,C,D) \tag{14}$$

The applications of the optimization procedure using the GRG algorithm give the values shown in Table 7.

Table 7. Optimal values of polymer concrete

Optimal values of parameters (%)		Optimal value of FC	Optimal values of parameters (%)		Optimal value of AS
A	13.94	70.23	A	13.88	11.93
B	7.98		B	7.92	
C	38.86		C	38.80	
D	39.09		D	39.03	

Using the proposed method the optimum setting parameters for CS was A = 13.94 %, B = 7.98%, C = 38.86% and D = 39.09% in the real values and $Y_{CS} = 70.23$. For the second response (AS) analyzed the optimum setting parameters are A = 13.88 %, B = 7.92%, C = 38.80% and D = 39.03% in the real values and $Y_{AS} = 11.93$.

Analyzing the experimental results we can observe the following:

- The values of CS varied from 65.32 N/mm² (for concrete type PC13 with 13.2 % polymer) to 43.47 N/mm² (for concrete type PC7 with 15.6% polymer). The compressive strength has high value for small polymer content.
- The values of AS varied from 10.25 N/mm² (for concrete type PC6 with 15.6% polymer) to 5.18 N/mm² (for concrete type PC2 with 12.4% polymer). The adherence is higher for big dosage of polymer.

From the predicted values it can observe that for CS the maximum value is for PC11 (with 16.4% polymer) and for AS the maximum value is for PC6.

The optimal composition for high value of compressive strength (CS=70.93 N/mm²) is with epoxy resin of 13.94%, silica fume with a dosage of 7.98%, aggregate sort 0-4 mm of about 38.86% and aggregate sort 4-8 mm of about 39.09%

For AS the optimum composition for AS=11.93 N/mm² is with 13.88% epoxy resin, silica fume with a dosage of 7.92%, aggregate sort 0-4 mm of about 38.80% and aggregate sort 4-8 mm of about 39.03%.

6. CONCLUSIONS

This paper described a mixture process optimization method for mechanical characteristics of polymer concrete that combines mixture design of experimental responses, response surface method and generalized reduced gradient optimization algorithm. In the present work, the optimization computation is carried out with a Microsoft Excel Worksheet using the generalized reduced gradient method. In the first phase, polynomial models are generated with the available mixture design of experiments data obtained by experimental tests. In the second phase, the optimizer uses the objective function during the search for the optimum until the final converged solution is obtained. Polymer concretes were made with epoxy resin in a reduced dosage, silica fume and aggregates. Response surface method has been used for a better understanding of the influence of the deviation of the polymer concrete parameters on mechanical strength evolution. The analyzed properties of PC were experimentally determined and compared with predicted values. The both

type of properties, compressive strength and adherence stress can be obtained with high values for optimum values of parameters.

References

1. Agarwal L.K., Thapliyal P.C., Karade S.R. Properties of polymer-modified mortars using epoxy and acrylic emulsions, *Construction and Building Materials* 21, pp: 379-383, 2007.
2. Varughese K.T., Chaturvedi B. K. Fly ash as Fine Aggregate in Polyester Based Polymer Concrete *Cement and Concrete Composites*, 18, pp: 105-108, 1996.
3. Muthukumar, M., and Mohan, D., Optimization of Mechanical Properties of Polymer Concrete & Mix Design Recommendation Based on Design of Experiments, *Journal of applied Polymer Science*, Vol. 94, pp: 1107-1116, 2004.
4. Muthukumar, M, Mohan, D., and Rajendran, D., Optimization of mix proportion of mineral aggregates using Box Behneken design of experiments, *Cement and Concrete Composites*, Vol. 25, pp: 751-758, 2003.
5. Marcia J Simon, Eria Slagergren, Kenneth A Snyder, Concrete mixture optimization using statistical mixture design method, *Proceedings of International Symposium of Height Performance Concrete*, New Orleans, Louisiana, October 20-20, 1997.
6. Cornell, J.A., How to Apply Response Surface Methodology, vol. 8, ASQC, Wisconsin, 1990.
7. Mayer RH and Montgomery DC, *Response Surface Methodology process and product optimization using design of experiments*, Wiley, New York, 1995.
8. Montgomery Douglas C., *Design and analysis of experiments*. – 5th edition by Wiley & Sons, Inc., New York., 2001.
9. Lepadatu D. et all, Optimization of springback in bending process using FEM and Response Surface Methodology, *International Journal of Advanced Manufacturing Technology*, 27, pp: 40-47, 2005.
10. Lepadatu D. et all, Statistical investigation of die wear in metal extrusion process, *International Journal of Advanced Manufacturing Technology*, 28, pp: 272-278, 2006.
11. Goupy J., *Plans d'expériences pour surfaces de réponse*. DUNOD, Paris, pp 253–294, 1999.
12. EN 12390/2001 - Testing hardened concrete. European Committee for Standardization, Brussels, Belgium - 2001.

Glass addition influence on cement-bound composite materials’ strength characteristics

Tomáš Melichar¹

¹Faculty of civil engineering, Institute of Technology of Building Materials and Components, Brno
University of Technology, Brno, 602 00, Czech Republic, melichar.t@fce.vutbr.cz

Summary

This paper deals with the brief summary of present research which is concerned a utilization of secondary raw materials in cement-bound composites problems. For the purposes of this article a recycled screen and monitor panel glass was used as the secondary raw material.

In the preamble of the paper is stated short developments retrieval of selected authors, who are engaged in the themes involved. Next subchapter then continues to a certain extent their science findings, whereas main care is paid a partial compensation of cement by secondary raw material.

Following paper section is focused on experimental research. Generally, fourth part of cement in test specimens was replaced by fine glass powder. Below there are stated some computational methods, which are cohering with some physical and mechanical properties determination.

KEYWORDS: cement, composite material, glass, compressive strength, bending tensile strength, grinding, secondary raw material

This paper was published with the financial contribution of research project CEZ - MSM 0021630511, “Progressive Building Materials with Utilization of Secondary Raw Materials and their Impact on Structures Durability and also a research project GA 103/05/H044, ”Stimulation of Doctorands Scientific Development in the Branch of Building Materials Engineering”.

1. INTRODUCTION

Waste problems and their processing or disposal question associated with it is often discussed theme in present, which there’s no need to convey too. A fact that growing bulk of waste produced of our human society has a negative environmental impact, leads to a development or implementation of quite new waste processing and recycling technologies. The secondary raw materials, which

can be used in various branches of industry, are rising by those procedures. An example of these secondary raw materials is e.g. slag or fly ash, which are used in building materials industry. However, the production of wastes not have to be account on manufacturing process such as aforementioned slag and fly ash, but it can be the cause of e.g. by a new manufacturing technologies implementation. The LCD screens, which are subsequently replacing the older types of screens (CRTs – Cathode Ray Tube screens) are by one of these cases. CRTs manufacturing in Czech Republic is rapidly turning off and a problem what to do about such bulk CRTs waste arises.

1.1. Recycled glass in cement-bound composites as an aggregate

The up to now research works how to utilize recycled glass (RG) have aimed at two main ways. A partial or full replacement coarse or fine aggregate by RG have been examined in the first case. Particularly physico-mechanical and micro structural material characteristic and next an appropriate rise of so much important alkali-silica reaction (ASR) were investigated on test specimens. Principle of ASR consists in long-term alkali (Na_2O , K_2O) effecting on active silica (SiO_2), thereby a reaction attended by expansion (alkali-silica gel formation Fig. 1). This expansive reaction can cause great problems of cracking and, consequently, it can be extremely deleterious for the durability of mortar and concrete. The reaction can be written in simplified form as follows:

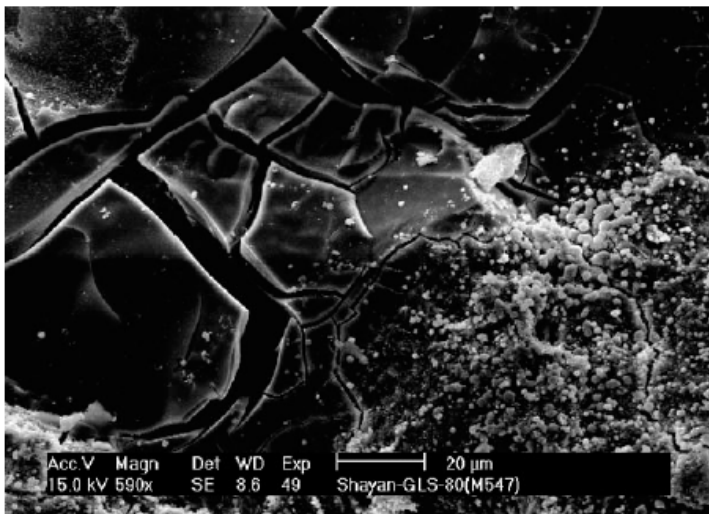
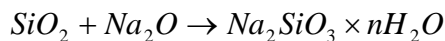


Figure 1. Site ASR gel formation in concrete and the composition of the gel [10]

There has been quite number of ASR determination. In [1], the comparison of chosen methods (i.e. according to ASTM C1260, ASTM C227 and ASTM C1293) with an autoclave method was carried out. Test specimens contained an aggregate wholly replaced by RG. It was founded that the test procedure suggested ASR screening test based on autoclaving exhibits sufficient sensitivity and accuracy to expose the reactivity of a certain mix or composition. Although absolute values are not determined, relative expansions due to ASR can be detected in comparison to reference samples of known reactivity [1].

During the experimental works in [2], where RG was considered as coarse aggregates in the concrete, an RG (fraction 4-16 mm) addition (in proportions of 0-60 %) effect was examined. Particularly effects of RG on workability and strength of the concrete with fresh and hardened concrete tests were analyzed. As a result of the study conducted, WG was determined not to have a significant effect upon the workability of the concrete, but the compressive strength decreased as much as 49% with a 60% of RG addition [2]. In article [3], three different fractions of the waste glass were examined, characterized by distinct grain size distributions: the finest fraction is characterized by particle size up to 36 μm ; the medium fraction is characterized by particle size ranging from 36 up to 50 μm and the coarsest fraction is characterized by particle size ranging from 50 up to 100 μm . Prismatic specimens (40 \times 40 \times 160 mm) were manufactured, cast, wet cured for 24 h and air cured at 20 C for further 27 days. Then the specimens were immersed in water for 100 days. Finally, they were maintained for 4 h in boiling water at 100 °C and subsequently cooled, always in water. On the basis of the results obtained the authors reached fact, is quite evident that no deleterious effect can be detected at a macroscopic level due to the reaction between cement paste and ground RG with particle size up to 100 μm . On the contrary, a strong improvement of the mortar mechanical performance was detected, due to the positive contribution of the RG to the micro-structural properties [3]. In [4], scientists the extensive research about RG (particle size up to 5 mm) and polymer (SBR latex) containing concrete carried out. Utility RG in proportions of 30 % (as aggregate) and SBR latex in proportion of 10 % results from the study, with regard to ASR risk of course.

1.2. Recycled glass in cement-bound composites as a pozzolanic material

A second featured way how to utilize RG for production of cement-bound composites results from its chemical composition, which in principle similar (silica content) to aforementioned fly ash. Fly ash is latently-hydraulic substance, which is used in cement industry for its pozzolana properties. This feature consists in sufficient so-called active SiO_2 content, that in necessary for running or support of hydration reactions and subsequent formation of hydration products (CSH I, CSH II), which are made during the cement-bound composites setting and hardening. It's necessary to grind RG to required particle size (specific surface area).

According to various literature sources the ASR rise is suppressed, when particle size of RG is up to 75 μm (according to [4] up to 100 μm). In [5], test specimens containing fine glass powder (specific surface area 264, 467 and 582 m^2/kg) and fly ash as a cement replacement (20 % of cement). The specimens were maintained at two different temperatures namely: 23 $^{\circ}\text{C}$ and 35 $^{\circ}\text{C}$. A strength activity index after 28 days and ASR (according to ASTM C1260) were determined. On the basis of reached results was founded that finely ground glass powders exhibited very high pozzolanic activity. Mortar strength testing results indicated that curing temperature has a greater influence on the pozzolanic activity of glass powder than on that of fly ash. Results from ASTM C1260 testing indicated that the replacement of Portland cement with ground glass powder also reduces the ASR-induced expansion, although it is not as effective as coal fly ash [5].

2. EXPERIMENTAL PART

All in all 36 test specimens were manufactured and analyzed, whereas 25 % of cement was replaced by finely ground CRT glass powder on 18 of them. Pozzolanic reactivity was observed implicitly, namely on compressive and bending tensile strength development, i.e. at the age of 28, 60 and 90 days.

2.1. Glass preparation

Chemical composition of CRT glass as a secondary raw material is to a certain extent variables, which is very hard influence able with regard to sort out work difficulty (i.e. economic and time). The chemical composition of CRT glass with which is operating its compilers is reported in Table 1.

Table 1. Cullet from panel of CRTs chemical composition

Chemical composition	Min. (%)	Max. (%)
SiO_2	53,9	69,1
Al_2O_3	1,7	4,0
Fe_2O_3	0,0	0,1
BaO	1,9	14,6
PbO	0,0	3,0
Na_2O	6,5	10,2
K_2O	6,5	10,3
CaO	0,8	4,6
MgO	0,0	1,8

It was used CRT fine glass powder, whereof was attained by two-step grinding. The first stage of grinding was carried out in a ball mill, where the beforehand cleaned and crushed CRT glass has been ground for 60 seconds. Then the glass has

been ground in vibrating mill (Fig. 2) for 1, 2, 4, 6 and 8 minutes to sufficient specific surface area was obtained. For this purpose the specific-gravity bottles and Blain’s apparatus were used. Relation between a time of grinding and specific surface area is shown in Fig. 3.



Figure 2. Sight to vibrating mill mouth (left) and grinding chamber with medium (right)

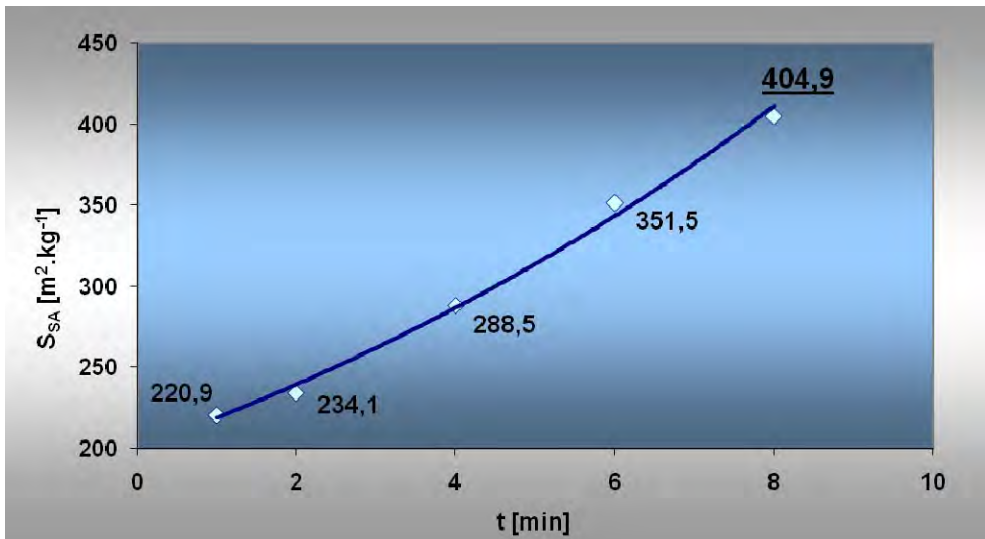


Figure 3. Relation between a time of grinding and specific surface area of RG

Exponential function describes a dependence of RG grinding time and specific surface evidently the best. Regress ratio criterion is a correlation coefficient in our case. The value of correlation coefficient takes a high values. Form of the relation can be described as following:

$$S_{SA} = 199,95.e^{0,0902.t} ; R=0.9973 \quad (1)$$

where:

S_{SA} is specific surface area [m^2/kg]

t is grinding time [min]

R is correlation coefficient [-]

The next needs to be remark, that aforementioned relation is applicable only in case of the used vibration mill and a weight shot (sample - glass) of 120 g.

With regard to aforementioned authors' results and specific surface area of cement, the glass powder, whose specific surface area reached value $405 m^2/kg$ was used for experimental work.

2.2. Test specimens preparation

The prismatic specimens ($40 \times 40 \times 160$ mm) were manufactured, cast, wet cured and tested according to Czech standard ČSN EN 196-1. CEM I 42,5 R and Standardized sand CEN EN 196-1 were used for manufacturing. Specific proportion of each component for both types of batch, i.e. reference marked Ref and partial cement replacement marked Glass, is reported in Table 2.

Table 2. Specific proportion of each component for both types of batch

component	mixture	
	Ref	Glass
	m [g]	m [g]
cement	450	337,5
aggregate	1350	1350
water	225	225
glass	0	112,5

2.3. Test data evaluation

For simplicity only average compressive and bending tensile strength values are imported. The next figures show a compressive (Fig. 4) and bending tensile (Fig. 5) strength development of reference (marked Ref) and recycled glass (marked Glass) containing samples. Positive influence is obvious in case of bending tensile strength, where the strength values of Glass samples at 60 days age are actually higher than values of Ref samples, at the age of 90 days the strength values are almost identical.

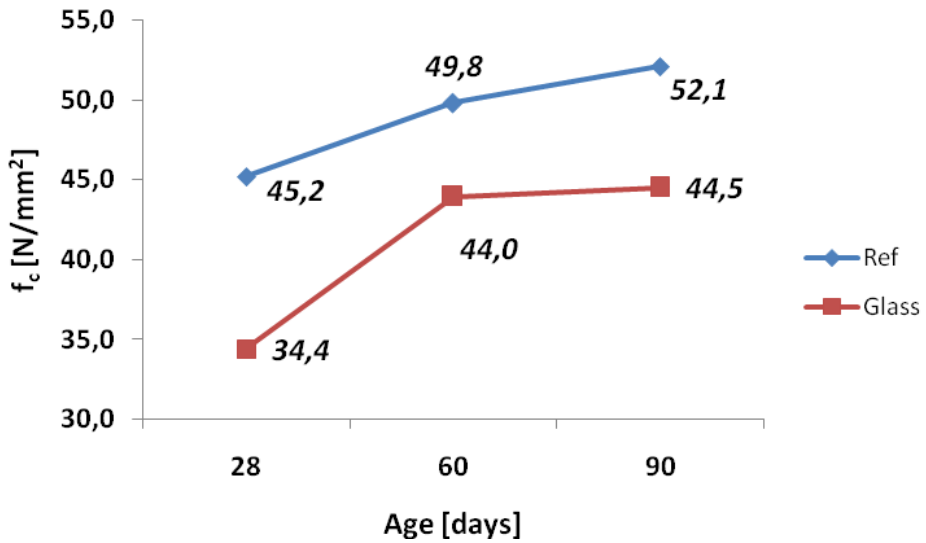


Figure 4. Compressive strength development of Ref and Glass samples comparison

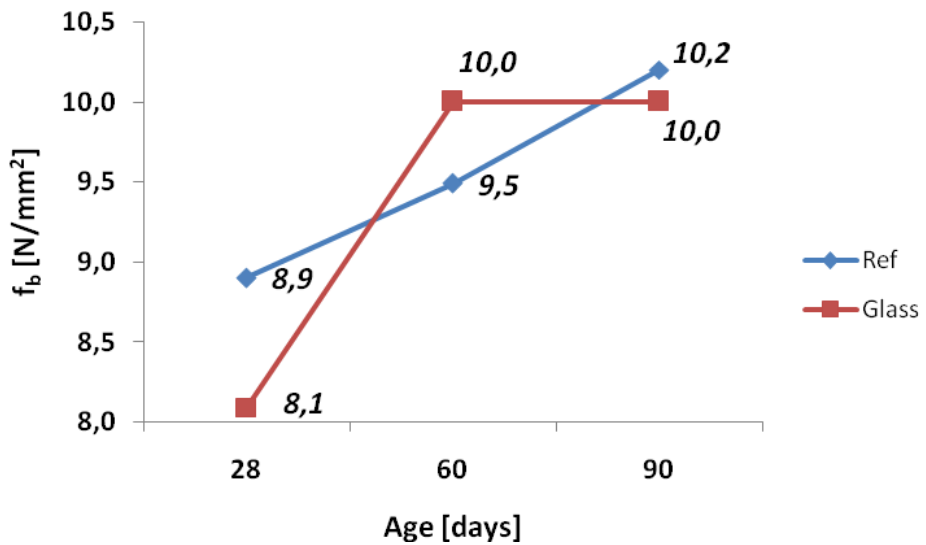


Figure 5. Bending tensile strength development of Ref and Glass samples comparison

3. CONCLUSIONS

In the first experimental work stage the dependence of recycled CRT glass grinding time on final product specific surface area was observed. From graphical analysis an exponential function (1) was derived by virtue of regression analysis. The function describes surveyed dependence best. High value of correlation coefficient acknowledges this fact. The coefficient is one of the most important function availability assessment criterions. Correlation coefficient expressing interdependence measure of investigated quantities. In term of resilience and workability (of fresh composite batch) a sample with specific surface of 405 m²/kg area value was chosen as an optimal.

In the following research, the partial replacement (25 %) of cement binder by recycled CRT glass influence on final strength characteristics was investigated. The strength parameters are one of main cement-bonded composites usability requirements in the structures construction field. Findings are interesting partly in term of samples age and partly in light of strength type development. It stands to reason, that strength difference of samples marked Ref and Glass is lowers with increasing age. In the case of compressive strength, Glass strength values attain 85 % of Ref strength values. As regards bending tensile strength, it is possible to state, that strength values of both sample types are almost identical after 90 days.

By the research and its evaluation in the paper a positive influence of partial cement binder replacement by CRT glass on strength characteristics. Replacement of 25 % is advantageous in light of environmental and economical aspects. Conclusion and evaluation of the article would be served as groundwork for another research in the field of glass secondary raw materials applied in cement-bound composites. Above all an attention would be paid to appropriate ASR (alkali-silica reaction) inception, durability characteristics, workability of fresh batch, microstructure (DTA, RTG, Chemical analysis) etc. On the basis of aforementioned it is possible to claim, that cement partial replacement by recycled CRT glass is practicable and even for certain aspects convenient.

Acknowledgements

This paper was published with the financial contribution of research project CEZ - MSM 0021630511, "Progressive Building Materials with Utilization of Secondary Raw Materials and their Impact on Structures Durability and also a research project GA 103/05/H044, "Stimulation of Doctorands Scientific Development in the Branch of Building Materials Engineering".

References

1. Pytlík P.: Technologie betonu, VUTIUM, Brno, 2000.
2. Hela R.: Technologie betonu I, *Studijní opory pro studijní programy s kombinovanou formou výuky*, Brno, 2005
3. ČSN EN 196-1: Metody zkoušení cementu: Stanovení pevnosti
4. ČSN EN 450-1: Popílek do betonu - Část 1: Definice, specifikace a kritéria shody
5. A suggested screening test for ASR in cement-bound composites containing glass aggregate based on autoclaving, *Cement & Concrete Composites* 26, 2004, 827-835
6. Properties of concrete containing waste glass, *Cement & Concrete Research* 34, 2004, 267-274
7. Reuse of ground waste glass as aggregate for mortars, *Waste Management* 25, 2005, 197-201
8. Studies on mechanical properties of concrete containing waste glass aggregate, *Cement and Concrete Research* 34, 2004, 2181-2189
9. Characteristics and pozzolanic reactivity of glass powders, *Cement and Concrete Research* 35, 2005, 987-993
10. Value-added utilisation of waste glass in concrete, *Cement and Concrete Research* 34, 2004, 81-89

The influence of damping ratios on earthquake response of steel frame structures

Horatiu Alin Mociran¹, Alexandra Denisa Stan¹

¹Faculty of Civil Engineering, Technical University, Cluj-Napoca, 400027, Romania

Summary

This paper provides a comparison of the seismic performance indices of a five story steel frame building with three different damping ratios (5%, 20% and 30%) and two structural systems (moment frame and viscously damped frame). A novel approach for earthquake hazard mitigation is the use of viscous dampers. The objective of this approach is to dissipate earthquake-induced energy in devices designed especially for this purpose, and to eliminate or minimize energy dissipation demand and inelastic action in primary structural members. The non-dimensional performance indices considered for the models are: Peak Drift ratio, Pick Base Shear and Peak Level Acceleration.

The moment frame structure is situated in Iași and was designed according to Romanian seismic code P100-1/2006. The structure was then modified by addition of fluid viscous dampers to improve the seismic performance, with no attempt made to redesign the main frame elements.

Linear viscous dampers of Taylor Devices type will be installed with a diagonal brace configuration. The inherent damping ratio of the structure is assumed to be 5%, and the total effective damping ratio of the whole system is designated at 20% and 30% of critical.

The seismic performance of these structures was studied using nonlinear response-history analysis. Three artificial earthquakes of Vrancea type, that matched P100-1/2006 Provisions response spectrum were used for analysis.

The results of the time history analysis are presented and discussed. Comparisons are made of estimated base shear, interstory drift and floor acceleration.

The numerical results are presented in both, graphical and tabular form.

The seismic performance indices show that these viscous dampers when incorporated into the structure reduce the earthquake response significantly in proportion to the amount of damping supplied in these devices.

KEYWORDS: steel frames, damping ratio, viscous damper, time history analysis.

1. INTRODUCTION

Recent earthquakes in Turkey (1999) and Taiwan (1999) have resulted in severe damages to civil infrastructures, in addition to a loss of lives. Today, one of the main challenges in structural engineering is to develop innovative design concepts to better protect civil structures, including their material contents and human occupants, from earthquakes [1].

Conventionally, structures have been designed to resist natural hazards through a combination of strength, deformability, and energy absorption. These structures may deform well beyond the elastic limit, for example, in a severe earthquake. They may remain intact only due to their ability to deform inelastically, as this deformation results in increased flexibility and energy dissipation. Unfortunately, this deformation also results in local damage to the structure, as the structure itself must absorb much of the earthquake input energy. It is ironic that the prevention of the devastating effects from earthquakes, including structural damage, is frequently attained by allowing certain structural damage.

Alternatively, some types of structural protective systems may be implemented to mitigate the damaging effects of these environmental forces. These systems work by absorbing or reflecting a portion of the input energy that would otherwise be transmitted to the structure itself. Considering the following energy conservation relationship [2] as an illustration of this approach:

$$E = E_k + E_s + E_h + E_d \quad (1)$$

where E is the total input energy from the earthquake motion, E_k is the absolute kinetic energy, E_s is the recoverable elastic strain energy, E_h is the irrecoverable energy dissipated by the structural system through inelastic or other forms of action, and E_d is the energy dissipated by supplemental damping devices. From this equation, one can see that, with certain input energy, the demand on energy dissipation through inelastic deformation can be reduced by using structural protective systems.

The level of damping in a conventional elastic structure is very low, and hence the amount of energy dissipated during transient disturbances is also very low. The concept of supplemental dampers added to a structure assumes that much of the energy input to the structure will be absorbed by supplemental devices. An ideal damper will be able to reduce both stress and deflection in the structure. Fluid viscous dampers operate on the principle of fluid flow through orifices. A stainless steel piston travels through chambers that are filled with silicone oil. The pressure difference between the two chambers cause silicone oil to flow through an orifice in the piston head and seismic energy is transformed into heat.

2. DESCRIPTION OF STRUCTURE, VISCOUS DAMPERS AND INPUT GROUND MOTION

2.1. Description of structure

A five story steel frame was selected as a reference frame. The structure was designed as a conventional SMRF (Figure 1) to provide a benchmark for seismic performance comparison with passive control systems.

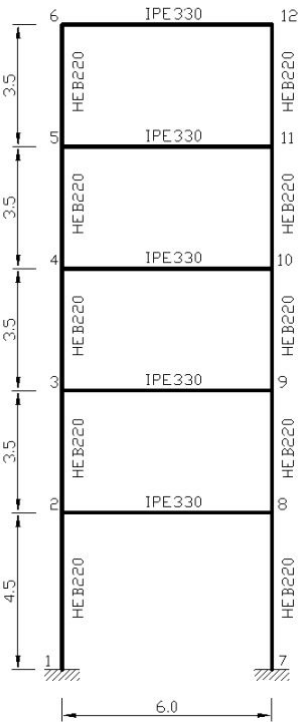


Figure 1. Five Story Reference Frame

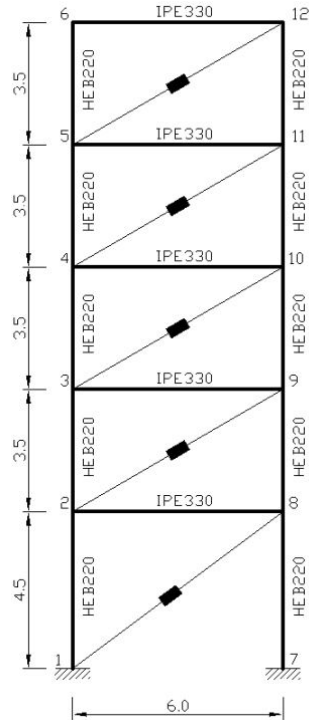


Figure 2. Five Story Frame with Linear Viscous Dampers

The following parameters according to P100-1/2006 were used to design SMRF [3]: importance class II $\gamma=1,2$; design ground acceleration $a_g=0,20g$; $TC=1,6$ sec and behavior factor $q=6$.

All connections between beams and columns are assumed rigid connections. The structure was then modified by the addition of fluid viscous dampers (Figure 2) to

improve the seismic performance, with no attempt made to redesign the main frame elements.

2.2. Description of viscous dampers

Linear viscous dampers are added at each floor. Figure 3 shows the internal construction of a viscous damper manufactures by Taylor Devices. The dampers will be installed with a diagonal brace configuration. The inherent damping ratio of the structure is assumed to be 5%, and the total effective damping ratio of the whole system is designed as equivalent to 20% and 30% of critical damping for the first mode.

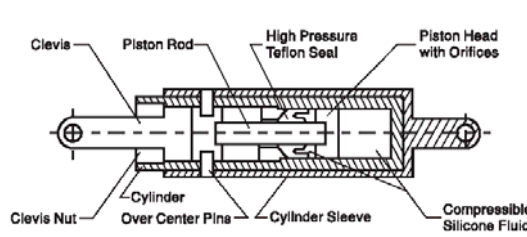


Figure 3. TAYLOR DEVICES Viscous Damper

The damping coefficient of each damper is $c=300\text{kN}\cdot\text{sec}/\text{m}$ for the case of a damping ratio of 20% and $c=505\text{kN}\cdot\text{sec}/\text{m}$ for a damping ratio of 30%. In this example, the linear effective stiffness is set to zero so that pure damping behavior is achieved.

2.3. Input ground motion

The seismic performance of these structural systems was studied using nonlinear response-history analysis. Three artificial earthquakes of Vrancea type, that matched P100-1/2006 [2] Provisions response spectrum for Iasi were used for analysis.

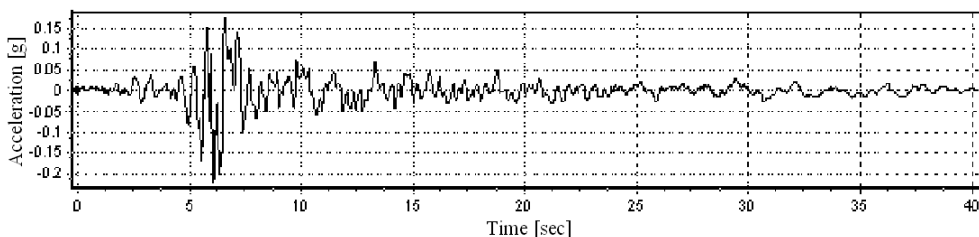


Figure 4. Artificial accelerogram of Vrancea Type

3. NUMERICAL RESULTS AND DISCUSSIONS

The results of the time history analyses are presented and discussed. Comparisons are made of estimated base shear, interstory drift and floor acceleration.

3.1. Base shear

Figure 5 demonstrate significant base shear reduction when dampers are added to the structural frame. As expected, best performance is achieved for a damping ratio of 30%, although the case of 20% damping ratio produces important response reduction. It should be mentioned that these results apply for an elastic structural system.

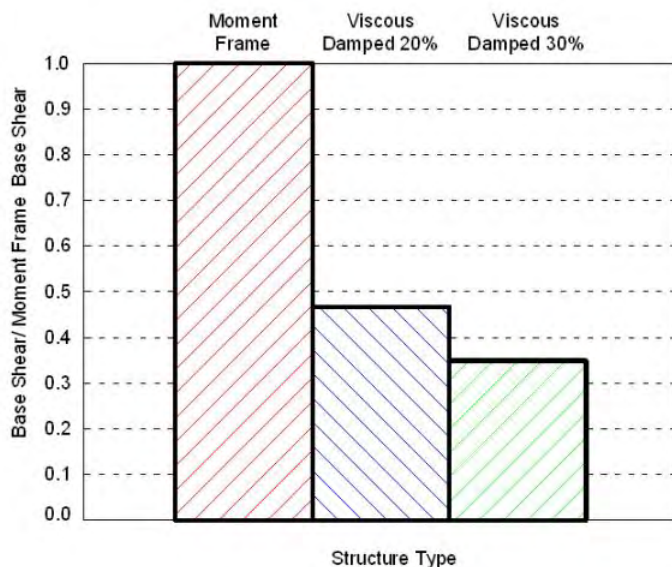


Figure 5. Normalized Maximum Value of Base Shear

3.2. Interstory drift

This is a code design parameter and is something most engineers focus upon during the design process. From a damageability perspective, it is a measure that impacts damage to the framing system, building façade and windows, piping, ductwork and partitions.

The obtained results indicate that the maximum interstory drift values were reduced in proportion to the amount of damping supplied in the structure. Figure 6 presents ratios of peak interstory drift of the structure with dampers to the structure without dampers.

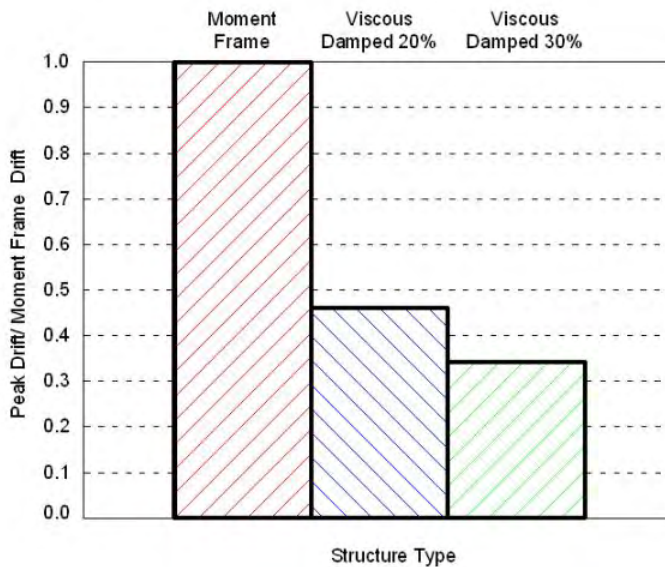


Figure 6. Normalized Maximum value of Interstory Drifts

3.3. Floor accelerations

This parameter is almost never taking into account in the design process, because it requires a time history analyses to obtain it. From the damageability perspective it is the measure that impacts damage to the ceiling and lights, electrical and mechanical equipment, elevators and the building contents.

Results indicated that viscous dampers have the potential to significantly diminish the floor accelerations in the structure. The viscous dampers reduced the floor accelerations by 50.50% for a damping ratio of 20% and with 60.20% for a damping ratio of 30%. Figure 7 shows a comparison of maximum values of floor accelerations for all framing schemes, normalized to the moment frame.

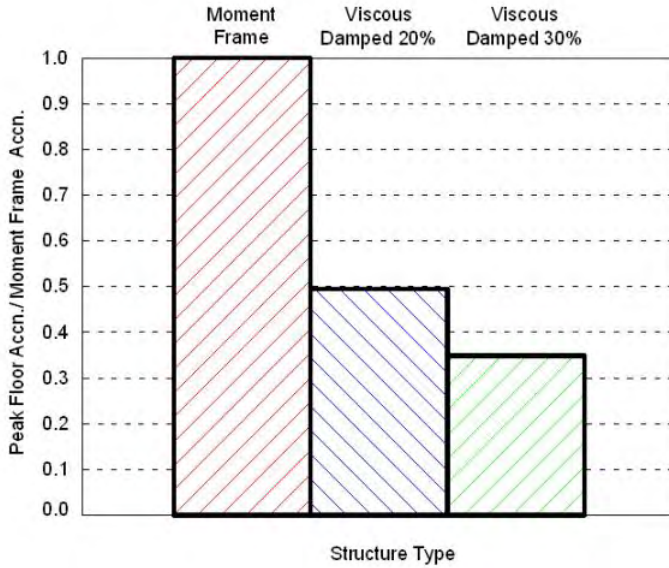


Figure 7. Normalized Peak Floor Accelerations

3.4. Performance indices

Three performance indices are introduced to assess the seismic efficiency of viscous dampers for different damping ratios. These indices compare peak response quantities of the five story structure without and with viscous dampers for the same earthquake input [4].

The non-dimensional performance indices considered in this study are Peak Base Shear (PI_1), Peak Drift ratio (PI_2), Peak Level Acceleration (PI_3).

They are defined as follows: $PI_1 = \frac{F_{b,c}^{\max}}{F_{b,u}^{\max}}$; $PI_2 = \frac{\delta_c^{\max}}{\delta_u^{\max}}$; $PI_3 = \frac{\ddot{x}_c^{\max}}{\ddot{x}_u^{\max}}$; where:

$F_{b,u}^{\max}$; $F_{b,c}^{\max}$ - the maximum base shear of the uncontrolled/controlled frame;

δ_u^{\max} ; δ_c^{\max} - the maximum inter storey drift ratio of the uncontrolled/controlled frame;

\ddot{x}_u^{\max} ; \ddot{x}_c^{\max} - the maximum absolute floor acceleration of the uncontrolled/controlled frame.

These indices are always positive and their values range between 0 and 1; values close to 0 indicate good performance, while values close to 1 mean poor performance.

The results presented in Table 1 demonstrate significant response reduction when the damping ratio of the structural frame is increased.

Table 1. Performance indices for peak base shear, peak drift and peak acceleration

Case	Performance Index			% Reduction		
	PI ₁	PI ₂	PI ₃	Base Shear	Story Drift	Acc
Viscous Damped 20%	0.467	0.460	0.495	53.30	54.00	50.50
Viscous Damped 30%	0.349	0.342	0.398	65.10	65.80	60.20

4. CONCLUSIONS

A numerical study has been conducted in order to asses the influence of damping ratios on earthquake response of steel frame structures..

The moment frame structure is situated in Iași and was designed according to Romanian seismic code P100-1/2006. The structure was then modified by addition of fluid viscous dampers to increase the damping ratio, with no attempt made to redesign the main frame elements. The inherent damping ratio of the structure is assumed to be 5%, and the total effective damping ratio of the whole system is designated at 20% and 30% of critical.

The seismic performance of these structures was studied using nonlinear response-history analysis. Three artificial earthquakes of Vrancea type, that matched P100-1/2006 Provisions response spectrum were used for analysis.

The non-dimensional performance indices considered for the models are: Peak Drift ratio, Pick Base Shear and Peak Level Acceleration.

The obtained results indicate that base shear, interstory drift and floor accelerations were reduced significantly in proportion to the amount of damping supplied in the structure.

References

1. Soong, T. T., Spencer J.R., Supplemental energy dissipation: state – of - the - art and state – of - the - practice, *Engineering Structures*, vol.24, 2002.
2. Christopoulos, C., Filiatrault, A., *Principles of Passive Supplemental Damping and Seismic Isolation*, IUSS Press, Pavia, 2006.
3. P100-1/2006, *Cod de proiectare seismică – Partea I. Prevederi de proiectare pentru clădiri*, Bucharest, 2006 (in Romanian).
4. Rama Raju, K., et al., Optimum Distribution of Viscous Fluid Dampers in Multi-Storied Buildings, *International Conference on Structural Stability and Dynamics*, Florida, 2005.

The simulation of weakening of steel columns` cross-sections caused by welding when strengthening under load

Mohamad Al Ali

Institute of Structural Engineering, Technical University of Košice, Košice, 04200, Slovakia

Summary

During welding, the weldment undergoes complex temperature changes that cause transient thermal stresses and non-elastic strains are produced in nearby the weld. After welding is finished, the remaining residual stresses are the result of the strains.

The strengthening of steel members under loading by means of additional parts is connected with many problems. Welding effects and high temperatures during the welding process cause a temporary local reduction of heated area. This problem becomes complicated thereby that these members rapidly get to the elastic-plastic zone. The displacement of the original centroid caused by temporary local reduction of heated cross-sectional area creates an additional moments. Because of listed reasons a vast investigation at home and abroad is absent.

This article deals with simulation of the cross-sectional weakening of steel columns during the welding process and brings out some comparing with experimental results. The paper also presents the actual state of this problem, some explanations for welding stress formation and creation of additional moments and deformations when the strengthening is realized under loading. Some recommendations for calculation and appraisal process are also presented here [1-7].

KEYWORDS: Welding stress, repair welding, strengthening of steel members, strengthening under loading, weakening of cross-sections, influence of the temperature.

1. INTRODUCTION

Strengthening of steel structures under loading is topical problem, which includes a lot of unanswered questions. The severity of analytical solution is residing in the complexity of identification of actual stress' pattern, which incessantly changes during welding process of new parts to original cross-section until finishing of Strengthening process and sequential loading.

During welding process high temperature is bringing into base material, which causes a melting-down of cross-sectional part in weld surroundings. Consequence of that is the temporary weakening of steel cross-section and changes of cross-sectional characteristics. After thermal wave's passage and stabilization the weakening of cross-section fade and the weld's shrinking develops in the welded member residual stresses and additional moments caused by eccentric location of the weld. The paper presents basic information about welding stress formation and creation of additional moments and deformations when the strengthening is realized under loading.

2. ANALYSIS OF CREATION AND REDISTRIBUTION OF WELDING STRESSES

For determination of welding stresses in welded member and regarding to technological conditions of welding, the following procedure can be considered:

- Analysis of thermal flow and amount of thermal energy,
- analysis of transient thermal stress and physical changes during welding process,
- determination of plastic strain and deformation,
- analysis of welding stresses.

The cardinal, but very difficult and demanding process is third step and the result is determination of non-continuous plastic deformations, which cause the hardening of base material around the weld.

Figure 1 allows better understanding of presented procedure, displays changes of stresses in dependence on temperatures changes around the weld, schematically represents weld along x-axis and actual position of welding electrode in point "0".

Position 1 is far from welding electrode station; thermal changes ΔT as well as thermal stresses caused by welding equal zero. Position 2 underlies on welding electrode station, therefore there's extreme of temperatures and their distribution is non-uniform. In this location of electrode, molten material cannot resist the loading and stress converges to zero. Stress in regions near welding electrode is

compressive, because the extension of these regions is restricted by surrounding material with lower temperatures. Intensity of compressive stresses has a yield stress value of material, heated up to relevant temperature. Stresses in regions far from the weld are tensile and they are in balance with compressive stresses.

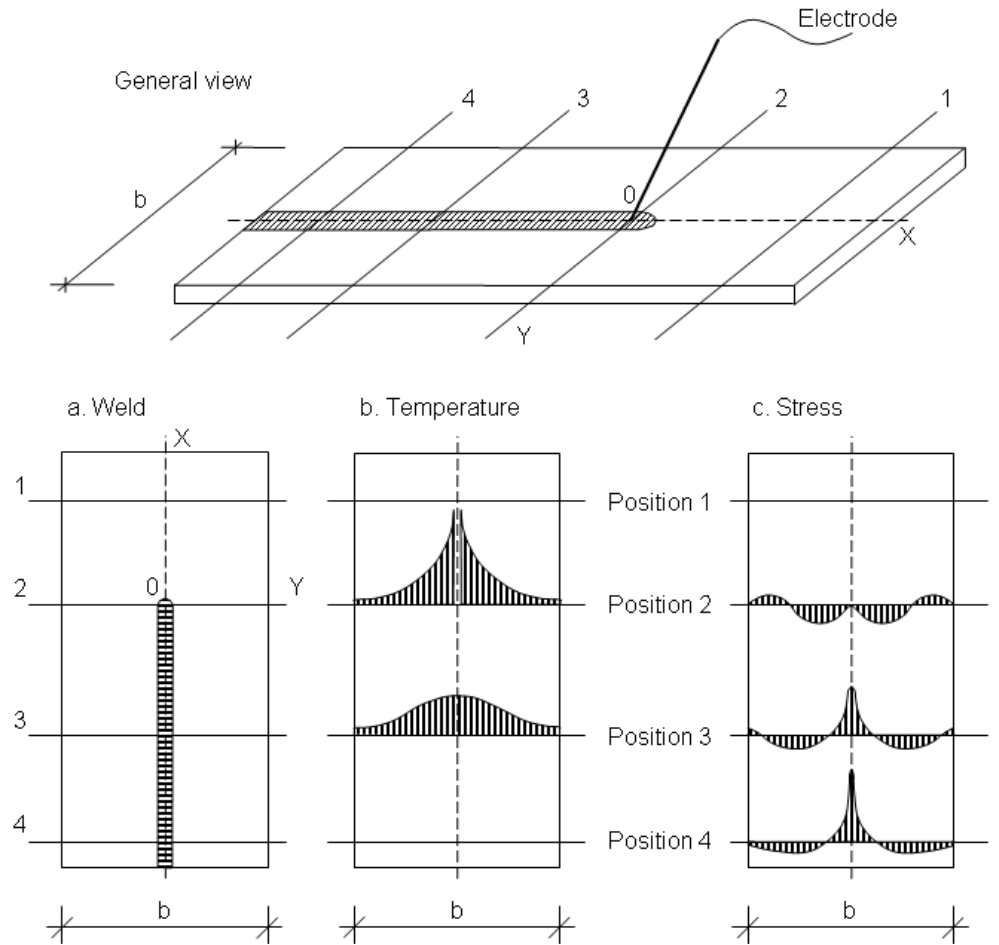


Figure 1. Interaction between temperature's changes and welding stress

Position 3 underlies after the welding electrode station, but the region is thermal affected and the temperature differences are smaller. This cooling causes shrinking of weld, as well as base material. Result of that is creation of tensile stresses near the weld. By increasing the distance from weld's region, stresses transform to compressive and they allowed transforming again to tensile. In position 4, temperature is steady and welding stresses acquire their final shape.

3. VERIFICATION REQUIRED FOR WELDING UNDER LOAD

According to above mentioned theory and because of the temporary weakening of the cross-section, the redistribution of the stress pattern, and the time-dependent changes in deformations, the loading capacity of the structural member must be checked at three different stages.

3.1. First stage

At this time the maximum reduction in effective area occurs. But resolidification already takes place a few seconds after the passing of the heat source. Deformations caused by temperature are still unimportant. For eccentric weld locations the centroid of the cross-section is shifted.

3.2. Second stage

At this time the member is subjected to maximum deformations caused by temperature gradients. According to test results, the maximum of these deformations occurs between 1 and 2 minutes after the passage of the heat source. Weakening of the cross-section is already receding considerably.

3.3. Third stage

This time signifies the complete cooling of the member. Shrinkage effects have attained their final and maximum stage.

This three-stage analysis gives a complete picture of the effects of welding under load and assures a safe performance of such operations.

4. SUBJECT OF SIMULATION AND DESCRIPTION OF THE MODEL

Welding new parts to the existing steel column under load causes temporary weakening of the original area along the certain length, displacement of centroid of the affected part and rising of additional moment from the external load.

On the basis of this idea strengthening was simulated, using column made from material grade G40.21-M-300W ($f_y = 300$ MPa), with cross-section W150x22 ($h = b = 152$ mm, $d = 138.6$ mm, $t_w = 5.8$ mm, $t_f = 6.7$ mm) by means of two plates ($b_l = 132$, $t_p = 8$ mm) welded to its flanges from the external sides, Figure 2. On the

basis of standard temperature field and reduction nomogram of the affected area, size of the reduced area, the form and size of the weakened cross-section were determinate.

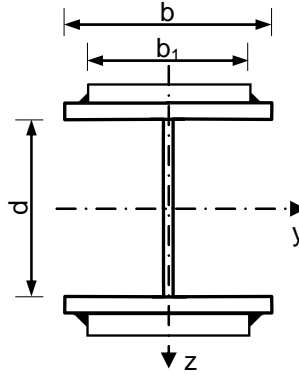


Figure 2. The shape of strengthened cross-section

For results comparing, modelling was realized according to procedures and parameters of accessible experiment. Column with mentioned cross-section and length 2980 mm was two-side hinged and strengthened under effect of centric force $N_{sd} = 440$ kN. Modelled column consist of thirty parts, to be able to insert different types of cross-sections according to strengthening stage, Figure 3.

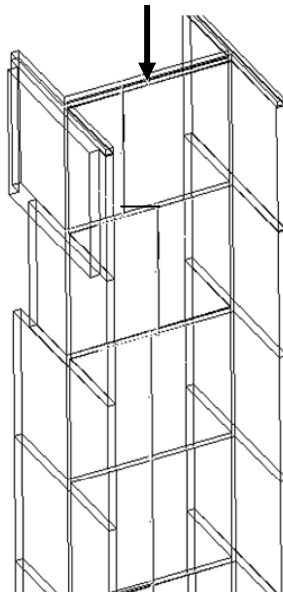


Figure 3. Part of the model: process of defining different cross-sections according to the strengthening stage

The software Feat 2004 was used for the simulation. The main advantage of the software lies in enabling defining cross-sections with shifted centroids together with the possibility of joining them with stiff arms for uniform behaviour of different parts of the column.

4.1. Simulation procedure and calculation

The above mentioned experiment was realized in the following way:

- In the first stage one of the steel plates was welded to the flange of the column along its whole length,
- in the following stage the second plate was welded to the second flange.

In this way, weakening in the first stage on the left side was alternated by weakening on the right side of column’s flange in certain length (approx. 100 mm). In a course of welding, weakening was appearing in different places of original cross-section. Previous weakening of other places is disappeared and the welded part of new plate started to cooperate with the original cross-section, Figure 3.

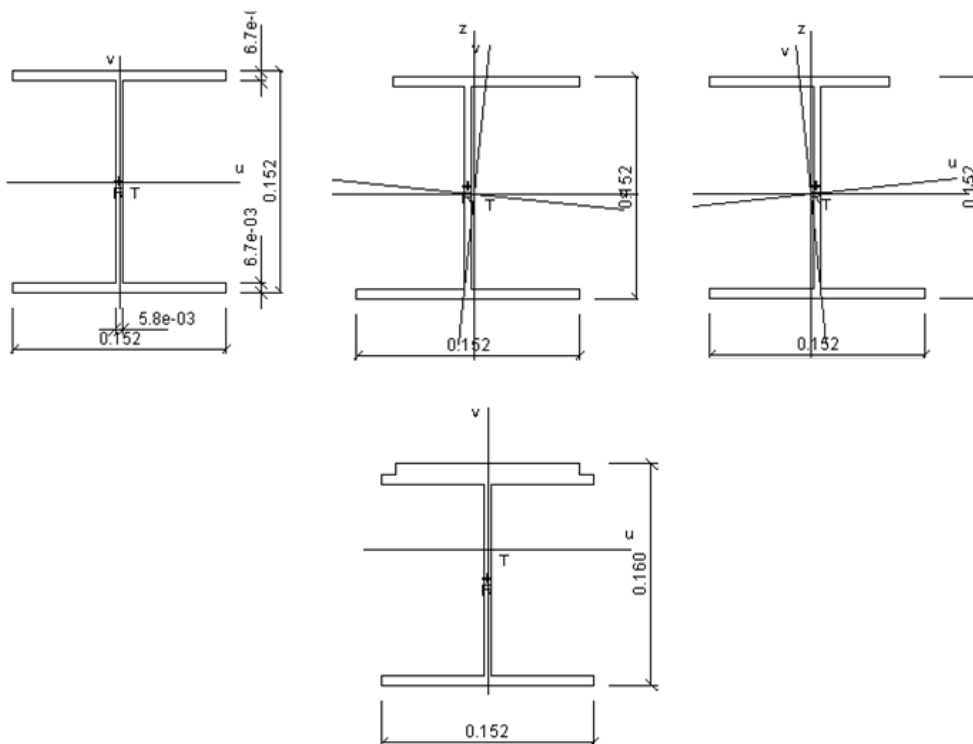


Figure 4. Procedure of defining cross-sections during simulation, sequential welding of the first plate

During simulation of the first stage, four types of cross-sections were defined, according to Figure 4. Calculation was carried out step by step with each change of the cross-sections and deflection's data from the previous step was added to the model. From the above mentioned it is evident that the simulation of first stage required repeating the calculation 60 times.

In the second stage, defining of the cross-sections was simulated analogically. From Figure 4 it is evident, that the column's flange from first stage is already strengthened along the whole length and weakening is alternated along the second flange until strengthening finishing, Figure 5.

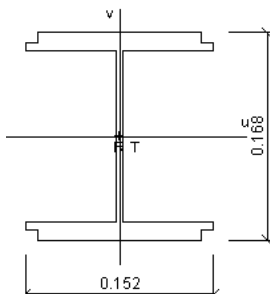


Figure 5. The final shape of strengthened cross-section

The aim was to obtain resulting deformations caused by external load when taking into account the influence of additional arms caused by Shifted centroids of the affected areas. These initial deformations were taken into account at increasing the values of loading in the final stage.

5. RESULTS AND COMPARISON WITH THE EXPERIMENT

After finishing of initial deformations calculation, the column was consecutively overloaded until obtaining the material yield stress ($f_y = 300$ MPa).

The maximum loading of the simulating model was $N_{Sd, max} = 990$ kN and the maximum loading of the experiment $N_{Sd, exp.} = 1100$ kN. The different between results was 10.0 %

6. CONCLUSIONS

- With increasing load the results of the simulating calculation show a lower carrying capacity in average 10 %.
- Higher carrying capacity obtained by the experiment is a result of the interaction between favorable and unfavorable effects of the several imperfections.
- At the strengthening of steel member under loading, three-stage theory has to be considered.

Acknowledgements

Presented paper was supported by Scientific Grant Agency of the Ministry for Education SR and the Slovak Academy of Sciences No. 1/4220/07. The author would like to acknowledge with thanks the financial support.

References

1. Masubuchi, K., *Analysis of welded structures*, PERGAMON PRESS, USA, 1980.
2. Tokuzawa, N., Horikawa, K., Mechanical behaviors of structural members welded under loading, *Transaction of JWRI*, VOL.10, No. 1, Welding Research Institute, Osaka – Japan, 1981.
3. Suzuki, H., Horikawa, K., Experimental study of the reshape of a plate girder under loading, *Transaction of JWRI*, VOL.14, No. 1, Welding Research Institute, Osaka – Japan, 1985.
4. Masubuchi, K., *Joint evaluation and quality control*, PERGAMON PRESS, USA, 1990.
5. HUNERSEN, G., HAENSCH, H., AUGUSTYN, J., Repair welding under load, *Welding in the world*, VOL.28, No. 9/10, P. 174-182, 1990.
6. Marzouk, H., Mohan, S., Strengthening of wide – flange columns under load, *CAN. J. CIV. ENG.*, VOL.17, P. 835-843, 1990.
7. Al Ali, M., The influence of welding process on strengthening of centrally compressed steel members under loading, *PhD. dissertation work*, Košice – Slovak republic, 2005.

Soft computing based approaches for lime-microsilica stabilized clayey soils

M. Moradi¹, A.H. Alavi², M.A. Pashabavandpour², A.H. Gandomi³, A. Askarinejad⁴

¹ Civil Engineering Department, Engineering Faculty, Tehran University, Tehran, Iran

² College of Civil Engineering, Iran University of Science & Technology (IUST), Tehran, Iran

³ College of Civil Engineering, Tafresh University, Tafresh, Iran

⁴ Department of Civil, Environmental and Geomatic Engineering, Swiss Federal Institute of Technology, Zurich, Switzerland

Summary

A range of stabilizers can be added to soil to stabilize it such as Lime, cement, microsilica, or a combination of these in order to improve the engineering properties of soil. Unconfined compressive strength (UCS) as a quality of stabilized soil is generally determined from laboratory tests. For appropriate selection of stabilizers and to avoid the need for the extensive and cumbersome experimental stabilization tests on soils for every new construction situation, it is desirable to develop a mathematical model to be capable of predicting the strength from the properties of natural soil before compaction and stabilization and stabilizer quantities and types. Hence, in the present study, we investigated the application of soft computing techniques namely, multilayer perceptron (MLP) and genetic programming (GP) for the first time in the literature in order to develop the mathematical models to be able to predict the UCS of lime-microsilica stabilized clayey soils from the influencing parameters. Subsequently, a comparison between these methods was performed in terms of prediction performance. The data for developing the models were generated through an experimental study that was conducted to obtain the UCS of some inland clayey soils.

KEYWORDS: stabilized soil; multilayer perceptron; genetic programming; lime; microsilica; unconfined compressive strength.

1. INTRODUCTION

Microsilica is one of the most plentiful waste materials in steel production process. Based on geotechnical engineering literature, the stabilization of soil by using stabilizers such as Lime, cement, microsilica, or a combination of these considerably changes and improves the engineering properties of soils such as UCS, compressibility, durability and permeability [1]. Stabilization can be considered as an alternative approach for road construction, foundation and other

earthwork purposes on the existing unstable soil that often leads to savings in high cost of cutting out and replacing the poor soil with higher quality fill material. Besides the emphasis on other characteristics of stabilized soil, the experts generally agree on compressive strength as the most important outcome of stabilization and as an important structural consideration in construction because of measuring the load-bearing capacity of stabilized materials. UCS of lime-microsilica stabilized soil is influenced by many parameters such as soil type, lime and microsilica contents and types, optimum moisture content, maximum dry density, liquid limit, plastic limit and plasticity index, liquidity index, curing conditions and duration, compaction and environmental conditions of the soil. For effective utilization of stabilizers and to avoid the need for extensive experimental stabilization tests for determination of UCS on every new occasion there is a need to develop a mathematical model relating the gain in strength in terms of the variables responsible. Some work has been done on developing the empirical models in this field [2, 3, 4]. They developed the models to predict the strength of cement stabilized soft ground based on cement content, water content and curing period and also to improve the performance of the models the effects of other parameters were considered. Their empirical models required the reference strength and assumed linear variation of normalized strength with logarithm of the curing period. The necessity to develop different empirical models for different conditions of the same soil, incorporating several assumptions into the models and nonlinearity in strength development that causes the accuracy of strength prediction using linear models to be dissatisfying, are the significant limitations of such empirical models that imply the need to develop the comprehensive mathematical models to be capable of predicting the strength.

Despite many years of stabilization with cementitious materials, there has been only limited research with the specific objective of utilizing computational intelligence techniques. There are also very little attempts on the basis of using the properties of natural soil before compaction and stabilization and stabilizer quantities and types to predict the strength while some more research has been done investigating the alterations in material properties before or after stabilization.

Hence, in the present study, soft computing techniques namely, multilayer perceptron (MLP) and linear genetic programming (LGP) as a particular subset of genetic programming (GP) for the first time in the literature are employed in order to develop the mathematical models to be able to predict the UCS of lime-microsilica stabilized clayey soils from the influencing parameters. At the last section of this paper, a comparison between these methods was performed in terms of prediction performance. The data for developing generic models were generated through an experimental study that was conducted to obtain the UCS of inland clayey soils namely, Hamadan clay (CL), Kermanshah clay (CH) and Tehran clay (CH).

2. EXPERIMENTAL STUDY

The materials used in the investigation and the experiments carried out in order to obtain 202 test results of the UCS of lime-microsilica stabilized clayey soils to develop the prediction models are described in the following subsections.

2.1. Materials used

Stabilizers. To cover a range of stabilizer contents different percentages of industrial lime (0 %, 1 %, 2 %, 3 %, 4, 5 %, 6 %, 7%, and 8 %) with different percentages of microsilica (0 %, 1 %, 2 %, 3 %, 4, 5 %, 6 % and 7%) ,that was obtained from Iran Ferroalloy Industries, were mixed with the soil. The properties of microsilica designated as (MS) is shown in Table 1. In order to analyze the effect of sulphates on the physical properties of the stabilized samples, they were mixed with different percentages of sulphate (gypsum) (0 %, 1 %, 2 %, 3 %, 4, 5 %, 6 % and 7%).

Soils. Three different inland soils are used in order to develop generic models. Hamadan clay (CL) and Kermanshah clay (CL) designated as (HC) and (KC) are obtained from Nam and Kord porcelain factories. Tehran clay which is classified as CL and designated as (TC) is obtained by open excavation from a depth of 1 m from the natural ground from the south lands of Tehran, Iran. The geotechnical properties of clayey soil are shown in Table 2.

Table 1. Properties of microsilica

Chemical composition (%)	MS
SiO ₂	94.04
Al ₂ O ₃	1.32
Fe ₂ O ₃	0.87
CaO	0.49
MgO	0.97
Na ₂ O	0.31
K ₂ O	1.01
SO ₃	0.1
Loss on ignition (LOI)	1.42
Free CaO	0.3
7-day strength activity index with PC (%)	131

Table 2. Geotechnical properties of soils

Properties	HC	KC	TC
Chemical composition (%)			
SIO ₂	62	51.11	55.32
AL ₂ O ₃	25	38.21	15.1
Fe ₂ O ₃	0.56	1.96	7.25
CaO	1.3	0.21	8.11
MgO	0.6	1.65	2.36
Na ₂ O	0.3	2.3	2.1
k ₂ O	0.4	3.54	2.56
Index properties			
Liquid limit (%)	55.3	40	34
Plastic limit (%)	27.02	18.41	26.5
Plasticity index (%)	28.28	22	7.5
Specific weight, G _s	2.62	2.6	2.79
Maximum dry density (kN/m ³)	14.83	15.4	18.05
Optimum moisture content (%)	18.79	23.47	16.5
Classification	CL	CL	CL

2.2. Sample preparation

A series of specimens (50×100 mm, cylindrical) for UCS tests according to ASTM D2166 were cast for each mixture. The specimens were wrapped up with the stretch film after removing from molds and cured for curing period (D) of 7,14 and 28 days at 70% humidity. The ranges of different parameters obtained through the experimental study involved in this study for the model development are given in Table 3. The cited information in Table 3 consists of curing period (D), liquid limit (%LL), plasticity index (%PI), liquidity index (%LI), lime content (%LC), microsilica content (%MC), sulphate content (%SC) and UCS (KPa). It is noteworthy that although optimum moisture content of the mixtures can considerably influence the strength improvement, it is a quality of stabilized soil and can be preferred as an outcome of the stabilization and based on the aims of this study it was decided not to use it as input parameter to the models.

Table 3. The ranges of different input and output parameters

Parameters	Minimum	Maximum	Mean	STD
Liquid limit (%)	28.3	55.3	38.90	7.83
Plasticity index (%)	2	28.28	15.88	6.74
Liquidity index (%)	1.12	2.46	1.87	0.41
UCS (KPa)	12	2850	423.4	548.23
Lime (0 %, 2 %, 3 %, 4 %, 5 %, 6 %, 7 %, 8 %)				
Microsilica (0 %, 1 %, 2 %, 3 %, 4, 5 %, 6 %, 7%)				
Sulphate (0 %, 1 %, 2 %, 3 %, 4, 5 %, 6 %, 7%)				
Curing period (7,14 ,28 days)				

3. SOFT COMPUTING TECHNIQUES

Soft computing as a foundation for the growing field of computational intelligence (CI) [5] includes evolutionary algorithms (EA) [6] and all of their different branches with artificial neural networks and fuzzy logic. Soft computing techniques have wide ranging applications as important tools for approximating the nonlinear relationship between the model inputs and corresponding outputs. In this paper, we aim at employing two of these approaches namely, MLP and LGP in order to develop the prediction models.

3.1. Artificial neural network (ANN)

Artificial neural networks (ANNs) [7] are a branch of computational intelligence that have been applied to many civil engineering tasks such as triaxial compression behavior of sand and gravel [8], stress–strain modelling of soils [9], capacity of driven piles in cohesionless soils [10], settlement of shallow foundations [11], earthquake induced liquefaction [12], and seismic lateral spreading [13]. As a powerful tool for prediction of nonlinearities, they can overcome the considerable limitations of the conventional methods. One of the most widely used ANN models in literature namely, MLP is described briefly in the following subsection.

3.1.1. Multilayer perceptron network (MLP)

MLPs [7] are class of ANN structures using feedforward architecture and usually applied to perform supervised learning tasks, which involve iterative training methods to adjust the connection weights within the network. They are trained with back propagation (BP) algorithm. BP [14] provides a means of adjusting the weights in an MLP, given a set of training data and allows the gradient of the error function to be calculated. MLP networks consist of an input layer, at least one

hidden layer of neurons and an output layer that each of these layers has several processing units and each unit is fully interconnected with weighted connections to units in the subsequent layer. Each layer contains a number of nodes that every input is multiplied by each of them using its interconnection weight. The output (h_j) is obtained by passing the sum of the product through an activation function as follows:

$$h_j = f\left(\sum_i x_i w_{ij}\right) \quad (1)$$

where $f()$ is activation function, x_i is the activation of i^{th} hidden layer node and w_{ij} is the weight of the connection joining the j^{th} neuron in a layer with the i^{th} neuron in the previous layer. For nonlinear problems, the sigmoid functions (Hyperbolic tangent sigmoid or Log-sigmoid) are usually adopted as the activation function. However, MLPs are universal approximators, that is, they are capable of approximating essentially any continuous function to an arbitrary degree of accuracy. Further details of MLPs can be found in [7].

3.2. Genetic programming (GP)

Genetic programming (GP) [15, 16] is one of the approaches of evolutionary methods that creates computer programs to solve a problem using the principle of Darwinian natural selection. GP was introduced by Koza as an extension of the genetic algorithms, in which programs are represented as tree structures and expressed in the functional programming language LISP [15]. A comprehensive description of GP is beyond the scope of this paper and can be found in [15, 16]. GP has been applied to some of the geotechnical engineering problems such as determination of liquefaction induced lateral spreading [17] and analysis of ground movements due to underground mining [18].

3.2.1. Linear genetic programming (LGP)

Linear genetic programming (LGP) [19] is a subset of GP that has been emerged recently. Comparing LGP to the traditional Koza's tree-based GP, there are some main differences such as the graph-based functional structure of linear genetic programs (LGPs), the coexistence of structurally noneffective code with effective code in LGPs and evolvement of these programs in an imperative language (like C/C++) [20] and machine code [21] rather than in expressions of a functional programming language (like LISP). The imperative instructions from these languages operate on registers or constants and assign the result to a destination register.

Automatic Induction of Machine code by Genetic Programming (AIMGP) is a particular form of LGP. AIMGP induces binary machine code directly without any

interpreting steps that results in a significant speedup in execution compared to interpreting GP systems. This LGP approach searches for the computer program and the constants at the same time. The evolved program is a sequence of binary machine instructions [21]. The machine-code-based, LGP uses the following steps to evolve a computer program that predicts the target output from a data file of inputs and outputs [19, 22]:

Step1: Initializing a population of randomly generated programs.

Step2: Running a Tournament. In this step four programs are selected from the population randomly. They are compared and based on fitness two programs are picked as the winners and two as the losers.

Step3: Transforming the winner programs. After that two winner programs are copied and transformed probabilistically as follows:

- Parts of the winner programs are exchanged with each other to create two new programs (crossover); and/or
- Each of the tournament winners are changed randomly to create two new programs (mutation).

Step4: Replacing the loser programs in the tournament with the transformed winner programs. The winners of the tournament remain without change.

Step5: Repeating steps two through four until convergence. A program defines the output of the algorithm that simulates the behavior of the problem to an arbitrary degree of accuracy.

A brief description on basic parameters used to direct the search for the linear genetic program is explained below.

Population size. The numbers of programs in the population that LGP will evolve are set by the population size. A larger population can solve more difficult problems and also can cause a run to take longer.

Crossover rate. Crossover transforms programs in the population and exchanges sequences of instructions between two tournament winners. Two offsprings are the outcomes of this exchange that are inserted in place of the loser programs in the tournament. Crossover occurs between Instruction blocks and it can be either homologous or non-homologous. Reproducing natural evolution is more closely in homologous crossover as a novel approach than traditional crossover.

Mutation rate. Mutation is used to transform programs in the algorithm and random changes of involved parameters in programs from the population that have won a tournament are a result of mutation. It is probabilistically applied to all winner programs. Three different types of mutation in LGP are block mutation, instruction mutation and data mutation.

Reproduction rate. Reproduction is another search operator that is used to copy a program and insert the copy into the population as well as the source program. The reproduction rate is related to the mutation and crossover as follows:

$$\text{Reproduction rate (\%)} = 100 - \text{mutation} - (\text{crossover} * (1 - \text{mutation}))$$

Demes. Based on the EA, the population of individual solutions may be subdivided into multiple subpopulations that migration of individuals among these subpopulations causes evolution to occur in the population. This mechanism was described by biologists as the island model [23]. Demes are semi-isolated subpopulations that in comparison to a single population of equal size, evolution proceeds faster in them. The percentage of individuals allowed to migrate from a deme into another deme during each generation is limited. They are widely used in the field of EA and GP. The number of them is related to the way the population of programs is divided.

4. MODEL DEVELOPMENT

The details of developing the models including the available data and using the intelligence techniques and also the performance of these models are presented in the following subsections.

4.1. Selection of training data

In the present study, curing period (D), liquid limit (%LL), plasticity index (%PI), liquidity index (%LI), lime content (%LC), microsilica content (%MC) and sulphate content (%SC) are selected as seven input parameters for the computational intelligence techniques to predict the UCS (KPa). As explained in Section 2, 202 data sets for development of the models are generated experimentally in laboratory.

The ranges of different input and output parameters involved in this study are summarized in Table 3. Some of the testing data used for comparing the prediction performance of these techniques are illustrated in Table 4. The details of data division for each model are discussed in the following sections.

Table 4. Some of the testing data

D	LL (%)	PI (%)	LI	LC(%)	MC(%)	SC(%)	UCS(KPa)
HC Soil							
7	36.2	11.2	2.2	6	3	0	198
7	36	11	2.2	6	5	0	250

Table 4. (continued)

D	LL (%)	PI (%)	LI	LC(%)	MC(%)	SC(%)	UCS(KPa)
7	35.2	10	2.3	6	0	1	104
7	35	9.8	2.3	6	1	1	135
7	35	9.8	2.3	6	3	1	188
7	34.9	9.9	2.3	6	5	1	330
7	34.9	9.9	2.35	6	0	3	96
7	34.9	9.9	2.35	6	1	3	123
7	34.5	9.6	2.35	6	3	3	200
7	34.5	9.6	2.35	6	5	3	304
7	34	9.2	2.36	6	0	6	105
7	33	16.3	1.74	5	2	0	109
7	34	9.3	2.36	6	1	6	110
28	37.6	14.8	2.17	2	5	1	552
28	37.9	14.9	2.18	2	0	3	191
28	37.4	14.9	2.18	2	1	3	254
28	37.6	15.3	2.19	2	3	3	381
28	36.9	15.1	2.18	2	5	3	410
28	36	14.6	2.19	2	0	6	193
28	36.2	14.8	2.18	2	1	6	235
28	35.8	14.9	2.17	2	3	6	421
28	37.1	14.1	2.16	2	5	6	589
28	37.2	13.6	2.2	4	0	0	102
28	37.3	13	2.19	4	1	0	392
28	37.4	15.2	2.18	4	3	0	942
28	38	15	2.21	4	5	0	1173
28	36.2	14.2	2.24	4	0	1	205
28	36.1	16	2.15	4	1	1	592
KC Soil							
7	32.5	16	1.76	5	2	2	168
7	32.5	16	1.78	5	2	4	150
7	32	15.8	1.79	5	2	7	148
7	35	17	1.66	3	4	0	115
7	36	17	1.67	3	4	2	239
7	35.3	16.8	1.69	3	4	4	192
7	35	16.5	1.7	3	4	7	188
7	36	18	1.6	2	5	0	145
7	35.9	17.6	1.62	2	5	2	261
7	35.8	17.4	1.63	2	5	4	152
28	35.2	19.8	1.65	0	7	2	35
28	35.1	19.2	1.69	0	7	4	38
28	35.6	19	1.7	0	7	7	40
TC Soil							
7	34	7.5	1.13	0	0	0	325
7	32.5	4.1	1.25	4	3	0	472
7	32.8	4.05	1.26	4	5	0	623

Table 4. (continued)

D	LL (%)	PI (%)	LI	LC(%)	MC(%)	SC(%)	UCS(KPa)
28	28.5	3.5	1.52	8	1	0	1432
28	28.9	3.6	1.35	8	3	0	1658
28	29.5	3.8	1.36	8	5	0	1932
14	28.6	3.56	1.62	8	3	0	1923
14	29.8	3.98	1.63	8	5	0	2100
28	28.5	3.5	1.52	8	1	0	1432

4.2. Development of MLP model

The seven soil characteristics and one bias are used for the MLP network model as the input variables while the single output is the UCS. Therefore, the input layer has eight neurons and the output layer has only one neuron. The number of neurons in the hidden layers as an important character in the performance of ANNs can be determined, using trial and error approach [24]. In the current study, the model architecture that gave the best results for the prediction of strength was built with two hidden layer, 12 neurons in the first layer and 11 neurons in the second layer, and a learning rate of 0.01 and the network was trained for 5,000 epochs. Neural network toolbox 5.1 in MATLAB was used to construct and train the MLP networks. For the analysis, the available data sets are randomly divided into training and testing subsets. Of the 202 data, 151 data were used as training and 51 data for testing the generalization capability. In order to evaluate the capabilities of the MLP model, the coefficient of determination (R^2), mean squared error (MSE), and mean absolute error (MAE) are used as the criteria between the actual and predicted values and given in the form of formulas as follows:

$$MAE = \frac{1}{n} \sum_{i=1}^n |h_i - t_i| \tag{2}$$

$$MSE = \frac{\sum_{i=1}^n (h_i - t_i)^2}{n} \tag{3}$$

$$R^2 = 1 - \frac{\sum_{i=1}^n (h_i - t_i)^2}{\sum_{i=1}^n (h_i - \bar{h}_i)^2} \tag{4}$$

where h_i and t_i are respectively the actual output and the calculated output value for the i^{th} output, \bar{h}_i is the average of the actual outputs, and n is the number of sample.

4.3. Development of LGP model

The seven input parameters to the LGP model were used to create models to be able to estimate UCS as the single output variable. The parameter selection will affect the model generalization capability of LGP. For the current study the parameter settings are shown in Table 5.

Table5. Parameter settings for LGP

Parameter	Settings
Number of generation	250,500
Population size	250,500
Maximum program size	256
Initial program size	80
Crossover rate	0.5,0.95
Homologous crossover	0.95
Mutation rate	0.9
Block mutation rate	0.3
Instruction mutation rate	0.3
Data mutation rate	0.4
Function set	+, -, *, /, $\sqrt{\quad}$, log, sin, cos
Number of demes	10

For the LGP modeling, we used the Discipulus software [25] which is based on the AIMGP approach. After completing a project, the Discipulus software in addition to the creation of single programs, combines these single programs into team programs [26] to produce better results and writes these programs in Java, C, or Intel assembler code automatically and the resulting code may be compiled into a DLL or COM object and called from the optimization routines [25]. For the analysis, the data sets are randomly divided into training, validation and testing subsets. Training data are used for learning. The validation data are used to specify the generalization capability of the evolved programs on data they did not train on. In other words, the training and validation data sets are used to select the best evolved programs. The testing data are used to measure the performance of program evolved by LGP. Out of the available data, 100 data are selected for training, 51 data for validation and 51 data for testing the generalization capability. Similar to the MLPs, the criteria for LGP model evaluation are R2, MSE and MAE.

5. RESULTS AND DISCUSSIONS

As mentioned previously, R^2 , MSE and MAE are selected as the target statistical parameters to evaluate the performance of the models using the available database. For the chosen MLP model, Figure 1 represents the predicted and the actual UCS values for training and testing data sets. The results of predicted UCS values using the best single and the best team solution that have been found by LGP, using different combination of parameters, for training and testing with their corresponding values of R^2 are illustrated in Figures 2 and 3, respectively. It can be seen that the best performance is obtained by the MLP model for both of the training ($R^2=0.9527$, MSE = 0.31%, MAE = 1.48%) and testing data ($R^2=0.8933$, MSE = 1.1%, MAE = 7.48%) followed by the best team solution and the best single solution that have been found by LGP. For the best team program the R^2 value for testing data is 0.8719 while those of the best single program is 0.8536. As can be observed in these figures, all the models have performed acceptable in predicting the UCS values.

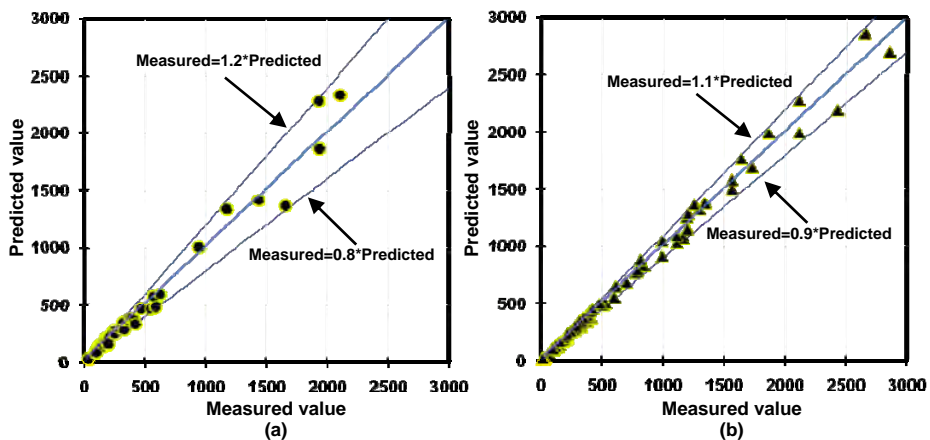


Figure 1. Results of MLP model (a) Training data (b) Testing data

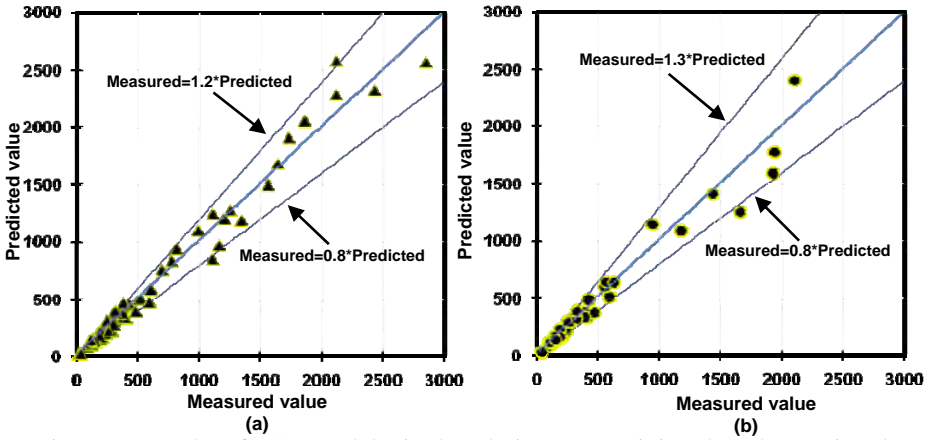


Figure 2. Results of LGP model (single solution) (a) Training data (b) Testing data

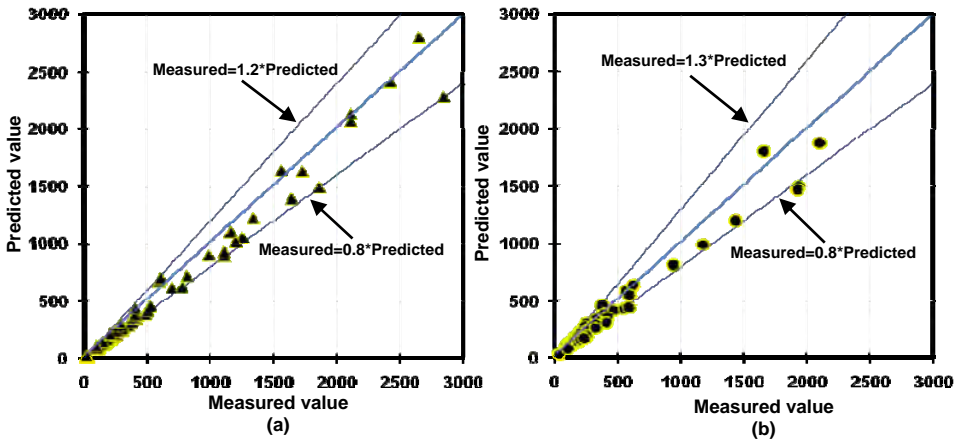


Figure 3. Results of LGP model (team solution) (a) Training data (b) Testing data

The results for all element test data can be seen in Figure 4. Performance statistics of these models in terms of their prediction capabilities are summarized in Table 6. Validation data sets results of the predicted UCS using LGP models are also included in this table. Concerning the values of performance indices for training and testing data, presented in Table 6, specifies that MLP outperforms both types of the LGPs. From this table, it also can be seen that the best team program solution created by LGP has produced slightly better results in comparison with the best single solution. It is noteworthy that although MLP has better performance than LGP, LGPs are white-box models that often provide elucidatory solutions, which are in Java, C, or Intel assembler code.

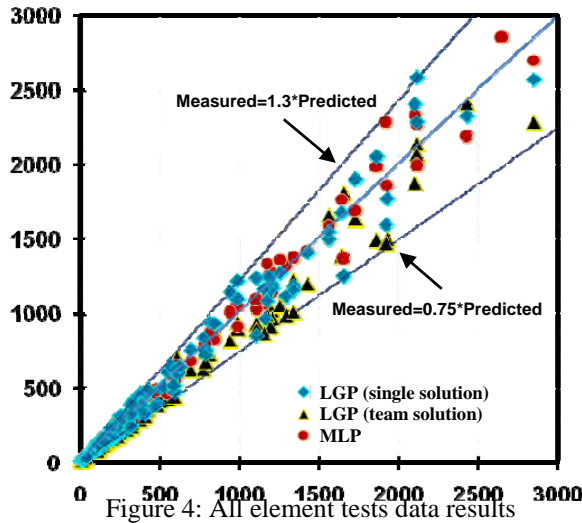


Figure 4: All element tests data results

Table 6. Performance statistics of models

Models	Training			Validation			Testing		
	R ²	MSE (%)	MAE (%)	R ²	MSE (%)	MAE (%)	R ²	MSE (%)	MAE (%)
MLP	0.9527	0.31	1.48	—	—	—	0.8933	1.1	7.48
LGP (Single solution)	0.8854	2.52	11.96	0.8612	3.45	15.3	0.8536	2.91	16.78
LGP (Team solution)	0.9122	1.71	8.13	0.869	4.05	13.42	0.8719	2.03	10.43

6. CONCLUSIONS

In the present study, two branches of computational intelligence techniques namely, multilayer perceptron (MLP) and linear genetic programming (LGP), are employed to simulate the behavior of the strength improvement in lime-microsilica stabilization process. Due to a need to avoid extensive and cumbersome experimental stabilization tests on soils on every new occasion, it was decided to develop mathematical models to be able to estimate the UCS as a quality of stabilized soil after both compaction and curing by using liquid limit, plasticity index, liquidity index as the properties of natural soil before compaction and stabilization and quantities and types of stabilizer. Data for training, validation and testing the prediction models were generated through an experimental study that was conducted to obtain the UCS of inland clayey soils. Based on the values of

performance measures for the models, presented in Table 6, it can be observed that all models are able to predict the UCS value to an acceptable degree of accuracy. The results demonstrate that the optimum MLP model with the values of R2, MSE and MAE equal to 0.8933, 1.1% and 7.48%, respectively, outperforms both the best single and the best team program that have been created by LGP. It can also be concluded that the best team program evolved by LGP ($R^2 = 0.8719$) has slightly better performance than the best single evolved program ($R^2 = 0.8536$). It can be concluded from this investigation that LGP is averagely able to reach a prediction performance similar to MLP model. Moreover, LGP as a white-box model provides the programs of an imperative language or machine language that can be inspected, and evaluated to provide a better understanding of the underlying relationship between the different interrelated input and output data.

References

1. McKennon, J.T., Hains, N. L., Hoffman, D.C, Methods for producing enhanced soil stabilization reactions between lime and clay soils due to the effect of silica addition, U.S. patents documents, patent number: 5,336,022, 1994.
2. Tan, T.S., Goh, T.L. and Yong, K.Y., Properties of singapore marine clays improved by cement mixing, *Geotech Testing J ASTM*, Vol. 25, 422–433, 2002.
3. Narendra, B.S., Sivapullaiah, P.V., Suresh, S. and Omkar, S.N., Prediction of unconfined compressive strength of soft grounds using computational intelligence techniques: A comparative study”, *Comput Geotech*, Vol. 33, 196–208, 2006.
4. Horpibulsuk, S., Analysis and assessment of engineering behavior of cement stabilised clays, PhD Thesis, Saga University, Japan, 2001.
5. Schwefel, H.-P., Wegener, I., and Weinert, K. (eds.), *Advances in Computational Intelligence – Theory and Practice*, Springer-Verlag, Berlin, 2002.
6. Bäck, T., *Evolutionary Algorithms in Theory and Practice: Evolution Strategies, Evolutionary Programming, Genetic Algorithm*, Oxford University Press, ISBN: 0195099710, 1996.
7. Haykins, S., *Neural networks – A comprehensive foundation* (2nd ed.), Prentice Hall International Inc., Englewood Cliffs (NJ), 1999.
8. Dayakar, P. and Rongda, Z., Triaxial compression behavior of sand and gravel using artificial neural networks (ANN), *Comput Geotech*, Vol. 24, 207–230, 1999.
9. Ellis, G.W., Yao, C., Zhao, R. and Penumadu, D., Stress strain modelling of sands using artificial neural networks, *J Geotech Eng ASCE*, Vol. 121, 429–435, 1995.
10. Abu Kiefa, M.A., General regression neural networks for driven piles in cohesionless soils, *J Geotech Geoenviron Eng ASCE*, Vol. 124, 1177–1185, 1998.
11. Shahin, M.A., Maier, H.R. and Jaksa, M.B., Predicting settlement of shallow foundations using neural networks, *J Geotech Geoenviron Eng ASCE*, Vol 128, 785–793, 2002.
12. Young-Su K, Byung-Tak K, Use of artificial neural networks in the prediction of liquefaction resistance of sands, *J Geotech Geoenviron Eng ASCE*;132(11):1502–1504, 2006.
13. Baziar, MH., Ghorbani, A., Evaluation of lateral spreading using artificial neural networks, *J Soil Dyn Earthquake Eng*;25:1–9, 2005.
14. Rumelhart, D. E., Hinton, G. E., and Williams, R. J., Learning internal representations by error propagation, In *Parallel Distributed Processing*, volume 1, chapter 8, pages 318–362. MIT Press, Cambridge, MA, 1986.
15. Koza, J.R., *Genetic programming: On the programming of computers by means of natural selection*, MIT Press, Cambridge (MA) ,1992.

16. Banzhaf, W., Nordin, P., Keller, R. & Francone, F., Genetic Programming – An Introduction. On the Automatic Evolution of Computer Programs and its Application, dpunkt/Morgan Kaufmann, Heidelberg/San Francisco, 1998.
17. Javadi, A.A., Rezani, M., Mousavi Nezhad, M., Evaluation of liquefaction induced lateral displacements using genetic programming . Comput Geotech, Vol. 33, pp. 222–233, 2006.
18. Lia, W., Daib, L., Houa, X., Leia, W. , Fuzzy genetic programming method for analysis of ground movements due to underground mining , Technical note ,International Journal of Rock Mechanics & Mining Sciences, Vol. 44 ,954–961, 2007.
19. Brameier, M., Banzhaf, W., Linear Genetic Programming, Springer Science + Business Media, LLC, 2007.
20. Brameier, M., Kantschik, W., Dittrich, P. & Banzhaf, W., SYSGP – A C++ library of different GP variants, Technical Report CI-98/48, Collaborative Research Center 531, University of Dortmund, Germany, 1998.
21. Nordin, P.J., A compiling genetic programming system that directly manipulates the machine code (Chapter 14), In Kenneth E. Kinnear, Jr., editor, Advances in Genetic Programming, MIT Press, pp. 311–331, 1994.
22. Deschaine, L.M., Tackling real-world environmental challenges with linear genetic programming, PCAI magazine, Vol.15, number 5, 35-37, 2000.
23. Wright, S., Isolation by Distance. Genetics, vol. 28, pp. 114–138, 1943.
24. Eberhart, R.C., Dobbins, R.W., Neural Network PC Tools: A Practical Guide. Academic, San Diego, 1990.
25. Francone, F., Discipulus Lite™ Owner’s Manual, Version 4.0, Register Machine Learning Technologies, 2004.
26. Brameier, M. & Banzhaf, W., Evolving teams of predictors with linear genetic programming. Genetic Programming and Evolvable Machines, 2(4), pp. 381–407, 2001.

People Presence Stochastic Model for Building Energy Simulations

Roman Musil¹

¹*Department of Environmental and Building Services Engineering, Czech Technical University in Prague, 166 29, Czech Republic, corresponding email: roman.musil@fsv.cvut.cz*

Summary

Currently are for object energy need calculation used dynamic simulation where given problem is formulated by set of input variables and their each other connected structures. Some input values aren't possible to describe only by one value or by one load profile. Those are random character magnitudes which depend on one variable – time. These magnitudes are called stochastic process and are linked with user activity and behaviour in the interior. This simulation input values are currently described like static (constant) loads profiles during the time but in the most cases it isn't true.

The main aim of this paper is to create universal probability model of presence user in interior. This model will serve for people behaviour influence assessment on total yearly energy need. Next aim is to create this model like base for next continues in more demanding stochastic process modeling.

KEYWORDS: people behaviour modeling, stochastic process, building energy simulations

1. INTRODUCTION

Stochastic process modeling doesn't belong to standard discipline of building energy simulations. What exactly stochastic process is? Stochastic process is possible to define like set of random magnitudes which depend on one variable – time. In other words it are activities where we can't to determine some magnitude process during the time step in advance. These magnitudes are in building energy simulations called loads profiles and are described like static profiles. This description is somewhat inaccurate because it claims that e.g. people presence profile in one year will be the same in next years. On analogical principle are described another loads profiles too. The main stochastic processes in building energy simulations are:

- person presence profile in the interior
- hot and cold water consumption profiles
- using lightings and electric appliances profiles
- natural ventilation profile
- pollutant production profile (heat gain, CO₂ production,...)

- heat and cooling system control profile – users interventions into system
- climatic dates

From previous list of main stochastic processes is evident dependence the most processes on people presence in interior. From this reason I started my work with creation of person presence in interior model.

Static person presence profiles are used in actual models which calculate building energy need. It is from 8 – 18:00 with one hour lunch break and two 15 minutes break during the work time for offices. All profiles are static – 100% presence during the work time and 0% from 18:15 to 7:45 and during lunch break. On the other side real people behaviour in interior is variable during the day. Main aim of this paper is to describe algorithm function which will generate user presence profiles in typical interior. User profile influences, especially at models with more numerous user representation, building energy need. Approximation user presence profile to more real behavior can help improve energy calculation results and simultaneously the profile serves like first stage for modeling next energy loads which depend on people presence.

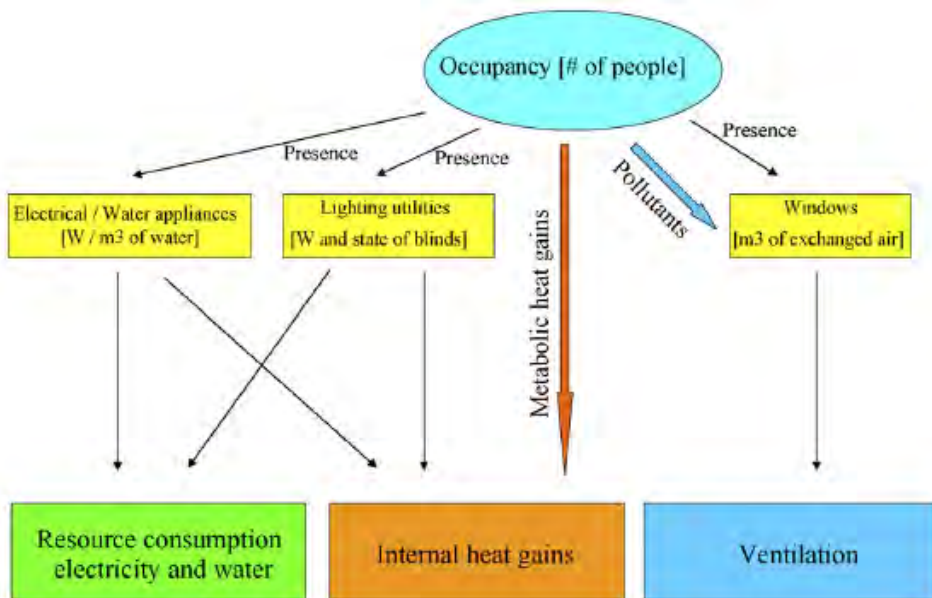


Figure 1. Schema of energy consumption in building effected by people presence

2. METHODS

2.1. Model inputs data

Inputs data for model are from monitoring single office during one year. Measured data was obtained during study stay at university TU Delft – Netherlands. People presence data was measured like by-product at adjudicates usage natural lighting of office spaces during the day. Measure equipment was given by firm the Watt Stopper. Resulting input presence profile is built from several dates files from several decade measured offices in various time intervals. Always work days and weekend days were respected and they are separated in model. Intervals are in quarter time-step and every day has 96 intervals. Model is universal, it is possible to generate profiles for different building types on the base of measured values. In measured dates was observed absence divided to the two categories – short term (less than 24 hour interval) and long term (bigger than 24 hour interval) where vacation and sickness days are calculated. Model within frame of long term absence generates 30 vacation days and 5 sickness days yearly. There are observed first arrivals and last departures in the office. Between first arrival and last departure is realized so-called short term absence. In sort-term absence interval we calculate for every quarter interval total time where is person present or absent at workplace and bigger value from this two values determines the interval state. We have two states in this profile 1 – present 0 – absent. In interval except short term absence is state 0.

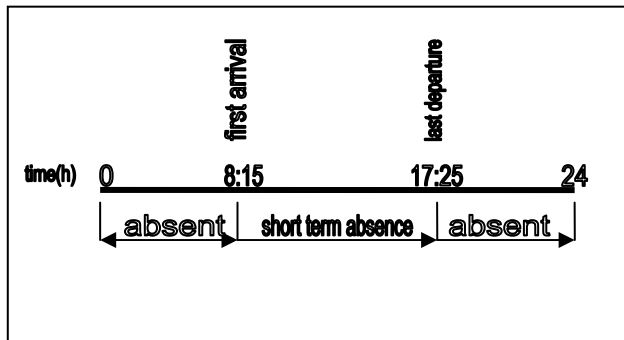


Figure 2. Graphic display of one day

Measured data it is necessary to replace by model with fit probability distribution for given data type. By help probability functions we need to describe these values:

- long term absence (vacation, sickness day)
- first arrival and last departure
- change in presence state (from 1 to 0 or from 0 to 1)

2.2. Mathematical input dates description

On base of processed dates it is possible to continue with mathematical description, I will describe probability functions creation on case of first arrival into the office for week days. Another variables description is similar. We get histogram of first arrivals from all year date processing.

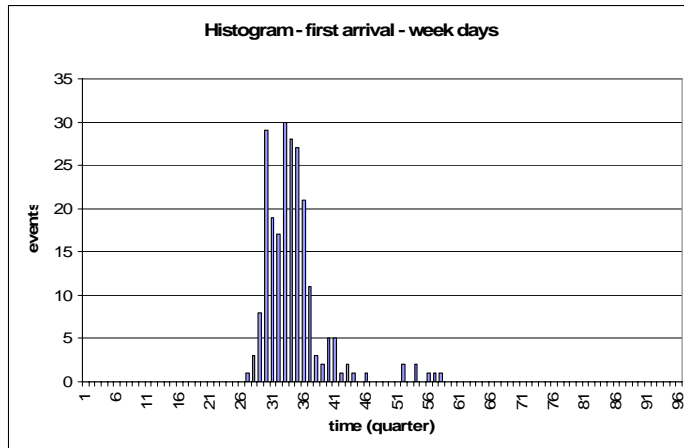


Figure 3. Histogram of first arrivals into the office – measured data

Now it is possible to find function which will describe this processed data. The most fitting is Poisson distribution from obtainable statistical model which describes measured data.

2.2.1. Poisson distribution

Poisson distribution is marked like scarce event distribution but it is driven event frequency which has very small occurrence probability on condition that:

- event can come in whatsoever time and number of this event occurrence depends only on the time interval length
- if λ is event average value in certain time then this value has distribution $Po(t*\lambda)$

Poisson probability distribution function is defined by relation (PPDF):

$$F(x) = P(X = x) = \frac{\lambda^x}{x!} e^{-\lambda}$$

This function shows probability that randomly chosen magnitude X will be equal x.

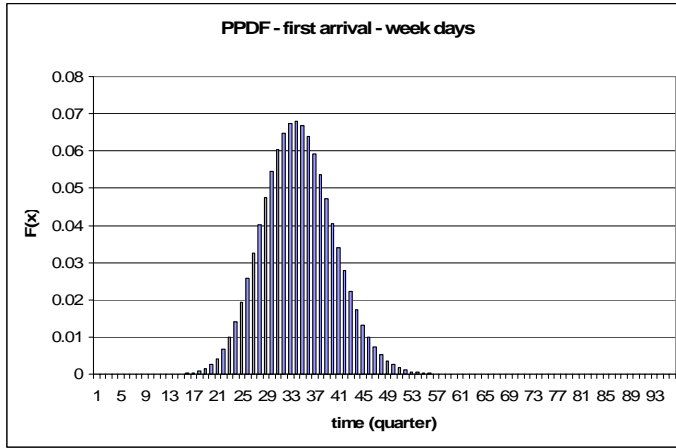


Figure 4. Poisson probability distribution function – measured data

Poisson cumulative distribution function (PCDF):

The word “cumulative” implies procedure PCDF creation, which is adding of probabilities function. PCDF is defined like:

$$F(x) = P(X \leq x)$$

$$F(x) \geq 0$$

This function shows probability that randomly chosen value X will not be bigger than x.

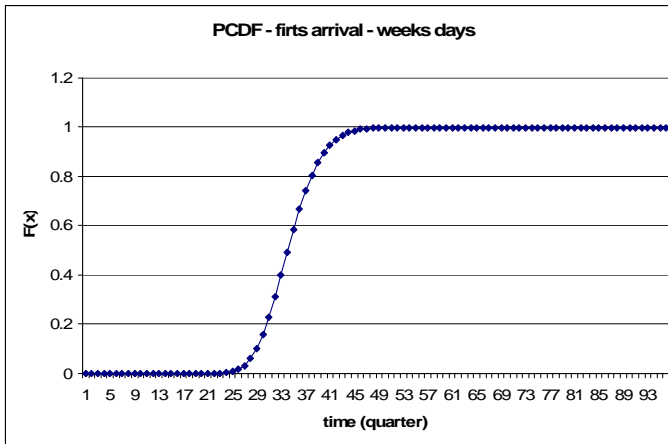


Figure 5. Poisson cumulative distribution function – measured data

2.2.2. Good agreement test

It is necessary to use good agreement test which compare given measured data deviation with theoretical deviation for preferably more precise replacing all measured values by probability distribution. We will formulate zero hypothesis H_0 “measured data has Poisson distribution (eventually another distribution)” and alternative hypothesis H_1 ”measured data don’t have Poisson distribution (eventually another distribution)“ If next equation is valid so zero hypothesis will be confirmed and tested distribution will be able for our data:

$$\chi^2 = \sum_{i=1}^l \frac{(n_i - np_i)^2}{np_i} < \chi_{1-\alpha}^2(df)$$

np_i – expected probability distribution frequencies

n_i – real frequencies

χ^2 – we will compare the value of magnitude χ^2 with critical values relevant chí distribution on required surface of significant. Test is possible to use on condition that all values np_i has frequency minimally 5 elements.

2.3. Random values in model generation

Modeling of stochastic process is specific by unpredictable variable events during the time. It isn’t possible accurately predict future state by modeling people presence in interior from reason of input random number. Random number is possible to model from relatively outmoded random number table over physical generator next to pseudo-random numbers. Real random numbers are given only from physical generators which are linked with some random process (throw cube, roulette, shuffle cards, etc.) and it is written. Obtaining random numbers by this way is relatively demandingness from reason of these complications and so pseudorandom numbers was developed. Pseudorandom numbers aren’t real random numbers, but they are generated by help algorithm which expressively influences quality of this numbers. I used Matlab random number in model of people presence. Events will be chosen by help generated random number which will occur during solved time-step interval. This selection will be done by help of method which uses inverse transformation. If required random magnitude has distribution function $F(x)$ and if we have continuous uniform distribution generator U on interval $(0,1)$, it is possible to get random number X with required distribution from this equation:

$$X = F^{-1}(U)$$

Necessary assumption for existing function F^{-1} is growing function $F(x)$.

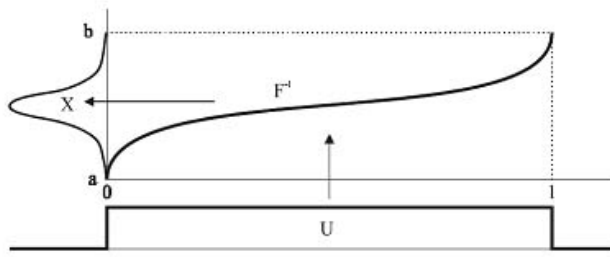


Figure 6. Number generation according to inverse function method

In our case is inverse function equal cumulative distribution function relevant events which perform growing inverse function.

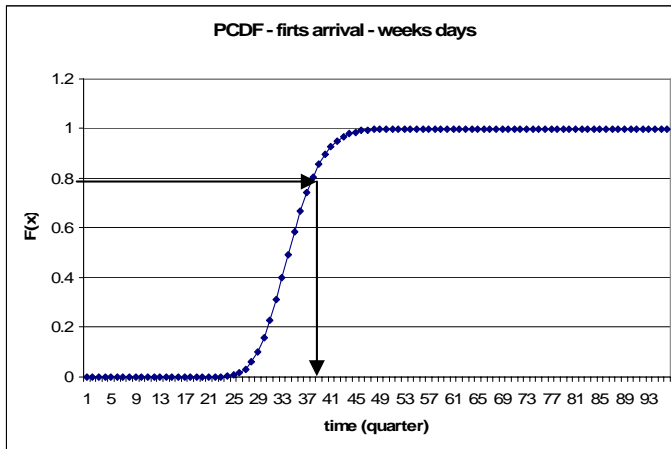


Figure 7. First arrival by help random and cumulative distribution function generation

Inverse function method is base element of model. First arrivals, last departures, date and length long term absence, short term absence change are generated using inverse function method.

4. ALGORITHM REALIZATION

User presence probability model in one office room is processed like set of each other scripts in Matlab program. Model works on base of pseudo-random numbers, probability distribution function and empiric probability functions. Algorithm connects computational Matlab core with excel file from where data are taken for

own calculation and there is place for saving profile results. Excel provides easy access to results and their processing.

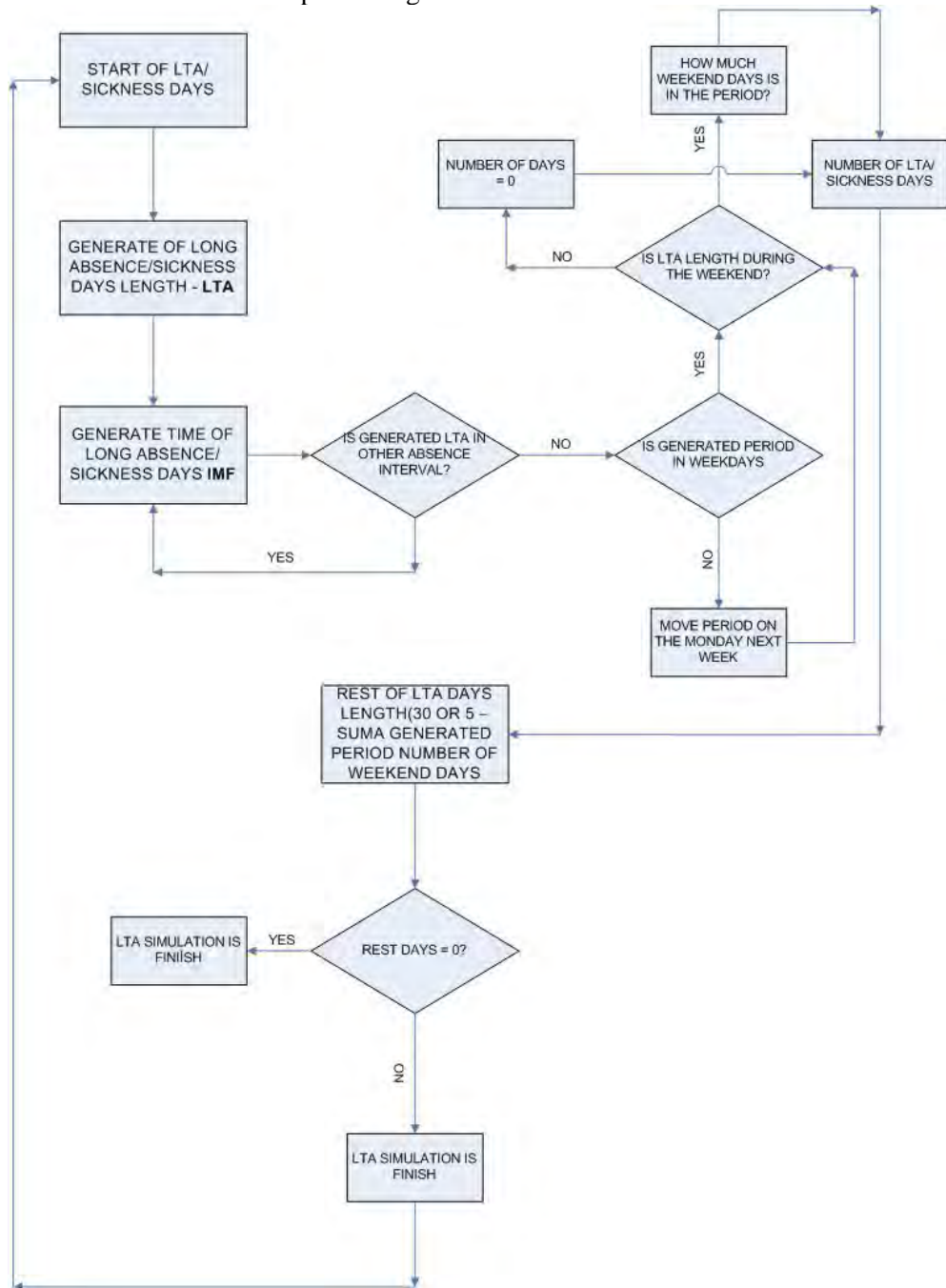


Figure 8. Long Term Absence (LTA) Generation

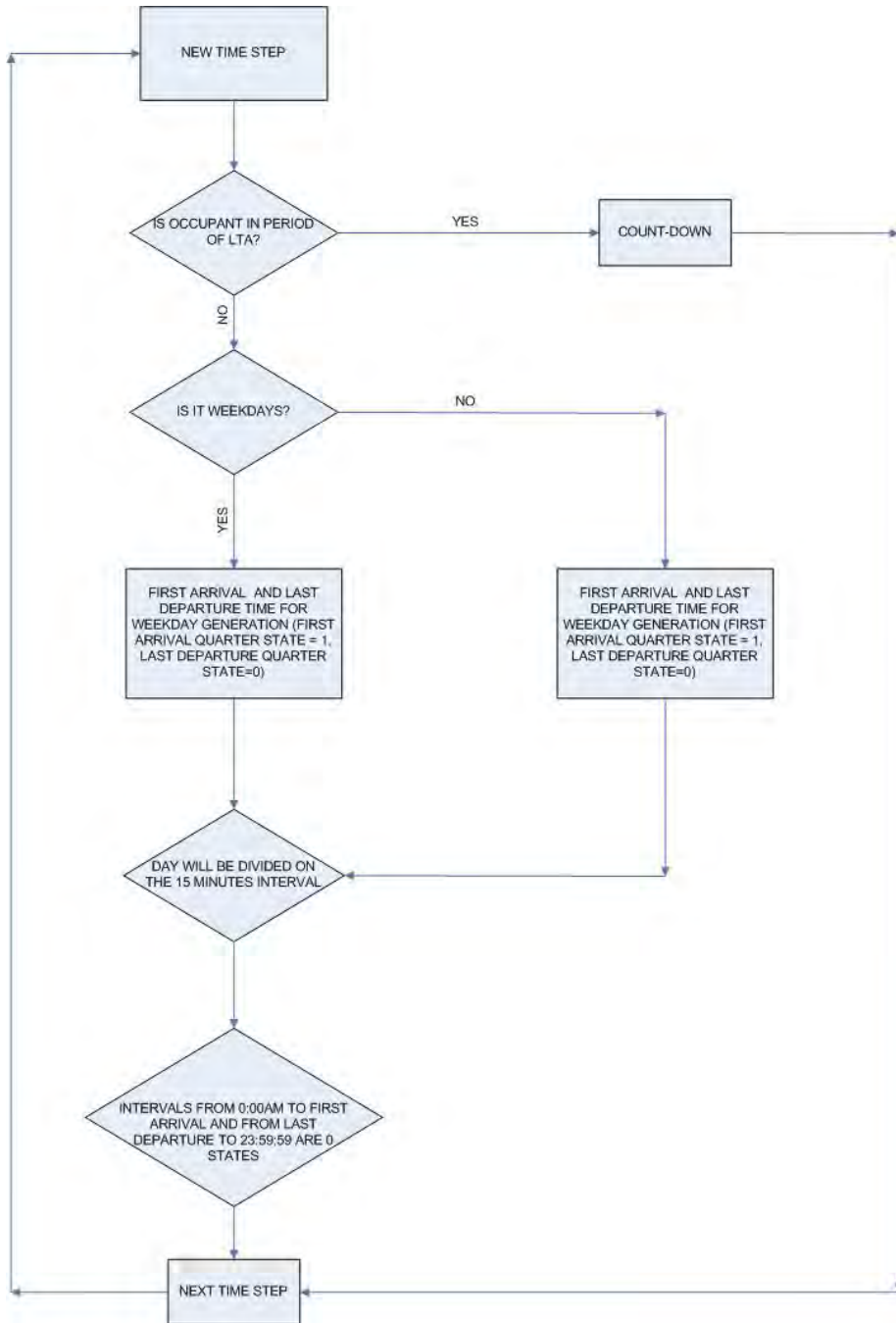


Figure 9. First Arrival (FA) and Last Departure (LD) Algorithm Generation

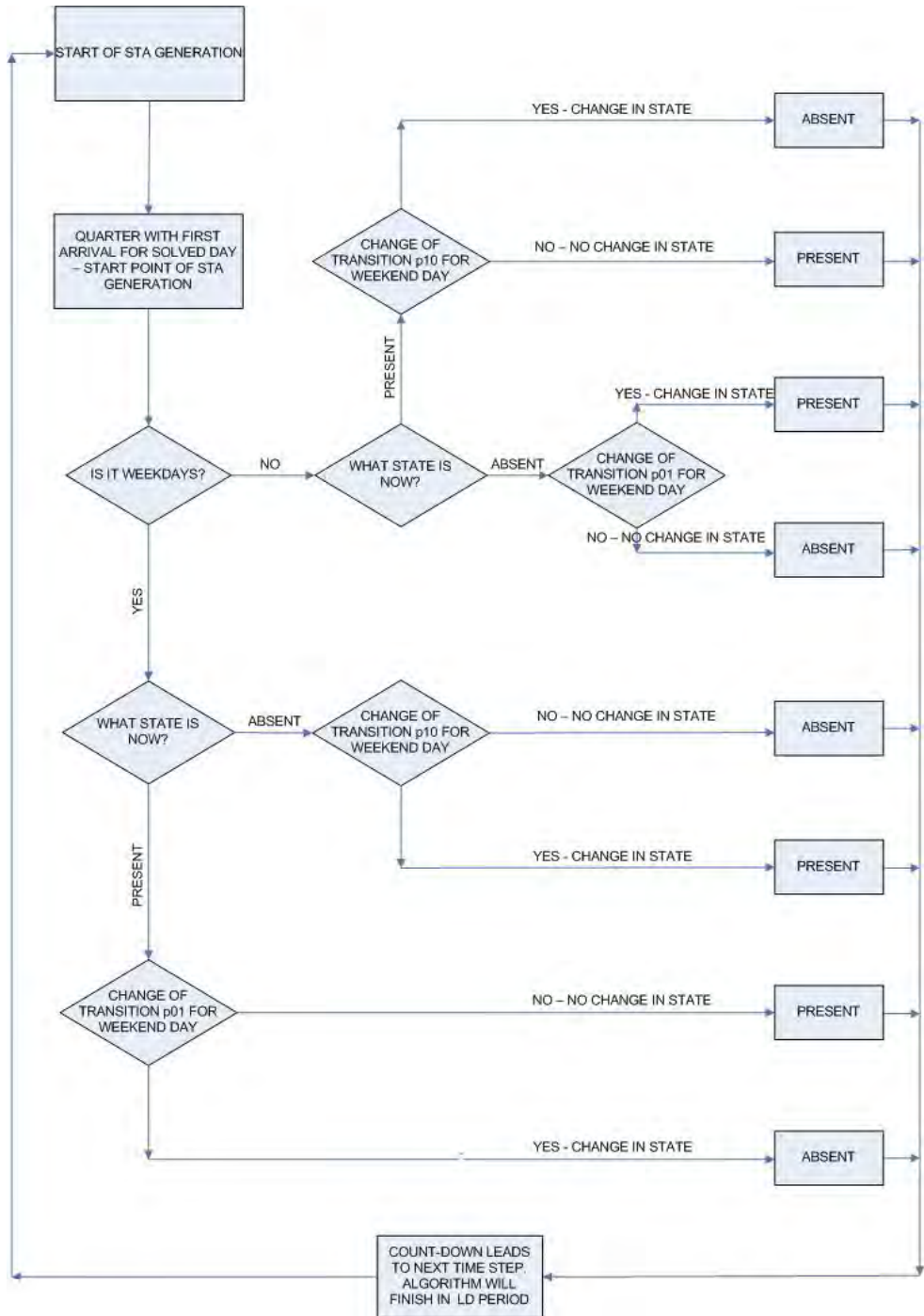


Figure 10. Short Term Absence (STA) and Presence Algorithm Generation

5. VALIDATION

Algorithm validation verifies total yearly presence sum with confrontation first arrival and last departure dates. 50 profiles was generated from algorithm for validation needs and it is possible to see average underestimate total yearly presence about 0,7% compared to source dates from results. It is regarding to great numbers of generated values vary good result and we don't continue with model improvement.

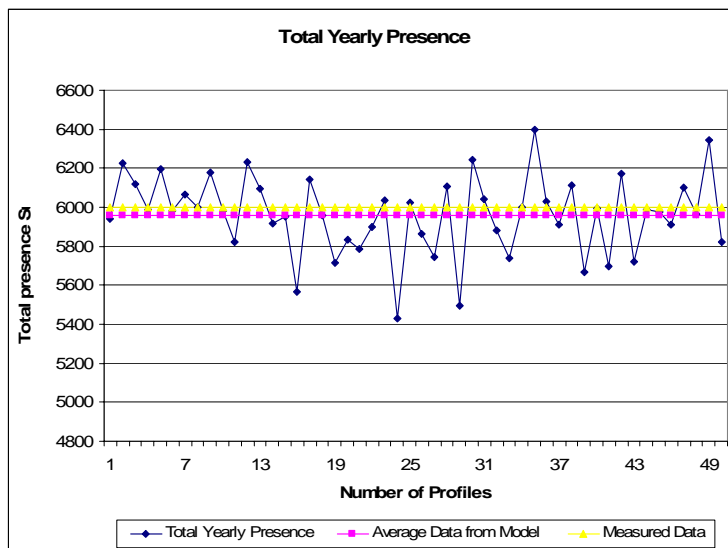


Figure 11. Total Yearly Presence Validation

6. CONCLUSIONS

Model was created like universal which will generate user profile presence for one person after input presence of typical building and its processing. If we have more than one person in the interior then the algorithm will calculate so often how many times people is in the interior and total result will sum. Primary algorithm aim is to create input user profiles for energy simulations where by multiple simulations dispersion and improvement total yearly energy need in dependence on human factor user presence in typical building type will be determined. Next aim was creation this model like base for next continues in more demanding stochastic process modeling like hot water consumption, ventilation, lightings operation, heating a cooling systems user operation etc. How it was mentioned stochastic

process are from big measure depended on random number during the time which we cannot influence and isn't possible these processes describe by constant profiles from this reason.

Acknowledgements

Paper was created with support of investigative intention CEZ MSM 6840770003. Very big thank to prof. Kees van der Linden and Ericu van den Ham for possibility cooperation at university TU Delft and their counsel during creation probability model presence.

References

1. Page J., Robinson D., Morel N., Scartezzini J.-L. 2007. A Generalised Stochastic Model for the Simulation of Occupant Presence. Switzerland: LESO-PB, Ba'timent LE, Station 18, E'cole Polytechnique Fe'derale de Lausanne, CH-1015 Lausanne
2. Jarůšková D. 1986. Probability and Mathematical Statistic. Czech republic: CTU Prague
3. Measured presence data 2007. Netherlands: TU Delft, Faculty of Technology, Department of Architecture
4. Gušnar M. 2000, Czech republic: Random Values Generation in Monte Carlo Method, In: Proceedings I. Year Nation Conference: Reliability Construction 2000, pp 5-8
5. program Matlab, CTU Prague License

People Behaviour Influence for Total Yearly Energy need in one Person Office Room

Roman Musil¹

¹*Department of Environmental and Building Services Engineering, Czech Technical University in
Prague, 166 29, Czech Republic*

Summary

This paper deals about practical application probability model of presence user into energy simulations. User presence probability model in one office room is processed like set of Matlab scripts. Model works on base empiric probability functions and pseudo-random numbers. It will ensure non-repetitive one generated profile from each other like it is in real life. By help the multiple simulations in energy simulation tool will be determined energy need dispersion in dependence on user human factor presence (and other direct activities depending on user presence) in office and these simulations will be compared with currently used static profile for office facilities.

KEYWORDS: people behaviour modeling, stochastic process, building energy simulations

1. INTRODUCTION

This paper comes out from previous paper “People Presence Stochastic Model for Building Energy Simulations“. In previous paper are specified basic stochastic processes in energy building modelling and next possibilities for current stochastic models extension. This paper deals about practical connection stochastic probability model with energy simulation for obtaining people presence influence on building energy need.

2. ENERGY SIMULATION

Energy simulation was created by connection three parts: generated profile presence model, TRNBuildu where are described individual model parts (engineering construction and boundary condition) and TRNSYS program which calculate own energy simulation. Structural model for next energy simulations is single office space oriented to the outdoor space with two windows on the southern side.

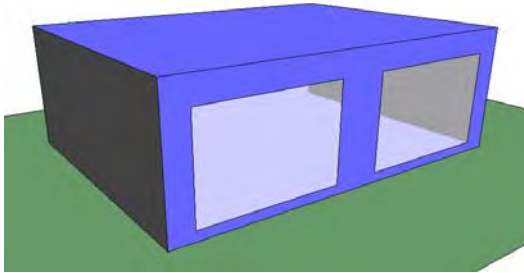


Figure 1. Schema of one persone office model

Table 1. Information about model boundary conditions

<i>dimension and orientation</i>		
office area	8x6x2,7	m
windows area	12	m ²
wall orientation with windows	south	
<i>boundary condition</i>		
climatic database	CZ-Prague - TM2	
outside temperature	from database	
ground temperature	5	°C
indoor temperature in winter	20	°C
indoor temperature in summer	27	°C
multiplicity exchange air	0,5	hour ⁻¹
<i>engineering construction</i>		
<i>wall construction</i>	thickness (m)	Conductivity - U (W/m ² K)
plasterboard	0,1	5,1
thermal insulation	0,0615	0,651
wood siding	0,009	15,556
<i>roof</i>		
plasterboard	0,01	16
thermal insulation	0,1118	0,358
Roof deck	0,019	7,368
<i>floor</i>		
concrete slab	0,08	14,125
thermal insulation	1,007	0,04
<i>windows</i>		
glass-U = 2,8W/m ² K, g = 0,755, 15% from area is frame-U = 2,27W/m ² K		

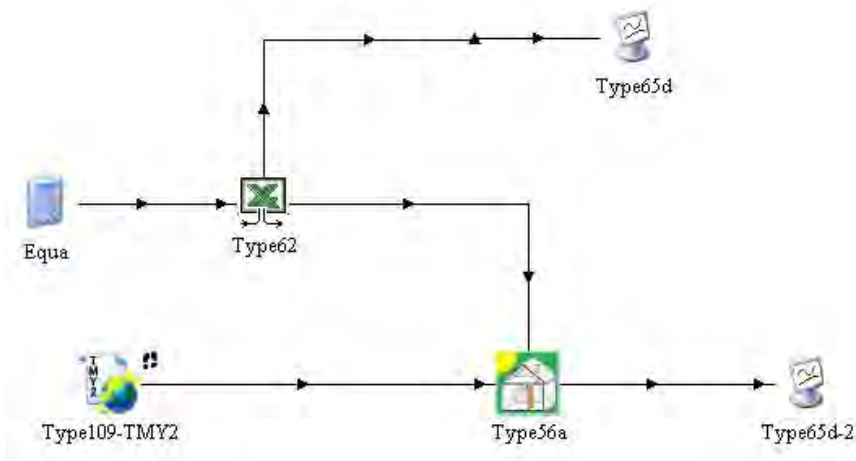


Figure 2. TRNSYS model connecting TRNbuild and excel file with profile presence model

DISCUSSION

Graphs No. 3 and 4 show summary separated outputs of energy simulation from TRNSYS and represent dispersion heat and cold need in dependence on one user in interior presence profile. One human heat production is taken according to specification ISO7730 for sitting lightly working man – office activity 150W. Average heat need for heating office room 1173 ± 6 kWh and for cooling 306 ± 2 kWh is from graphs results. It is heat need 1187kWh and cooling need 298kWh at model office place without present man in interior during whole year. On the other side at people presence modeling with respect actual legislation it means presence from 8:00 to 18:00 including two 15 minutes breaks is yearly heat need 1152kWh and cooling need 318kWh.

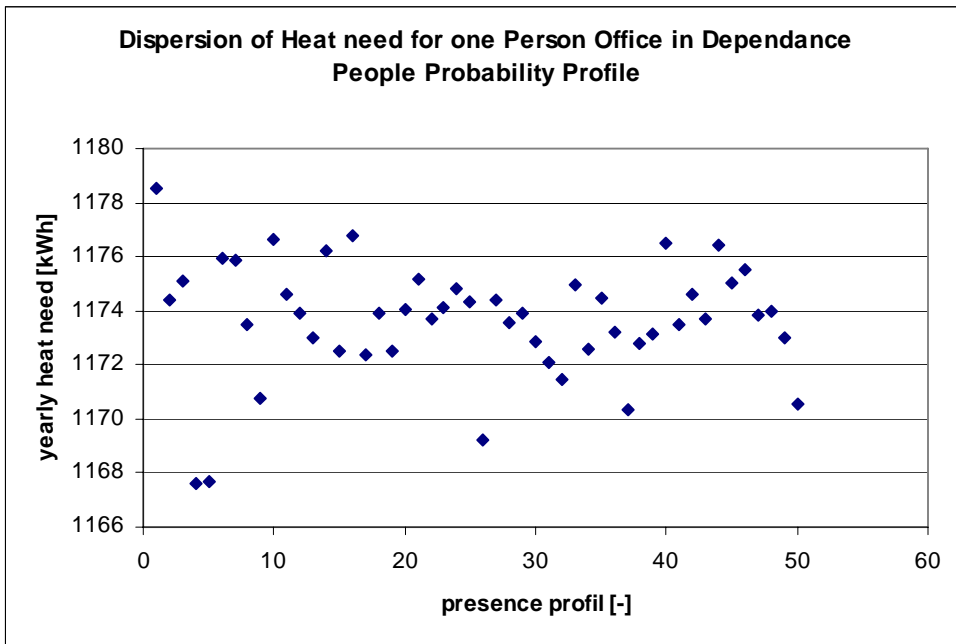


Figure 3. Yearly heat need in dependence on interior occupancy

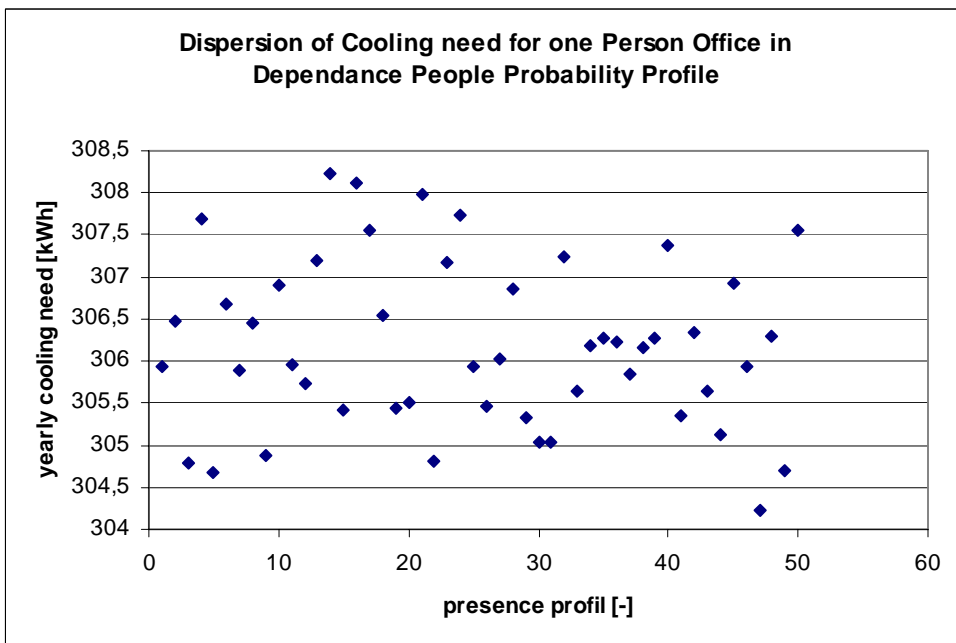


Figure 4. Yearly cooling need in dependence on interior occupancy

CONCLUSIONS

1% dispersion outcome results for yearly heating need and 0,5% for yearly cooling need is evident from energy simulations people activity influence on the total heat need. That all influence only pure people presence in actual model and it isn't take into account influence of people activity on using electric appliance, lighting, ventilation, heating and cooling systems control etc. At comparison average heat and cooling need at using profile generated by model and current static profile is deviation for heating 1,8% and for cooling 3,8%. It isn't fundamental difference but more precisely presence has significant influence for next stages people activity.

Acknowledgement

Paper was created with support of investigative intention CEZ MSM 6840770003.

Very big thank to prof. Keesovi van der Lindenovi and Ericu van den Hamovi for possibility cooperation at university TU Delft and their counsel during creation probability model presence.

References

Measured presence data 2007. Netherlands: TU Delft, Faculty of Technology, Department of Architecture
program Matlab, CTU Prague
program TRNSYS, CTU Prague

Seismic analysis using Robot Millennium

Mihai Nedelcu

Department of Structural Mechanics, Technical University of Cluj-Napoca, 400020, Romania

Summary

The paper presents the modelling and structural analysis of a complex structure under seismic loads using the Robot Millennium software package. In order to test the output results, the author chose a building already designed in the documentation [1].

The above mentioned documentation was created as a guideline for applying the design standard P100-1/2006. Following the given structure architecture and loads, the author of this paper remodelled the structure using Robot Millennium v.20.1.

The objective of the paper is to show:

- 1. the Robot Millennium instruments used for modelling this type of structures*
- 2. various modelling ways for the same structure highlighting the most convenient one (in the author's opinion)*
- 3. the results accuracy of the analysis in comparison with the output given by the work of Professor Tudor Postelnicu*

KEYWORDS: seismic analysis, modal analysis, stories, rigid links, panel cut, reinforced concrete walls.

1. INTRODUCTION

The chosen building is fully described in the 3rd example of a very professional and useful documentation: "P100-1/ Building seismic design, volume 2-B. Comments and calculus examples", responsible author: Tudor Postelnicu, Ph.D., Prof., U.T.C.B. For the seismic analysis, the authors of the above mentioned documentation used the lateral force method and 3D linear-elastic computation generated by means of the ETABS program. The author of this paper wanted to see if the Robot Millennium software package could be a good alternative in this kind of structures analysis.

The analyzed building is located in Bucharest and has:

- 3 underground levels (h=3m) + ground floor (h=6m) and 10 stories (h=3m)
- 5 longitudinal spans x 8m and 5 transversal spans 2x7+1x4+2x7m

The structural characteristics:

- R.C. walls (both uncoupled and coupled by spandrel walls), columns and beams
- concrete class C25/30
- steel PC52
- $a_g=0.24g$, $T_c=1.6\text{sec}$, ductility class H, importance coefficient $\gamma_1=1.2$

A current floor plan is shown in Figure 1.

2. MODELLING PRESENTATION

For the seismic analysis, the structure is considered fixed at the ground floor base. Using Robot Millennium v.20.1, the author modeled the structure using bars for columns/beams and panels for slabs/ R.C. walls (see Figure 2). Of course after the mesh generation (even with large finite elements) the great number of equations (of order 10^5) led to a significant slowing down of the analysis. As a good alternative the Rigid Links additional attribute can be used instead of panels for the slabs modeling. By introducing the Membrane rigid link, the user can connect the nodes of each floor according to any DOF, in this case the X,Y displacements and the RZ rotation. And so the slab effect as a rigid body is fully covered. At the same time the beams have to be modeled as T-section, taking into account the corresponding slab rigidity. A slab width of 3xhp (the slab thickness) was taken on each side for the interior beams and of 2xhp on each side for the marginal beams. Having no slab finite elements reduces considerably the analysis time with absolutely no damage to the results. The model is presented in Figure 3.

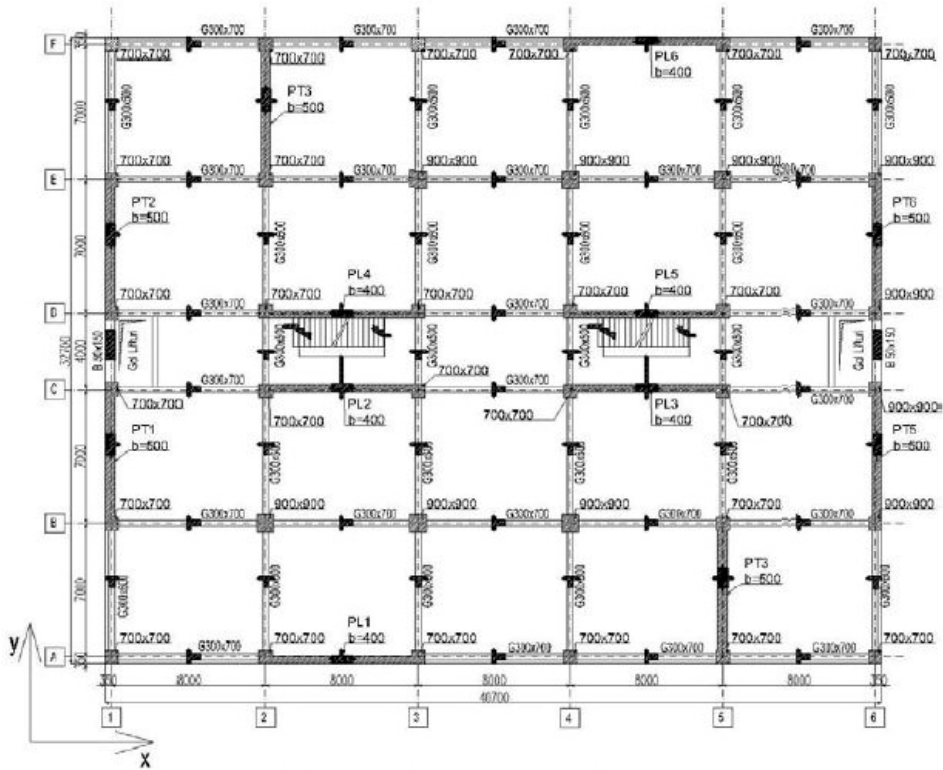


Figure 1. The building current floor plan

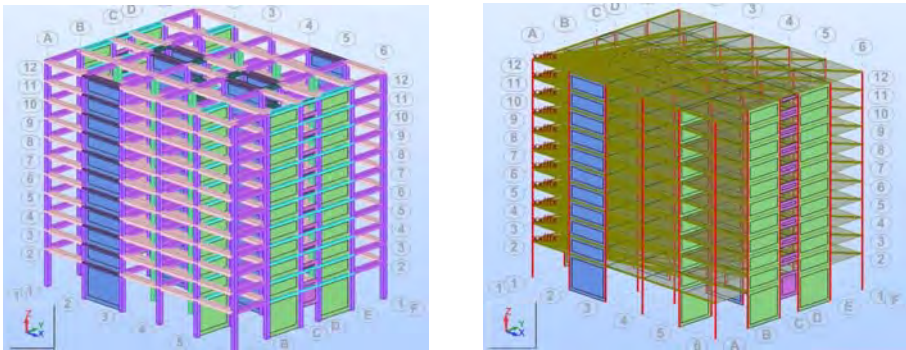


Figure 2. The structure model showing: a) section shapes, b) rigid links

Following the instructions of P100-2006, the rigidity of the elements is taken differently, depending on the type of analysis. First, the goal is to make the modal analysis, in which the rigidity of walls, columns and beams is taken $EI=0.5E_cI_c$. As for the spandrel walls, their Young modulus is $E_{\text{spandrel}}=0.4 \cdot E_{\text{walls}}$ and the other

sectional characteristics: $A=0.2A_c$, $I=0.2I_c$. Reducing the rigidity of the elements, the elements are considered in a plastic stage and so the building behavior during an earthquake is well approximated according to P100-2006. To achieve that the user can define a new material with a modified Young modulus, in this case named C25/30_0.5 (*Job Preferences/Materials/Modification*). The characteristics of a longitudinal wall are set as presented in Figure 3. As for the spandrel walls the double reduction is achieved by multiplying the thickness of 50cm with the 0.2 factor.

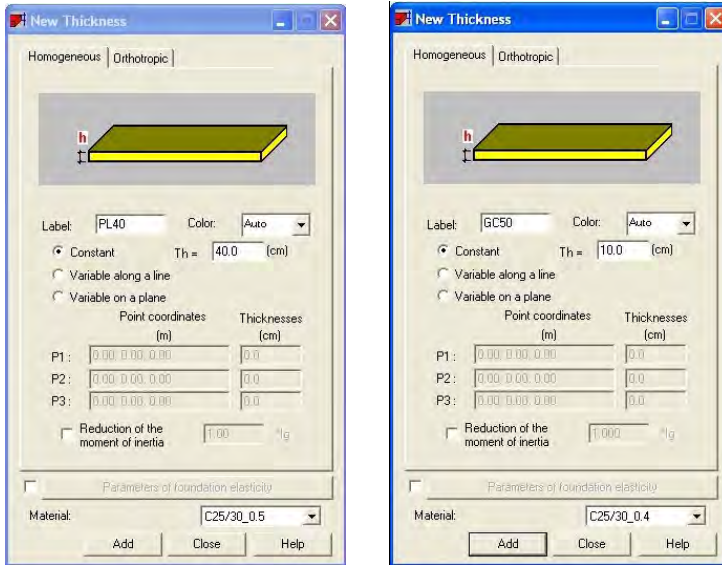


Figure 3. Defining the section properties of: a) longitudinal walls, b) spandrel walls

As for the bar elements, there is an alternative. The program allows the reduction of moment of inertia according to local axes x, y, z (see Figure 4).

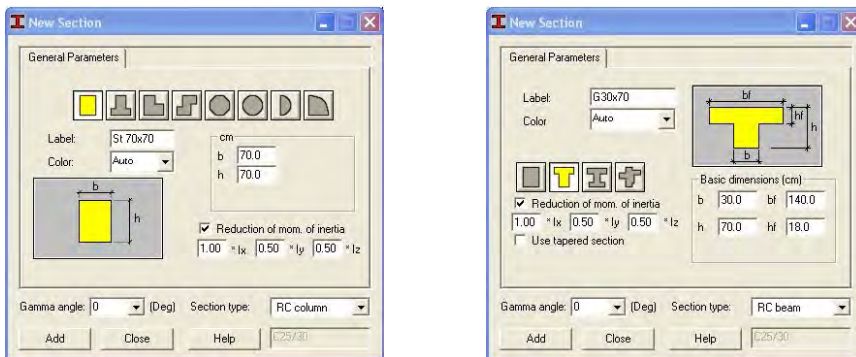


Figure 4. Defining the properties of: a) columns 70x70cm, b) beams 30x70cm

Another problem in the modal analysis is the modeling of the additional eccentricities: $\pm 5\%$ in each direction. The code explains in detail how their effect has to be taken into account. The level seismic forces, computed by hand or by some user defined computer program have to be applied to the resistance elements depending on their rigidity. Because there are 2 main directions, for each one 2 signs and the mass eccentricities can also be positive or negative, there are 8 combinations to be made. This work is time consuming and the probability of user errors is highly increased. A good alternative seems to be the *Modal Analysis Parameters/Definition of mass eccentricities* that the program offers (see Figure 5). The sign of eccentricity can be changed but is impossible to have both signs in the same model. So, different models have to be made. Of course, if the structure is somehow symmetrical, the work is much reduced.

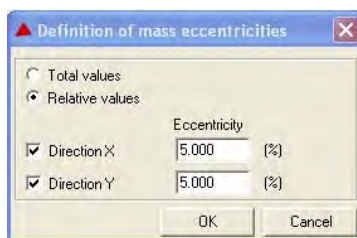


Figure 5. Introducing the additional mass eccentricities

In the 3rd example the loads are generally given. Because of this “generality” the results of this paper are not identical to the original ones, but the differences are acceptable. Given the loads, the load to mass conversion is made automatically. The size of FE-s should be set as big as possible, since from the modal analysis point of view the mesh refinement will not change the results. Doing that the modal analysis was made in a few seconds. The results are compared to the original ones (see Figures 6 and 7). Also the shape of the eigenvectors for the first 3 modes is shown in XY view (see Figure 8). The additional eccentricities effect for the first two modes can be seen.

Mode	Frequency (Hz)	Period (sec)	Rel.mas.UX (%)	Rel.mas.UY (%)	Cur.mas.UX (%)	Cur.mas.UY (%)
1	1.369	0.731	70.757	0.230	70.757	0.230
2	1.552	0.644	71.106	71.161	0.349	70.931
3	2.042	0.490	71.517	73.206	0.412	2.046
4	5.900	0.170	88.945	74.492	17.428	1.285
5	6.115	0.164	90.565	90.305	1.620	15.814
6	7.973	0.125	90.829	90.825	0.264	0.520
7	12.562	0.080	93.355	93.294	2.526	2.469
8	13.144	0.076	95.783	95.461	2.428	2.168
9	13.179	0.076	95.798	95.497	0.015	0.036

Figure 6. The Robot Millennium modal analysis results

Mod propriu	T_k (sec)	directie X m_k	directie Y m_k	directie R_z m_k	cumulat X Σm_k	cumulat Y Σm_k	cumulat R_z Σm_k
1	0.728	73.53	0.04	0.00	73.53	0.04	0.00
2	0.650	0.04	75.01	0.00	73.57	75.05	0.00
3	0.517	0.00	0.00	74.98	73.57	75.05	74.98
4	0.172	19.17	0.03	0.00	92.73	75.08	74.98
5	0.168	0.03	17.62	0.00	92.76	92.71	74.98
6	0.134	0.00	0.00	17.75	92.76	92.71	92.73
7	0.078	0.01	5.03	0.00	92.77	97.73	92.73
8	0.078	5.05	0.01	0.00	97.82	97.74	92.73
9	0.063	0.00	0.00	5.05	97.82	97.74	97.78

Figure 7. The original modal analysis results

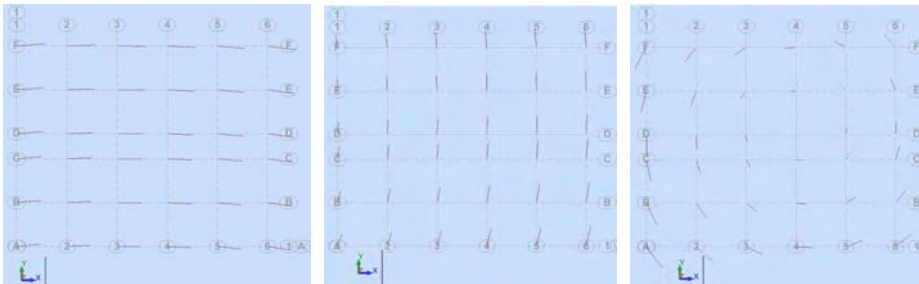


Figure 8. The shape of the eigenvectors for the first 3 modes in XY view

The next step is to define the seismic analysis (see Figure 9). The behavior factor (q) has different values according direction X and Y. For the ductility class H, on X-longitudinal direction, the walls are considered as cantilevers ($q = 4\alpha_u / \alpha_1$) while on Y-transversal direction, the walls are coupled, and so results a higher q ($q = 4\alpha_u / \alpha_1$).

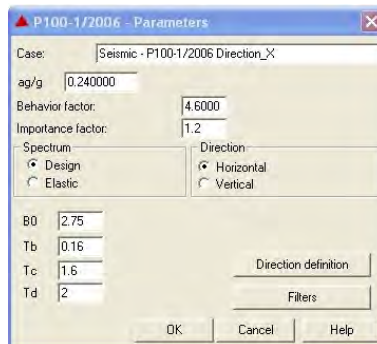


Figure 9. Introducing the seismic analysis parameters

Since the seismic analysis is concerned, only the special load combinations are introduced. To assess the deformations, no changes are made to the FE mesh or to the sectional rigidities. The allowed displacements are given by P100-2006 in relation to the elastic drift.

The program offers another useful tool by allowing the user to define the stories of the building: *Geometry/Code Parameters/Stories*. The elements of each storey are presented in a different color in the Figure 10. The walls are not colored because of the large FE mesh.

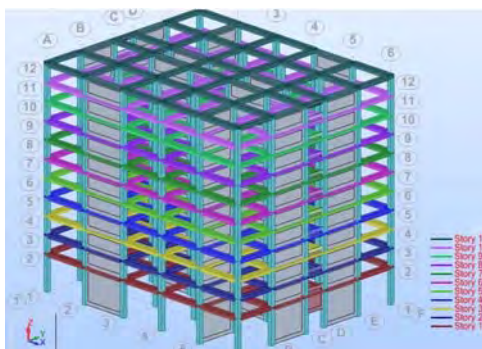


Figure 10. The stories display

The characteristics of each storey can be seen by the *Story Table/Values* option. In the Figure 11, are presented the mass, the gravity and torsion centers, eccentricity e_0 and the applied additional eccentricities e_2 .

Itame	Mass (kg)	G (x,y,z) (m)	T (x,y,z) (m)	Ix (kgm ²)	Iy (kgm ²)	Iz (kgm ²)	ex0 (m)	ey0 (m)	ex2 (m)	ey2 (m)
Story 1	589008.071	20.00 16.00 5.6	20.00 16.00 5.6	48458578.237	137822167.335	185487768.660	0.0	0.00	2.00	1.60
Story 2	481217.949	20.00 16.00 9.0	20.00 16.00 9.0	44481317.600	94352002.734	136747026.140	0.0	0.00	2.00	1.60
Story 3	481217.949	20.00 16.00 12.0	20.00 16.00 12.0	44483548.229	94354233.363	136747026.140	0.0	0.00	2.00	1.60
Story 4	481217.949	20.00 16.00 15.0	20.00 16.00 15.0	44485778.858	94356463.992	136747026.140	0.00	0.00	2.00	1.60
Story 5	481217.949	20.00 16.00 18.0	20.00 16.00 18.0	44488009.488	94358694.622	136747026.140	0.0	0.00	2.00	1.60
Story 6	481217.949	20.00 16.00 21.0	20.00 16.00 21.0	44490240.117	94360925.251	136747026.140	0.0	0.00	2.00	1.60
Story 7	481217.949	20.00 16.00 24.0	20.00 16.00 24.0	44492470.746	94363155.880	136747026.140	0.0	0.00	2.00	1.60
Story 8	481217.949	20.00 16.00 27.0	20.00 16.00 27.0	44494701.375	94365386.509	136747026.140	0.0	0.00	2.00	1.60
Story 9	481217.949	20.00 16.00 30.0	20.00 16.00 30.0	44496932.005	94367617.139	136747026.140	0.0	0.00	2.00	1.60
Story 10	481217.949	20.00 16.00 33.0	20.00 16.00 33.0	44499162.634	94369847.768	136747026.140	0.00	0.00	2.00	1.60
Story 11	433533.572	20.00 16.00 35.0	20.00 16.00 35.0	42832327.656	75262000.722	118019847.868	0.0	0.00	2.00	1.60

Figure 11. Story Table: Values

Using *Story Table/Displacements* option, the stories maximum absolute and relative displacements ($d_{r,c}$) can be seen (Figure 12).

	MAX UX (cm)	Node	MAX UY (cm)	Node	dr UX (cm)	dr UY (cm)	MIN UX (cm)	Node	MIN UY (cm)	Node
Case 7	seismX									
Story 1	0.3073	563	0.0279	563	0.2436	0.0594	0.0637	1206	-0.0315	580
Story 2	0.5406	627	0.0464	627	0.1864	0.0965	0.3543	579	-0.0521	644
Story 3	0.8121	691	0.0670	691	0.2295	0.1420	0.5826	619	-0.0750	708
Story 4	1.1158	755	0.0890	755	0.2664	0.1886	0.8494	683	-0.0997	772
Story 5	1.4414	819	0.1117	819	0.2986	0.2368	1.1428	747	-0.1251	836
Story 6	1.7808	883	0.1345	883	0.3257	0.2650	1.4551	811	-0.1505	900
Story 7	2.1265	947	0.1568	947	0.3478	0.3323	1.7786	875	-0.1755	964
Story 8	2.4725	1011	0.1781	1011	0.3655	0.3776	2.1070	939	-0.1995	1028
Story 9	2.8125	1075	0.1983	1075	0.3785	0.4204	2.4340	1003	-0.2221	1092
Story 10	3.1507	1139	0.2171	1139	0.3929	0.4604	2.7577	1091	-0.2433	1147
Story 11	3.4344	10	0.2288	393	0.3672	0.4854	3.0671	1131	-0.2566	12

Figure 11. Story Table: Values

And so the elastic and inelastic drift can be computed. Table 1 is showing a comparison between the results of this paper and the original ones for X direction.

Table 1. Name of the table

Level	Robot Millennium			Example 3	
	dreX (cm)	driftSLS <0.005	driftULS <0.025	driftSLS <0.005	driftULS <0.025
GF	0.1470	0.0009	0.0042	0.0009	0.0040
E1	0.1309	0.0016	0.0075	0.0015	0.0070
E2	0.1590	0.0020	0.0091	0.0018	0.0084
E3	0.1801	0.0022	0.0103	0.0020	0.0095
E4	0.1948	0.0024	0.0111	0.0022	0.0102
E5	0.2041	0.0025	0.0116	0.0023	0.0105
E6	0.2086	0.0026	0.0119	0.0023	0.0107
E7	0.2090	0.0026	0.0119	0.0023	0.0106
E8	0.2063	0.0025	0.0118	0.0022	0.0104
E9	0.2018	0.0025	0.0115	0.0022	0.0102
E10	0.1940	0.0024	0.0111	0.0021	0.0098

The next step is to calculate the internal forces. The elements rigidities are to be changed. For walls and bar elements CR 2-1-1.1 gives $EI = E_c I_c$ and for the spandrel walls $EI = 0.4(E_c I_c)$. As the building flexibility is decreasing, the internal forces will be calculated on the hypothesis of the uncracked sections and so they are higher than the most probable ones. The FE mesh of the walls was now refined up to a 50cm size. Further refinement gave no substantial modification of the results. Of course the challenge is to find the internal forces concerning the walls and the spandrel walls. For this reason the program has the option *Reduced Results for Panels*. With the sign convention from Figure 12 the user can choose the section (the cut) where moments, shear forces and stresses will be displayed (see Figure 13).

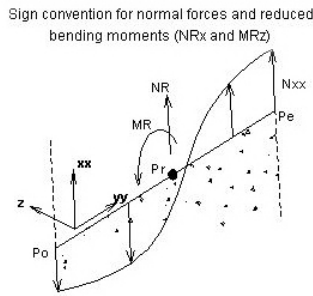


Figure 12. Sign convention

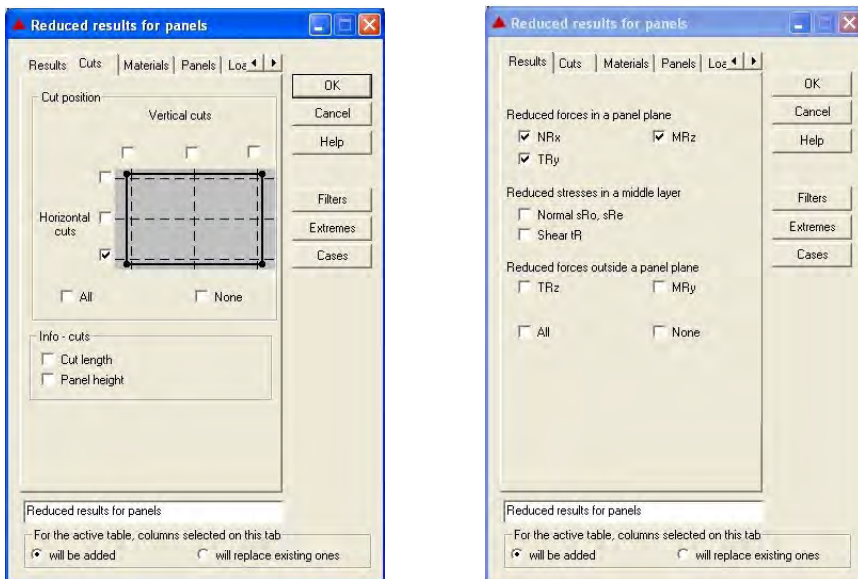


Figure 13. Choosing a) the cut position, b) the reduced forces to be displayed

There are two possibilities for modeling the wall columns. Until now they were modeled as bars. In this case, for a RC wall the internal forces of both wall and wall columns must be combined in order to have the result for the entire wall section. A second possibility is to eliminate the wall columns and to use an equivalent wall section from the primary moment of inertia point of view. The building stiffness will slightly decrease due to the lack of compression/tension absorbed by the wall columns. Comparison of the 2 modeling methods with the original results is given for a longitudinal wall (Table 2). The forces are calculated at the ground floor level from one seismic combination on X direction. The difference between the axial forces has to come from the lack of knowledge in the

loads distribution over each storey since the evaluation of the building total weight was checked and almost perfect similarity was achieved.

Table 2. Final internal forces for a longitudinal wall

Wall PL1	N (kN)	M (kNm)	T (kN)
Wall	-7741.22	-32648.3	2986.15
Wall column 1	-2760.13	-178.81	324
Wall column 2	5175.29	-251.61	389
Final forces	-10156.4	64389.96	3699.15
Wall without columns	-9939.21	-63955.5	3468.02
Example 3	-11456	65463	3778

3. CONCLUSIONS

The Robot Millennium software package gives us a reliable and elegant alternative for seismic analysis. Its features fully cover the demands of P100-2006. However, careful examination of its tools has to be done in order to choose the optimal modeling strategy.

References

1. Postelnicu Tudor, **P100-1/Proiectarea Seismica a cladirilor vol.2-B. Comentarii si exemple de calcul** – *ctr. U.T.C.B. nr. 158/02.08.2005 M.T.C.T.*
2. **Robot Millennium v.20.1.** Autodesk Inc, 2008
3. **CR 2-1-1.1, Cod de proiectare a constructiilor cu pereti structurali de beton armat**
4. **P100-1/2006, Cod de proiectare seismica**

Computational Approaches for Life Cycle Cost Analysis

Nicuta Alina Mihaela¹

¹“Gheorghe Asachi” Technical University, Iasi, 700050, Romania

Summary

In order to perform an optimal economic evaluation of a construction project the research institutes have considered necessary to develop different computer software. This is due to the great diversity of information and for the facilitation of man’s work. This is why in the last years have been created complex databases with different price information, construction details and other. This stored information was introduced in different computer software which realizes an automatic calculation and analysis.

The present paper will present some of the software which realizes computer analysis of investments and cost – benefit analysis for construction projects. Some of the software will have a more detailed presentation due to the accessibility of the software and the capacity to download it.

KEYWORDS: computer software, HERS-ST, Real Cost, BridgeLCC, economic analysis, costs.

1. INTRODUCTION

Some of the obstacles in realizing a cost analysis for a construction work is considered the lack of a general accepted methodology and the difficulty to access a basic cost database and personnel services.

In order to facilitate the economic analysis process for the construction projects have been realized different computer software packages. The main producers of these computer software are also the initiators of LCCA – Life Cycle Cost Analysis, more exactly FHWA – Federal Highway Administration and AASHTO – American Association of State Highway and Transportation Officials from USA.

Some examples of software are HERS-ST – Highway Economic Requirements System, HDM-4 – Highway Development and Management Tools, FHWA LCCA model – Federal Highway Administration Life Cycle Cost Analysis, DarWin, CES – Cost Estimation System, Estimator – Highway Cost Estimation Workstation etc.

The majority of these computer software have high prices of acquisition. On the official sites of the producers mainly can be found only demo versions or the software can be bought. Some of the computer software can benefit from a price reduction in the case in which a Research Institution or University asks for the software in order to use it only for research or academic purpose.

There are also some exemptions such as HERS-ST or FHWA-LCCA that can be downloaded for free from the official internet pages of the producers. As for their structure, HERS-ST comes with a new interface and FHWA-LCCA is structured as an information database in Excel.

1. OVERVIEW ON THE MAIN ECONOMIC ANALYSIS SOFTWARE MODELS

HERS and HERS-ST

Highway Economic Requirements System (HERS) is an analysis system for cost – benefit analysis developed by the Office of Goods Management from the Federal Administration of Highway Infrastructure. This is used to compare the improvements of highway segments including surface reconstruction, enlargement etc.

Initially, it has been applied at national level; the states from Oregon and Indiana have adopted this software in order to analyze the large investments of the state. These elements have been adopted in a new version at state level under the name of HERS-ST.

HDM 4

Highway Development and Management Tools (HDM-4) has been developed by the World Bank consequently after a serial of previous versions. It is used to estimate the benefits of roads users, infrastructure costs and externalities including accidents, energy consume and emissions for alternative investment strategies.

Previous versions of the model have been used at international level in order to evaluate the changes between the highways development and their conservation. The new HDM-4 offers a strong system for roads managements analysis and investment alternatives.

The system can be applied in several areas such as roads management, roads network development prevention, funds needs estimation, budgetary allocation, project evaluation and politics studies impact.

This is one of the most costly computer software for cost analysis.

FHWA LCCA model

It has been developed in 2002. It is based on the Technical Bulletin FHWA LCCA from 1998. Has a friendly interface for the required level of complexity and in the same time easy to use. It's based on Microsoft Excel interface.

APA model - asphalt pavement analysis

The APA model is same based on the Technical Bulletin FHWA. It has the capacity to realize LCCA in a probabilistic or deterministic determination for till four alternatives. For the probabilistic analysis are necessary information regarding the medium value, distribution of discount rate, traffic increase and construction time. When the estimation of these distributors is impossible it can be used the deterministic model. This allows the consideration of the users costs resulted from delays due to the time spent in the work zones and determines the detailed analysis of the results in graphics or excel.

Each and every of these computer software includes specific models in order to face several functions such as the users costs and roads pavement development.

The majority of these models can be used in the states which have developed them only if can't be realized certain changes of sub – modules in conformity with the state project specifications. The models realize LCCA as a component part of their objective which is the network rehabilitation, previous model planning and establishment of economical viability for the future.

CES - Cost Estimation System

The Cost Estimation System (CES) is the primary Transport module for construction cost estimation. It provides a highly productive environment for preparation of parametric, cost-based and bid-based cost estimates, and it is fully integrated with the other modules of the Transport system. CES provides a full range of cost estimating capabilities from conceptual estimation to the final engineer's estimate.

CES comes with a standard set of cost groups for parametric estimation and tools to upload existing labor, equipment, material, and crew data. Estimators can migrate their work though each stage of estimation, splitting and combining jobs as required, moving smoothly from parametric to detailed estimation, creating projects and producing the final estimate.

ESTIMATOR

Highway Cost Estimation Workstation Transport Estimator is an interactive, PC-based, stand-alone cost estimation system for transportation construction that provides a graphical user interface for the preparation of detailed estimates. Estimator supports generation of cost estimates using cost-based and bid-based techniques.

All the data for these estimates, such as wages, equipment and material costs, production rates, and historical item price estimation data is stored and maintained on the PC. Estimator can import bid-based item price estimation data and supports multiple bid histories from which the user can choose.

TRACER - Transportation Cost Estimator

Earth Tech and the American Association of State Highway & Transportation Officials (AASHTO) have developed a new cost estimating tool that will make it easier and more time efficient to estimate transportation project costs.

Traditionally, transportation planners have had to input their historical costs, including bid information, to build a database of knowledge that can be used to create a plan or budget for highway and bridge construction, renovation, and demolition projects in the pre-design and preliminary design phases.

TRAnspOrtation Cost EstimatoR (TRACER) is a parametric cost engineering tool that streamlines this process by employing pre-engineered model parameters and construction criteria in conjunction with location-specific cost data to create accurate project cost estimates utilizing limited design information. This is achieved through default quantities which are built into the software and based on similar projects and experienced engineering assumptions.

TRACER is an interactive cost estimating software solution that is PC based. All parametric algorithms and cost data are inherent to the software and the turnkey package allows the user to begin creating cost-based estimates from the moment the software is launched.

BridgeLCC

Life cycle cost software for bridge design. BridgeLCC is user-friendly life-cycle costing software developed by the National Institute of Standards and Technology (NIST) to help bridge engineers assess the cost effectiveness of new, alternative construction materials. The software uses a life-cycle costing methodology based on both ASTM standard E 917 and a cost classification developed at NIST.

BridgeLCC is created to compare new and conventional bridge materials but works equally well when analyzing alternative conventional materials. Also, it can be used to analyze pavements, piers, and other civil infrastructure.

BridgeLCC runs in Windows 95, 98, 2000, NT, and XP.

DARWin 3.1

DARWin represents the series of AASHTO's computer software programs for pavement design and is an implementation of the 1993 AASHTO publication - Guide For The Design of Pavement Structures.

DARWin 3.1 is metric-compliant AASHTOWare computer software that conforms to and is compliant with the pavement design models. The overlay design module provides a fully automated means of performing all of the different overlay design calculations, including automated file processing and back calculation.

The module on life-cycle costs in DARWin is designed so that the user can input costs in the same format as they are made available for initial construction, rehabilitation, and maintenance. Outputs are customizable and can be presented several ways. DARWin also has enhanced calculation procedures, report generation capabilities, display graphics, extensive on-line help, and many other features.

DARWin 3.1 is designed to run under Microsoft Windows 95, Windows 98, and Windows NT. DARWin 3.1, is a full 32-bit application which takes advantage of the multi-tasking environment of Windows and provides excellent screen graphics.

A user's guide with descriptions of the various software features and extensive examples help explain the capabilities of DARWin 3.1. While the software has extensive on-line help facilities, the first-time user of DARWin is strongly encouraged to use and reference both DARWin user's guides and the appropriate edition of the pavement design guide.

DARWin releases prior to July 1999 are equipped with a hardware security device, called Hardlock, to prevent unlicensed users from running unauthorized copies of DARWin. The Hardlock must be installed for DARWin to run.

DARWin releases after July 1999, will be equipped with a software security device that replaces the Hardlock.

2. HERS-ST

The Highway Economic Requirements System (HERS) has been used by the Federal Highway Administration's (FHWA's) Office of Legislation and Strategic Planning to develop future highway investments in order to either improve the highway system or maintain user cost levels on the system. HERS provides cost estimates for achieving economically optimal program structures. HERS can also predict system condition and user cost levels resulting from a given level of investment.

The HERS model uses incremental benefit cost analysis to optimize highway investment. HERS addresses these deficiencies by selecting a set of alternative improvements to satisfy performance objectives. Each potential improvement is subjected to a rigorous benefit-cost analysis that considers travel time, safety, and vehicle operating and emissions costs.

When funding is not available to achieve "optimal" spending levels, HERS prioritizes economically worthwhile potential improvement options according to relative merit and selects the "best" set of projects. When funding is available, HERS recommends all projects having benefits. Given funding constraints or users needs, HERS minimizes the expenditure of public funds while simultaneously maximizing highway user benefits.

HERS-ST the improved version of HERS uses engineering standards to identify highway deficiencies and applies economic criteria to select the most cost-effective mix of highway system improvements.

The Highway Economic Requirements System - State Version (HERS-ST) is a software package that predicts the investment required to achieve certain highway system performance levels. Alternatively, the software can be used to estimate the highway system performance that would result given various investment levels.

The HERS-ST model is an extension of the HERS model. It was developed by the Federal Highway Administration (FHWA) to examine the relationship between national investment levels and the condition and performance of the highway system.

HERS-ST has many applications in a State transportation agency such as:

- Long Range Planning
- What-if Analysis
- Programming
- Performance Measures
- Congestion Management
- Needs Assessment
- Data Management
- Legislative Decision Support
- Software Description

The HERS-ST software is an easy to use Microsoft Windows based application. Interview screens or "wizards" are used to facilitate the entry and editing of input data.

HERS-ST is also flexible. When it comes time to run the HERS-ST analysis, the user selects the type of scenario to be performed and clicks a button.

Users of all skill levels can create a wide variety of maps, charts, tables, and reports. HERS-ST has a built-in graphical information system (GIS), so that the user can spatially view the HERS-ST input and analysis output. There are built-in

charts and reports for the novice user, "wizards" and queries for the intermediate user, and the ability to create ad-hoc charts and reports for the experienced user.

The HERS-ST software simulates the selection and implementation of highway capital improvements consistent with the principles of incremental benefit-cost analysis. The analysis considers travel time, safety, vehicle operating, emissions, and highway agency costs. The model optimizes highway investment given funding constraints or performance objectives.

When funding is available, HERS-ST will implement all projects having benefits in excess of costs. Given funding constraints or user-specified performance objectives, HERS-ST selects those projects with the highest benefit/cost ratios until the public agency funds are exhausted, therefore maximizing the combined highway user and highway agency benefits.

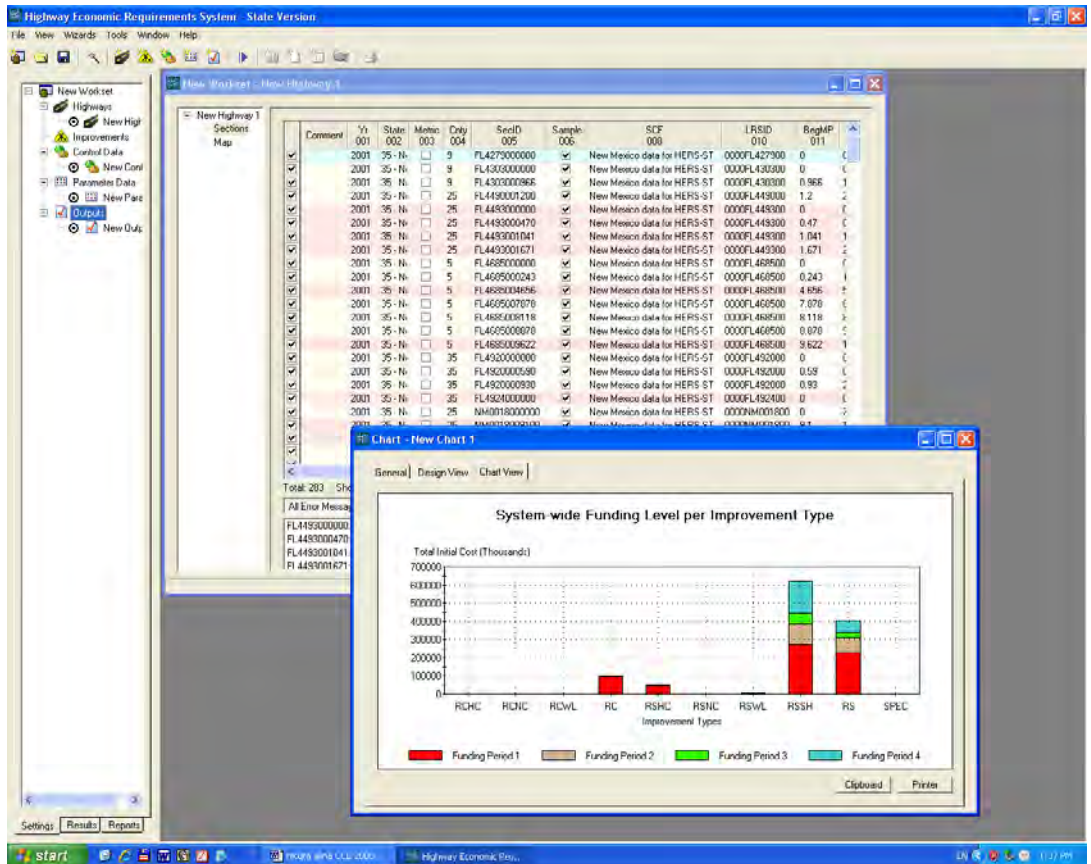


Fig. 1 Example of HERS-ST Window

3. REAL COST SOFTWARE

RealCost has the purpose of providing a tool for pavement design and in the same time to incorporate the costs elements in the process. The software allows the user to investigate the effects of cost, service life, and economic inputs on life-cycle cost.

RealCost automates FHWA’s LCCA methodology as it applies to pavements.

The software calculates life-cycle values for agency and user costs associated with construction and rehabilitation. The software can perform deterministic and probabilistic modeling of pavement problems.

RealCost supports deterministic sensitivity analyses and probabilistic risk analyses.

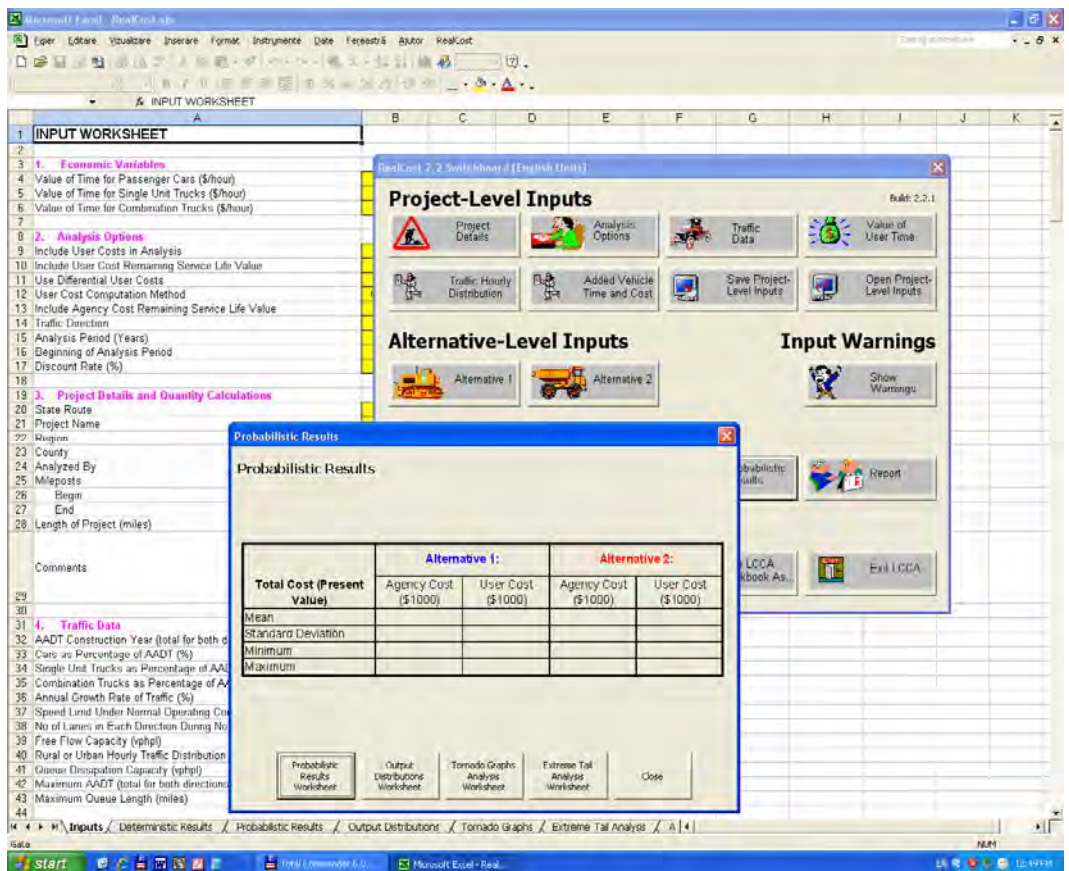


Fig. 2 RealCost window

4. BRIDGELCC

BridgeLCC 2.0 uses an economic methodology based on the ASTM Standard Practice for measuring the life-cycle costs of buildings and building systems (E 917). The software includes a cost classification scheme that helps insure that all costs are accounted for and are well organized so that useful comparisons can be made quickly between project alternatives.

BridgeLCC 2.0 can operate in two alternate modes: (1) a *Basic Mode* where the amounts and timings of costs are best-guess values without any uncertainty, and (2) an *Advanced Mode* where uncertainty in amounts and timings of costs can be taken into consideration. The analyst can switch back and forth between the two modes without any loss of data.

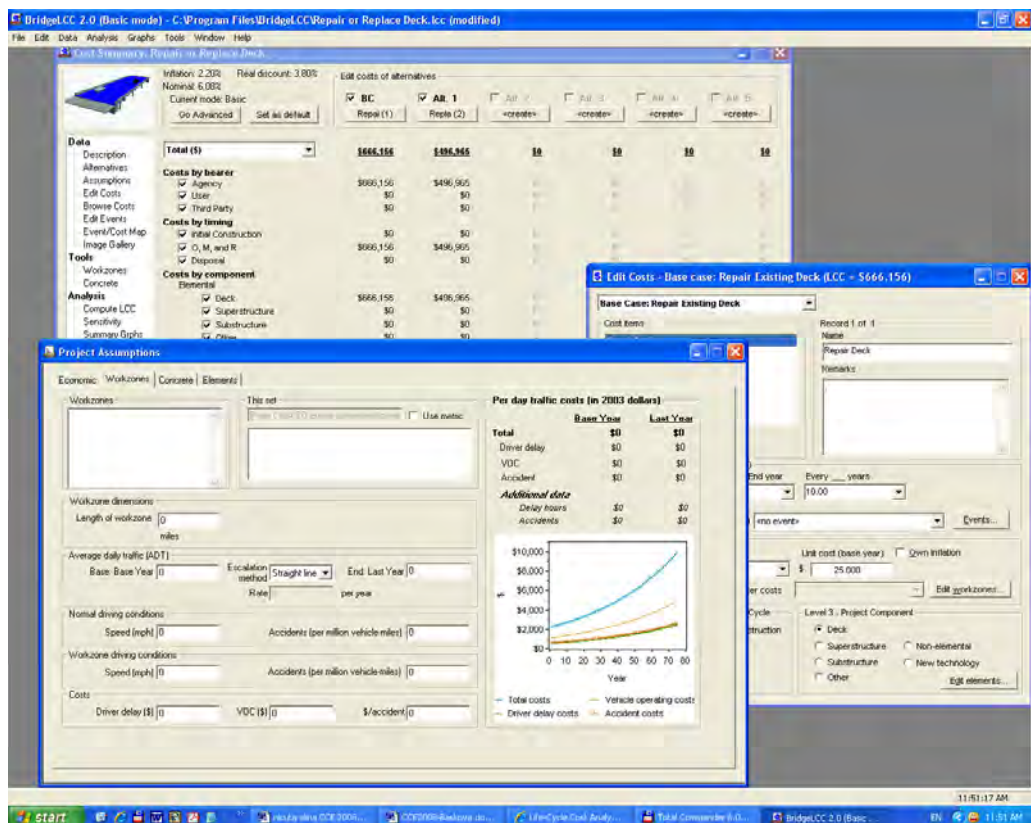


Fig. 3 BridgeLCC window

BridgeLCC includes tools that support life-cycle cost analysis of bridges. The Workzones window allows the user to estimate the per-day cost of road

construction and repair to drivers on and under a bridge, in terms of driver delay costs, vehicle operating costs, and accident costs.

BridgeLCC 2.0 offers features such as:

- analyzing up to 6 alternatives at a time;
- creating life-cycle 'events' that affect many agency, user, or third-party costs;
- creating and using multiple work zones (with driver delay, vehicle-operating costs, and accident costs);
- improved sensitivity analysis of interest rates, life-cycle events, and costs;
- select non-U.S. currencies (British, Japanese, Euro, General).

CONCLUSIONS:

The software programs in the area of construction cost analysis addresses the needs of the transportation agency during a particular phase in the construction life cycle.

The release of the computer software is willing to provide support and analysis in easy to understand and use formats.

The software programs presented in this paper have the role of explaining the evolution of the cost analysis for construction works. Due to the great variety and quantity of information necessary to make the analysis this computer software have the purpose to facilitate the work for the analysis, to take into considerations different alternatives, to access new funding opportunities and to take optimal investment decisions.

References:

1. <http://www.fhwa.dot.gov/infrastructure/asstmgmt/lccasoft.cfm>
2. <http://www.bfrl.nist.gov/bridgelcc/overview.html>
3. <http://www.fhwa.dot.gov/infrastructure/asstmgmt/rc210704.pdf>
4. <http://aashtoware.org/?siteid=28&pageid=76>

Comparative study regarding three standardized European methods for estimation on horizontal loads that act on formworks

Eugen Pamfil¹, Vasile Iacob² Ioan Paul Voda³

¹BMTO, “Gheorghe Asachi” Technical University, Iasi, 700050, Romania

²BMTO, “Gheorghe Asachi” Technical University, Iasi, 700050, Romania

³BMTO, “Gheorghe Asachi” Technical University, Iasi, 700050, Romania

1. METHODS FOR ESTIMATION OF HORIZONTAL LOADS THAT ACT ON FORMWORKS

1.1 According to method from normative c140-86, Romania [1]

According to normative C140-1986, effectual for year 2008, for formworks and theirs timbering computation the next values of horizontal loads will be considered:

f. *Horizontal static load, p_f* coming from lateral concrete pressure (casted and then compacted by vibration) applied on formwork walls, this is an area load and its value is distributed on formwork height depending on concreting speed v (m/h), according to diagrams from figure 1.1

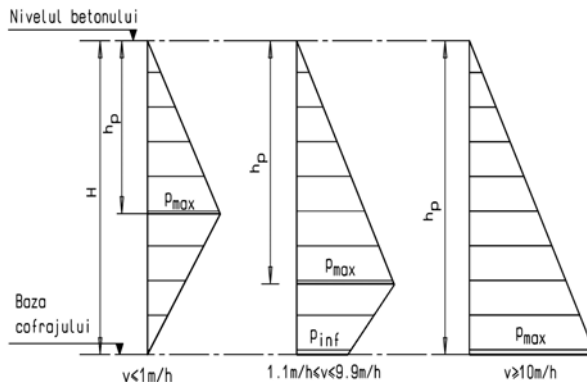


Fig. 1.1 Distribution of lateral concrete pressure applied on formwork height depending on concreting speed

Concreting actual speed represent the ratio between height H of casted concrete element and time period, t_b , estimated for filling the formwork with concrete up to

respective height H . For continue casting, without accidental working joints, the following condition must be fulfilled:

$$v_t = \frac{H}{t_b} \geq v_{t_{\min}} = \frac{h_{str}}{t_2 - t_1} \quad (1.1)$$

where:

$v_{t_{\min}}$ – the minimum concreting speed , [m/h];

h_{str} – the height of concrete layer casted in one reprise, [m];

t_1 – the age of concrete at the end of creation, in hours; $t_1 \leq t_i$ (time when concrete starts to harden, in hours).

t_2 – the age of concrete at the cover of one concrete layer with another, without accidental working joints, in hours; $t_2 \leq t_r$ (time of re-vibration, $t_r \cong 2 \cdot t_i$, in hours).

In computation, the conventional values t_i și t_r are used, this values are different depending on cement type and environmental temperature at the time when concrete is made (tab. 1.1), [2].

Table 1.1 Characteristic ages of concrete, from time of concreting

The age of concrete	Cement type	Environmental temperature (°C)			
		+5	+10	+20	+30
t_i time when concrete starts to harden	a) unitary cement, type I, SR388, SR 3011	1,50	1,25	1,00	0,75
	b) composite cement, type IIA, SR 1500; SR 3011	1,75	1,50	1,25	1,00
	c) composite cement, type IIB, IIIA,IVA SR 1500; SR 3011	2,00	1,75	1,50	1,25
t_r maxim type of re-vibration, after one concrete layer was covered with another concrete layer	a) unitary cement, type I, SR 388, SR 3011	3,00	2,50	2,00	1,50
	b) composite cement, type IIA, SR 1500; SR 3011	3,50	3,00	2,50	2,00
	c) composite cement, type IIB, IIIA,IVA SR 1500; SR 3011	4,00	3,50	3,00	2,50
t_p time of end (ending of the concrete hardening)	a)unitary cement, type I, SR388, SR 3011	10,00	8,00	6,00	4,00
	b) composite cement, type IIA, SR 1500; SR 3011	12,0	10,0	8,00	5,00
	c) composite cement, type IIB, IIIA,IVA SR 1500; SR 3011	16,0	12,0	10,0	6,00

The age t_3 is the minimum age of concrete after which the concreting with working joint can be resumed $t_3 \geq t_p$ (ending of the concrete hardening, in hours, when the concrete lateral pressure on formwork disappeared).

The maximum concreting speed is actuated depending on the effective debit (capacity of concreting) of the driving equipment from the complex flux of concreting and on the effective surface in the horizontal plan of the working front, with relation:

$$v_{t \max} = \frac{C_{b \max}}{S_{b \min}} \quad (1.2)$$

where:

$v_{t \max}$ – the maximum concreting speed [m/h];

$C_{b \max}$ – the maximum concreting capacity [m^3/h];

$S_{b \min}$ – the maximum surface in horizontal plan of concrete casted in one round, for the minimum working front between two technological joints [m^2];

The condition that must be fulfilled for the assurance of concreting quality and continuity is:

$$v_{t \min} \leq v_t \leq v_{t \max} \quad (1.3)$$

The depth where the maximum concrete pressure is manifested is actuated with the following relation:

$$h_p = \lambda_1 \cdot H \quad (1.4)$$

where:

h_p – the height (the depth) where the maximum lateral pressure of the concrete is manifested, the height is measured from the upper part of the casted concrete column [m];

λ_1 – member of relation with values between 0,55 – 1,00, depending on the concreting speed, see table 1.2;

H – height of the casted concrete column [m];

Value of the maximum pushing force, that is manifested as hydrostatic pressure of the fresh concrete at the depth h_p , is actuated with the following relation:

$$p_{f \max} = \lambda_1 \cdot \lambda_2 \cdot \lambda_3 \cdot \lambda_4 \cdot H \cdot \rho_b \quad (kN/m^2) \quad (1.5)$$

where:

λ_2 – member of relation that depends on the working properties of concrete, this property is evaluated by Abrams test (testing of cone, $T[cm]$), table 1.2;

λ_3 – member of relation that depends on the minimum dimension [cm] of the fresh casted concrete section, table 1.2;

λ_4 – member of relation that depends on the fresh casted concrete temperature ($^{\circ}\text{C}$), see table 1.2;

H – the height of the column of casted concrete [m];

ρ_b – the volume of the casted and compacted concrete;

$\rho_b = 2400 \text{ kg/m}^3$ (the average).

The concrete lateral pressure at the bottom layer of the formwork, p_{inf} , is actuated with the following relation:

$$p_{\text{inf}} = \alpha \cdot p_{\text{fmax}} \quad (1.6)$$

where the values for α are from table 1.3.

Table 1.2 Values of members $\lambda_1, \lambda_2, \lambda_3$ and λ_4 [1]

Characteristic	λ_1	λ_2	λ_3	λ_4
Concreting speed (m/h)	≤ 1	0,55		
	2	0,65		
	3	0,75		
	4	0,85		
	6	0,90		
	8	0,95		
	≥ 10	1,00		
Working property of concrete, compaction T_i (cm)	<1 (T_1)		0,85	
	1...4 (T_2)		0,95	
	5...9 (T_3)		1,00	
	10...15 ($T_3/T_4, T_4$)		1,05	
	>15 ($T_4/T_5, T_5$)		1,10	
Minimum dimension of the section (cm)	≤ 15		0,90	
	16...54		0,95	
	≥ 55		1,00	
Temperature of the fresh concrete ($^{\circ}\text{C}$)	≤ 5			1,00
	6...24			0,95
	≥ 25			0,90

Table 1.3 Values of α depending on the concreting speed [1]

Concreting speed (m/h)	≤ 1	2	3	4	6	8	≥ 10
A	0,00	0,25	0,45	0,70	0,80	0,90	1,00

g. *The horizontal dynamic load on the formwork walls*, accrue from the concussions that are produced at the concrete discharge in formwork, p_g . The value of this load will be considered as described bellow:

- for a capacity q of the transportation from which the concrete is discharged into the fromwork of:

$q < 0,2 \text{ m}^3 \dots\dots\dots 200 \text{ daN/m}^2$;

$q = 0,2\dots0,7 \text{ m}^3 \dots\dots\dots 400 \text{ daN/m}^2$;

$q > 0,7 \text{ m}^3 \dots\dots\dots 600 \text{ daN/m}^2$;

- for the casting with gutters and gates. 200 daN/m²;

- for the casting with pump. 600 daN/m².

h. *Wind load, p_w* . This load (STAS 10101/2 – 90) will be considered only in case of computation of formwork timbers higher than 6,0 m.

Loads group

The combination of loads must contain those loads that can act simultaneously, in the same sense derogatory to the formwork fullness. In the table 1.4 are the recommendation of C140-1986 normative, regarding the combination of loads that act on formworks.

Table 1.4 Group of horizontal loads that act on formworks [1]

No.	Elements denomination	Loads considered for:	
		Resistibility computation	Stiffness computation
1	Formworks for concrete poles with arms with maximum dimension of 30 cm and formworks for walls with maximum thickness of 10 cm	f+g	F
2	Formworks for concrete poles with arms higher than 30 cm and formworks for walls with thickness higher than 10 cm; the formworks of beamy elements	f	F
3	Side parts of formworks, beams or arches	f	F

1.2. According to standards DIN 18202/18218, Germany [3], [6], [7]

1.2.1 Hypothesizes:

- the concrete consistency is $\gamma_b = 25 \text{ kN/m}^3$;
- the formwork is tight;
- concrete is compacted through interior vibration;
- the concrete temperature is of $+15^\circ\text{C}$, constant for the period of hardening;
- hardening period, $T_E = 5 \text{ h}$;
- after hardening period T_E passes, the lateral pressure of the fresh concrete upon the formworks stops growing; the depth h_E from where the lateral pressure of concrete stops growing is actuated with the following relation:

$$h_E = v_b \cdot T_E \tag{1.7}$$

where:

- v_b is the concreting speed (m/h) and $T_E = 5 \text{ h}$, – hardening period.
- up to the depth of vibration h_r , it is considered that the fresh concrete, condensed through vibration, is producing hydrostatic pressure upon the vertical formwork; $h_r = 0,90 \text{ m}$, so $p_r = 0,9 \cdot \gamma_b \text{ (kN/m}^2\text{)}$
- variation in time of the fresh concrete lateral pressure will be:

$$dp = \gamma_b \cdot v_b \cdot dt \cdot \lambda_{(t)} \tag{1.8}$$

- it is accepted that the pressure decrease to zero for T_E , $0 \leq \lambda \leq \lambda_o$, $\lambda_o < 1,0$

The variation (distribution) of fresh concrete pressure on the height of the formwork, with the maximum value at the depth h_E , is described in the figure fig. 1.2.

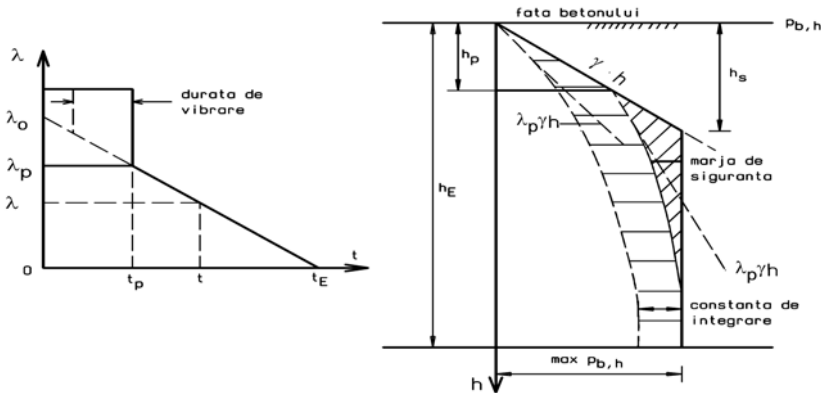


Fig. 1.2 Variation of fresh concrete pressure on the height of the formwork, DIN 18218/80

The simplification of the diagram by adding the hachured surface means more safety for the situation when the vibration depth exceed 0,90 m.

1.2.2 Evaluation of the maximum lateral pressure

For the actuation of the lateral pressure on the formwork the working property of the concrete is introduced through curves K_1, K_2, K_3 liquid concrete. At the end results the diagram for computation of fresh concrete lateral pressure, p_b (kN/m^2), depending on the hydrostatic height h_s (m), on the concreting speed V_b (m/h) and on the compaction value W_{alz} , for vertical formworks it depends on poles and walls – fig. 1.3.

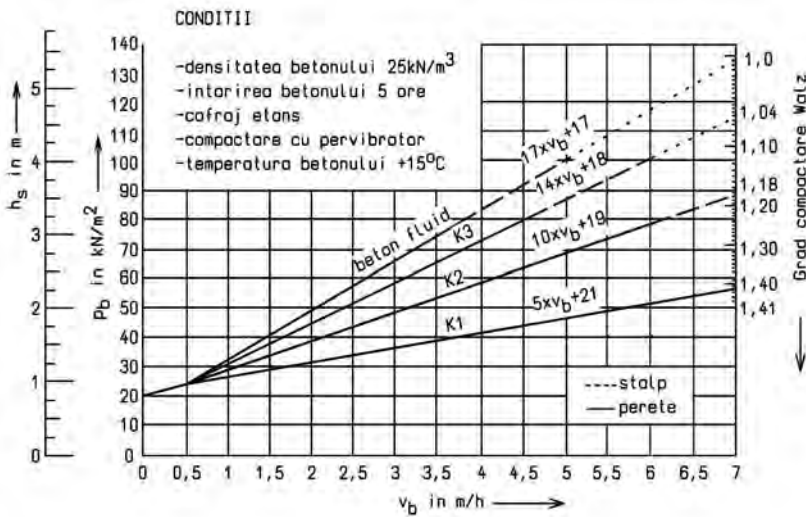


Fig. 1.3 Diagrams for computation of the fresh concrete lateral pressure, DIN 18202/18218

Considering $h_r = 0,90$ m, $T_E = 5$ h, $\gamma_b = 25 \text{ kN/m}^3$, the maximum lateral pressure will have the following expressions (where V_b [m/h] and $p_{b,h}$ [kN/m^2]):

- for $K_1(G_c \leq 1,4)$, $p_{\max} = p_{b,h} = 5 \cdot V_b + 21$ (1.9)

- for $K_2(G_c \leq 1,18)$, $p_{\max} = p_{b,h} = 10 \cdot V_b + 19$ (1.10)

- for $K_3(G_c \leq 1,04)$, $p_{\max} = p_{b,h} = 14 \cdot V_b + 18$ (1.11)

- for liquid concrete ($G_c \approx 1,0$), $p_{\max} = p_{b,h} = 17 \cdot V_b + 17$ (1.12)

The relations are consistent when $V_b \leq 4,0$ m/h, and are corresponding to the distribution of pressure on the vertical size of the formwork from fig. 1.4.

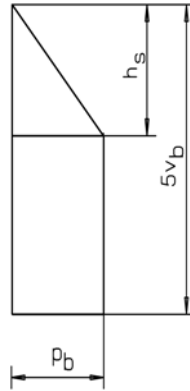


Fig. 1.4 Distribution of the fresh concrete on the vertical size of the formwork for $V_b \leq 4,0$ m/h

When the concreting speed is lower or higher than $h/T_E = h/5$, the distribution of lateral pressure on the vertical size of the concrete is described in fig. 1.5.

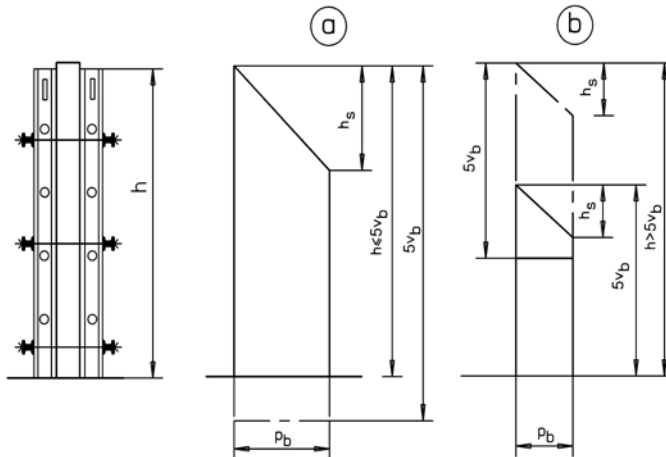


Fig. 1.5 Distribution of fresh concrete lateral pressure on the vertical size of the formwork for:

(a) $V_b \leq h/T_E = h/5$, (b) $V_b > h/T_E = h/5$

1.2.3 Corrections

If hypothesis from point a) aren't accomplished, the fresh concrete lateral pressure on the formwork, actuated as described at point b), will be corrected as bellow:

- if the vibration depth h_r exceeds the hydrostatic depth h_s , the lateral pressure will raise up to value $p_{b,h} = 25 h_r$ kN/m²;
- if the fresh concrete temperature is different from +15°C, the pressure $p_{b,h}$ and the hydrostatic depth h_s will be modified; they will increase with 3% for every 1°C bellow +15°C or they will decrease with 3% for every 1°C after +15°C (diminution mustn't exceed 30%).

The hypothesis that the temperature stays constant while the concrete is hardening (period T_E) is kept if:

- the environmental temperature exceeds +15°C and the formwork can be warmed up above this temperature, can be omitted the influence of the higher environmental temperature upon the fresh concrete lateral pressure (the hypothesis of +15°C concrete temperature will be kept)
- if at the preparation of concrete are used plasticizer additives, the fresh concrete lateral pressure will be modified considering the new values for K_1 , correspondig to the real working property of the concrete;
- if are used hardening retarders additives, will be used the coefficients from table 1.5 for multiplying of $p_{b,h}$ and h_s ;

Table 1.5 Multiplication coefficients of pressure $p_{b,h}$ and of height h_s

Hardening delay (ore)	Consistency		
	K_1	K_2	K_3
5	1,15	1,25	1,40
15	1,45	1,8	2,15

- if the concrete volume γ_{b1} is different from $\gamma_b = 25$ kN/m³, the pressure $p_{b,h}$ is calculated again with the relation: $p_{b,h(\gamma_{b1})} = \alpha \cdot p_{b,h(25)}$, where $\alpha = \gamma_{b1}/\gamma_b$; h_s – the same.

1.3. According to methods CIB and CIRIA, France–England [3], [5]

Table 1.6 The lateral pressure of the fresh concrete on the formworks

<p>„Le Manuel de Technologie: Coffrage“ -CIB- Comité International du Bâtiment, France. „Concrete Pressure on Formwork“ - CIRIA - Construction Industry Research and Information Association, UK.</p> <p>Factors that are considered:</p> <ol style="list-style-type: none"> 1. concrete consistency (kg/m^3) 2. working property of concrete – compaction – mm 3. concreting speed, R (m/h) 4. concrete temperature ($^{\circ}\text{C}$) 5. the height of the casted concrete, H (m) 6. the minimum dimension of the section, d (mm) <p>The considered pressure P_{\max} is between 5 kN/m^2 and 150 kN/m^2 and has the minimum value from P_1, P_2, P_3</p>	1. Pressure P_1 , from the height effect (concrete consistency: 2500 kg/m^3)												
	H (m)	1	2	3	4	5	>6						
	P_1 (kN/m^2)	25	50	75	100	125	150						
	2. Pressure P_2 , from the arch effect												
	d (mm)	R (m/h)											
		0,75	1	2	3	4	5	6	8	10	15	20	30
	150	$P_2=35$	35	35	40	45	45	50	55	60	75	90	120
	200	35	40	40	45	50	50	55	60	65	80	95	125
	300	45	50	50	55	60	60	65	70	75	90	105	135
	400	55	60	60	65	70	70	75	80	85	100	115	145
	500	65	70	70	75	80	80	85	90	95	110	125	125
	3. Pressure P_3 , from the hardening concrete effect												
	Comp action (mm)	Temp. concrete ($^{\circ}\text{C}$)	R (m/h)										
			0,75	1	1,2	1,5	1,8	2	2,5	3	4	5	
	50	5	$P_3=40$	50	60	70	85	95	115	135	150	150	
		10	35	40	45	55	65	70	85	100	135	150	
		15	35	40	40	45	50	55	65	75	100	125	
20		35	35	35	40	45	45	50	55	70	90		
75	5	45	60	70	85	100	110	140	150	150	150		
	10	35	50	55	65	75	85	105	125	150	150		
	15	35	40	45	50	60	65	80	95	125	150		
	20	35	35	35	40	45	50	60	70	90	115		
100 la 150	5	55	70	85	100	120	130	150	150	150	150		
	10	40	55	65	75	90	100	120	150	150	150		
	15	35	45	50	60	70	75	90	110	150	150		
	20	35	35	40	45	50	55	70	80	110	130		

2. NUMERICAL EXAMPLES OF EVALUATION OF FRESH CONCRETE LATERAL PRESSURE

The evaluation of the fresh concrete lateral pressure on the vertical side of the formwork through numerical examples is necessary for can make precise comparisons between the results obtained using the evaluation methods described above.

2.1. For concreting speeds lower than 1,0 m/h

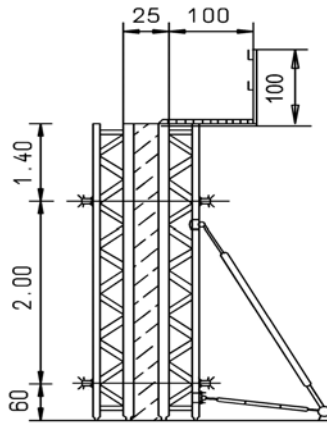


Fig. 1.6 Structural wall formwork from reinforced concrete

Measure the concrete maximum lateral forces and the pressure distribution on the vertical size of the formwork from figure 1.6, knowing:

Construction element: **structural wall**, longitude 7,20m, height 4,0m, width 25 cm.

Fresh casted concrete: C20/25 – T₃ – II/A-S-32,5R-16 (with self-compacting Abrams cone, T = 70 ± 20 mm, compacting degree Walz, G_c = 1,04 – 1,10, K₂, γ = 24 kN/m³). Concreting time t_b = 5 hours, v_b = $\frac{4,0m}{5,0h} = 0,80 \text{ m/h} > v_{bmin}$

$$\frac{h_{str}}{t_2 - t_1} = 0,35 - 0,60 \text{ m/h.}$$

2.1.1. According to normative C140-86

$$p_{fmax} = \lambda_1 \cdot \lambda_2 \cdot \lambda_3 \cdot \lambda_4 \cdot H \cdot \rho_b \text{ (kN/m}^2\text{)}$$

$$v_b = 0,8 \text{ m/h, } \rightarrow \lambda_1 = 0,55 \rightarrow h_p = \lambda_1 \cdot H = 0,55 \cdot 4,0 = 2,20 \text{ m. } \alpha = 0 \rightarrow p_{inf} = 0$$

The concrete property of working: class T₃ (self-compacting 70 ± 20 mm) → λ₂ = 1,00; d_{min} = 25 cm → λ₃ = 0,95;

Concrete temperature: θ_b = +5°C → λ₄ = 1,00;

Results, p_{fmax} = 0,55·1,00·0,95·1,00·4,0·24 = **50,16 kN/m²**, h_p = **2,20 m**, and the lateral pressure distribution on the vertical size of the formwork is represented in fig. 1.7A1.

2.1.2. According to standards DIN 18202/18218

For interior vibration, tight formwork, θ_b = +15°C, T_E = 5 hours, γ_b = 25 kN/m³, and K₂,

P_{b,h} = 10·V_b + 19 = 10·0,8 + 19 = 27 kN/m² h_s = 27/25 = 1,08 m

Corrections: - θ_b = 5°C → p_{b,h,max} = 3%·Δθ·p_{b,h} + p_{b,h} = 0,3·27 + 27 = 35,10 kN/m²
 - γ_br = 24 kN/m³ → p_{b,h,max} = p_{b,h}· γ_br / γ_b = 35,10·24/25 = 33,70 kN/m²; h_s = 33,70/24 = 1,40 m

p_{max} = 33,70 kN/m², h_s = 1,40 m, and the lateral pressure on the vertical size of the formwork is described in fig. 1.7A2.

2.1.3. According to method CIB and CIRIA

H = 4,0 m; ρ_b = 2500 kN/m³ → P₁ = 100 kN/m²; for ρ_b = 2400 kN/m³ →

P₁ = 100 · $\frac{2400}{2500}$ = 96 kN/m²

d = 250 mm; v = 0,8 m/h; → P₂ = **40 kN/m²**, h_s = 40/24 = 1,67 m.

T = 75 mm; θ_b = 5°C, v = 0,8 m/h → P₃ = 45 kN/m²

P_{max} = 40 kN/m², h_s = 1,67 m, and the lateral pressure on the vertical size of the formwork is described in fig. 1.7A3.

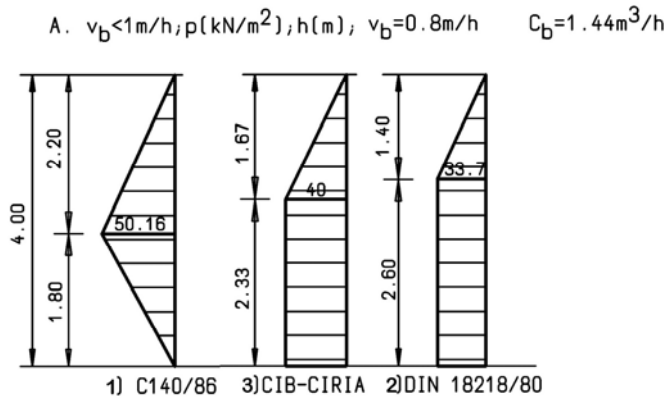


Fig. 1.7.A Diagrams for concrete lateral pressure on the vertical size of the formwork, v_b ≤ 1 m/h

2.2. For concreting speeds higher than 1,0 m/h, but lower than 10m/h

Measure the maximum lateral force of the concrete and the distribution of the lateral pressure on the vertical size of the formwork from fig 1.6, knowing:

Construction element: structural wall, longitude 7,20m, height 4,0m, width 25 cm.

Fresh casted concrete: C20/25 – T₃ – II/A-S-32,5R-16, (with self-compacting Abrams cone, T = 70 ± 20 mm, compacting degree Walz, G_c = 1,04 – 1,10, K₂, γ = 24 kN/m³). C_b = 7,2 m³/h.

Concreting time t_b = 1 oră, v_b = $\frac{4m}{1h} = 4,00 \text{ m/h} > v_{bmin} = \frac{h_{str}}{t_2 - t_1} = 0,35 - 0,60 \text{ m/h}$.

2.2.1. According to normative C140-86

$$p_{fmax} = \lambda_1 \cdot \lambda_2 \cdot \lambda_3 \cdot \lambda_4 \cdot H \cdot \rho_b \text{ (kN/m}^2\text{)}$$

$$v_b = 4,00 \text{ m/h}, \rightarrow \lambda_1 = 0,85 \rightarrow h_p = \lambda_1 \cdot H = 0,85 \cdot 4,0 = 3,40 \text{ m. } \alpha = 0,70 \rightarrow p_{inf} = 0,7 \cdot p_{fmax}$$

The concrete property of working: class T₃ (self-compacting 70 ± 20 mm) → λ₂ = 1,00; d_{min} = 25 cm → λ₃ = 0,95;

Concrete temperature θ_b = +5°C → λ₄ = 1,00;

Results, p_{fmax} = 0,85 · 1,00 · 0,95 · 1,00 · 4,0 · 24 = 77,52 kN/m², h_p = 3,40 m,

p_{inf} = 0,70 · 77,52 = 54,26 kN/m², and the lateral pressure on the vertical size of the formwork is described in fig. 1.7B1.

2.2.2. According to standards DIN 18202/18218

For interior vibration, tight formwork, θ_b = +15°C, T_E = 5 hours, γ_b = 25 kN/m³, și K₂, V_b = 4,0 m/h, P_{b,h} = 10 · V_b + 19 = 10 · 4,0 + 19 = 59 kN/m² h_s = 59/25 = 2,36 m

Corrections: - θ_b = 5°C → p_{b,h,max} = 3% · Δθ · p_{b,h} + p_{b,h} = 0,3 · 59 + 59 = 76,7 kN/m²

- γ_{b,r} = 24 kN/m³ → p_{b,h,max} = p_{b,h} · γ_{b,r} / γ_b = 76,7 · 24 / 25 = 73,63 kN/m²; h_s = 73,63 / 24 = 3,06 m

p_{max} = 73,63 kN/m², h_s = 3,06 m, and the lateral pressure on the vertical size of the formwork is described in fig. 1.7B2.

2.2.3. According to method CIB și CIRIA

$$H = 4,0 \text{ m; } \rho_b = 2500 \text{ kN/m}^3 \rightarrow P_1 = 100 \text{ kN/m}^2;$$

$$\text{for } \rho_b = 2400 \text{ kN/m}^3 \rightarrow P_1 = 100 \cdot \frac{2400}{2500} = 96 \text{ kN/m}^2$$

$$d = 250 \text{ mm}; v = 4,0 \text{ m/h}; \rightarrow P_2 = 55 \text{ kN/m}^2, h_s = 55/24 = 2,29 \text{ m.}$$

$$T = 75 \text{ mm}; \theta_b = 5^\circ\text{C}, v = 4,0 \text{ m/h} \rightarrow P_3 = 150 \text{ kN/m}^2$$

$P_{\max} = 55,0 \text{ kN/m}^2$, $h_s = 2,29 \text{ m}$, and the lateral pressure on the vertical size of the formwork is described in fig. 1.7B3.

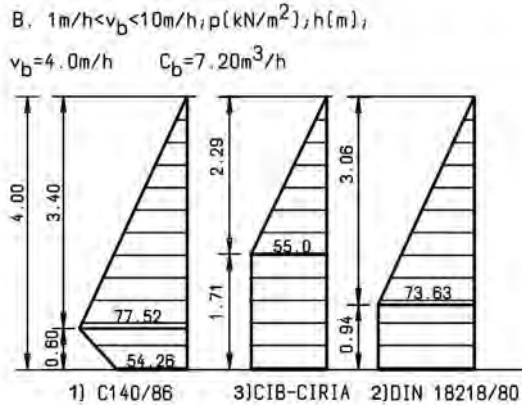


Fig. 1.7.B Diagrams for concrete lateral pressure on the vertical size of the formwork, $1 \text{ m/h} < v_b < 10 \text{ m/h}$

2.3. For concreting speeds higher than $10,0 \text{ m/h}$

Measure the maximum lateral concrete forces and the distribution of the lateral pressure on the vertical size of the formwork from figure 1.6, knowing:

Construction element: structural wall, longitude $7,20 \text{ m}$, height $4,0 \text{ m}$, width 25 cm .
 Fresh casted concrete: C20/25 – T₃ – II/A-S-32,5R/0-16, (with self-compacting Abrams cone, $T = 70 \pm 20 \text{ mm}$, compacting degree Walz $G_c = 1,04 - 1,10$, K_2 , $\gamma = 24 \text{ kN/m}^3$). $C_b = 20,55 \text{ m}^3/\text{h}$.

$$\text{Concreting time } t_b = 0,35 \text{ ore}, v_b = \frac{4 \text{ m}}{0,35} = 11,42 \text{ m/h} > v_{b\min} = \frac{h_{str}}{t_2 - t_1} = 0,35 -$$

$0,60 \text{ m/h}$.

This concreting rate suppose one concreting capacity $C_b \geq 20,55 \text{ m}^3/\text{h}$, characteristic to concrete pumping. In these conditions the fresh concrete must have the working property T_3/T_4 (self-compacting cone $100 \pm 20 \text{ mm}$) and the compacting degree $G_c \leq 1,04 \rightarrow K_3$;

one liquefying additive will be used.

2.3.1. According to normative C14-/86

$$p_{fmax} = \lambda_1 \cdot \lambda_2 \cdot \lambda_3 \cdot \lambda_4 \cdot H \cdot \rho_b \quad (\text{kN/m}^2)$$

$v_b > 10,0 \text{ m/h}$, $\rightarrow \lambda_1 = 1,00 \rightarrow h_p = \lambda_1 \cdot H = 1,0 \cdot 4,0 = 4,0 \text{ m}$. $\alpha = 1,00 \rightarrow p_{inf} = p_{fmax}$
 hydrostatic pressure; the working property of concrete : class T₃/T₄ (self-compacting 100 ± 20 mm) $\rightarrow \lambda_2 = 1,05$; $d_{min} = 25 \text{ cm} \rightarrow \lambda_3 = 0,95$; concrete temperature $\theta_b = +5^\circ\text{C} \rightarrow \lambda_4 = 1,00$;

Results, $p_{fmax} = 1,0 \cdot 1,05 \cdot 0,95 \cdot 1,00 \cdot 4,0 \cdot 24 = 95,76 \text{ kN/m}^2$, $h_p = 4,0 \text{ m}$, $p_{inf} = 95,76 \text{ kN/m}^2$, and the lateral pressure on the vertical size of the formwork is described in fig. 1.7C1.

2.3.2. According to standards DIN 18202/18218

For interior vibration, tight formwork, $\theta_b = +15^\circ\text{C}$, $T_E = 5 \text{ ore}$, $\gamma_b = 25 \text{ kN/m}^3$, $\xi_i K_3$, $V_b = 11,42 \text{ m/h}$, $p_{b,h} = 14 \cdot V_b + 18 = 14 \cdot 11,42 + 18 = 177,88 \text{ kN/m}^2$ $h_s = 177,88/25 = 7,11 \text{ m} > H = 4,0 \text{ m}$

In this conditions, $p_{b,h} = 4,0 \cdot 25 = 100 \text{ kN/m}^2$

Corections: - $\theta_b = 5^\circ\text{C} \rightarrow p_{b,h,max} = 3\% \cdot \Delta\theta \cdot p_{b,h} + p_{b,h} = 0,3 \cdot 100 + 100 = 130 \text{ kN/m}^2$

$$- \gamma_b r = 24 \text{ KN/m}^3 \rightarrow p_{b,h,max} = p_{b,h} \cdot \gamma_b r / \gamma_b = 130 \cdot 24 / 25 = 124,8 \text{ kN/m}^2;$$

$h_s = 124,8/24 = 5,2 \text{ m} > H = 4,0 \text{ m} \rightarrow p_{max} = 100 \cdot 24 / 25 = 96 \text{ kN/m}^2$, hydrostatic pressure.

$p_{max} = 96 \text{ kN/m}^2$, $h_s = 4,0 \text{ m}$, and the lateral pressure on the vertical size of the formwork is described in fig. 1.7C2.

2.3.3. According to method CIB and CIRIA

$H = 4,0 \text{ m}$; $\rho_b = 2500 \text{ kN/m}^3 \rightarrow P_1 = 100 \text{ kN/m}^2$; for $\rho_b = 2400 \text{ kN/m}^3 \rightarrow$

$$P_1 = 100 \cdot \frac{2400}{2500} = 96 \text{ kN/m}^2$$

$d = 250 \text{ mm}$; $v = 11,42 \text{ m/h}$; $\rightarrow P_2 = 85 \text{ kN/m}^2$, $h_s = 85/24 = 3,54 \text{ m}$.

$T = 120 \text{ mm}$; $\theta_b = 5^\circ\text{C}$, $v = 11,42 \text{ m/h} \rightarrow P_3 = 150 \text{ kN/m}^2$

$P_{max} = 85,0 \text{ kN/m}^2$, $h_s = 3,54 \text{ m}$, and the lateral pressure on the vertical size of the formwork is described in fig. 1.7C3.

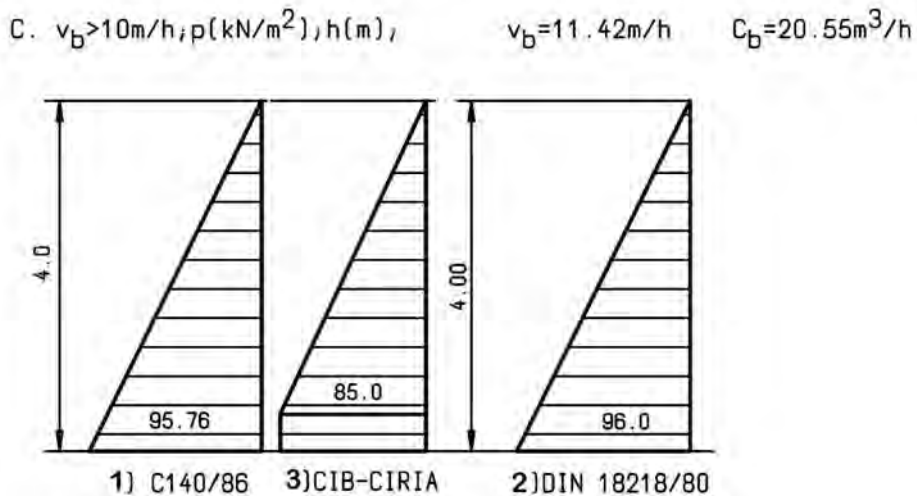


Fig. 2.13.C Diagrams for concrete lateral pressure on the vertical size of the formwork, $v_b > 10 \text{ m/h}$

3. CONCLUSIONS AND PROPOSALS

Observing the prescriptions from the technical normative regarding the evaluation and the grouping of loads that act on the formworks in mandatory in Romania.

The three methods of evaluation of lateral forces of the fresh concrete on the vertical sizes (or a little bit skewed) of the formwork and the numerical applications described above are leading to the next conclusions:

- In evaluation of the maximum pressure on the vertical formworks are interfering many influence factors, and it is difficult to translate this factors in mathematical relations, to describe accurately the physical phenomenon;
- The resulted values for the maximum pressure, measured through different methods, are totally different, from very small values (methods CIB-CIRIA) to very big values (C140-86, DIN 18202/18218); the maximum pressure values are influenced by the concreting speed in every method of evaluation presented. Sometimes, through computations results maximum pressures higher than the hydrostatic pressure, it is in contradiction with the real situations.
- Doesn't exists an unique rule of limiting the maximum value of the pressure, even hydrostatic pressure; it can be limited only the adequacy height, depending on the maximum value of measured hydrostatic pressure.

- For frequently encountered heights of the vertical formworks result, for some computation methods, very small lateral pressures against the hydrostatic pressure, this produces the oversize risk for the formwork (CIB-CIRIA, for concreting speeds higher than 1,0 m/h and DIN 18218, for concreting speed lower than 1,0 m/h). For example, in case of form working with Peri (Germany) formworks, concreting conditions (the concreting speed mostly) must be adapted so as the lateral concrete forces not to get over the evaluated values through standards DIN18218.
- As a general rule, in case of vertical formworks for buildings construction, where the height of the formworks is about equal with one floor height, the hydrostatic pressure on the height of the fresh concrete column is recommended to be taken into account, without the risk of over sizing the formwork, but the safety coefficient regarding the formwork allowable abnormality will grow up. For this load, the optimal form working solution is to use primary horizontal retaining walls and on unequal distances and rigid vertical headmistress, at equal distances and only with two secondary retaining wall on every headmistress.
- The maximum pressure limiting on the height of the formwork, as a part of the hydrostatic pressure, can be accepted for higher formworks, height that correspond on the fresh concrete column from the formwork, if through the concreting technology used can be reduced the value of the fresh casted concrete maximum hydrostatic pressure (through the adequacy height). It can be asserted, that the Romanian standards from normative
- C140-86 and the German standards DIN 18202/18218 are presenting near values for the maximum fresh concrete pressure for the same concreting conditions (concrete type, environmental and concrete temperatures, concreting speeds, formwork conditions). The pressure distribution on the vertical size of the formwork is the same, even if in the Romanian normative, for concreting speeds below 10,00 m/h the pressure is decreasing below the proportionality depth h_p , pressure that can reach 0 (for $v_b \leq 1,0$ m/h). It is well-known that in formwork designing, from the formwork foundation (depth H) and to the proportionality depth (depth h_p), the pressure is considered constant, equal with the maximum value p_{max} . (see fig.1.7A1 și 1.7B1).
- In evaluation and grouping of horizontal loads that act on the vertical formworks must be observed the technical prescription that exists in every country, the requirements of legal technical settlements must be applied correctly and with judgment.

References

1. *** Normativ pentru executarea lucrărilor din beton și beton armat, indicativ C 140/86, Buletinul Construcțiilor vol. 12, ICCPDC București, 1986
2. Trelea, A., Giușcă, N., Pamfil, E., Tehnologia și mecanizarea lucrărilor de construcții civile, industriale și agricole, vol. 1, 2, Institutul Politehnic Iași, Iași, 1988.

3. Domșa, J., Ionescu, A., Utilaje, echipamente tehnologice și procedee performante de betonare, Editura Oficiul de informare documentară pentru industria construcțiilor de mașini, București, 1994.
4. Cod de practică pentru executarea lucrărilor din beton, beton armat și beton precomprimat, indicativ NE 012-99, Buletinul Construcțiilor vol. 8-9, INCERC București, 1999.
5. *** Annales N° 78 de l'ITBTP, La Poussée du béton sur les Coffrages.
6. *** Coffrages, Livre 2002, Catalog PERI, 2002.
7. *** System H Hünnebeck: Tekko, Manto, Rasto, Topec, Tunnel, ID15, Compact-Lift, Catalog Hünnebeck, 2005.
8. *** Goliath, armatura di solai con travi e puntelli ad alta portata, catalog Faresin, Italia, 2005.

Modeling and simulation of ventilation in fire emergency situations

Popa Constantin¹, Ion Anghel² and Valeriu Panaitescu³

¹Fire Officers Faculty, "Alexandru Ioan Cuza" Police Academy, Bucharest, Romania

²Fire Officers Faculty, "Alexandru Ioan Cuza" Police Academy, Bucharest, Romania

³Energetic Faculty, Universitatea „Politehnica”, Bucharest, Romania

Abstract

The article below treats the problem of ventilation in fires, as it is in Romania, a rather new and modern technique to keep the evacuation hallways and stairwells free of smoke and hot gases resulted from fires.

The computer simulations made in this work prove that using this method can really make a difference in a fire emergency situation.

The program used (Fire Dynamic Simulator) offers information about the temperature, concentration of gases and visibility in the compartments of the simulation.

KEYWORDS: ventilation in fires, FDS, smoke and hot gases.

1. INTRODUCTION

In the firefighting domain, the term “ventilation” is used to define the removal of heated air, smoke and other airborne contaminants from a structure, and their replacement with fresher air. Tactical ventilation of a fire requires the intervention of the fire service to open up the building, releasing the products of combustion and allowing fresher air to enter. Positive Pressure Ventilation (PPV) is achieved by forcing air into a building using a fan, to increase the pressure inside, relative to outside atmospheric pressure.

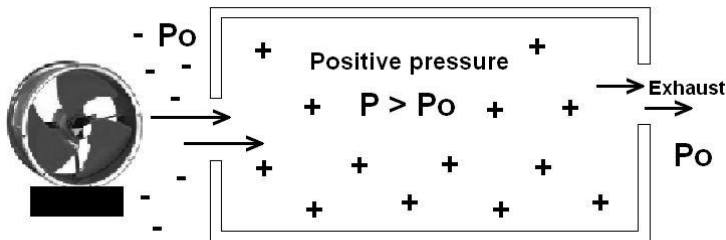


Figure 1. Basic principle of Positive Pressure Ventilation

Extracting smoke from the fire compartment as a part of operational fire fighting would be most beneficial, but sometimes it involves certain risks when initiated during the fire. In some cases the smoke ventilation is advantageous: the hot gases are removed from the fire enclosure, the visibility improves and the enclosure cools down. But, of course, in other cases the opposite happens: with the accelerated burning rate, more smoke is spread around, and the temperatures rise. The basic principles of PPV are relatively simple, as can be seen in figure 1.

All researches taken in this area concluded that PPV can contribute to the effective tackling of incidents - in the case of the present research, involving multi-storey buildings, both for smoke clearance and to keep means of escape clear for evacuation.

2. PRACTICAL CONSIDERATIONS

As said, Positive Pressure Ventilation is accomplished by using high powered fans outside the burning building – typically close to a door opening – to force heat and smoke out of the building. An exhaust opening, e.g. a window, is required to direct the smoke out in a controlled way. At its best, the PPV technique rapidly reduces temperatures, and the removal of smoke and toxic gases improves visibility inside the structure, increasing in the same time, the survivability for potential victims.

2.1. Experimentally verified advantages of PPV [1]

The experimentally verified advantages of using PPV in a fire emergency situation are:

- reduced temperatures: at key fire fighting positions, for example, PPV contributed to temperature reductions from 450 °C to 50 °C within 1 minute;
- improved air quality: PPV was shown to contribute to oxygen addition and carbon monoxide removal;
- faster smoke removal and faster restoration of visibility: when PPV was used, fire fighters had water on a residential fire 6 min after it began and were walking upright in a cool, high-visibility environment. By contrast, 8 min after the start of a second, identical fire in which PPV was not used, fire fighters were still crawling around a hot, smoke-filled environment;
- reversal of the direction of flames away from the fire fighting location: for example, flashover flames that entered a hallway were pushed back into the burning room soon after the start of PPV;
- no spread of heat damage.

If, when we talk about the reasons why PPV is not widely used in the developing countries, such as Romania, the answer is obvious. On one hand, the infrastructure

of buildings and city housing are not so complex, and on the other hand, fire service is still caught in a developing stage, and do not find the reserves to properly invest at large scale in PPV; The mechanical basis respectively power fans, exist as firefighting equipments, but the “know how” to use them and create PPV in order to use it during a fire, and not only after it is suppressed, to exhaust the smoke, is not fully developed. Therefore, this research proves once again that the development of fire system in Romania and all developing countries should evolve, but, if finances are invested only in equipment, but not in tactical firefighters education also, the evolution is not a real and healthy one.

As well as for developing countries, but mainly for Western Europe and American fire services, we can find two more reasons why, although PPV has its benefits, still it is not commonly used by fire departments.

First, the fire service tradition is typically such that it is difficult to get new technologies or methods accepted; fire fighters are resistant to change. Second, the concept of introducing large amounts of fresh air into a burning building is not popular. [2]

2.2. Stair shaft venting analysis

The authors chose to underline ventilation of a stair shaft, as it is a very important part of a building, in case a fire or other emergency situation occur, that’s because it is the most usual and rapid way to get out of the building (civilians), but also to get into it (firefighters).

Escape stairs need to have a satisfactory standard of fire protection if they are to fulfill their role as areas of relative safety during a fire evacuation, and that is why every internal escape stair, as standards demand, should be a protected stairway (i.e. it should be within a fire-resisting enclosure). [4,5,9]

In an assessment of stair shaft pressurization, it was found that it may be advantageous to use PPV to assist firefighters to reach the fire floor, locate and fight the fire, clear the stair shaft of smoke or maintain a stair shaft free of smoke for evacuation. [3,10]

In some pioneering fire brigades in the USA, PPV has become a standard operating procedure. The Los Angeles department is already routinely using PPV to pressurize stair shafts in high-rise buildings. Based on experience, probably the most amazing benefit of PPV to the fire fighter is the increase in visibility. [1]

If the aim of PPV was to ensure that smoke does not permeate into an initially clear stairwell, a small vent should be created beyond the fire, on the fire floor, and the stairwell pressurized by deploying the fan in the ground floor doorway while keeping all vents in the stairwell closed.

This reduces the likelihood of smoke entering the stairwell. It may be possible to clear the stairwell of any existing smoke by creating an outlet vent at the top, small enough so that the pressure in the stairwell does not drop too much.

All this information was used in the following simulations, to verify the need and the advantages of using PPV in pressuring a stair shaft, in the event of a fire.

3. FDS SIMULATIONS ON A STAIR SHAFT. RESULTS, DISCUSSIONS.

Fire Dynamics Simulator (FDS) is a computer program designed by the specialists at National Institute for Standards and Technology (NIST) in U.S.A., and is used by fire researchers all over the world, to simulate the development and all involved characteristics of fires, with given primary conditions (fire enclosure, fuel, wind current, etc.).[6,7]

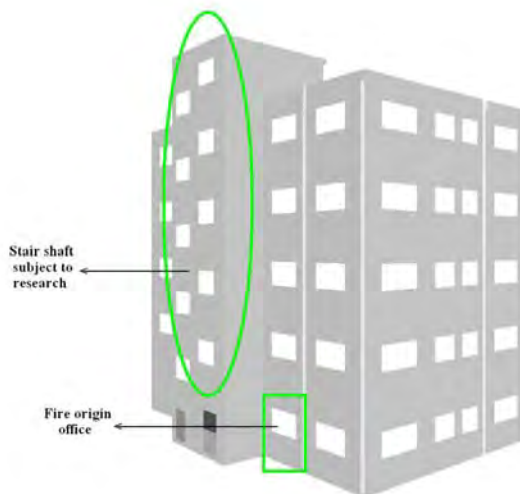


Figure 2. The building subject of the fire modeling. Emphasize on the fire origin office and on the stair shaft (in section) to be pressurized

Two simulations were made, both of them on the same building, with the same conditions. The only difference is that in the first - which will be called standard simulation – no PPV was used; the second, PPV simulation, is the same as the first one, with PPV acting in the stair shaft, pressuring it. The stair shaft subject to this research, and the fire compartment as explained in the following, are highlighted in figure 2.

The fire origin office is situated close to the fire shaft, as it can be seen in the figure above. The room has 3m x 3m x 3m dimensions, an open door of 2m x 0,8m and a closed window of 1m x 1,6m x 0,004m. The fire load is considered to be 511 MJ/m², and the heat release rate (HRR) 250 KW/m², according to the destination of the enclosure (see Euro Code 1).[8]

Simulations are made in a computational domain of 14 m wide, 18 m long and 18 m height. The total number of cells inside who are made hydrodynamic calculus is 656.100. The fire ignites on the locker in the office; the ambient temperature is 20 °C. The simulations were done on a computer with 2400 MHz Intel Core 2 Duo processor and 1024 MB DDRAM memory. In the table 1 can be seen few parallel information about the two simulations.

As a real story of this hypothetically situation, we can have the following: during a normal work day, the office situated at the first floor of the four storey building, burst on fire, because of an electric malfunction. With the door being open, the smoke soon fill up the hallway (see figure 3) situated at the first floor, and begin to evolve on the stair shaft, through the imperfections of the door situated between the hallway and the stair shaft. Smoke emerges also through the toilet window (0,3 m²) which was left open (see figure 3).

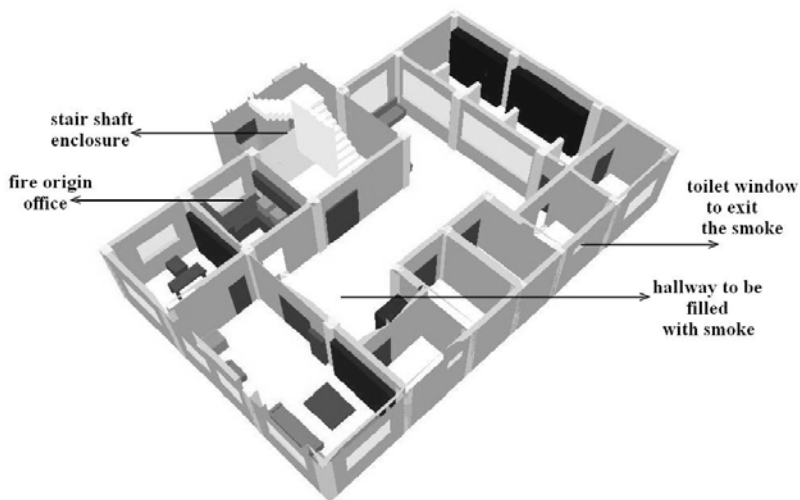


Figure 3. The building subject of the fire modeling. Plan of the first floor (in section)

Firefighters soon arrive, (120 seconds after the initiation of the fire) and in order to allow people at upper floors to use the stairs to evacuate the building, pose at the entry into the stair shaft, a powerful fan which generates a great air flow current,

pressuring the enclosure, stopping the smoke to dissipate outside the hallway, on the stair shaft, in large quantities.

Table 1. Parallel information for the two simulations

No.	Item to compare	Standard simulation	PPV simulation	Observations
1	Total time of simulation	600 s	600 s	The real time of computer working differs from one simulation to another, because in the second one, a new condition was introduced, the pressure produced by the fan
2	Real time of computer working	9,34 hours	10,49 hours	
3	Total number of iterations	8936	9521	

As previously said, standard simulation shows what could have happened if no PPV would have been used, and the PPV one shows what happened when firefighters used the fan to create a safer exit for the building users.



Figure 4. FDS Slice - Image of the two simulations at 140 s fire time. Only smoke visible. Standard simulation (left), and PPV one (at the right side of the figure)

The stair shaft was approximately 17, 5 m high with a footprint of 20 m². The total volume of the stair shaft was approximately 350 m³. This does not take into consideration the volume filled by the stairs and landings.

Assuming the airflow through the exterior doorway produced by the PPV fan was 1 m³ /s, results an air change on the stair, once at 350 seconds.

The venting rate for the stair shaft provided by the PPV system was approximately 10,2 air changes per hour (ACH). This is high compared with the 6 ACH required by the NBC for venting floor areas in high-rise buildings to aid firefighting. [3]

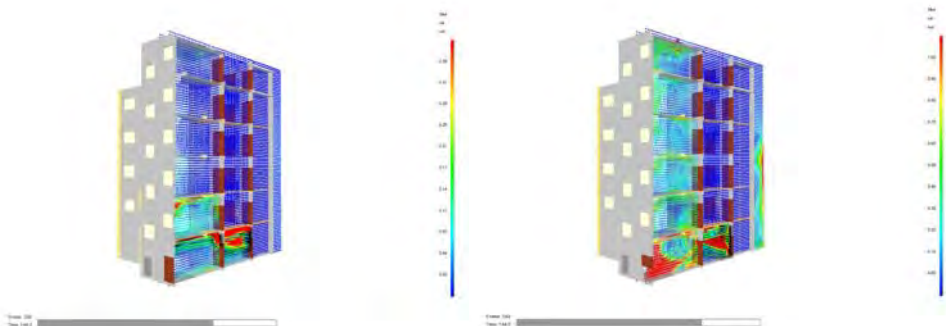


Figure 5. FDS Slice - Image of the two simulations at 144 s fire time. Only air flow speed vectors. Standard simulation (left), and PPV one (at the right side of the figure)

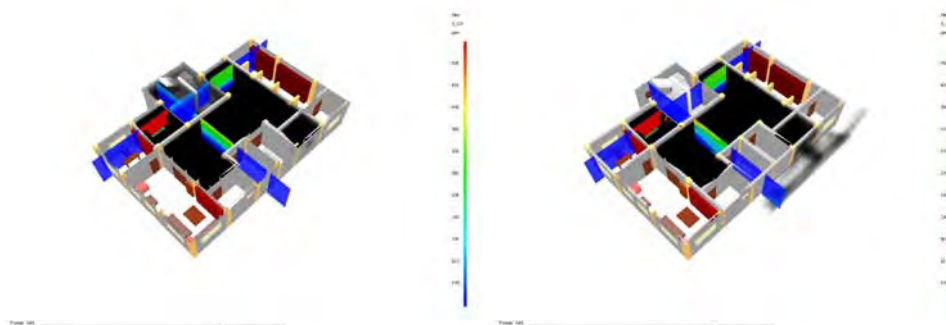


Figure 6. FDS Slice at the level of the first floor - Image of the two simulations at 144 s fire time. Only levels of carbon monoxide. Standard simulation on the left, and PPV one on the right side of the figure

In these conditions, it can easy be seen in the parallel pictures (see figure 4) that smoke is allowed in a large quantity inside the stair shaft in the standard simulation, while the pressure in the stair shaft produced by the fan (firefighters fan or the fan which the construction is provided with, no matter) do not permit smoke

to dissipate in large quantity. Also the same, in figure 5 can be observed the real differences between the air flow speed vectors, in the 6th figure the differences in levels of carbon monoxide, and in the 7th one, levels of temperature.

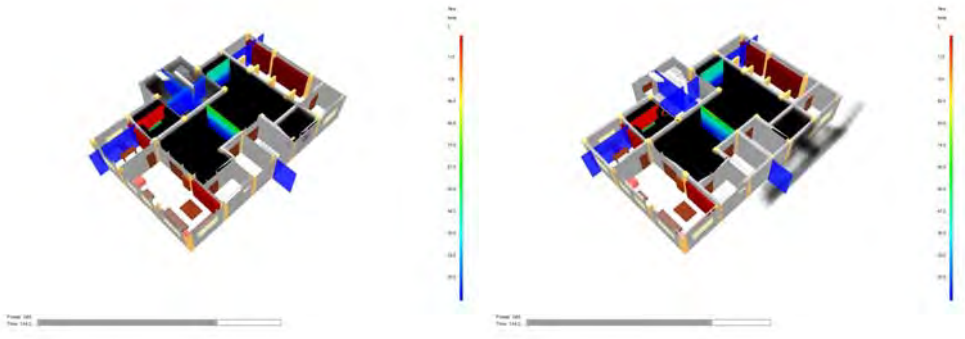


Figure 7. FDS Slice at the level of the first floor - Image of the two simulations at 144 s fire time. Only levels of temperature. Standard simulation on the left, and PPV one at the right side of the figure

A comparison of the results in the two simulations can be viewed in table 2. Analyzing the table, we can conclude:

- If a level of 100 ppm causes severe sickness [11], then for sure, the diminishing (starting at 120 s of PPV simulation) from 40 ppm to 15 ppm is more than welcome, when we think about usual people that need that exit, and are not wearing breathing apparatus;
- The level of smoke is quickly dissipated, finally is drawn out of the building through the small venting outlet way on the top of the shaft (0,25 m²);
- Pressure, by using the fan, rises from 0,45 Pa to 15 Pa;
- Temperatures are cooled down from approximate 35 °C in the standard simulation, to 20 °C in the PPV one.
- Visibility. An important item, it rises from minimum of 0, 5 meters to a minimum of 16 meters.

Table 2. Comparison of the two simulations results, at chosen simulation time of 144 seconds, analyzed on the stair shaft

	Items to compare	Standard simulation	PPV Simulation
1	Levels of Carbon Monoxide	Max 40 ppm	Max 15 ppm
2	Level of smoke	Approx. upper half of the 1 st floor, evolving to the 2 nd	dissipated to upper floors
3	Pressure into the shaft	15 Pa	0,45 Pa
4	Temperatures	35 °C	20 °C
5	Visibility	Min 0,5 m	Min 16 m

4. CONCLUSIONS – WHY IS PPV A LIFE SAVER?

The information and simulations above proved the expected: when a fan is used to pressurize a stair shaft, that space which have a greater pressure than the enclosure directly connected with the fire, do not permit the smoke and hot gases to permeate in large quantities into the shaft. The fire incidents history is filled with sadly stories about casualties in a high rise buildings at the top floors (intoxicated with smoke), while the real fire occurred at the lower ones. That’s why using a fan can make all the difference in saving human life and property.

References

1. Maarit T.- *Smoke ventilation in operational fire fighting*, VTT Building Technology Technical Research Centre of Finland, Espoo, 1997.
2. Martin T. - *The use of positive pressure ventilation in firefighting operation*, Home Office Research into Positive Pressure Ventilation, 2002.
3. Loughheed G.D., McBride P.J. and Carpenter D.W. - *Positive Pressure Ventilation for High-Rise Buildings NRC-CNRC Research*, Institute for Research in Construction National Research Council, Canada, 2002.
4. Rimen, J.G. - *An assessment of the use of positive pressure ventilation in an unpressurised Stairwell*. London, 1997.
5. Brian H. - *Firefighting in under-ventilated compartments*, Fire Statistics and Research Division Office of the Deputy Prime Minister, London, 2005.
6. McGrattan K. B. - *Fire Dynamics Simulator (Version 4) Technical Reference Guide*, NIST Special Publication 1018, Fire Research Division, Building and Fire Research Laboratory in cooperation with VTT Building and Transport - Finland, NIST, 2006.
7. Anghel I., Darie E. și Flucuș I. - *Simularea numerică a unui incendiu într-o clădire cu structură ușoară* - The IXth Scientific Communications Session with international participation of “Al. I. Cuza” Police Academy – Fire Officers Faculty, p. 101-108, Bucharest, 2006.
8. *** Eurocod 1: *Acțiuni asupra structurilor Partea 1-2: Acțiuni generale-Acțiuni asupra structurilor expuse la foc*, p. 43-44, 2004.
9. *** *Normativ de siguranță la foc a construcțiilor*, P 118- Institutul de proiectare, cercetare și tehnică de calcul în construcții, Bucharest, 1999.
10. *** NFPA 204 - *Standard for Smoke and Heat Venting*, National Fire Protection Association, U.S.A., 2002.
11. Flucuș I., Anghel I. and Popa C. - *Human incapacitation in fires - the XIth Scientific Communications Session with international participation „Man in the organization based on knowledge” -Technical sciences section - „Nicolae Bălcescu” Land Forces Academy*, p. 232-239, Sibiu, 2006.

Gamma Radiation Shielding

David Procházka¹, Dalibor Beneš²

^{1,2} *Institute of Building Materials and Components, Faculty of Civil Engineering, Brno University of Technology, 602 00 Brno, Czech Republic*

Summary

The paper concerns the shielding of gamma and X-ray radiation. We are confronted with this problem for instance in hospitals, nuclear plants or in departments for non-destructive testing. With respect to the fact, that these radiations are in greater doses harmful for the man it is necessary to protect adequately persons working in these plants. This protection is realized by shielding of the given radiation. The here tested shielding material is barite.

KEYWORDS: barite, shielding, ionizing radiation, ionizing radiation protection, shielding plasters.

1. INTRODUCTION

This paper concerns one of the radiation shielding methods in workplaces and plants exposed to the effect of X-ray and gamma radiation. We can be confronted with both these types of radiation first of all in hospitals and in nuclear plants. This radiation is produced by apparatuses such as X-ray equipments, linear accelerators, mammographs, research or industrial reactors etc.

Considering the fact that this radiations have ionization character they have in greater extend harmful influence on the human organisms. The excessive exposure of persons to these radiations can cause health troubles. The effect of these troubles can be in the extreme the sc. radiation sickness which means direct danger for bodily organs of vital importance.

It is necessary to secure the exposed workplaces in an adequate way to prevent these dangerous effects. This is made by the sc. shielding i.e. the whole room or only the mentioned equipment is surrounded by a layer from protective material. This material must be chosen according to the character of the radioactive radiation and according to local conditions. We have tested barite sand as shielding material in this work.

2. IONIZING RADIATION

The ionizing radiation is the radiation which is able to ionize the material. It means that this radiation is able to furnish to the particles of the material energy which causes the liberation of electrons from the atom shell. If the particle is neutral, it splits into two differently charged ions. The energy necessary for the fission is called the ionization energy. It is normally expressed in electronvolts ($1 \text{ eV} = 1.602 \times 10^{-19} \text{ J}$). The formation of the ionizing radiation is given by complicated processes, which take place at the atomic level.

The sources of the ionizing radiation are either natural or artificial. The natural sources are the non-stable nuclides of certain elements (e.g. uranium, thorium, radium, radon etc.) and the stars, as the source of so-called cosmic radiation. The artificial sources are the equipments constructed by the man (atomic power stations, particle accelerators, X-ray apparatuses, etc.)

The alpha, beta, gamma and neutron radiations are classified as ionizing radiations.

Alpha radiation: It is the stream of helium nuclei – i.e. of two protons and two neutrons. This radiation is formed in the case of the heaviest nuclei (uranium and trans-uranium). These elements when they penetrate into the substance extract, owing to their “double charge”, very effectively the electrons from the atom shells, whereby they lose quickly their energy and they stop after about 0.1 mm in substances which have the density of water or of tissue. Consequently this radiation penetrates weakly and it can be stopped even by a sheet of paper. However it can be as harmful as radiation inside the organism.

Beta radiation: It is the stream of electrons or positrons. These particles are moving with very high speed and they are formed in atomic nuclei as the result of neutron ($n^0 \rightarrow p^+ + e^- + \bar{\nu}$) and proton ($p^+ \rightarrow n^0 + e^+ + \nu$) disintegration. This radiation stops after 1 – 4 mm in substances with the density of water and in heavy metals after about 0.1 mm.

Gamma radiation: It is the most penetrating radiation. It is not the stream of particles but energy which is emitted by the atoms nuclei having excess of energy. It is strongly ionizing. It liberates from substance charged particles as the result of photo effect, Compton effect and the formation of electron-positron pairs. It can be weakened by the layer of materials containing the nuclei of heavy metals (lead, tungsten, barite, limonite etc.)

Neutron radiation: It is the stream of neutrons which are formed during the fission of nuclei. The neutrons have no charge and they don't ionize during the penetration through the material. The ionization of the medium is caused only by secondary particles which are formed during the interaction of neutrons with the atomic nuclei (the neutrons react after entering into the material exclusively with

the atomic nuclei). The protection against this radiation is formed by light atoms (hydrogen, boron) and by substances containing these elements (water, paraffin, concrete). The shielding with materials containing heavy elements is not effective – the heavy nuclei reflect the neutrons.

3. INTERACTION OF RADIATION WITH THE SUBSTANCE

Generally interactions take place between quanta of radiation with electron shells and the atomic nuclei during the transit of different ionizing radiation. All these interactions and processes cause that during the transit of ionizing radiation quanta through the substance these particles lost their energy, they retard and finally they stop (if the medium of the material is sufficiently large). The quanta of radiation mark the ionizing track formed by free negative electrons and positive ions. A part of these ions and electrons interacts with each other but another part can initiate new chemical bindings and reactions in the surrounding material.

Table 1: Specific Ionization of Radiation

RADIATION	RANGE IN AIR [cm]	SPEEDS [km·h ⁻¹]	SPECIFIC IONIZATION [ion pairs/cm]
Alpha	5 – 7	3 200 – 32 000	20 000 – 50 000
Beta	200 – 800	25 – 99 % speed of light	50 – 500
Gamma	use of half-thickness	300 000	5 – 8

The following interactions with the material take place during the gamma radiation:

Photoefekt: The γ radiation “comes into collision” with the electron e^- bound in the atom shell and transmits to it all its energy and disappears. The electron which received this energy is liberated from the atom bound and blows up from it.

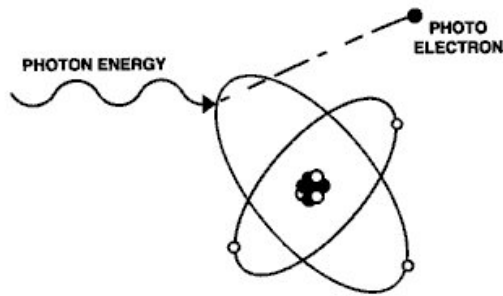


Figure 1. Gamma interaction by photoelectric effect

Compton effect (scattering): It takes place in cases, when the γ radiation comes into “collision” with the free or weakly bound electron. The photon transmits to the electron a part of its energy, it reflects softly and moves further in other direction and with lower energy. The electron accelerates after this collision.

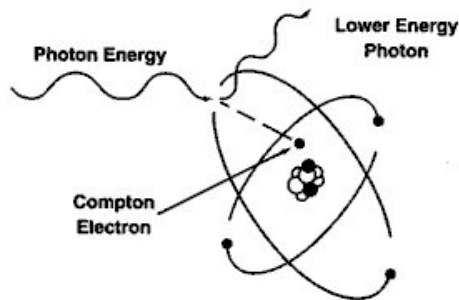


Figure 2. Gamma interaction by Compton scattering

The formation of electron – positron pairs: If the photon enters into the material with sufficiently high energy, the collision with the nucleus can cause the disintegration into an electron and positron. The electron becomes the part of the atom and the positron annihilates with another electron of the atom under formation of two photons and gamma radiation.

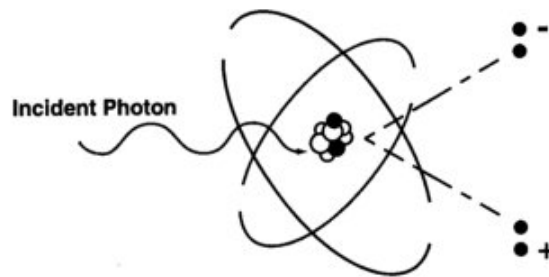


Figure 3. Gamma interaction by pair production

The above described mechanism of γ radiation with the mass causes that at least a part of ionizing radiation is absorbed during the transmission through the material. In the case of radiation with weak penetration everything is absorbed, in the case of penetrating radiation a part of quanta is absorbed and a part passes through.

The shielding of γ radiation: The most useful shielding materials for the gamma and X-ray radiation are materials with high density – first of all lead, tungsten, uranium (it is necessary to consider that uranium is not only very expensive but it is also radioactive). It is necessary to use the thicker shielding layer the higher is the photons energy of gamma radiation. Lead glass with high lead oxide content in the melt is used if it is necessary to maintain the optic visibility. It is sometimes more advantageous for economical reasons to apply a higher layer of material with lower shielding capacity, if it is possible following the configuration of the radiator, of the radiated materials and of the detector. This is as the rule in the building conception of workplaces with ionizing radiation where in addition to the brick masonry more dense materials are used – concrete with the admixture of barite, barite plasters etc.

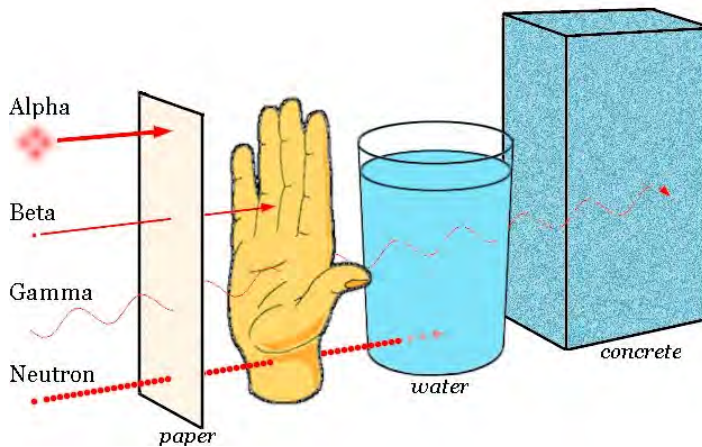


Figure 4. Radiation penetration

4. MEASUREMENTS OF THE RADIATION EFFECT

The dosimetry is concerned with the measurement and research of the radiation effects on materials. The basic values in dosimetry are:

- The radiation dose D : it is the energy of the ionizing radiation absorbed in the given place of the radiated material per mass unit. It is given by the relation $D = \Delta E / \Delta m$. The unit is gray = Gy = J/kg.
- The dose rate D' : it is the dose received in the given place by the radiated material in the unit of time i.e. the relation between the increase of the dose ΔD during the time interval Δt : $D' = \Delta D / \Delta t$. The unit is Gy / s.
- The dose equivalent: it is given in the considered tissue by the product of the absorbed dose D in the given place and of the quality factor Q : $H = Q \cdot D$. The unit is sievert (Sv)

5. BARITE

Barite is a natural mineral with high density ($\approx 4\,500 \text{ kg} \cdot \text{m}^3$). The chemical composition is barium sulfate (BaSO_4). Barite contains often admixtures of celestite (SrSO_4) and of anglesite (PbSO_4) – see figure below. It exists in different colours – most often white, yellowish, pinkish, greenish, red, brown etc. The hardness is 3.5 following Mohse, the streak is white. The crystals are tabular or pillarlike, mostly oblong in different directions. The barite is used mostly for shielding of X- and gamma rays. Further it is a raw material for the production of

glazes, enamels and special glasses. It is also utilized in the paper production in pyrotechnics or in the oil industry. The world resources are about 300 million tons. The finding places are mainly in Poland, Germany and in the USA.



Figure 5. Barite mineral

For the production of mixtures we have used aggregates from Slovakia. These aggregates were sieved to the fraction 0 – 4 mm.

6. PROPOSAL AND TESTING OF THE BARITE MIXTURE

The barite is as mentioned above suitable for the shielding of the gamma radiation. The barite sand was selected for the actual shielding system. This sand can be used as aggregate into dense concrete or into plasters. It was necessary, considering the non-traditional aggregate to design a suitable and functional formulation. The greatest problem during the work with the barite mortar was the segregation of the heavy aggregate and the difficult workability of the fresh mixture. It was therefore necessary to use a suitable admixture to change this unfavorable situation. The formulation following table 2 was designed after some unsuccessful proposals and tests.

Table 2: The proposed formula

PARAMETER		VALUE
COMPOSITION [%]	cement	12
	barite sand 0-4 mm	88
	admixture A	1
	admixture B	0,12
DRY MASS VOLUME WEIGHT OF THE DRY MIXTURE IN SHAKED STATE [kg·m ⁻³]		2 830
WATER-CEMENT RATIO [-]		0,29
BULK DENSITY OF CONCRETE [kg·m ⁻³]	fresh mixture	3 140
	after 28 days of maturing	3 070

The testing of technological parameters started after the successful design. The testing was made with prisms 40 x 40 x 160 mm. The values are in the table 3.

Table 3: Technological properties

VLASTNOST		VALUE
WATER-CEMENT RATIO [-]		0,29
BENDING TENSILE STRENGTH [MPa]	after 1 day	1,6
	after 28 days	3,3
COMPRESSION STRENGTH [MPa]	after 1 day	6,6
	after 28 days	22,4

Samples with the thickness 10, 20, and 30 mm were prepared following the designed formula. These samples were tested by X-ray radiography. The intensity of X-ray radiation was gradually increased by voltage change of the X-ray tube. The resulting shielding values are in the tables below.

Sample thickness 10 mm

VOLTAGE <i>U</i> [kV]	DOSE RATE <i>D</i> [pGy/s]					mean value
	measurement No.1	measurement No.2	measurement No.3	measurement No.4	measurement No.5	
60	3 200	3 130	3 120	3 120	3 210	3 160
80	32 300	30 300	32 100	30 800	31 400	31 400
100	364 000	358 000	368 000	371 000	342 000	360 600
135	3 060 000	3 250 000	3 180 000	3 160 000	3 220 000	3 174 000

Sample thickness 20 mm

VOLTAGE <i>U</i> [kV]	DOSE RATE <i>D</i> [pGy/s]					mean value
	measurement No.1	measurement No.2	measurement No.3	measurement No.4	measurement No.5	
60	61	62	59	62	60	61
80	190	201	185	198	181	191
100	7 730	7 540	7 480	7 610	7 280	7 530
135	360 000	330 000	325 000	316 000	338 000	334 000

Sample thickness 30 mm

VOLTAGE <i>U</i> [kV]	DOSE RATE <i>D</i> [pGy/s]					mean value
	measurement No.1	measurement No.2	measurement No.3	measurement No.4	measurement No.5	
60	39	39	40	40	41	40
80	57	56	57	56	58	57
100	642	650	653	645	651	648
135	68 800	69 800	70 100	67 600	69 000	69 100

Sample thickness 40 mm

VOLTAGE <i>U</i> [kV]	DOSE RATE <i>D</i> [pGy/s]					mean value
	measurement No.1	measurement No.2	measurement No.3	measurement No.4	measurement No.5	
60	29	34	30	29	32	31
80	49	57	52	51	56	53
100	159	155	149	158	150	154
135	10 100	10 600	9 800	12 100	10 300	10 600

Sample thickness 50 mm

VOLTAGE <i>U</i> [kV]	DOSE RATE <i>D</i> [pGy/s]					mean value
	measurement No.1	measurement No.2	measurement No.3	measurement No.4	measurement No.5	
60	23	24	24	26	23	24
80	50	51	48	53	46	50
100	146	132	142	140	138	140
135	2 260	2 350	2 340	2 160	2 280	2 280

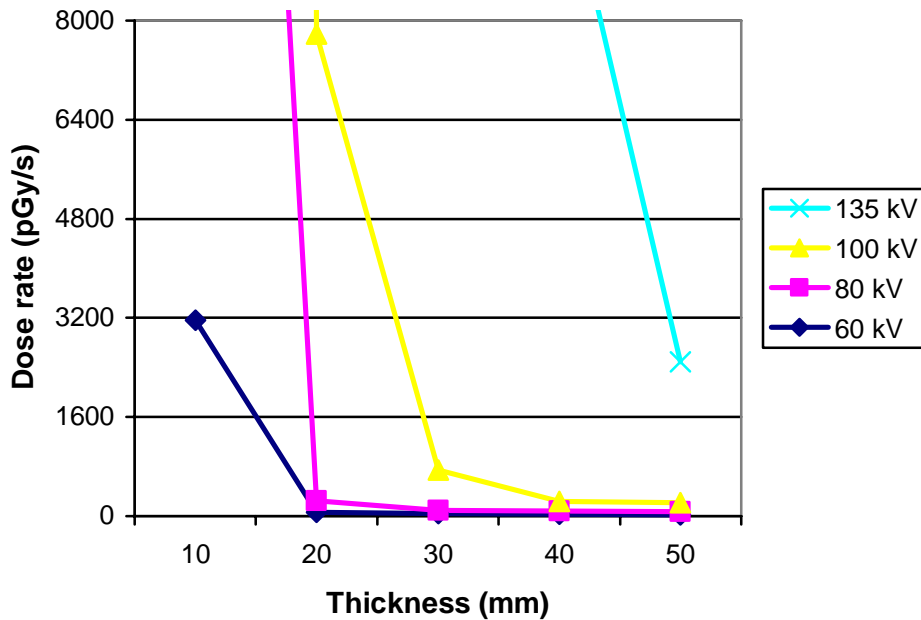


Figure 6: Comparison of shielding properties for individual thicknesses

The graph shows that the radiation to which the body is exposed has exponential character. This is very important information! In the case that the proposal of the radiation shielding is undersized the dose received by the man grows exponentially. This can cause a quick process of the radiation sickness symptoms.

The graph further shows that the stronger is the radiation (the stronger is its energy), the thicker must be the protective layer. In addition the protection against this radiation is more difficult.

7. CONCLUSION

The measured values show that the above tested formula has relatively good strength characteristics. The designed mixture is suitable among others also for bearing purposes.

Heavy concrete or plaster can be prepared from this mixture and the shielded space will be relatively effectively protected against the effects of X-ray and γ radiations.

Acknowledgements

The work was supported by the MSM 0021630511 plan: Progressive Building Materials with Utilization of Secondary Raw Materials and GA 103/05/H044 project.

References

1. RNDr. Vojtěch Ullmann: Nuclear and Radiation Physics (online), (in Czech).
2. Ivan Štoll: Physics of the Micro-world , Prometheus, Praha, (in Czech).
3. Pavel Schmid et al.: Quality Control, Cerm, Brno 2001 (in Czech).

Computer Simulations for Physics Laboratory

Irina Radinschi¹, Cristian Damoc²

¹Department of Physics, “Gh. Asachi” Technical University, Iasi, 700050, Romania,
radinschi@yahoo.com

²Faculty of Automatic Control and Computer Science, “Gh. Asachi” Technical University, Iasi,
700050, Romania

Summary

In the recent years computer simulations have become an integrated part of basic physics and engineering education, and have also been used together with the experiments. They don't replace the traditional methods of learning physics but are powerful tools for the understanding of physics laws and phenomena, and developing skills of measurement and analysis. Furthermore, they are not affected by the errors generated by the measurement process and the sensibility of apparatus. One of our main targets is to develop and improve our physics course level targeting students' difficulties, and including the computational methods as efficient tools to assist them in learning physics. In this way we develop an open window to the virtual labs and simulations, and also allow the students to use a comparative mode of learning: experiments and software applications. Moreover, our set of physics simulations can be implemented in the distance learning through internet (e-learning) which is partially or entirely based on Web and Internet courses and homework's delivery.

In this paper we present a computer simulation elaborated in Adobe Flash CS3, which is designated for the study of virtual evolution of the photoelectric effect. The aim of the application is to check the experimental verification of the laws of photoelectric effect. These laws are given by the dependence between the photoelectric current intensity I_f and the voltage U , $I_f = f(U)_{E=const.}$ for constant values of the illuminance E , and the dependence between the photoelectric current intensity I_f and the illuminance E , $I_f = f(E)_{U=const.}$ at constant values of the voltage U . The computer simulation provides the

calculations for the values of illuminance $E = \frac{I}{r^2}$, with I the luminous intensity

of light which is considered $I = 1 \text{ cd}$ and the plotting of these two graphs. The application also works as a checking tool of the results yielded by experimental work. Screen-shot pictures of the application interface are presented.

KEYWORDS: computer simulations, physics learning, computational methods

1. INTRODUCTION

The recent years of experience in the field of physics learning and the development of the programmable web and new computational technologies have pointed out the necessity of implementation of the computer simulations [1]-[2]. More, these computational methods do not imply the renunciation at the traditional methods even in the future a rapid and efficient way of improving knowledge would consist in the using at large scale of the Web technology. Computer simulations of physics phenomena are powerful tools for learning physics concepts and developing skills of measurement and analysis. The simulations will not substitute for laboratory experience, but can be used for improving such experience and for a better understanding of the physics phenomena. They are not affected by the errors generated by the measurement process and the sensibility of apparatus.

In the last two years we have implemented some courses and computational tools [3]-[9] to assist our students and to improve the learning process. In a first stage we proposed some “teaching-while-quizzing” tests [10]-[12] that are already used by our students. The next stage will consists of a set of computer simulations [13], and we have already started the implementation of physics simulations in our physics laboratory with the simulation of the photoelectric effect laws using Adobe Flash CS3 [14] program. One of our main targets is to develop and improve our physics course level targeting students’ difficulties, and including the computational methods as efficient tools to assist them in learning physics. For making experiments and demonstrations at the physics laboratory the students use the computers as scientific tools for collecting, analyzing, visualizing and modeling real data. For students is very important to be familiarized with the physics laws and phenomena described in our physics course, and with some computational programs that will make easier the understanding of physics concepts, and facilitate the developing of their ability to apply these physics concepts to physical situations and reason with them. The students will be able to apply the ideas and skills.

The purpose of this paper is to present a physics simulation elaborated in Adobe Flash CS3 [14] program and which is designated for the study of virtual evolution of the laws of photoelectric effect. Two important laws are verified, the current voltage curve, which is given by the dependence between the photoelectric current intensity I_f and the voltage U , $I_f = f(U)_{E=const.}$ for constant values of the illuminance E , and the dependence between the photoelectric current intensity I_f and the illuminance E , $I_f = f(E)_{U=const.}$ at constant values of the voltage U .

2. COMPUTER SIMULATION USING ADOBE FLASH CS3

Through the process of making experiments and demonstrations at the physics laboratory, students came to understand the physics laws and phenomena at a deeper level than at simply attending a course. We want to explore how they interact and learn during a computer-based simulation and for this purpose a total of 175 students have interacted with a computer-based simulation of the laws of photoelectric effect in which they had control over the values of the voltage U and the distance between the source of light and the photoelectric cell. We used modern software and technologies [14], our physics simulation computer application is elaborated in Adobe Flash CS3 program [14] and two simulation conditions are implemented: the study of the current voltage curve $I_f = f(U)_{E=const.}$ and of the dependence between the photoelectric current intensity I_f and the illuminance

E , which is given by the law $I_f = f(E)_{U=const.}$. Adobe Flash CS3 software is featuring a streamlined user interface, advanced video tools, and impressive integration with related software [14] and several updates for integrating into other Adobe products. For making our computer simulation running the students have to know some theoretical notions about the photoelectric effect. These are presented both in English and Romanian in the program and screen-shots. In the following, the screen-shots of the application interface are presented in Figure 1, Figure 2, Figure 3 and Figure 4. Within this application, the user must choose a value for the distance r between the source of light and the photoelectric cell, after which the value of the voltage U starts rising, in order to observe the evolution of the diagram that shows the dependence of I_f on the voltage U

$I_f = f(U)_{E=const.}$. The light-red line unites the obtained points for values of the voltage U , values that are within the range 0-70 V and have a rising step of 5V. The black curve is the diagram of the dependency $I_f = f(U)_{E=const.}$. For the dependence between photoelectric current intensity I_f and the illuminance E , which is described by the law

$I_f = f(E)_{U=const.}$, the students have to read the values of the photoelectric current intensity for the values of the illuminance E , which has a rising step of 0.03 m between 0.2 m and 0.9 m (or between 0.15 m and 0.77 m), at a constant value of the voltage $U=50V$. The black curve represents the diagram of the dependency $I_f = f(E)_{U=const.}$.

Lab Objectives

Lab objectives are the experimental verification of the laws of photoelectric effect. These are:

1. The dependence $I_f = f(U)_{E=const}$, where I_f is the photoelectric current intensity, U is the voltage and $E = \frac{I}{r^2}$ is the illuminance (in lx) and I the luminous intensity of light and r the distance between the source of light and the photoelectric cell. The distance between the source of light and the photoelectric cell is constant.
2. The dependence $I_f = f(E)_{U=const}$, and in this case the voltage U is constant.

Measurements and procedure:

- picking-up the values of the photoelectric current intensity I_f for different values of the voltage $0V \leq U \leq 70V$. Calculations of $E = \frac{I}{r^2}$ with $I = 1cd$. Making the graph with U on x-axis and I_f on y-axis.
- picking-up the values of the photoelectric current intensity I_f for different values of the distance r between the source of light and the photoelectric cell $0,15m \leq r \leq 0,70m$. Calculations of $E = \frac{I}{r^2}$ with $I = 1cd$. Making the graph with E on x-axis and I_f on y-axis.

OK

Figure 1. Lab objectives and measurements and procedure

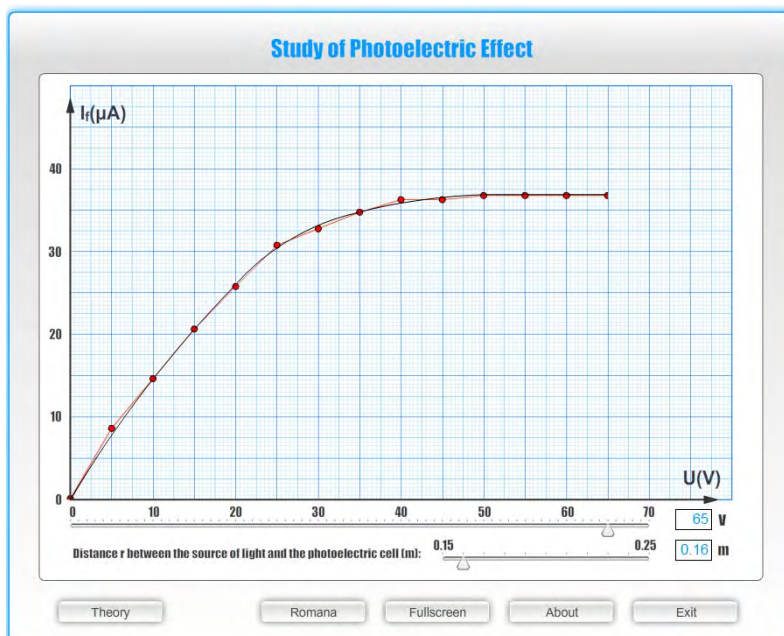


Figure 2. Photoelectric current intensity versus voltage for $r = 0.16 m$

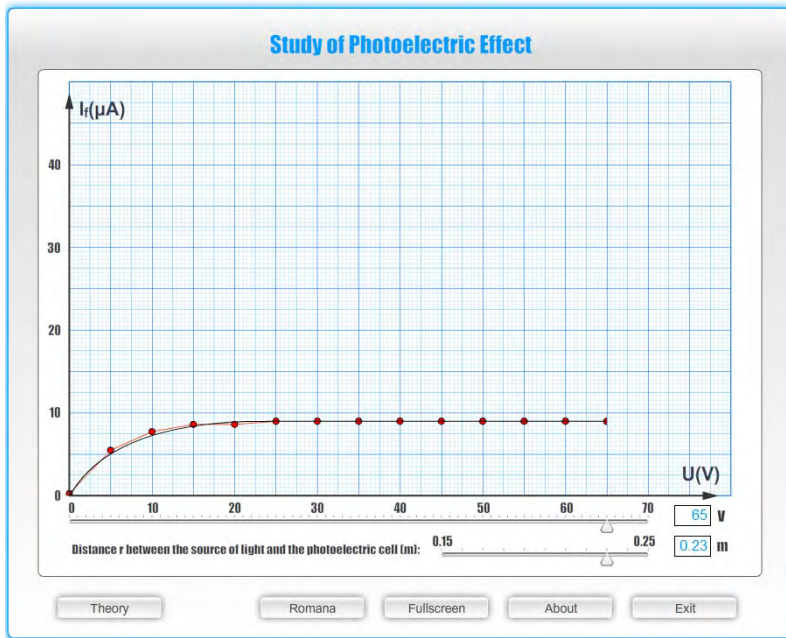


Figure 3. Photoelectric current intensity versus voltage for $r = 0.23\text{ m}$

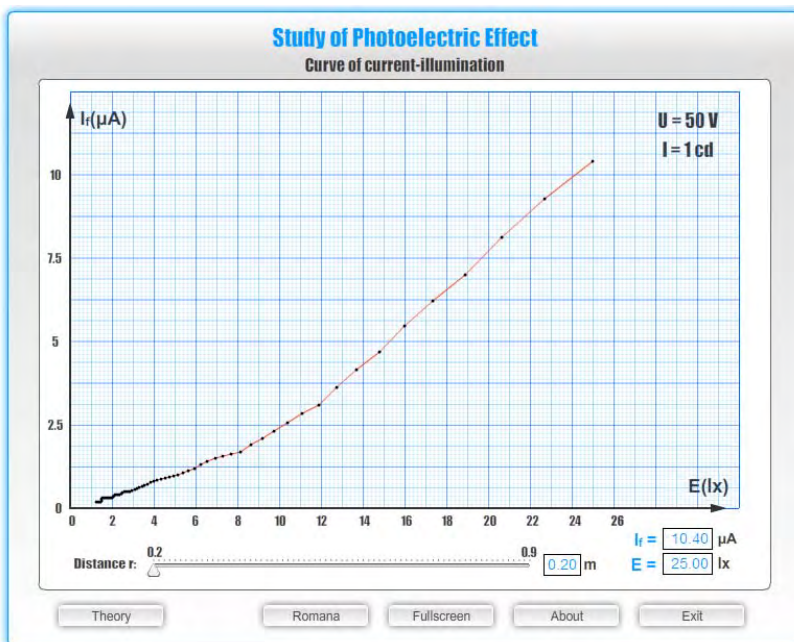


Figure 4. Photoelectric current intensity versus illuminance

At several illuminance levels (see the curves drawn above) one obtains the shape of the photoelectric current intensity versus voltage. In the case of the dependence between the photoelectric current intensity I_f and the illuminance E , which is described by the law $I_f = f(E)_{U=const.}$ the screen-shot of the application interface is given in the Figure 4. The computer simulation gives the possibility of using the experimental data acquired for performing calculations and plotting.

3. CONCLUSIONS

In the last years we have added to the traditional methods of learning physics some computer-based tools like “teaching-while-quizzing” tests and physics simulation computer applications.

The physics interactive simulation computer application that describes two laws of the photoelectric effect was done using the animation and programming environment Adobe Flash CS3 [14], which is professional software by means of which applications, animations and web pages may be created and processed [13]. The application has two menus, a menu in Romanian and one in English, which may be used depending on necessity of preference. Moreover, the application is developed to simulate the values obtained using the laboratory apparatus. The computer simulation is a copy of the real device and can be used at the same time with the experiment, and gives the possibility of making a comparative study between experiment and simulation. It can be also used as a checking tool of the results yielded by experimental work.

Our goal is to allow students to use computer simulations as a method of discovery in physics. The students have in this way an open access to the virtual labs and simulations, and can work with a comparative mode of learning: experiments and software applications. Furthermore, our set of physics simulations can be implemented in the distance learning through internet (e-learning) which is based on Web and Internet delivery of the applications.

Moreover, a complete set of physics simulation of experimental works elaborated in Adobe Flash CS3 program will be implemented in our physics laboratory for improving the learning process. We have elaborated these physics interactive simulation computer applications for describing some important physics phenomena and verifying some important laws of physics. We point out that taking into account the circumstances in our country, our computer simulations will be good new computational tools because they represent a cheaper kind of physics learning.

References

1. sip.clarku.edu; Hennessy, S., Deaney, R. & Ruthven, K., Situated expertise in integrating use of multimedia simulation into secondary science teaching, *International Journal of Science Education*, 28 (7), 701-732, 2006; Jones A., Issroff K., Learning technologies: Affective and social issues in computer-supported collaborative learning, *Computers & Education*, 44, 395-408, 2004.
2. phet.colorado.edu/web-pages/simulations-base.html ; www.mypysicslab.com/; Murariu G., Toma D., A Note About the Simulation Programs for Heat and Molecular Physics Laboratory, physics/0505053; Murariu G., Interactive computer simulations of electrokinetic physics phenomena, physics/0609215, Proceedings of CCP 2007, September 5-8, Brussels, Belgium, 2007.
3. Radinschi I., Ciobanu B., Teste de Fizica, Editura Junimea Iasi, 2006, ISBN (10)973-37-1166-7, ISBN (13)978-973-37-1166-7; Radinschi I., Ciobanu B., Fizica pentru ingineri, Editura Junimea Iasi, 2006, ISBN (10)973-37-1167-5, ISBN (13)978-973-37-1167-4
4. Ciobanu B., Radinschi I., Implementation of Physics Teaching in Engineering Education, The 6-th International Balkan Workshop on Applied Physics, July 5-7, 2005, Constanta, Romania.
5. Ciobanu B., Radinschi I., Computational Method for Study of Hall Effect in Physics Laboratory, The 6-th International Balkan Workshop on Applied Physics, July 5-7, 2005, Constanta, Romania.
6. Ciobanu B., Radinschi I., One Computational Algorithm for Physics Modeling, Proceedings of 5th International Conference on Electromechanical and Power Systems, SIELMEN, October 6-8, 2005-Chisinau, Rep. Moldova.
7. Ciobanu B., Radinschi I., Implementation of some teaching tools in physics education, Proceedings of International Symposium Present and Perspective in Textile Engineering, November 10-12, 2005, Iași, Romania, p. 607-611, ISBN 2973-730-120-X
8. Radinschi I., Ciobanu B., Improving Engineering Physics Teaching-Learning with Mathematica 5.1, Proceedings of International Symposium Computational Civil Engineering 2007, CCE 2007, Iasi, Romania, May 25, pp. 180-190, 2007.
9. Radinschi I., Ciobanu B., Physics Studies - Computational Methods, a Strong Connection, Proceedings of International Symposium Computational Civil Engineering 2007, CCE 2007, Iasi, Romania, May 25, pp. 200-211, 2007.
10. Radinschi I., Frunza M. D. and Ciobanu B., Online Virtual Model for Testing the Knowledge, Proceedings of International Technology, Education and Development Conference INTED 2007 edited by IATED, Valencia, Spain, March 7-9, pp. 42-47, 2007.
11. Radinschi I., Scripcariu L., Ciobanu B., Frunza M., Online Quizzes, an Application of PHP-Triad and MySQL, *Romanian Journal of Physics*, 53, No.1-2, pp. 391-396, 2008.
12. Frunza M. D. and Radinschi I., A Virtual Model for Testing Mathematics, Physics and Chemistry Student's Knowledge, Proceedings of International Symposium for Design and Technology of Electronic Packages, SIITME 2006, Iași, România, pp. 154-160, 2006.
13. Radinschi I., and Damoc C., Computer Simulations of Physics Phenomena Using Flash, prepared for CCP 2008, August 5-9, Ouro Preto, Brazil, 2008.
14. www.adobe.com/products/flash.

Management Program for Urban Traffic Road

Voichița Roib

Roads, Bridges and Railways Department, University of Cluj-Napoca, Civil Engineering Faculty,
Cluj-Napoca, Romania

Summary

The paper present the methodology of implementing a traffic management program, in Cluj-Napoca city. The economic and demographic development of Cluj-Napoca city led to the amplification of traffic in the city, a thing which stressed the inadequacy of the present traffic networks which manifests itself by the overflow of the traffic ways. To satisfy the present and the perspective movement needs, the proposition refers to the application of a traffic management program by the use of a new technology for the collection, organization and transmission of information related to the infrastructure and traffic status.

The great numbers of factors which influence traffic require the processing of a huge volume of data and the performance of multiple calculations to determine optimal solutions. All these are carried out with the aid of computer software and of certain advanced traffic management systems. The traffic management system has the role of securing the traffic control and monitoring as well as to supply information to the travellers, its aim being to reduce traffic congestions and agglomerations, travel and intervention time in case of accident.

In order to optimize the traffic, a data processing program was created, which determines traffic parameters by collecting traffic data, processing these data and ascertaining the main traffic indicators. The designation of the main traffic indices is accomplished by gathering and adjusting the traffic data in the program created. With the aid of the Management Program for urban traffic road, was adjused the traffic data from some streets of Cluj-Napoca municipality.

In order to prove the utility of this program, traffic data gathered during a fixed period of time from Regele Ferdinand Street in Cluj-Napoca city was adjusted. The results of the processed data basis of Management program have a special importance by the information sent related to traffic conditions, and for the decisions related to traffic optimizing.

KEYWORDS: management program, traffic road, computer software, to monitor.

1. INTRODUCTION

The transport system is the infrastructure of any economy, conditioning its efficiency and the architecture of the whole system. Economic development led to the increase of movements, transport being an important factor, merchandise and persons mobility having a major impact on every field of activity. The greatest part of displacements is done on the road network which offers a greater freedom for the organization of the trip or of the transport, but with negative consequences in what concerns traffic safety and comfort.

Cluj-Napoca City is one of the main urban centers of Romania by its political, administrative, industrial, commercial and cultural functions. The economic and demographic development of the city of Cluj-Napoca led to the amplification of traffic in the city, a thing which stressed the inadequacy of the present traffic networks which manifests itself by the overflow of the traffic ways. To ensure the access and mobility possibilities, to satisfy the present and the perspective movement needs, necessity arise to propose new ways of fluidization of the road traffic in the city, with the observance of the use requirements of the urban area and of the environment conditions.

To solve such issues the proposition refers to the application of long term transport policies related to the management of the road traffic by the use of a new technology for the collection, organization and transmission of information related to the infrastructure and traffic status. It is thus proposed the implementation in the city of Cluj-Napoca of a traffic management system.

This system is based on a complex infrastructure which contains sensors, video tracking cameras, data transmission network and exact position detection equipment (GPS).

It is composed of multiple subsystems which are integrated into a system coordinated through the transport management centers [1]. To send the necessary services to users, the system uses a chain of information which contains data acquisition from the transport system, data communication, data processing, information distribution to the system users and the use of information to back up decision and control.

Data processing, integration and results representation under a graphic form is done in the control centers offering information in real time on the current traffic conditions of a network.

The traffic management system has the role of securing the traffic control and monitoring as well as to provide information for the travelers, the aim being to decrease traffic congestions and agglomerations, of the time to travel and the time of intervention in case of accidents. For traffic safety and mobility information is handled with reference to transport manner, route and travel duration.

The local authorities look for the best administration of the existing urban transport infrastructure by developing and implementing long-term transport policies to be correlated with the economic development, the population growth, the urbanism plan and the traffic needs.

The Municipality Council aims at regularizing the traffic at the crossroads by creating an integrated, modern and intelligent system to manage the traffic flows; this amendment was set within the Program for the modernization of the streets network on a medium-term between 2005 and 2014. Thus the authorities from the Cluj-Napoca municipality initiated a study of the circulation in 2005 in order to identify the traffic problems and some methods to decrease and regularize the traffic of the vehicles by ensuring a coordinated system of traffic lightening. A first part of the study was ended with the traffic regularization Plan in the centre of the municipality, which was approved by the City Council. This study was made by the company called Search Corporation Bucharest, which sub-contracted the Technical University of Cluj-Napoca. Therefore, the Technical University carried out monitored traffic measurements on various arteries and crossroads of the Municipality. The large amount of data resulting from the traffic recordings imposes their storage in a data base that can be adjusted through the computerized program and can ensure the information needed by the decision factors for the optimization of the traffic. Therefore during a first stage it was created a computerized program for the management of the traffic parameters.

2. THE STRUCTURE OF THE PROGRAM

2.1. Application programming language

The Management Program for urban traffic road is a computer application that automatically organizes and adjusts the data following the territorial surveys.

The application consists of creating charts where the gathered data are stocked in fixed sections, the adjustment of the data, the displaying of the results and the graphic representation of the traffic characteristics obtained. The program can be installed on a PC, it is easy to access, it facilitates the analyzing and decision-making process.

The designation process for traffic elements, the methodology of adjustment for the gathered data, the technical terminology are according to the effective standards and laws [2], [3], [4], [5] and [6].

The application was developed using JAVA programming language. The data is stored in a MySql database.

MySQL is the most popular open source relational database management system. It is based on the structure query language, which is used for adding, removing, and modifying information in the database. MySQL was owned and sponsored by a single for-profit firm, the Swedish company MySQL AB, now a subsidiary of Sun Microsystems. The project's source code is available under terms of the GNU General Public License, as well as under a variety of proprietary agreements.

Java is a programming language originally developed by Sun Microsystems and released in 1995 as a core component of Sun Microsystems' Java platform. The language derives much of its syntax from C and C++ but has a simpler object model and fewer low-level facilities. Java applications are typically compiled to bytecode that can run on any Java virtual machine (JVM) regardless of computer architecture.

The design of the application is object oriented. The objects and the relations between them can be observed in the application diagram, as shown in Figure 1.

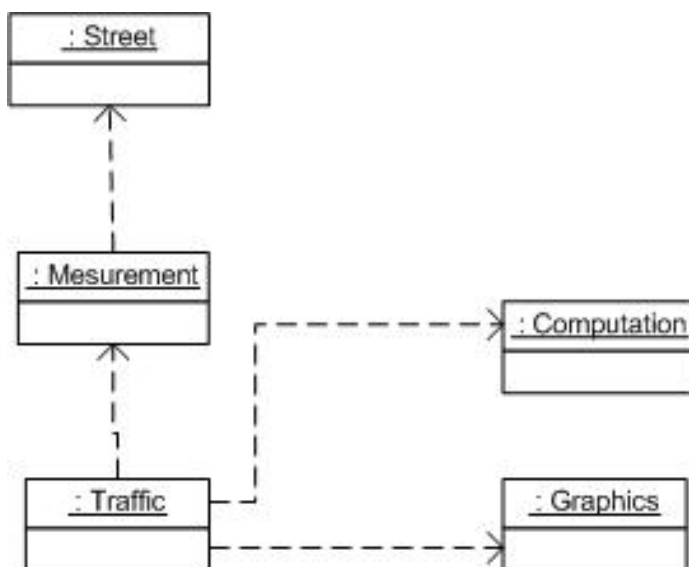


Figure 1. The application diagram.

Data collected by user regarding traffic information is inserted into the database using the application interface. Relevant computation and graphics for the traffic analyze is performed.

The menu of the programme comprises the following options: Data entering, Data changes, Data display, Choose the measurement, Calculations, Graphics, Statistic indices.

2.2. Entering and Organizing the Data

The entering of the data is made by accessing the option **Data entering** from the Menu bar. It comprises:

- the basic data of the street where the survey is made (the locality, the name, the geometric elements, the technical group)
- the basic data of the traffic survey (the beneficiary, the locality, the street, the date, the location, the kilometric position, the ways, the types of surveyed vehicles, the time spans, the reference span, the indices of turning into standard vehicles, the meteorologic conditions, the condition of the road). The surveyed vehicles are entered in the system by the operator based on the filled in survey charts.

Subsequent to the data entering, as shown in Figure 2, one can also access other options from the Menu bar which allow the modification or the access of the data base.

The screenshot displays the 'Gestione trafic' application window. The menu bar includes 'Introducere date', 'Modificare date', 'Vizualizare date', 'Calcul', 'Grafice', and 'Indicatori statistici'. The main area contains three overlapping windows:

- Recenzare trafic:** Fields for Localitate, Strada, Data (zi/luna/an), Post nr., and Pozitie kilometrica. Includes a 'Cauta' button.
- Inserare strada:** Fields for Denumire strada, Localitate, Cartier, Lungime (m), Latime (m), Viteza medie(km/h), and Clasa tehnica (dropdown menu). Includes a 'Salveaza' button.
- Inserare date de baza recenzie trafic:** Fields for Beneficiar, Localitate, Strada, Data (zi/luna/an), Post nr., Pozitie kilometrica, Sens (dropdown menu), Vehicule inregistrate (dropdown menu), and Recenzor. Includes time-related fields: Interval de timp (min) (dropdown menu), Durata de referinta (ore), Interval orar, and weather/road condition dropdowns (Conditii meteo, Starea drumului). Includes a 'Salveaza' button.

Figure 2. The options from the Menu bar. Choosing the Data entering option.

Data changes: allows the changing of the measurements and the traffic data.

Data display: allows the view of the measurements and the traffic data.

Choose the measurement: allows the choosing from the data base.

2.3. The Data Adjustments. Results

The adjustment of the traffic data gathered during a fixed period of time is made according to an algorithm that obeys the effective standards and laws, [5] and [6].

In order to initiate the data adjustment option **Calculations** is accessed from the menu bar. The programme accomplishes the data adjustment and the acquiring of the following traffic parameters: standard vehicles, the model of the equivalent traffic, traffic densities and the rush-hour (the time-span of the highest traffic intensity, of the medium traffic intensity, and of the minimum intensity).

Graphics. After the adjustment, by choosing option **Graphics**, the programme allows the display of the data obtained in a graphical representation of the resulting values: the diagram on types of vehicles, the diagram for the equivalent traffic hour variation, the frequency of occurrence on groups, the cumulated frequency.

Statistic indices. By accessing option **Statistic indices** from the Menu bar tendency parameters are obtained (the arithmetic average of the survey, the average value of the survey, the survey type, the main value) and the diffusion parameters (the square average deviation of the survey, the diffusion of the data chain, the amplitude of the data chain, the variation indice of the survey chain, the absolute average deviation of the data chain).

The statistic parameters are also useful for the designation of some specific tendencies typical for the load on the traffic arteries. These parameters allow the estimation with a higher degree of approximation of the traffic prognosis (the distribution of the vehicle flow), [7].

3. APPLICATION MADE IN THE MANAGEMENT PROGRAM

3.1 The Recording

Following the traffic study and based on the monitored traffic data, suggestions were made for the regularization of the traffic, which consist in the change of the traffic directions, parking restrictions, creating new traffic lanes. In order to know the evolution of traffic since 2005, in March 2008 traffic measurements have been made in the central area, on Regele Ferdinand Street. These have been necessary in order to take decisions on the opportunity of introducing a one-way on the mentioned street for creating a traffic ring in the central area.

The recordings were manually made through the direct countings of the traffic participants and consisted of the countings of the vehicles that passed by a fixed area (the Regele Ferdinand street) within a well determined period; the

composition and the intensity of traffic flows were established based on these variables.

The measurements were made during 12 hours in a working-day, between 7.30 and 19.30, on each of the circulation ways and with a differentiation on categories of traffic participants. The sustained countings during the day allow the designation of the most intensely circulated intervals (the rush-hour). During the interval of traffic recording subdivisions of the traffic were pointed out in intervals for 15 to 15 minutes.

3.2 Data Entering

In the next part the basic data of the street and of the traffic survey were entered by using the previously mentioned options that are to be found in the Menu bar.

3.3 The Results Obtained

The features of the traffic were reached to after adjusting the data: standard vehicles, the model of the equivalent traffic, traffic intensities and the rush-hour, as shown in Figure 3 and statistic indices.

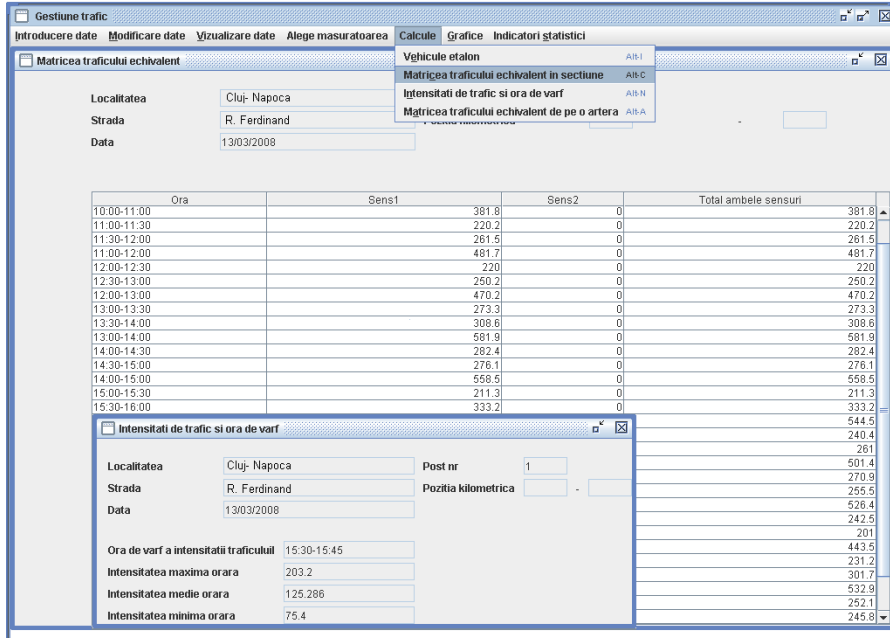


Figure 3. Choosing the Calculations option. The model of the equivalent traffic, traffic densities and the rush-hour.

The graphic representation of the results values is made by selecting the Graphics option: the diagram on types of vehicles as shown in Figure 4, the diagram for the equivalent traffic hour variation as shown in Figure 5.

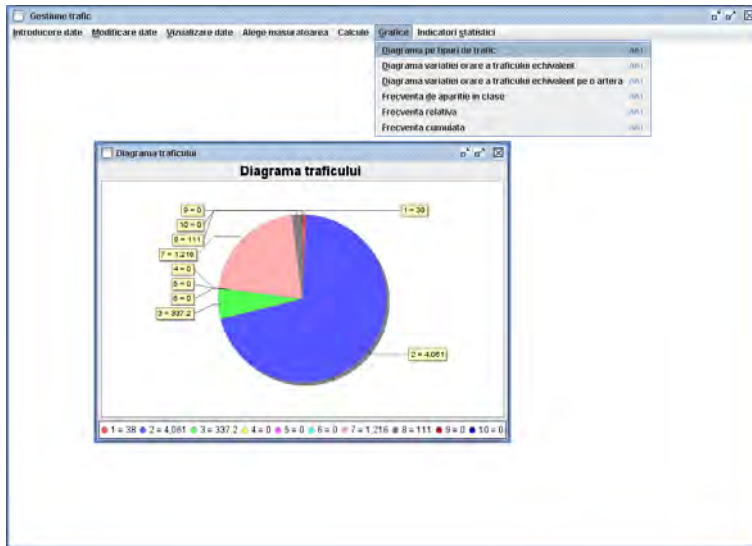


Figure 4. Choosing the Graphics option. The diagram on types of vehicle.

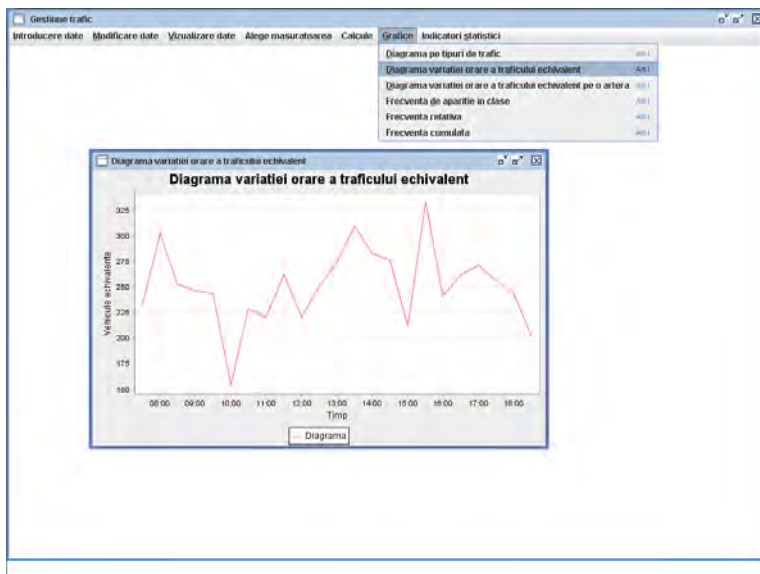


Figure 5. Choosing the **Graphics** option. The diagram for the equivalent traffic hour variation.

By accessing option **Statistic indices** from the Menu bar tendency parameters are obtained, as shown in Figure 6 and the diffusion parameters, useful for the designation of some specific tendencies typical for the load on the street.

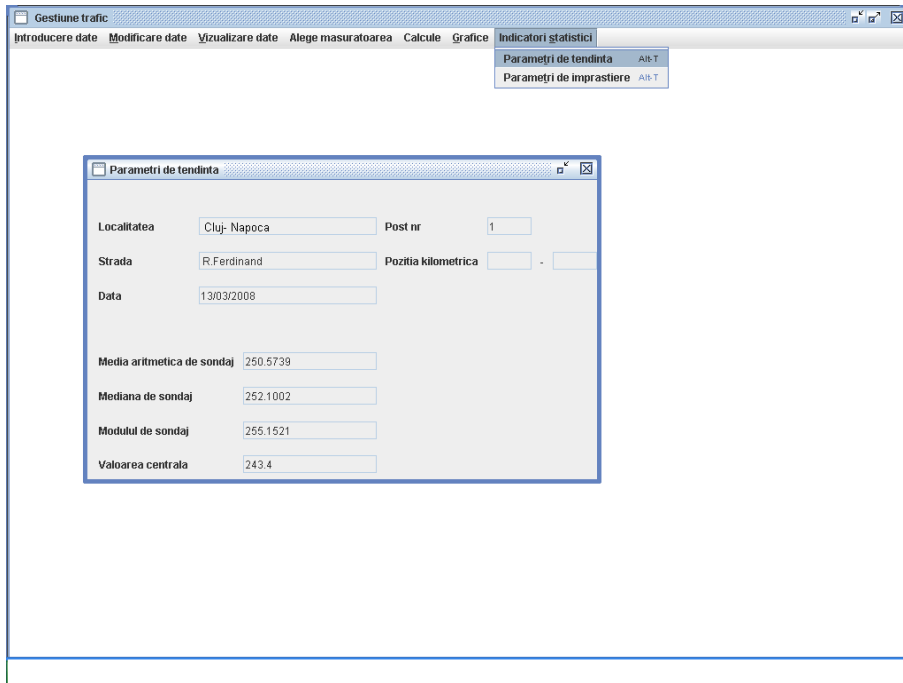


Figure 6. Choosing the **Statistic indices** option. Tendency parameters.

The results obtained are necessary in order to be able to designate the effective and perspective traffic, for calculating the circulation capacity of the street.

The Regele Ferdinand Street is situated in the historical centre of the Cluj-Napoca city, is a central link street between two important squares of the city, Unirii Square and Mihai Viteazu Square, ensuring the transit on North-South axe of the city. The street is 317 m length, 13 m wide, and side-walks with 4-5 m wide. For the most part of the day, the traffic is a continuous vehicle flow. The features of the traffic were reached to after adjusting the data gathered from Regele Ferdinand Street, direction Mihai Viteazu Square to Unirii Square were: standard vehicles, the model of the equivalent traffic, traffic intensities and the rush-hour. Based on the information acquired regarding the traffic conditions, a traffic monitoring is achieved; this can lead to the optimization of the circulation due to the decisions taken after interpreting the resulting indices.

3. CONCLUSIONS

The very large amount of data obtained within the traffic studies and the numerous calculations impose that they be organized in a data base. This data base must be adjustable within some informatic programmes that can provide the necessary information for the decision-making factors in the traffic optimization. Thus we have created a computerized programme for the administration of the traffic parameters which was implemented on a street from the Cluj-Napoca Municipality.

The programme allows the structuring of a data base with detailed access, the automatic generation of reports regarding the traffic parameters, expressed graphically and through charts, very useful in the activity of traffic management. Through this programme the users are offered information about the traffic and the possibility of some traffic analyses and prognoses.

The analyses and the prognoses of the traffic tendencies will allow the elaboration of some traffic optimization policies by the decision-making factors.

References

1. Banciu, D., Hrin, R., Mihai, G., Eşanu, A., Alexandrescu, M., Anghel, L. *Sisteme Inteligente de Transport - ghid pentru utilizatori și dezvoltatori*, Ed. Tehnică, București, 2003. (in Romanian)
2. STAS 4032-2-92. *Tehnica traficului rutier. Terminologie*. (in Romanian)
3. STAS 10795-1-76. *Tehnica traficului rutier. Metode de investigare a circulației. Clasificare*. (in Romanian)
4. AND 557-1999. *Instrucțiuni pentru efectuarea înregistrării circulației rutiere pe drumurile publice*. (in Romanian)
5. SR 7348-2001. *Lucrări de drumuri. Echivalarea vehiculelor pentru determinarea capacității de circulație*. (in Romanian)
6. C 243-93. *Instrucțiuni tehnice pentru efectuarea de sondaje, recensăminte, măsurători și anchete de circulație în localități și teritorii de influență*. (in Romanian)
7. N. Filip, N. Cordos, I. Rus, *Zgomotul urban și traficul rutier*, Ed. Todesco, Cluj-Napoca, 2001, pp.136-149. (in Romanian)

Simplified Inventory for Road Culverts and Bridges

Claudiu Romanescu¹, Cristina Romanescu², Rodian Scînteie³

¹Bridge Management System Office, CESTRIN, Bucharest, 061101, Romania

²Road Bridges Dept., CESTRIN, Bucharest, 061101, Romania

³CERT-CESTRIN, CESTRIN, Bucharest, 061101, Romania

Summary

Road bridges management compulsory implies an exhaustive knowledge of the managed inventory at a technical level, in order to have an accurate view of the measures to be implemented.

A software system capable to rapidly and efficient provide information of the technical condition of bridges is the necessity of any road administrator. The decisions regarding each structure must be taken accordingly to its specific and these must be sustained by precise information on the bridge.

This paper presents The Simplified Inventory for Road Culverts and Bridges (SIRCUB) program that wishes to be the answer to specialist's basic requests, delivering data related to structure identification, geometrical and material characteristics and a brief set of functional information. It is available to all users having usual database software (MS Access) and may constitute the basis for further developments to include data about technical condition, a basic intervention prioritization of bridges, etc.

SIRCUB is very flexible, allowing displaying data of selected structures, modifications of records, and also modifications of the graphical user interface to permit more information to be viewed and assessed.

KEYWORDS: bridges, database, inventory.

1. INTRODUCTION

Road bridges management compulsory implies an exhaustive knowledge of the managed inventory at a technical level, in order to have an accurate view of the measures to be implemented. In this respect, the administrators needs to have a fast, reliable, small software tool capable to rapidly and efficiently provide information of the technical condition of bridges. This is the necessity of any road administrator wishing to spent time and money as less as possible on solutions regarding the electronic inventory. Also, the decisions regarding each structure

must be taken accordingly to its specific and these must be sustained by precise information on the bridge.

This paper presents The Simplified Inventory for Road Culverts and Bridges (SIRCUB) program that wishes to be the answer to specialist's basic requests, displaying data related to structure identification, geometrical and material characteristics and a brief set of functional information. It is available to all users having usual database software (like MS Access) and may constitute the basis for further developments to include data about technical condition, a basic intervention prioritization of bridges, a more sophisticated user interface, etc.

SIRCUB is very flexible, allowing displaying data of selected structures, modifications of records, and also modifications of the graphical user interface to permit more or less information to be viewed and assessed.

The main objectives are to provide a handy tool to verify information coming to the administrator from various sources (in field inspections and investigations, contractors, consultants, etc.). Thus, two different activities are to be done in the process of management: the management and the administration of the electronic form. The management requires the use and interpretation of data in the purpose of fulfilling the scope of the activities and the administration shall be done by input, validation and actualization of the data.

2. DESCRIPTION OF THE FORM

The user must open the form and the main window appears (figure 1). One has the possibility to choose the road needed to be viewed and the following window will open (figure 2).

Data included in the SIRCUB are as follows:

- DN – the identification of the road where the structure is located (i.e. DN 7A);
- Pozitia kilometrica – is the mileage where the structure is located on the given road (i.e. 42+700, meaning that the bridge can be found at kilometer 42 and 700 meters). This position is established from the beginning of the guardrail on the bridge;
- Obstacol – the name of the surpassed obstacle is written here (i.e. Râul Olt or Railway);
- Localitate – the name of the closest human settlement is to be found here;
- Materiale Suprastructura – the main constructions materials used for the superstructure, such as concrete, metal, etc. must be written here (i.e. BP, meaning pre-stressed concrete);

- Materiale Infrastructura – the main construction materials used for the infrastructure, such as concrete, metal, etc. must be written here (i.e. B, meaning concrete);
- Tip Fundatii – one must write in this field the type of foundations of the bridge (i.e. D meaning direct foundations);
- Nr total deschideri – the total number of spans is to be written here;
- Lung deschidere 1 – the length of the span no. 1, in meters;
- Lung deschidere 2 – the length of the span no. 2, in meters;
- Lung deschidere 3 – the length of the span no. 3, in meters;
- Lung deschidere 4 – the length of the span no. 4, in meters;
- Lungime totala – contains the total length of the bridge, in meters;
- Latime carosabil – is the width of the carriage way, in meters;
- Latime intre parapeti – is the width between two opposite guardrails, in meters;
- H etiaj – the measured height, in meters from the ground to the lower part of the superstructure will be found here; in the case that the bridge overpasses a railway the height will be measured from the rail;
- Indice stare tehnica – the aggregate index that takes into account the degradation condition of the bridge and also its functionality indexes will be written in this field;
- Clasa tehnica – the technical class where the bridge must be classified according to its aggregate index, in conformity with the Romanian Instructions for establishing the technical condition of the bridge, AND 522-2006.

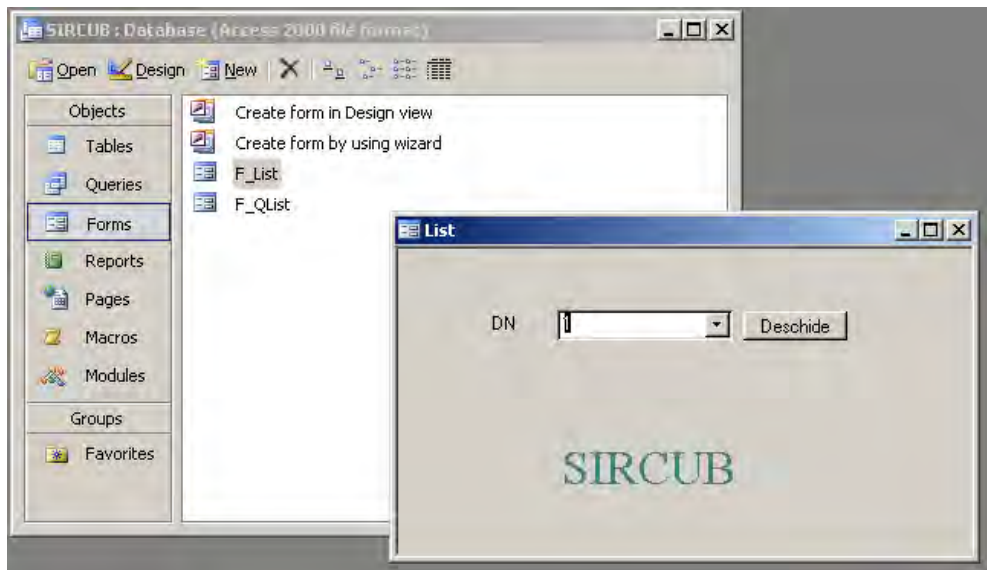


Figure 1. The main window of the form

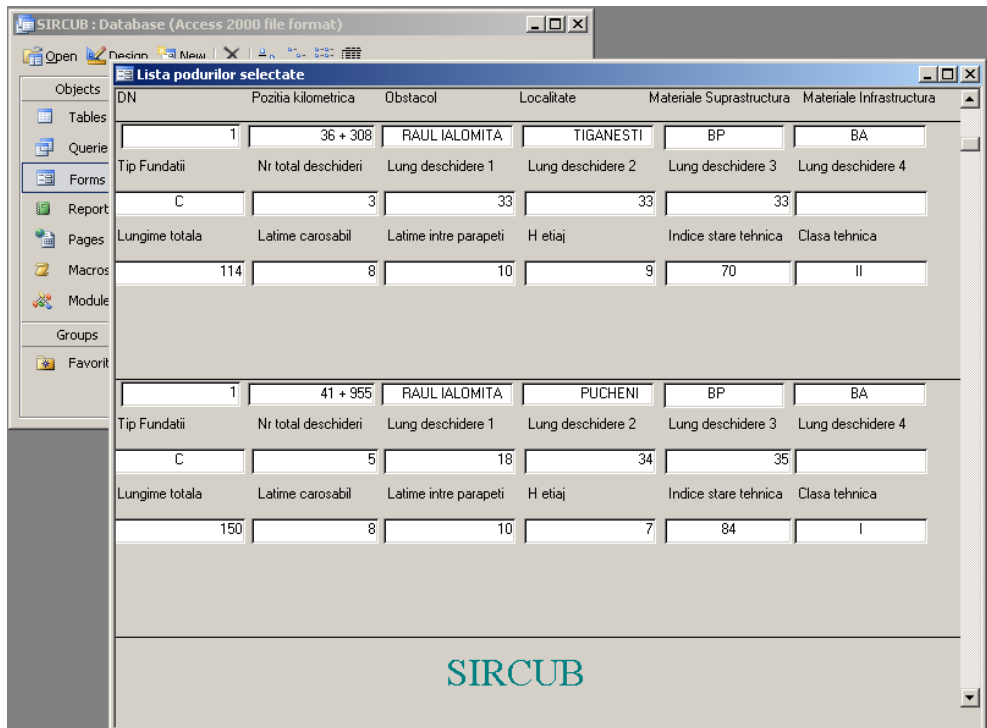


Figure 2. The window containing the information on the bridges

3. CONCLUSIONS

The Simplified Inventory for Road Culverts and Bridges addresses the bridge administrator with the only scope to provide a fast, reliable and totally inexpensive tool needed in their work. Being free of any charge (General Public License), this electronic form requests the possession of a database managing software such as Microsoft Access or similar and a minimum of computer knowledge to input and manipulate data.

References

1. Instructiuni pentru stabilirea starii tehnice a unui pod, indicative AND 522-2006 (in Romanian).
2. Scinteie, R., Baze de date si algoritmi pentru cai de comunicatie, 2003 (in Romanian).

Analysis of repair works assignment to create the BMS works database

Cristina Romanescu¹, Claudiu Romanescu² and Rodian Scînteie³

¹Road Bridges Department, CESTRIN, Bucharest, 061101, Romania, bridge@cestrin.ro

²Road Bridges Department, CESTRIN, Bucharest, 061101, Romania, cromanescu@gmail.com

³CERT-CESTRIN, Bucharest, 061101, Romania, rodian.scinteie@gmail.com

Summary

STELA-R is the bridge management system developed at CESTRIN for CNADNR, between 2000 and 2007 with the aim:

- *to preserve existing infrastructure investments,*
- *to ensure safety of the users and*
- *to maintain mobility.*

STELA-R stores inventory and inspection information of the bridges situated on the Romanian national road network in a relational database that supports a set of analysis procedures used in evaluating the needs of each structure.

The Romanian Bridge Management process starts with the building of a relational database that includes inventory data and inspection information.

STELA-R uses a group of elements at inspection level data as follows: superstructure - main elements; superstructure - elements that sustain the deck; substructure elements; channel and road approaches elements; carriageway elements.

Bridge inventory and inspection data are managed using the STELA-R Inspection Module. It consists of a set of relational tables and user graphical interface for creating new records, entering new inspection data, modifying existing ones and eventually erasing the obsolete data.

Through field inspections CESTRIN personnel quantifies the technical condition of structures. All defects and degradation are pointed out, evaluated and for each of them one or more intervention works are attached, works that could be maintenance, repair, rehabilitation or replacement of elements or groups of elements.

Works are assigned to defects in the Analysis Module.

This paper is dealing with the issues of creating a repair works database. To create this database Romanian experience was considered and comparison has been made toward other systems like (Pontis - American bridge management system, Gepeto - French bridge administration software belonging to GETEC Company).

KEYWORDS: defects, assessment, deterioration processes and repair works

1. INTRODUCTION

A software system is designed to perform a series of operations to the database. It is composed by:

- software;
- database.

The realization of a database implies:

- the analyses of the system that will use the database;
- database design;
- data input into the database;
- exploitation and maintenance of the database.

The effective realization of an application supposes:

- establish the goal, considering the activities to be modeled;
- the goal analysis, meaning the identification of the information types, its connections and the necessary management operations;
- designing the software, exactly the data and software structure designing
- modules testing, detecting and correcting errors
- implementation of the software consists in building the final form of the application through the step-by-step integration of the tested functioning modules
- the maintenance of the application consists in removing the users pointed out errors.

The result of the analysis supposes describing inputted data kept within the database, the list of processed data and description of information within the reports.

Designing the software structure supposes detailing the modules for files creation, data input processing and using the results.

The users of a database may not be specialists having a communication mode close to the usual talking and specialist users knowing the database structure.

Creating the table that includes all repair/rehabilitation or replacement works is directly related with the degradations and its working costs. Thus this table had to take into account that for each defect included in the Romanian Instruction for Establishing the Technical Condition of a Bridge (named from now on as the Instruction) one has to assign a certain reparation work and for each work a certain cost.

In this respect a series of bridge specific software have been identified, including lists of maintenance, repair and rehabilitation works. Therefore one may have: Pontis - American bridge management system, Gepeto - French bridge administration software belonging to GETEC Company, Doclib – software used for resources management, works estimate creation, preparing and organization of the production.

Each of this software has its own methodology specific to the works execution technologies, being structured on bridge elements and types of materials and also on degrees of severity for the observed degradations.

2. PONTIS

Pontis is exhaustive bridge management system software that can assist agencies in allocating restrained resources to protect existing infrastructure investments. Pontis includes inventory and inspection information about bridges, culverts and other structures in a relational database that permits the use of modeling, analysis and reporting tools to facilitate project, budget and program development. It also analyzes the impact of different project options on the overall condition of individual structures or a network of structures.

The Pontis Database consists of a relational database that includes importing inventory data and adding element-level inspection information. The process continues with development of a preservation policy for each element and environment combination in the database.

Data regarding bridge inventory and inspection consists of a set of relational tables and graphical user interfaces for managing new structures, deleting structures, reviewing existing data, entering new inspection data with comments or checking data out or into the system. This is a highly flexible data structure, having detailed element-level condition inspection data.

Pontis uses inspection data for each element level as the basis for bridge analyses. The main components of a typical bridge, such as deck, superstructure, and substructure are sub-divided into numerous elements to add more detail and precision. A superstructure might contain several elements such as steel girders, steel floor beams, bearings, etc. Elements are also classified by material types, such as concrete, steel, or timber. Through element-level inspections can be quantified the condition of structures. Pontis uses this information to compute the costs and benefits of bridge repair or rehabilitation.

The user may run analysis within the inspection module for a bridge, a group of bridges or all bridges in the database. The most recent data from this module is

used to determine network-level and bridge-level preservation and improvement needs.

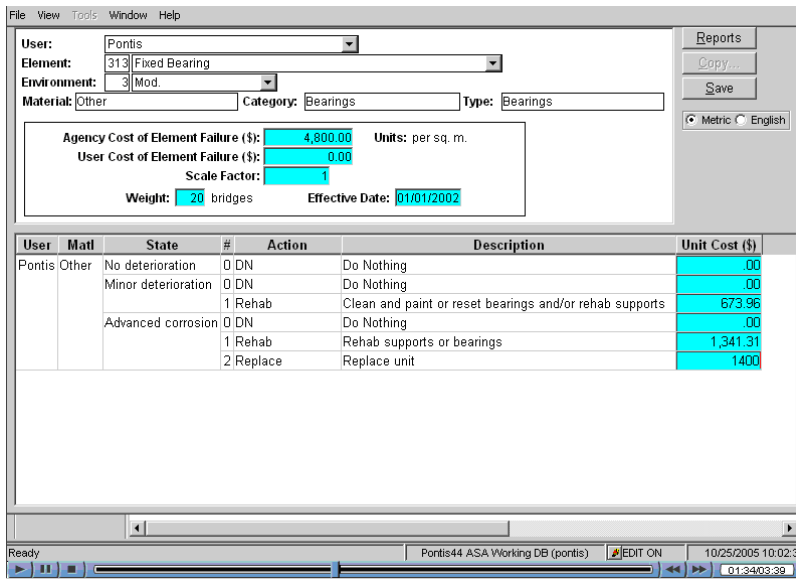


Figure 1. Pontis software repair and rehabilitation works

Pontis makes a distinction between preservation actions and functional improvements. Preservation actions seek to maintain or restore the physical condition of structure elements to its best condition. Improvement actions are aimed at making the structure satisfy the current and future functional demands. Preservation actions include maintenance, repair, rehabilitation or replacement of elements or groups of elements. The preservation model identifies the optimal preservation actions based on the objective of minimizing costs and maximizing benefits. Standard types of functional improvement actions include bridge widening, raising, strengthening and replacement. Programming of improvement actions is based on policy standards, such as lane and shoulder widths, vertical and horizontal clearances, and unit costs and benefits supplied by the user. Pontis is designed to support testing of different combinations of functional improvement policies, and cost and benefit assumptions. Pontis analyzes preservation and improvement alternatives separately, and brings them together in a network analysis.

PONTIS element tables include:

- deck and slab elements;
- superstructure elements;
- substructure elements;
- culvert elements;

- joint elements;
- bearing elements;
- smart flags.

User	Element	Matl	Env	#	State	#	Action	Med Yrs	P. St.1	P. St.2	P. St.3	P. St.4	P. St.5
Pontis	Fixed Bearing	Other	Mod.	1	No deterioration	0	DN	15.0	95.48	4.52			
				2	Minor deterioration	0	DN	7.0		90.57	9.43		
						1	Rehab		95.00	5.00	0		
				3	Advanced corrosion	0	DN	4.0			84.09		
						1	Rehab		90.00	9.00	1.00		
						2	Replace		100.00	0	0		

Figure 2. Pontis software: preservation policy for each element and environment combination

The deck and slab elements may be built using different materials (stone or brick masonry, concrete, reinforced concrete, pre-stressed concrete, steel, timber) thus resulting in different specific degradations. Therefore the list of repair/rehabilitation works includes specific techniques of reparation of the material. These works consists primary on reparations and in case of advanced degradations the replacing action is recommendable.

For the concrete elements one may have: repair spalls and delaminations, and add a protective system on the entire deck and replace deck.

For the steel elements one may have: surface clean and restore top coat, spot blast, clean and paint, rehab connectors and replace paint system and replace unit.

For the timber elements one may have: rehab and/or protect deck and replace deck.

For all other elements of the infrastructure and superstructure and also for joints and bearings the recommended works depends on the degradation stage and indicates simple actions, without any constructive details.

3. GEPETO

GEPETO is bridge inventory software that performs analysis on the current condition of the structures at the very moment of the in field inspections. It have been developed by a French company, GETEC, that has a good reputation in the field of bridge inspecting, evaluating and works recommendations. The software is capable to make an intervention prioritization of the bridges at the level of the entire inventory, based on the technical condition and functionality. It also possesses a statistics module allowing the user to have a general view of the bridges from one or another point of view (i.e. age of the bridge, length, etc). Gepeto does not make any predictions on the future condition of bridges, so no strategies are available. One may not have a cost-benefit ratio calculated on a long term basis and may not be able to have an analysis on the optimum funds to be spent each year.

It shows the bridges in the database on the left side of the panel, and for each structure, the data is separated into structure's data and visual inspection data.

The structure's data is input with 8 screens:

- General description (location, obstacle type of structure, ...)
- Geometric characteristics, including the description of the opening
- Piers and Abutments
- Equipment
- Environmental data, including traffic, utilities and load restrictions
- Design and History, including data on the initial design and eventual available documentation, history of the works and access means required for the inspections
- Functional index
- General images (elevation, view of the carriageway or of the intrados)

Almost all data lists can be defined by the user with the parameters, meaning that the lists seen in the inputs can be adapted to the manager's requirement.

This is the case for instance for the equipments, where the list of equipments can be increased where required; similarly, the different types and natures defined for each equipment in the list can be adapted.

The visual inspection data is input with 7 screens:

- General conditions of the visit (data, weather, access ...)
- Functional index, in case the functional index has changed between the initial input of the structure's data and the visit
- Quality index, meaning the quality rating of the structures according to Romanian standard
- Repair form, display of the works and costs selected
- Emergency actions
- Diagnostic and Conclusion

- Distress images, linked to the visit.

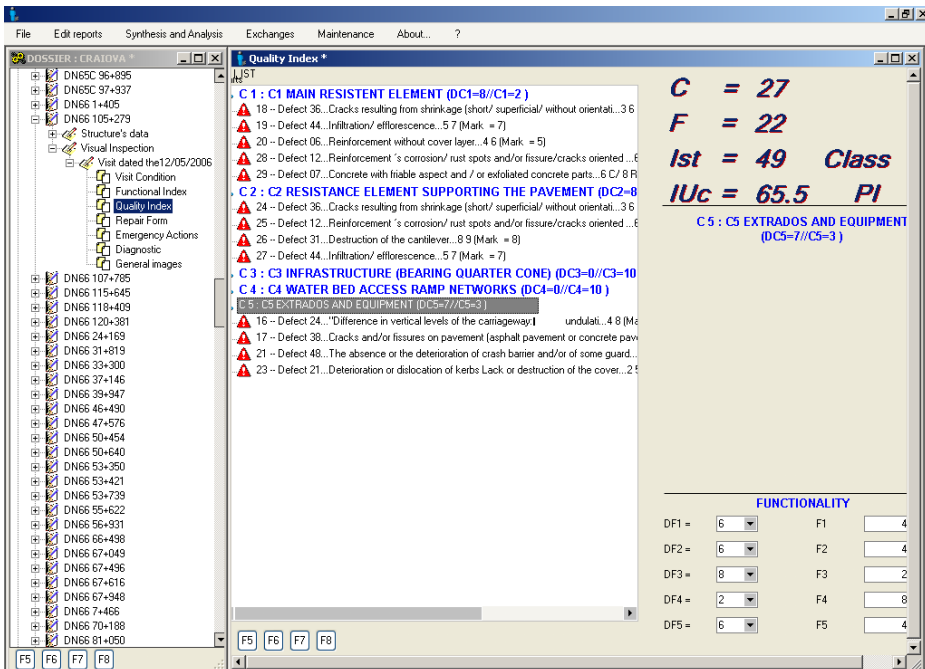


Figure 3. Gepeto software: reparation and rehabilitation works for each degradation

In the Figure 4 it is shown how the user inputs first the defects seen on site. For some defects, where judged appropriate, the user chooses to repair. In this case, a default action (which can be changed) is proposed, and a quantity must be inputted.

These works and quantities form the core part of the repair form, where additional works can be selected, and small works and Maintenance value can be added (see next section).

In the diagnostic screen, a general evaluation is given, the type of maintenance / repair action, as well as the type of recommended surveillance, is proposed.

The visit is completed with the relevant distress pictures that will be part of the visit report.

Based on the data collected in the software, 3 families of reports can be generated:

- Structures and visit notebooks, summarizing and illustrating the findings for each individual structure
- Statistical analysis of the bridges on the network, in terms of structure, materials etc. as well as bridge condition

N° of Price	LABEL	U	QTY	Unit Price	Total Value
4.640.020	D37 C1/C2/C3... Repair of line and open cracks... Filling / injection... Inje	ml	40.00	180.00 €	7.200.00 €
7.810.010	D68 C1/C2/C3... Precasted elements (Cornice, intrados, deck slab, side m	ml	36.00	140.62 €	5.062.32 €
2.110.010	D12 C1/C2/C3... Repair of concrete surface... Concrete repair and reinfo	m2	4.00	765.00 €	3.060.00 €
2.110.010	D12 C1/C2/C3... Repair of concrete surface... Concrete repair and reinfo	m2	1.00	1.275.00 €	1.275.00 €
4.640.020	D37 C1/C2/C3... Repair of line and open cracks... Filling / injection... Inje	m	5.00	540.00 €	2.700.00 €
3.210.010	D23 C4... Repair of scour... Repair of verges... Verges in concrete	m2	80.00	68.20 €	5.456.00 €
2.020.010	D11 C5... Pavement or Shoulder repair... Trottoir... Repair of pavem	m2	360.00	28.60 €	10.296.00 €
5.110.050	D42 C5... Guard rail... Metallic / paint... Complete reconstruction	ml	78.00	120.00 €	9.360.00 €
6.020.020	D50 C5... Dilation Joints and Waterproofing... Flexible sealed in situ... Cc	ml	30.00	600.00 €	18.000.00 €

Value BT	62,409.32 €
Various Value (5%)	3,120.47 €
Value prep. works	3,572.58 €
Value Maint.	3,540.41 €

Figure 4. Gepeto software: list of works and correspondent costs

- Synthesis of the data, including the pre-programming of the works, based on the calculation of the quality indexes and functional indexes, combined into priority indexes and the economic index (cost of the works).

Taking into consideration that that the analyzed GEPETO version has been adapted to fulfill the requirements of the Romanian regulations (The Instruction) the structure of repair and reconstruction works started from degradations, continued by the necessary work then by its effective realization way according to the material that the analyzed element has been built of.

4. DOCLIB

This software is used for assessment, bidding process and construction works pursuance. It includes the estimates collection and the access to the providers actualized costs databank and it is the only Romanian software that can describe a work from a technical, technological and production organization the point of view. It also permits the economical evaluation (obtaining the estimates) based on the automated, correct and transparent description of works.

DocLib is also as assisted designing software. It permits the automated calculus of the articles quantities (having the recipe), of the estimate associated to a parametric drawings allowing the user the automated economical assessment based on the drawing on the technical project. This software has its own programming language that can be modified by the user to have his/her engineering formulas/or algorithms to automatically compute quantities in the estimate or in the drawing the dimensions of some segments, angles, or curvature radius.

This software has its own drawing system for “double parameters” sections. The dimensions on the drawing aren’t numbers but variable names; to some of the variable dimensions one may associate the computing formula associated to the dimension written during the drawing process with its own programming language. Drawings may be done during building the estimate and the drawing is attached to an articles group having the same current number and also having quantity computing formulas depending on the “variable dimensions” on the prototype drawing.

Table 1. DocLib works with costs

Doclib

NR. CR	DESCRIERE	UM	CANTITATE	PRET UNITAR
0	1	2	3	4
	LUCRARI DE POD			
	INFRASTRUCTURA			
1	Sapatura pentru fundatii cu adâncimea mai < de 4.00 m	mc	30	13.50
	Sapatura pentru fundatii cu adancimea mai > de 4.00 m	mc		29.40
	Forarea pilotilor cu diametrul de:1080mm	m		472.10
	Forarea pilotilor cu diametrul de:1500mm	m		655.69
	Forarea pilotilor cu diametrul de:2000mm	m		874.26
	Forarea pilotilor cu diametrul de:800mm	m		349.70
	Armături din oțel beton OB 37 la infrastructuri în fundații, radiere, etc.	t		3350.00
2	Armături din oțel beton OB 37 la infrastructuri în elevații	t	0.5	3350.00
1	Armături din oțel beton PC 52 la infrastructuri în fundații, radiere, etc	t		3460.00
3	Armături din oțel beton PC 52 la infrastructuri în elevații	t	0.5	3460.00
1	Armături din oțel beton OB37 în piloți forăți de diametru mare	t		3371.00
1	Armături din oțel beton PC52 în piloți forăți de diametru mare	t		3493.00
1	Cofraje plane obisnuite la infrastructuri	mp		36.00
4	Cofraje plane pt.fata vazuta la infrastructuri	mp	50	39.60
3	Cofraje curbe obisnuite la infrastructuri	mp		45.00
2	Cofraje curbe pt.fata vazuta la infrastructuri	mp		49.50
4	Beton in fundatii la infrastructură C 8/10	mc		282.00
2	Beton in fundatii la infrastructură C 12/15	mc		302.60
5	Beton in fundatii la infrastructură C 16/20	mc	30	320.00
2	Beton in fundatii la infrastructură C 20/25	mc		344.20
5	Beton in fundatii la infrastructură C 25/30	mc		378.00
4	Beton in elevatii la infrastructură C 8/10	mc		282.00
3	Beton in elevatii la infrastructură C 12/15	mc		302.60
5	Beton in elevatii la infrastructură C 16/20	mc		320.00

The prototype drawing together with the articles associated to the drawing forms a “designing unit” that may be appealed in any estimate. Giving then values to the “variable dimensions” these will be computed automatically in the caller estimate the quantities for the articles from the designing units attached to the project redrawing it automatically rescaled on the screen and on the printer the sections of the designing units according to the numerical values for the given work. The designing unit addresses to the designer, but mostly to the constructor as the only mean of automated calculation.



Photo 1. Widening of a bridge to fulfill the actual traffic requests

One may observe that this software can be used on real projects and may not be inputted in a works database to have an estimate of necessary funds.

For estimates drafting DocLib offers an extended works list specific to bridge construction: diggings, drillings, type of reinforcements, frameworks, classes of concrete, precast elements, types of pavements for the carriageway, types of joint covering systems, etc.

3. CONCLUSIONS

The list of analyzed software is not as wide as it could be, but the authors preferred to focus on the main available items on the market. It is important to bear in mind that a good estimation of works costs would lead to a more correct contracting process and a faster way to reach the goal of a better infrastructure. In the

repair/rehabilitation works quality materials must be used, advanced technologies and experienced engineers must be brought on site. Thus the durability of the performed works will increase and the overall costs will be lowered.

STELA-R presently includes repair/rehabilitation/replacement works and costs from the Gepeto software, but the authors are willing to change them according to the Romanian regulation “Normativul de proiectare pentru lucrări de reparații și consolidare ale podurilor rutiere în exploatare” (Designing norm for repair and consolidation works of under traffic bridges).

The repair/rehabilitation works must take into account the importance of the architectural and aesthetics of the bridge in order to preserve the patrimony. Therefore technologies, materials and methods able to extend the lifetime of bridges are recommendable.



Foto 2. Replacement of an existing small bridge

References

1. New Jersey Department of Transportation, *Pontis Coding Guide Manual*, 2003.
2. Getec Manual degradari metodologia ce sta la baza Gepeto,
3. DRAPEAU, A. et M. Bélanger *Manuel d'inspection des structures – Évaluation des dommages* , Direction des Structures, Ministère des Transports, Québec, 1995.
4. Ionescu C., Scînteie R., Considerații privind integrarea calculatorului electronic în ingineria podurilor, *Journal Intersections/Intersecții, Lumea podurilor*, vol.1, No.7, 2004. (in Romanian)
5. Scînteie R., Baze de date și algoritmi pentru căi de comunicație, 2003
6. Instrucția de satbilire s stării 522/2006

7. Normativ privind alcătuirea și calculul structurilor de poduri și podețe de șosea cu suprastructuri monolit și prefabricate, PD 165 – 2000, *Buletinul tehnic Rutier volumul 10-11 din 2002*
8. Instrucțiuni tehnice privind repararea și întreținerea podurilor și podețelor de șosea din beton, beton armat, beton precomprimat și zidărie de piatră, indicativ CD 99-2001, *Buletinul tehnic Rutier volumul 3 din 2001*
9. Normativ de proiectare pentru lucrări de reparații și consolidare ale podurilor rutiere în exploatare, indicativ NP 103-04, *Buletinul construcțiilor volumul 6 din 2005*
10. Normativ pentru proiectarea podurilor din beton și metal. Suprastructuri pentru poduri de șosea, cale ferată și pietonale, precomprimate exterior” – indicativ NP 104-05, *Buletinul Construcțiilor volumul 10-13 din 2005*
11. Normativ privind proiectarea infrastructurilor de beton și beton armat pentru poduri – indicativ NP 115-04, *Buletinul Construcțiilor volumul 16 din 2005*

Appendix 1. Pontis works (sample)

012 Concrete Deck – Bare
Do nothing
Add a protective system
Repair spalled/delam areas
Repair spalled areas and add a protective system on entire deck
Replace deck
013 Concrete Deck - Unprotected w/AC Overlay
Do nothing
Repair potholes and substrate
Replace overlay & repair substrate
Repair substrate & replace overlay
Replace deck
014 Concrete Deck - Protected w/AC Overlay
Do nothing
Repair potholes
Replace overlay
Replace overlay and protective
Replace deck
018 Concrete Deck - Protected w/Thin Overlay
Do nothing
Repair spalls/delams
Replace overlay
Replace deck

Appendix 2. Gepeto works (sample)

Defect	Place	Work	Unit	RefCant
74	C1/C2/C3	Different small works; Different small works; Cleaning dirt zones	m2	100
14	C1/C2/C3	Different structures and works; Partial reconstruction; Estimation of works for reconstruction	m2	50
16	C1/C2/C3	Different structures and works; Partial reconstruction; Estimation of works for reconstruction	m2	50
68	C1/C2/C3	Precast elements (cornice, soffit, deck slab, sidewalks); Cement concrete; Repair of joinings	m	40
37	C1/C2/C3	Repairing fissures and cracks; Joinings; Crack filling	m	10
37	C1/C2/C3	Repairing fissures and cracks; Stone; Crack filling	m	10
37	C1/C2/C3	Repairing fissures and cracks; Cracks; Crack filling	m	10
37	C1/C2/C3	Repairing fissures and cracks; Filling / injection; Crack filling	m	10
37	C1/C2/C3	Repairing fissures and cracks; Filling / injection; Injection of cracks	m	10
06	C1/C2/C3	Repairing of cement concrete surfaces; Concrete surface repair without repairing rebar; Cement mortar	m2	30
06	C1/C2/C3	Repairing of cement concrete surfaces; Concrete surface repair without repairing rebar; Remove the calcite	m2	50
07	C1/C2/C3	Repairing of cement concrete surfaces; Concrete surface repair without repairing rebar; Cement mortar	m2	30
07	C1/C2/C3	Repairing of cement concrete surfaces; Concrete surface repair without repairing rebar; Remove the calcite	m2	50
08	C1/C2/C3	Repairing of cement concrete surfaces; Concrete surface repair without repairing rebar; Cement mortar	m2	30
08	C1/C2/C3	Repairing of cement concrete surfaces; Concrete surface repair without repairing rebar; Remove the calcite	m2	50
12	C1/C2/C3	Repairing of cement concrete surfaces; Repair concrete surface and rebar; Cement mortar	m2	10
17	C1/C2/C3	Repairing of cement concrete surfaces; Concrete surface repair without repairing rebar; Sand blasting	m2	200
17	C1/C2/C3	Repairing of cement concrete surfaces; Concrete surface repair without repairing rebar; Cement mortar	m2	30
35	C1/C2/C3	Repairing of cement concrete surfaces; Concrete surface repair without repairing rebar; Cement mortar	m2	30
67	C1/C2/C3	Repairing of cement concrete surfaces; Concrete surface repair without repairing rebar; Cement mortar	m2	30
09	C1/C2/C3	Repairing of cement concrete surfaces; Consolidation	m2	50

Defect	Place	Work	Unit	RefCant
		with gunite; Without repairing rebar		

Appendix 3 DocLib works (sample)

Performing holes for evacuation of water and air	Pcs.	72	15.00
Stone packing demolition at cones quarter, embankments ...	m2	110	25.00
Bridge demolition for superstructure length $L < 12\text{m}$	Pcs.		600 000
Bridge demolition for superstructure length $12.00\text{ m} < L < 30.00\text{ m}$	Pcs.		1200000
Bridge demolition	Pcs.		
Concrete and reinforced concrete supporting walls	m3		
Injectare pentru impermeabilizarea suprafeței de contact dintre structură și teren	m2		700
Dismantle of existing metal elements	t		18
Replacement of pre-stressed precast beams $L=14\text{m}$ $h=0,72\text{m}$	Pcs.		
TOTAL			
TOTAL – BRIDGE WORKS			
HYDRO-TECHNICAL WORKS			
Concrete beam as foundation for stone packing	m3		2 300
Geo-textile as filtering support	m2		81
Gravel as draining layer	m3		665
Protection with precast concrete slabs -15cm	m2		345
Stone matrix - 0.30m thick	m3		1 026
Stone matrix - 0.50m thick	m3		1 710
Stone packing structures	m3		1 550
Demolition of cement concrete elements	m3		600
Repairs with concrete class C18/22.5	m3		2 000
Channel re-aligning	m3		218
TOTAL – HIDROTECHNICAL WORKS			
Stone packing	m3	1700	185.00
Digging for foundation: > de 4.00 m deep	m3		29.40
Drilling foundations for piles - 1080mm diameter	m		472.10
Drilling foundations for piles - 1500mm	m		655.69

Numerical implementation of meshless methods for beam problems

Victoria E. Roșca¹, Vitor M.A. Leitão²

¹Civil Engineering Faculty, Technical University of Iasi, 700050, Romania

²DECivil, Instituto Superior Técnico, TULisbon, Lisbon, 1049-001, Portugal

Summary

In the last decade a family of methods called meshless methods has been developed both for structural and fluid mechanics problems.

After these ideas, a possible classification for numerical formulations may be to separate the methods that make use of a standard finite element mesh from those that do not need a standard mesh, namely the meshless methods.

For solving a partial different equation by a numerical method, a possible alternative may be either to use a mesh method or a meshless method.

A flexible computational procedure for solving 1D linear elastic beam problems is presented that currently uses two forms of approximation function (moving least squares and kernel approximation functions) and two types of formulations, namely the weak form and collocation technique, respectively, to reproduce Element Free Galerkin (EFG) and Smooth Particle Hydrodynamics (SPH) meshless methods.

The numerical implementation for beam problems of these two formulations is discussed and numerical tests are presented to illustrate the difference between the formulations.

KEYWORDS: numerical methods; meshless formulation, EFG, SPH, beam discretisation.

1. INTRODUCTION

In engineering and science, one often has a number of data points, as obtained by sampling or some experiment, and tries to construct a function, which closely fits those data points. The so-called meshless methods construct approximations from a set of nodal data without the need for any (finite - element) *a priori* connectivity information between the nodes. In general, it is recommendable to preserve the local character of the numerical implementation. Meshless method allows to use local interpolation or approximation to represent the trial function with the values (or the fictitious values) of the unknown variable at some randomly located nodes.

There are two ways to construct approximations of a function using meshless methods:

- a continuous form, or reproducing kernel (RK) approximation.

A reproducing kernel K is a function $K(x,y) \rightarrow \mathbb{R}$, such that all evaluation functions are continuous, and the functions can be reproduced by the kernel:

$$\forall f, \quad \langle f(\mathbf{y}), K(\mathbf{x}, \mathbf{y}) \rangle = f(\mathbf{x}) \quad (1)$$

Accordingly, a function $u(\mathbf{x})$ can be approximated with $u^h(\mathbf{x})$ in a continuous way, by the integral transformation:

$$u(\mathbf{x}) \approx u^h(\mathbf{x}) = \int_{\Omega_y} K(\mathbf{x}, \mathbf{y}) u(\mathbf{y}) d\Omega_y \quad (2)$$

Smoothed Particle Hydrodynamics (SPH) [1] and Reproducing Kernel Particle Method (RKPM) [2] are two representative methods of RK.

- discrete form

There are several types of discrete approximation functions. Among these are: Moving least square (MLS) functions, Partition of unity (PU) functions, or hp-cloud functions, as representatives. Surveys can be found in [3].

The domain is discretized by a set of N nodes, and the solution, $u(\mathbf{x})$, is approximated by a linear combination of nodal coefficients, \hat{u}_{lj} , and of approximation functions, $h_{lj}(\mathbf{x})$,

$$u(\mathbf{x}) \approx u^h(\mathbf{x}) = \sum_{l=1}^N \sum_{j=1}^m h_{lj}(\mathbf{x}) \hat{u}_{lj} \quad (3)$$

where m denotes the number of coefficients per node.

In addition to these requirements, one often forces the approximation functions to satisfy other properties. For example, if the approximation functions satisfy the interpolation property (functions associated with a node are unity at that node and zero at all other nodes) and $m = 1$ (see eq. (3)), then nodal coefficients can be interpreted as the solution evaluated at the node. In this case, we refer to the approximation function as an interpolation function.

The approximations functions constructed in continuous or in discrete way are used as approximations of the *strong forms* of partial differential equations (PDEs), and those serving as approximations of the *weak forms* of PDEs to set up a linear system of equations.

To approximate the strong form of a PDE, the partial differential equation is usually discretized by specific *collocation technique*. The SPH is a representative method for the strong form collocation approach.

To approximate the weak form of a PDE various *Galerkin weak formulations* are used. Another imposed attribute arises from the condition that the resulting matrix system equation obtained by strong or weak form to be banded. This is possible when the approximation functions exhibit local support. In this case, each node has a domain of influence, a region of the domain in which the approximation functions for that node are non-zero. A large domain of influence will result in a node being influenced by nodes far away, while a small domain of influence will result in a node being influenced only by close neighbors. If the support is small, there is less coupling between nodes, and the system matrix has a small bandwidth.

In this paper, we will describe how the meshless approximation is constructed for two representative families: interpolations based on kernel methods and interpolations based on Moving Least Squares (MLS) functions.

Kernel methods are briefly summarized in section 2; MLS approximation functions are derived from a generalization of a weighted least square fit and are described in section 3.

Some concepts weak formulations are recalled in section 4, with special attention on the Galerkin formulation and, in particular, on the Element-Free Galerkin (EFG) method.

Numerical comparison between these two formulations is performed in section 5. Numerical applications for beam problems are obtained by implementing various quadrature techniques to perform the integrations of the system equations in EFG method or for discretize the continuous form of the displacement of the SPH.

2. SMOOTH PARTICLE HYDRODYNAMICS (SPH)

The kernel estimate of a function is the integral transformation of a function $u(\mathbf{x})$ to $u^h(\mathbf{x})$:

$$u(\mathbf{x}) \approx u^h(\mathbf{x}) = \int_{\Omega_y} w(\mathbf{x} - \mathbf{y})u(\mathbf{y})d\Omega_y \quad (4)$$

where $u^h(\mathbf{x})$ is the ‘reproduced’ function of $u(\mathbf{x})$, and eq. (4) is called the *reproducing equation* and $w(\mathbf{x} - \mathbf{y})$ is known as the *kernel* (or *weight*) of the transformation.

If the kernel (or weight function) is equal to the Dirac function $\delta(\mathbf{x} - \mathbf{y})$, then $u^h(\mathbf{x}) \rightarrow u(\mathbf{x})$. In SPH, the kernel is selected to have a small compact support, such that $u^h(\mathbf{x})$ approximates $u(\mathbf{x})$. Note that the eq.(4) is a continuous form of an approximation. Usually a positive function, such as the Gaussian function or spline functions are usually employed.

For the purposes of developing approximation, discrete analogs of eq. (4) are needed. The discrete form of eq. (4) is obtained by numerical quadrature of the right-hand side.

For an arbitrary PDE given by eq. (4), using SPH approximation leads to:

$$u(\mathbf{x}) \approx u^h(\mathbf{x}) = \int_{\Omega_y} w(\mathbf{x} - \mathbf{y})u(\mathbf{y})d\Omega_y = \sum_{I=1}^N w_I(\mathbf{x})\Delta V_I u(\mathbf{x}_I) \quad (5)$$

Commonly used weight functions are exponential, the cubic spline and the quartic spline. Once the quadrature is performed, the approximation can then be rewritten in the readily recognized form:

$$u^h(\mathbf{x}) = \sum_I^N \phi_I(\mathbf{x}) \cdot \hat{u}_I \quad (6)$$

where

$$\phi_I(\mathbf{x}) = \sum_I^N w_I(\mathbf{x}) \cdot \Delta V_I \quad (7)$$

From eq. (7), because ΔV_I stands for integration weights, consistency cannot be reached at boundaries, where $\sum_{I=1}^N w_I(\mathbf{x})\Delta V_I \neq 1$. The lack of consistency near boundaries leads to a solution deterioration near the domain boundaries.

In spite of absence of linear consistency, SPH methods have provided good solutions to second-order partial differential equations.

Improvements of the standard SPH method are still an active research area. There exist a number of proposed ideas for correction of SPH addressing issues such as instability, boundary conditions and consistency. An overview and further references can be found in [3], [4], and [5].

3. CONSTRUCTION OF MLS INTERPOLANTS

As in the corrected SPH methods commented in the previous section, the interpolations based on a Moving Least Squares (MLS) development can be considered as an improvement of the SPH method. However, the MLS interpolations are usually used to discretize a Galerkin formulation, and thus, accuracy and consistency in both the interpolation and its derivatives are needed in the entire domain.

Given a set of scattered nodes in ($d=1-3$) with prescribed nodal data, a surface approximation can be constructed without the need for any (finite - element) a priori connectivity information between the nodes. This viewpoint is adopted in meshless Galerkin methods, where well-known methods from data approximation theory [6] are used to construct the trial and test spaces. We touch upon a moving least squares (MLS) approximants that are used in EFG method [7], [8] as well as in many of the other meshless methods [4].

In the MLS approximation, the trial function u^h is defined as:

$$u_L^h(\mathbf{x}, \bar{\mathbf{x}}) = \sum_{j=0}^k \mathbf{p}_j(\mathbf{x}) \mathbf{a}_j(\bar{\mathbf{x}}) = \mathbf{p}^T(\mathbf{x}) \mathbf{a}(\bar{\mathbf{x}}) \quad (8)$$

where $\mathbf{p}(\mathbf{x})$ is a complete polynomial of order k . In order that the local approximation is the best approximation to $u(\mathbf{x})$ in a least-squares sense, the coefficient vector $\mathbf{a}(\bar{\mathbf{x}})$ is selected to minimize the following least square discrete L_2 norm:

$$\begin{aligned} \mathbf{J}(\mathbf{a}(\bar{\mathbf{x}})) &= \sum_I \mathbf{w}(\mathbf{x} - \mathbf{x}_I) \left[\mathbf{u}_I^h(\mathbf{x}, \bar{\mathbf{x}}) - \mathbf{u}(\mathbf{x}_I) \right]^2 \\ &= \sum_I w(\mathbf{x} - \mathbf{x}_I) \left[\mathbf{p}^T(\mathbf{x}_I) \mathbf{a}(\bar{\mathbf{x}}) - \mathbf{u}_I \right]^2 \end{aligned} \quad (9)$$

where $w(\mathbf{x} - \mathbf{x}_I)$ is the weighting function. The functional $J_{\bar{\mathbf{x}}}(\mathbf{a})$ can be minimized by setting the derivative of $J_{\bar{\mathbf{x}}}(\mathbf{a})$ with respect to \mathbf{a} equal to zero, hence $\partial J(\mathbf{a})/\partial \mathbf{a} = 0$.

In EFG method, each node is associated with a domain of influence r , which is the support of the isotropic weight function $w(\mathbf{x} - \mathbf{x}_I)$, with $w(\mathbf{x} - \mathbf{x}_I) > 0$ in its interior and $w(\mathbf{x} - \mathbf{x}_I) = 0$ outside it. Typically, domains of influence are circular or rectangular in 2D. Several weight functions can be used. A review of some of the possibilities can be found in [4]. In this work, we use cubic spline weight functions with circular domain.

The approximation can be written shortly as:

$$u^h(\mathbf{x}) = \sum_{I=1}^N \phi_I(\mathbf{x}) \hat{u}_I = \Phi^T(\mathbf{x}) \hat{\mathbf{u}} \quad (10)$$

The EFG shape function $\Phi(\mathbf{x})$ is defined as:

$$\Phi^T(\mathbf{x}) = \mathbf{p}^T(\mathbf{x}) \cdot [\mathbf{M}(\mathbf{x})]^{-1} \cdot \mathbf{B}(\mathbf{x}) \quad (11)$$

with

$$\mathbf{M}(\mathbf{x}) = \sum_{I=1}^N w(\mathbf{x} - \mathbf{x}_I) \mathbf{p}(\mathbf{x}_I) \mathbf{p}^T(\mathbf{x}_I) \quad (12)$$

$$\mathbf{B}(\mathbf{x}) = [w(\mathbf{x} - \mathbf{x}_1) \mathbf{p}(\mathbf{x}_1) \quad w(\mathbf{x} - \mathbf{x}_2) \mathbf{p}(\mathbf{x}_2) \quad \dots \quad w(\mathbf{x} - \mathbf{x}_N) \mathbf{p}(\mathbf{x}_N)] \quad (13)$$

The continuity of the shape function is governed by the continuity of the basis function $\mathbf{p}(\mathbf{x})$.

4. DISCRETE EQUATIONS OF THE GALERKIN WEAK FORM

We consider the following two-dimensional problem, on the domain Ω bounded by Γ :

$$\Delta \boldsymbol{\sigma} + \mathbf{b} = \mathbf{0} \quad \text{in } \Omega \quad (14)$$

$$\begin{aligned} \mathbf{n} \boldsymbol{\sigma} &= \bar{\mathbf{t}} \quad \text{on } \Gamma_t \\ \mathbf{u} &= \bar{\mathbf{u}} \quad \text{on } \Gamma_u \end{aligned} \quad (15)$$

where $\boldsymbol{\sigma}$ is the stress tensor, which corresponds to the displacement field \mathbf{u} and \mathbf{b} is a body force vector, $\bar{\mathbf{t}}$ is the prescribed traction vector on Neumann boundary

Γ_t , \bar{u} is the vector of prescribed displacements on Dirichlet boundary Γ_u , Δ is a linear gradient operator and \mathbf{n} is the matrix of direction cosine components of a unit normal to the domain boundary.

One of main characteristic of the meshless methods is that the shape functions do not satisfy the Kronecker delta condition at each node, i.e., $\phi_i(x_j) \neq \delta_{ij}$.

So, the imposition of essential boundary conditions is more complicated than for the standard FEM. To enforce the essential boundary conditions, Lagrange multipliers are used in the potential energy functional.

Substituting the approximate solution $u^h(\mathbf{x})$ and the test function δv constructed according to equation (8) into the variational principle using Lagrange multipliers, given by:

$$\int_{\Omega} \boldsymbol{\varepsilon}_v : \boldsymbol{\sigma} d\Omega - \int_{\Omega} \mathbf{v} \mathbf{u} \mathbf{b} d\Omega - \int_{\Gamma_t} \mathbf{v} \bar{\mathbf{t}} d\Gamma - \int_{\Gamma_u} \delta \lambda (\mathbf{u} - \bar{\mathbf{u}}) d\Gamma + \int_{\Gamma_u} \lambda \mathbf{v} d\Gamma = 0 \quad (16)$$

the following discrete equations of the weak form for regular EFG is obtained:

$$\begin{bmatrix} \mathbf{K} & \mathbf{G} \\ \mathbf{G}^T & \mathbf{0} \end{bmatrix} \begin{Bmatrix} \mathbf{u} \\ \lambda \end{Bmatrix} = \begin{Bmatrix} \mathbf{f} \\ \mathbf{q} \end{Bmatrix} \quad (17)$$

and:

$$\mathbf{K}_{ij} = \int_{\Omega} \mathbf{B}_i^T \mathbf{D} \mathbf{B}_j d\Omega \quad (18)$$

$$\mathbf{f}_i = \int_{\Gamma_t} \varphi_i \bar{\mathbf{t}} d\Gamma + \int_{\Omega} \varphi_i \mathbf{b} d\Omega \quad (19)$$

$$\mathbf{G}_{ik} = - \int_{\Omega} \varphi_i \mathbf{N}_k d\Gamma, \quad \mathbf{q}_k = - \int_{\Omega} \mathbf{N}_k \bar{\mathbf{u}} d\Gamma \quad (20)$$

where:

$$\mathbf{B}_i = \begin{bmatrix} \phi_{i,x} & 0 \\ 0 & \phi_{i,y} \\ \phi_{i,y} & \phi_{i,x} \end{bmatrix} \quad \mathbf{N}_k = \begin{bmatrix} N_k & 0 \\ 0 & N_k \end{bmatrix} \quad (21)$$

To integrate the terms \mathbf{K}_{ij} in the discrete equations, it is necessary to use numerical quadrature since the integrals cannot be evaluated analytically. To overcome the difficulties and the errors due to Gauss quadrature, we employ the idea of quasi-Monte Carlo integration [11] (used also in the original formulation of the SPH).

5. NUMERICAL EXAMPLES

For comparison of the integration purpose, we generalize the above formulation for the approximation of an arbitrary function. Let $u(x) = 1-x^2$.

In this numerical example we consider isotropic weight function, where the support is circular. In this investigation, a cubic spline window function [10] is used:

Using the approximation given by eq. (4), the discrete form is obtained by numerical quadrature of the right hand side.

By Monte-Carlo Techniques:
$$u^h(\mathbf{x}) = \frac{1}{N} \sum_{I=1}^N w_I \cdot \hat{u}_I \tag{22}$$

or Gauss rule:
$$u^h(\mathbf{x}) = \sum_{I=1}^N w_I(\mathbf{x}) \cdot \Delta V_I \cdot \hat{u}_I \tag{23}$$

Various choices for the quadratures will be tested:

- random Monte-Carlo technique [9] (as in original form of SPH);
- quasi-random Monte-Carlo sequences [9];
- Gaussian quadrature.

For EFG formulations, the integration of the coefficients of the system equation given by eq. (18) to eq. (20) is performed using Gauss quadrature

Figure 1 to Figure 3 present comparison of the SPH solution to the exact solution for the displacements along the bar.

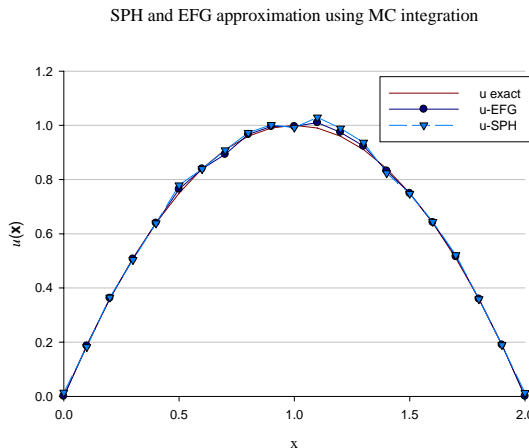


Figure 1: SPH approximation of $u(x) = 1 - x^2$ with Monte Carlo approximation, for $r_I/L = 0.02$.

These results are obtained using eleven nodes equal distributed along the length of the bar. The integration was performed using the random Monte Carlo integration the quasi-random Monte-Carlo techniques and Gauss quadrature. For integration with Monte-Carlo techniques, a simple random generator was used; for Quasi-random Monte-Carlo integration, Weyl-sequences are adopted, while for Gauss integration, 4th order quadrature rule are used.

Since Monte Carlo methods are statistical, for the integration with random Monte-Carlo, a high number of integration points are necessary. Even so, the results do not show a good accuracy.

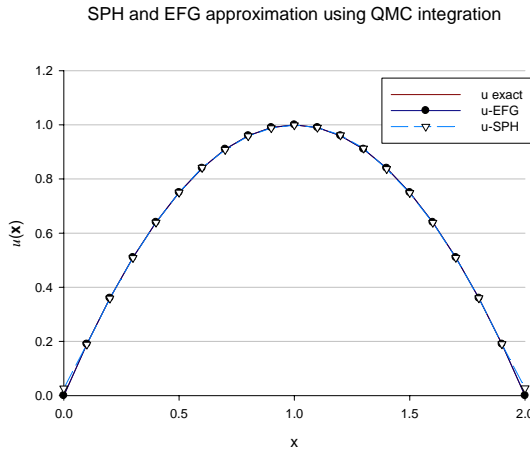


Figure 2: SPH approximation of $u(x) = 1 - x^2$ with Quasi Monte Carlo approximation, for $r_I / L = 0.02$.

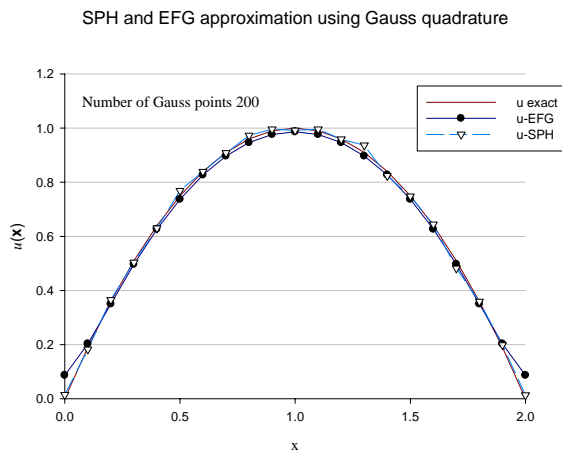


Figure 3: SPH approximation of $u(x) = 1 - x^2$ with Gauss quadrature for $r_I / L = 0.02$.

The integration by quasi Monte Carlo techniques and Gauss quadrature give better results. We note that the numbers of integrations points used by Gauss and QMC techniques are comparable: for Gauss rule, a total of 200 integration points is enough, while for QMC to achieve the same accuracy, 500 integration points are needed.

In multidimensions, using Gauss quadrature, it is more difficult to come to grips with the need to increase the number of integration points, whereas for QMC the convergence rate, despite being always low, is independent of the dimension. This makes the use of QMC integration to be promising.

5. CONCLUSIONS

Although the two principles MLS and RKPM have their roots in very different areas, (the first has its origin in data fitting, the second in wavelet theory), the resulting interpolation functions are virtually the same [3]. The original SPH method usually provides not so accurate approximations when applied for solving PDEs with boundary conditions, and thus, it is necessary to improve the interpolation, or its derivatives, in some way.

The test has clearly demonstrated that the proposed Quasi Monte Carlo integration technique provides accurate results in and can be utilized successfully for these problems. The method may be extended for 3D meshless problems without too many problems.

References

1. Lucy, L.B. A numerical approach to the testing of the fission thesis. *Astron. J.*, 82(12), 1013-1024, 1977.
2. Liu, W.K., Jun, S., Zhang, Y.F. Reproducing Kernel Particle Methods. *Int. J. Numer. Methods in Fluids*, 20, 1081 - 1106, 1995
3. Li, S., Liu, W. K Meshfree and particle methods and their applications. *Applied Mechanics Review*, 55(1), 1–34, 2002.
4. Belytschko, T., Krongauz, Y., Organ, D., Fleming, M., Krysl, P., Meshless methods: An overview and recent developments, *Comput. Methods Appl. Mech. Engrg.*, 139, pp. 3–47, 1996.
5. Randles, P.W., Libersky, L.D. Smoothed Particle Hydrodynamics: Some recent improvements and applications. *Comp. Methods Appl. Mech. Engrg.*, 139, 375 - 408, 1996.
6. Lancaster, P., Salkauskas, K. Surfaces generated by moving least squares methods. *Mathematics of Computation*, 37:141–158, 1981.
7. Belytschko, T., Lu, Y.Y., Gu, L., 1994. Element-Free Galerkin Methods, *International Journal for Numerical Methods in Engng.*, vol. 37, 229-256
8. Dolbow, J., Belytschko, T., 1998. An Introduction to Programming the Meshless Element Free Galerkin Method, *Archives of Computational Methods in Engineering*, Vol.5, 3, 207-241.
9. Sobol, I.M., 1974. The Monte Carlo Method, *University of Chicago Press*
10. Monaghan, J.J., 1988. An introduction to SPH. *Computer Physics Communications*, 48, 89 – 96
11. Roşca, V.E., Leitão, V.M.A., A simple and less-costly integration of meshless Galerkin weak form. *III ECCOMAS*, 5-8 June, Portugal, 529-540, 2006.

Pushover analysis of reinforced concrete structures (Damage theory)

Salim Sadi¹

¹ PhD student, Department of reinforced concrete, Technical University of Civil Engineering,
Bucharest 2 38RO72302, Romania

1. INTRODUCTION

The recent earthquakes, including the one that hit the region of **Boumerdes (Algeria)**, have seriously damaged and destroyed many reinforced concrete structures; they pointed out the necessity of performing an assessment of the actual seismic behavior of the existent buildings. Particularly when it comes to the seismic renovation of the reinforced concrete structures existing in the areas with high seismicity – and this is a topic of high interest – the vulnerable structures must be identified and an acceptable protection level must be established. In order to perform an assessment, the classical linear elastic methods are not appropriate, and the structure engineers had to resort to non-linear techniques, such as the static «pushover» analysis. This pushover analysis is a relatively simple way of exploring a structure’s design. The pushover analysis consists in pushing the mathematical model of a structure, imposing a displacement in order to plan the sequence of the damage in the inelastic field and to detect the weak links.

2. METHODOLOGY OF THE PUSHOVER ANALYSIS

In a pushover analysis, a nonlinear inelastic model is being subjected to a lateral load until a moving target is reached or the model is destroyed. The displacement of the target represents the maximum displacement that could take place during the seismic calculation. The control knot or the displacement of the target is set at the centre of the terrace’s level mass. Various forms of lateral load can be considered a uniform charge, a modal charge or any other form defined by the analyst. The model of the structure must be developed starting from the law-bending moments of the elements.

These properties must reflect in an accurate way their current behavior both in the elastic field, with an elastic stiffness flexional that does not crack and also in the plastic field to collapse. If the value “moment-curvature” of an element cannot be determined with precision, then experimental trials become a must. The main

results of a pushover analysis are curves in terms of capacity and demand. Fig. 1 shows the representation of the capacity relative to demand. If the demand curve intersects the capacity curve, near the elastic field, then the concept is reassured, otherwise the design is not an adequate one.

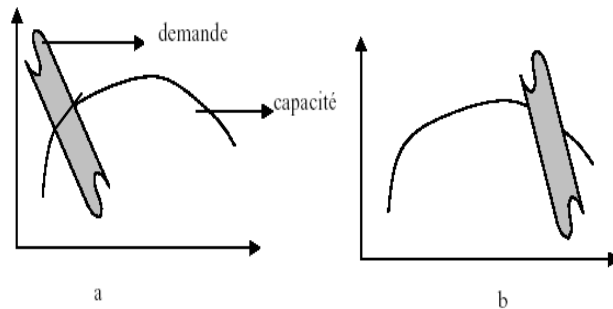


Figure 1 Seismic demand relative to the capacity
(a) reassured design, (b) non-reassured design

Under the action of an incremental charge, certain elements can be gradually plasticizing. As a result, for each event, the rigidity of the structure will be modified as shown in, where IO, LS and CP represent the beginning of the exploitation, the state of the safety exploitation and the collapse prevention.

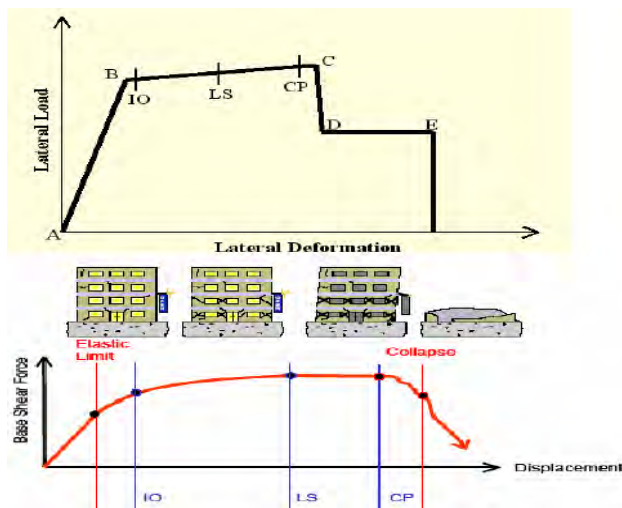


Figure 2

Capacity curve" CC " can be achieved for all kinds of buildings and infrastructures, such as bridges, warehouses and so forth. The advantage provided by this approach lies in the easiness of interpreting the state of the damaged structure. However, from the technical point of view, the steps which have to be undertaken in order to develop them often require very complex and expensive analysis in terms of time, and carried out by researchers or experienced engineers. Provided that the emergence of software suitable for this type of approach does not diminish the complexity level of the analysis, it influences the working time. Because of the calculation's iterative nature, information technology hence improves the delays in obtaining results.

In order to estimate the damages caused by earthquakes, CC averages for different types of constructions will be needed for a comprehensive study of the building. As a result, various analyses for the same type of constructions, but with different configurations, will be carried out in order to extract values defining the average of these curves. The development of CC presents, from a general point of view, the same steps of a general calculation, regardless of the type of construction. However, each type of structure has its specific features.

Obtaining CC lies in the analysis of structures, such as "pushover," or the method of spectrum capacity. The advanced method of civil engineering, originally developed in the late 70s (Freeman, 1975; Freeman, 1978), took off in the middle of the 90s (ATC 40, 1996; Chopra, 1995; Mahaney, 1993; Paret, 1996).

The techniques for the analysis of structures primarily consist in comparing a requested parameter with another parameter of capacity. The base share was the parameter traditionally used for the paraseismic conception of buildings. The engineer calculates the solicitation (force) caused by a given earthquake (or more given earthquakes) at the very base of the building, and then he compares it with the strength of the building. When using the traditional method of calculation, the forces are being reduced in an artificial way, in order to keep the design in the elastic field. In the post-elastic field, the damage appears gradually, in various parts of the building, hence causing the plastification of certain elements. Therefore a redistribution of the efforts emerges, as the demand also depends on the behavior of each element.

This way, generally speaking, the damage is more sensitive to movement than to force. These factors have led to the development of nonlinear analytical tools, such as the method «of the secant» analysis or« time-history» nonlinear analysis (ATC 40,1996)

However, these two analyses are relatively complex when it comes to widespread use. In order to facilitate the access to this type of analysis, several simplified approaches have been developed, such as the method of displacement coefficients, the method of equivalent displacement or the one of the spectrum capacity (ATC

40, 1996; Comartin et al., 2000; Fajfar, 1999, 2000; Chopra & Goel, 1999; 2002; Priestley, 2000).

Hence, the method of spectrum capacity is a pseudo-static, non-linear, simplified method of analysis. It is not a dynamic method because the request has no variations in time, and the deformation is related only to the first mode of vibration, yet the parameters specific to the dynamic analysis are taken into account, such as modal participation factor, the coefficient of effective mass, or the amplitude of the vibration mode. This is why we have called this method a "pseudo static" one.

The non-linear character is given by the taking into account of the plastic behavior of the structure, where its distortion is no longer proportional to the solicitation. The mathematical model of the structure is modified so it can take into account the decrease of the resistance of plastic components,

following a significant dissipation of hysterical energy.

This behavior is translated into very significant deformations because of the minor increments of the request. In the case of structures "beams – columns" the damage usually occurs through the formation of plastic hinge.

By using this method, the displacement becomes the first parameter, not the force. So the criterion is the maximum displacement of the structure (the resistance) against the reference imposed request (the demand). The resistance must be more important than the demand, but the reasoning is done in terms of displacement. The request is determined through the representation of the response spectrum, derived from the traditional format "period-acceleration" in the "displacement-acceleration", through a simple

change of variable.

A capacity curve is representing graphically the behavior of a building subjected to a horizontal static solicitation (Fig. 3).

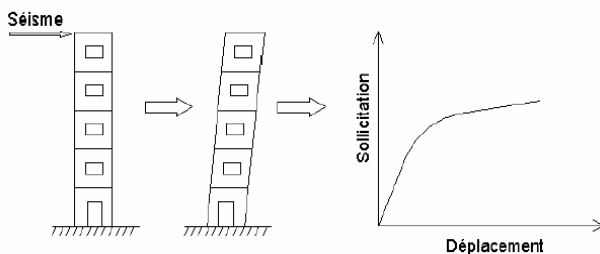


Figure 3

This method of the nonlinear analysis corresponds to a simplified pseudo static approach. The seismic strength does not vary in time, so the analysis does not have

a dynamic character. At the same time, one approximates the building's behavior in the first mode of vibration. In order to simplify: obtaining CC , from the technical point of view, consists in two changes of variables.

In the first case of changing the variables, the seismic force (taken into consideration at the superior level of the building) is transformed into acceleration, being divided by the weight of the construction:

$$\vec{F} = m \cdot \vec{a}$$

Where:

- M - is the mass of the building.
 \vec{a} - is the acceleration imposed by the earthquake to the structure

The second change of variable, the real movement at the level of the roof is transformed into spectral moving, divided by two parameters: a modal factor of modal contribution and a factor related to the amplitude of the first mode of vibration.

$$S_d = \frac{u_n}{\Gamma_1 \cdot \phi_{1,n}}$$

3. APPLICATION EXAMPLE

From the analysis to the case of frame reinforced by RC Walls.

- Description of the original building
 the analysed building has 5-floors, reinforced frame while the height of each floor is 3.06 m and the plan dimensions are shown in Fig. 4. The masses are concentrated at each floor's level and $G_t = 22.35$ KN/ml; $Q_t = 3$ KN/ml; $G_{ec} = 18.3$ KN/ml; $Q_{ec} = 4.5$ KN/ml.
- Description of the modified structures
 In order to examine the effect of reinforcing the frame by RC Walls, we will consider the following modified structures, ST1, ST2 and ST3.

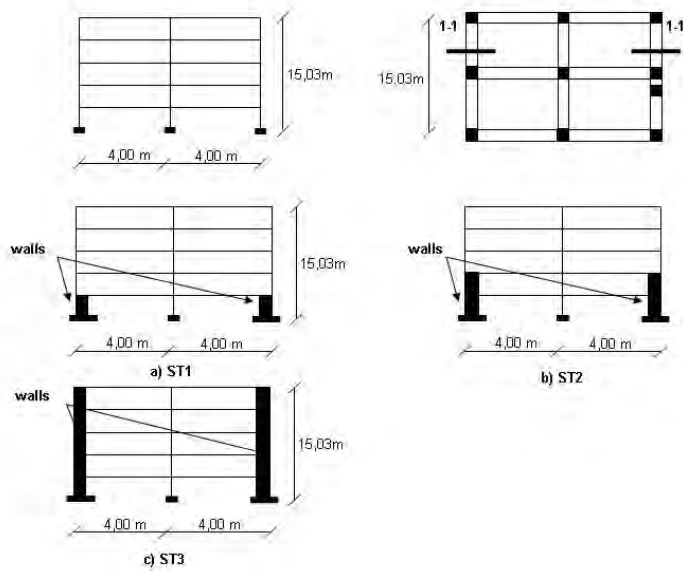


Figure 4

• Pushover analysis:

The building is designed in the post-elastic field, in accordance with the Algerian code for the III-rd zone, a region of highly seismic activity, and the nonlinear pushover analyses have been made using the ETABS software, by submitting the original and modified buildings to an acceleration in the direction X, representing the forces that the structure will be subjected to, under the action of an earthquake.

- Pushover curves:

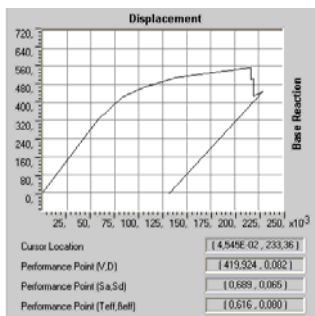


Figure 5
Pushover curve original building

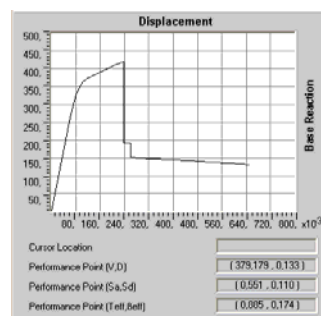


Figure 6
Pushover curve ST1

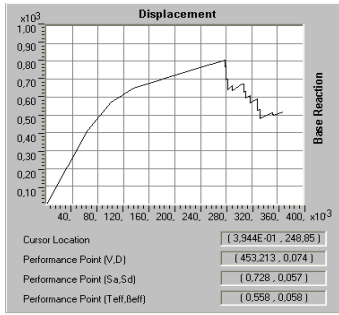


Figure 7
Pushover curve ST2

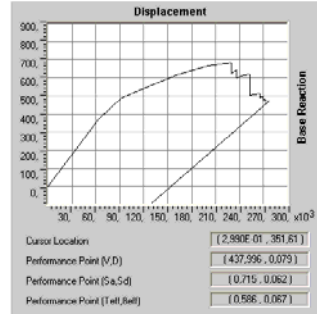


Figure 8
Pushover curve ST3

- Curve demand – capacity:

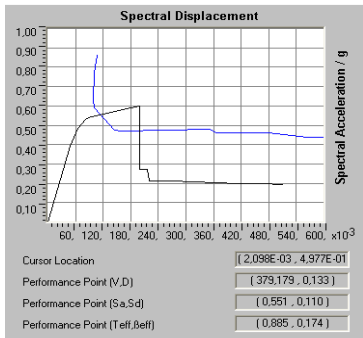


Figure 9
Demand-capacity curve ST3

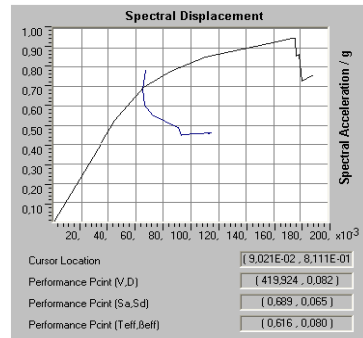


Figure 10
Demand -capacity curve ST1

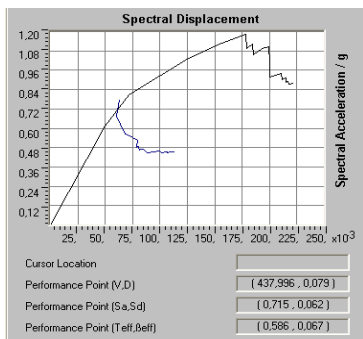


Figure 11
Demand-capacity curve ST2

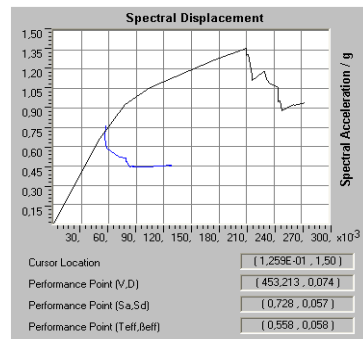


Figure 12
Courbe demande-capacite ST3

- One notes that:

1. The figures 5, 6, 7 and 8 indicate that the original building can be moved until a target movement greater than the one of the modified buildings, since it is flexible. There is a marked decrease in the capacity of shearing at the base, due to the formation of plastic hinge for a displacement of 0.13m, 0.082m, 0.079m and 0.074m for the original buildings, respectively for the modified ones. There is a rigidity for the structure ST1, ST2 and ST3, and the safety margin of these buildings has been improved.
2. The figures 9, 10, 11 and 12 show the demand-capacity curves for the original buildings, respectively the modified ones. The demand is important for the original building, since it intersects the capacity curve near the event point LS. For the modified building, ST1, the intersection occurs near the Event point B.

For ST2 and ST3 in particular, the demand curve intersects the capacity curve near the event point B, and this means an elastic reply and that the margin of safety is improved. Thus adding RC Walls before the event, not only at the first level, increases the level of security since the demand curve tends to intersect the curve near the elastic capacity field. Accordingly, one can conclude that the margin of safety vis-à-vis the collapse of the original building is small as compared to the modified buildings ST1, ST2 and ST3, since there are sufficient reserves of strength and movement.

- Formation or the plastic hinge

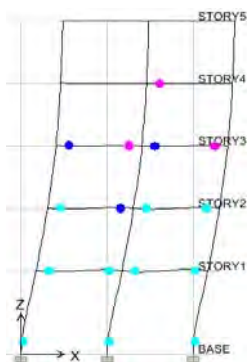


Figure 13
Original building



Figure 14
ST1

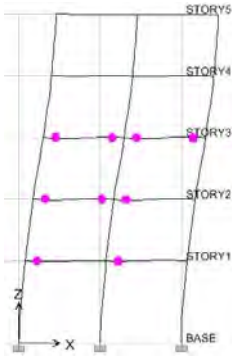


Figure 13
ST2

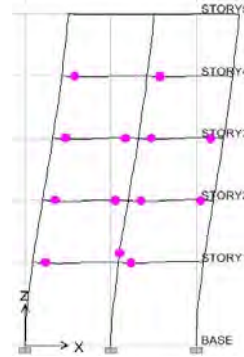
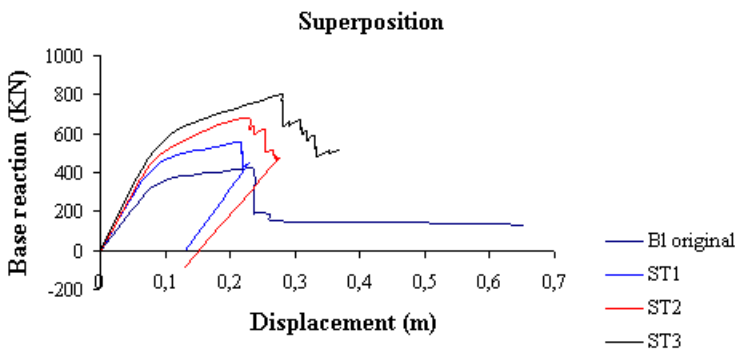


Figure 14
ST3

3. The formation of plastic hinge in the structures clearly shows that the original building will suffer great damages, especially at the first level, where the Columns are getting plastified when the LS event occurs (Fig. 13) and for the modified buildings ST1, ST2, (Fig.14, 15.16) and ST3, the improvement in great.
4. The performance point that represents the global behavior for each building is given in table 1.

Table 1 Point of movement performance – Demand	
Sd(demand in displacement)	
Original building	0,13
ST1	0,082
ST2	0,079
ST3	0,074

From table 1 one can see that the demand of moving decreases in relation to the number and the height of RC Walls.



• Summary of the obtained results

<u>Standard typologies of the buildings taken into account</u>	We have taken into consideration only the structure type «beams-Columns», «RC Walls», reinforced concrete. There has been made a distinction based on the height of RC Walls.
<u>Modelling hypothesis</u>	Several hypotheses have been made for the pushover analysis. Hence, one postulates that: 1) - The first vibration mode is the predominant reply of the structure. 2) - The post-elastic behaviour of structures is defined through plastic hinges of moment – rotation type. 3) - The plastic hinges are formed at all nodes of the structure.
<u>Results</u>	The results show a significant change in the capacity curve with the height of RC Walls. <ul style="list-style-type: none"> ➤ The displacement varies between 13.3cm and 7.4 cm. ➤ The base share varies between 379.17 and 453.213KN. Original structure : <ul style="list-style-type: none"> ➤ $V/V_{cod}=1.16$. ST1: <ul style="list-style-type: none"> ➤ $V/V_{cod}=1.28$. ST2 : <ul style="list-style-type: none"> ➤ $V/V_{cod}=1.34$. ST3 : <ul style="list-style-type: none"> ➤ $V/V_{cod}=1.38$.

CONCLUSION

The seismic behavior of the original buildings is not very adequate since the structure is of the strong beams-weak columns type, which is typical in the structural design of Algeria. By adding RC walls, and not only at the first level, one can considerably improve the behavior of the building; the studies have shown a significant improvement when it comes to the safety margin. Adding RC walls might be considered to be a solution to this problem, but one has to study a wide range of situations, in order to find the ideal solution. One has to pay attention to

the posts under the RC walls when this type of walls is not available in the whole building.

Adding RC Walls not only at the first level can greatly improve the behavior of the building, and the modified building **ST3** clearly shows a great improvement of the safety margin, because it behaves in an elastic way. Although it is costly, one has to work in the post elastic field, except for the nuclear bases or very important structures. Thus, strengthening the buildings by adding RC Walls can be considered to be a solution, but one must study a wide range of cases, in order to find the optimum solution and great attention must be paid to the study of columns located just above the RC Walls, in case the RC Walls are not provided for the entire height of the structure. The pushover analysis is a powerful and extremely useful tool, able to allow structure engineers to seek several patterns for comfort of the existing buildings and to study new structures that will behave in an appropriate manner during future earthquakes. The results obtained from a pushover analysis in terms of demand, capacity and plastic hinge offers an overview on the physical behaviour of the structure.

References:

- [1]. FEMA-273'NEHRP guidelines for the seismic rehabilitation of building's, federal emergency management agency publication 273, 1997
- [2]. ATC, seismic evaluation and retrofit of concrete buildings, vol1, ATC-40 report applied technology council, redwood city, California, 1996.
- [3]. Post-elastic calculation of matrix structures rom Bucuresti « Liviu Crainic Iliina Stanciulesc »
- [4]. Reinforced concrete structures.
- [5]. Doctorate thesis modelling of damages following earthquakes. Extension to other natural hazards (Lucian CHIROIU)
- [6]. The earthquake of May 21, 2003 in Algeria – preliminary report of the AFPS mission Parasismic Algerian rules (RPA 99)

Seismic Assessment and Strengthening of Intermediate Moment Resisting Concrete Frames

Meisam Safari Gorji¹, Masoud Taribakhsh² and Amirhossein Gandomi³

¹School of Civil Engineering, College of Engineering, University of Tehran, Tehran, Iran

²Department of Civil and Environmental Engineering, Amirkabir University of Technology, Tehran, Iran

³Department of Civil Engineering, Tafresh University, Tafresh, Iran

Summary

The objective of this study was to investigate the seismic evaluation and strengthening of Intermediate Moment Resisting Concrete Frames (IMRCF) designed according to the Iranian concrete code of practice (ABA) and Iranian Seismic Code (Standard No. 2800).

This type of RC frames is excessively used in Iran while their vulnerability in earthquake prone area and their performance level is not clearly known for designers.

In this study, several intermediate moment resisting concrete frames have been selected and subjected to seismic evaluation according to the Iranian Guidelines for the Seismic Rehabilitation of Existing Buildings.

In this study, to determine the target point of frames, the Capacity Spectrum Method (CSM) has been used. CSM method works with capacity curves of the structural system. Such curves can be obtained by means of static non-linear analysis (the so-called pushover analysis) that is for sure much less time-consuming than time-history analysis. The pushover analysis was performed using the SAP2000 computer program.

The results indicate that the frames having lesser spans are weak and some of structural elements are not able to fulfil the acceptance criteria given by the guidelines.

In the present paper to improve the seismic performance of such frames, one frame has been selected as a control frame and strengthened by adding different lateral load resisting systems.

The effects of proposed strengthening methods on performance of the frames have been investigated, pointing out the differences between the various strategies.

KEYWORDS: Seismic Assessment, Strengthening, Concrete Frame, Pushover Analysis, Capacity Spectrum Method

1. INTRODUCTION

Moment frames have been widely used for seismic resisting systems due to their superior deformation and energy dissipation capacities. The evaluation of seismic safety of existing buildings is one of the matters that are being investigated by the researchers especially in countries of high seismic risk.

In recent years, efforts have begun to establish methods to evaluate the seismic safety of buildings to determine risks and to suggest strengthening of existing buildings. The seismic repair and/or strengthening philosophy generally consist of a) system behavior improvement and b) member repair/strengthening. Although these two general approaches can be applied separately in some cases, they generally are combined. In the system behavior improvement technique, the general philosophy is to introduce a new lateral load resisting system, which will increase the lateral strength and the lateral stiffness of the existing system, which is generally a non-ductile frame with inadequate lateral stiffness. Various techniques based on this principle have been developed and applied in the past.

Many researches have been directed to rehabilitation of RC frames with different strengthening methods. Bush et al. [1], Ghobarah & Abou Elfath [2], Masri & Goel [3], Tasnimi [4] and Negro & Verzeletti [5] conducted some experimental investigations on behaviour of RC frames strengthened with steel bracing system. Perera [6] and Mehrabi et al. [7] have evaluated the seismic performance of masonry-infilled RC frames. Younfei et al. [8] and Sugano [9] investigated the behaviour of RC frames strengthened using reinforced concrete infills.

In this study several intermediate moment resisting concrete frames (IMRCF) designed according to the Iranian concrete code of practice (ABA) and Iranian Seismic Code (Standard No. 2800) have been selected and subjected to seismic evaluation.

After assessing of the performance levels of the frames and the identification of their structural defects, different strengthening strategies have been proposed and investigated based on the both experimental and analytical researches.

To achieve the aim, one frame selected as a control frame and strengthened with the following methods: adding steel bracing, masonry infills and reinforced concrete infills. The performance of the strengthened frames obtained by nonlinear static analysis using SAP2000 program and compared with each other. Furthermore, the effects of each type of strengthening method on behaviour of frames have been investigated.

2. DESCRIPTION AND CASE STUDY

2.1. Assessment procedure

Assessing of seismic behavior of existing building can be faced according to main focuses, namely in terms of either maximum strength against the horizontal seismic actions and maximum ductility, consisting in the capability for plastic displacements. Seismic assessment of structures generally results in pointing out structural deficiencies related to a general lack of strength and ductility of both a certain number of members and the structural system as a whole.

To investigate the performance level of structure, it is necessary to specify the performance point on the capacity curves of the structural system. In this study, to determine the performance point of frames, the Capacity Spectrum Method (CSM) has been used. CSM method works with capacity curves of the structural system. Such curves can be obtaining by means of static non-linear analysis (the so-called pushover analysis) that is for sure much less time-consuming than time-history analysis. So, CSM has been widely adopted by Code of Standards, because it represents a reasonably adequate procedure for design and evaluation purposes. Software for determining capacity curves of structures by means of pushover analysis are no more confined to the academic framework, but is getting more and more popular between the practicing structural engineers.

2.2. Frames description used in this study

In order to investigate the performance of the buildings designed according to the Iranian Concrete Code, the following plan depicted in Fig. 1 was selected as the base plan. To investigate the performance of different stories, the design was carried out for 6, 8, 10 stories.

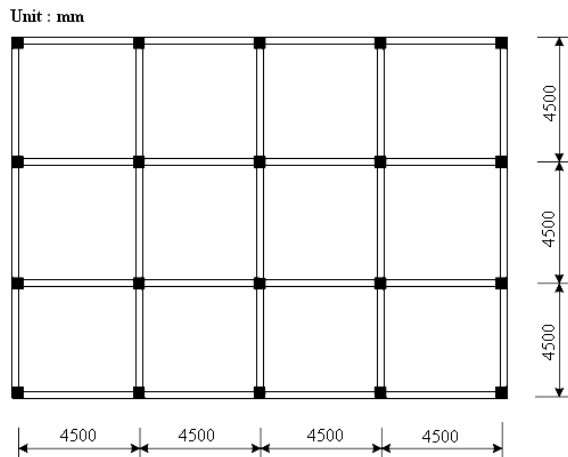


Figure 1. Floor scheme of the considered structure

This is a B group structure (offices) and rectangular type plan with 18x13.5 m dimensions. The buildings have uniform storey height of 3.2m. The design was based on the Intermediate Moment Resisting Concrete Frames (IMRCF) and all the criteria regarding the Iranian Concrete Standard (ABA) and Iranian Seismic Code (Standard No. 2800) was taken into account. The mentioned buildings were designed in a region with relatively very high seismic probability. For purposes of the modeling, two critical frames presented in the plan in X (four bays) and Y (three bays) directions were selected as based frames to be studied. With respect to the above mentioned variables (number of stories and bays) 6 frames were selected for the analysis as given in Table 1.

Table 1. Different frames type evaluation studies

Frame type	A ₁	A ₂	A ₃	A ₄	A ₅	A ₆
No. of stories	6	8	10	6	8	10
No. of bays	3	3	3	4	4	4

3. ANALYTICAL STUDY FOR EVALUATION OF FRAMES

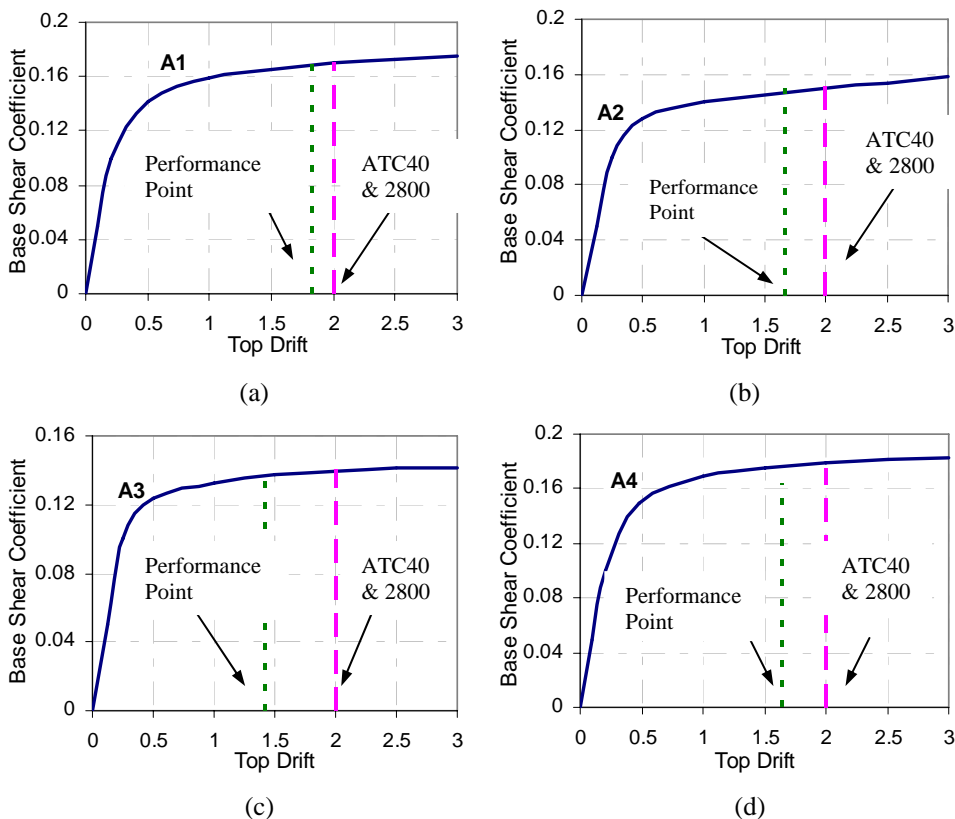
3.1. Modeling of frames for pushover Analysis

The SAP2000 static pushover analysis capabilities, which are fully integrated into the program, allow quick and easy implementation of the pushover procedures prescribed in the ATC-40 [12] and FEMA-273 [13] documents for both two and three-dimensional buildings. The criteria pertaining to the intermediate ductility has been considered in the modeling. The combination of critical loading has been

considered for the gravity loads. The accuracy of a pushover analysis is also depends on using an appropriate distribution of the lateral loads. The lateral load distribution system was according to the Iranian guidelines for the seismic rehabilitation of existing buildings and the most critical state was chosen as a basis for the distribution of lateral loading. The P- Δ effect has also been taken into consideration in the modeling. In order to model nonlinear behavior in any structural element, a corresponding nonlinear hinge was assigned in the building model.

3.2. Analysis results

The resulting capacity curves for the frames are shown in Figure 2 and performance points have specified on these curves. All curves show similar features. They are linear initially but start to deviate from linearity when inelastic actions start to take place in the beams and later in the columns. When the frames are pushed well into the inelastic range, the capacity curves again become essentially linear, but with a much smaller slopes.



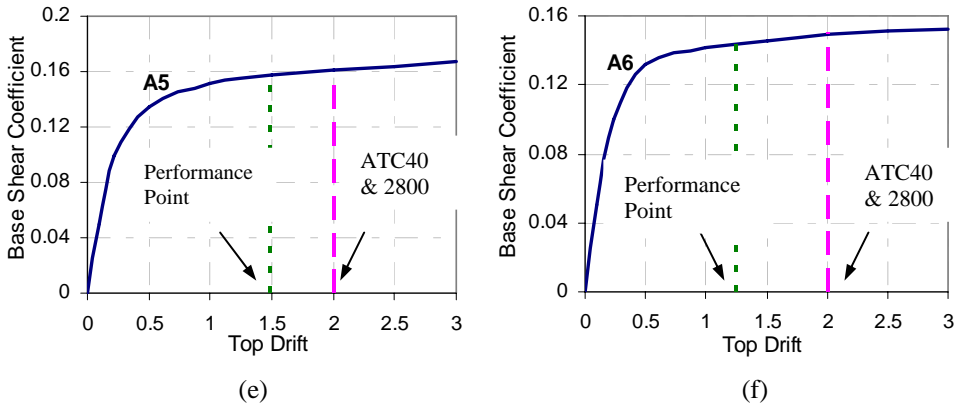


Figure 2. Pushover (capacity) curves of the analyzed frames

3.3. Determining the performance points of the frames

According to the CSM, to estimate the performance point of frames, pushover curves resulted from the analyses, have been converted to capacity diagrams in A-D (Acceleration-Displacement) format. According to the chosen β (damping ratio 5%) and the behavior type (B), the CSM spectral reduction factors have been located from ATC-40 or Iranian Guidelines for the Seismic Rehabilitation of Existing Buildings. The demands have been recalculated by accounting the spectra reductions. Furthermore, the demand diagram and capacity diagram have been plotted together in A-D system and intersection point gave displacement demand. Table 2 shows the performance points of the frames resulted from the CSM.

Table 2. Performance points of the frames resulted from the CSM

Frame Type	δ_i in A-D system (mm)	δ_i (mm)	Top Drift
A1	254	352	1.85
A2	303	425	1.71
A3	308	454	1.45
A4	231	330	1.69
A5	270	380	1.5
A6	276	402	1.28

3.4. Assessment of performance levels of structural elements

In order to evaluate the performance levels of structural elements of the frames, deformations and forces of each element (resulted from the pushover analysis) in performance points have been investigated. These results have been compared to

limiting values for different performance levels according to the Iranian Guidelines for the Seismic Rehabilitation of Existing Buildings.

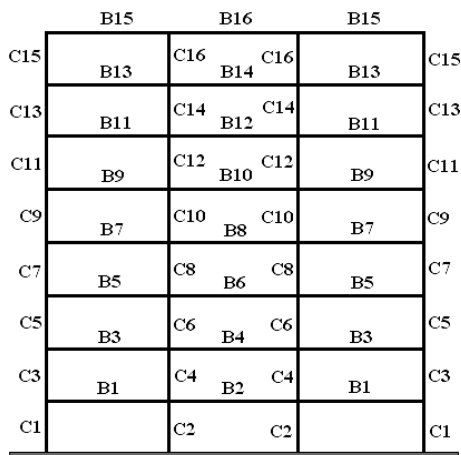


Figure 3. Different types of beams and columns in A2 frame.

Different types of beams and columns in A2 frame are shown in Fig. 3. Tables 3 and 4 show the performance levels of the beams and columns of A2 frame, respectively.

Tables 5 and 6 show the percentage of beams and columns existing in different performance levels for all of the frames.

Table 3. Evaluation of Performance levels of the beams in A2 frame.

Beam Type	$3.77 \frac{V}{b_w d \sqrt{f_c}}$	Transverse bars	$\frac{\rho - \rho'}{\rho_{bal}}$	Acceptance Criteria			Rotation	Performance Level
				IO	LS	CP		
B1	0.44	NC	0.07	0.0050	0.0100	0.0199	0.005	IO
B2	0.34	C	0.07	0.0099	0.0199	0.0249	0.004	IO
B3	0.45	NC	0.07	0.0050	0.0100	0.0199	0.013	LS-CP
B4	0.35	C	0.07	0.0099	0.0199	0.0249	0.011	IO-LS
B5	0.45	C	0.14	0.0099	0.0197	0.0249	0.021	IO-LS
B6	0.34	C	0.14	0.0099	0.0197	0.0249	0.018	IO-LS
B7	0.45	C	0.14	0.0099	0.0197	0.0249	0.0226	LS-CP
B8	0.35	C	0.14	0.0099	0.0197	0.0249	0.0201	LS-CP
B9	0.42	C	0.14	0.0099	0.0197	0.0249	0.026	CP(OVER)
B10	0.33	C	0.14	0.0099	0.0197	0.0249	0.0235	LS-CP
B11	0.36	C	0.17	0.0098	0.0197	0.0248	0.025	CP(OVER)
B12	0.28	C	0.17	0.0098	0.0197	0.0248	0.0215	LS-CP
B13	0.32	C	0.21	0.0098	0.0196	0.0248	0.021	LS-CP
B14	0.24	C	0.21	0.0098	0.0196	0.0248	0.0198	LS-CP
B15	0.23	C	0.08	0.0099	0.0199	0.0249	0.014	IO-LS
B16	0.13	C	0.08	0.0099	0.0199	0.0249	0.003	IO

Table 4. Evaluation of Performance levels of the columns in A2 frame.

Column Type	$3.77 \frac{V}{b_w d \sqrt{f_c}}$	Transverse bars	$\frac{\rho}{A_g f_c}$	Acceptance Criteria			Rotation	Performance Level
				IO	LS	CP		
C1	0.39	C	0.13	0.0047	0.0146	0.0193	-0.002	IO
C2	0.57	NC	0.09	0.0050	0.0050	0.0060	-0.002	IO
C3	0.33	C	0.11	0.0049	0.0148	0.0197	-0.003	IO
C4	0.6	NC	0.09	0.0050	0.0050	0.0060	-0.003	IO
C5	0.42	C	0.11	0.0049	0.0148	0.0197	0.004	IO
C6	0.64	NC	0.10	0.0050	0.0050	0.0060	0.004	IO
C7	0.40	C	0.09	0.0050	0.0050	0.020	0.004	IO
C8	0.63	NC	0.08	0.0050	0.0150	0.006	0.005	IO
C9	0.46	C	0.09	0.0050	0.0150	0.020	0.004	IO
C10	0.66	C	0.08	0.0050	0.0150	0.020	0.004	IO
C11	0.35	C	0.07	0.0050	0.0150	0.020	-0.005	IO
C12	0.56	C	0.07	0.0050	0.0150	0.020	-0.005	IO
C13	0.39	C	0.04	0.0050	0.0150	0.020	-0.004	IO
C14	0.51	C	0.05	0.0050	0.0150	0.020	-0.006	IO-LS
C15	0.19	C	0.03	0.0050	0.0150	0.020	-0.004	IO
C16	0.32	C	0.03	0.0050	0.0150	0.020	-0.012	IO-LS

Table 5. Percentages of beams existing in different performance levels.

Performance level	Frame Types					
	A1	A2	A3	A4	A5	A6
IO	11.1%	16.66%	30%	29.17%	21.88%	47.5%
IO-LS	44.44%	25%	26.66%	41.67%	50%	17.5%
LS-CP	33.33%	41.6%	23.33%	29.17%	28.12%	32.5%
OVER CP	11.1%	16.66%	20%	0	0	2.5%

Table 6. Percentages of columns existing in different performance levels.

Performance level	Frame Types					
	A1	A2	A3	A4	A5	A6
IO	54.16%	87.5%	72.5%	83.33%	92.5%	74%
IO-LS	37.5%	12.5%	17.5%	13.33%	5%	16%
LS-CP	8.33%	0	7.5%	3.33%	2.5%	6%
OVER CP	0	0	2.5%	0	0	4%

4. STRENGTHENING STRATEGIES

In order to investigate the effects of different strengthening methods, the A₂ frame is selected as a control frame. With respect to the performance levels of the structural elements of the selected frame, it is clear that this frame has some deficits regarding the lateral stiffness and as the deficits are distributed in many stories, the lateral strength and stiffness of the system should be improved. In this

study, to improve the performance of the frame, different strengthening methods have been investigated as shown in Fig 4.

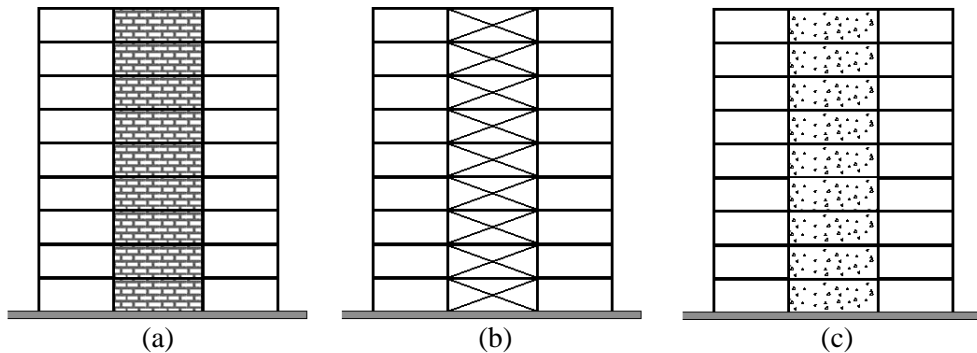


Figure 4. Added different lateral load resisting systems considered in this study. (a), (b) and (c) are masonry infills, steel bracing and reinforced concrete infills, respectively.

4.1. Steel Bracing System

In this part, the characteristics of the added steel bracings are such that the failure of the frame first occurs in bracings, then in beams and after that in columns. In order to add steel bracing system, 2U10 (channel section) was used for the first four stories and 2U8 was used for the last four stories. In order to model nonlinear behavior in any structural element, a corresponding nonlinear hinge was assigned in the frame models. PMM hinges at the columns, P hinges at the steel braces and moment hinges at the beams were assigned in the models according to modelling criteria of Iranian Guidelines for the Seismic Rehabilitation of Existing Buildings. The pushover curves of the control frame (A2) and strengthened frame with steel bracing are shown in Fig. 5. It can be observed that the strength and stiffness of the frame has well increased. The ductility of the strengthened frame in this case has decreased were compared to the control frame. The Analysis results show that first the braces buckled in compression and then hinges occurred in some braces and beams and ultimately the failure mechanism were transmitted to the columns. After evaluation of performance levels of the structural elements of the strengthened frame, it was observed that the steel bracing system was able to improve the performance of the frame significantly and provided Life Safety performance level intended by the code.

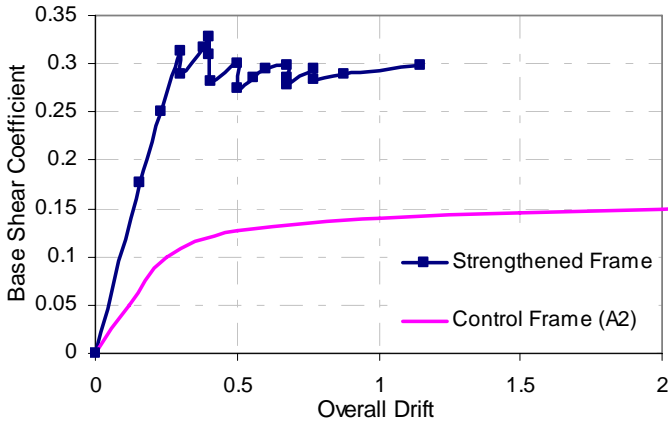


Figure 5. Pushover (Capacity) curves of the frames.

4.2. Shear wall

In this strengthening method, the reinforced concrete infills were added to the middle bay of the control frame. It was assumed that the added shear wall to the system interact completely with the frame beams and columns by stitching the reinforcements. In this case, it can be considered that the added shear wall and the two side columns work monolithically. Given that the shear wall in the frame are slender with wall height-to-length ratio well above 3 and therefore seismic response of the shear wall is expected to be dominated by flexure, as well as because modeling nonlinear behavior in SAP2000 pushover analysis is limited to frame elements, the shear walls were modeled as equivalent frame elements. According to the Iranian Concrete Code, the minimum values for thickness of the wall and reinforcement ratio are 0.15cm and 25%, respectively. Fig. 6 shows the pushover curves resulted from the analysis. It can be observed that the lateral strength of the system has been increased significantly. After determining the performance levels of the structural elements of the strengthened frame with the shear wall, it is concluded that all structural elements of the strengthened frame are in the Immediate Occupancy (IO) performance level. Adding the shear wall to the frame not only has met the performance level of Life Safety (LS), but also has increased the performance level of the frame and let the frame to lie in the Immediate Occupancy performance level.

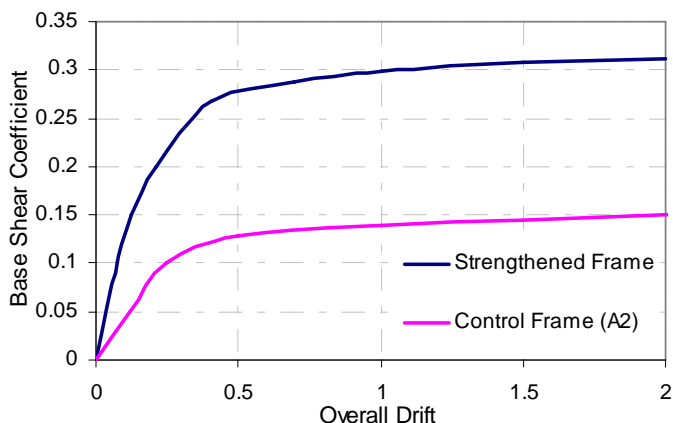


Figure 6. Pushover (Capacity) curves of the frames.

4.3. Masonry Infills (MI)

The third strategy for strengthening of the frame in this study was added masonry infills. There is strong evidence that masonry infills enhance the lateral strength of framed building structures under severe earthquake loads and have been successfully used to strengthen the existing moment-resisting frames in some countries. In order to use masonry infills and regarding the diversity of using these materials as well as different characteristics of them, the results of laboratory tests of Tasnimie et al. [4] was used. It should be noted that because the axial load effects in providing the cohesive bond is not high, this effects has been ignored according to Iranian Guidelines for the Seismic Rehabilitation of Existing Buildings. Hence, only the cohesive bond of masonry has been taken into account. According to the Iranian Guidelines, Behavior of frame with masonry infills was modeled with a diagonally braced frame model in which the columns act as vertical chords, the beams act as horizontal ties, and the infill is modeled using the equivalent compression strut analogy. Characteristics of the equivalent compression strut are shown in Table 8. The combined behavior of MI-RC frames is such that the total seismic design force is resisted in proportion to the lateral stiffnesses of the RC frame and MI walls at all story levels. The analysis results show that plastic hinges were formed almost in all beams and compressive strut. The failure mechanism occurred in beams concurrently with the compressive strut. Thus introduction of Masonry infills in RC frames changes the lateral-load transfer mechanism of the structure from predominant frame action to predominant truss action. Results show that by placing masonry wall in building, the lateral strength of the system have been increased and the performance level of the structural

elements of the frame have been improved. Fig. 7 shows the pushover curves resulted from the analysis.

Table 7. Characteristics of the equivalent compression strut.

Story	T_{inf} (cm)	λ	a (cm)	A_{ni} (cm^2)	F_{vie} ($\frac{kg}{cm^2}$)	Q_{CE} (kg)
1	20	0.0137	76.7	9325	2.17	20200
2	20	0.0137	76.7	9325	2.17	20200
3	20	0.0121	79.75	9225	2.17	19980
4	20	0.0121	79.75	9225	2.17	19980
5	25	0.0114	80.6	11400	2.17	24700
6	25	0.0114	80.6	11400	2.17	24700
7	30	0.0109	80.25	13525	2.17	29320
8	30	0.0109	80.25	13525	2.17	29320

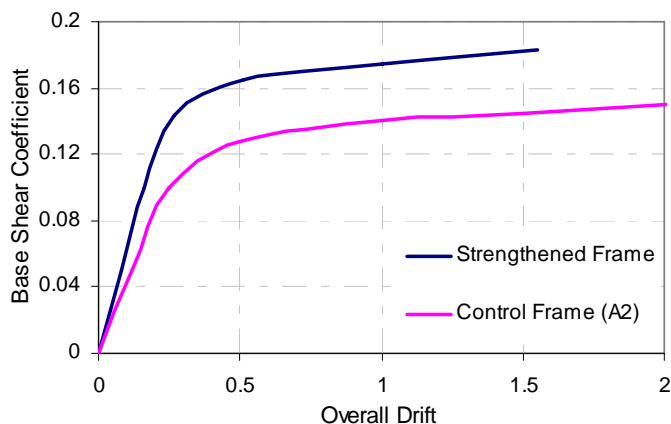


Figure 7. Pushover (Capacity) curves of the frames.

4.3. Comparison between Different Strengthening Methods

CSM spectral reduction factors and target points of the frames are shown in Table 8. Fig. 8 shows the pushover curves resulted from the analyses for different type of strengthened frame. By comparing the curves it can be observed that by adding steel bracings the most increase in the lateral strength of the system was achieved and after that the shear wall, masonry infills had the most effects on the lateral strength of the system, respectively.

Table 8. CSM spectral reduction factors and performance points of the frames

Frame type	K	β_{eff}	β_0	SRV	SRA	δ_t in A-D system (mm)	δ_t (mm)	Top drift
------------	---	---------------	-----------	-----	-----	-------------------------------	-----------------	-----------

Control (A2)	0.7	37.68	46.8	0.56	0.44	303	425	1.71%
Strengthened with steel bracing	0.77	22.28	22.32	0.60	0.52	86.2	120	0.50%
Strengthened with shear wall	0.77	22.88	23.21	0.62	0.50	95.7	142	0.62%
Strengthened with masonry infills	0.73	30.68	36	0.56	0.44	230	291.5	1.18%

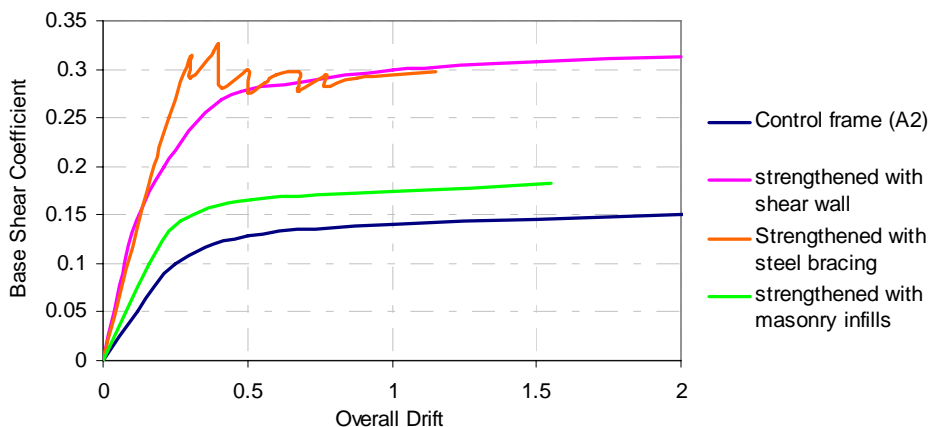


Figure 8. Comparison of pushover curves before and after the strengthening

5. CONCLUSIONS

This article presents an analytical investigation of the effects of different strengthening methods on the seismic performance of the Intermediate Moment Resisting Concrete Frames (IMRCF) using rational displacement-based analytical method (nonlinear static pushover analysis) based on realistic and efficient computational models of the structural components. On the basis of results, the following conclusions can be drawn:

Assessment of the performance levels of the frames structural elements according to the Iranian guidelines, shows that some of the beams and columns were seismically deficient in terms of life safety.

The frames including four spans have a better performance as compared with the frames having three spans.

Comparison between the three strengthening strategies, shows that the most increase in the lateral strength were related to using steel bracing system.

With regards to the performance levels of the structural elements in strengthened frames, the best strengthening system was adding shear wall.

By utilizing reinforced concrete infills to strengthen the frame, the performance level of the frame has been improved significantly. In this case, the Immediate Occupancy (IO) performance level was reached and the relative displacement corresponding to the performance point decreased significantly owing to the increase in lateral stiffness of the strengthened frame.

In the strengthened frame with steel bracing system, the compressive bracings buckle rapidly. In order to prevent the buckling of braces, if stronger braces were used, the failure mechanism may transferred to columns and beams owing to the increase in axial load of columns as well as the increase in shear forces of beams and columns. In this case study, in order to improve the performance level up to the Immediate Occupancy, only adding bracing is not sufficient but also some of the structural element should be strengthened along with adding steel bracings to resist the increase of forces in these structural elements.

The analyses results show that ordinary masonry infills can increase the lateral strength of the frames and improve the performance level of the system to some extent.

References

1. Bush, T., Jons, E., Jirsa, J., Behavior of RC Frame Strengthening Using Structural Steel Bracing, *Journal of Structural Engineering*, 1991, Vol. 117, No. 4, April 1991, pp. 1115-1126.
2. Ghobarah, A., Abouelfath, H., Rehabilitation of a Reinforced Concrete Frame using Eccentric Steel Bracing, *Journal of Engineering Structures*, Vol. 23, No. 7, July 2001, pp. 745-755.
3. Masry, A. C., Subhash, C. G., Seismic Design and Testing of an RC Slab-Column Frame Strengthened by Steel Bracing, *Journal of Earthquake Spectra*, Vol. 12, No. 4, November 1996, pp. 645-666.
4. Tasnimi A. A., Strengthening of Reinforced Concrete Frames Using Steel Bracing, *Building and Housing Research Center, research report*, September 2000, Tehran, Iran.
5. Negro, P., Verzeletti, G., Effect of Infills on the Global Behavior of R/C Frames: Energy Considerations Pseudo-Dynamic Tests, *Earthquake Engineering & Structural Dynamics*, 1996, Vol. 25, No. 8, pp. 753-773.
6. Prera, R., Performance evaluation of masonry-infilled RC frames under cyclic loading based on damage mechanics, *Journal of Engineering Structures*, Vol. 27, No. 8, July 2005, pp. 1278-1288.
7. Mehrabi, A. B., Shing, P. B., Schiller M. P., Noland, J. L., Experimental Evaluation of Masonry-Infilled RC Frames, *Journal of Structural Engineering*, 1996, No. 3, pp. 228-237.
8. Yunfei, H., Yufeng, C., Changs, S., Bainian, H., The Experimental Study of a two-Bay Tree Story Reinforced Concrete Frame Under Cyclic Loading, *Proceeding of the Eight Symposium on Earthquake Engineering*, 1986, Roorkee, India.
9. Sugano, S., Seismic Strengthening of Existing Reinforced Concrete Building in Japan, International Institute of Seismology and Earthquake Engineering Building Research Institute Ministry of Construction, 1992.

10. Mohele, J. P., State of Research on Seismic Retrofit of Concrete Building Structures in US, *Pacific Earthquake Engineering Research Center*, University of California Berkeley, 2000.
11. Iranian Guidelines for the Seismic Rehabilitation of Existing Buildings, *International Institute of Earthquake Engineering and Seismology*, 2002, Tehran, Iran.
12. ATC-40, “Seismic Evaluation and Retrofit of Concrete Buildings”, *Applied Technology Council*, 1996.
13. FEMA-273, “Seismic Rehabilitation Guidelines”, *Federal Emergency Management Agency*, September 1996.

The Comparison of the Dynamic Parameters of the Rail Fastening Vossloh W 14 and Pandrol FC

Jaroslav Smutny¹, Lubos Pazdera² and Ivo Moll³

¹Department of Railway Structures and Constructions, Brno University of Technology,
Brno, 602 00, Czech

² Department of Physics, Brno University of Technology, Brno, 602 00, Czech

³Department of Mathematics and Descriptive Geometry, Brno University of Technology,
Brno, 602 00, Czech

Summary

The paper deals with the analysis and comparison of the dynamic parameters of the rail fastening used in a standard way in the trunk line of the high-speed lanes of the Czech Rail, i.e. the elastic rail fastening Vossloh W 14 and Pandrol FC. The paper also includes the description of the methods of measurement and a suitable mathematical apparatus for the evaluation of the measured parameters. The conclusion of the paper is devoted to recommendations for further measurement and practical applications.

KEYWORDS: Dynamic Analysis, Rail Fastening, Vossloh, Pandrol, Time Frequency Analysis, Rihaczek Transform

1. INTRODUCTION

The fundamental claim put on particular parts of the railway superstructure is their operation ability and the connected minimum costs for their production, maintenance and repairs. In spite of the fact that the railway superstructure during its more than one hundred and fifty year history has developed almost to its perfection, new technical improvements can still be found.

Even if the primary aim of the modernisation of the main railway lines in the network of the Czech Rail, J.S.C. is not the reduction of the noise emissions and vibrations caused by the operation but preferably the creation of the corresponding infrastructure in a way to be able to become a part of the standard European railway network using the transportation speed up to $160 \text{ km}\cdot\text{h}^{-1}$, the introduction of modern structures of the railway superstructure itself causes an interesting secondary effect of the modernisation, which is the reduction of noise emissions and in particular, the vibrations spreading through the ground. [1]

2. EXPERIMENTAL SET UP

It is appropriate to observe that the vibration spreading through the ballast bed to the structural layers of the line are of cardinal importance from the stability of the engineering structure stability viewpoint. [2] The task of the optimally designed rail fastening is, besides others, to eliminate maximally these vibrations, which results in slowing down the process of degradation of the line structure, especially the railway superstructure. Therefore, besides the sensors placed on the track length, another indicator of the acceleration of vibrations was placed in the railway bed on a special rail pad of a hemisphere shape. The surface of this measuring hemisphere is fitted with 21 small pyramids wedged in the aggregates.

The measuring places were chosen so that the parameters of the horizontal alignments, slope conditions and gravel bed of these sections may be as similar as possible. A complete measurement in the field was carried out in the following four measuring situations:

➤ *Locality Hranice na Moravě, Vossloh fastening*

The measuring place was situated in the circular part of the right-side curve between the stopping point Bělotín and the railway station Hranice na Moravě (Figure 1 and Figure 2).

➤ *Locality Hranice na Moravě; Pandrol fastening*

The measuring place was situated in the circular part of the left-side curve between the railway stations Drahouše and Lipník nad Bečvou (Figure 3).



Figure 1 General view of the working place

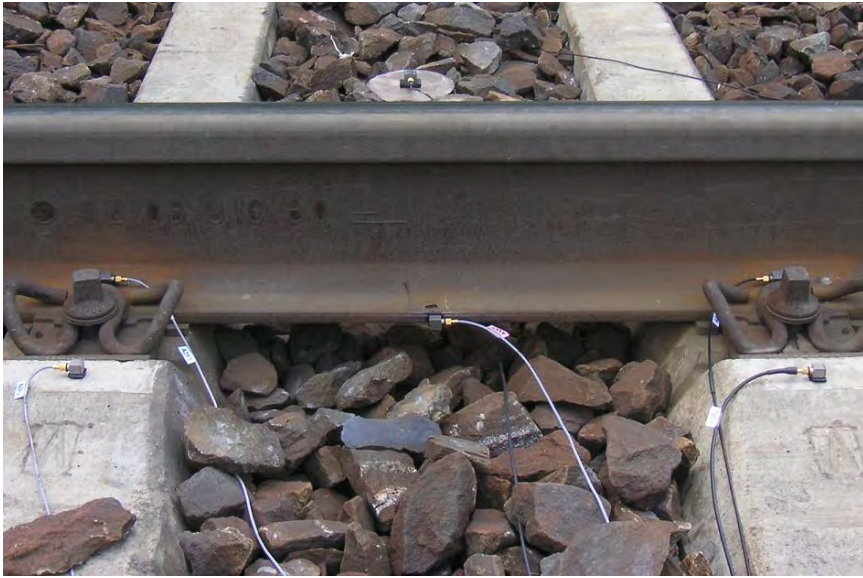


Figure 2 Sensors location, the elastic rail fastening Vossloh W 14



Figure 3 Sensors location, the elastic rail fastening Pandrol FC

3. JOINTED TIME FREQUENCY TRANSFORMATION

In many applications, analyses are interested in the frequency content of a signal locally in time. Non-linear methods present next fundamental class of time frequency distributions. These methods are based upon estimating an instantaneous power spectrum using a bilinear operation on the signal $x(t)$ itself. The class of all non-linear time-frequency distributions to time shifts and frequency-shift is called Cohen’s class. Similarly, the class of all quadratic time-frequency distributions covariant to time-shift and scales is called the Affine class. The intersection of these two classes contains time-frequency distributions, like the Wigner-ville distribution, that are covariant to all operators. One of them Zhao-Atlas-Marks transform is defined by [2, 3]

$$C_x(t, f) = \iiint q(\theta, t', \tau, t, f) \cdot \psi(\theta, \tau) \cdot x\left(t' + \frac{\tau}{2}\right) \cdot x^*\left(t' - \frac{\tau}{2}\right) \cdot d\theta \cdot dt' \cdot d\tau \quad (1)$$

where

$$q(\theta, t', \tau, t, f) = e^{-j \cdot 2\pi \cdot \theta \cdot t - j \cdot 2\pi \cdot f \cdot \tau + j \cdot 2\pi \cdot \theta \cdot t'} \quad (2)$$

and Kernel function is [3]

$$\psi(\theta, \tau) = h(\tau) \cdot \frac{\sin a \cdot \theta \cdot \tau}{a \cdot \theta \cdot \tau} \quad (3)$$

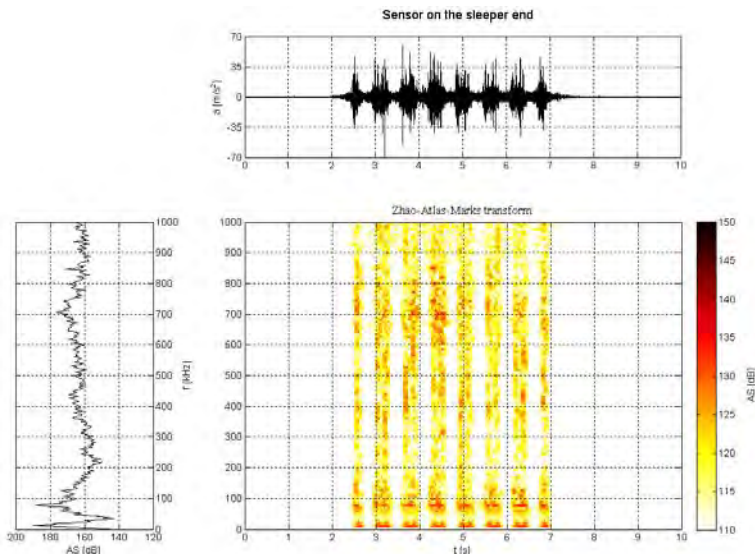


Figure 4 Time history of acceleration, amplitude spectrum and time-frequency spectrum, train set Pendolino, fastening Vossloh, 140 km/h

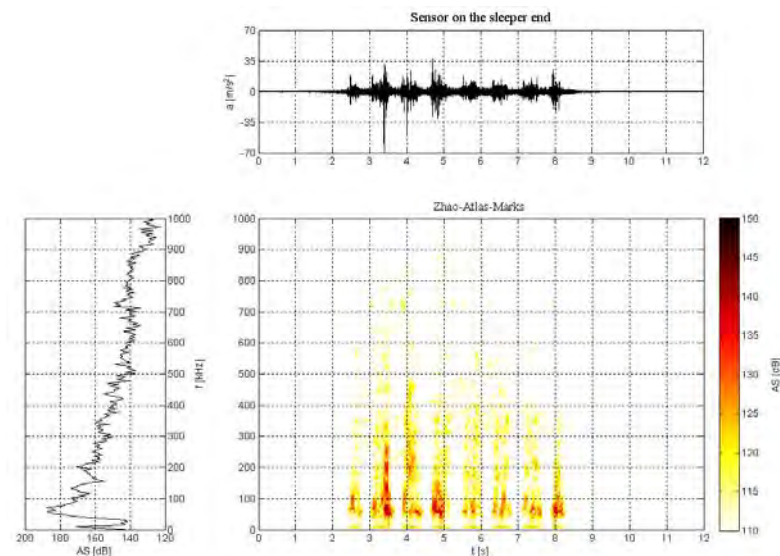


Figure 5 Time history of acceleration, amplitude spectrum and time-frequency spectrum, train set Pendolino, fastening Pandrol, 140 km/h

4 RESULTS OF THE MEASUREMENT AND ITS INTERPRETATION

The signals measured on the sleeper end were plotted on graphs. The specimens of the graphs which were used for the analysis and the following comparison are presented in Figure 4 and Figure 5. Zhao-Atlas-Marks transform was applied for analysis of signal from Pendolino train. The results are shown in Figure 4 for fastening Vossloh and Figure 5 for fastening Pandrol. There are three graphs in Figure 4 and Figure 5. The upper graphs show time history of acceleration and left ones show frequency spectrum. Last graph included time frequency distribution of spectrum computed by using Zhao-Atlas-Marks transform. Note horizontal axis is time, vertical is frequency and color (or shade gray) mean spectra values.

Based upon the comparison of both fastening structures, the following conclusions are clearly shown in particular measuring places:

- From the point of view of vertical vibrations measured on the base of the rail, 2÷3times higher values are observed in case of the Pandrol fastening.
- The comparison based upon vertical vibrations on the heads of rails, the Pandrol fastening offers much better values. With this fastening the energy effects of these vibrations is roughly of a half value compared with the Vossloh fastening.

- In the ballast bed, the fastening structure Pandrol offers better values both in acceleration and in the speed of vibrations while just the speed of vibrations is the most important parameter in the railway bed. This is most evident in case of the vibrations perpendicular to the rail axis.
- The conclusions described above are evident both from the time and frequency analyses.

5. CONCLUSIONS

Based upon the comparison of both fastening structures, the following conclusions are clearly shown in particular measuring places:

- From the point of view of vertical vibrations measured on the base of the rail, 2÷3times higher values are observed in case of the Pandrol fastening.
- The comparison based upon vertical vibrations on the heads of rails, the Pandrol fastening offers much better values. With this fastening the energy effects of these vibrations is roughly of a half value compared with the Vossloh fastening.
- In the ballast bed, the fastening structure Pandrol offers better values both in acceleration and in the speed of vibrations while just the speed of vibrations is the most important parameter in the railway bed. This is most evident in case of the vibrations perpendicular to the rail axis.
- The conclusions described above are evident both from the time and frequency analyses.

Acknowledgements

This research has been supported by the research project GACR 103/07/0183 ("The investigation of dynamic effects due to the rail transport by the method of quadratic time and frequency invariant transformations ") and by research project MSM 0021630519 ("Progressive reliable and durable load-bearing structural constructions")

References

1. Smutný J., Pazdera L. New techniques in analysis of dynamic parameters rail fastening, *InSight, The Journal of The British Institute of Non-Destructive Testing*, Vol. 46, No 10, October, 2004, pp. 612-615, ISSN 13542575
2. Melcer, J, Kucharova, D, Mechanical properties of rubber pads under static and dynamic load, *International Conference on Materials Science and Engineering, BRAMAT 2003, Romania, Brasov, 3/2003, University of Brasov, 2003, pp 18-314.*
Smutný J., Pazdera L., *Time frequency analyses of real signals*, 2003
3. Cohen L. Time-frequency distributions - a review, *Proc. IEEE*, Vol. 77 No. 7, 941-981, 1989

The Analysis of Dynamic Effects in Turnout Structures by the Method of Quadratic Time and Frequency Invariant Transformations

Jaroslav Smutný¹, Lubos Pazdera², Ivo Moll³ and Miroslav Bajer⁴

¹Department of Railway Structures and Constructions, Brno University of Technology,
Brno, 602 00, Czech

² Department of Physics, Brno University of Technology, Brno, 602 00, Czech

³Department of Mathematics and Descriptive Geometry, Brno University of Technology,
Brno, 602 00, Czech

⁴Department of Metal and Timber Structures, Brno University of Technology,
Brno, 602 00, Czech

Summary

The subject of the paper is focused on the analysis of dynamic parameters of turnout structures. The paper also deals with the comparison of the parameters measured in the turnout provided with the spring movable frog and with their comparison with the fixed crossing frog. A part of the paper also includes the description of the methods of measurement and a suitable mathematical apparatus for the evaluation of the parameters measured. The conclusion of the paper will deal with the recommendations for further measuring and practice.

KEYWORDS: Time, Frequency, Transform, Dynamic, Structures, Quadratic Transform

1. INTRODUCTION

The vibration of the superstructure is particularly affected by its quality, by operational technical conditions, by climatic phenomena and above all by the dynamic loading due to the wheelsets of the railway vehicles. The weight on the axle, the speed of the railway vehicles, the arrangement of axles, their spring mounting and the spring mounting of the coach body and last but not least also the quality of the running surface of the wheel tyre also affect vibration. [2]

The optimum design of new turnout structures requires the knowledge of their dynamic behaviour directly in the terrain. Laboratory measurement or the computer simulations do not offer sufficiently accurate results due to the complexity of the whole structure and a very strong non-stationary dynamic load. Therefore the measurement of dynamic effects in turnouts under the real operation is important. Furthermore, an experimental analysis of dynamic effects in turnout structures

focused on the comparison of the turnout provided with the spring crossing movable frog (SCMF) with the standard turnout structure with a fixed frog point (FFP) is described.

2. EXPERIMENTAL SET UP

The compared types of turnouts are to be found in the Břeclav deviation of the railway station Vranovice (Fig. 1). These are the turnouts No.5 and No. 3 which form a simple crossover and both of them are run in the straight direction against the frog point. Since the aim was to compare the turnout structure provided with the fixed frog point with the spring movable frog, the measurement was arranged in the way so that both turnout structures may be mutually compared. So, it was necessary to find such measuring points that are approximately the same or which are at the same distance and position because of the frog point. Therefore the following measuring points were chosen:

- wing rail - both in vertical and cross directions
- frog point – both in vertical and cross directions
- sleeper under the frog point – in vertical direction (centre and the sleeper head)
- ballast bed – in vertical direction, in cross direction and in longitudinal direction

Since the dynamic effects are best captured by the acceleration time behaviour (or by the speed), the method of measuring these quantities by means of the piezoelectric accelerometers was used. The sensors used were fixed at chosen point by means of the plastic rail pads which were glued on the chosen spots with the “second glue”. In total, 11 accelerometers by the firm Bruel&Kjaer were used. The measurement of vibration acceleration took place on 30th March 2007 (a turnout provided with the spring crossing frog) and on 3rd April 2007 (a turnout with fixed frog point). For measuring vibrations, a 48-channel measuring exchange DEWE – 2502 was used. During the passage of a set of wagons the speed of the passage was measured by the manual speed meter Bushnel.

The measured signals were divided based on the kind of trains (SC, EC, ET, PT, FT). The measurement was evaluated in the time, frequency and time-frequency regions.

In the time region, the values of the maximum, minimum and especially the RMS (effective acceleration values) were calculated. In the frequency region, the Welch method was used, which is essentially the averaging method based upon the Fourier transformation. Furthermore, the time-frequency analysis was also used, which offers the analysis of frequency components in time. As a basic time frequency method, the short-time Fourier transformation was used. Let us observe

that the third-octave analysis was also used for the comparison of particular measured points.



Figure 1. Measured part of railway



Figure 2. Experimental set up of 3 axis sensor



Figure 3. Experimental set up of sensors

3. ANALYSIS

Jointed time frequency transform Rihaczek was applied to analysis of measured signals (Figures 4 and 5). Its definition equation is given [1, 3, 4]

$$C_x(t, f) = \iint A_x(\theta, \tau) \cdot \psi(\theta, \tau) \cdot e^{-j \cdot 2\pi \cdot f \cdot \tau} \cdot e^{-j \cdot 2\pi \cdot \theta \cdot t} \cdot d\tau \cdot d\theta \quad (1)$$

where

$$A(\theta, \tau) = \int x\left(t + \frac{\tau}{2}\right) \cdot x^*\left(t - \frac{\tau}{2}\right) \cdot e^{-j \cdot \theta \cdot t} \cdot dt \quad (2)$$

and

$$\psi(\theta, \tau) = e^{\frac{j \cdot \theta \cdot \tau}{2}} \quad (3)$$

The signals measured on the center of sleeper under the frog point – in vertical direction were plotted on graphs. Figure 4 and 5 represent the analysis during the passage of the Pendolino set of wagons by Rihaczek transform. There are three graphs in Figure 4 and Figure 5. The upper graphs show time history of acceleration and left ones show frequency spectrum. Last graph included time frequency distribution of spectrum computed by using Rihaczek transform. Note horizontal axis is time, vertical is frequency and color (or shade gray) mean spectra values.

Based upon the comparison of both turnout structures, the following conclusions are perceptible at particular measuring points:

- A positive effect of the movable frog point can unambiguously be observed on the wing rail. In the turnout provided with the spring crossing movable frog, the values in the 1 – 400Hz frequency band in the vertical and cross directions are as much as 2 times lower compared with the structure with the fixed frog point.
- The same situation is on the sleeper. On the sleeper under the crossing point, a positive effect of the spring crossing movable frog (SCMF), especially in the sleeper centre can be observed. Here, the values of SCMF in the frequency band 1 – 400 Hz are as much as 5 times lower.
- In the longitudinal direction, at the frog point, a better turnout is that one provided with the fixed fog point. In the cross and vertical directions, both structures are comparable.
- In the ballast bed, both structures are comparable, both in acceleration values and in the calculated values of vibration. In the vertical direction, the vibration speed is almost twice as big as that one compared to the cross direction and as

much as threefold compared to the longitudinal direction. Based upon the frequency analysis it is evident that in the vertical direction, the SCMF shows the dominant frequencies between 45 – 55 Hz and between 90 – 105 Hz. In the turnout with the fixed frog point, the dominant frequencies in the vertical direction are between 75 – 135 Hz.

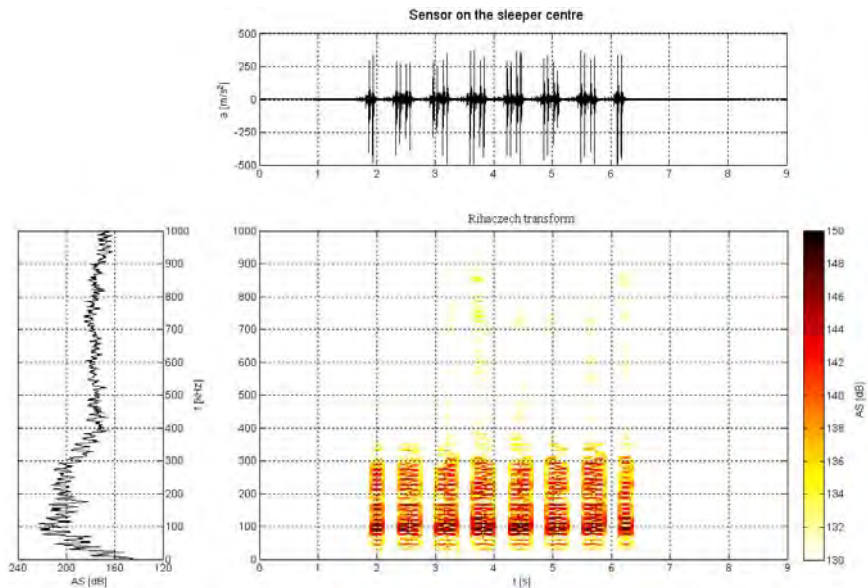


Figure 4. Time history of acceleration on sleeper under turnout – fixed frog, amplitude spectrum and time-frequency spectrum, train set Pendolino, 160 km/h

3. CONCLUSIONS

In conclusion, based upon the measurement and analyses made, we may state that the methods of measurement analyses used offer good results and conclusions. Both the measured and calculated values show sufficient accuracy and informative capabilities. Within the framework of the frequency analysis, the Welch method proved to be very reliable. This method, together with time frequency procedures, offers a comprehensive view on the dynamic behaviour of the turnout structures.

Based upon the measurement made, for the reason of further analysis, especially the measurement of shunting on centres and on sleeper heads may be recommended. It would be very interesting to measure the shunting of the point machine in the turnout provided with the spring crossing movable frog. Based upon the analyses made, the springing of the whole system may be recommended by inserting rail pads, which could decelerate the process of the disintegration of the

gravel bench under the sleeper heads in the turnout provided with the fixed frog point.

For the most part it may be stated that the advantage of the turnout provided with the spring crossing movable frog point will fully reveal at speeds higher than $160 \text{ km}\cdot\text{h}^{-1}$. Up to this speed, both investigated structures are almost comparable.

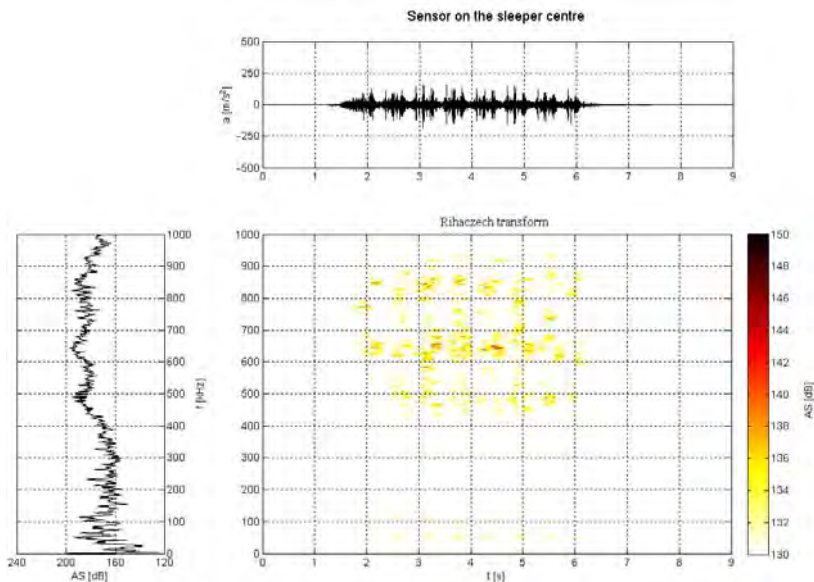


Figure 5. Time history of acceleration on sleeper under turnout – spring movable frog, amplitude spectrum and time-frequency spectrum, train set Pendolino, 160 km/h

Acknowledgements

This research has been supported by the research project GACR 103/07/0183 ("The investigation of dynamic effects due to the rail transport by the method of quadratic time and frequency invariant transformations ") and by research project MSM 0021630519 ("Progressive reliable and durable load-bearing structural constructions")

References

1. Smutný J., Pazdera L. New techniques in analysis of dynamic parameters rail fastening, *InSight, The Journal of The British Institute of Non-Destructive Testing*, Vol. 46, No 10, October, 2004, pp. 612-615, ISSN 13542575
2. Melcer, J, Kucharova, D, Mechanical properties of rubber pads under static and dynamic load, *International Conference on Materials Science and Engineering, BRAMAT 2003, Romania, Brasov, 3/2003, University of Brasov, 2003*, pp 18-314.
3. Smutný J., Pazdera L., Time frequency analyses of real signals, 2003
4. Cohen L. Time-frequency distributions - a review, *Proc. IEEE*, Vol. 77 No. 7, 941-981, 1989

Modeling lateral earth pressure on concrete retaining walls

Alexandra Stan¹ and Horatiu Mociran²

¹Department of Structural Mechanics, Technical University of Cluj-Napoca, Cluj-Napoca, 400020, Romania

² Department of Structural Mechanics, Technical University of Cluj-Napoca, Cluj-Napoca, 400020, Romania

Summary

Retaining walls prevent the embankment sliding or erosion and provide support for the near vertical grades. Because of this, these structures are commonly used in all branches of civil engineering – from houses and buildings to roads, railways, bridges and banks protection.

The real estate in Romania, in the past few years, has grown substantially, the big cities are in continuous expansion and therefore the authorities have to keep up with growing their infrastructure in order to meet the city’s needs. But, because of the rough terrain in most of the Transylvanian cities, a number of the new streets that have to be designed and built are supported by retaining walls.

This article’s focus is on the development of a simple and easy to implement model of cantilever retaining walls, with an emphasis on the modeling of lateral earth pressure.

KEYWORDS: numerical methods, cantilever retaining walls, active earth pressure, passive earth pressure, at-rest earth pressure

1. INTRODUCTION

Lateral earth pressure is the pressure exerted by the soil in the horizontal plane. In order to describe this pressure, a lateral earth pressure coefficient, K , is used. K represents the ration between the lateral normal (effective) stresses to the vertical (effective) stresses, equation (1). The value of K depends upon the material and also on the geological history of the soil. Lateral earth pressure coefficients are of three kinds: active, at-rest and passive.

$$K = \frac{\sigma_x}{\sigma_z} \quad (1)$$

K – lateral earth pressure coefficient

σ'_x - horizontal effective stress

σ'_z - vertical effective stress

As for the theories that predict earth pressure, there are two commonly used – Rankine and Coulomb, but a lot of research is being put into a better understanding of soil behavior.

In the following chapters, Rankine and Coulomb theories will be summarized and an example of modeling the lateral earth pressure on typical cantilever retaining walls will be presented.

2. RANKINE THEORY

Rankine theory was developed in 1857 [1] and it does not take into account the friction of the soil and it assumes that the soil-structure interface is vertical.

The possible stresses in the soil are limited by Mohr-Coulomb failure criterion. The criterion is that the shear stresses on any plane are limited by condition (2):

$$\tau < \tau_f = c + \sigma tg\phi \quad \tau < \tau_f = c + \sigma tg\phi \quad (2)$$

c – cohesion,

ϕ - the angle of internal friction.

The criterion can be illustrated using Mohr's circle, Figure 1.

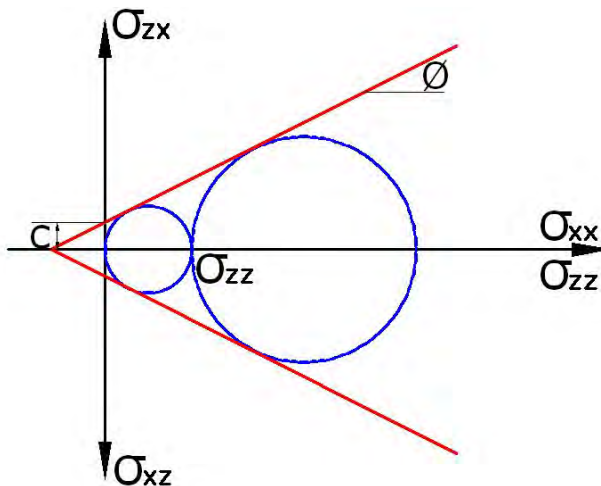


Figure 1. Mohr's circle

If σ_{xx} and σ_{zz} are the principal stresses, σ_{zz} is known, it follows that the horizontal stress can not be smaller than indicated by the small circle and not larger than the large circle. The principal stresses can be computed, the following values being obtained, equation (3.a) and (3.b):

$$\sigma_1 = K_p \sigma_3 + 2c\sqrt{K_p} \tag{3.a}$$

$$\sigma_3 = K_a \sigma_1 - 2c\sqrt{K_a} \tag{3.b}$$

In equations (3.a) and (3.b), the coefficient K_a and K_p are defined by equations (4.a) and (4.b):

$$K_p = \frac{1 + \sin \phi}{1 - \sin \phi} = tg^2 \left(45 + \frac{\phi}{2} \right) \tag{4.a}$$

$$K_a = \frac{1 - \sin \phi}{1 + \sin \phi} = tg^2 \left(45 - \frac{\phi}{2} \right) \tag{4.b}$$

These two coefficients, K_a and K_p , known as the active earth pressure (K_a) and the passive earth pressure (K_p), give the smallest and the largest ratio of the two principal stresses.

Active earth pressure appears when a retaining structure is being pushed away by the soil, while passive earth pressure appears when a structure is being pushed into the ground.

3. COULOMB THEORY

Before the analysis of Rankine, the French scientist Coulomb presented a theory of limiting stress states in soil, in 1776 [2]. The theory has as its main assumption the idea that the soil fails along straight slip planes. Also, wall friction is taken into account.

The active earth pressure and the passive earth pressure coefficients are given in equations (5.a) and (5.b):

$$K_p = \frac{\cos^2(\phi + \alpha)}{\cos^2 \phi \cos(\delta - \alpha) \left(1 - \sqrt{\frac{\sin(\phi + \alpha) \sin(\phi + \beta)}{\cos(\delta - \alpha) \cos(\beta - \alpha)}} \right)^2} \tag{5.a}$$

$$K_a = \frac{\cos^2(\phi - \alpha)}{\cos^2 \alpha \cos(\delta + \alpha) \left(1 + \sqrt{\frac{\sin(\phi + \alpha) \sin(\phi - \beta)}{\cos(\delta + \alpha) \cos(\alpha - \beta)}}\right)^2} \tag{5.b}$$

4. NEUTRAL EARTH PRESSURE

In a homogeneous natural soil deposit the ratio σ'_x / σ'_z is a constant known as the coefficient of neutral earth pressure or of earth pressure at rest (K_o). In this state, there are no lateral strains. The value of this coefficient may be estimated using the formula proposed by Jaky [3], equation 6:

$$K_o \approx 1 - \sin \phi \tag{6}$$

In an elastic material the value of K_o would be $K_o = \nu / (1 - \nu)$, but this is not a very good estimate as the soil is not an elastic material.

5. CANTILEVER RETAINING WALLS

In Figure 2 two types of cantilever retaining walls frequently used are presented.

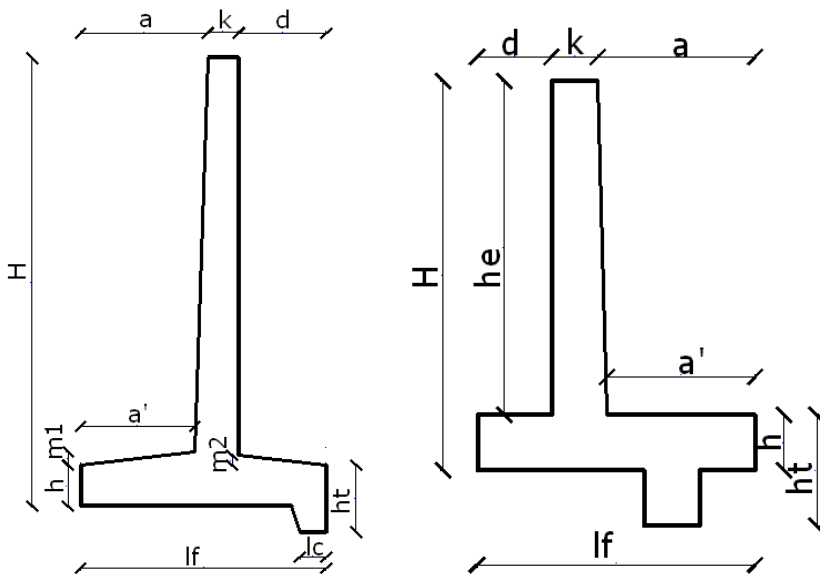


Figure 2. Cantilever retaining walls

For cantilever walls, Rankine active condition is assumed along a vertical plane that goes through the edge of the heel of the base slab. The weight of the soil above the heel and the weight of the concrete are taken into account.

For the retaining wall on the left side of Figure 2, with the geometry presented in Figure 3, numerical results based on the Rankine theory are presented:

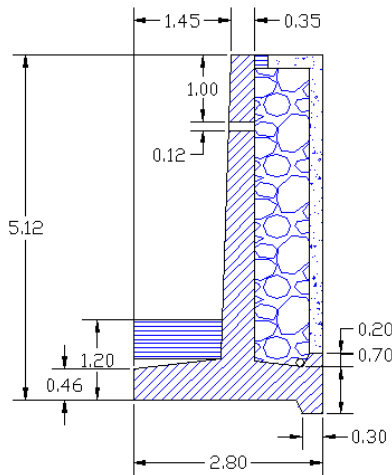


Figure 3. Geometry of the retaining wall

No overload due to traffic was taken into account, as the street is in front of the retaining wall.

The soil behind the wall has the following characteristics:

the soil weight: $\gamma_p=17.9\text{kN/m}^3$,

the cohesion $c=15\text{ kN/m}^3$,

$\Phi=18^\circ$;

There is only one layer of soil behind the retaining wall.

The active earth pressure coefficient, computed using Rankine’s theory, is $K_a=0.528$, while the passive earth pressure coefficient is $K_p=1.894$. The neutral earth pressure coefficient, after Jaky, equals 0.691.

In Figure 4, based on the values obtained for the earth pressure coefficients, a possible relation between the horizontal stress against the retaining wall and its horizontal displacements is given. If the displacement is zero, the lateral stress coefficient will be K_o . If the structure moves away from the soil, the lateral stresses are decreasing until the lowest value is reached, value defined by the active earth

pressure coefficient K_a . If the structure is pressed towards the soil, the lateral stresses will increase, until K_p is reached.

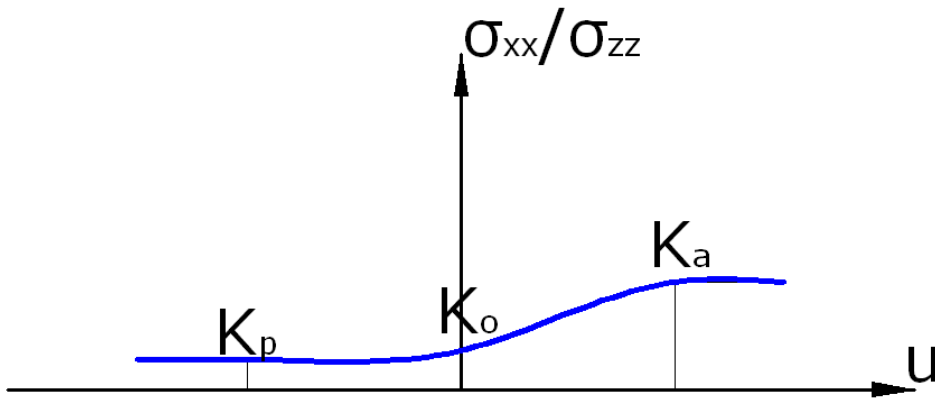


Figure 4. Horizontal stress as a function of the displacement

6. CONCLUSIONS

Due to the high number of cases where retaining walls have to be used, it is important to understand and to be able to easily use the different methods used to evaluate the earth pressure. Moreover, a look should be taken into the issue of predicting the neutral earth pressure using artificial neural networks [4]. These networks are adaptive algorithms that have, as a first input, the results obtained from the dilatometer test.

References

1. Rankine, W., *On the stability of loose earth*. **Philosophical Transactions of the Royal Society of London**, Vol, 147, 1857
2. Coulomb C. A., *Essai sur une application des regles des maximis et minimis a quelques problemes de statique relatifs a l'architecture*. **Memoires de l'Academie Royale pres Divers Savants**, Vol. 7, 1776
3. Jaky J., *Pressure in soils*, 2nd ICSMFE, London, Vol.1, pp 103-107, 1948
4. Das S. K., Baudhar P. K., *Prediction of Coefficient of Lateral Earth Pressure using Artificial Neural Networks*, **EJGE**, Vol 10, 2005.

The seismic force development related to romanian designing codes

Doina Stefan, Gabriela Covatariu

Structural Engineering, “Gh. Asachi” Technical University, Iasi, Romania

Summary

The seismic calculus researches in the past 50 years also based on experimental recordings are led to changes in the building design standards.

Major changes were made in estimating the dynamic amplification coefficient β which is established in relation to the spectral composition of the seismic movements generated by the Vrancea source and in relation with the reduction coefficient ψ , which accounts for the ductility of the structure.

This paper aims evolution of global seismic coefficient for 3 types of structures situated in Iasi and Bucharest.

By analyzing the results of the seismic force calculus according to the present standards one can notice the major increase of the seismic force value according to the P100-2006 Standard, in comparison with the former ones. Seismic force values representing 40-60% of the seismic force according to P100-2006 for various types of buildings designed in period 1963 - 1992 can be alarming if we think about the number of buildings are made in this time interval.

KEYWORDS: seismic force, global seismic coefficient, building design standards.

1. INTRODUCTION

After the earthquake in November 1940, the first norms of seismic design appeared in Romania in December 1941, and it was called „*Temporary Instructions Regarding the Prevention of Construction Damages Caused by Earthquakes and For Rehabilitation of the Damaged Ones*”. A new edition of these instructions appeared in 1945. In 1963 it was published the first „*Standards for Civil and Industrial Constructions Designing in Seismic Areas (P13-63)*”.

In 1970 was published the improved edition of these standards and it considered the specific characteristics of Romania.

The 1977 earthquake was led to the modification of the existent standards due to the registrations made during the earthquake. Thus, in 1978 „*The Seismic*

Standards for Designing of Civil, Socio-Cultural, Agricultural and Industrial Constructions P100-78” and in 1981 a slightly improved edition P100-81 was published.

The years between 1980 and 1990 was a period of extended theoretical and experimental research which also used registrations of the seismic movements and these led to the improvement of the existent standards in order to assure a higher degree of seismic protection. Thus, in 1991 appears the P100-91 standard, modified and completed in 1992. In this latter version appears for the first time concepts such as *corner period*, *importance coefficient* and a detailed classification of the structures, in order to establish the *reducing factors* for the earthquake.

The Seismic Design Code P100-2006 is applied since 2006 and combines the Romanian and European regulations. In it appears some differences in seismic action representation, in establishing the requirements of performance and in specific regulations for structures of various materials.

2. THE ROMANIAN CODES - THE SEISMIC REPRESENTATIONS AND ITS INTERPRETATIONS

The seismic forces are conventionally considered to act according to the directions of the dynamic freedom degrees and represent the maximum values of the inertia forces. These depend on the dynamic characteristics of the structure and on the characteristics of the seismic action represented by the response spectrums.

For the nDOF systems, the seismic force corresponding to the k module of vibration can be determined by using the following:

2.1. P13-63, P13-70, P100-78 Standards

This standard computes seismic force with relation (1)

$$S_k = c_k G, \quad c_k = \alpha k_s \psi \beta_k \varepsilon_k, \quad \varepsilon_k = \frac{\left(\sum_{i=1}^n m_i u_{ik} \right)^2}{\sum_{i=1}^n m_i \sum_{i=1}^n m_i u_{ik}^2} = \frac{\left(\sum_{i=1}^n G_i u_{ik} \right)^2}{\sum_{i=1}^n G_i \sum_{i=1}^n G_i u_{ik}^2} \quad (1)$$

where: c_k is the global seismic coefficient corresponding to vibration k mode.

k_s is the seismic intensity coefficient corresponding to the seismic protection degree of the building (tab. 1 and fig. 1)

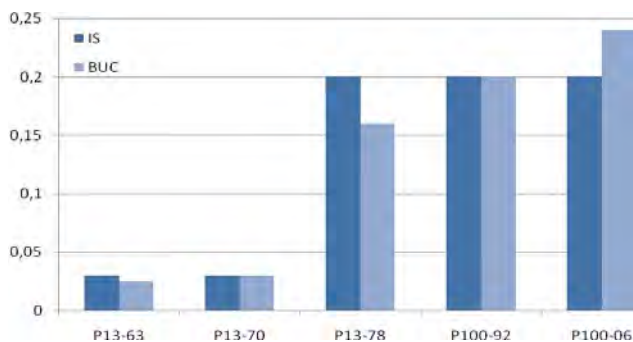


Figure 1. Seismic coefficient intensity variation

Table 1. Seismic intensity coefficient k_s

Antiseismic protection degree	9 - A	8.5-B	8-C	7.5-D	7-E	6.5-F	6
P13-63	0,100		0,050		0,025		
Very important buildings	0,12		0,08		0,05		0,03
P13-70							
Buildings with a medium importance	0,08		0,05		0,03		
P100-78 (81)	0,32	0,26	0,20	0,16	0,12	0,09	0,07
P100-92	0,32	0,25	0,20	0,16	0,12	0,08	
P100-2006	0,32	0,28	0,24	0,20	0,16	0,12	0,08

where: β_k is the dynamic coefficient corresponding to vibration k mode (tab. 2)

ψ is the coefficient of the seismic loading effects reduction which takes into consideration the ductility of the structure, the capacity of stress redistribution and the cooperation between the structure and the nonstructural and damping elements. (tab. 3)

ε_k is the coefficient of equivalence between the real system nDOF and the system sDOF having a proper period of vibration T_k

u_{ik} is the ordinates of the eigenvector.

2.2. P100-92

The P100-92 norms determines the entire horizontal seismic loading depending on the coefficient of importance of the building, (eq. 2)

$$S_k = c_k G ; c_k = \alpha k_s \psi \beta_k \varepsilon_k ; \varepsilon_k = \frac{\left(\sum_{i=1}^n m_i u_{ik} \right)^2}{\sum_{i=1}^n m_i \sum_{i=1}^n m_i u_{ik}^2} = \frac{\left(\sum_{i=1}^n G_i u_{ik} \right)^2}{\sum_{i=1}^n G_i \sum_{i=1}^n G_i u_{ik}^2} \quad (2)$$

Table 2. Dynamic coefficient

	β_k	β_{min}	β_{max}
P13-63	ground: type <i>a</i> (cliffs) $\beta_k = 0,90/T$	0,60	3,00
	type <i>b</i> (normal) $\beta_k = 1,25 * 0,90/T$		
	type <i>c</i> (clay) $\beta_k = 1,5 * 0,90/T$		
P13-70	ground: type <i>a</i> $\beta_k = 0,8 * 0,80/T_k$	0,60	2,00
	type <i>b</i> $\beta_k = 0,80/T_k$		
	type <i>c</i> $\beta_k = 1,5 * 0,80/T_k$		
P100-78 (81)	ground: type <i>a</i> $\beta_k = 0,8 * 3 / T_k$	0,75	2,00
	type <i>b</i> $\beta_k = 3 / T_k$		
	type <i>c</i> $\beta_k = 1,3 * 3 / T_k$		
P100-92	$\beta_r = 2.5$ for $T_k < T_c$	1,00	2,50
	$\beta_r = 2.5 - (T_k - T_c)$ for $T_k > T_c$		
P100-06	$T_c = 0,7s; 1,0s; 1,5s$		
	$\beta(T) = 1 + \frac{(\beta_0 - 1)}{T_B} T$ $T \leq T_B$		2,75
	$\beta(T) = \beta$ $T_B < T \leq T_C$		
	$\beta(T) = \beta_0 \frac{T_C}{T}$ $T_C < T \leq T_D$		
	$\beta(T) = \beta_0 \frac{T_C T_D}{T^2}$ $T > T_D$		
$T_c = 0,7s; 1,0s; 1,6s$			

2.3. P100-2006

Regulation determines the seismic force (the base shear force) with the expression:

$$F_{bk} = \gamma_I S_d(T_k) m_k \quad (3)$$

$S_d(T_k)$ represent the ordinate of the response spectrum of design corresponding to the k mode;

$$S_d(T) = a_g \left[1 + \frac{\frac{\beta_0 - 1}{q} T}{T_B} \right] \text{ or } S_d(T) = a_g \frac{\beta(T)}{q} \quad (4)$$

where: γ_I - the importance-exposure factor of the building;

T_k - vibration period corresponding to the k mode;

q - coefficient of behavior (tab. 4)

m_k - the modal mass associate to the proper mode of vibration k ;

$$m_k = \frac{\left(\sum_{i=1}^n m_i s_{ik} \right)^2}{\sum_{i=1}^n m_i s_{ik}^2} \quad (5)$$

s_{ik} – the eigenvector component in the k mode which is corresponding to the dynamic free i degree (iDOF)

Table 3. Reduction coefficient ψ

Reinforced concrete structures	P13-63	P13-70	P100-78 (81)	P100-92
Rigid structure buildings (brickwork bearing walls or reinforced concrete diaphragm) or semirigid (semipermanent)	1,00	1,30 1,20	0,30 0,25	0,25 0,20
Storey framed buildings	1,20	1,00	0,25 0,20	0,20 0,15
Industrial buildings	1,00		0,20 0,15	0,20 0,15
Silo	1,00	-	0,25	0,25
Very flexible and high buildings (towers and chimneys)	1,50	1,80	0,35	
Water tower	1,50	2,00	0,35	0,35

Table 4. Coefficient of behaviour q - **P100-2006**

Reinforced concrete structures	Ductility class H	Ductility class M
Frames. Dual system. Coupling walls	5 α_u / α_1	3,5 α_u / α_1
Walls	4 α_u / α_1	3,0
Nucleus flexible at stress	3,0	2,0
Inverted pendulum structures	3,0	2,0

Table 5. Overstrength factor - **P100-2006**

		α_u / α_1
Frames or	Buildings with one storey and single aperture	1,15
Dual structures with main frames	Buildings with multiple stores and single aperture	1,25
	Buildings with multiple stores and multiple apertures	1,35

Structural wall or	Structures with only two walls in each direction	1,0
Dual systems with main walls	Multiple walls structures	1,15
	Coupled walls structures and dual structures with preponderant walls	1,25
For structures having complete regularity and perfectly controlled execution conditions q can be increased with max.20%		

3. THE SEISMIC FORCE EVOLUTION RELATED TO THE ROMANIAN CODES

3.1. Reinforced concrete frame structure

Consider a reinforced concrete frame with P+7E. The structure was designed according to the ductility class M . The fundamental period of the structure is 0.6s.

In tab. 6 and fig. 2 is represented variation of global seismic coefficient for reinforced concrete frame structure localized in Iasi and Bucharest.

Table 6. Variation of global seismic coefficient

P+7E Reinforced concrete frame structure	P13 -	P13 -	P100 -	P100 -	P100 -	P13 -	P13 -	P100 -	P100 -	P100 -
	63	70	78 (81)	92	06	63	70	78 (81)	92	06
	IASI					BUCURESTI				
$\alpha ; \gamma_1$	-	-	-	1.00	1.00	-	-	-	1.00	1.00
κ_s	0.03	0.03	0.20	0.20	0.20	0.025	0.03	0.16	0.20	0.24
β_k	1.875	1.33	2.00	2.50	2.75	1.875	1.33	2.00	2.50	2.75
ψ	1.20	1.00	0.20	0.20	-	1.20	1.00	0.20	0.20	-
$3^* \alpha_u / \alpha_1$	-	-	-	-	4.725	-	-	-	-	4.725
α_u / α_1	-	-	-	-	1.35	-	-	-	-	1.35
$\varepsilon_k ; \lambda$	0.85	0.85	0.85	0.85	0.85	0.85	0.85	0.85	0.85	0.85
c_k	0.0574	0.034	0.068	0.085	0.0989	0.0478	0.034	0.054	0.085	0.1187
	58%	34%	69%	86%	100%	40%	29%	45%	72%	100%

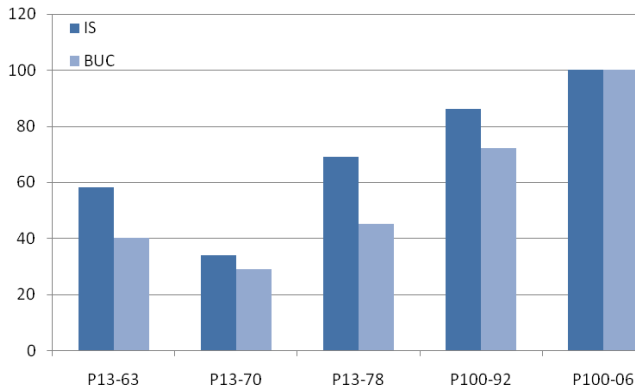


Figure 2. Global seismic coefficient variation

3.2. Structural Walls - Structure of Reinforced Concrete

Consider a structure of reinforced concrete structural walls with P+7E. The structure was designed according to the ductility class *M*. The proper fundamental period of the structure is 0.4s. In tab. 7 and fig. 3 is represented variation of global seismic coefficient for buildings with reinforced concrete structural walls localized in Iasi and Bucharest.

Tab. 7. Variation of global seismic coefficient

P+7E Structure of reinforced concrete structural walls	IASI					BUCURESTI				
	P13-63	P13-70	P100-78 (81)	P100-92	P100-06	P13-63	P13-70	P100-78 (81)	P100-92	P100-06
$\alpha ; \gamma_1$	-	-	-	1.00	1.00	-	-	-	1.00	1.00
κ_s	0.03	0.03	0.20	0.20	0.20	0.025	0.03	0.16	0.20	0.24
β_k	2.00	2.00	2.00	2.50	2.75	2.00	2.00	2.00	2.50	2.75
ψ	1.00	1.20	0.25	0.25	-	1.00	1.20	0.25	0.25	-
q	-	-	-	-	3.00	-	-	-	-	3.00
α_u/α_1	-	-	-	-	-	-	-	-	-	-
$\varepsilon_k ; \lambda$	0.75	0.75	0.75	0.75	0.75	0.75	0.75	0.75	0.75	0.75
c_k	0.045	0.054	0.075	0.09375	0.1375	0.0375	0.054	0.06	0.09375	0.165
	33%	39%	55%	68%	100%	23%	33%	36%	57%	100%

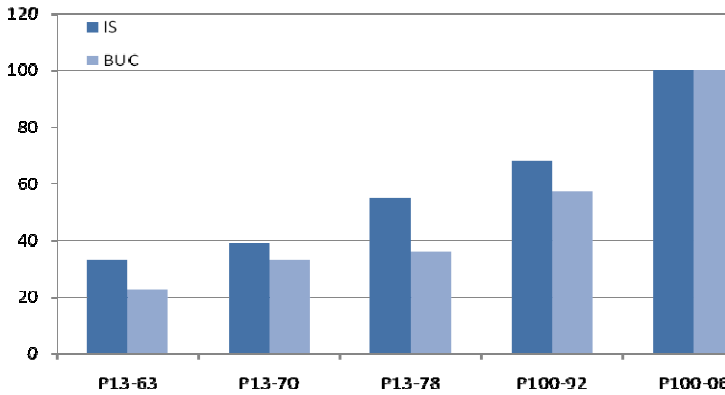


Figure 3. Global seismic coefficient variation

3.3. Structural Walls - Structure of Brick Masonry

Consider a structure of brick masonry structural walls with P+4E. The fundamental period of the structure is 0.4s. In tab. 8 and fig. 4 is represented variation of global seismic coefficient for buildings with structure of brick masonry structural walls situated in Iasi and Bucharest.

Table 8. Variation of global seismic coefficient

P+4E Structure of brick masonry structural walls	P13-63	P13-70	P100-78	P100-81)	P100-92	P100-06	P13-63	P13-70	P100-78	P100-81)	P100-92	P100-06
	IASI						BUCUREȘTI					
$\alpha ; \gamma_1$					1.00	1.00					1.00	1.00
κ_s	0.03	0.03	0.20	0.20	0.20	0.20	0.025	0.03	0.16	0.20	0.20	0.24
β_k	2.00	2.00	2.00	2.50	2.75	2.75	2.00	2.00	2.00	2.50	2.50	2.75
ψ	1.30	1.00	0.30	0.25			1.30	1.00	0.30	0.25		
$q = 3 \times \alpha_u / \alpha_1$	-					3.75	-					3.75
α_u / α_1	-					1.25	-					1.25
$\varepsilon_k ; \lambda$	0.75	0.75	0.75	0.75	0.75	0.75	0.75	0.75	0.75	0.75	0.75	0.75
C_k	0.059	0.045	0.09	0.094	0.11	0.11	0.0487	0.045	0.072	0.094	0.094	0.132
	54%	41%	82%	85%	100%	100%	37%	34%	55%	71%	71%	100%

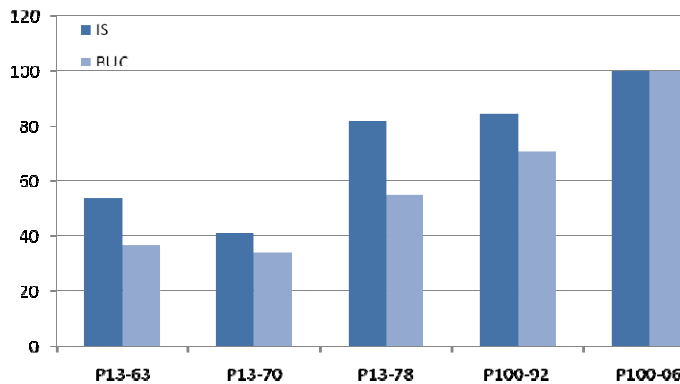


Figure 4. Global seismic coefficient variation

4. FINAL CONCLUSIONS

The seismic calculus researches in the past 50 years also based on experimental recordings are led to changes in the building design standards.

Were made major changes in estimating the dynamic amplification coefficient β (which is established in relation to the spectral composition of the seismic movements generated by the Vrancea source) and in relation with the reduction coefficient ψ (which accounts for the ductility of the structure).

Analyzing the results of the seismic force calculus according to the present standards one can notice the major increase of the seismic force value according to the P100-2006 Standard, in comparison with the former ones. Seismic force values representing 40-60% of the seismic force according to P100-2006 for various types of buildings designed in period 1963 - 1992 can be alarming if we think about the number of buildings are made in this time interval. This fact can become even more alarming if we take into account the effects of the earthquakes produced in 1977, 1986 and 1990. The structures of the buildings have been more or less affected by those earthquakes.

This can be proved with the results obtained after the evaluations on various types of buildings made before 1992. Thus:

- structures made of bearing brick masonry - the bearing capacity being reduced with 22%.
- structures with reinforced concrete prefabricated diaphragms - real medium reduction of 25 to 28% (major problems with joints);

- reinforced concrete framed structures - real reduction of almost 6% (constant degradation mainly present in beams).

By corroborating the effects of the designing standards changes with the degradations caused by the earthquakes it could draw the alarming conclusion for the heritage witch was built before 1992 – the most of the buildings do not meet the terms of seismic insurance.

REFERENCES

1. P13-63 - *Conditioned Standards for Civil and Industrial Constructions Design in Seismic Regions*
2. P13-70 - *Standards for Civil and Industrial Constructions Design in Seismic Regions*
3. P100-78 - *The Seismic Standards for Design of Civil, Socio-Cultural, Agricultural and Industrial Constructions*
4. P100-92 - *The Seismic Standards for Design of Civil, Socio-Cultural, Agricultural and Industrial Constructions*
5. P100-1/2006 - *Seismic Design Code - part I – Building Design Provisions*

Different numerical methods using for analysis of historical masonry structures

Jerzy Szołomicki¹

¹*Department of Civil Engineering, Wrocław University of Technology, Wrocław, 50-370, Poland*

Summary

In this paper author investigated different numerical techniques for the analysis of historical masonry structures. The following approaches are taken into account:

- *standard FEM modeling method, based on concept of homogenized material and smeared cracking,*
- *FEM with discontinuous elements which are used for modeling vertical and horizontal mortar joints,*
- *Discrete element modeling.*

An overview of presented such numerical methods with their specific theoretical aspects can have practical usefulness in analysis of behavior of historical masonry structures.

KEYWORDS: Masonry structures, numerical models, computational simulations

1. INTRODUCTION

Many historical buildings and monumental structures are made of masonry material. In recent years growing attention has been paid to providing theoretical and numerical methods for better understanding the mechanical behaviour of such structures. The complex mechanical behaviour of masonry structures depends on the composite nature of masonry material. Masonry is a composite material made of brick units and mortar joints. The large number of variables influencing the mechanical behaviour of masonry. The development of numerical techniques led to more refined models which separately model bricks and joints and allow for local failure inside these components. The numerical modeling of masonry structures by using FEM is a very difficult task. The typological characteristics of masonry structures do not allow to refer to simplified static schemes and mechanical properties of the material lead to a widely non-linear behaviour. Besides the incomplete characterization of the material renders uncertain the calibration of numerical models. Due to this intrinsic geometrical complexity, it is necessary to assume a homogenised material and perform the analyses applied FEM, when the

global behaviour of structure is base of investigation. When a single structural element is being analysed , the finite element method with discontinuous elements and the discrete element method are most effective. The computational mechanics of masonry structures used to be approached in two different ways: the discrete and the smeared crack models. The smeared approach is preferred over the discrete one, since in large scale structures it is quite impossible to track each individual crack.

2. DIFFERENT NUMERICAL METHODS FOR ANALYSIS OF MASONRY STRUCTURES

2.1. Application of FEM

The analysis of masonry structures is a complex problem since several peculiar features have to be kept into account: the orthotropy along the two directions of the masonry, the different strengths of components, the friction effects and the sliding along an open crack, the irreversible deformation under compression, and finally the stiffness recovery at crack closure under alternate loading. The finite element method is usually adopted to achieve sophisticated simulations of the structural behavior. A mathematical description of the material behavior, which yields the relations between the stress and strain tensor in a material point of the body is necessary for this purpose. In general, the approach towards its numerical representation can focus on the micro-modeling of the individual components, or the macro-modeling of masonry as a composite (Figure 1).

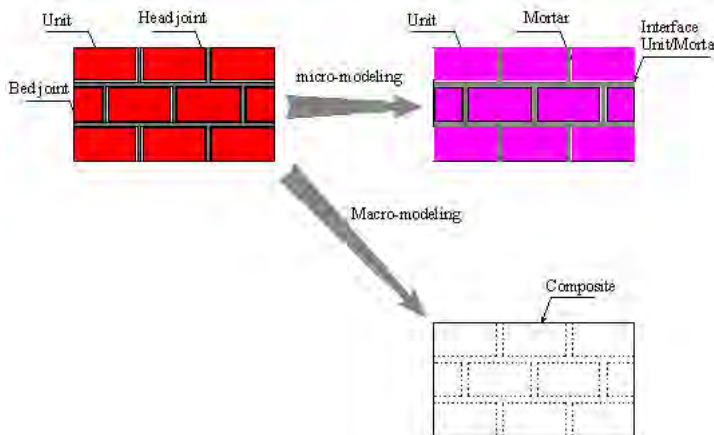


Figure 1. Micro and macro-modelling of masonry structures

Micromodelling consists of simulating the global behaviour of a composite material by means of detailed geometrical discretization, based in the finite element method, and providing non-linear constitutive laws for each component. In the micromodels bricks, bed and vertical mortar joints are simulated separately. Micro-model can include all the basic types of failure mechanisms that characterize masonry. The main attention must be paid in the modelling of mortar joints, since the sliding at joint level often starts up the crack propagation. The fault of this method comes from the extremely large number of elements to be generated as the structure increases in size and complexity.

The macromodel assumes that the masonry structures is a homogeneous continuum to be discretized with a finite element mesh. In macro-modelling masonry can be regarded as a combination of two material phases constituted by bricks and a series of mortar joints arranged regularly. In the latter, the joints follow the boundaries of the bricks forming two main groups: horizontal and vertical. The constitutive model is based on the formulation, for each of the deformation modes of the basic cell, of the equilibrium and compatibility equations. These are introduced in the constitutive equations of each material component, obtaining expressions for the stress-strain behaviour of the composite, as well as the homogenized mechanical parameters. Nevertheless the equivalent material models have proven to be able to grasp certain aspects of the global behaviour without the number of parameters needed in the micromodel.

2.2. Application of FEM with discontinuous elements

The micro-modelling approach analyses the masonry material as a discontinuous assembly of blocks, connected each other by joints at their actual position, the later being simulated by appropriate constitutive models of interface. The interface constitutive models are usually expressed in terms of contact of tractions and conjugate generalized joint strains, the latter being derived from the displacements discontinuities at the joint. In the finite element analysis, the mechanical description of the interaction between two bodies, in contact through a surface is developed by means:

- link elements between two opposite nodes of the elements in contact;
- continuum finite elements of small and finite thickness,
- zero thickness interface elements in which the displacement discontinuities between opposite nodes represent the primary kinematic variables.

The introduction of the joint is easy to implement in a software programme, since the nodal unknowns are the same for continuum and joint elements, though for the latter the stress tensor must be expressed in terms of nodal displacements instead of deformation components. For continuum elements the relevant quantities at the

Gauss integration points are the components of the local stress tensor, the relevant quantities for the joint element are the component of the local stress vector at the interface. Therefore a constitutive law for the shear component S and the normal component N of this vector shall be defined (Figure 2). Those components depend on the opening δ and the sliding component γ of the displacement jump across the joint. Two constitutive laws of this kind are known. The first model is a simple elasto-plastic Coulomb friction law with small dilatancy and no cohesion. In this model the joints are intended to behave elastically within the domain defined by the criterion $|S| < (N_t - N) \tan \phi$ (Figure 3), where N_t is the maximum normal stress in tension and ϕ is the friction angle. A second constitutive model for the joints features the elastic domain as in previous $|S| < (N_{t0} - N) \tan \phi_0$, but both the maximum normal stress and the friction angle are allowed to vary with plastic strain.

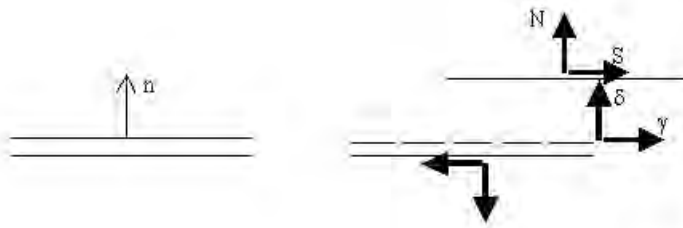


Figure 2. Characteristic quantities at the Gauss integration points for joint elements

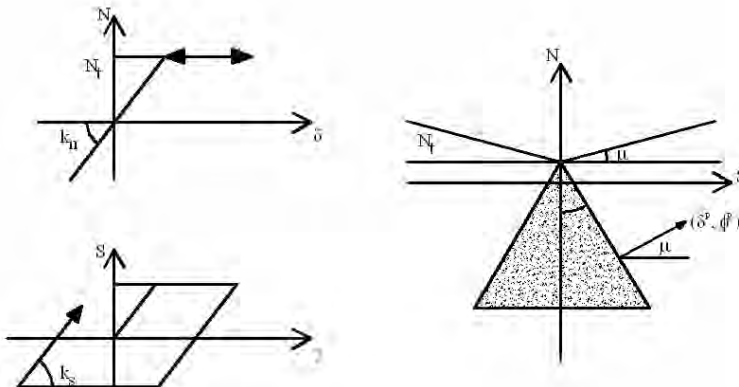


Figure 3. Interface joint model

2.3. Application of Discrete Element Method

In this method, the structure is considered as an assembly of distinct blocks, rigid or deformable, interacting through unilateral elasto-plastic contact elements which follow Coulomb slip criterion for simulating contact forces. The approach is based on a formulation in large displacement (for the joints) and small deformations (for the blocks), and can correctly simulate collapse mechanisms due to sliding, rotations and impact. The contacts are not fixed, like in the FEM with discontinuous elements, so that during the analyses blocks can loose existing contacts and make new ones. In this method different types of contacts can be handled, depending on the initial geometry and on the displacement history during the analysis. Typically , the general types of contacts are: a) face to face; b) edge to face; c) vertex to face; d) edge to edge; e) vertex to edge; f) vertex to vertex. All of them can be represented by sets of point contacts of two elementary types: VF and EE (Figure 4). The main advantage of this approach is the possibility of following the displacements and determining the collapse mechanisms of structures made up of virtually any number of blocks. The fault is that the method is not accurate for the analysis of stress states within the blocks.

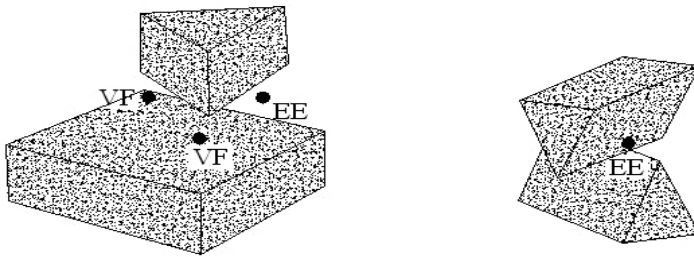


Figure 4. Different types of contacts

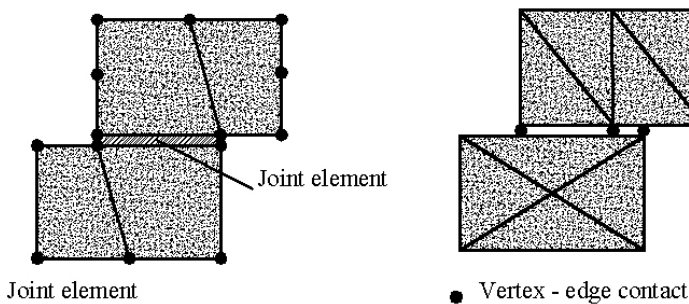


Figure 5. Comparison of joint elements and point contacts

3. CONCLUSION

In spite of the specific limitations of each model, all three methods are able to correctly grasp the global behaviour of analysed masonry structures. The actual ultimate strength in monotonic loading can be predicted with good approximation performing non-linear analysis. For computer model, nevertheless, major concerns derives from the inability to predict cyclic behaviour, so that further investigations are needed, possibly involving the development of a fully masonry oriented constitutive model. The main difficulty is connected with the necessity of providing an easy methodology to remesh contacts when large displacement are to be allowed. The limits of these models are overcome by discrete element method that features straightforward handling of compatible meshes and large displacement. It must be said that for FEM with discontinuous elements and discrete element method the actual distribution of brick and mortar joints is needed, which in most practical cases is not easy to detect, since the masonry elements are usually covered by finishing materials. The lack of experimental data on real-scale structures renders the validation of numerical results very difficult.

References

1. Genna, F., Di Pasqua, M. Numerical analysis of masonry structures: a comparison between 'no tension' and 'softening' constitutive laws. *Proc. VII Convegno Italiano di Meccanica Computazionale*, Trieste, Italy, 1993.
2. Genna, F., Di Pasqua, M., Veroli, M. Numerical analysis of old masonry buildings: a comparison among constitutive models. *Engineering Structures*, vol. 20: p. 37-53, 1998.
3. Giambanco, G., Rizzo, S., Spallino, R. Numerical analysis of masonry structures via interface models. *Comput. Methods Appl. Mech. Engrg.*, vol. 190: p. 6493-6511, 2001.
4. Gierson, D.E., Franchi, A., De Donato, O., Corradi, L. Mathematical programming and nonlinear finite element analysis. *Comp. Meth. Appl. Mech. Engrg.*, vol. 17/18: p. 497-518, 1979.
5. Zucchini, A., Lourenço, P.B. A micro-mechanical model for the homogenization of masonry. *International Journal of Solids and Structures*, vol. 39: p. 3233-3255, 2002.

Slab stiffness influence in design of reinforced concrete frame system

George Țăranu¹, Mihai Budescu²

^{1,2} *Department of Structural Mechanics, Faculty of Civil Engineering and Installations,
Technical University “Gh. Asachi”, Iași, 70050, Romania*

Summary

The paper summarizes and analyses the basic requirements associated with initial conceptual design and hypothesis of reinforced concrete structural frames that are included in Eurocode 8, Eurocode 2 (EC8, EC2), SR EN 1992-1, P100/2006 into an easily understandable synopsis accompanied with one numerical model and pictures. One of the principal hypotheses is stiffness slab and the product EI which has influence on the model analyse and the structure behaviour.

KEYWORDS: reinforced concrete structural frames, slab, stiffness, modulus of elasticity, product EI

1. INTRODUCTION

Reinforced concrete structural frames have multiple advantages. Many buildings have this kind of structure. In analyse and design of these structures is necessary little completion. Software models give the response of structures. The response can be correct or incorrect, that's depend on how the hypothesis is made. The importance of stiffness consists in strain results. The most important action on these structures situated in seismic regions is horizontal forces. In the next part is presented some specific rules for concrete building according to EC 8 and P100/2006.

2. STRUCTURAL ANALYSIS

2.1. Modelling

The model of the building shall adequately represent the distribution of stiffness and mass in it so that all significant deformation shapes and inertia forces are properly accounted for under the seismic action considered. In the case of non-

linear analysis, the model shall also adequately represent the distribution of strength. The model should also account for the contribution of joint regions to the deformability of the building, e.g. the end zones in beams or columns of frame type structures. Non-structural elements, which may influence the response of the primary seismic structure, should also be accounted for.[1]

When the floor diaphragms of the building may be taken as being rigid in their planes, the masses and the moments of inertia of each floor may be lumped at the centre of gravity.

In concrete buildings the stiffness of the load bearing elements should, in general, be evaluated taking into account the effect of cracking. Such stiffness should correspond to the initiation of yielding of the reinforcement.

2.2. Specific rules for concrete buildings

The frame system is a structural system in which both the vertical and lateral loads are mainly resisted by spatial frames whose shear resistance at the building base exceeds 65% of the total shear resistance of the whole structural system.

The design of earthquake resistant concrete buildings shall provide the structure with an adequate capacity to dissipate energy without substantial reduction of its overall resistance against horizontal and vertical loading. In the seismic design situation adequate resistance of all structural elements shall be provided, and non-linear deformation demands in critical regions should be commensurate with the overall ductility assumed in calculations.

Concrete buildings may alternatively be designed for **low dissipation capacity** and **low ductility**, by applying only the rules of EN 1992-1-1:2004, (SR EN 1992-1). For buildings which are not base-isolated, design with this alternative, termed ductility class L (low), is recommended only in low seismicity cases.

Earthquake resistant concrete buildings other than those with low dissipation shall be designed to provide energy dissipation capacity and an overall ductile behaviour. Overall ductile behaviour is ensured if the ductility demand involves globally a large volume of the structure spread to different elements and locations of all its storeys. To ductile modes of failure (e.g. flexure) should precede brittle failure modes (e.g. shear) with sufficient reliability.

Concrete buildings designed to ensure dissipation, are classified in two ductility classes DCM (medium ductility) and DCH (high ductility), depending on their hysteretic dissipation capacity. Both classes correspond to buildings designed, dimensioned and detailed in accordance with specific earthquake resistant provisions, enabling the structure to develop stable mechanisms associated with large dissipation of hysteretic energy under repeated reversed loading, without suffering brittle failures.[1],[2]

2.2.1. Design action effects

The design values of bending moments and axial forces shall be obtained from the analysis of the structure for the seismic design situation in accordance with EN 1990:2001 6.4.3.4, SR EN 1990:2004, taking into account second order effects. Redistribution of bending moments in accordance with EN 1992-1-1 is permitted.

In primary seismic beams the design shear forces shall be determined in accordance with the capacity design rule, on the basis of the equilibrium of the beam under: a) the transverse load acting on it in the seismic design situation and b) end moments $M_{i,d}$ (with $i=1,2$ denoting the end sections of the beam), corresponding to plastic hinge formation for positive and negative directions of seismic loading. The plastic hinges should be taken to form at the ends of the beams or (if they form there first) in the vertical elements connected to the joints into which the beam ends frame (Figure 1).

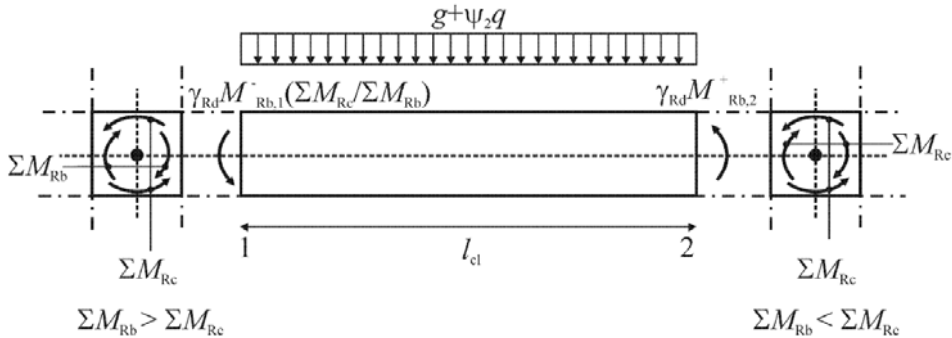


Figure 1. Capacity design values of shear forces on beams [1]

At end section i , two values of the acting shear force should be calculated, i.e. the maximum $V_{Ed,max,i}$ and the minimum $V_{Ed,min,i}$ corresponding to the maximum positive and the maximum negative end moments $M_{i,d}$ that can develop at ends 1 and 2 of the beam.

End moments $M_{i,d}$ may be determined as follows:

$$M_{i,d} = \gamma_{Rd} M_{Rb,i} \min \left(1, \frac{\sum M_{Rc}}{\sum M_{Rb}} \right) \quad (1)$$

γ_{Rd} is the factor accounting for possible over strength due to steel strain hardening, which in the case of DCM beams may be taken as being equal to 1,0;

$M_{Rb,i}$ is the design value of the beam moment of resistance at end i in the sense of the seismic bending moment under the considered sense of the seismic action;

ΣM_{Rc} and ΣM_{Rb} are the sum of the design values of the moments of resistance of the columns and the sum of the design values of the moments of resistance of the beams framing into the joint, respectively. The value of ΣM_{Rc} should correspond to the column axial force(s) in the seismic design situation for the considered sense of the seismic action.

In primary seismic columns the design values of shear forces shall be determined in accordance with the capacity design rule, on the basis of the equilibrium of the column under end moments $M_{i,d}$ (with $i=1,2$ denoting the end sections of the column), corresponding to plastic hinge formation for positive and negative directions of seismic loading. The plastic hinges should be taken to form at the ends of the beams connected to the joints into which the column end frames, or (if they form there first) in the columns (Figure 2).

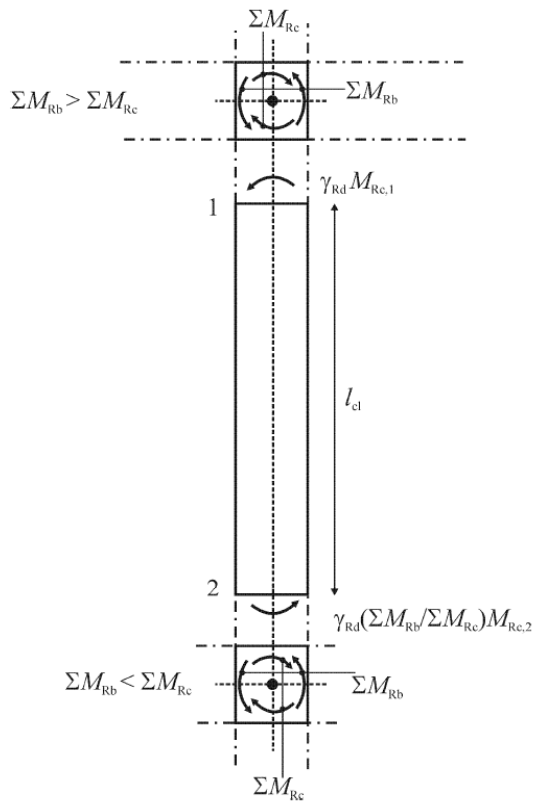


Figure 2. Capacity design shear force in columns

End moments $M_{i,d}$ may be determined from the following expression [1],[2]:

$$M_{i,d} = \gamma_{Rd} M_{Rc,i} \min \left(1, \frac{\sum M_{Rb}}{\sum M_{Rc}} \right) \quad (2)$$

γ_{Rd} is the factor accounting for over strength due to steel strain hardening and confinement of the concrete of the compression zone of the section, taken as being equal to 1,1 according with EC 8 and 1,3 for first level at the base of structure and 1,2 for the up levels according with P100/2006;

$M_{Rc,i}$ is the design value of the column moment of resistance at end i in the sense of the seismic bending moment under the considered sense of the seismic action;

$\sum M_{Rc}$ and $\sum M_{Rb}$ are the sum of the design values of the moments of resistance of the columns and the sum of the design values of the moments of resistance of the beams framing into the joint, respectively. The value of $\sum M_{Rc}$ should correspond to the column axial force(s) in the seismic design situation for the considered sense of the seismic action.

2.2.2. Design verifications

Depending on the elements verification the hypothesis of the stiffness elements are different to simulate the cracks in concrete.

On the beams ULS verifications the bending and shear resistances should be computed in accordance with EN 1992-1-1:2004, SR EN 1992-1, STAS 10107/0-90.

The top-reinforcement of the end cross-sections of primary seismic beams with a T- or L-shaped section should be placed mainly within the width of the web. Only part of this reinforcement may be placed outside the width of the web, but within the effective flange width b_{eff} .

The effective flange width b_{eff} may be assumed to be as follows:

a) for primary seismic beams framing into exterior columns, the effective flange width b_{eff} is taken, in the absence of a transverse beam, as being equal to the width b_c of the column (Figure 3b), or, if there is a transverse beam of similar depth, equal to this width increased by $2h_f$ on each side of the beam (Figure 3a);

b) for primary seismic beams framing into interior columns the above widths may be increased by $2h_f$ on each side of the beam (Figure 3c and d).

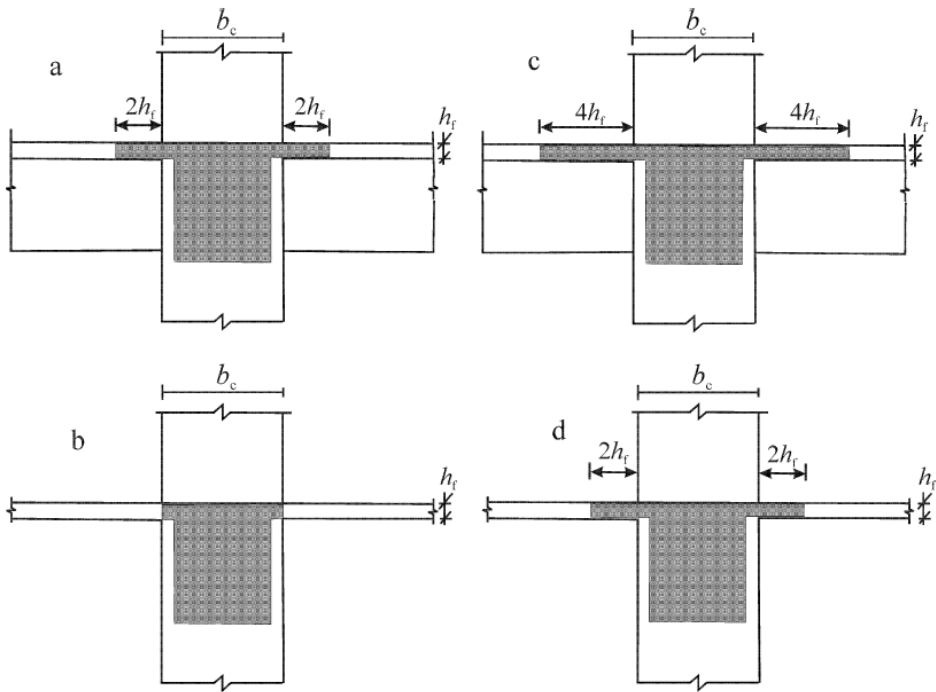


Figure 3, Effective flange width b_{eff} for beams framing into columns [1]

In accordance with EN 1992-1-1:2004 the effective flange width b_{eff} for a T beam or L beam shown in figure 4, may be derived as [3]:

$$b_{eff} = \sum b_{eff,i} + b_w; \quad (3)$$

where

$$b_{eff,i} = 0.2b_i + 0.1l_0 \leq 0.2l_0; \quad (4)$$

and

$$b_{eff,i} \leq b_i \quad (5)$$

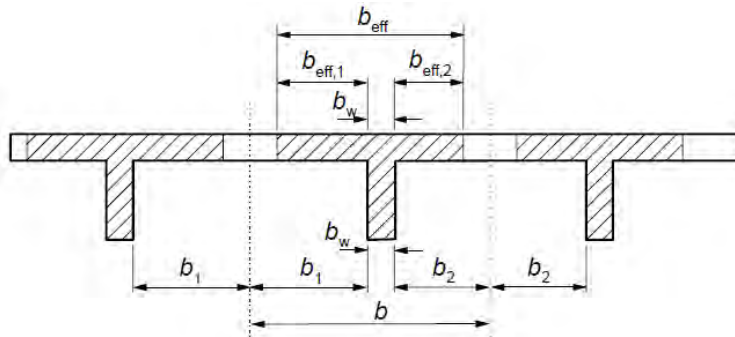


Figure 4, Effective flange width parameters [3]

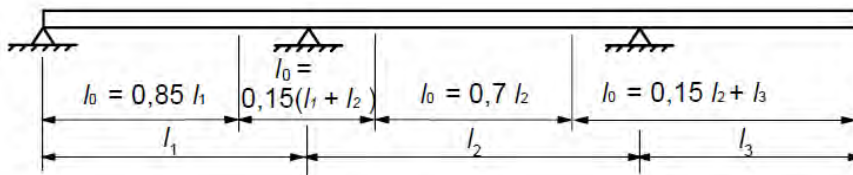


Figure 5, Definition of l_0 , for calculation of flange width [3]

3. CONCRETE FRAME SYSTEM ANALYSE

In order to see how the stiffness slabs has importance in strain results of frame's elements, in the next part a current plane frame system it will be analyzed. The frame system is composed from 2 storeys. The columns have 45x45 cm section, and beams 25x45cm. Span is 5.00 m long, and height is 3.00 m. The properties of materials are shown in table 2. To modify the value of stiffness elements (product EI) are 2 possibilities. One is to reduce the moment of inertia or to reduce the modulus of elasticity. The reduction of these depends on what kind of verification or analyze is did it. For strain results the product EI must be 0.8EI for columns, and 0.5EI for beams. In case of displacement verification depends on type of elements of structure. It will be considered the influence of stiffness slab on strain results so the value of this is presented in table 2. The next step is to analyze 2 models which will have the properties presented in table 2 and the section of beams it will be T. The moment of inertia of beams section is calculated and the product EI is modified by reducing the modulus of elasticity in 2 hypotheses [4].

Table 1. Value of product EI in case of displacement verification

Type of structure	The nature of links between non-structural elements and structure	
	The non-structural elements have influence on behaviour of structure	The non-structural elements have not influence on behaviour of structure
Frame system	$E_c I_c$	$0.5E_c I_c$
E_c - concrete modulus of elasticity		
I_c - concrete section moment of inertia		

Table 2. Value of product EI in structure analyzed

Element	Product EI	Material used
	strain analyze	Concrete C20/25 $E=300000,00 \text{ daN/cm}^2$
Beam	$0.5EI$	$0.5E=150000 \text{ daN/cm}^2$
Slab	$0.5EI$	$0.5E=150000 \text{ daN/cm}^2$
Beam	$0.6EI$	$0.6E=180000 \text{ daN/cm}^2$
Slab	$0.6EI$	$0.6E=180000 \text{ daN/cm}^2$
Column	$0.8EI$	$0.8E=240000 \text{ daN/cm}^2$

3.2. Current frame model

First model analyzed is a current frame. Being a seismic beam framing into interior columns, the flange width is in according with EC8 rules:

$$b_{eff} = b_c + 4h_f = 45 + 4 \cdot 15 = 105 \text{ cm} \quad (6)$$

In the figure 6 is presented the beam section parameters.

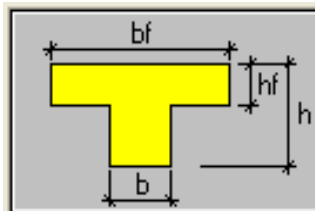


Figure 6, beam section parameters

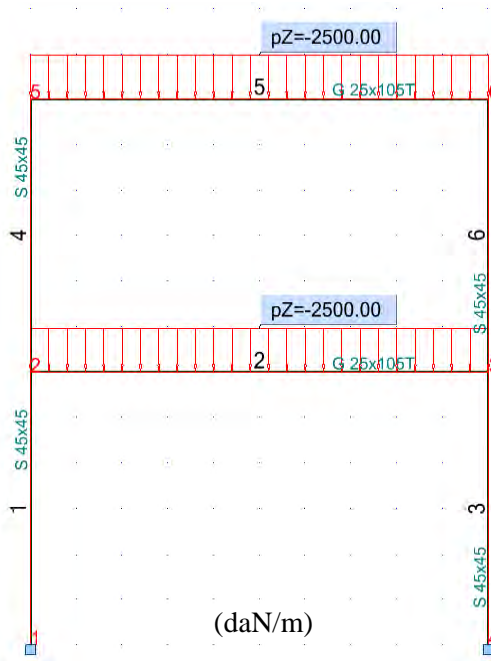


Figure 7, Geometrical and static loading schema of the model analyzed

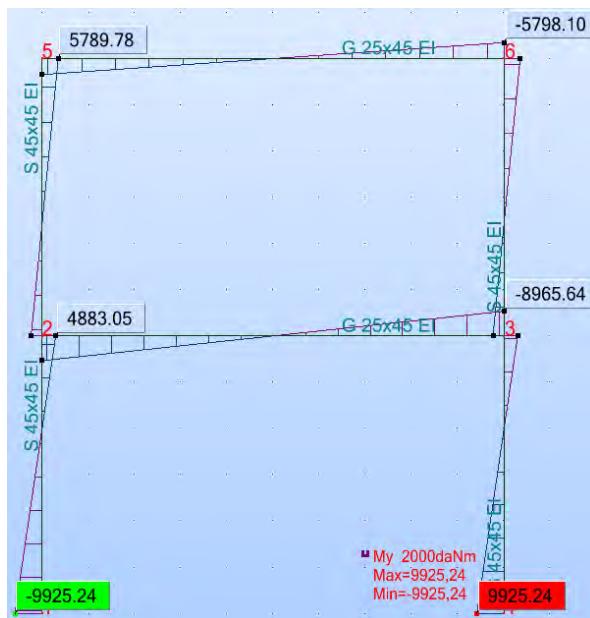


Figure 8, M diagram when product EI is not modified

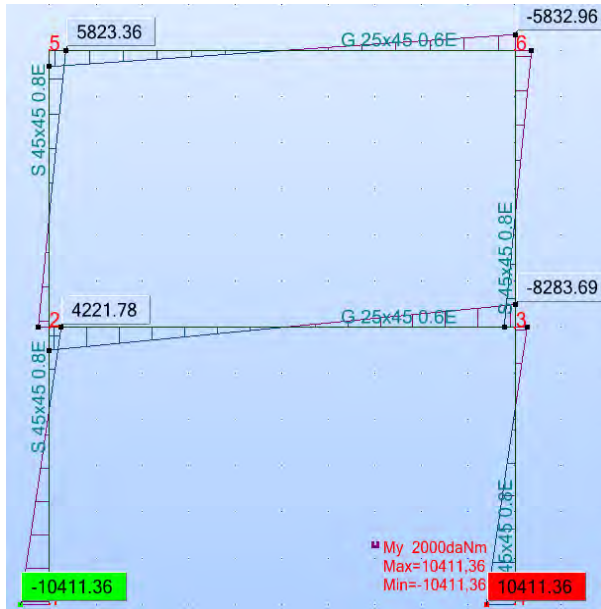


Figure 9, M diagram when product EI is 0.8EI for column and 0.6EI for beam

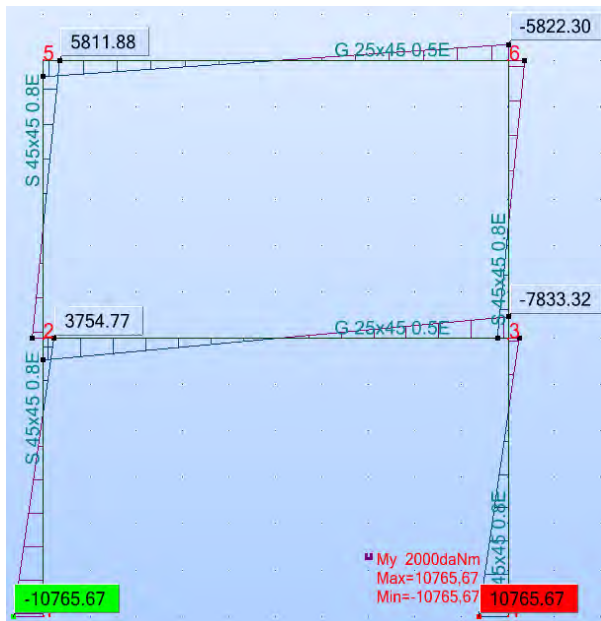


Figure 10, M diagram when product EI is 0.8EI for column and 0.5EI for beam

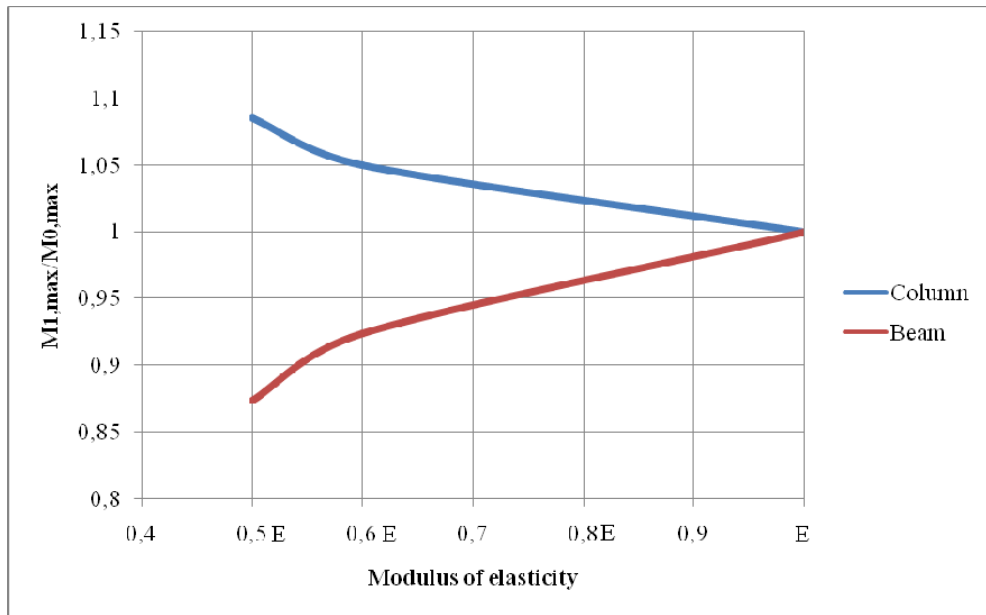


Figure 11, Influence of Modulus of elasticity on Bending Moments

4. CONCLUSIONS

After the models analyze observes that the value of bending moment on column is increasing while the modulus of elasticity is reduced. On beams, the modification of product EI makes that the value of bending moment to reduce. This knowledge is important because in reality the structure behaviour is affected by the concrete condition, and that must be provided in simulation model. Because the slab and beam pull together is necessary that the slab have same stiffness like beam.

References

1. Eurocode 8: *Design of structures for earthquake resistance Part 1: General rules, seismic actions and rules for buildings*, EN 1998-1-1-2003
2. P 100/2006 *Cod de proiectare seismică - Partea I-Prevederi de proiectare pentru cladiri*
3. Eurocode 2: *Design of concrete structures -Part 1: General rules and rules for buildings*, EN 1992-1-1-2002
4. Postelnicu, T., *P 100/1 Proiectarea seismică a cladirilor – vol. 2A Comentarii si exemple de calcul*, M.T.C.T, 2005.

The detection of singular points in the stability analysis of structures

Teodorescu Mircea-Eugen, Topala Cristina-Alexandra

Department of Mechanics, Static and Dynamic of Structures, Technical University of Civil Engineering, Bucharest, 38RO-020396, Romania

Summary

Depending of the history of loading, the stiffness of the structure may be softening or stiffening, the equilibrium path may be stable or unstable and the structure itself may be on a stage of loading or unloading.

All such phenomena are typified by the occurrence of singular points (limit points and bifurcation points) which tend to bring us numerical difficulties in the solution process.

For tracing the entire load deflection path is necessary an automatically incremental-iterative procedure using control parameters for guiding the direction of the loading and the presence of the singular points, also.

The paper describes a methodology for detection of the singular points in the stability analysis of structures.

Using an original program for 3D – truss structures, two numerical examples are presented. The results are compared with the analytical solution or given by others authors.

KEYWORDS: stability analysis, singular points, incremental-iterative method

1. INTRODUCTION

The finite element method is an important tool for the analysis of non-linear problems, such as geometrical and material non-linear behaviour of solids and structures.

The behaviour of the structure can be represented by load-deflection response for certain degree of freedom (fig.1).

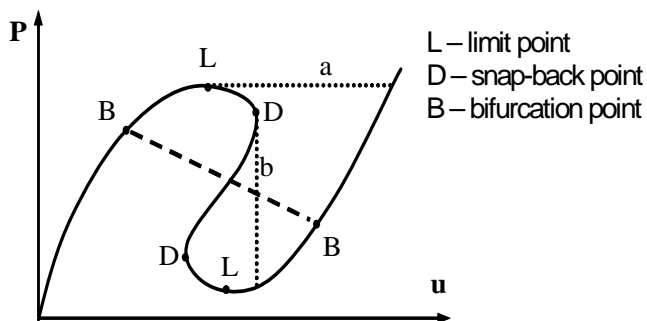


Figure 1

It can be observed that, depending on the history of loading, the stiffness of the structure may be softening or stiffening, the equilibrium path may be stable or unstable, and the structure itself may be on a stage of loading or unloading. All such phenomena are typified by the occurrence of singular points (limit points and bifurcation points) and snap-back points in the load-deflection curve, which tend to bring us numerical difficulties in the solution process.

A typical nonlinear system can be represented by the following equation:

$$\mathbf{K}\delta\mathbf{u}=\delta\lambda\mathbf{P}-\mathbf{R} \tag{2}$$

where \mathbf{K} is the tangent stiffness matrix, $\delta\mathbf{u}$ represents the iterative correction of the nodal displacement vector, $\delta\lambda$ the iterative change of load, \mathbf{P} is the reference load vector and \mathbf{R} is the out-of-balance force vector.

The system of nonlinear equation described by Eq.(2) has (N+1) variable, but only N equations, where N is the number of degrees of freedom of the finite element model. In order to solve the system of nonlinear equations a constraint equation is added.

To obtain the complete load-deflection response of the structure, an automatically incremental-iterative procedure based on arc-length method is used. The arc-length method [3] is probably the most used procedure to trace the post-buckling path of nonlinear structures since it can easily overcome limit points and snap-backs points.

The basic idea of the arc-length approach is to constraint the size of incremental changes $\Delta\mathbf{u}$ and $\Delta\lambda$, leading to

$$\Delta\mathbf{u}^T \Delta\mathbf{u}+\psi^2 \Delta\lambda^2-\Delta\ell^2=0 \tag{3}$$

where $\Delta\ell$ is the prescribed arc-length and ψ is a scaling parameter (for spherical arc-length ψ is 1 and for cylindrical arc-length ψ is 0).

In order to obtain a stable and efficient procedure the arc-length should be updated at the beginning of each step according to the nonlinearity of the equilibrium path. The simplest measure of the nonlinearity is the number of iterations required to achieve convergence in the previous step (I_n). therefore, the new arc-length can be computed from:

$$\Delta \ell_{n+1} = \Delta \ell_n \left(\frac{I_d}{I_n} \right)^\alpha \quad (4)$$

where I_d is the desired number of iterations (2 to 5) and the parameter α is generally set to 0.50. A minimum ($\Delta \ell_{\min}$) and a maximum ($\Delta \ell_{\max}$) arc length should be specified to control the adaptive process.

The load increment automatically chosen must also be of the correct sign necessitating measures capable of detecting when the maximum and the minimum points on the load-deflection path have been passed. The correct sign is chosen according to the criteria in Section 3 [5].

2. STABILITY ANALYSIS. DETECTING THE SINGULAR POINTS

The analysis of a given structure is not complete without the determination of its load carrying capacity, which requires to compute the singular points of the load-displacement curve and to trace the secondary paths.

There are two different types of singular points, as depicted in Fig.1. A limit point arises when the equilibrium path reaches a local extremum as points L, while a bifurcation occurs when different equilibrium paths cross at a certain point, as points B. Moreover, bifurcation points can be simple or multiple.

A point of the load-displacement curve is a singular point when the stiffness matrix of the finite element model is singular. Thus, a singular point can be detected using the condition:

$$\det \mathbf{K}(\mathbf{u}, \lambda) = 0 \quad (5)$$

An alternative approach to the singular point detection is to use the zero eigenvalue condition

$$\mathbf{K}(\mathbf{u}, \lambda) \boldsymbol{\Phi} = 0 \quad (6)$$

where $\boldsymbol{\Phi}$ is the associated eigenvector which represents the buckling mode of the structure.

To classify the singular points the following criterion (7) can be used :

$$\begin{aligned} \Phi^T \mathbf{P} \neq 0 &\rightarrow \text{limit point} \\ \Phi^T \mathbf{P} = 0 &\rightarrow \text{bifurcation point} \end{aligned} \quad (7)$$

In order to study the stability of the post-buckling state it is necessary to trace the secondary paths at a bifurcation point. One of the branch-switching techniques consists in the application of a predictor according with the eigenvector mode with arc length method for iterations.

3. CLASSIFICATION OF SINGULAR POINTS BY CONTROL PARAMETERS

For the detection of singular points the followings control parameters are used:

- *the number of negative pivots of stiffness matrix.* The number of negative pivots of \mathbf{K} (noted by NPIV) can be obtained very easy from the elements of diagonals matrix \mathbf{D} from $\mathbf{L}^T \mathbf{D} \mathbf{L}$ factorization of \mathbf{K} (stiffness matrix corresponding to the equilibrium state $i-1$). If structure has no bifurcation points then, in the stable path $\text{NPIV}=0$ (minimum pivot >0) and in the unstable path $\text{NPIV}=1$ (minimum pivot <0). For the structures with multiple bifurcation points, this control parameter is inefficient.

- *current stiffness parameter.* This parameter, proposed by Bergan [1] is defined as follows:

$$CSP_i = \frac{\{\Delta \mathbf{u}\}_i^{1T} \cdot \{P\}}{\{\Delta \mathbf{u}\}_1^{1T} \cdot \{P\}} \quad (8)$$

where $\{\Delta \mathbf{u}\}_1^1$ and $\{\Delta \mathbf{u}\}_i^1$ denote the displacements increments associated with the first iteration in the first step and respectively in i^{th} step, and \mathbf{P} represents the reference load.

The parameter has an initial value of unity for any non-linear structure. One general property of this parameter is that it tends to increase for structures that are loaded into the stage of stiffening and to decrease for structures on the stage of softening. For structures reaching the limit points in the load-deflection curves, the current stiffness parameter becomes exactly equal to zero.

Thus, a positive CSP refers to a stable region on load-deflection curves, for which the external loads can be increasingly, apply. A negative CSP corresponds to an unstable region on load-deflection curves for which the external loads should be decreasingly applied. Despite these useful characteristics, the CSP is not suitable for application to problems involving snap-back.

The CSP changes the sign at both limit point and snap-back point, thereby making impossible to distinguish between two types of points. Realizing that the directions of loading need to reverse only when passing the limit points it can see that CSP is not a proper indicator for guiding the direction of loading.

Moreover, the CSP varies in an abrupt manner whenever any displacement component snaps-back.

-general stiffness parameter. The general stiffness parameter (noted by GSP) is defined as the scalar product of the displacements increments vectors associated with the iteration $j=1$ for two consecutive steps

$$\text{GSP}_i = \{\Delta \mathbf{u}\}_{i-1}^1 \cdot \{\Delta \mathbf{u}\}_i^1 \quad (9)$$

This control parameter has several important characteristics:

- GSP turns out to be negative only for the incremental steps immediately after the limit points, whereas for the other incremental steps it will always remain positive;
- GSP can predict the occurrence of limit points, it serves as a good indicator for changing the direction of loading, as follows:

If $\text{GSP}_i < 0$ then $\Delta \lambda_i^1$ and $\Delta \lambda_{i-1}^1$ have different signs,

If $\text{GSP}_i > 0$ then $\Delta \lambda_i^1$ and $\Delta \lambda_{i-1}^1$ have the same sign

- GSP tends to increase for structures on the stage of stiffening and to decrease for structures on the stage of softening. However, the GSP is superior to CSP in that it remains bounded throughout the entire history of loading, regardless of the presence of snap-back points.

The nature of singular point can be determined using the values of control parameters above discussed, as follows [3]:

- if the current stiffness parameter CSP and the minimum pivot PIVMIN switch signs, the singular point passed is a limit point (figure 2,a);
- if only the minimum pivot PIVMIN has switched signs, with no change in the sign of current stiffness parameter CSP, then the singular point passed is a bifurcation point (figure 2,b).

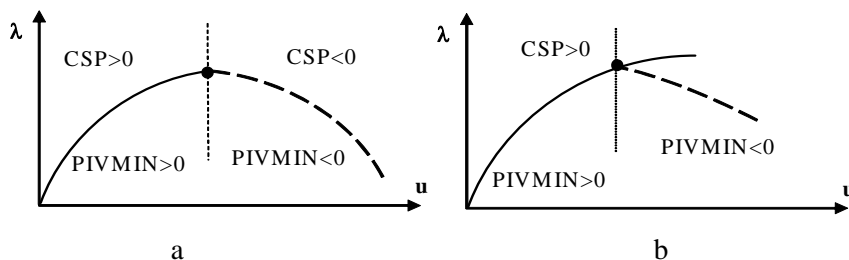


Figure 2

4. NUMERICAL EXAMPLES

In this section, two examples of different characteristics will be used to validate the techniques presented in this work. The examples are concerned with the post buckling behaviour of truss structures. The convergence of the finite element solution is established on the Euclidean norm of the out of balance force. An original program GEONEL [4] using an automated incremental-iterative procedure based on arc length method (cylindrical version) has been realized.

4.1. A three-dimensional arch truss

Figure 3 shows the arch truss, with $EA=1000N$, that have several singular points including four bifurcation points and a limit point.

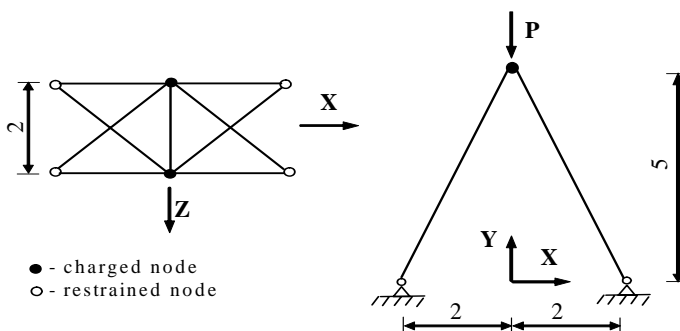


Figure 3

The values of the load corresponding to singular points are presented in Table 1.

Table 1

	GEONEL	Crisfield [3]
Bifurcation point	1222	1228
Bifurcation point	6902	6913
Limit point	9890	9926
Bifurcation point	9105	9105
Bifurcation point	2296	2294

The computed relationship between the load and the three deflections of one of the top nodes under the vertical loading are shown in figures 4,a,b,c where it's only plotted the post-buckling path for the first two bifurcation points beyond the limit point.

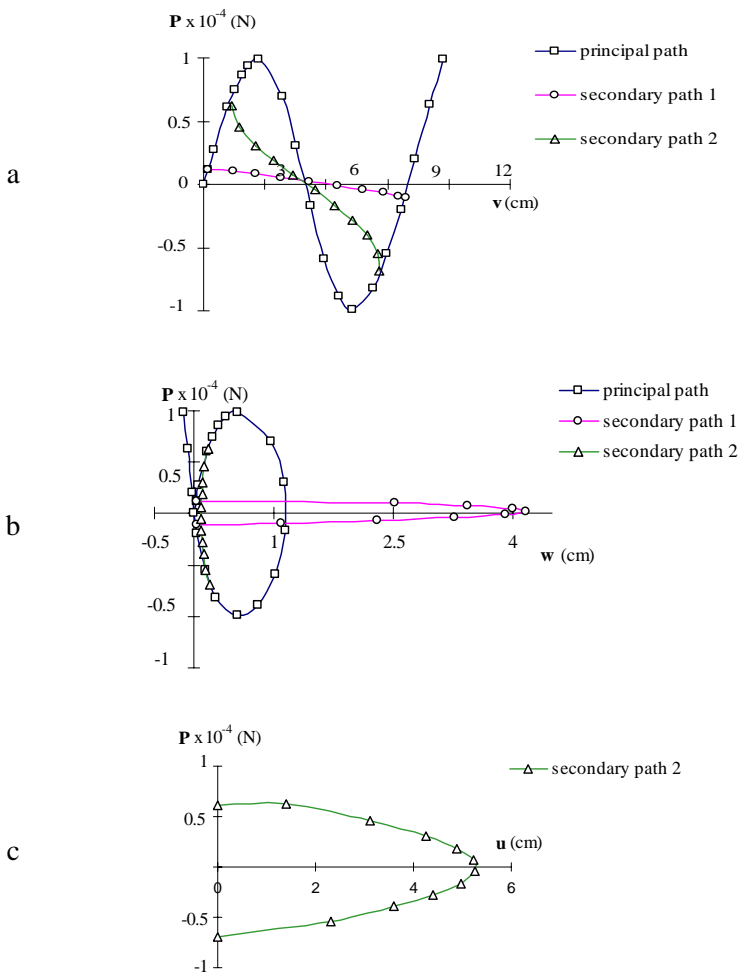


Figure 4

All the bifurcation points are ‘simple’, and, as results there are no particular difficulties either in ‘bracketing’ or ‘branch switching’.

At the first bifurcation point the structure buckles in the yz plane (fig.4,b) with no displacement in the x-direction; at the second bifurcation point, it buckles in the xy plane (fig.4,c) so that the z-displacements are symmetric at the top nodes.

4.2. 24 member hexagonal star-shaped shallow dome

The structure shown in figure 5 was analyzed by various authors [3], [4], [5] as a space truss to trace its load deflection behaviour into the post-buckling range. The characteristics of the shallow are $E= 3.03 \times 10^5 \text{ N/cm}^2$, $A= 3.17 \text{ cm}^2$. The supports of the dome are assumed to be pinned and restrained against translational motion. The dome is subjected to a vertical load $P/2$ at the central node and vertical loads P at the others nodes.

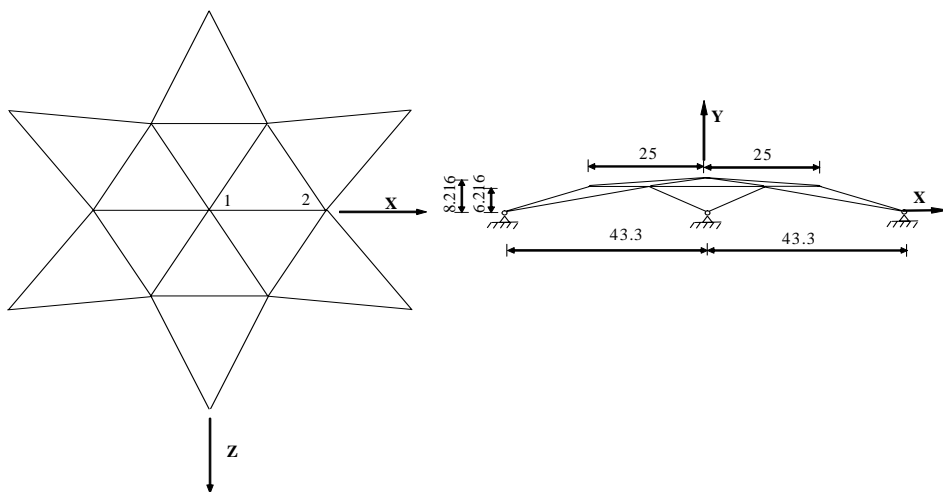


Figure 5

The load – deflection path for the apex point (fig.6) is very interesting, because there are a lot of singular points (8 limit points and 7 simple bifurcation points and 11 double bifurcation points).

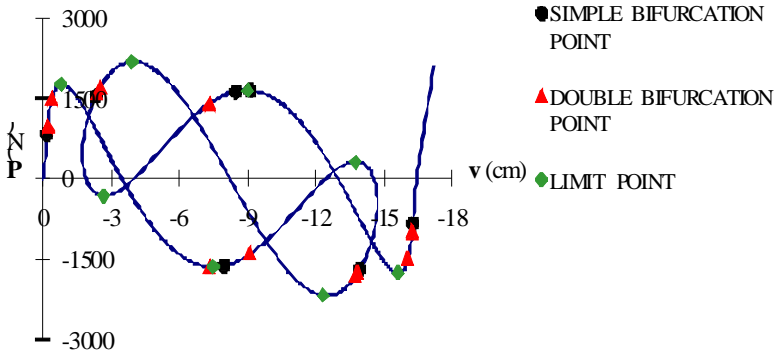


Figure 6

A same response was obtained by Fujii [4] using control displacement method. The bifurcation points are simple or double. The same results was obtained by Healey [5] using group theory and by Crisfield [3] using an iterative incremental strategy based on Newton Raphson method and arc length method which is leaded by CSP.

Unfortunately, Crisfield [3] gives only the results before first limit point. Using the program of Crisfield, it's not possible to trace the entire path because there are snap-back points.

5. CONCLUSIONS

For tracing the entire load deflection path is necessary an automatically incremental-iterative technique using control parameters for guiding the direction of the loading and the presence of the singular points, also. The control parameter is computed in the predictor phase and characterized the equilibrium position of the structure and the degree of non-linearity.

For the detection of singular points the followings control parameters are used:

the number of negative pivots of the tangent stiffness matrix of the structure, the current stiffness parameter and the general stiffness parameter.

The number of negative pivots (NPV) is inefficient for structures, which present multiple bifurcation points. This control parameter can be used to determine the nature of singular points.

The current stiffness parameter (CSP) is used for determine the nature of singular points (limit or bifurcation) and is not suitable for application to problems involving snap-back.

The general stiffness parameter (GSP) can predict the occurrence of limit points, it serves as a good indicator for changing the direction of loading.

Using an original program for 3D – truss structures, two numerical examples are presented. The results obtained are very closed with the results given by others authors.

References

1. B.G.Bergan, G. Horrigmoe, B. Krakeland and T.H. Soreide -Solution techniques for non-linear finite element problems, *Int. J.Numer. Methods Eng.*, 12, 1677-1696, (1978)
2. Clarke, M.J., Hancock, G.J. - A study of incremental-iterative strategies for non-linear analysis. *Int. J. Num. Meth. & Engng.*, 29, 1365-1391 (1990)
3. Crisfield, M.A. - *Non-linear Finite Element Analysis of Solids and Structures*, Vol.1 Essentials, John Wiley&Sons 1991, Vol.2 Advanced topics, John Wiley&Sons 1997
4. Fujii,F., Perez, B.G., Choong, K.K. - Selection of the control parameter in displacement incrementation. *Comput. & Struct.*, 42, 167-174 (1992)
5. Healey, T.J. – A group – theoretic approach to computational bifurcation problems with symmetry. *Comp. Meth. Appl. Mech. & Engng.*, 67, 257-295 (1984)
6. Teodorescu, M.E. - *Studiu comparativ al metodelor pentru determinarea solutiilor in calculul neliniar al structurilor* Teza de doctorat, 1999

The Seismic Soil-Structure Interaction Effect for Pile-Raft Systems

Nicolae Ungureanu¹, Mihai Vrabie¹ and Iancu Bogdan Teodoru²

¹Department of Structural Mechanics, TU “Gh. Asachi”, Iasi, 700050, România

²Department of Transportation Infrastructure and Foundations, TU “Gh. Asachi”, Iasi, 700050, România

Summary

The horizontal displacement and the base rotation for a structural system resting on general vertical pile-raft foundation is evaluated. Two different cases for the boundary condition at the top of the pile are considered: pinned and fixed head. The effect of these displacements about the shear force in the seismic design of the structural system is analysed. The influence on the twisting of the structure is discussed too.

KEYWORDS: pile-raft system, soil-structure interaction, vibration period, base displacement

1. INTRODUCTION

The analysis of the structural seismic response includes, in a more generalised case, the influence of the Soil Structure Interaction (SSI). The equivalent fixed-base models for SSI systems can be accepted only for those sufficiently rightful cases. In fact, a more developed analysis is necessary. The analysis must take into account the displacements of the base because of the surrounding soil flexibility. A practical case is the structures standing on a pile-raft system, which following are analysed.

The piled rafts, subjected at strong horizontal forces, such as the base shear force from the seismic action, moves in horizontal direction because of the piles deformation. The raft is very stiff (with respect to the piles) and all the piles have the same displacement by translation. The action of the moment transmitted by the structure to the foundation system leads to its rotation. It is considered the case when the moment is placed in the vertical principal plane of inertia. Because of the piled raft stiff, the ends of the piles after the foundation rotation will be situated in a plane, which can be adequately fixed.

By the translation of the piled raft, the same displacement is transmitted on the height of the building and by its rotation; the displacement on height will be

proportional with the distance from the base. These displacements correct the displacements from the fixed-base model and accordingly the dynamic response of the structural system is modified.

2. THE INFLUENCE OF THE BASE DISPLACEMENTS ON THE VIBRATION PERIOD

If we refer to the vibration periods, these depend of the real displacements which take place in the system. Thus, at a certain level, at one point, the displacement can have the following components:

- the displacement because of the structure bending considered with a fixed base (x_M);
- the displacement because of the shear force of the structure with fixed base (x_Q);
- the displacement generated by the translation (sliding) of the piled raft (x_R);
- the displacement caused by the rotation of the piled raft (x_ϕ).

If it is assumed that the analysis for the determination of the fundamental period T_1 is made in the principal plane of inertia xOz , we can use, for example, the Rayleigh method to obtain the expression [1]:

$$T_1 = \frac{2\pi}{\omega_1} = 2\pi \sqrt{\frac{x_{ST,max}}{gA_{n1}}} \quad (1)$$

where:

T_1 is the fundamental period of vibration, in seconds;

ω_1 is the fundamental circular frequency, in radians per second;

$x_{ST,max}$ is the maximum static displacement of structure, which is produced by the gravitational forces applied in the degrees of freedom directions;

g is the gravity acceleration ($= 981 \text{ cm/s}^2$);

A_{n1} is the shape coefficient corresponding to the degree of freedom.

Particularly, for a multistory structure can be shown that the medium value of the shape coefficient is approximate 1,41 [1].

In this conditions the fundamental period T_1 may be expressed as:

$$T_1 = \xi_n \sqrt{x_{ST,max}} \quad (2)$$

where ξ_n is a dimensionless coefficient which depends on the gravitational loads and number of levels.

For instance, if the gravitational loads are the same for each floor, ξ_n is between 0,2 for $n = 1$ and 0,165 for $n \geq 12$ [1].

From (2) we find out directly that the period T_1 depends on maximum static displacement and, implicitly on the flexibility degree of the structure, respectively on its stiffness.

The displacement $x_{ST,max}$, as well as the displacement $x_{n,max}$ at the n level, consists of those foregoing displacements:

$$x_{ST,max} = x_M + x_Q + x_R + x_\varphi \quad (3)$$

The displacement x_M and $x_Q = x_V$ are produced by the gravitational forces applied to horizontal direction on the structure with fixed base.

The displacements x_R and x_φ depend on the boundary conditions because the piles may be considered with pinned or fixed head.

3. THE CALCULUS OF DISPLACEMENTS $x_R = x_0$ AND

$$x_\varphi = \varphi_0$$

3.1 Vertical pinned-head pile

3.1.1. The displacement x_0 produced by the level horizontal forces

The pile is considered as a beam of semi-infinite length on elastic foundation, subjected at the upper end by a horizontal force q_i [2], [3], (Fig. 1.a.). From elementary beam theory, the deflection under the load, at the end ($z = 0$) is:

$$x_{0i} = \frac{2q_i\alpha_i}{b_i c_h} \quad (4)$$

where:

b_i is the width or diameter of the pile in the normal direction on the bending plane, in cm;

c_h is the coefficient of horizontal subgrade reaction, in N/cm^3 , considered constant on depth; this coefficient can be determined by using the horizontal loading test, for which the displacement of the upper end acted by a horizontal force is measured;

α_i is a dimensionless parameter given by the expression:

$$\alpha_i = \sqrt[4]{\frac{c_h b_i}{4EI_{pi}}} = (c_h b_i / 4EI_{pi})^{1/4} \quad (5)$$

where

E is the modulus of elasticity for constitutive material of the pile;

I_{pi} is moments of inertia with respect to the bending axis of the pile cross-section.

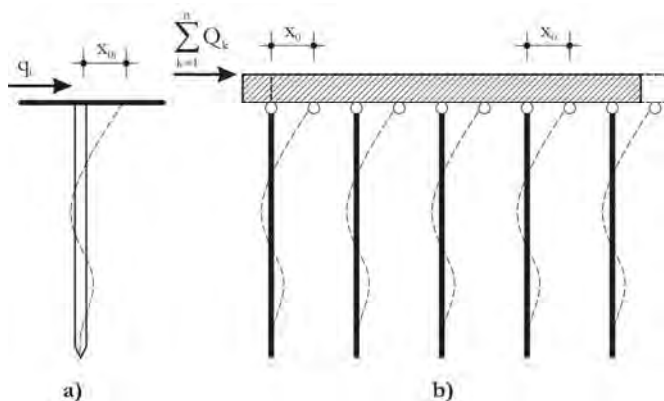


Figure 1. Vertical pinned-head pile: **a)** pile subjected by a horizontal force q_i ; **b)** the horizontal displacement x_0 of the raft

For $q_i = 1$, the translation stiffness of the pile, can be expressed as [2], [4-5]:

$$k_i^* = \frac{1}{x_{oi}} = \frac{b_i c_h}{2\alpha_i} \quad (6)$$

The stiffness of a m piles group will be:

$$K^* = \sum_{i=1}^m k_i^* = \sum_{i=1}^m \frac{b_i c_h}{2\alpha_i} \quad (7)$$

The horizontal displacement x_0 of the raft (Fig. 1.b), produced by the shear force

$$V = Q = \sum_{k=1}^n Q_k \quad (8)$$

where n is the number of levels, can be expressed as:

$$x_0 = \frac{\sum_{k=1}^n Q_k}{\sum_{i=1}^m \frac{b_i c_h}{2\alpha_i}} = \frac{Q}{K^*} \quad (9)$$

If the piles have the same cross-section and orientation, the previous expression becomes:

$$x_0 = \frac{\sum_{k=1}^n Q_k}{mk^*} = \frac{2\alpha \sum_{k=1}^n Q_k}{mbc_h} \quad (10)$$

3.1.2. The raft rotation produced by the bending moment

Considering that the centroid of the building coincides, on the vertical direction, with the centroid of the piles cross-sections, the raft will be acted by the bending moment (Fig. 2)

$$M_0 = M_{Q_k} + \sum_{k=1}^n Q_k \cdot h_r \quad (11)$$

which is a vector in y - y direction (h_r is the height of the raft foundation). The axial force acted on the i pile, produced by the moments M_0 is:

$$N_{pi} = \frac{M_0 x_i}{\sum_{i=1}^m A_{pi} x_{pi}^2} A_{pi} \quad (12)$$

where:

A_{pi} is the area of the i pile cross-section;

$x_{pi} = x_i$ is the distance from the i pile to the y - y axis;

The endmost piles, with respect to the y - y axis, (Fig. 2), will be most loaded (identical piles); if the m piles in the group are identical, it results:

$$N_{pi} = N_{p\max} = \frac{M_0 x_{\max}}{\sum_{i=1}^m A_{pi} x_{pi}^2} A_{pi} = \frac{M_0 x_{\max}}{\sum_{i=1}^m x_{pi}^2} \quad (13)$$

where x_{\max} is the distance from the y - y axis to the endmost piles.

In the relations (12) and (13), the denominator is the pile moment of inertia, if we ignore the moments of inertia with respect to own axis:

$$I_y = \sum_{i=1}^m A_{pi} x_{pi}^2 \quad (14)$$

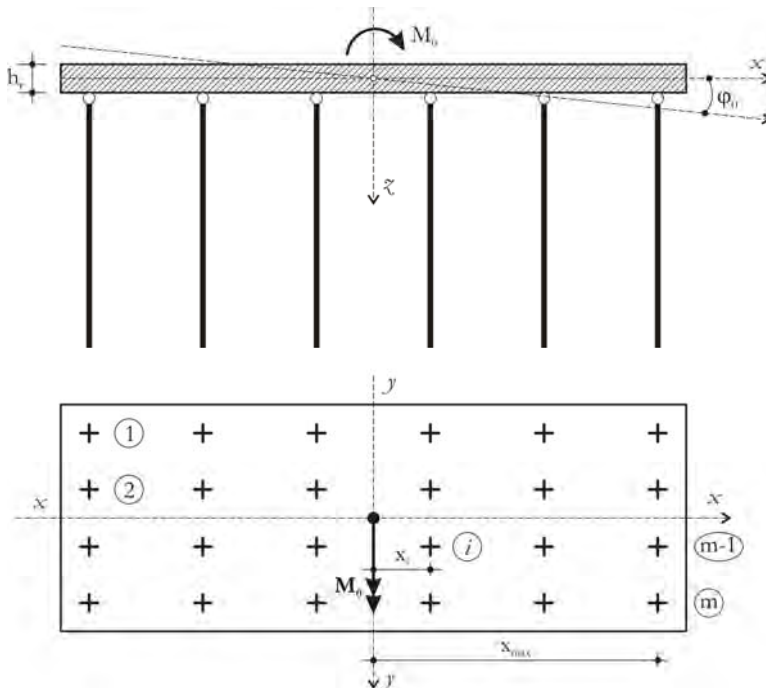


Figure 2. Raft subjected by a bending moment M_0

The raft rotation φ_0 can be expressed, from geometrical considerations, as:

$$\varphi_0 \cong \text{tg} \varphi_0 = \frac{\Delta l_{\max}}{x_{\max}} \quad (15)$$

where Δl_{\max} is the shortening (or elongation) of the endmost pile, and it has the expression:

$$\Delta l_{\max} = \frac{N_{p \max} \cdot l_p \cdot s}{E_p A_p} \quad (16)$$

where:

l_p is the pile length;

s is a coefficient which takes into consideration the settlement of the pile tip and the skin friction effect; it is determined on testing piles;

E_p, A_p are the elasticity modulus of the constitutive material, respectively the cross-sectional area of the pile.

Therefore, the rotation of the raft results:

$$\varphi_0 = \frac{M_0 s l_p}{\left(\sum_1^m A_p I_p \right) E_p x_{\max}} = \frac{M_0 s l_p}{E_p x_{\max} \sum_{i=1}^m A_{pi} I_{pi}} \quad (17)$$

For a group of m identical piles results:

$$\varphi_0 = \frac{M_0 s}{m x_{\max} E A_p} \quad (18)$$

3.2. Vertical fixed-head pile

3.2.1. The displacement x_0

By the raft translation, at the pile head appear horizontal shear forces and bending moments. From the invariability condition of the angle in the fixed section of the pile (Fig. 3a), the value of the bending moment at the pile head can be expressed as:

$$m_i = \frac{q_i}{2\alpha_i} \quad (19)$$

The displacement of the pile head is obtained:

$$x_{0i} = \frac{2q_i \alpha_i}{b_i c_h} - \frac{2m_i \alpha_i^2}{b_i c_h} = \frac{q_i \alpha_i}{b_i c_h} \quad (20)$$

For $q_i = 1$ the translation stiffness of the pile can be written [2], [4-5]:

$$k_i^* = \frac{1}{x_{0i}} = \frac{b_i c_h}{\alpha_i} \quad (21)$$

and the translation stiffness of the piles group results:

$$K^* = \sum_{i=1}^m k_i^* = \sum_{i=1}^m \frac{b_i c_h}{\alpha_i} \quad (22)$$

Therefore, the raft displacement x_0 is (Fig. 3.b):

$$x_0 = \frac{\sum_{k=1}^n Q_k}{K^*} = \frac{\sum_{k=1}^n Q_k}{\sum_{i=1}^m \frac{b_i c_h}{\alpha_i}} \quad (23)$$

For the case of the identical piles, the raft displacement can be expressed as:

$$x_0 = \frac{\alpha}{mbc_h} \sum_{k=1}^n Q_k \quad (24)$$

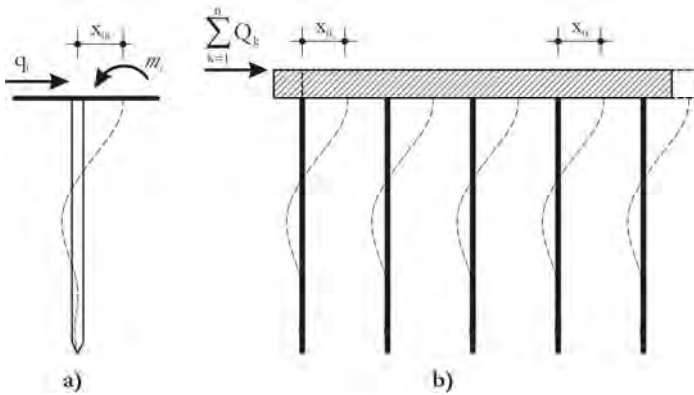


Figure 3. Vertical fixed-head pile: **a)** pile subjected by a horizontal force q_i ; **b)** the horizontal displacement x_0 of the raft

3.2.2. The global rotation of the raft produced by the structure bending

The bending moment M_0 which acts on the raft (Fig. 4) is given by the horizontal forces Q_k at the floors level, and by eventually eccentric gravitational forces ($M_{Q,P}$). Adding the effect of the thickness of the foundation raft, for Q_k forces, the M_0 bending moment can be expressed as:

$$M_0 = M_{Q,P} + h_r \sum_{k=1}^n Q_k \quad (25)$$

The rotation φ_0 of the raft induces axial forces in piles by the displacement

$$\Delta l_i = \varphi_0 x_i \quad (26)$$

The axial forces in piles will be:

$$N_i = \frac{E_p A_p}{sl_p} \Delta l_i = \frac{E_p A_p}{sl_p} x_i \varphi_0 \quad (27)$$

Also, the rotation φ_0 will give a bending moment at the pile head, expressed as

$$m_\varphi = \frac{c_h b}{4\alpha^3} \varphi_0 \quad (28)$$

This moment corresponds to a beam on elastic foundation acted by a φ_0 rotation at the upper end.

The moment's equation with respect to the y - y axis will give

$$\frac{EA_p}{sl_p} x_i \varphi_0 x_i + m \frac{c_h b}{4\alpha^3} \varphi_0 = M_0 \quad (29)$$

where m is the number of piles.

So the φ_0 rotation can be written as:

$$\varphi_0 = \frac{M_0}{\frac{EA_p}{sl_p} \sum_{i=1}^m x_i^2 + \frac{mc_h b}{4\alpha^3}} \quad (30)$$

Knowing the rotation of the piled raft we can compute the displacement because of it at a point at h height, being $\varphi_0 h$.

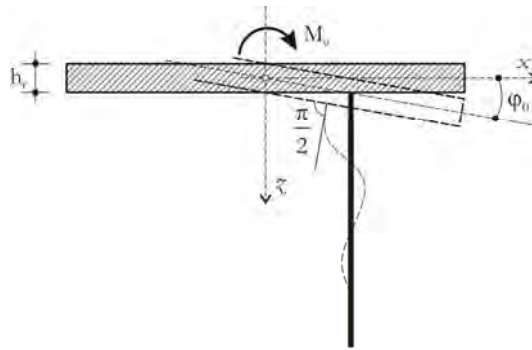


Figure 4. The global rotation of the raft

4. CONCLUSIONS

The made analysis allows to take into account, in design, the interaction of structure with the foundation system (piled raft type) for the determination of the fundamental vibration period.

To extend the analysis in the spatial case, a similar calculus in yOz plane is needed at first, and then a vectorial superposition of the resultants, or according to some recommendations prescribed in the Design Codes, can be made.

If the mass centre of the building doesn't coincide with the centroid of the piles sections, at the inferior level of the piled raft, a torsional moment appears, that makes modifications in the structural seismic response and in the internal forces and moments of the piles.

References

1. Ifrim, M., *Dinamica structurilor și inginerie seismică*, Editura Didactică și Pedagogică, București, 1984, pp. 470-473. (in Romanian)
2. Ungureanu, N., Contribuții privind analiza radierelor rezemate pe piloți, *teză de doctorat*, Institutul Politehnic Iași, 1969, pp. 7-14. (in Romanian)
3. Ungureanu, N., Elastic Plates Supported on Piles, *Buletinul I. P. Iasi*, Tomul XIX (XXIII), 1973, pp. 9-16.
4. Ungureanu, N., Lungu, I., Raileanu, P., On the Definition and Estimation of Pile Stiffness, *Buletinul IPI*, Tomul XLII (XLVI), 1996.
5. Ungureanu, N., Vrabie, M., Missir-Vlad, I., Studies concerning the analysis of flexible pier on pile foundations, *Buletinul IPI*, Tomul XL (XLIV), 1994, pp. 59-66.

Study of durability prediction of concrete structures using computer’s software

Ioan Paul Voda¹, Nicolae Florea² and Vasile Iacob³

¹Faculty of Civil Engineering- BMTO, “Gh. Asachi” Technical University, Iasi, Romania

²Faculty of Civil Engineering- BMTO, “Gh. Asachi” Technical University, Iasi, Romania

³Faculty of Civil Engineering- BMTO, “Gh. Asachi” Technical University, Iasi, Romania

Summary

Over the past decades, an enormous amount of effort has been expended in laboratory and field studies on concrete durability estimation. The results of this research are still either widely scattered in the journal literature or mentioned briefly in the standard textbooks. A significant step forward could be the development of appropriate software for computer-based estimation of concrete service life, including reliable mathematical models and adequate experimental data.

The main objective of this paper consists in presenting the basis of a computer estimation of the concrete service life. The prediction is focused on the basic deterioration phenomena of reinforced concrete, such as carbonation and chloride penetration, that initiate the reinforcing bars corrosion.

KEYWORDS: *computer, concrete, software, durability*

1. INTRODUCTION

Concrete service life (or working life) is the period of time during which the performance of the concrete structure will be kept at a level compatible with the fulfilment of the performance requirements of the structure, provided it is properly maintained. The ability of a structure to resist environmental attacks, without its performance dropping below a minimum acceptable limit, is called durability. The following three main factors affect the durability of concrete: the initial mixture proportions, the design, construction and maintenance of the structure, and the specific environmental conditions. Deterioration of concrete in service is every loss of performance, and it may be the result of a variety of mechanical, physical, chemical or biological processes.

All mechanical and physical mechanisms for concrete deterioration, except direct loading and imposed deformations, may exhibit their effect on concrete performance during the first year of the service life. Chemical and biological mechanisms actually start from the beginning; however, their detrimental results are observed typically long after the first year. In reinforced concrete, the most serious deterioration mechanisms are those leading to corrosion of the reinforcement, which occurs after depassivation due to carbon dioxide or chloride ion penetration. It is therefore necessary, if a long service life is required, that the modelling attempts to address corrosion initiation mechanisms and chemical/biological attack processes.

The EUCON software for prediction of concrete service life was developed at Patras Science Park S.A. Greece, fig. 1 shows the logic diagram used in this software development :

First, the essential parameters that characterize a concrete composition (mixture proportions) are selected, and this is the main source on which all other concrete characteristics depend. Thereafter, the main chemical and volumetric characteristics of concrete are calculated (chemical composition of hydrated cementitious materials, porosity and related characteristics) and this is also another source to receive more information. Based on the selected mixture proportions (cement type and strength class, cement content, water-cement ratio, air content, aggregate type, type and activity of additions, etc.), the compressive strength class of concrete is further estimated.

For each significant deterioration mechanism, according to the specific environment where the structure would be found, an appropriate proven predictive model is used. Concrete carbonation and chloride penetration are the most common causes for reinforcement corrosion onset, and for further concrete deterioration.

The service life of the structure found in these environments, which cause either carbonation or chloride penetration, is calculated. The degree of deterioration from a possible chemical attack (future development) is also estimated, either as a reduction in the effective concrete section (in the case of acid or biological attack) or as a reduction in strength of the affected concrete (in the case of sulphate or alkali attack). Finally, cost and environmental aspects regarding concrete composition are analysed. Now, for the initially selected concrete composition, the most essential properties have been predicted, such as strength, service life and cost. The designer can then modify the concrete composition accordingly to improve further every required property.

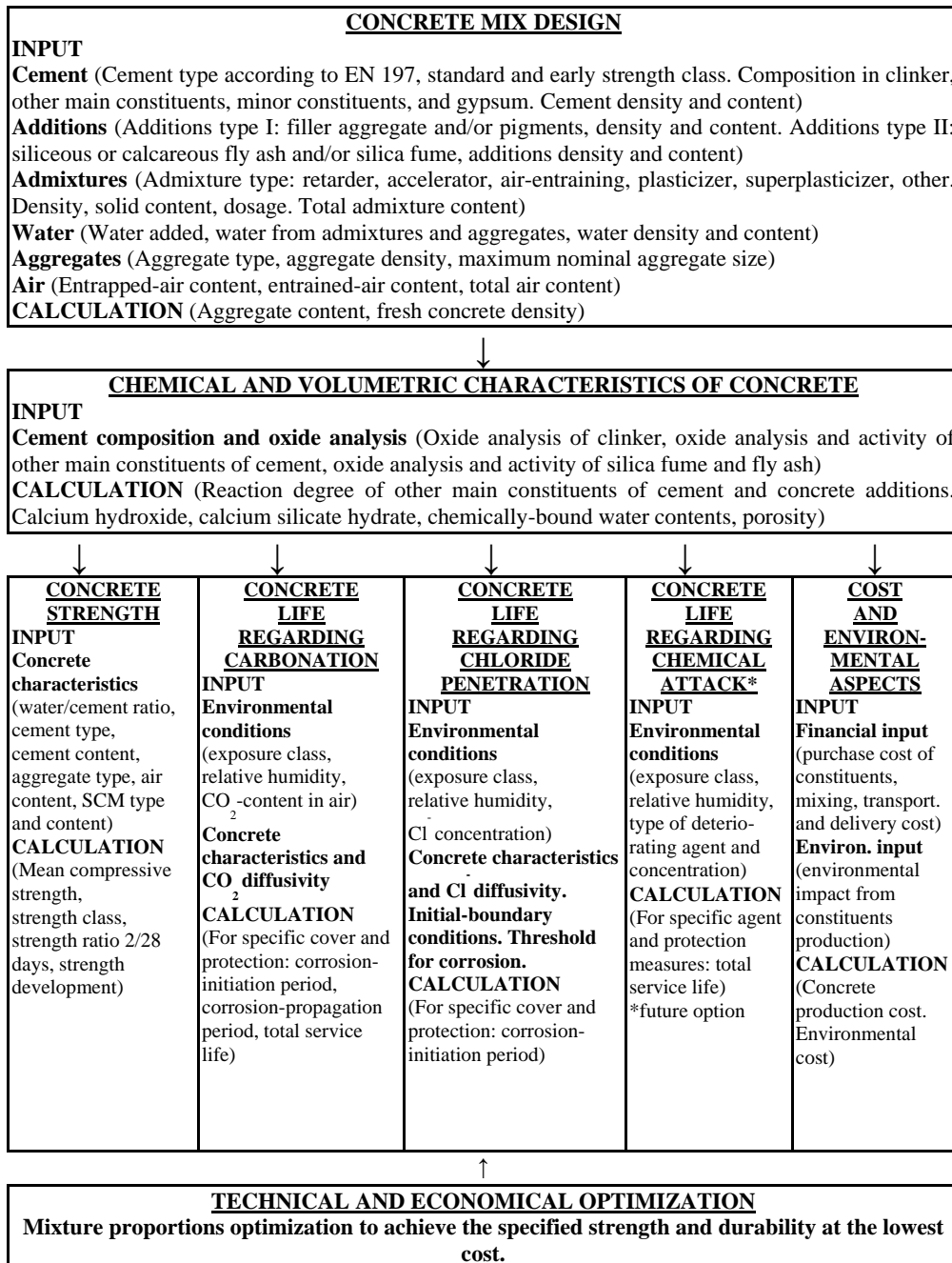


Figure 1. Logic diagram for computer-based estimation of concrete service life.

2. MODELLING OF DETERIORATION RATE

2.1. Mix design and basic calculation

For the present application, a concrete volume is assumed that contains certain amounts of cement, additions (optional), aggregates, water, and admixtures (optional) only. To the above materials entrained or entrapped air should be added. All these materials have to comply with the corresponding standards for the constituent materials. As the basis for concrete composition, the volume unit of 1 m³ of the fresh concrete is selected.

The composition of 1 m³ of fresh concrete is given as follows:

- C: kg cement / m³ of concrete;
- d_C : cement density (kg/m³);
- S: kg silica fume / m³ of concrete;
- d_S : silica fume density (kg/m³);
- F: kg fly ash / m³ of concrete;
- d_F : fly ash density (kg/m³);
- A: kg aggregates / m³ of concrete;
- d_A : aggregate density (kg/m³);
- W: kg effective water / m³ of concrete;
- d_W : water density (kg/m³);
- D: kg admixtures (solid) / m³ of concrete;
- d_D : admixture density (kg/m³);
- ϵ_{air} : m³ of entrained and/or entrapped air / m³ of concrete;

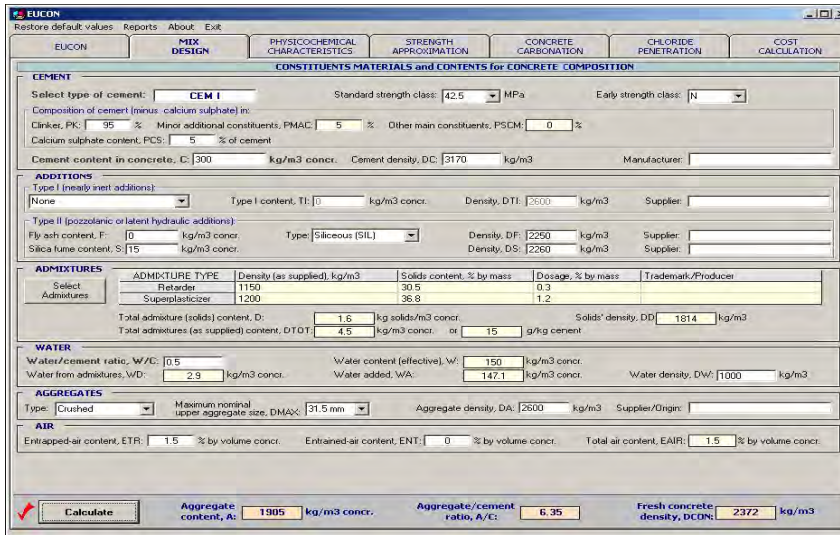
The following mass balance equation has to be fulfilled:

$$\frac{C}{d_C} + \frac{S}{d_S} + \frac{F}{d_F} + \frac{A}{d_A} + \frac{W}{d_W} + \frac{D}{d_D} + \epsilon_{air} = 1 \quad (1)$$

Fig. 2 shows the tab of the logic flowchart of the concrete mix design. As it is easy to see, there are several important fields :

- a field that the user introduces the input data for cement, additions, admixtures, water, aggregates;

- a calculation button;
- a field of the output results including the aggregate content in order to achieve the mass balance requirements, according to Eq. (1).



EUCON
Restore default values Reports About Exit

EUCON MIX DESIGN PHYSICO-CHEMICAL CHARACTERISTICS STRENGTH APPROXIMATION CONCRETE CARBONATION CHLORIDE PENETRATION COST CALCULATION

CEMENT
Select type of cement: **CEM I** Standard strength class: **42.5** MPa Early strength class: **N**
Composition of cement (minus calcium sulphate) in:
Clinker, PK: **95** % Minor additional constituents, PMAC: **5** % Other main constituents, PSCM: **0** %
Calcium sulphate content, PCS: **5** % of cement
Cement content in concrete, C: **300** kg/m³ concr. Cement density, DC: **3170** kg/m³ Manufacturer: _____

ADDITIONS
Type I (early strength additions)
None Type I content, TI: **0** kg/m³ concr. Density, DTI: **2500** kg/m³ Supplier: _____
Type II (pozzolanic or latent hydraulic additions)
Fly ash content, F: **0** kg/m³ concr. Type: **Siliceous (SIL)** Density, DF: **2260** kg/m³ Supplier: _____
Silica fume content, S: **15** kg/m³ concr. Density, DS: **2260** kg/m³ Supplier: _____

Select	ADVERTISEMENTS TYPE	Density (as supplied), kg/m ³	Solids content, % by mass	Dosage, % by mass	Trademark/Producer
Retarder		1160	30.5	0.3	
Superplasticizer		1200	36.8	1.2	

Total admixture (solids) content, D: **1.6** kg solids/m³ concr. Solids' density, DD: **1814** kg/m³
Total admixtures (as supplied) content, DTD: **4.6** kg/m³ concr. or **15** g/kg cement

WATER
Water/cement ratio, W/C: **0.5** Water content (effective), W: **150** kg/m³ concr.
Water from admixtures, W/D: **2.9** kg/m³ concr. Water added, W/A: **147.1** kg/m³ concr. Water density, DW: **1000** kg/m³

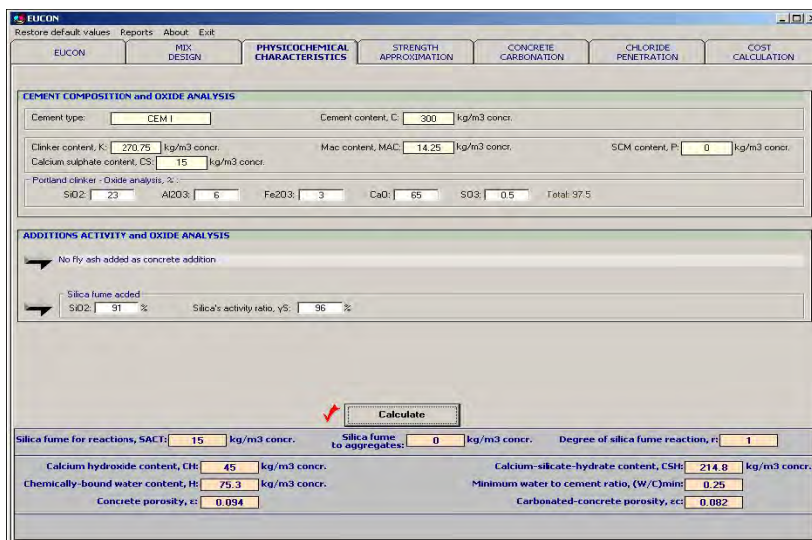
AGGREGATES
Type: **Crushed** Maximum nominal upper aggregate size, DMAX: **31.5** mm Aggregate density, DA: **2800** kg/m³ Supplier/Org: _____

AIR
Entrapped-air content, ETR: **1.5** % by volume concr. Entrained-air content, ENT: **0** % by volume concr. Total air content, EAIR: **1.5** % by volume concr.

Calculate Aggregate content, A: **1905** kg/m³ concr. Aggregate/cement ratio, A/C: **6.35** Fresh concrete density, DC0N: **2372** kg/m³

Figure 2. General view of the tab “MIX DESIGN” of the EUCON program.

In fig. 3 is estimated the chemical and volumetric composition of concrete.



EUCON
Restore default values Reports About Exit

EUCON MIX DESIGN PHYSICO-CHEMICAL CHARACTERISTICS STRENGTH APPROXIMATION CONCRETE CARBONATION CHLORIDE PENETRATION COST CALCULATION

CEMENT COMPOSITION and OXIDE ANALYSIS
Cement type: **CEM I** Cement content, C: **300** kg/m³ concr.
Clinker content, K: **270.75** kg/m³ concr. Mac content, MAC: **14.25** kg/m³ concr. SCM content, P: **0** kg/m³ concr.
Calcium sulphate content, CS: **15** kg/m³ concr.
Portland clinker - Oxide analysis, %:
SiO₂: **23** Al₂O₃: **6** Fe₂O₃: **3** CaO: **65** SO₃: **0.5** Total: **97.5**

ADDITIONS ACTIVITY and OXIDE ANALYSIS
No fly ash added as concrete addition
Silica fume added
SiO₂: **91** % Silica's activity ratio, yS: **96** %

Calculate

Silica fume for reactions, SACT: **15** kg/m³ concr. Silica fume to aggregates: **0** kg/m³ concr. Degree of silica fume reaction, r: **1**

Calcium hydroxide content, CH: **45** kg/m³ concr. Calcium-silicate-hydrate content, CSH: **214.8** kg/m³ concr.
Chemically-bound water content, H: **75.3** kg/m³ concr. Minimum water to cement ratio, (W/C)_{min}: **0.25**
Concrete porosity, ε: **0.094** Carbonated-concrete porosity, ε_c: **0.082**

Figure 3. General view of the tab “PHYSICO-CHEMICAL CHARACTERISTICS” of the EUCON program.

The tab contains:

- a field that the user introduces the input data for cement composition and oxide analysis, and additions activity and oxide analysis;
- a calculation button;
- field of the output results including the reaction degree of supplementary cementing materials and the various additions (either in cement or concrete), the calcium hydroxide and calcium-silicate-hydrate (CSH) content, the chemically-bound water content and the concrete porosity .

2.2. Reinforced corrosion induced by carbonation

Reinforcing bars in concrete are protected from corrosion by a thin oxide layer that forms on their surface due to the high alkalinity, i.e., the high pH-value, of the surrounding concrete. Corrosion may start when this protective layer is destroyed:

- either by chloride penetration (and the chloride content exceeds a critical value), or
- due to a reduction in the pH value of concrete to values below 9. Such a reduction in alkalinity is the result of carbonation of the $\text{Ca}(\text{OH})_2$ in the concrete mass, i.e., of its reaction with the atmospheric CO_2 that diffuses through the concrete pores.

The evolution of the carbonation depth, x_c (m), with time, t (s), is given by the following analytical expression, proven widely by many laboratory and field measurements:

$$x_c = \sqrt{\frac{2D_{e,CO_2}(CO_2/100)t}{0.33CH + 0.214CSH}} \quad (2)$$

where:

- CO_2 -content in the ambient air at the concrete surface (%),
- D_{e,CO_2} : the effective diffusivity of CO_2 in carbonated concrete (m^2/s),
- CH and CSH: the content of calcium hydroxide and calcium-silicate-hydrate, respectively, in concrete volume (kg/m^3).

In an ambient relative humidity, RH (%), the diffusivity is given by the empirical equation:

$$D_{e,CO_2} = 6.1 \times 10^{-6} \left(\frac{\varepsilon_c - \varepsilon_{air}}{1 - \frac{A}{d_A} - \varepsilon_R} \right) (1 - RH/100)^{2.2} \quad (3)$$

where:

- ε_c : the porosity of the carbonated concrete;
- ε_{air} : the content of concrete in entrapped or entrained air;
- A: the aggregate content in concrete volume (kg/m^3);
- d_A : the aggregate density (kg/m^3).

The critical time, $t_{cr,carb}$ (s), required for the carbonation front to reach the reinforcement located at a distance c (concrete cover to reinforcement, m), can be estimated by ($RH \geq 55\%$):

$$t_{cr,carb} = \frac{(0.33CH + 0.214CSH)c^2}{2D_{e,CO_2}(CO_2/100)} \quad (4)$$

The approach of Eq. (2-4) is the basis in the software (Papadakis and Efstathiou, 2005) for estimation of the corrosion-initiation period. In Fig. 4, the part of the logical flowchart of the program is presented for the calculation of the concrete carbonation depth and the estimation of the service life as regards corrosion induced by the carbonation-initiation mechanism.

The screenshot shows the EUCON software interface for the 'CONCRETE CARBONATION' tab. The interface is organized into several sections:

- ENVIRONMENTAL CONDITIONS:** Exposure class according to EN206: XC3 Moderate humidity; Mean relative humidity, RH: 70 %; Environment type: Urban area; CO2-content in the ambient air, CO2: 0.08 %.
- CONCRETE CHARACTERISTICS AND CO2 DIFFUSIVITY:** Carbonatable constituents: Calcium hydroxide, CH: 45 kg/m3 concr.; Calcium-silicate-hydrate, CSH: 214.8 kg/m3 concr.; Carbonated concrete porosity, ε_c : 0.082; Effective diffusivity of CO2, D_{e,CO_2} : 0.908 E-08 m2/s.
- ESTIMATION OF CONCRETE SERVICE LIFE:** Concrete cover, c : 30 mm; Corrosion - initiation period, $t_{cr,carb}$: 134.2 years; Corrosion - propagation period, $t_{pr,carb}$: 3 years; Total service life of concrete, Z_{carb} : 137.2 years.
- ESTIMATION OF CARBONATION DEPTH:** Concrete age, t : 50 years; Carbonation depth, x_c : 18.3 mm.

At the bottom of the interface, there are radio buttons for 'No Protection' and 'Protection'.

Figure 4. General view of the tab “CONCRETE CARBONATION” of the EUCON program.

The tab contains:

- a field that the user introduces the input data as regards the environmental conditions where the concrete structure is exposed;
- a field that the user is informed on the main concrete characteristics and CO₂ diffusivity that influence concrete carbonation;
- a calculation button, for estimation of concrete service life for a given cover to reinforcement;
- a calculation button, for estimation of carbonation depth at a given concrete age;
- There is also the possibility to estimate the above results in the case of use of a protection measure, such as waterproof sealants or cement – lime mortar coatings .

2.3. Reinforced corrosion induced by chlorides

Chlorides, transported through the concrete pore network and microcracks, depassivate the oxide film covering the reinforcing steel and accelerate the reaction of corrosion and concrete deterioration. Chloride penetration is a process which takes place in totally or partly water-filled pores. This is the main reason that as a process is much slower than carbonation, where CO₂ molecule may penetrate faster via air-filled pores.

The physicochemical processes of diffusion of Cl⁻ in the aqueous phase, their adsorption and binding in the solid phase of concrete, and their desorption therefrom are described by a nonlinear partial differential equation for the concentration of Cl⁻ in the aqueous phase [Cl⁻(aq)] (in kg/m³ pore solution), from which that of Cl⁻ bound in the solid phase [Cl⁻(s)] (kg/m³ concrete) can be computed algebraically:

$$\frac{\partial [Cl^{-}(aq)]}{\partial t} = \frac{D_{e,Cl^{-}}(1 + K_{eq}[Cl^{-}(aq)])^2}{K_{eq}[Cl^{-}(s)]_{sat} + \varepsilon(1 + K_{eq}[Cl^{-}(aq)])^2} \frac{\partial^2 [Cl^{-}(aq)]}{\partial x^2} \quad (5)$$

$$[Cl^{-}(s)] = \frac{K_{eq}[Cl^{-}(aq)]}{1 + K_{eq}[Cl^{-}(aq)]} [Cl^{-}(s)]_{sat} \quad (6)$$

initial condition: $[Cl^{-}(aq)] = [Cl^{-}(aq)]_{in}$ at $t = 0$ (initial concentration) (7a)

boundary conditions: $[Cl^{-}(aq)] = [Cl^{-}(aq)]_0$ at $x = 0$ (concrete surface) (7b)

$$\partial [Cl^{-}(aq)] / \partial x = 0 \text{ at } x = M \text{ (axis of symmetry)} \quad (7c)$$

where:

- x is the distance from the concrete surface (m);
- t is the time (s);
- $D_{e,Cl}$ - denotes the intrinsic effective diffusivity of Cl^- in concrete (m^2/s);
- K_{eq} the equilibrium constant for Cl^- binding (m^3 of pore volume/kg);
- $[Cl(s)]_{sat}$ the saturation concentration of Cl^- in the solid phase (kg/m^3 concrete);
- ε the concrete porosity (m^3 pore volume/ m^3 concrete).

Eq. (5) can be solved only numerically, e.g., using a finite difference method as does the aforementioned software.

A general view of the relevant tab is given in Fig. 6. The user has to fill in the “white boxes” within the permitted limits or to accept the default values, and then to press the calculation button in order to have an estimation of Cl^- profiles into concrete at various ages, as well as the corrosion-initiation period.

The screenshot shows the EUCON software interface with the following sections and values:

- ENVIRONMENTAL CONDITIONS:**
 - Corrosion induced by chlorides from: Sea water
 - Exposure class according to EN206: XS2 Permanently submerged
 - External source of chlorides: Marine environment-Mediterranean Sea
 - Chloride concentration at the concrete surface, $[Cl(aq)]_0$: 20 kg/m³ sol.
 - Exposure degree, ρ : 1
 - Cation: Na+
- CONCRETE CHARACTERISTICS and Cl- DIFFUSION BINDING:**
 - Silica fume added as concrete addition: No
 - Efficiency factor regarding chloride penetration, k : 5
 - No fly ash added as concrete addition: Yes
 - Concrete porosity, ε : 0.034
 - Effective porosity, ε_{eff} : 0.068
 - Effective diffusivity of Cl^- , $D_{e,Cl}$: 0.2828 E-12 m²/s
 - Equilibrium constant for Cl-binding, K_{eq} : 0.1 m³ sol/kg
 - Cl- saturation concentration in solid phase, $[Cl(s)]_{sat}$: 3.2 kg/m³ concr.
- INITIAL-BOUNDARY CONDITIONS and THRESHOLD for CORROSION:**
 - Initial concentration of chlorides, $[Cl(aq)]_i$: 0 kg/m³ sol.
 - Component (semi-)thickness, M : 200 mm
 - Critical value for corrosion $[Cl]_{total}$: 2.41 kg/m³ concr.
- SOLUTION and OUTPUT PARAMETERS:**
 - Space cells, N : 100
 - Spacestep, DX : 2 mm
 - Time values for intermediate results (years): t1: 10, t2: 25, t3: 50, t4: 75
 - Timestep, DT : 36000 s
 - Maximum time, $TMAX$: 100 years

A "Calculate" button with a red arrow is located at the bottom right of the input area. The bottom of the window shows tabs for "Parameters", "Results", and "Protection".

Figure 5. General view of the tab “CHLORIDE PENETRATION” and sub-tab “Parameters” of the EUCON program.

More specifically, the tab contains:

- a field that the user introduces the input data as regards the environmental conditions where the concrete structure is exposed;
- a field that the user is informed on the main concrete characteristics, the Cl⁻ diffusivity, and Cl⁻ binding characteristics, which all influence significantly the penetration;
- a field that the user introduces the initial-boundary conditions and the threshold for corrosion, and another field that the user introduces the solution and output parameters;
- a calculation button, for estimation of Cl⁻ profiles into concrete at various ages, as well as the corrosion-initiation period for a given cover to reinforcement (on results subtab);
- There is also the possibility to estimate the above results in the case of use of a protection measure, such as waterproof sealants (on protection subtab).

3. CONCLUSIONS

The software offers the possibility of investigating the efficiency of various protection measures, such as waterproof sealants, cement-lime mortar coatings, inhibitors, etc. Using these software packages, including the present one, an optimum concrete design can be achieved by estimating reliably the concrete strength, durability and production cost.

References

1. Papadakis, V.G., Efstathiou, M.P., Computer-aided approach of parameters influencing concrete service life and field validation, *Computers & Concrete* (Manuscript Number: CAC0123), 2007
2. Neville, A.M., *Properties of Concrete*, Longman, Essex, U.K., 1995
3. Richardson, M.G., *Fundamentals of Durable Reinforced Concrete*, Spon Press, London, 2002 .
4. European Standard EN 206-1 (2000), *Concrete – Part 1: Specification, Performance, Production and Conformity*, CEN, Brussels.

Computational modeling development for radionuclide decay study

Iulia Brîndușa Ciobanu

Physics Department, "Gh. Asachi" Technical University, Iasi, 700050, Romania

Summary

The aim of the present contribution is to perform a computational program in C++ language, adapted to the study of beta radiation interaction with substance. The program computes the linear absorption coefficient, mass absorption coefficient of beta radiation, maximum mass range, and maximum distance of radiation penetration into substance as well as maximum energy. The program was run for a set of experimental data obtained by measurements with the help of a Geiger type radiation counter, using a Cs-137 radionuclide source and as absorbent substance, aluminum (Al).

Our computational method can be used for nondestructive density measurements of cylindrical specimens. This method has several important applications in civil engineering. Many specimens in civil engineering laboratory testing are usually in the form of cylinders. One can show that for solid cylindrical specimens of the materials tested, the radiation attenuation law is satisfied to a very high degree [1].

The parameters of the two equivalent linear representations of radionuclide decay law were calculated, that derive by logarithmation of disintegration law. The processing of experimental data is computed by using the least squares method. One of coefficients represents the crossing of the lines with Oy axes, and the another parameter is slope of the linear function. It is observed the fact that the two foofs of lines with Oy axes are equal in a good approximation. They differ only at the 6th decimal. The linear absorption coefficients calculated by the two methods lead to a rather good coincidence and are in agreement with the recent experimental results, obtained by Sieglaff in 2007 [2]. The last statement is sustained also by the small values of the percentage relative errors that do not exceed the value of 0.5%. Consequently, the computational program designed by us proves to be correct and useful in studying the beta radiation absorption by substances.

We engage students collaboratively in making and using computational programs to describe, to evaluate, to design, and simulate physical phenomena. We involve students in using computers as scientific tools for collecting, analyzing, visualizing, and modeling data [3], [4].

KEYWORDS: computational program, C++ language, beta decay.

1. INTRODUCTION

The nucleus of an atom is a very dense area of the centre, consisting of protons and neutrons. The nucleus dimension is much smaller than the dimension of atom itself. The mass of an atom is approximately determined only by proton and neutron mass and with almost no contribution on behalf of the electrons [5].

The isotope of an atom is determined by the number of neutrons of the nucleus. Various isotopes of the same element have very similar chemical properties because the chemical reactions depend almost entirely on the number of electrons that atom have. The arrangement of electrons in the shells and sub-shells of an atom depends to a great extent on their number in the atom. Various isotopes of a particular chemical sample can be separated using a centrifugal plant or a mass spectrometer. For example, the first method is used in producing the enriched uranium from natural uranium, and the second method is used with carbon aging determination [5], [6].

The number of protons and neutrons determine, together, the nuclide or the nucleus type. The protons and neutrons have almost equal masses and their number, that is the mass number, is approximately equal with the mass of the atom. The mass of the electrons is very small compared to the mass of the nucleus, as soon as the proton and the neutron are each, of approximately 1836 times more massive than the electron. Two or more nuclides having the same number of nucleons in their nuclei, and having therefore identical mass number and about the same atomic mass are called nuclear isobars [5], [6].

An atomic nucleus is more stable as the average binding energy between the nucleons is higher, situation encountered especially at the nucleus containing: 2, 8, 20, 28, 50, 82, 126... ("magic numbers") protons or neutrons. The Pb-208 isotope, for example, has 82 protons and 126 neutrons. If a nucleus has too many or too few neutrons, it can be unstable and it will disintegrate after a certain period of time. For example, after several seconds after they were created, the nitrogen-16 atoms (7 protons, 9 neutrons) are beta disintegrating towards oxygen-16 atoms (8 protons, 8 neutrons). During this decay, the low nuclear force transforms a neutron from the nitrogen nucleus in a proton and an electron. The element (the atom) changes as initially had seven protons (fact for which it was “nitrogen”), and now has eight protons (fact for which it is oxygen”). Many elements have isotopes remaining stable for weeks, years or billion of years [5].

The discovery of the electron was the first indication that the atom has an internal structure. At the crossing of the XIX and XX centuries, the accepted atom model was “raisin cake” of J.J. Thompson, where the atom was considered a positively charged big ball, where small negative charges were included. In a short time, the physicists discovered, also, three types of radiation coming out from atoms, that they named alpha, beta and gamma radiations (Fig.1) [5], [7]. The experiments

conducted in 1911 by Lise Meitner and Otto Hahn and the ones carried out by James Chadwick in 1914 lead to the discovery that the spectral characteristics interpretation of beta disintegration should involve the supposition of admitting the non-conservation of energy. This issue leads to the discovery, later, of the neutrino. [5].

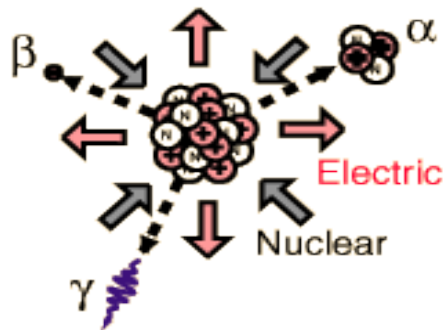


Figure1. Types of radionuclide decay [7]

In 1930, failing to reach the German town Tübingen to attend a meeting on radioactivity issues, Wolfgang Pauli sent to the participants a letter suggesting there is the possibility that in the nucleus to be a third particle which he named it “neutron”. He suggested that this particle should be very light (lighter than an electron), that it has not an electric charge and it does not interact with the substance, fact for which it was not still detected. This desperate way solved both problems: the one of energy conservation and that of nuclear spin of nitrogen-14, firstly because the “neutron” of Pauli was carrying with it the extra-energy of beta decay and then because that an extra-“neutron” mated with the seventh electron in the nucleus of nitrogen-14 gave the 1 spin. The “neutron” of Pauli was renamed neutrino by Enrico Fermi in 1931, but only after 30 years it was demonstrated that the neutrino really exists in beta decay [5], [8].

With the works of Fermi and Yukawa, the modern model of the atom was completed. The centre of the atom consists of a compact ball of neutrons and protons that are kept together by the hard nuclear forces. The unstable nuclei can endure alpha decay, in which they emit helium energetic nuclei, or beta decay, in which they emit electron or positrons. After one of these disintegrations, the resulted nucleus can be also in an excited state and in this case it is disintegrated also to a basic state emitting high energy photons (gamma decay) [5], [9].

Experiments have shown that all radioactive radiations cause chemical effects, blacken photographic plates, ionize gases and, sometimes, condensed materials on passing through them, and cause some solids and liquids to fluoresce. These properties are at the basis of experimental techniques for the detection and investigation of radioactive rays [6], [10].

2. THEORETICAL APPROACH

2.1. Beta decay

Fermi accepted the hypothesis of Pauli, rendering it in a theory of low interactions, that can explain even today many of the experimental results. Fermi changed the name of the particle, calling it neutrino, referring to its very small mass [8], [9]. He suggested a quantitative theory of beta ray emission where the existence of neutrino is admitted and it is treated the emission by a nucleus of electrons and of neutrino by beta decay which takes place by a similar process to the one described in the radiation theory by emission of a light quantum by an excited atom. There are deducted the formulas for the average life time and for the form of the continuous spectrum of beta rays and were compared with experimental data.

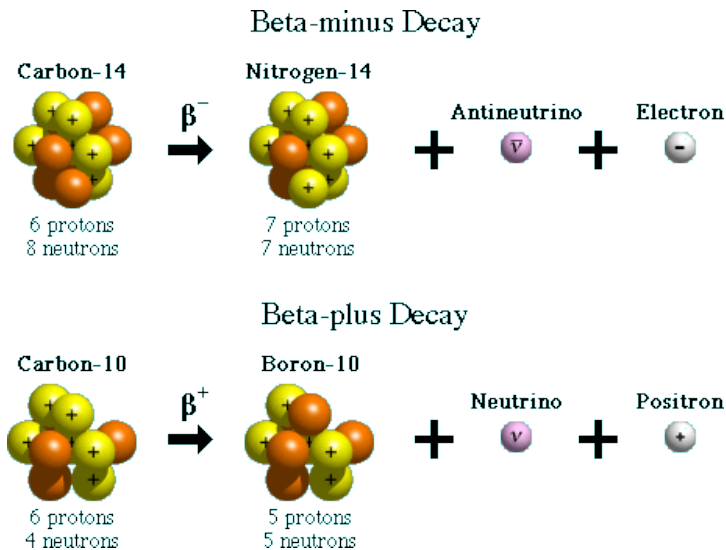


Figure 2. Two types of beta decay, beta-minus and beta-plus [11]

Beta decay is the process of spontaneous transmutation of unstable nuclei in isobaric nuclei whose atomic number varies with a unit, $\Delta Z = \pm 1$, by electron or positrons emission (Fig. 2.) or by electron capture from the outer cover of the atom. The half-time life of active beta nuclei varies from 10^{-2} seconds to 2×10^{15} years, and the maximum energy of the emitted beta particles is in the range of 18 keV (for 3_1H) and 16.6 MeV (for ${}^{12}_7N$) [11], [12].

There are known three types of beta decay:

- beta-minus decay (electron emission, e^-);

- beta-plus decay (positron emission, e^+);
- electron capture.

Trying to build a theory of nuclear electrons and of beta ray emissions it faced two major difficulties. The first one depends on the fact that the primary beta rays are emitted by the nuclei with a continuous distribution of velocity. If it doesn't want to abandon the principle of energy conservation, it has to admit that a fraction of energy released in the process of beta decay misses the present observing possibilities. According to the suggestion of Pauli that it can admit for example the existence of new particle, so-called neutrino that has a zero load and the mass of an order equal in size with that of the electron or smaller. It is admitted also that in each beta decay process simultaneously are emitted an electron, which is observed as a beta ray, and a neutrino that cannot be observed, but which bears a fraction of released energy. In the present theory, we rely on the existence of neutrino. A second difficulty for nuclear electron theory is related to the present relativist theories of light particles (electrons and neutrinos) that cannot offer a satisfactory explication of the fact that such kind of particles are connected on orbits of nuclear dimensions [8], [9].

The phenomenon of neutron beta decay is presented in Fig. 3, and Fig. 4. A neutron (udd) is transformed in a proton (uud), an electron and an antineutrino [13], [14].

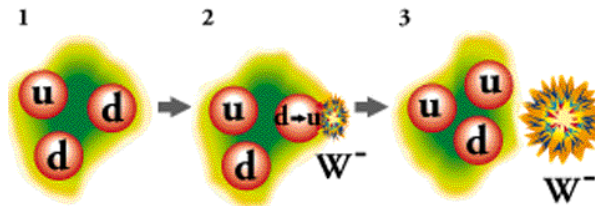


Figure 3. Theoretical model of neutron beta decay. Frame 1, 2, 3. [13]

Frame 1: The neutron (electric charge 0) made of a quark up and two quarks down;
 Frame 2: One of the quarks down is transformed in a quark up. As the quark down has a charge of $-1/3$ and the quark up has a charge of $2/3$, that means that the process is mediated by a virtual W particle that transports in distance a charge of -1 (so that the charge is conserved!);

Frame 3: The new quark is reunited away of emitted W⁻. The neutron became now a proton (Fig.3).

Frame 4: An electron and an antineutrino appear after virtual boson W⁻ disappearance.

Frame 5: The proton, the electron and the antineutrino are moving apart each other. The intermediary stages of this process occur in about a billionth of billions of billions of second and they are not observed (Fig.4), [13], [14].

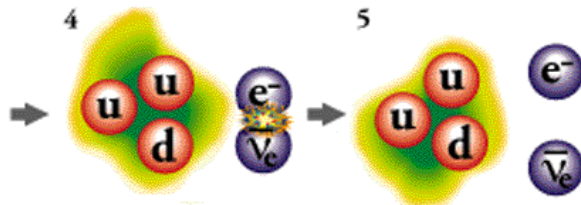


Figure 4. Theoretical model of neutron beta decay. Frame 4, 5. [13]

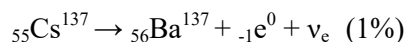
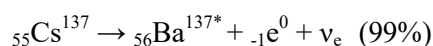
Some nuclei can undergo double beta decay ($\beta\beta$ decay) where the charge of the nucleus changes by two units. In most practically interesting cases, single beta decay is energetically forbidden for such nuclei, because when β and $\beta\beta$ decays are both allowed, the probability of β decay is (usually) much higher, preventing investigations of very rare $\beta\beta$ decays. Thus, $\beta\beta$ decay is usually studied only for beta stable nuclei. Like single beta decay, double beta decay does not change number of nucleons, A . Thus, at least one of the nuclides with some given A has to be stable with regard to both single and double beta decay [16], [17].

2.2. Cs-137 radionuclide decay

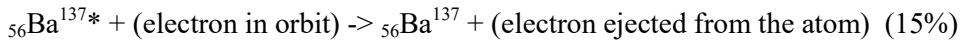
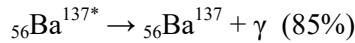
The study of beta radiation interaction with substance has been investigated using Cs-137 sources. The sources were mounted on thin foils in such a manner that they did not accumulate charge.

Caesium-137 is a radioactive isotope of Caesium which is formed mainly by nuclear fission. It has a half-life of 30.23 years, and decays by pure beta decay to a metastable nuclear isomer of barium-137 (Ba-137m). Barium-137m has a half-life of 2.55 minutes and is responsible for all of the gamma ray emission. The ground state of barium-137 is stable [15].

There are two possible final states after the beta decay: the ground state of Ba¹³⁷, or an excited state of Ba¹³⁷. The final state is the excited state 99% of the time:



The excited state of Ba^{137} can also decay in two different ways: via gamma emission or internal conversion. The gamma decay occurs 85% of the time, and internal conversion happens 15% of the time:



If ${}_{56}\text{Ba}^{137*}$ does undergo internal conversion, a hole is left in the inner electron orbit. Another electron quickly fills the hole and an X-ray is emitted. Thus for every ${}_{55}\text{Cs}^{137}$ decay, there are a lot of particles that can be emitted.

There is an 85% chance that a gamma will be emitted. We call 0.85 the gamma yield factor. There is always an electron emitted in beta decay, and there are also electrons emitted when internal conversion occurs. In addition, characteristic X-rays are emitted [18], [19], [20].

Cs-137 is used in small amounts for calibration of radiation-detection equipment, such as Geiger-Mueller counters. In larger amounts, Cs-137 is used in medical radiation therapy devices for treating cancer; in industrial gauges that detect the flow of liquid through pipes; and in other industrial devices to measure the thickness of materials, such as paper, photographic film, or sheets of metal [21].

Caesium-137 is water-soluble and extremely toxic in minute amounts. Once released into the environment, it remains present for many years as its radiological half-life is 30.23 years. It can cause cancer 10, 20 or 30 years from the time of ingestion, inhalation or absorption provided sufficient material enters the body.

Biological behavior of Cs-137 is similar to potassium. After entering the organism, all Cs gets more or less uniformly distributed through the body, with higher concentration in muscle tissue and lower in bones. The biological half-life of caesium is short at 70 days [15], [21].

3. PROGRAM IMPLEMENTATION

Beginning in the 1970s, computers played a role in nuclear science that developed from relatively minor to significant. Before this time, computers were used for calculations to develop and refine theories in nuclear science. As computers moved to being interfaced with detectors and accelerators, they became inseparable from the experiment. Indeed, the design of detectors for large experiments includes the integration of computer systems into each detector element.

Computers are still used to calculate predictions of experiments based on various theories. Only the most powerful computer systems can generate simulations of the expected data from today’s giant experiments. Similarly, only the most powerful computers can process the data that come from these experiments [22].

Some fundamental Physics topics are not well understood by the students that arrive to the university levels which are observed by the low performance of the students in the basic subjects of Physics during the first course of the science and enginery degrees. This indicates the need to develop new pedagogical methodologies that help students to increase their knowledge, abilities, and skills. Computer-assisted instruction is a good pedagogical tool to obtain these objectives. It is necessary to develop programs that permit a high level of interaction with the students [23], [24].

We present now our new computational program in C++ code, adapted for study of beta decay in physics laboratory.

The magnitude values are introduced in the computational program (Fig. 5):

- substance density, $D = \rho$;
- dead time correction, $M = \tau$ = the minimum time from the beginning of a completely developed impulse until the beginning of the next impulse that could be still separately recorded; the small time (but finite) needed for recording a radiation implies a non-zero probability so that some radiations to reach the detector, just in time for the counting installation to be locked with the recording of the previous impulse [25];
- background correction = F = counting rate corresponding to the radiations coming out of environment (cosmos, earth, construction materials);

The number of determinations is introduced, N .

At each of the N determinations the following are introduced:

- $d(i)$ = thickness of attenuating layer, where $i = \overline{1, N}$;
- $n(d(i))$ = uncorrected counting rate = number of impulses recorded in time unit; $d(i)$ representing the variable;

The thickness of the attenuating layer substance (Al) is increased and it is measured with the help of a radiation detector the number of impulses in time unit, $n(d(i))$.

The program computes and displays for each $i = \overline{1, N}$ determinations:

- $$R(i) = D \cdot d(i) = x(i) \tag{1}$$

where $R(i)$ is mass range (it are calculated the components of the vector which components are represented by the products between density and thickness of the attenuating layer);

- $$n(i) = [n(d(i)) - F] + M[n(d(i)) - F]^2 \tag{2}$$

- $$y(i) = \ln(n(i)) \tag{3}$$

The program calculates and displays the coefficients of the linear representation (a , b) by the least squares method (Fig. 6). Law of decay in its logarithmic form expresses a linear dependence from a theoretical point of view:

$$\ln(n(i)) = b \cdot d(i) + a \tag{4}$$

$$a = \frac{\sum_{i=1}^N x_i^2 \sum_{i=1}^N y_i - \sum_{i=1}^N x_i \sum_{i=1}^N x_i y_i}{N \sum_{i=1}^N x_i^2 - (\sum_{i=1}^N x_i)^2} \tag{5}$$

$$b = \frac{N \sum_{i=1}^N x_i y_i - \sum_{i=1}^N x_i \sum_{i=1}^N y_i}{N \sum_{i=1}^N x_i^2 - (\sum_{i=1}^N x_i)^2} \tag{6}$$

where b represents the mass absorption coefficient of radiation and also is the slope of tangent to the graph of linear function.

The program calculates and displays, [26]:

- linear absorption coefficient

$$C = \mu = -b \cdot D \tag{7}$$

- maximum mass range

$$R(\max) = \frac{D \cdot a}{C} \tag{8}$$

- maximum energy

$$E(\max) = \frac{(42.9R(\max) + 44.15) + \sqrt{(42.9R(\max) + 44.15)^2 + 858R(\max)}}{429} \tag{9}$$


```

PROGRAM_CPP
1=[1]
if (y2[i] > maxy) {maxy = y2[i];}
}
if (maxx < 1) {for (i = 1; i < n + 1; i++) {x2[i] = x2[i] * 200; y2[i] = y2[i]
else {if (maxx < 10) {for (i = 1; i < n + 1; i++) {x2[i] = x2[i] * 50; y2[i]
for (i = 1; i < n + 1; i++) {if (x2[i] < minx) {minx = x2[i];}
if (x2[i] > maxx) {maxx = x2[i];}
if (y2[i] < miny) {miny = y2[i];}
if (y2[i] > maxy) {maxy = y2[i];}
}
if (maxy < 1) {for (i = 1; i < n + 1; i++) {x2[i] = x2[i] * 100; y2[i] = y2[i]
else {if (maxy < 10) {for (i = 1; i < n + 1; i++) {x2[i] = x2[i] * 50; y2[i]
if (maxx > 700) {for (i = 1; i < n + 1; i++) {x2[i] = x2[i] / 10; y2[i] = y2[i] / 4
for (i = 1; i < n + 1; i++) {if (x2[i] < minx) {minx = x2[i];}
if (x2[i] > maxx) {maxx = x2[i];}
if (y2[i] < miny) {miny = y2[i];}
if (y2[i] > maxy) {maxy = y2[i];}
}
if (maxy > 700) {for (i = 1; i < n + 1; i++) {x2[i] = x2[i] / 10; y2[i] = y2[i]
for (i = 1; i < n + 1; i++) {if (x2[i] < minx) {minx = x2[i];}
if (x2[i] > maxx) {maxx = x2[i];}
if (y2[i] < miny) {miny = y2[i];}
if (y2[i] > maxy) {maxy = y2[i];}
}
}
}
d = h * minx + a;
f = h * maxx + a;

initgraph(&gdriver, &gmode, "");
al = getmaxx();
bl = getmaxy();
line(al / 2 - 100, 0, al / 2 - 100, bl);
line(0, bl / 2 + 100, al, bl / 2 + 100);
moveto(al / 2 - 112, 0);
outtext("0");
moveto(al / 2 - 103, 0);
outtext("A");
moveto(al - 8, bl / 2 + 97);
outtext("");
moveto(al - 8, bl / 2 + 103);
outtext("W");
e = al / 2 - 100 + minx;
g = al / 2 - 100 + maxx;
line(e, bl / 2 + 100 - d, g, bl / 2 + 100 - f);
for (i = 1; i < n + 1; i++) {putpixel(al / 2 - 100 + x2[i], bl / 2 + 100 - y2[i], 4);}
getch();
closegraph();
}
86:77
F1 Help F2 Save F3 Open Alt-F9 Compile F9 Make F10 Menu

```

Figure 6. Screen capture of computational algorithm (C++ code). Part 2.

3. RESULTS AND DISCUSSION

The mass absorption coefficient in Al ($D = 2.7 \text{ g/cm}^3$) for 0.52 MeV beta rays from a Cs-137 sample was measured using a Geiger detector (Fig.7).

The Geiger counter has the following characteristics [27]:

- portable, compact, easy to use instrument;
- selectable filters for determining alpha, beta, gamma radiations;
- large display, integrated RS 232 interface;
- with cable, software for Windows, operating manual;
- types of radiations: alpha (from 4 MeV), beta (from 0.2 MeV), gamma (from 0.02 MeV);
- measured variables: equivalent dose in Sv/h, mSv/h, microSv/h, pulses/sec,

pulses/ time interval;

- detector: probe counting tube type, from stainless steel with neon filling, length 31,1 mm, diameter 9,1 mm with mica window;

-internal memory 2kB;

-dimensions 163x72x30 mm.



Figure 7. Radiation detector. Geiger counter [27]

Table 1. contains experimentally measured magnitude values which were introduced in the computational program, as well as the values of some magnitude determined by program running.

Table 1. Experimental data

Nr.	d(i) [mm]	n(i) [imp/min]	R(i) [g/cm ²]	ln(n(i))
1	0	59874	0	11.0
2	0.20	22026	0.054	10.0
3	0.40	7332	0.108	8.9
4	0.60	1480	0.162	7.3
5	0.80	403	0.216	6.0
6	0.98	148	0.2646	5.0

The program computes the linear absorption coefficient, mass absorption coefficient of beta radiation, maximum mass range, and maximum distance of radiation penetration into substance (Fig.8).

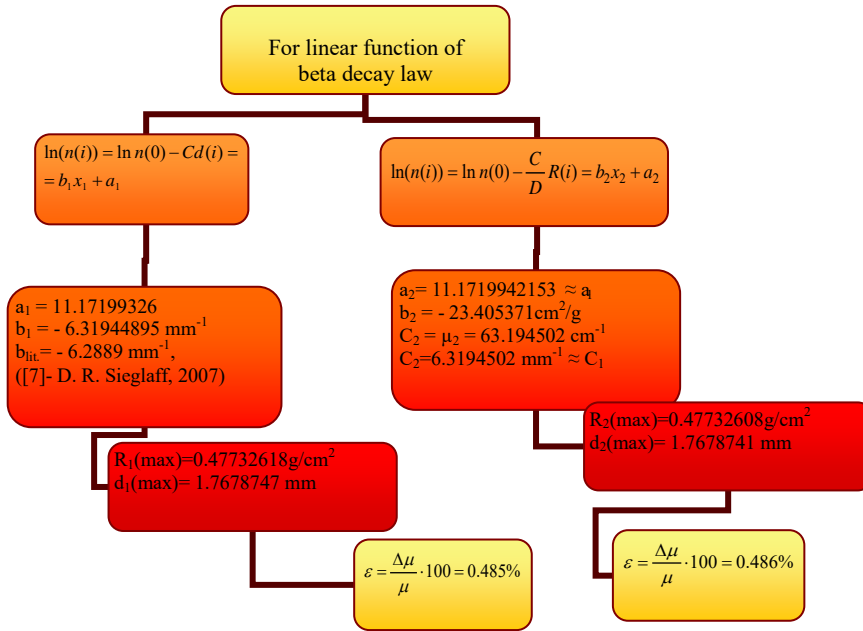


Figure 8. Computational results

Figure 8 summarizes the absorption coefficients and mass absorption coefficients determined for each case. One obtains:

$$\begin{aligned}
 a_2 &= 11.1719942153 \approx a_1 = 11.1719942153 \\
 C_1 = \mu_1 &= 6.31944895 \text{ mm}^{-1} \approx C_2 = \mu_2 = 63.194502 \text{ cm}^{-1} \\
 R_1(\text{max}) &= 0.47732618 \text{ g/cm}^2 \approx R_2(\text{max}) = 0.47732608 \text{ g/cm}^2 \\
 d_1(\text{max}) &= 1.7678747 \text{ mm} \approx d_2(\text{max}) = 1.7678741 \text{ mm}.
 \end{aligned}$$

It is observed the fact that the two foots of lines with Oy axes are equal in a good approximation. They differ only at the 6th decimal. The linear absorption coefficients calculated by the two methods lead to a rather good coincidence and are in agreement with the recent experimental results, obtained by Sieglaff in 2007 [2]. The last statement is sustained also by the small values of the percentage relative errors that do not exceed the value of 0.5% (Fig.8).

Consequently, the computational program designed by us proves to be correct and useful in studying the beta radiation absorption by substances.

Our computational method can be used for nondestructive density measurements of cylindrical specimens. This method has several important applications in civil

engineering. Many specimens in civil engineering laboratory testing are usually in the form of cylinders. One can show that for solid cylindrical specimens of the materials tested, the radiation attenuation law is satisfied to a very high degree [1].

3. CONCLUSIONS

All course and laboratory activities have to be designed to build structural knowledge and develop the students' abilities. Also, the better and faster method for processing the physics data, the computational method is enriched with one powerful C++ program. The idea of monitoring and modeling of the physical phenomena surely help to educate new generations.

Code written in C++ is very short in comparison with other languages, since the use of special characters is preferred to key words, saving some effort to the programmer. The resulting code from a C++ compilation is very efficient, due indeed to its duality as high-level and low-level language and to the reduced size of the language itself.

Acknowledgements

The work was supported by the Scientific Grant CEX05-D10_08/03.10.2005.

References

1. S. A. Tan, T. F. Fwa, *Nondestructive density measurements of cylindrical specimens by gamma-ray attenuation*, Journal of Testing and Evaluation, Vol. /Issue: 19:2, pp. 155-160, 2001.
2. D. R. Sieglaff, Augustana College, Rock Island, Illinois, USA, *Determination of Mass Absorption Coefficients in Pb and Al, and the Range in Al, for Radiations from Co-60 and Cs-137, Nuclides*, http://helios.augustana.edu/~drs/PHYS351%202007_2/Sample%20Formal%20Write-up.doc, 2007.
3. B. Ciobanu, I. Radinschi, *One Computational Algorithm for Physics Modeling*, Proceedings of 5th International Conference on Electromechanical and Power Systems- SIELMEN 2005, Chisinau, Republic of Moldova, Vol. 1, pp. 222-225, 2005.
4. B. Ciobanu, I. Radinschi, *Implementation of Physics Teaching in Engineering Education*, The 6th International Balkan Workshop on Applied Physics, Constanta, Romania, pp. 161, 2005.
5. http://ro.wikipedia.org/wiki/Nucleu_atomic.
6. B. M. Yavorsky, A. A. Pinsky, *Fundamentals of Physics*, Vol. II, MIR Publisher Moscow, Second printing, 1979.
7. C. R. Nave, B. C. Nave, *Physics for the Health Sciences*, 3rd Ed., W. B. Saunders, 1985, <http://hyperphysics.phy-astr.gsu.edu/Hbase/nuclear/beta.html#c1>.
8. ScienzaPerTutti 2002-2005.
9. E. Fermi, *Tentativa unei teorii a razelor beta*, 1934.
10. H. D. Young, *Physics*, Eighth Edition, Addison- Wesley Publishing Company, 1992.
11. <http://education.jlab.org/glossary/betadecay.html>

12. S. Muscalu, *Fizica atomica si nucleara*, Editura Didactica si Pedagogica, Bucuresti, 1975. (in Romanian)
13. http://fizicaparticulelor.ro/index.php?option=com_content&task=view&id=248&Itemid=1
14. N. Pacachoff, *Marie Curie and the Science of Radioactivity*, Oxford University Press, 1997.
15. <http://en.wikipedia.org/wiki/Caesium-137>.
16. http://en.wikipedia.org/wiki/Beta_decay.
17. F. N. D. Curie, J. R. Richardson, H. C. Paxton, *The Radiations Emitted from Artificially Produced Radioactive Substances*, I. The Upper Limits and Shapes of the β -Ray Spectra from Several Elements". *Physical Review* **49** (5): 368-381. doi:10.1103/PhysRev.49.368, 1936.
18. H. M. Agnew, *The Beta-Spectra of Cs¹³⁷, Y⁹¹, Pm¹⁴⁷, Ru¹⁰⁶, Sm¹⁵¹, P³², and Tm¹⁷⁰*, Phys. Rev. **77**, pp. 655 – 660, 1950.
19. <http://www.csupomona.edu>
20. Yu.A.Baurov, A.A.Konradov, V.F.Kushniruk, E.A.Kuznetsov, Yu.V.Ryabov, A.P.Senkevich, Yu.G.Sobolev, S.V.Zadorozsny, *Experimental Investigations of Changes in beta-decay rate of Co-60 and Cs-137*, Mod.Phys.Lett. **A16**, pp. 2089-2102, 2001.
21. www.bt.cdc.gov/radiation, *Radiation Emergencies, Radioisotopes Brief, Cesium-137(Cs-137)*, Department of Health and Human Services Centers for Disease Control and Prevention Safer. Healthier.People, August 2004-2005.
22. <http://lbl.gov/abc/wallchart/chapters/03/2.html>, *Guide to the Nuclear Wallchart*, 2000.
23. B. Ciobanu and I. Radinschi, *A Computational Program for the Performance Prediction of Yarns*, International Symposium Present and Perspective in Textile Engineering Proceedings, 10-12 November 2005, Iasi, Romania, pp. 563-569, 2005.
24. J. M. Sanchez, M. Hidalgo, V. Salvado, VALORA: A PC Program for the Self- Learning of Acid Base Titrations, International Technology, Education and Development Conference Proceedings, March 7th-9th, 2007, Valencia, pp. 52-57, 2007.
25. D. Mihailescu, E. Lozneau, *Lucrari practice de fizica nucleara*, Editura Universitatii "Alexandru Ioan Cuza, Iasi, 2003. (in Romanian)
26. S. Oancea, *Absorbția beta în aluminiu și determinarea energiei maxime prin metoda absorbției totale*, *Indrumar de lucrari practice de fizica*, Tipografia Insitutului Politehnic Iasi, pag. 309-313, 1977. (in Romanian)
27. [http:// www.telecomed.ro](http://www.telecomed.ro).

“Computational Civil Engineering 2008”, International Symposium
Iași, România, May 30, 2008



Photo 1. Symposium poster



Photo 2. Opening session - prof. Constantin Ionescu



Photo 3. Image from the audience



Photo 4. Image from the audience



Photo 5. Prof. Mihai Budescu read the order of the Senate of Technical University “Gh. Asachi” granting Diploma of Excellence to prof. Alex. Horia Barbat from University of Catalonia, Barcelona, Spain



Photo 6. Handing of diploma



Photo 7. Prof. A.H. Barbat thanking the University Senate for the diploma of excellence



Photo 8. Image from the audience



Photo 9. Dr. eng. Rodian Scînteie present synthesis



Photo 10. Dr. eng. Octavian Victor Roșca present synthesis



Photo 11. Dr. eng. Irina Baran present synthesis



Photo 12. Prof. Assoc. Marinela Barbuta present synthesis



Photo 13. Drd. Alina Nicuta present synthesis



Photo 14. Prof. Doina Ștefan present synthesis



Photo 15. Prof. Alex.Horia Barbat present scientific report

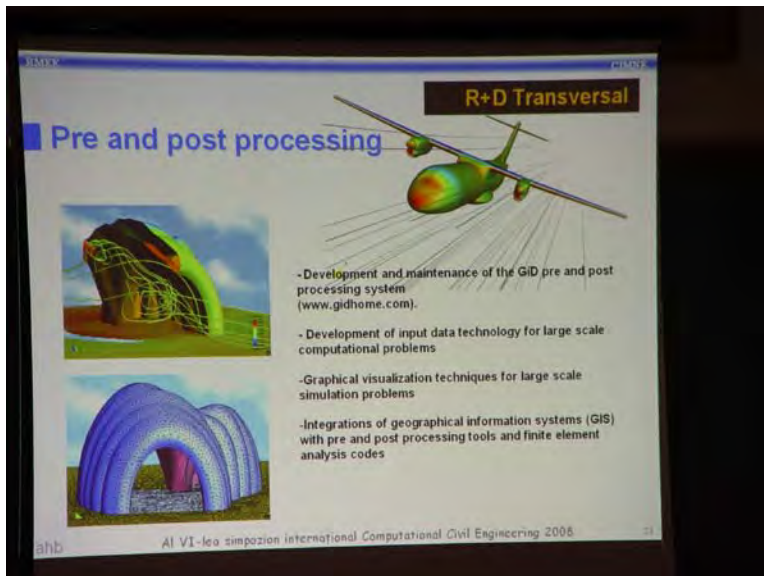


Photo 16. Picture form prof. A.H. Barbat report

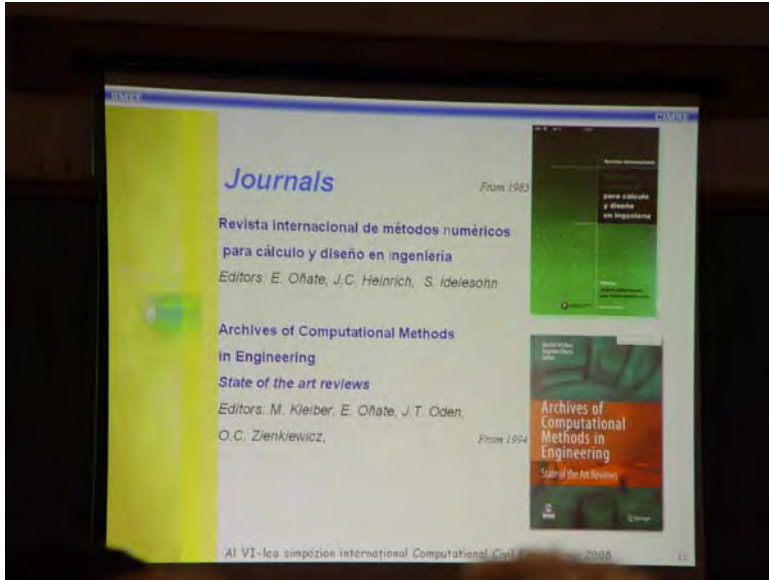


Photo 17. Picture form prof. A.H. Barbat report



Photo 18. Prof. Andrei Radu – view point

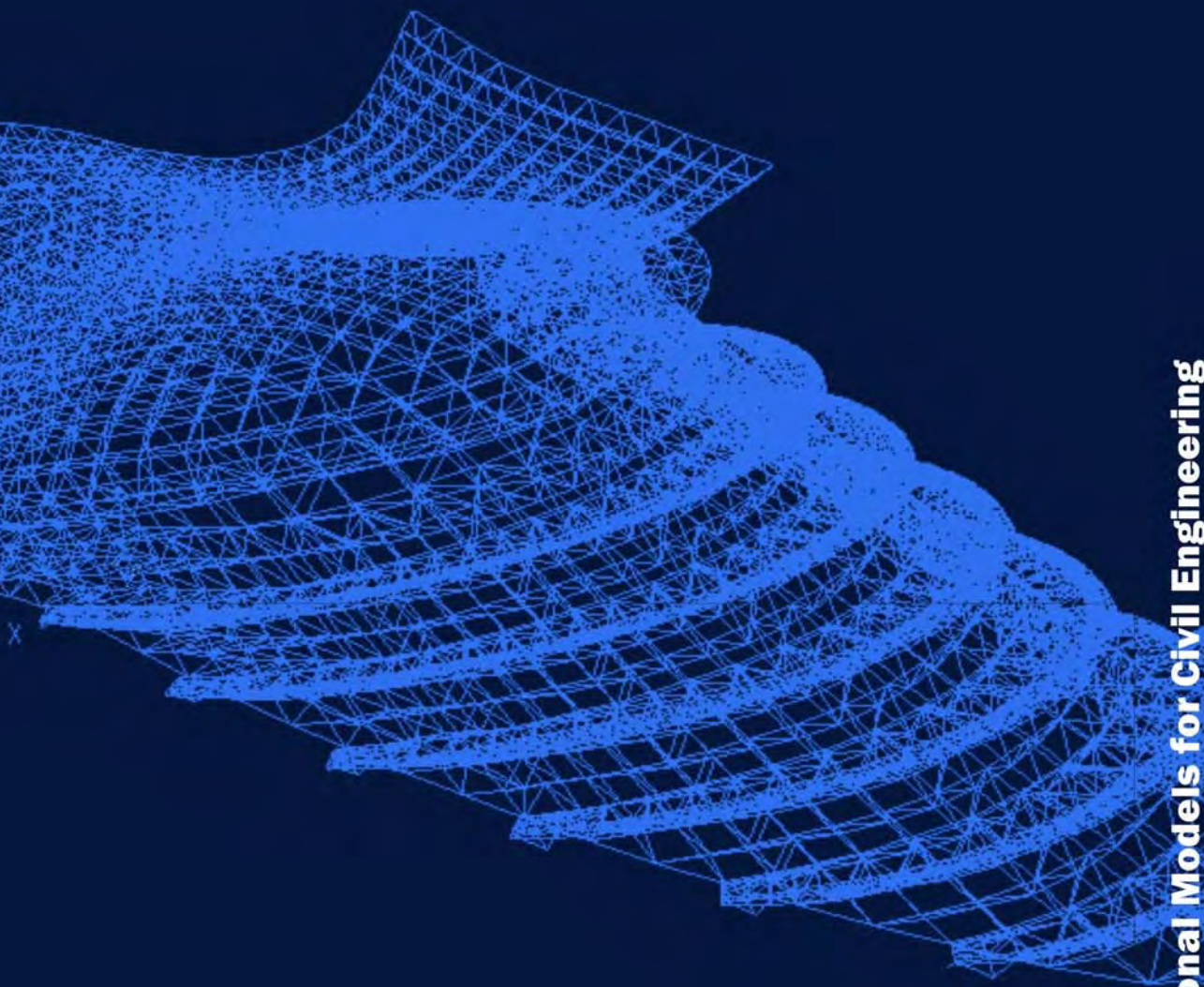


Photo 19. Prof. Cristian Comisu – view point



Photo 20. Prof. Dan Diaconu – view point

COLECȚIA
MANIFESTĂRI ȘTIINȚIFICE



Computational Models for Civil Engineering



ISBN 978-973-8955-41-7